

AD-A242 580



DREDGING RESEARCH PROGRAM

TECHNICAL REPORT DRP-91-3

vm (2)

MOBILE, ALABAMA, FIELD DATA COLLECTION
PROJECT, 18 AUGUST - 2 SEPTEMBER 1989

Report 1

DREDGED MATERIAL PLUME
SURVEY DATA REPORT

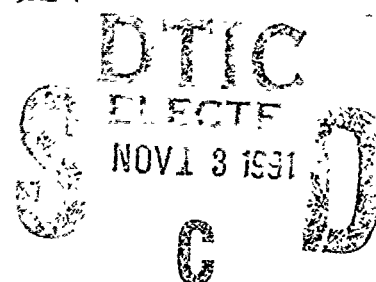
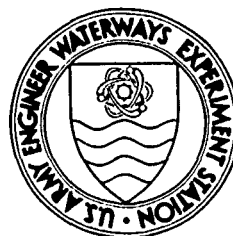
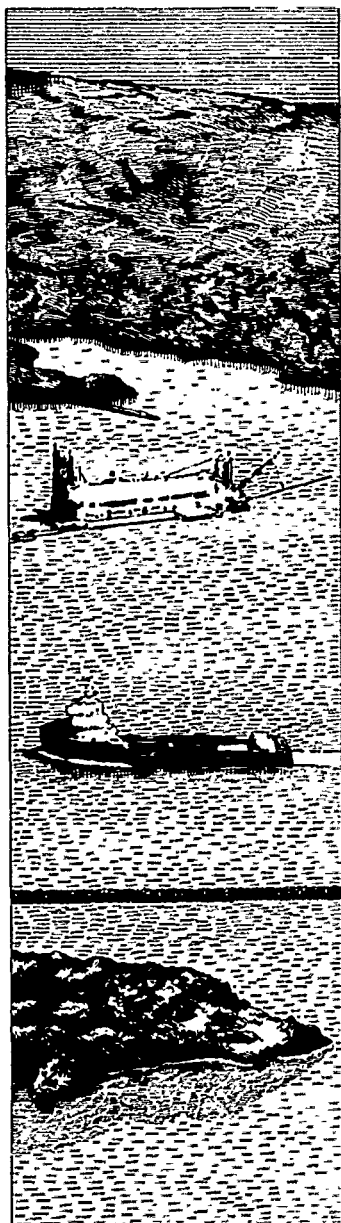
edited by

Nicholas C. Kraus

Coastal Engineering Research Center

DEPARTMENT OF THE ARMY

Waterways Experiment Station, Corps of Engineers
3909 Halls Ferry Road, Vicksburg, Mississippi 39180-6199



September 1991

Report 1 of a Series

Approved For Public Release; Distribution Is Unlimited

Prepared for DEPARTMENT OF THE ARMY
US Army Corps of Engineers
Washington, DC 20314-1000

Under Measurement of Entrainment and Transport
(Noncohesive Sediments) Work Unit 32464

91 1113 012

91-15548



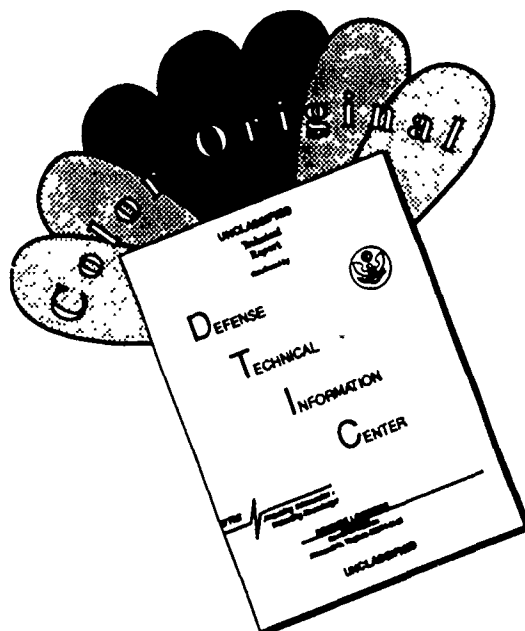
The Dredging Research Program (DRP) is a seven-year program of the US Army Corps of Engineers. DRP research is managed in these five technical areas:

- Area 1 - Analysis of Dredged Material Placed in Open Waters
- Area 2 - Material Properties Related to Navigation and Dredging
- Area 3 - Dredge Plant Equipment and Systems Processes
- Area 4 - Vessel Positioning, Survey Controls, and Dredge Monitoring Systems
- Area 5 - Management of Dredging Projects

Destroy this report when no longer needed. Do not return
it to the originator.

The contents of this report are not to be used for
advertising, publication, or promotional purposes.
Citation of trade names does not constitute an official
endorsement or approval of the use of such
commercial products.

DISCLAIMER NOTICE



THIS DOCUMENT IS BEST QUALITY AVAILABLE. THE COPY FURNISHED TO DTIC CONTAINED A SIGNIFICANT NUMBER OF COLOR PAGES WHICH DO NOT REPRODUCE LEGIBLY ON BLACK AND WHITE MICROFICHE.

REPORT DOCUMENTATION PAGE			Form Approved OMB No. 0704-0188	
Public reporting burden for this collection of information is estimated to average 1 hour per response, including the time for reviewing instructions, searching existing data sources, gathering and maintaining the data needed, and completing and reviewing the collection of information. Send comments regarding this burden estimate or any other aspect of this collection of information, including suggestions for reducing this burden, to Washington Headquarters Services, Directorate for Information Operations and Reports, 1215 Jefferson Davis Highway, Suite 1204 Arlington, VA 22202-4302, and to the Office of Management and Budget, Paperwork Reduction Project (0704-0188), Washington, DC 20503				
1. AGENCY USE ONLY (Leave blank)		2. REPORT DATE September 1991		3. REPORT TYPE AND DATES COVERED Report 1 of a series
4. TITLE AND SUBTITLE Mobile, Alabama, Field Data Collection Project, 18 August - 2 September 1989; Report 1, Dredged Material Plume Survey Data Report			5. FUNDING NUMBERS WU 32464	
6. AUTHOR(S) Nicholas C. Kraus, Editor				
7. PERFORMING ORGANIZATION NAME(S) AND ADDRESS(ES) USAE Waterways Experiment Station Coastal Engineering Research Center 3909 Halls Ferry Road, Vicksburg, MS 39180-6199			8. PERFORMING ORGANIZATION REPORT NUMBER Technical Report DRP-91-3	
9. SPONSORING / MONITORING AGENCY NAME(S) AND ADDRESS(ES) US Army Corps of Engineers, Washington, DC 20314-1000			10. SPONSORING / MONITORING AGENCY REPORT NUMBER	
11. SUPPLEMENTARY NOTES Available from National Technical Information Service, 5285 Port Royal Road, Springfield, VA 22161				
12a. DISTRIBUTION / AVAILABILITY STATEMENT Approved for public release; distribution is unlimited			12b. DISTRIBUTION CODE	
13. ABSTRACT (Maximum 200 words) The Dredging Research Program Technical Area 1 entitled "Analysis of Dredged Material Placed in Open Water" conducted the Mobile, Alabama, Field Data Collection Project (MFDCP) in 1989 off Mobile, Alabama, with the objectives of testing acoustic instrumentation for measuring sediment plume dynamics and bottom boundary layer processes, and to develop and refine plume tracking procedures for monitoring the movement of dredged material placed in shallow water. This report, consisting of six separately authored chapters, collectively provides an overview of equipment and procedures used during the MFDCP together with a presentation of the MFDCP data and analyses results. The MFDCP produced an extensive, high-quality data set by monitoring 18 dredged material plumes, from which eight events were selected for detailed analysis in this report. Components of the MFDCP include: acoustic backscatter measurements from two systems; water current measurements by an acoustic-Doppler current profiler; in situ water sampling; pre- and post-dredged material sampling; aerial photography; accurate ship and barge positioning; and local oceanographic and meteorological conditions.				
14. SUBJECT TERMS See reverse			15. NUMBER OF PAGES 350	
			16. PRICE CODE	
17. SECURITY CLASSIFICATION OF REPORT UNCLASSIFIED	18. SECURITY CLASSIFICATION OF THIS PAGE UNCLASSIFIED	19. SECURITY CLASSIFICATION OF ABSTRACT	20. LIMITATION OF ABSTRACT	

14. (Concluded).

acoustic-Doppler current profiler
acoustic profiler
dredged material
Mobile, Alabama

sediment concentration
sediment plumes
sediment transport
suspended sediment

PREFACE

The study described herein was authorized as part of the Dredging Research Program (DRP) by Headquarters, U.S. Army Corps of Engineers (HQUSACE). Work was performed under the Measurement of Entrainment and Transport Work Unit 32464 of DRP Technical Area 1 (TA1), Analysis of Dredged Material Placed in Open Water, at the Coastal Engineering Research Center (CERC), U.S. Army Engineer Waterways Experiment Station (WES). Messrs. Robert H. Campbell and Glenn R. Drummond were the HQUSACE Chief and TA1 Technical Monitors, respectively, for the DRP. Mr. E. Clark McNair, CERC, was DRP Program Manager (PM), and Dr. Lyndell Z. Hales, CERC, was Assistant PM. Dr. Nicholas C. Kraus, Senior Scientist, CERC, was Technical Manager of DRP TA1, which includes Work Unit 32464. Dr. Kraus was also Principal Investigator of Work Unit 32464 and technical editor of this report.

This report contains a compilation and preliminary analysis of data obtained during a DRP field data collection project conducted off Mobile Harbor, Alabama, in the Gulf of Mexico, during 18 August to 2 September 1989. This report was written over the period January to November 1990 by the investigators who participated in the data collection project and colleagues: Ms. Carol A. Coomes, Evans-Hamilton, Inc. (EHI), Seattle, Washington; Mr. W. Paul Dammann, Ocean Acoustics Division (OAD), Atlantic Oceanographic and Meteorological Laboratories (AOML), National Oceanographic and Atmospheric Administration (NOAA), Miami, Florida; Dr. Curtis C. Ebbesmeyer, EHI; Mr. Christopher Humphrey, RD Instruments (RDI), San Diego, California; Dr. Kraus, CERC; Mr. Atle Lohrmann, RDI; Ms. Terri L. Prickett, Coastal Processes Branch (CPB), Research Division (RD), CERC; Dr. John R. Proni, Chief, OAD, AOML; and Dr. Orson P. Smith, Smith Ocean Science and Engineering, Inc., Clayton, North Carolina. Dr. Kraus was under the supervision of Dr. James R. Houston, Chief, CERC, and Mr. Charles C. Calhoun, Jr., Assistant Chief, CERC. Ms. Prickett was under the supervision of Mr. Bruce A. Ebersole, Chief, CPB.

Onsite coordination and assistance at the U.S. Army Corps of Engineer District (USAED), Mobile, were provided by Mr. Pat Langan, Operations Division (OD), Navigation Branch; Dr. Susan Ivester Rees, Planning and Environment Division, Environment and Resources Branch, and Mr. Steven Sema, OD, Mobile Area Office. Dr. Thomas E. White, Prototype Measurement and Analysis Branch (PMAB), Engineering Development Division (EDD), CERC, was the EHI Contract Monitor and CERC coordinator between WES; EHI; USAED, Mobile, and the USAED,

Mobile, contract dredger, Great Lakes Dredge & Dock Company (GLD&D). Dr. White also participated in the field data collection. Mr. Timothy L. Fagerburg, Estuarine Processes Branch, Estuaries Division, Hydraulics Laboratory (HL), WES, led an HL team that obtained dredged material sediment samples from the disposal scows. Principal contacts at GLD&D were Mr. John Zenga, Project Superintendent; Mr. Kevin Holt, Project Engineer; and Mr. Ken Lago, Captain of the dredge *Chicago*. Mr. Steven Rabelais, Louisiana Universities Marine Consortium, Cocodrie, Louisiana, was the coordinator for the *R/V Pelican* used in the Mobile, Alabama, Field Data Collection Project, and Mr. Robert Cutting was the Captain. Appreciation is expressed to the captains of the GLD&D tug *Paul Candies*. Mr. Sam Corson, PMAB, EDD, CERC, and Ms. Sandra Staggs, Contracts Division, WES, assisted in EHI contract arrangements. Ms. Lee T. Byrne, Information Technology Laboratory, WES was the publications editor of the final report.

COL Larry B. Fulton, EN, was Commander and Director of WES. Dr. Robert W. Whalin was Technical Director.

Additional information can be obtained from Mr. E. Clark McNair, Jr., DRP Program Manager, at (601) 634-2070 or Dr. Nicholas C. Kraus, Principal Investigator, at (601) 634-2018.

CONTENTS

	<u>Page</u>
PREFACE	1
CONVERSION FACTORS, NON-SI TO SI (METRIC) UNITS OF MEASUREMENT .	5
SUMMARY	6
CHAPTER 1. INTRODUCTION TO THE MOBILE, ALABAMA, FIELD DATA COLLECTION PROJECT, <i>by Nicholas C. Kraus, Curtis C. Ebbesmeyer, and Orson P. Smith</i>	7
Introduction	8
Objectives of the MFDCP	11
Project Organization	12
Project Site	15
Plume Tracking Procedure	14
Data Set	19
Concluding Discussion	20
Acknowledgments	21
References	21
Tables	23
Figures	25
Appendix 1A: Coordinated Summary of Surveys	39
CHAPTER 2. AMBIENT METEOROLOGIC AND OCEANOGRAPHIC CONDITIONS, <i>by Orson P. Smith, Carol A. Coomes, Terri L. Prickett, and Nicholas C. Kraus</i>	53
Introduction	54
Regional Meteorological and Oceanographic Conditions	54
Moored Current Meter Array (Tidal Current)	55
Local Waves, Currents, and Weather	59
References	61
Table	62
Figures	63
Appendix 2A: Current Vector Plots and Time Histories During Releases	99
CHAPTER 3. SHIP AND BARGE POSITIONING, <i>by Carol A. Coomes and Terri L. Prickett</i>	111
Introduction	112
Ship Positioning During Survey Operations	112
Hopper Barge Tracking During Survey Operations	115
Acknowledgment	117
Tables	118
Figures	125

CHAPTER 4. PROJECT MEASUREMENTS: IN SITU WATER PROPERTIES, SUSPENDED AND BOTTOM SEDIMENT, AND AERIAL PHOTOGRAPHY, by Orson P. Smith, Terri L. Prickett, and Nicholas C. Kraus	135
Introduction	136
In Situ Water Property Measurements, Samples, and Analysis	136
Prerelease Dredged Material Samples and Analysis	144
Postrelease Bottom Grab Samples and Analysis	145
Aerial Photography	146
Acknowledgments	147
References	147
Tables	148
Figures	174
Appendix 4A: Depth Profiles of Temperature, Salinity, Sigma-Theta, Velocity of Sound, Light Transmission, and Brunt-Väisälä Frequency	177
Appendix 4B: Suspended Sediment Sample Grain Size Density Functions	201
CHAPTER 5. MEASUREMENTS WITH AN ACOUSTIC DOPPLER CURRENT PROFILER (ADCP), by Atle Lohrmann and Christopher A. Humphrey	219
Introduction	220
ADCP System: Hardware and Software	222
Measurement of Sediment Concentration	223
Simple Models of the Acoustic Backscatter	226
Bottom Tracking and Navigation	228
Current Velocity	232
Vertical Velocity, Backscattering, and Internal Waves	233
Conclusions and Recommendations	237
References	238
Tables	239
Figures	244
Appendix 5A: Beam Amplitude Calibration	301
CHAPTER 6. SEDIMENT PLUME MEASUREMENTS WITH AN ACOUSTIC CONCENTRATION PROFILER, by W. Paul Dammann and John R. Proni	311
Introduction	312
Background	313
Equipment and Procedures	313
Analysis and Results	316
Conclusions	321
Discussion and Recommendations	322
References	324
Tables	325
Figures	328
Appendix 6A: Theoretical Background	345

CONVERSION FACTORS, NON-SI TO SI (METRIC) UNITS OF MEASUREMENT

Non-SI units of measurement used in this report can be converted to SI (metric) units as follows:

<u>Multiply</u>	<u>By</u>	<u>To Obtain</u>
cubic yards	0.7645549	cubic meters
degrees (angle)	0.01745329	radians
Fahrenheit degrees	5/9	Celsius degrees or kelvins*
feet	0.3048	meters
inches	25.4	millimeters
knots (international)	0.51444444	meters per second
miles (U.S. nautical)	1.852	kilometers
miles (U.S. statute)	1.609347	kilometers
ounces (U.S. fluid)	0.02957353	cubic decimeters

Accession For	
NTIS GRA&I	<input checked="" type="checkbox"/>
DTIC TAB	<input type="checkbox"/>
Unannounced	<input type="checkbox"/>
Justification	
By	
Distribution/	
Availability Codes	
Dist	Avail and/or Special
A-1	



* To obtain Celsius (C) temperature readings from Fahrenheit (F) readings, use the following formula: $C = (5/9) (F - 32)$. To obtain kelvin (K) readings, use: $K = (5/9) (F - 32) + 273.15$.

SUMMARY

This report consists of six separately authored chapters that collectively provide a data compilation and introduction to measurements made and procedures used during the Mobile, Alabama, Field Data Collection Project (MFDCP). The MFDCP was a major data collection project conducted during 18 August to 2 September 1989 in the Gulf of Mexico, off Mobile Harbor, Alabama, under the auspices of the Dredging Research Program (DRP). The MFDCP had four objectives: (a) to collect comprehensive data on sediment plume dynamics for verifying and improving numerical simulation models of the short-term fate (minutes to hours after release) of dredged material placed in open water; (b) to investigate and refine sediment plume monitoring procedures; (c) to evaluate acoustic instrumentation for measuring sediment plume dynamics, and (d) to collect field data on coastal bottom boundary layer processes.

This report presents MFDCP data for meeting the first three objectives and provides numerical simulation components of the DRP and the research community with reliable and comprehensive measurements of sediment plume dynamics in shallow water. It also contains information for conducting similar field data collection exercises. The data set on plume dynamics is believed to be superior to previous plume surveys in accuracy, length of measurement, capture of key features, and variety. Simultaneous measurement of backscatter intensity from the suspended sediments by two independent and different acoustic systems, made together with water sampling, allows inter-comparison of the acoustic instruments and provides a first step toward field calibration.

Excellent weather and instrument functioning resulted in a successful project yielding a high-quality data set of 18 dredged material plumes, of which 8 plume events are extensively analyzed in this report. Local oceanographic and meteorological conditions are also given. Plume monitoring was performed at two locations within the authorized disposal area at Mobile, nominally of 42- and 27-ft depths. The monitoring characterized the growth and decay of the main body of plumes generated in shallow water during dredged material placement operations. The recorded plume dynamics include the initial descent, bottom surge, generation of internal waves, and evolution of the plume under different current conditions.

CHAPTER 1
INTRODUCTION TO THE MOBILE, ALABAMA,
FIELD DATA COLLECTION PROJECT

NICHOLAS C. KRAUS

*Coastal Engineering Research Center
Waterways Experiment Station, Corps of Engineers
Vicksburg, Mississippi 39180-6199*

CURTIS C. EBBESMEYER

*Evans-Hamilton, Inc.
Seattle, Washington 98103*

ORSON P. SMITH

*Smith Ocean Science and Engineering, Inc.
Clayton, North Carolina 27520*

Contents

1. Introduction
2. Objectives of the MFDCP
3. Project Organization
4. Project Site
5. Plume Tracking Procedure
6. Data Set
7. Concluding Discussion

Acknowledgments

References

Tables

Figures

Appendix

1. Introduction

Background and Motivation

The U.S. Army Corps of Engineers (USACE) is responsible for assuring the navigability of the Nation's waterways, a responsibility that includes both dredging and managing dredged material disposal sites. This mission requires removal of sediments deposited within channels, inlets, and harbors and subsequent disposal in open-water sites. All types of sedimentary material are encountered in dredging projects, including rock, sand, and marine silt and clay, and mixtures of these components. The texture of this material includes large cohesive clay clumps, clastic rocks, sands composed of individual particles, and colloidal solutions of very fine particles. Proper disposition and management of dredged material into the ocean environment are conducted following regulatory guidelines administered by the U.S. Environmental Protection Agency and other Federal and State agencies.

Recognizing the dual responsibility of maintaining navigability of U.S. waters and protecting the environment in the process of dredging, transporting, and disposing or placing of dredged material, the USACE conducted a major research effort called the Dredged Material Research Program (DMRP) during the years 1973 through 1978 to study environmental effects associated with dredging (Saucier et al. 1978; Lazar, Calhoun, and Patin 1984). As one of its many contributions to the understanding of environmental effects of dredging, the DMRP issued a numerical simulation model of the short-term fate of dredged material released in open water (Johnson and Holliday 1978) that has seen widespread use and periodic updating (Johnson 1990). However, only limited field data have been available to verify and refine this model.

In 1988, the USACE established the Dredging Research Program (DRP) as a 7-year interlaboratory research effort to develop technologies to reduce the cost of dredging (McNair 1989). The DRP is organized into five technical areas that encompass the various aspects of dredging. Among these, DRP Technical Area 1 (TA1), "Analysis of Dredged Material Placed in Open Water," includes two activities: development of improved numerical simulation models to predict the movement of dredged material introduced to coastal and estuarine waters and development of techniques and equipment to monitor the movement of this material. The monitoring component encompasses data collection for model verification as well as production of equipment for dredged material monitoring at the project level. These research activities are

intended to reduce dredging costs by providing systematic, objective, and verified procedures capable of categorizing the physical behavior of material placed in disposal sites.

One of the most difficult aspects of monitoring dredged material in open water is measurement of the movement, type, and amount of material in the water column during the minutes to hours immediately following release from a barge or scow. The volume of material released is typically 500 to 5,000 cu yd³ and consists of both solids and water. Model predictions and laboratory and field observations, including observations described herein, indicate that the majority of the material falls to the bottom as a collective body at a rate much greater than the fall speed of an individual sediment particle (e.g., Biggs 1968; Sustar, Wakeman, and Ecker 1976; Bokuniewicz et al. 1978; Tsai and Proni 1985; Nichols, Diaz, and Schaffner 1990). A small portion of the fine-grained particles remains in the water column to disperse and settle as individual particles at relatively low concentration. The amount of material remaining in the water column and its movement must be known before dredged material disposal sites can be managed effectively.

The result of a typical placement operation is a plume of material, shown schematically in Figure 1.1, consisting of the combination of a cloud of particles (often visible on the water surface) and the main mass of material descending through the water column and spreading along the bottom. In this report, the term "plume" refers to all material in the water column. The shape and evolution of the plume depend upon the type of material, motion of the barge, method of discharge, local currents and waves, density structure of the water column, water depth, and other factors. Because of the many factors governing plume dynamics and the rapid changes in a plume occurring over substantial spatial extent, measurement of the short-term plume behavior is extraordinarily difficult, and such data are lacking. In fact, both the instrumentation and the procedures for making these measurements are in their infancy.

Field Data Collection Project

To progress beyond limited measurement capabilities, as well as to collect high-quality data on the dynamics of dredged material plumes for simulation model verification, personnel of DRP TA1 planned and conducted a major field data collection project in the Gulf of Mexico at the site of dredged material placement operations carried out for Mobile Harbor deepening and improvement. This field effort, called the Mobile, Alabama, Field Data Collection Project (MFDCP), took place

* A table of factors for converting non-SI units of measurement to SI (metric) units is presented on page 5.

from 18 September to 2 August 1989. An overview of the MFDCP was given by Kraus and Prickett (1989), and a video documenting the MFDCP field activities was produced (Kraus 1990).

Scope of This Report

The MFDCP was conducted in three phases: preproject planning, field measurements, and data compilation and analysis. This report is a product of the third phase, but it also contains discussion of measurement procedures employed during the field data collection and logistical arrangements. It consists of six chapters written by the individuals responsible for the data collection activities during the MFDCP and subsequent data reduction and interpretation. As a coordinated and edited report, the chapters are structured to optimize completeness and usefulness of the data, yet not overlap in coverage. Appendices are included as necessary to supplement the text with data listings, graphics, and explanations of more technical and specialized matter. The MFDCP produced a large quantity of diverse measurements, and it is not possible to include all the data at this stage of analysis. The raw data may be requested from the DRP Program Manager, Coastal Engineering Research Center (CERC), at the U.S. Army Engineer Waterways Experiment Station (WES), or from the pertinent authors.

This report describes the scope of the MFDCP, procedures used in the field data collection, and data obtained during the observation of dredged material plumes. The intent is to provide sufficient documentation and analysis of the data set so that it may be used by modeling components of the DRP and others to test and refine numerical and physical models of plume dynamics and particle dispersion. The data are also useful for the intercomparison and testing of the plume-monitoring capabilities of acoustic instruments.

Chapter 1 describes the background of the MFDCP, orientation to the study site, and general procedures used in the data collection. It also introduces the remaining five chapters of the report containing the data and specific technical information. Chapter 2 presents the ambient meteorologic and oceanographic conditions that occurred during the MFDCP, including the wave, wind, and tidal current conditions. Chapter 3 concerns ship positioning and presents measurement procedures and results of accurate surveys of the positions of both the measurement vessel and the barges releasing the dredged material. Chapter 4 describes background measurements that provide basic information on the ambient water in which the dredged material was released, the sediment that was dredged, and sediment as it was found on the sea floor. Information pertaining to the aerial photographs taken during the MFDCP is also presented in Chapter 4.

Chapters 5 and 6 contain results obtained from two independent acoustic instruments forming the principal equipment suite used to measure plume dynamics and water current in the vicinity of the plumes. Chapter 5 presents results obtained with the Acoustic Doppler Current Profiler (ADCP). This instrument was originally developed to measure the three-dimensional current velocity field in an open-water, typically oceanic environment. A 1.2-MHz ADCP was operated by the manufacturer, RD Instruments. During the MFDCP, the ADCP was tested to provide ship positioning by bottom tracking and also, importantly, to measure backscatter intensity associated with the particles composing the plume, thereby providing estimates of sediment concentration.

Chapter 6 contains results obtained with the Acoustic Concentration Profiler (ACP), an acoustic instrument specifically designed to measure sediment concentration (more generally, any particle concentration such as sewerage discharge constituents or biomass) in open water (Proni et al. 1975, Proni et al. 1976a, 1976b). The ACP, consisting of 20- and 200-kHz transducers, was operated by personnel from the developing organization, the Ocean Acoustics Division, Atlantic Oceanographic and Meteorological Laboratory, National Oceanographic and Atmospheric Administration.

2. Objectives of the MFDCP

The scope of the MFDCP was broader than measurement of dredged material plumes. The MFDCP was designed to meet four objectives:

1. Collect comprehensive data on plume dynamics for use in verifying and improving numerical simulation models.
2. Investigate and refine plume monitoring procedures.
3. Evaluate acoustic instrumentation for measuring plume dynamics.
4. Measure bottom boundary layer processes.

Objective 4 involved deployment of the Acoustic Resuspension Measurement System (ARMS) being developed by Ohio State University under contract for DRP TA1. The ARMS obtains comprehensive and accurate measurements of sediment and fluid movement in the lower 1 m of the water column above the sea floor. For the MFDCP, the ARMS was configured as an instrumented tripod approximately 10 ft high with a 15-ft span between the legs. The tripod contained a 3-MHz acoustic transducer to measure sediment concentration, two electromagnetic current meters, a pressure gage for water surface elevation measurement, and other sensors to

measure water properties. The ARMS was deployed in shallow water away from the site of dredged material placement operations and is not discussed further in this report. A companion report for the MFDCP (Bedford et al., in preparation) describes the ARMS data and preliminary analysis results.

Objective 3, evaluation of acoustic instrumentation, will evolve from the initial data analyses made in preparation of this report. In future work, concentrations inferred from backscatter information available from the two acoustic instruments will be compared with each other and the water samples.

This report focuses on MFDCP activities related to Objectives 1 and 2, field data collection on plume dynamics. It provides comprehensive documentation on the data and procedures used in the plume tracking, and it is intended to serve as a data source for furthering basic understanding of dredged material plume dynamics and for testing and refining predictive numerical models.

3. Project Organization

Scientific Staff

An experienced team of oceanographic and coastal engineers and scientists was assembled to plan and conduct the MFDCP. Measurements at the dredged material placement site were made by this team operating onboard an oceanographic research vessel. Shipboard operations were supported by land-based surveyors providing accurate positioning (Chapter 3), by WES personnel who sampled the dredged material in the barge (Chapter 4), and by staff of the U.S. Army Engineer District (USAED), Mobile, who coordinated operations with the dredging contractor and with pertinent maritime organizational entities.

Research Vessel

A major logistical requirement for conducting the MFDCP was acquisition of a suitable vessel. It was necessary that the vessel support all scientific objectives and serve as a base for deploying equipment and making measurements without time lost in returning to port each day. Major considerations entering the vessel selection included:

1. Capability of supporting 12 scientific crew members and associated equipment for at least 2 weeks of continuous operations at sea.
2. Experience of crew with oceanographic measurement procedures.

3. Facilities meeting power, space, and cleanliness requirements for two independent sets of data loggers and peripheral computers and equipment associated with the acoustic instrumentation.
4. Capability of deploying simultaneously two independent sets of acoustic measurement instruments, together with collection of suspended sediment (water) samples through the water column.
5. Capability of deploying and recovering large instruments such as a moored current meter array (described below and in Chapter 2) and the ARMS.
6. Least cost for combined ship rental, transportation to and from the measurement site, and transportation for the scientific crew and equipment.

A vessel satisfying these requirements, the *R/V Pelican*, was contracted from the Louisiana Universities Marine Consortium (LUMCON), Cocodrie, Louisiana. LUMCON is located 6 hr by ground travel from WES, which enabled most heavy equipment, such as chains, weights, and buoys, to be transported by truck. Moreover, Cocodrie is an 18-hr cruise from the project site. LUMCON also had facilities and experienced personnel to analyze the sediment samples immediately upon return from the data collection cruise, which substantially reduced associated logistical costs and possible sources of error in handling the considerable number of samples.

Figure 1.2 illustrates the configuration of the *R/V Pelican*, in which locations of MFDCP instrumentation is indicated in parentheses. The ship is 105 ft long, has a 26-ft beam, and draws 9 ft fully loaded. For the MFDCP, the *R/V Pelican* carried a crew of six: a captain, one mate, two deck hands, one specialist familiar with electronic and electrical equipment onboard, and a cook. The crew had considerable experience in conducting oceanographic research cruises and was quite competent at deploying and recovering unique, sensitive, and unwieldy instruments.

Schedule

The crew and a 12-person scientific team remained at sea for the 12-day cruise period of the 16-day project. The project schedule is summarized in Table 1.1, and a detailed chronology of major events occurring during the 22-31 August data collection period is given in Appendix 1A.

4. Project Site

The MFDCP took place at a dredged material placement site west of the navigation channel leading to Mobile Harbor, Mobile, Alabama (Figure 1.3). This site is an integral part of the National Berm Demonstration Project (NBDP) established by the USACE in 1988 in cooperation with local sponsors and navigation and environmental interests (McLellan and Langan, in preparation).

The objective of the NBDP is "to assess and document potential physical and fishery benefits associated with underwater berms as a beneficial-uses application of dredged material" (McLellan and Langan, in preparation). (In the present context, the word "berm" refers to an artificially constructed and well-defined subaqueous feature, such as a linear bar or a mound.) The MFDCP benefitted from the umbrella of background data and local instrumentation at the NBDP. The extensive data set, ongoing dredging operations, and excellent cooperation from all concerned parties fostered by the NBDP were the central reasons the MFDCP was conducted near Mobile.

Two notable subaqueous features have been created with dredged material at the NBDP site (Figure 1.4). The feeder berm was constructed as part of routine dredging and consists of beach-quality sand placed along the 18- and 19-ft depth contours along its central crest to an elevation reaching 7 or 8 ft above the original bottom. The feeder berm is intended to migrate onshore and enter the littoral zone. The ARMS was placed at the feeder berm, and this feature was also surveyed with the acoustic instrumentation.

All measurements of dredged material plumes were conducted in the vicinity of the stable berm, where placement operations were then taking place. The stable berm consists of estuarine mud, clay, silt, and sand and serves as a wave break and fish habitat. For the MFDCP, the dredging contractor arranged for disposal at two fixed locations, one in deeper water at a nominal depth of 40-ft and the other in shallower water at nominal 25-ft depth. To monitor releases at precise locations and closely coordinate the tug and monitoring vessel, the two locations were marked by a temporary buoy deployed from the *R/V Pelican*.

5. Plume Tracking Procedure

Tracking Instrumentation

Plume tracking was conducted by four teams aboard the *R/V Pelican* (navigation, ACP, ADCP, and deck crew that handled sediment sampling). These teams were closely coordinated via the *R/V Pelican's* internal phone system, via hand-held radio receivers for communication on deck, and via a marine radio on the bridge to shore and other vessels. Successful monitoring of a plume required knowledge of the exact location and time of disposal, rapid entry into the plume, and accurate tracking of the main plume body as it drifted with the current.

Plume tracking centered around three instruments: the ADCP, the ACP, and a rosette containing twelve 5-l sampling bottles activated electronically at specified depths. The rosette, referred to as a "CTD" for Conductivity, Temperature, and Depth-measuring capability, contained other instruments and is described in Chapter 4. The CTD yielded samples of suspended material in the water prior to the disposal (background) and in the plume to calibrate the acoustic instruments, and provided salinity samples at selected depths. The three instruments were deployed near each other amidship off the starboard side of the *R/V Pelican*, shown schematically in Figure 1.2.

Figures 1.5, 1.6, and 1.7 show the ADCP, ACP, and CTD, respectively, as they were deployed aboard the *R/V Pelican*. The ADCP was mounted on a 4-in.-diam pipe held vertical during monitoring. The depth of the 1.2-MHz ADCP sensor head when the pipe was fully vertical was approximately 3 m. The four ADCP transducers were arranged with one sensor aimed vertically and the other three aimed obliquely at 30 deg to vertical and directed forward, aft, and starboard. The ACP was mounted in a fish-shaped tow body tethered by a rope and suspended from a boom extending 15 ft off the starboard side. The towed body travelled about 1 m under the water surface with both the 20- and 200-kHz transducers directed vertically. Similarly, the CTD was also lowered and raised between the ACP and ADCP by a winch. Figure 1.8 is a photograph showing the ADCP, ACP, and CTD deployed during a plume monitoring operation.

Plume Tracking

The barge was towed by the tug boat *Paul Candies* at speeds of 4 to 6 knots, and usually released material over a time interval from 10 to 20 sec, although slower releases also occurred. A surface plume was usually evident as a long, thin cloud of material, and the acoustic instruments indicated a localized column of material descending to the bottom in the region of the predominant discharge from the barge. For releases believed to consist primarily of sand, the surface plume was

barely detectible owing to the absence of fine particles, whereas releases believed to consist mainly of clay and silt were often accompanied by a milky grey surface plume. Figure 1.9 shows four photographs taken during the MFDCP at varying stages of release that form a sequence illustrating the dredged material placement process.

Two tracking procedures were used to monitor the evolution of the plumes (Figure 1.10). One is called transverse tracking and involves maneuvering the monitoring vessel such that the plume is entered perpendicular to its major axis produced by the motion of the barge in release of the material. After the perimeter of the plume is passed, the survey ship turns and attempts to reenter the plume at a right angle. In longitudinal tracking, the survey vessel follows the barge and passes through the plume along its major axis, turning to re-enter the plume after its perimeter is passed. These procedures are continued until the plume is no longer detected or another type of measurement, in particular a CTD cast, interrupts the survey.

Figure 1.11 displays two aerial photographs showing the *R/V Pelican* in initial entry to plumes on transverse and longitudinal transects. In Figure 1.11a, the *R/V Pelican* has begun crossing the plume as the tug begins a turn executed to both free the material rapidly and change course to return to Mobile Harbor. In Figure 1.11b, the *R/V Pelican* is entering behind the barge to follow it just prior to the release. This barge contained a mound of dry sand in its middle, with water ponded fore and aft.

The plume tracking procedure is not as straightforward as Figure 1.10 might suggest, because a plume will be advected by existing currents. Wind shear at the water surface and horizontal currents in the water column can translate the plume and shear it into separate bodies at various depths. For these reasons, visual observations of the plume at the water surface do not usually indicate the location of the main body of material settling through the water column. During MFDCP plume tracking, therefore, the plume was monitored visually and by the ADCP and ACP. Because of the capability of the ADCP software to display backscatter from the plume, current speed, and ship track in real-time (see Chapter 5), this instrument was often used to provide guidance to the bridge of the *R/V Pelican* on the best course for tracking the plume. Figure 1.12 is a photograph of the ADCP recorder and computer monitor located in the Dry Laboratory (Figure 1.2) of the *R/V Pelican* taken while course changes were being communicated to the bridge based on signals from the monitor. Figure 1.13 is a photograph of the ACP recorder system in the instrument room, the paper readout displaying passage through the plume in two transverse transects with the plume appearing as the narrow dark bands (see Chapter 6).

The advantage of the transverse transect survey procedure is that time development of the vertical and lateral extent of a plume can be observed in a series of relatively rapid passes through the material. This enables, for example, the speed of the leading edge of the bottom surge to be recorded, as well as descent of the main body of the plume to the bottom. The advantage of longitudinal tracking is that the length of the plume is surveyed at least once (on the first transect following the scow), giving more complete areal coverage of the plume.

Variations of the transverse and longitudinal tracking procedures were also performed. For example, in some surveys the *R/V Pelican* entered the plume on a transverse transect, then stopped in an attempt to remain on the center of a plume to make a CTD cast (labeled "*in situ* sampling" in Figure 1.10). If there were no wind and horizontal currents were steady through the water column, the vessel would in theory move with the plume, allowing a CTD cast to be made in the plume and continuous recording by the acoustic instruments of the evolution of the plume. However, this idealized situation was never encountered, and the *R/V Pelican* and the plume typically drifted away from each other, preventing adequate sampling in the core of the plume at all depths. Other sampling variations included executing a series of transects followed by a CTD cast, or performing one or two longitudinal transects followed by a series of transverse transects, or vice versa.

During the planning phase, the CTD was conceived as a reasonable approach to obtain sediment concentration samples at specified depths in the same water volume covered by the acoustic instruments. Indeed, the CTD obtained samples over a wide range of concentrations (Chapter 4), as illustrated by the variations in the shade of the recovered samples shown in Figure 1.14. However, use of the CTD was found to suffer two disadvantages: relative drifting of the sampling platform (the *R/V Pelican*) and the plume, and loss of plume tracking time while the cast was made, which typically required 20 min. In future plume tracking exercises, it is recommended that the CTD rosette be replaced by or used as a supplement to a continuous pump-out system mounted on a towed body that can be operated at different depths. Two disadvantages of using a towed body, and main reasons why a pump-out system was not employed during the MFDCP, are that the sampling spaces of the towed body and acoustic systems may be separated, and the time interval for passing a towed body through a plume at different depths will be substantial.

Underway Procedure

This section gives an overview of procedures followed during a typical MFDCP plume tracking operation.

The approximate time of the survey was first determined through radio contact with the dredge and, later, the tug. A meeting of investigators and the ship's crew was then held to decide the type of plume survey as transverse or longitudinal and other particulars of the survey, such as if and when CTD casts will be made. The tug captain was contacted while the tug and barge were en route to the placement site, and confirmation was made of their approach and exact location of material release at the target buoy. The tug captain was also asked for estimates of the types and volume of material in the barge. During this standby period, instrument systems were checked, the CTD was prepared on deck, clocks were synchronized, and contact was established with the Mini-Ranger shore stations used to provide accurate positioning of the *R/V Pelican* (Chapter 3).

Approximately one-half hour before arrival of the tug at the release site, the *R/V Pelican* arrived on station, and range positioning of the tug and scow began (Chapter 3). The CTD was lowered to obtain background water samples at three depths in the water column (near-bottom, middepth, and near-surface), and, if time permitted, a grab sample of bottom sediments was taken (Figure 1.15). About 5 min before release of the dredged materials, the acoustic instruments were turned on to obtain background readings.

Through close coordination between the captains of the tug *Paul Candies* and the *R/V Pelican*, the position of barge opening was determined, and the *R/V Pelican* began the first transect as the barge opened. The time of barge opening and associated prerelease and postrelease drafts were recorded (Figure 1.16), as were other particulars of the release process (e.g., fast or slow release, texture and type of material in the barge, etc.). The main priorities of the two MFDCP navigation team members on the bridge were to record the position of the *R/V Pelican* from Loran-C (as a backup to the Mini-Ranger System), and measure the barge range and heading with respect to the *R/V Pelican*.

Several drogues were released from the deck of the *R/V Pelican* as it passed through the center of the surface plume as judged visually from the bridge. The drogues were used in attempts (sometimes successful, other times not) to track the surface plume, which became difficult to locate visually shortly after the release.

After the first transect, detection of the main body of the plume was usually made by the ADCP team using real-time readings of the current in the water column in the vicinity of the plume and the *R/V Pelican's* position obtained from bottom tracking displays incorporating headings via the ship's gyroscope (Chapter 5). By these means, an estimate of plume position was made to guide the *R/V Pelican* on a course for the next transect. During some surveys, the

R/V Pelican stopped to make a CTD cast in the plume, after which tracking was resumed. Other operations during the tracking included photographing the barge and plume from the bow of the *R/V Pelican* with a 35-mm camera, aerial photography for some surveys, and recovery, bottling, and logging of the CTD water samples. When the plume became weakly detectible and could no longer be tracked, the ship returned to the approximate location of the release, and another bottom grab sample was obtained.

During the survey, as time allowed, each individual measurement teams recorded observations about the survey, data, and procedures. These records were compared at the end of the survey to form a consistent overall description of the survey and to detect and correct simple errors in the records that might produce uncertainties in subsequent data interpretation. This coordinated summary of surveys is contained in Appendix 1A. Investigators met after the survey to discuss observed properties of the plume and critique performance of the monitoring effort with the aim of refining the measurement and recording procedures.

Dredged material samples were collected from two barges for use in calibrating the acoustic instruments and understanding in a qualitative manner the behavior of the plume in relation to its constituent material.

6. Data Set

Over the 10-day monitoring period, 18 plumes were surveyed. This number was almost double the anticipated 10 events (1 per day) originally estimated in MFDGP planning. The quality of the data collection improved as experience was gained and skills polished. Also, with the opportunity to monitor many plumes, variations in plume surveying were made to increase the content and features of the data set.

It was considered the most fruitful approach and use of resources to focus on the highest quality surveys for analysis in this data report. The selection process took place at a meeting of all investigators, with input from numerical modeling components of the DRP. Through this procedure, 8 plume surveys of the 18 described in Appendix 1A were identified and subjected to detailed analyses. The shallow-water berm survey was also analyzed as a test of extreme shallow-water measurement capabilities.

The eight target surveys are listed in Table 1.2, which introduces notation and numbering conventions used in the other chapters of this report. Surveys were assigned the number of the

Julian day, together with the letter A or B to designate the first and second, respectively, on that day. All data were recorded and analyzed as referenced to Greenwich Mean Time (GMT), which is related to the local Eastern Daylight Savings Time (EDST) as $\text{time (EDST)} = \text{time (GMT)} - 5 \text{ hr}$. The right-hand column in Table 1.2 gives the principal property of the plume that contributed to its selection for analysis.

7. Concluding Discussion

This chapter has served as an introduction to the MFDCP and the five technical chapters that follow in this report. The large and high-quality data set obtained by the MFDCP is the result of four factors: (a) careful planning and preparation, (b) favorable weather with calm seas, (c) full functioning of equipment, a factor in part due to experienced operators and technicians on board the *R/V Pelican*, and (d) excellent cooperation among all concerned parties. In summary, as presented in this and subsequent chapters, the following are considered to be the major accomplishments of the MFDCP:

1. A large, comprehensive, and varied data set on plume dynamics was obtained. Distinguishing features of the data set include: data collection at two shallow-water sites; simultaneous operation of two acoustic systems together with water and sediment sampling; measurement of the local current; precise measurement of monitoring vessel and hopper barge positions; and availability of bathymetric data and regional oceanographic and meteorological data provided by the NBDP.
2. The concept of an operational project-level plume monitoring instrument was verified. This instrument would have the capabilities, demonstrated in the MFDCP, of (1) measuring the three-dimensional plume concentration, (2) measuring the three-dimensional current velocity at the plume, and (3) tracking the position of the survey ship.
3. Data were collected that enable field calibration of the acoustic instruments used to infer sediment concentrations in the water column.
4. Plume monitoring procedures that can be recommended for future research and project-level use were tested and refined.
5. The ARMS obtained detailed and accurate information on boundary layer processes (wave, current, sand concentration) at a shallow-water berm site.

Other uses of the data and recommendations for further study are given in the succeeding chapters.

Acknowledgments

A complex and comprehensive field data collection project such as the MFDCP can be successfully accomplished only through the positive interest and assistance of a large number of people. The following individuals contributed substantially in providing resources and expertise, but did not write sections of this report: USAED Mobile: Mr. Pat Langan, Operations Division, Navigation Branch; Dr. Susan Ivester Rees, Planning and Environment Division, Environment and Resources Branch; and Mr. Steven Sema, Operations Division, Mobile Area Office; Great Lakes Dredge & Dock Company (GLD&D): Mr. Kevin Holt, Project Engineer; Mr. Ken Lago, Captain of the dredge *Chicago*; Mr. John Zenga, Project Superintendent; and all the captains of the GLD&D tug *Paul Candies*; Louisiana Universities Marine Consortium: Mr. Steven Rabalais, Coordinator for the *R/V Pelican*, and Mr. Robert Cutting, Captain of the *R/V Pelican*; Evans-Hamilton, Inc: Mr. Douglas Evans, who contributed valuable navigation and positioning skills on board the *R/V Pelican*; U.S. Army Engineer Waterways Experiment Station: Mr. Sam Corson and Dr. Thomas E. White, Prototype Measurement and Analysis Branch, Engineering Development Division, and Ms. Sandy Staggs, Contracting Division.

References

- Bedford, K. W., Wai, O., Van Evra, R., III, Velissariou, P., Lee, J., and Libicki, C. "The Local Near-Bottom Response of a Dredged Material Placement Site to Wind and Tide Effects," DRP Technical Report in preparation, U.S. Army Engineer Waterways Experiment Station, Vicksburg, MS.
- Biggs, R. B. 1968. "Environmental Effects of Overboard Spoil Disposal," *Journal of the Sanitary Engineering Division*, Vol. 94, No. SA3, pp. 477-487.
- Bokuniewicz, H. J., Gebert, R. B., Gordon, R. B., Higgins, J. L., Kaminsky, P., Pilbeam, C. C., Reed, M. W., and Tuttle, C. 1978. "Field Study of the Mechanics of the Placement of Dredged Material at Open-Water Disposal Sites," Technical Report D-78-F, Vol. I, U.S. Army Engineer Waterways Experiment Station, Vicksburg, MS.
- Johnson, B. H. 1990. "User's Guide for Models of Dredged Material Disposal in Open-Water," Technical Report D-90-5, U.S. Army Engineer Waterways Experiment Station, Vicksburg, MS.
- Johnson, B. H., and Holliday, B. W. 1978. "Evaluation and Calibration of the Tetra Tech Dredged Material Disposal Models Based on Field Data," Technical Report D-78-47, U.S. Army Engineer Waterways Experiment Station, Vicksburg, MS.

- Kraus, N. C. 1990. "Plume Tracking off Mobile, Alabama," WES Video File No. 90086, U.S. Army Engineer Waterways Experiment Station, Vicksburg, MS.
- Kraus, N. C., and Prickett, T. L. 1989. "Plume Chasing off Mobile Bay," *International Dredging Review*, Vol. 8, No. 11, pp. 6-7.
- Lazar, R. L., Calhoun, C. C., and Patin, T. R. 1984. "The Corps Environmental Effects of Dredging Programs," *Proceedings of Dredging and Dredged Material Disposal*, American Society of Civil Engineers, pp. 150-156.
- McLellan, T. N., and Langan, J. P. "National Berm Demonstration Project: Mobile, Alabama," *Proceedings of Beneficial Uses of Dredged Material*, in preparation.
- McNair, C. 1989. "Dredging Research Program of the U.S. Army Corps of Engineers," *Proceedings of the XIIth World Dredging Congress*, Western Dredging Association, pp. 44-50.
- Nichols, M., Diaz, R. J., and Schaffner, L. C. 1990. "Effects of Hopper Dredging and Sediment Dispersion on Chesapeake Bay," *Environ. Geol. Water Sci.*, Vol. 15, No. 1, pp. 31-43.
- Proni, J. R., Rona, D. C., Lauter, C. A., and Sellers, R. L. 1975. "Acoustic Observations of Suspended Particulate Matter in the Ocean," *Nature*, Vol. 254, pp. 413-515.
- Proni, J. R., Newman, F. C., Rona, D. C., Drake, D. E., Berberian, G. A., Lauter, C. A. Jr., and Sellers, R. L. 1976a. "On the Use of Acoustics for Studying Suspended Oceanic Sediment and for Determining the Onset of the Shallow Thermocline," *Deep-Sea Research*, Vol. 23, pp. 831-837.
- Proni, J. R., Newman, F. C., Sellers, R. L., and Parker, C. 1976b. "Acoustic Tracking of Ocean-Dumped Sewage Sludge," *Science*, Vol. 193, pp. 1005-1007.
- Saucier, R. T., Calhoun, C. C., Jr., Engler, R. M., Patin, T. R., and Smith, H. K. 1978. "Synthesis of Research Results, Dredged Material Research Program," Technical Report DS-78-22, U.S. Army Engineer Waterways Experiment Station, Vicksburg, MS.
- Sustar, J. F., Wakeman, T. H., and Ecker, R. M. 1976. "Sediment-Water Interaction During Dredging Operations," *Proceedings Dredging and Its Environmental Impacts*, American Society of Civil Engineers, pp. 736-749.
- Tsai, J. J., and Proni, J. R. 1985. Acoustic Study of Dredged-Material Dumping in the New York Bight," in B. H. Ketchum et al. (eds.) *Wastes in the Ocean*, Vol. 6, *Nearshore Waste Disposal*, John Wiley & Sons, New York, pp. 357-381.

Table 1.1
Schedule Summary for the MFDGP

<u>Activity</u>	<u>Date</u>	<u>No. of Days</u>
Mobilization	18-20 August	3
Transit to site	21 August	1
Data collection	22-31 August	10
Transit from site	1 September	1
Demobilization	2 September	1

Table 1.2
List of Surveys Selected for Detailed Analysis*

<u>Plume Survey</u>			
<u>Survey (Chron. Order)</u>	<u>Julian Day and Survey Designator</u>	<u>Starting Time GMT</u>	<u>Comments</u>
6	237A	14:18	Longitudinal sampling; deep site
8	238A	14:22	Transverse sampling; deep site
9	238B	21:55	Transverse sampling; many transects; deep site
10	239A	14:06	Three transverse transects followed by two longitudinal transects; strong shear current; deep site
11	239B	22:14	Transverse sampling (seven transects); good observation of plume dynamics and sediment fall behavior in a weak current; deep site
14	241A	11:44	Transverse sampling; rapid discharge and plume decay; shallow site
16	242A	16:06	Longitudinal sampling (six transects); high CTD concentrations; shallow site
18	243A	18:03	Transverse sampling (six transects over main plume); discharge may have been on edge of mound, not directly on top. Good quality plume dynamics at shallow site

<u>Shallow-Water Berm Survey</u>	
<u>Survey Time GMT</u>	<u>Comments</u>
18:00-21:00	Ten short diagonal transects over the shallow-water sand berm, going on and off the berm in zig-zag fashion

* Note: Information taken from Appendix 1A, Coordinated Summary of Surveys.

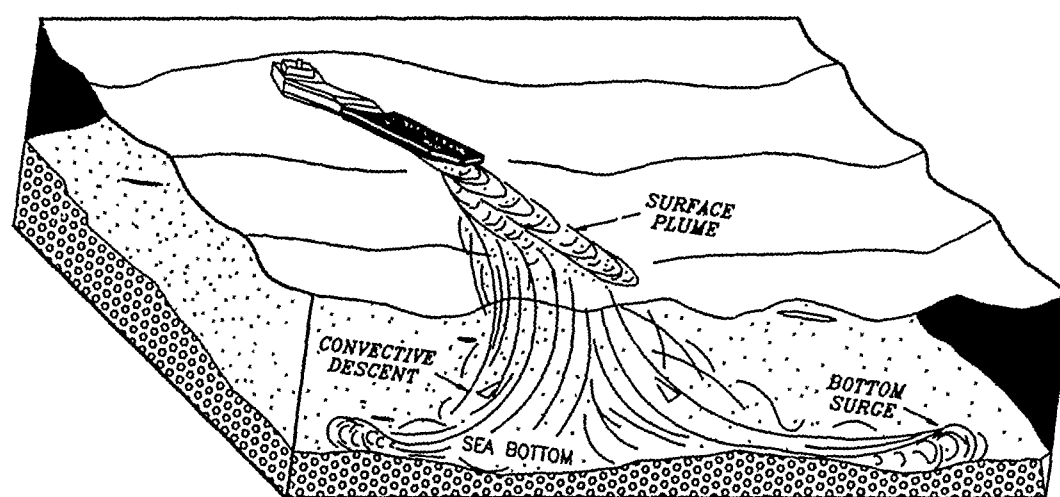


Figure 1.1. Schematic of dredged material plume.

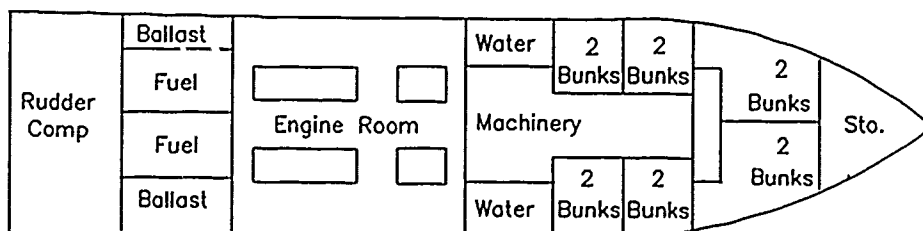
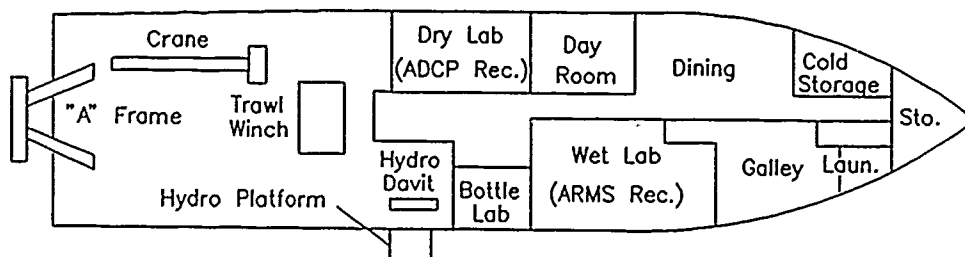
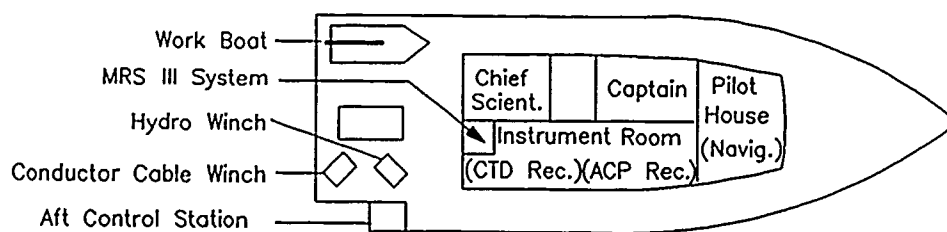
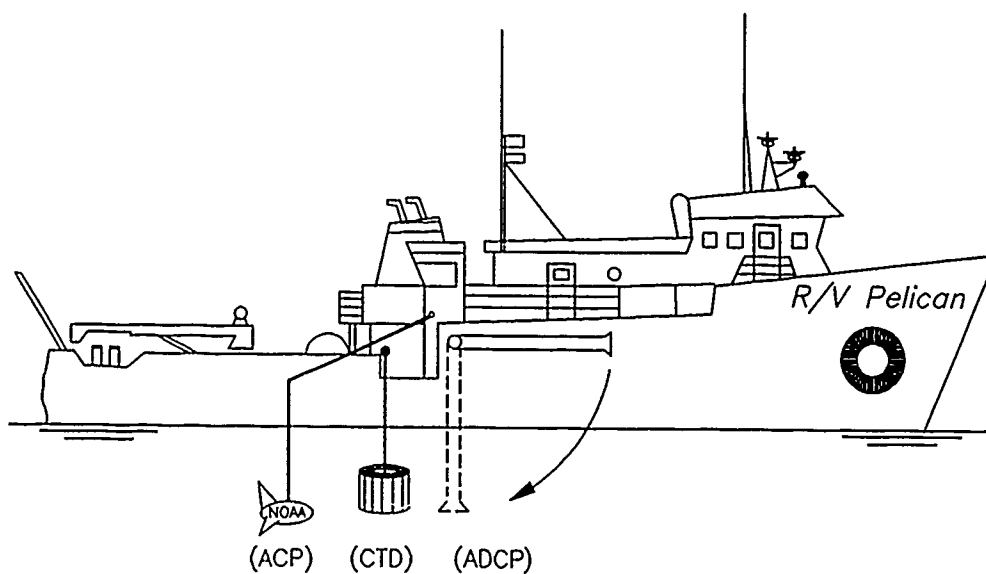


Figure 1.2. Schematic layout of the *R/V Pelican* and scientific equipment.

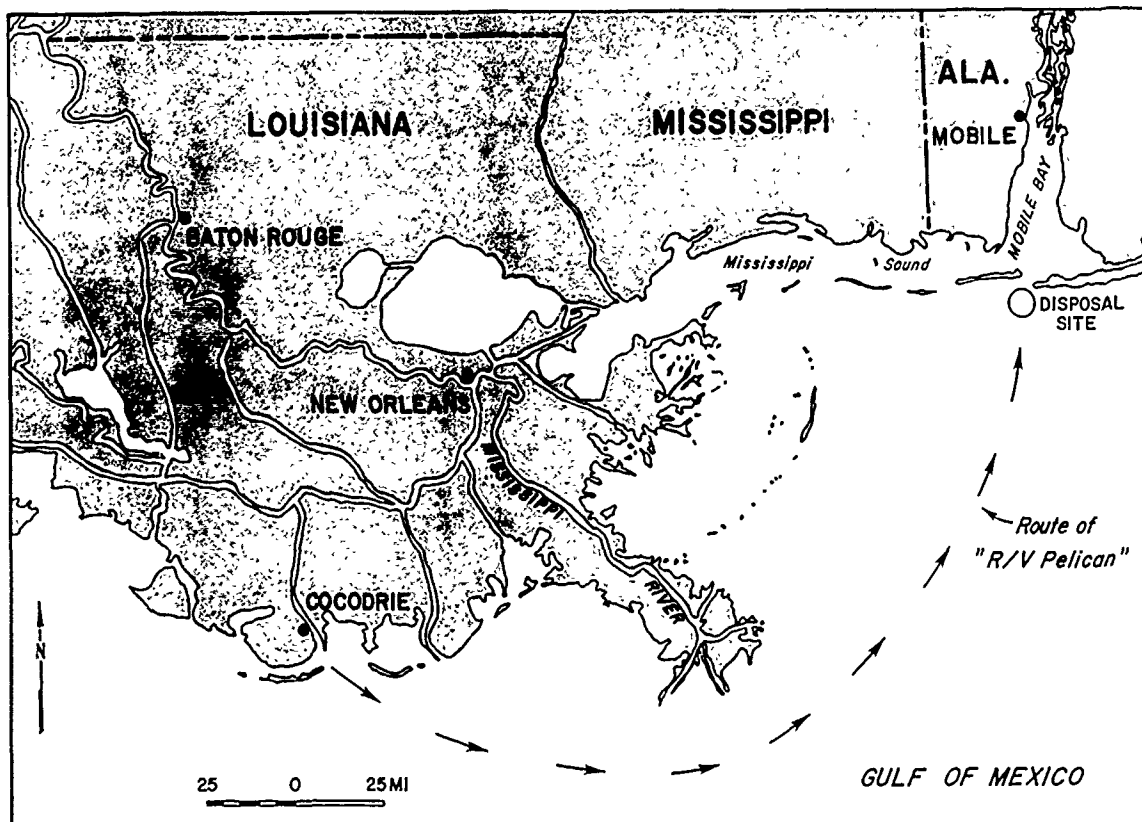


Figure 1.3. Location map for the MFDGP site.

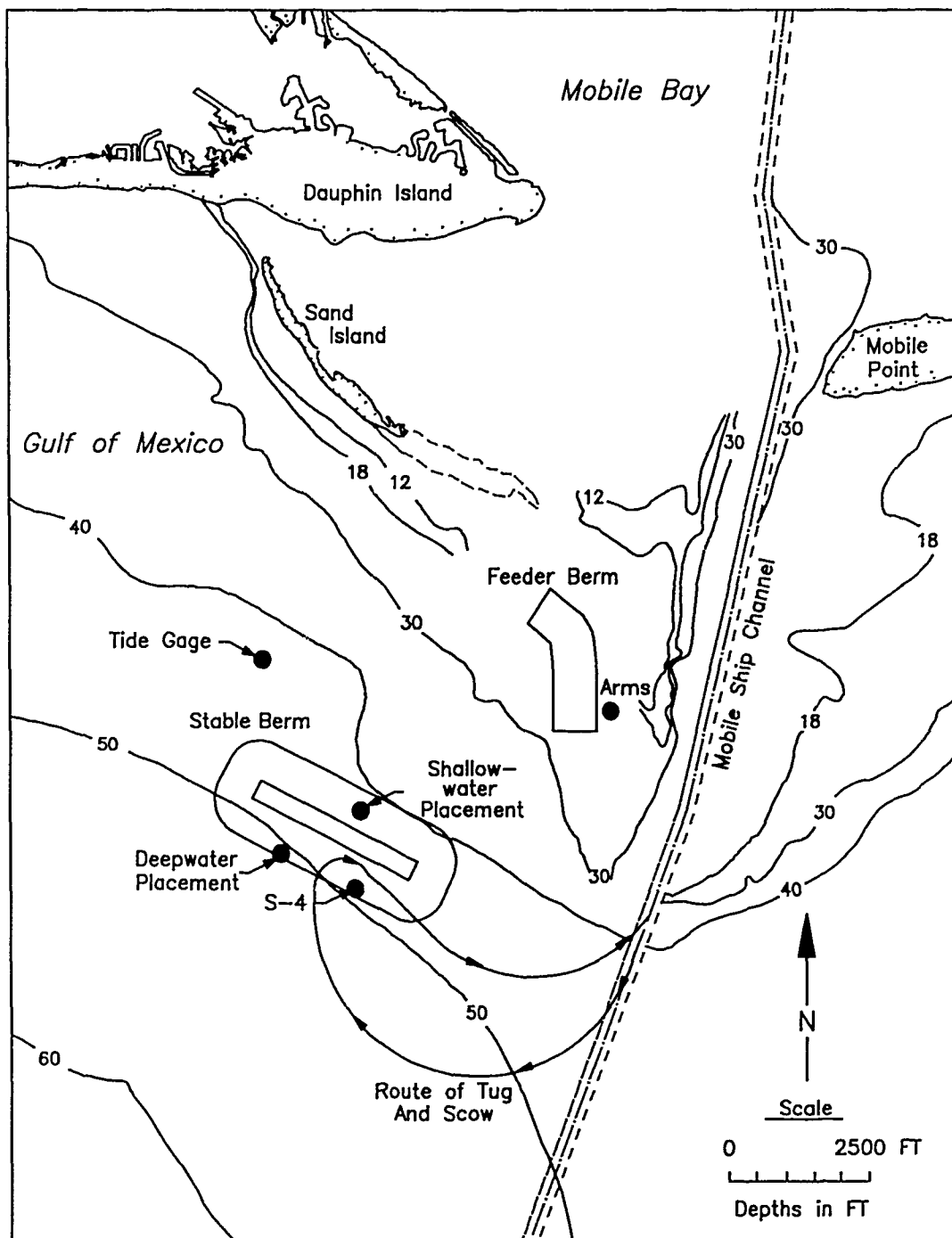


Figure 1.4. Dredged material placement sites, NBDP, Mobile, Alabama.

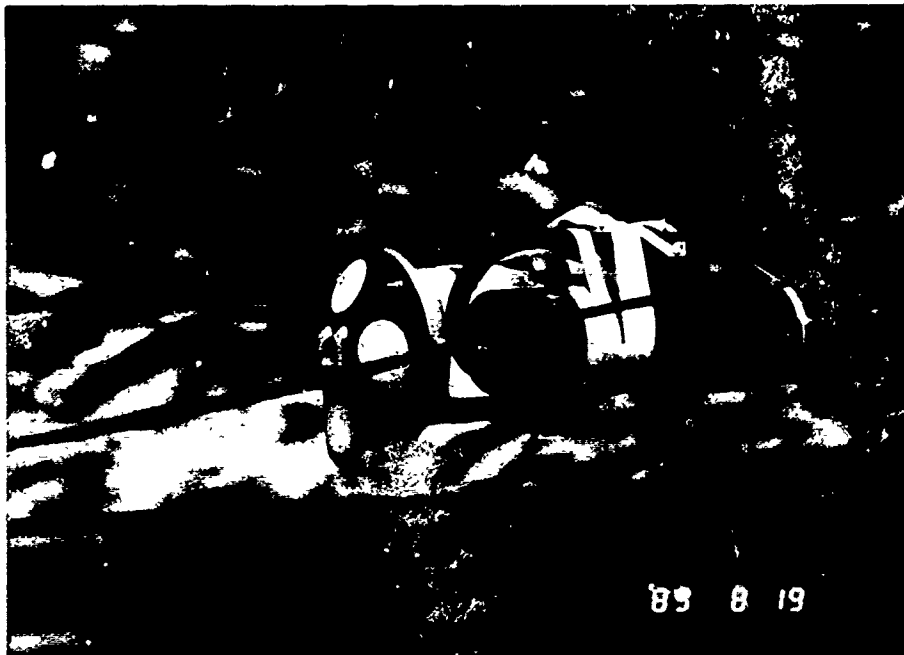


Figure 1.5. ADCP transducer head mounted on a pipe.

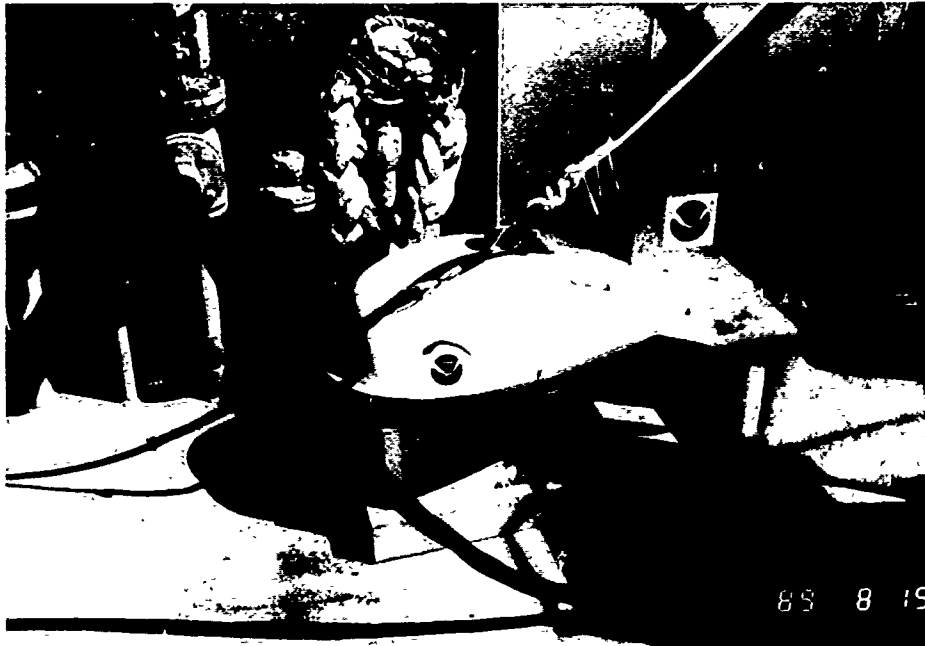


Figure 1.6. ACP tow body ready for deployment.

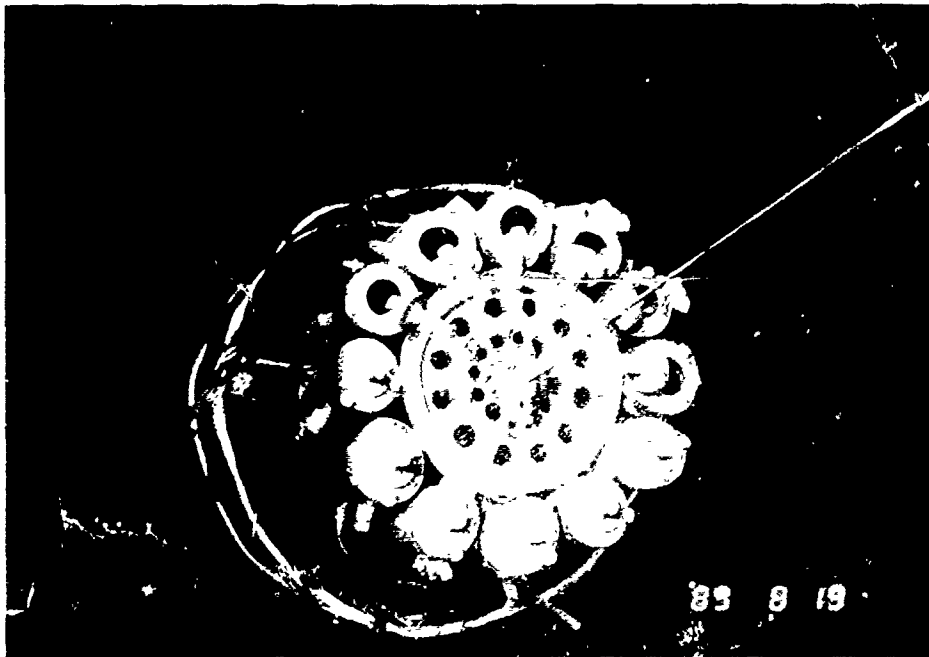


Figure 1.7. CTD sampling near the water surface.

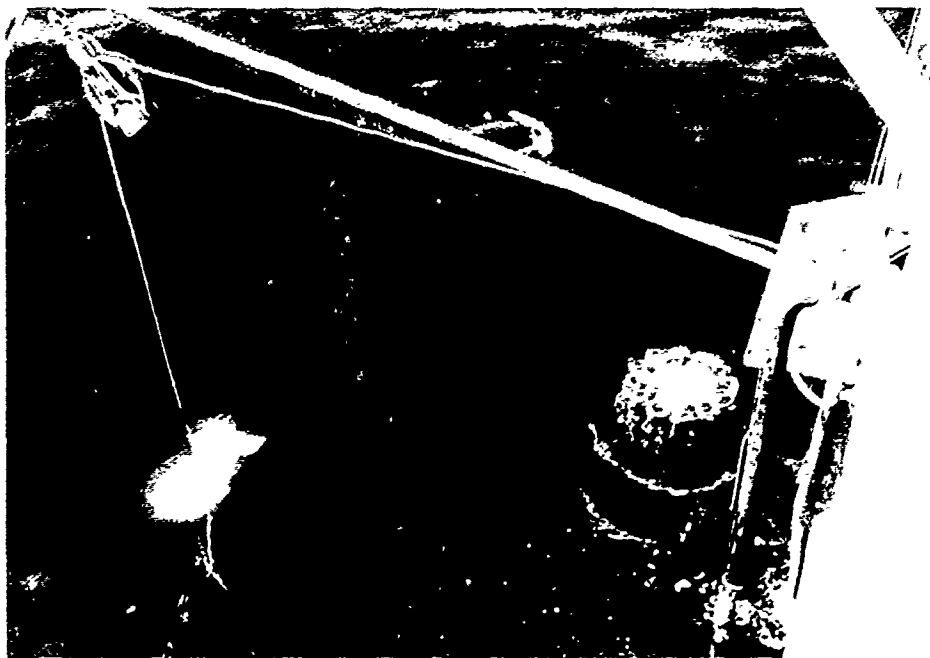
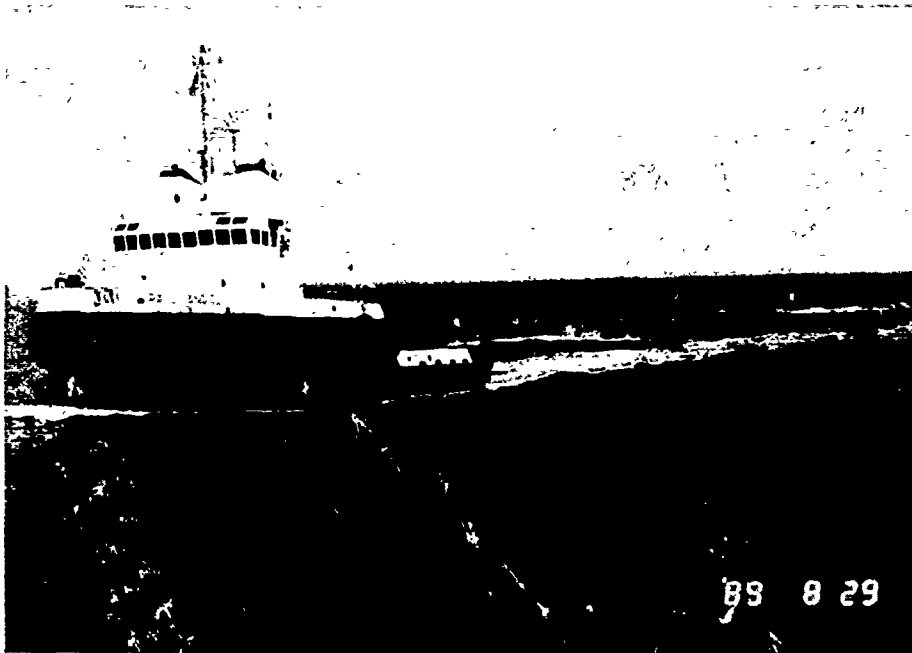
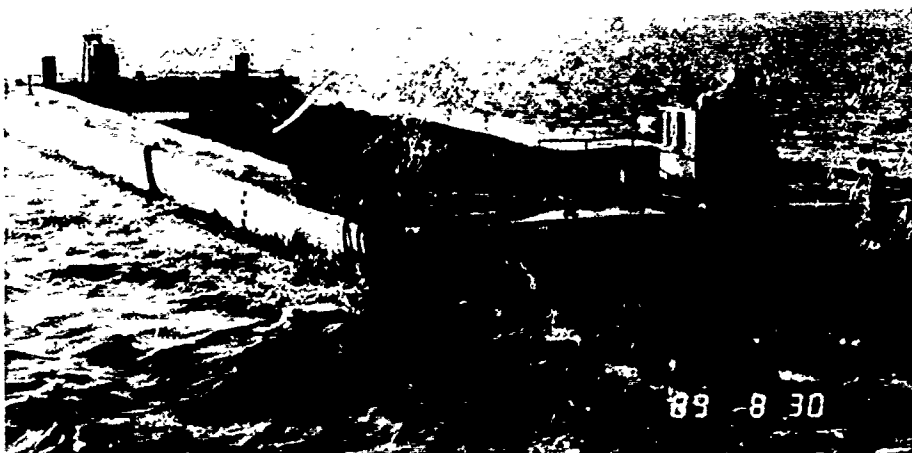


Figure 1.8. ADCP, ACP, and CTD deployed during a plume survey.

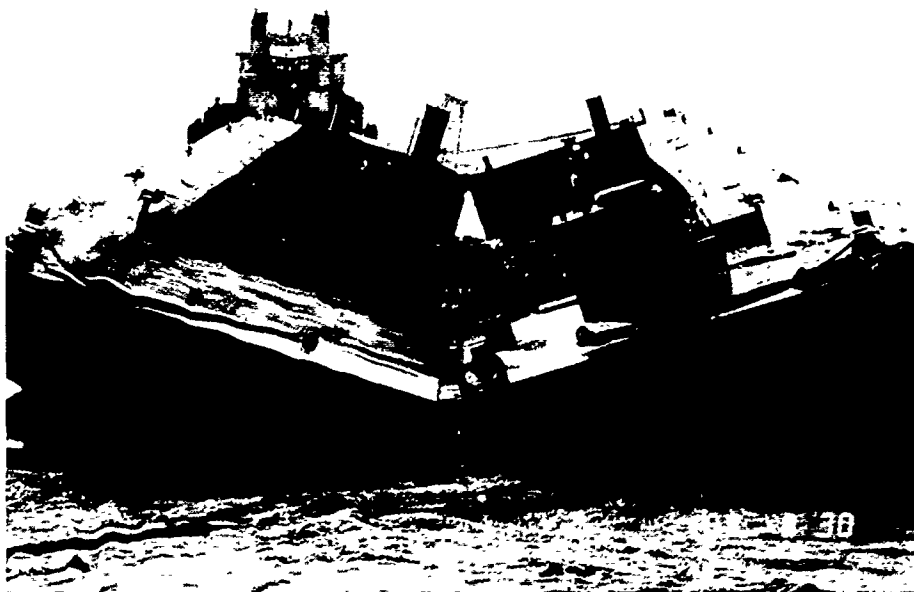


a. Tug with loaded scow prior to material release.



b. Closeup of loaded scow.

Figure 1.9. Dredged material placement during the MFDGP (Continued).



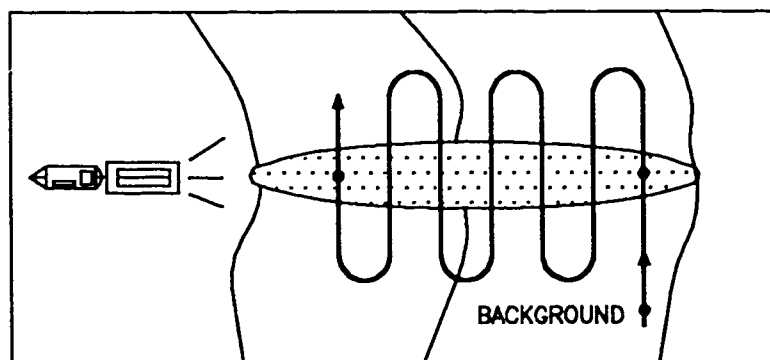
c. Release of material from scow.



d. Plume immediately after material release.

Figure 1.9. (Concluded)

TRANSVERSE SAMPLING



LONGITUDINAL SAMPLING

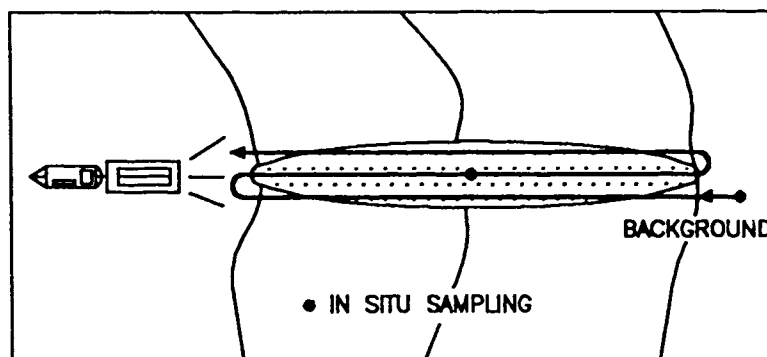
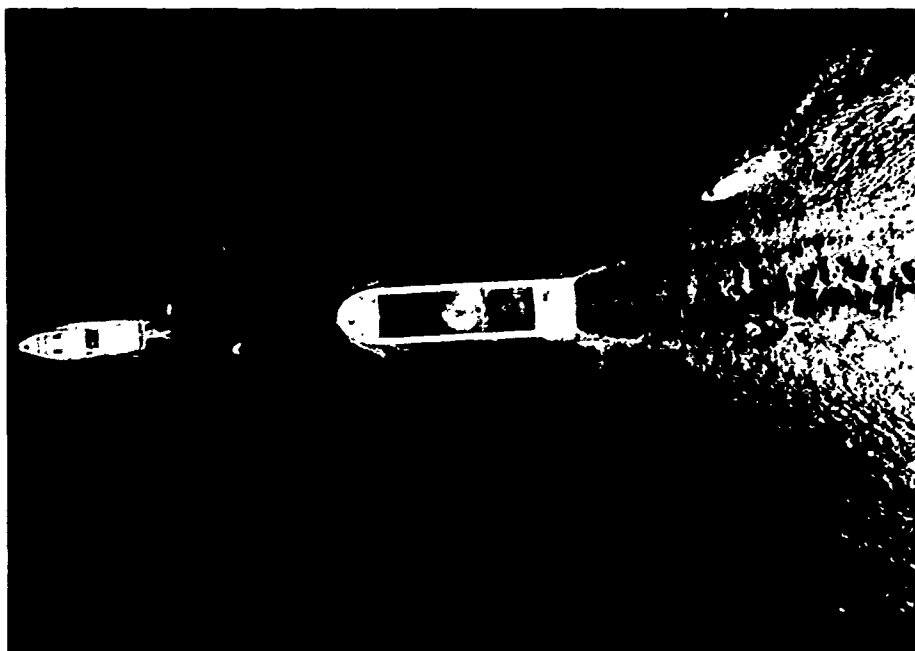


Figure 1.10. Schematic of two main plume sampling schemes.



a. Transverse entry.



b. Longitudinal entry.

Figure 1.11. Photographs showing start of plume surveys.



Figure 1.12. ADCP monitor during a plume survey.



Figure 1.13. ACP paper readout during a plume survey.

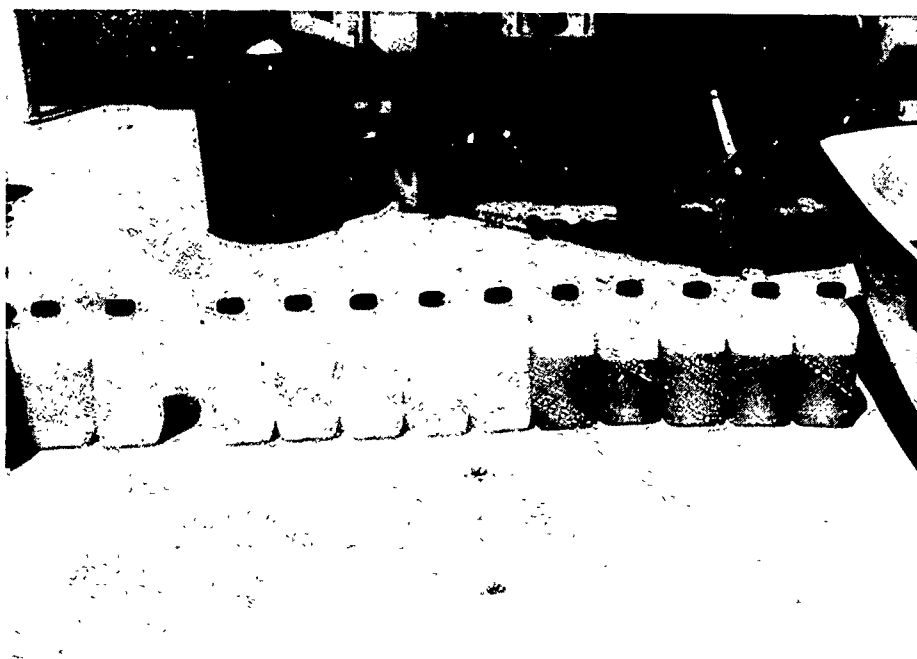


Figure 1.14. CTD water samples taken at various depths.



Figure 1.15. Bottom grab sampler being recovered.

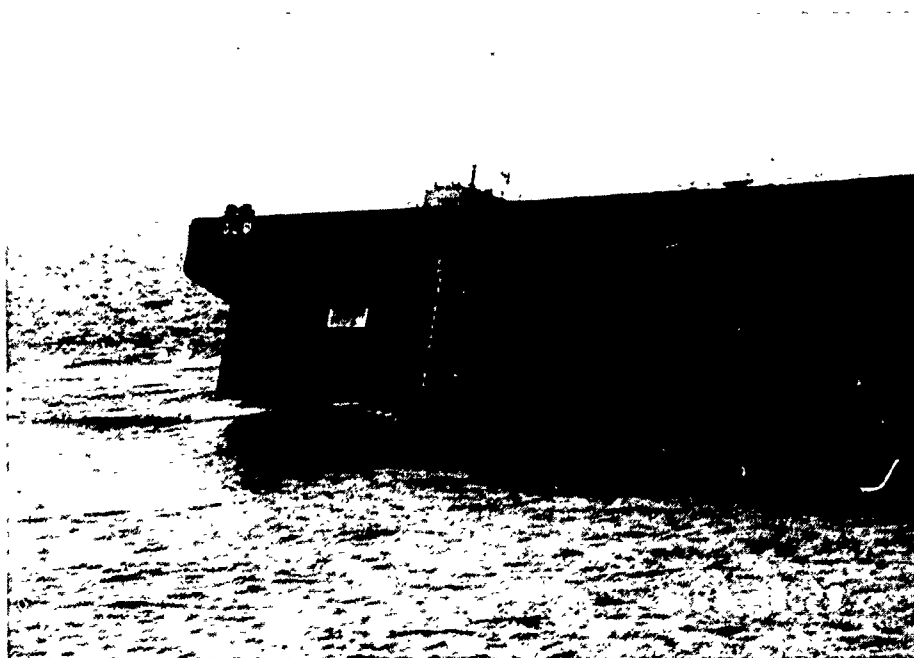


Figure 1.16. Draft marks exposed on an open scow.

Appendix 1A: Coordinated Summary of Surveys

This appendix contains summaries of the 18 dredged material plume surveys and other data collection activities performed during the Mobile, Alabama, Field Data Collection Project (MFDCP). The main source of information for compiling this appendix was a daily log maintained during the cruise. In keeping the log, an attempt was made to coordinate among the various data collection teams on board the *R/V Pelican* to obtain an integrated and consistent picture of operations being conducted. During writing of this appendix, information in the log was supplemented by information that became available after the cruise.

During compilation of the log, a quality rating of low, medium, or high (L, M, H) was assigned to each survey based on the performance of the survey, level of detail of the information obtained, and characteristics of the particular plume survey relative to other surveys. Every survey had one or more interesting features, however, and objectives of a particular analysis may change the quality rating of a survey and the associated data.

The quality rating of surveys was used, in part, to select the eight surveys targeted for the detailed analysis described in the main body of this report. For ease of reference, the titles of these eight plume survey events are marked by shadowing in the list given below.

The descriptions of the plume surveys are presented in chronological order and are designated by the number of the Julian Day (JD) and the letter A, B, or C to denote the first, second, or third survey of that day. Typically, two plume surveys were performed each day. Time of day is reported as Greenwich Mean Time (GMT). Local time at Mobile during the MFDCP was Eastern Daylight Savings Time (EDST) and is related to GMT by the relation $\text{time (EDST)} = \text{time (GMT)} - 5 \text{ hr.}$

Surveys were performed in regions of two different depths in the authorized placement area and are referred to in the following as the "deep" site (nominal water depth of 12 to 13 m) and the "shallow" site (nominal water depth of 8 to 9 m).

The remainder of this appendix provides a description of major data collection activities in chronological order.

Monday, 21 August 1989 (JD 233)

The S-4 current meter array was moored at 18:10 GMT. Prior to placement of the array, a bathymetric survey of the mooring area was performed using the *R/V Pelican's* fathometer.

Tuesday, 22 August 1989 (JD 234)

Acoustic Resuspension Measurement System (ARMS) Deployment

The first of two deployments and data collection by the ARMS commenced at 18:01 GMT at the Sand Island berm (located south-southwest of Shell gas well 113 JA) on a flat, fine sand bottom) at 19-ft depth. The ARMS was ringed by four guard buoys. Two divers took water sample in the ARMS profilometer beam during deployment. Another water sample was taken by the Conductivity-Temperature-Depth (CTD) rosette at 20:35 GMT, together with a grab sediment sample.

Survey 1 (234A) (Quality: M/II)

The survey started 18:58:42 GMT at the deep site. The barge speed and heading were 5.0 knot and 013 deg from True North, respectively, and the prerelease draft was 17 ft. The material in the barge could not be seen. The barge did not open completely, producing a semi-continuous discharge. The *R/V Pelican* entered behind the barge in a longitudinal sampling track. The first longitudinal transect ended at 19:14:35. The water depth beneath the *R/V Pelican* changed from 40 to 57 ft over the course of the first transect.

Wednesday, 23 August 1989 (JD 235)

ARMS Water Sample

A water sample was taken near the ARMS at 13:50 GMT.

Survey 2 (235A) (Quality: L/M)

The survey started at 16:59:40 GMT at the deep site. The barge speed and heading were 4.1 knot and 018 deg, respectively, with a prerelease draft of 20 ft. Small clumps of material were observed in the middle of the barge prior to release. The *R/V Pelican* entered the plume at an angle and stopped to cast the CTD rosette to obtain water and sediment samples.

The ACP showed a bottom surge of material. The first transect had an 18-min interval to remain onsite for the CTD cast, and the plume concentration decreased notably after about 11 min. The plume, extending from the water surface to the Gulf bottom, drifted with the current (at 170 deg) and away from the initial placement site. We could not track both the plume and material near the bottom at the initial site, and indecision caused data some gaps.

A plume from the Mobile River was observed from the *R/V Pelican's* bridge. The CTD was first cast in the river plume and then at the saltwater edge of the plume to obtain an idea of the range of salinities at the site. The Acoustic Doppler Current Profiler (ADCP) showed an increase in backscatter intensity in the salt water as compared with the fresh water.

ARMS Water Sample

A water sample was taken near the ARMS at 21:05 GMT.

Survey 3 (236A) (Quality: L)

The survey started at 00:19 GMT at the shallow site and proceeded along an irregular sampling pattern. The barge speed and heading were 7.1 knots and 290 deg, respectively, with a prerelease draft of 20 ft. The *R/V Pelican* entered the main plume at 00:20:35 (ACP), and the CTD was cast when the ship reached the center of the plume. The first exit of the major portion of the plume occurred at 00:27.

Thursday, 24 August 1989 (JD 236)

Survey 4 (236B) (Quality: M)

The survey started at 15:00 GMT at the deep site. Barge GL-64 approached with a speed and heading of 3.2 knots and 355 deg, respectively, and the prerelease draft was 20 ft. Large grey and black clumps were observed in the middle of the barge. The tug captain estimated the barge contents to be 20-percent sand and 80-percent fines. By visual observation, the barge discharged very rapidly (approximately 10 sec).

The *R/V Pelican* entered the plume at 15:01:45. The ACP showed a clear thin layer of sediment at approximate 4.5-m depth, suggesting a density difference or current reversal. The ADCP showed a strong current moving south from 3 to 8 m below the water surface, and the backscatter intensity indicated most material immediately fell to the bottom, with little material remaining in suspension. The *R/V Pelican* drifted on to the site and cast the CTD. The CTD was

in the plume on the way down, but out of the plume on the way up; the cast started at 15:03 and lasted 14 min.

Survey 5 (236C) (Quality: M/H)

The survey started at 22:09 GMT at the deep site, executed as a longitudinal sampling track. Barge GL-63 approached with a speed and heading of 6.5 to 7.0 knots and 350 deg, respectively; the barge appeared to be leaking slightly prior to the main release and had to be opened manually. The prelease draft was 16 ft. The tug captain reported 4500 cu yd estimated as 80-percent sand and 20-percent fines.

The *R/V Pelican* entered the plume at 22:11 according to the ACP. Twenty-four 35-mm photographs were taken of the placement operation over an approximate 10-min period. The material in the barge could not be seen. The tug executed a sharp turn, which appeared to loosen a portion of material remaining in the barge. The ACP showed two distinct peaks in the discharge, passing into and out of the first peak at 22:12 and 22:13, and into and out of second peak at 22:15 and 22:19. The ADCP also detected two main discharges. A CTD cast was made at the end of the survey; the ADCP indicated clear water during the cast.

Friday, 25 August 1989 (JD 237)

ARMS Water Sample

A water sample was taken near the ARMS at 01:00 GMT.

Survey 6 (237A) (Quality: M/H)

The survey started at 14:18 GMT at the deep site. Barge GL-61 (first time this barge appeared) approached with a speed and heading of 5.6 knots and 354 deg, respectively, and the prelease draft was 19 ft at the bow and 20 ft at the stern. The tug captain reported 5,600 cu yd estimated to consist of 80-percent sand and 20-percent fines. One clump of material was observed in the middle of the barge; otherwise, the material appeared relatively flat. The barge opened with a crisp sound and fairly rapidly (but not the fastest so far).

The *R/V Pelican* entered the plume on a longitudinal transect at 14:18:30 and exited at 14:25 (ACP), then reentered the plume at 14:27 and turned at 14:32. The main body of the surface plume by visual observation could not be seen after 2 min. The current was strong and uniform (30 to 50 cm/sec to the south-east) in the upper layer (ADCP). The ADCP detected bottom

suspended material, a middepth plume, and a surface plume at different locations. This release appeared to have high values of the sediment vertical fall speed (ADCP).

ARMS Recovery

The ARMS was recovered at 17:10 GMT to end the first deployment. Upon recovery, the data collection was found to have lasted 55 hr and 32 min. Data collection ceased at 01:33.

Sand Island Berm Survey

The survey of the Sand Island shallow-water berm took place over the period 17:42 to 20:57 GMT and consisted of 10 oblique and continuous transects over the berm on a predetermined track designed to cover prominent depth features from most shallow to most deep. Mini-Ranger readings were recorded verbally at minute intervals, supplemented by range and bearing readings during brief interruptions of Mini-Ranger transmission. A plotted record from the *R/V Pelican's* Fathometer was made, and depths ranged from approximately 25 ft at the side of the berm to 10 ft at the berm crest.

Survey 7 (237B) (Quality: L)

The survey began at 22:14:30 GMT at the deep site. Barge GL-64 approached with a speed and heading of 5.1 knots and 005 to 010 deg, respectively, and the prelease draft was 19.5 ft. The tug captain estimated 80-percent sand and 20-percent fines. The barge was fully loaded, and the surface of the dredged material was relatively flat. The material was light brown, appearing to be sand. Although the barge opened rapidly, the discharge became stalled at an early stage because the sand appeared to be dry. White sand could be seen clinging to the sides of the barge, collapsing in discrete release events as the barge continued to open. At 22:16:30, the barge tilt reached a sufficiently large angle that the sand collapsed as a sheet, causing the barge to rise rapidly. During the entire release, the barge was on a course to the starboard of the tug (eastward) apparently due to a strong cross-current. The surface trace of released sediment looked brown, as opposed to a grey-to-black chalky color usually associated with fine-grained sediments.

The *R/V Pelican* entered the plume at 22:14:30 and exited at 22:22 (ACP). The plume was well recorded but not systematically sampled. A longitudinal sampling track of two passes was made, followed by a CTD cast.

Saturday, 26 August 1989 (JD 238)

Survey 8 (238A) (Quality: H)

The survey started at 14:22:09 GMT at the deep site. Barge GL-64 approached with a speed and heading of 5.1 knots and 001 deg, respectively, and the prelease draft was 20 ft. The tug captain reported 65-percent sand and 35-percent fines. The release was slow, but not as slow as for the previous survey (237B).

Based on visual observations from the bridge, the *R/V Pelican* turned to port and entered the plume on a transverse transect at a right angle in the region judged to correspond to the major portion of the released material. The center of the plume was crossed at 14:24:22, and the surface plume was 50 to 75 ft wide. The *R/V Pelican* completed crossing the surface plume and proceeded to a point judged to be beyond its edge; the ship then did a sharp, 180-deg turn called a "twist" turn and re-entered the plume at a right angle, as judged visually. After the plume was traversed for a second time, detection of the plume for tracking was turned over to the ADCP team.

According to the ACP observation, the *R/V Pelican* entered the plume at 14:24. A bottom surge was recorded, and the plume was first exited at 14:26:00. The twist turn occurred at 14:36:30, and re-entry was at 14:27:50 followed by exit at 14:29:51.

The survey continued for four transects; on the fifth transect, a CTD cast was made. After the CTD cast, one longitudinal transect was performed, and the survey was ended with transverse transects over the down-current surface plume (ADCP). The ACP 20-kHz record showed material advection through the water column on several transects. The current was strongly sheared, with the top 3 to 7 m moving at almost 50 cm/sec and the bottom 7 to 10 m moving about 10 cm/sec, both layers moving to the southeast (ADCP). The sediment plume also became sheared (ADCP).

Survey 9 (238B) (Quality: H)

The survey started at 21:55 GMT at the deep site. Barge GL-61 approached with a speed and heading of 6 knots and 351 deg, respectively, and the prelease draft was 21 ft. The tug captain reported 5,600 cu yd estimated as containing 70-percent sand and 30-percent fines. A mound of what appeared to be sand was located in the middle of the barge, with water at the fore and aft ends. The release was relatively rapid.

The *R/V Pelican* reached the middle of the plume at 21:56 on a transverse transect, and the ACP showed a bottom surge at each side. Five transverse transects were made, followed by a CTD cast, then three longitudinal transects (which revealed little material according to the ADCP).

Bottom mounding and the plume were easily identifiable by the ADCP, which allowed many transects to be made. It was speculated that identification was easy because the dredged material consisted mainly of sand.

Sunday 27 August 1989 (JD 239)

Survey 10 (239A) (Quality: L/M)

The survey started at 14:06 GMT at the deep site, and the first aerial photographs were taken. Barge GL-61 approached with a speed and heading of 3.3 knots and 351 deg, respectively, and the prelease draft was 18.5 ft. The tug captain reported 75-percent sand and 25-percent fines.

The survey started with a CTD cast at 14:10 from a transverse entry, but the water samples did not contain appreciable sediment. After the cast was completed, there was difficulty finding the correct survey track to follow because surface marker buoys placed during the CTD cast had evidently drifted away from the plume. Three transverse transects were made followed by two longitudinal transects. A relatively strong wind (20 mph) moved the *R/V Pelican* out of the plume and also produced a 50 cm/sec current extending from the surface to 5 m (ADCP), with a strong shear at 5-m depth (ADCP). The ADCP showed that a plume extended approximately 300 m from the placement site on the first transect, and the plume grew to 500-m length on the second transect (the rapid increase attributed to the strong current and shear). The ADCP did rapid sampling to observe clumps. The ACP recorded a surge on both sides of the discharge during the first transect. The ADCP could clearly track the bottom and showed both peaked and flat mounds.

ARMS Second Deployment

The ARMS was deployed for the second time, and data collection commenced at 17:34 GMT. A water sample was taken in the profilometer beam at 17:37.

Survey 11 (239B) (Quality: H+)

The survey started at 22:14 GMT at the deep site. Barge GL-64 approached with a speed and heading of 6.5 knots and 340 deg, respectively, and the prelease draft was 17 ft at the bow and 18 ft at the stern. The tug captain reported 4,500 cu yd estimated to be 70-percent sand and 30-percent fines. The inside of the barge could not be seen during its approach, but at release the barge rose relatively rapidly and ridges of black-grey material were observed. A narrow black and chalk-colored plume appeared on the water surface after the release. Seven transverse transects

were made. There was minimal surface current and wind, and the water surface was flat. Light rain and fog precluded aerial photography. The ACP showed indications of internal waves through observation of trapping and movement of material in the water column; the presence of internal waves was verified by visual observation of the water surface. Several 35-mm photographs of the water surface were also taken. The internal waves appeared to originate at about 5-m depth (at 22:27:30) and had an amplitude on the order of 1.5 m. (The ACP gain was changed during mid-run for the first time to optimize the visual record; this procedure was followed in later runs as necessary.)

According to the ACP record, at later times of plume evolution the angle of the sides of plume was different, and it was hypothesized that the angle change was an indication of differential settling by particle classes of different grain size. The current was weak (less than 30 cm/sec, although there was a shear), and the suspended sediment pattern was considered as an almost perfect "laboratory plume" in postsurvey discussion. The pycnocline was located at depths of 3 to 5 m below the ADCP sensor. Widening of the plume near the water surface and at the bottom could be seen by the ADCP.

Monday, 28 August 1989 (JD 240)

Survey 12 (240A) (Quality: L/M)

The survey started at 13:35:14 GMT at the deep site. Barge GL-64 approached with a speed and heading of 5.5 knots and 335 deg, respectively, and the prelease draft was 18 ft at the bow and 19 ft at the stern. The tug captain reported 4,500 cu yd estimated to be 50-percent sand and 50-percent fines. One large black clump was visible in the barge, and 35-mm pictures were obtained of black material on the inside of the barge as it was splitting open. The CTD was cast on the first transverse entry; the *R/V Pelican* intentionally overshot the plume to drift back during the CTD cast, but the return took longer than expected. The CTD water samples visually showed the highest concentrations to date.

The plume exhibited typical behavior (ADCP). The wait for completion of the initial CTD cast precluded observation of the initial dynamic behavior of the plume. There was slight evidence of

bottom surge on the entry side of the plume, and there also appeared to be an indication of a shear on the sediment (ACP). Schools of large fish were observed in the ACP record.

Survey 13 (240B) (Quality: II)

The survey started at 20:35:17 GMT at the deep site, and the decision was made for this survey to be the last one at the deep site. Barge GL-61 approached with a speed and heading of 6.0 knots and 345 deg, respectively, and the prelease draft was 18 ft at the bow and 17 ft at the stern. At 19:06 the tug captain had reported a draft of 19.5 ft at the bow and 16.5 ft at the stern; it was speculated that the material had subsequently settled and redistributed. The tug captain reported 4,400 cu yd estimated to be 70-percent sand and 30-percent fines. The barge had large black and grey clumps in the middle and front and was fishtailing due to the skewed weight distribution. The release was rapid and lasted about 10 sec.

The CTD was cast from a transverse entry, and, after sampling was completed, the *R/V Pelican* continued with transverse transects followed by longitudinal transects. Visually, the CTD appeared to be in the vicinity of the plume for the entire cast, but it may have drifted away during initial portion of sampling, later returning to the plume. The current was relatively weak, and the material remained localized (ADCP). The ADCP recorded a steady decrease in backscatter amplitude over 4-1/2 longitudinal transects. (Interpretation of the ADCP record indicated that the transverse transects were made south of the main discharge, at the site of the marker buoys of the main plume. It was speculated that the main discharge moved north in the water column.) The longitudinal extent of the bottom discharge was approximately 700 m (ADCP). The ACP indicated a bottom surge on the entry side.

Tuesday, 29 August 1989 (JD 241)

Survey 14 (241A) (Quality: M/II)

The survey started at 11:44 GMT at the shallow site. Barge GL-61 approached with a speed and heading of 6.7 knots and 288 deg, respectively, and the prelease draft was 20 ft. The tug captain reported 5,600 cu yd estimated to be 90-percent fines (as 75-percent clay and 15-percent mud) and 10-percent sand. Many black clumps were observed in the barge, and the release was

rapid, on the order of 10 sec. The resultant surface plume had a narrow width compared with previously observed plumes. The *R/V Pelican* began sampling on a transverse entry at an oblique angle away from the direction of barge motion. The current was weak (10 to 20 cm/sec to east), and the plume decayed rapidly (ADCP). The ACP showed a bottom surge on both sides and clear signals on all transects.

Survey 15 (241B) (Quality: M/H)

The survey started at 18:46 GMT at the shallow site. Barge GL-64 approached with a speed and heading of 6.2 knots and 292 deg, respectively, and the prelease draft was 21 ft. The tug captain reported 5,600 cu yd estimated to be 70-percent sand and 30-percent fines (mud). Large brown clumps were located in the middle of barge, and the release lasted 30 sec. The CTD was cast on the first transverse entry. The *R/V Pelican* drifted out of the plume during the cast; therefore, the CTD was hoisted, and the ship was put on the track of the plume through guidance by the ADCP; the CTD samples contained several water samples of high concentration.

The plume suspension pattern was similar to others previously observed and had no unusual characteristics (ADCP). The ADCP did rapid sampling to obtain vertical velocities of sediment clumps. The ACP showed a surge upon entry during the first transect; also, the sediment concentration appeared to decay rapidly, but the ship track must be checked to see if this apparent decay is an artifact caused by ship drift.

Wednesday, 30 August 1989 (JD 242)

ARMS Recovered (Second Deployment)

Recovery of the ARMS was made at 03:35 GMT. Inspection of the data canister revealed that the collection had malfunctioned shortly after deployment, resulting in very limited data acquisition.

Survey 16 (242A) (Quality: M/H)

The survey started at 16:06 GMT at the shallow site. Barge GL-61 approached with a speed and heading of 5.5 knots and 292 deg. The tug captain reported that he had slightly "cracked" the hopper to provide us with a fast opening. In approach, the barge had a draft of 16 ft, slowly decreasing to approximately 14 ft upon start of full opening. The release was rapid, and a grey-brown plume emerged. The tug captain reported 4,000 cu yd estimated to be 80-percent sand and 20-percent fines (mud).

The CTD was cast from a longitudinal entry and was located slightly off the center of the plume as judged visually; however, it was always located well within the central portion of the surface plume. The CTD samples contained the highest concentrations obtained to date as estimated visually. After the CTD cast, sampling continued on longitudinal transects.

The plume was approximately 600 m long as judged by the ADCP. The ACP showed a bottom surge on the trailing edge of the longitudinal entry side, a phenomenon not previously noted. The ADCP showed a 30 to 40-cm/sec current near the water surface. Six longitudinal transects (largest number of longitudinal transects) were made. The backscatter of the ADCP signal decreased as the plume dissipated and became indistinct. Small concentrations over a wide area suggested that the plume consisted of fine-grained material.

Survey 17 (242B) (Quality: L/M)

The survey started at 23:30 at the shallow site. Barge GL-64 approached with a speed and heading of 5.5 knots and 295 deg, respectively, and the prelease draft was 19 ft. The tug captain reported 5,200 cu yd estimated to be 70-percent sand and 30-percent fines (mud). The barge contained several large brown clumps, but most material appeared to be black during the release. The load appeared to be dry or cohesive, and discharge took approximately 2 min. The last material remaining in the barge was black-colored and clung to the sides of the barge until the rising sides reached a large oblique angle (a 35-mm photograph was obtained of this material).

The CTD was cast from a longitudinal entry. The cast was in the center of a dense plume and remained in the plume; the resultant water samples were extremely dense and denser than any samples previously taken, including the Survey 242A samples. The area was very shallow (3 to 5-m depth), and the tug touched bottom shortly after completion of the release. The shallow water may have contributed to produce the high concentrations, but also the suspended material appeared to be fine grained with some lipids. No surge was evident in the ACP record. The CTD became entangled with the ADCP, and about 30 min of the ADCP record was lost. Three longitudinal transects were made after the CTD cast, but the backscatter level was weak because of the wait for disentanglement of the CTD. The survey was not considered valuable for characterizing plume dynamics in postsurvey discussion, but it is very important for calibrating the acoustic instruments with the water samples.

Thursday, 31 August 1989 (JD 243)

Survey 18 (243A) (Quality: H)

The survey started at 18:03 at the shallow site. Barge GL-64 approached with a speed and heading of 6.7 knots and 307 deg, respectively, and the prelease draft was 20 ft. The tug captain reported 5,600 cu yd estimated to be 60-percent sand and 40-percent fines (mud). The barge contained small brown clumps in the middle; the release was complete within 10 to 15 sec, and the plume was relatively narrow and readily visible.

Sampling began as a slightly diagonal transverse entry. Six transverse transects were made over the main plume and two over a more northerly smaller plume generated as the tug and barge turned back (ADCP). The ADCP showed a strong surge. The impression from the ADCP record was that the release was on the edge of the placement mound, not at the top. The current speed was approximately 25 cm/sec, and the current was toward the south-southeast in the surface layer. The plume had the characteristic inverted mushroom pattern found in previous MFDCP surveys (ADCP). This survey was considered to be of good quality because it contains many transects in shallow water. However, the first transect was on a slight diagonal, and second transect was believed to be slightly southeast of the main plume.

CHAPTER 2

AMBIENT METEOROLOGIC AND OCEANOGRAPHIC CONDITIONS

ORSON P. SMITH

*Smith Ocean Science and Engineering, Inc.
Clayton, North Carolina 27520*

CAROL A. COOMES

*Evans-Hamilton, Inc.
Seattle, Washington 98103*

TERRI L. PRICKETT, NICHOLAS C. KRAUS

*Coastal Engineering Research Center
Waterways Experiment Station, Corps of Engineers
Vicksburg, Mississippi 39180-6199*

Contents

1. Introduction
2. Regional Meteorological and Oceanographic Conditions
3. Moored Current Meter Array (Tidal Currents)
4. Local Waves, Currents, and Weather

References

Table

Figures

Appendix

1. Introduction

The Mobile Field Data Collection Project (MFDCP) incorporated a variety of measurements of ambient local conditions to fully define the physical setting and driving forces controlling the dispersion of dredged material at the site. These measurements include hydrographic surveys of the site (bathymetry), surface wave time series, water level time series, and current measurements at two depths. The locations of the measurements, details of the data collection equipment and procedures, and analysis of the data are described in this chapter. Ambient water properties were measured in the course of surveying dispersion events and are described in Chapter 4. No significant regional meteorological or oceanographic events affected the site from 21 August to 1 September 1989 during the field data collection effort. Conditions were quiescent on a regional scale, and any atmospheric or oceanic driving forces entering the measurements were probably of local origin.

2. Regional Meteorological and Oceanographic Conditions

Weather

Weather was mild throughout the field work because of the presence of a stable high-pressure system that extended from the tropical Atlantic across the southeastern United States and Gulf of Mexico (Climate Analysis Center 1989a, 1989b). Daily high temperatures were consistently in the 90's (deg F) and night time lows in the 70's. Wind direction was variable, but was often offshore, and the wind speed seldom exceeded 15 knots. Seas were usually calm, though periods of light chop occurred intermittently. No significant precipitation was encountered by the *R/V Pelican*.

Oceanographic Conditions

Sea surface temperatures over the Gulf of Mexico were essentially uniform, nominally 29 deg C, as interpreted on a large scale from satellite data (National Weather Service 1989). The monthly sea surface temperature anomaly, the difference between the monthly mean and the climatological mean, was less than 0.5 deg C, above average in the northern gulf along the Continental Shelf of Mississippi, Alabama, and Florida. The typically high seasonal sea surface temperatures precluded clear resolution of Gulf Loop Current features from satellite imagery, but a strong eddy, dubbed "Nelson Eddy," was reported during the period of the field data collection

by oil platforms much farther offshore in the Gulf of Mexico. There was no indication that this phenomenon had any direct effect on the measurements made near Mobile Bay.

Tides

The 1989 Tide Tables (National Oceanic and Atmospheric Administration (NOAA) 1989b) predict a mean diurnal range of tidal elevations of 1.3 ft at the entrance to Mobile Bay. Tidal elevations predicted for the period of the field data collection (21 August to 1 September 1989) were as low as 0.1 ft mean lower low water (mllw) and as high as 2.0 ft mllw. This extreme range was predicted for 25 August 1989 and decreased to lower low water of 0.7 ft mllw and higher high water of 1.4 ft mllw for 1 September 1989. Only diurnal predicted variations (i.e., high water levels 24.8 hr apart) were significant enough to report during this period. The 1989 Tidal Current Tables (NOAA 1989a) predict a maximum flood current of 2.5 knots and ebb of 2.6 knots 12.4 hr later for 25 August at the entrance to Mobile Bay. The predicted flood and ebb currents decreased to 0.9 and 0.7 knots, respectively, by 1 September. The long-term average speed and direction at this location are 1.4 knots flowing toward 27 deg for the flood and 1.5 knots toward 190 deg for the ebb. Directions in this chapter are defined with respect to True North.

3. Moored Current Meter Array (Tidal Current)

Introduction

Three InterOcean S4 current meters were deployed from the *R/V Pelican* at the start of the field data collection program (21 August 1989) on a fixed mooring in a vertical array located at 30°09.02' N 88°06.63' W (Figure 1.4). The centers of the three meters were located at 4.30, 7.68, and 11.09 m below the surface (Figure 2.1). The upper and middle current meters were equipped to record horizontal current speed components electromagnetically with a nominal accuracy of ± 1 cm/sec. These instruments recorded current direction with a flux-gate compass with a nominal accuracy of ± 2 deg. Internal clocks assigned a Julian date, hour, and minute (Greenwich Mean Time (GMT)) to the beginning of each of the records. The bottom (deepest) current meter contained sensors to measure temperature, conductivity, and pressure. Sampling intervals were set at 2 min for the top meter, 1 min for the middle meter, and 0.5 min for the bottom meter. The mooring was retrieved on the final day of field work at the project site (31 August), for a total deployment of 10 days.

Procedure

The digital data of the three current meters were downloaded to a microcomputer aboard the *R/V Pelican* immediately after retrieval. These data were subsequently checked for gaps and errors. For an undetermined reason, only temperature was recorded by the bottom meter. Complete data from the upper and middle meters were recorded.

Current directions from the upper and middle meters were converted from magnetic north to true north. A 1-min time correction was added to all records to account for a known offset from the NOAA clock aboard the *R/V Pelican* used as a time standard for other measurements during the project. Percent occurrence of current speed toward specific directions for the upper and middle meter records are listed in Table 2.1. Vector stick plots of the upper and middle meter records are shown in Figures 2.2 to 2.6, and time series are shown in Figures 2.7 to 2.16. In the lower panels showing the current direction, values appearing as spikes or bad data correspond to changes in the northerly current direction between 330 to 30 deg. Time series for the temperature record of the bottom meter are shown in Figures 2.17 to 2.19. Current vectors and time series from the meter records during each release are shown in an expanded scale in Appendix 2A.

The Julian date, hour, and minute format was converted to a single time variable as decimal Julian days. The cross-shore and longshore components (positive southward and eastward, respectively) were computed from speed and direction and then subjected to a 3-hr low-pass (digital convolution) filter, which further decimated the data to 1-hr intervals. The time series for the cross-shore and longshore components of the upper and middle meter records are shown in Figures 2.20 and 2.21, prior to low-pass filtering, and after filtering in Figures 2.22 and 2.23. Scattergrams of concurrent offshore and longshore components are shown in Figure 2.24 for the unfiltered records of the top and middle current meters. Auto-spectra for the cross-shore and longshore components of the currents were computed by Fourier transformation which averaged 10 of 129 frequency bands at equal intervals between 0 and 0.5 cycles per hour (cph) (Figure 2.25). A 10-percent cosine window was applied to the data before transformation by Singleton Fast Fourier Transform. For reference, the frequencies of the strongest diurnal (K1) and semidiurnal (M2) tidal components of the tidal tractive force are superimposed as vertical dashed lines.

Results

The low tidal energy of the study area was confirmed by the moderate peak of the auto-spectra at the M2 frequency and minimal response at K1 frequency. Atmospheric events (e.g., sea breeze or synoptic scale wind stress), long-period oceanographic phenomena in the Gulf of Mexico, or freshwater discharge from Mobile Bay could have significantly influenced the flow at the mooring. The limited duration of the measurements (10 days) precluded resolution of longer periods; therefore, synoptic effects were discernible to a limited degree as periodic phenomena. Sea breezes probably imparted energy with a diurnal period (approximately 24 hr), providing an explanation of the moderate response in otherwise mild conditions of the upper meter in a broad band surrounding the K1 frequency. The middle meter responded weakly at both the M2 and K1 frequencies.

Estimated water particle trajectories associated with tidal waves propagating along the coast most commonly appear as elliptical paths, with clockwise rotation in the Northern Hemisphere. In most cases, the major axes of ellipses are oriented with the direction of wave propagation. Bottom friction tends to exaggerate the major axis (i.e., cause water particle motion to be more rectilinear) and, as the bottom is approached, to veer its orientation in the counterclockwise direction. Bottom currents tend to reach their maxima earlier than near-surface currents; therefore, a phase lag is to be expected. A phase lag approaching 180 deg is evident by inspection of the superimposed time series of the offshore and longshore components of the top and middle meter records (Figure 2.26).

The rotary spectral characteristics of the current meter records were calculated by the procedure of Fofonoff (1969). The orientation of the major elliptical axes at each frequency is presented for the top current meter in Figure 2.27a and for the middle meter in Figure 2.28a. The top current meter shows a significant orientation at the M2 frequency of about 135 deg from the longshore direction (225 deg True North), whereas data from the middle meter indicate an orientation at the M2 frequency of about 45 deg (135 deg True North).

The average direction of the maximum cbb predicted by NOAA (1989a), which generally corresponds to a surface current, because the entrance to Mobile Bay is directed at 190 deg True. This predicted current lies roughly halfway between the M2 orientations of the data from the top and middle meters, along the channel orientation at the bay entrance. The top current meter thus indicates a dominant direction 35 deg clockwise from that predicted, or further toward the longshore direction. This measured current orientation reflects a transition from channel-oriented

tidal flow to that of the open Continental Shelf. The 90-deg counterclockwise veering of the axis orientation of the top to the middle current meter is explained in part by effect of bottom friction, but could also be related to the strong density stratification measured throughout the project.

Ellipse stability is displayed for the top and middle meters (Figures 2.26b, 2.27b). This parameter has a larger value if directionality is strong, and a smaller value if the direction is not a dominant factor. Directionality is shown to be relatively stronger for the top meter. The top meter shows a significant peak in stability at near-diurnal frequencies, which may be associated with sea breeze effects. The lower meter lacks this peak, possibly as a result of its being closer to the bottom and having stronger influence of friction.

Eccentricity is the ratio of the minor to the major elliptical axes. A ratio of zero corresponds to purely rectilinear motion, a ratio of one indicates circular motion, and a negative ratio denotes counterclockwise rotation. The ratio for the top meter is also plotted in Figure 2.26b and for the middle meter in Figure 2.27b. Without further analysis, the significance of the counterclockwise current vector rotation indicated by both meters at tidal frequencies is unclear.

Maximum and minimum rotary coherences are plotted in Figures 2.27c and 2.28c for each current meter. Simultaneously high minimum and maximum coherences indicate coherent elliptical motion; a low minimum and a high maximum indicate rectilinear motion. Simultaneously low minimum and maximum coherences denote incoherent motion. A tendency toward coherent elliptical motion at both diurnal and semidiurnal frequencies is evident for the top meter. The middle meter indicates less coherent motion in general, with motion tending to be rectilinear at the M2 frequency and incoherent at the K1 frequency.

In summary, tidal influences were clearly stronger in the upper portion of the water column than they were at middepth during the current meter deployment. The site was apparently located near a transition between channel-dominated and Continental Shelf tidal circulation. Tidal energy was confirmed to be low relative to many other coastal sites. Meteorological effects (in particular, sea breeze) appear to have influenced current speed and direction. The differences in directionality and overall response at tidal frequencies between the top and middle meters indicate that the strong stratification measured during the deployment may have also significantly affected the currents. Conditions at the surface, which tended to be more predictable, thus did not control the long-term (scale of days) fate of suspended matter at the site.

4. Local Waves, Currents, and Weather

Fair weather conditions were experienced during the MFDCP, with only a trace of precipitation and fog occurring on 27 August (Exxon Well MO-112-1). The National Data Buoy Center (NDBC), NOAA, provided local meteorological data and wave measurements for the project operating period from a pitch-roll buoy (NDBC-42016) located near the stable berm off Mobile Bay (Figure 2.29). The buoy was placed at the site in May 1988, in a depth of 42 ft to monitor the ambient wave and wind climate of the stable berm. For documenting climatic conditions during the project, information taken from the buoy consists of wave height and period, wind direction and speed, air and water surface temperature, and barometric pressure.

Significant wave heights (H_s) and the periods associated with the spectral peak (T_p) are presented in Figures 2.30 and 2.31, respectively. Figure 2.30 shows highest waves (approximately 1 m) were experienced during 21-23 August (Julian Days 233-235); thereafter, the sea was relatively calm for the remainder of the operating period with wave heights averaging 0.3 m.

Wind speed and direction were measured from an anemometer on the buoy at an approximate elevation of 5 m. Figure 2.32 shows peak wind speed of approximately 7 m/sec during the beginning of the cruise, corresponding with the period of peak wave heights, and averaging approximately 3 m/sec for the remainder of period on site. Figure 2.33 shows the wind was directed from the east and southeast during the period of maximum speed, changing to west and northwest directions during 25-28 August (Julian Days 236-240), then shifting from south to southwest direction towards the end of the cruise.

Figure 2.34 shows air temperatures ranged from 26 to 29 deg C, and sea surface water temperatures were slightly higher, averaging 28 to 32 deg C. Temperature gradually rose as the project proceeded. Atmospheric pressure at sea level was steady, varying between 1,014 to 1,017 mb.

Water elevations (Figure 2.35), given in feet, were obtained from a pressure-type tide gage mounted by the U.S. Army Engineer District, Mobile, on Exxon Well MO-112-1, located north of the monitoring operations (Figure 2.29). The water elevation reached a maximum of 2.6 ft mllw on 22 August (Julian Day 234), when wave heights were greatest, and a minimum of 0.4 ft mllw on 25 August (Julian Day 237). The mean water surface elevation was approximately 1.6 ft. Maximum fluctuation of the water elevation (2.1 ft), occurred on 25 August (Julian Day 237), and a minimum fluctuation of 0.5 ft occurred on 1 September (Julian Day 244).

Figure 2.36 presents the water level measurements of the tide gage at Exxon Well MO-112-1, corrected to meters with reference to the Julian Date (local time). These water level data were smoothed with a 3-hr low-pass convolution filter. Predicted high and low tide levels, connected by a cubic spline fit curve, for Station No. 3665, Fort Gaines, Mobile Bay Entrance at 30°15' N 88°04' W (NOAA 1989b) are superimposed for comparison. A 0.2-m adjustment was added to predicted water levels to match the predicted mean level with the measured mean level. The comparison shows that measured water level variations departed little from predicted tides. This conformance to predictions indicates that the astronomical tractive force, on which the predictions are based, was the only significant force controlling water level during the field measurements.

Figure 2.37 presents the auto-spectrum of the measured water levels, band averaged over each four adjacent frequency bands. The spectrum shows significant peaks at the principle diurnal (K1) and semidiurnal (M2) tidal frequencies. No energy peaks are discernible at lower frequencies, and energy levels at higher frequencies are not significant. This frequency domain treatment of the measured water levels supports the observation that only astronomical forces had significant effect on water levels during the field measurements offshore of Mobile Bay.

Current velocities during the project operating period were calculated using data obtained from a combined pressure gage (P) and two-component (u,v) current meter mounted on a steel frame and located southeast of the feeder berm (Figure 2.29). The Puv gage was deployed by the Dredging Research Program in June 1989 in a depth of 20 ft to monitor directional wave and current velocity characteristics in the outer boundary of the stable berm. Data were collected for 17 min at 6-hr intervals. Figure 2.38 shows an average current velocity of 0.09 m/sec at the beginning of the project and increasing to a maximum current velocity of 0.35 m/sec during the period 24-28 August (Julian Days 236-240). For the remainder of the project operating period, current velocities decreased to an average of approximately 0.10 m/sec.

Average current directions were calculated from the Puv data by taking the average of instantaneous current directions. Figure 2.39 shows that average current direction during the project was directed from a south-to-southeast direction during the beginning of the cruise, shifting to a southwest direction during the period of maximum current velocities (Julian Days 236-240). Thereafter, current directions shifted to the predominantly northeast direction for the remainder of the project period.

References

Climate Analysis Center. 1989a. "Daily Weather Maps, Weekly Series: August 21 - 27, 1989," U.S. Department of Commerce, Washington, D.C.

_____. 1989b. "Daily Weather Maps, Weekly Series: August 28 - September 3, 1989," U.S. Department of Commerce, Washington, D.C.

Fofonoff, N. P. 1969. "Spectral Characteristics of Internal Waves in the Ocean," *Deep Sea Research*, Vol. 16, Suppl., pp. 59-71

National Oceanic and Atmospheric Administration. 1989a. "Tidal Current Tables 1989, Atlantic Coast of North America," U.S. Department of Commerce, Rockville, MD.

_____. 1989b. "Tide Tables 1989, High and Low Water Predictions: East Coast of North and South America, Including Greenland," U.S. Department of Commerce, Rockville, MD.

National Weather Service. 1989. "Oceanographic Monthly Summary, August, 1989," Vol. IX, No. 8, U.S. Department of Commerce, Washington, D.C.

Table 2.1

Percent Occurrence for the Top and Middle Current Records

Speed cm/sec	Direction, deg True North																Total																				
	0- 20		20- 40		40- 60		60- 80		80- 100		100- 120		120- 140		140- 160			160- 180		180- 200		200- 220		220- 240		240- 260		260- 280		280- 300		300- 320		320- 340		340- 360	
	0- 5	5- 10	10- 15	15- 20	20- 25	25- 30	30- 35	35- 40	40- 45	45- 50	50- 55	55- >	0- 5	5- 10	10- 15	15- 20		20- 25	25- 30	30- 35	35- 40	40- 45	45- 50	50- 55	55- >	0- 5	5- 10	10- 15	15- 20	20- 25	25- 30	30- 35	35- 40	40- 45	45- 50	50- 55	55- >
Top Meter																		Middle Meter																			
0- 5	0.33	0.09	0.14	0.07	0.24	0.26	0.65	0.67	0.87	0.77	0.99	1.02	0.82	0.96	0.52	0.50	0.17	9.34																			
5- 10	0.29	0.37	0.23	0.19	0.40	1.02	1.03	1.58	3.54	1.51	0.72	0.86	1.12	1.58	1.12	0.76	0.66	17.79																			
10- 15	0.90	0.09	0.22	0.56	0.79	0.22	3.11	2.35	0.86	0.93	0.50	0.26	0.63	0.92	0.65	0.07	0.53	14.77																			
15- 20	0.72	0.17	0.00	0.72	0.72	0.63	2.38	2.54	1.15	0.72	0.69	0.17	0.62	0.37	0.13	0.13	0.52	14.13																			
20- 25	0.47	0.09	0.52	0.56	0.36	0.66	3.96	2.32	0.59	0.62	0.29	0.27	0.40	0.96	0.11	0.23	0.34	14.21																			
25- 30	0.03	0.00	0.00	1.38	0.43	1.51	2.52	3.21	1.48	0.01	0.01	0.01	0.56	0.30	0.00	0.00	11.57																				
30- 35	0.00	0.00	0.00	0.37	0.39	2.41	0.73	0.00	0.00	0.00	0.00	0.00	0.69	0.09	0.00	0.00	10.14																				
35- 40	0.00	0.00	0.00	0.04	1.52	2.60	0.82	0.00	0.00	0.00	0.00	0.00	0.07	0.33	0.01	0.00	5.45																				
40- 45	0.00	0.00	0.00	0.00	0.00	0.30	0.01	0.00	0.00	0.00	0.00	0.00	0.00	0.39	0.99	0.00	1.98																				
45- 50	0.00	0.00	0.00	0.00	0.00	0.00	0.00	0.00	0.00	0.00	0.00	0.00	0.00	0.49	0.03	0.00	0.52																				
50- 55	0.00	0.00	0.00	0.00	0.00	0.00	0.00	0.00	0.00	0.00	0.00	0.00	0.00	0.10	0.00	0.00	0.10																				
55- >	0.00	0.00	0.00	0.00	0.00	0.00	0.00	0.00	0.00	0.00	0.00	0.00	0.00	0.00	0.00	0.00	0.00	0.00																			
Total	2.74	0.80	1.10	3.89	5.13	9.60	14.31	15.13	10.94	7.13	4.56	3.20	2.60	6.48	3.56	1.69	2.22	100.00																			
0- 5	1.45	0.95	0.96	1.07	1.54	1.39	1.66	1.91	1.00	0.86	0.44	0.27	0.24	0.46	0.54	0.83	1.47	17.46																			
5- 10	1.63	0.50	0.44	0.74	2.53	4.03	4.34	4.91	3.62	1.23	0.30	0.13	0.04	0.85	1.20	1.07	1.78	30.24																			
10- 15	0.07	0.13	0.01	0.09	2.19	1.80	1.47	1.71	1.73	1.08	0.11	0.25	0.37	1.24	0.54	1.13	0.90	16.50																			
15- 20	0.00	0.00	0.00	0.13	1.82	2.18	5.30	3.89	0.45	0.07	0.00	0.32	1.07	0.47	0.63	0.04	0.00	16.80																			
20- 25	0.00	0.00	0.00	0.00	0.19	4.13	4.04	1.13	0.27	0.02	0.00	0.00	0.07	0.52	0.26	0.00	0.00	11.22																			
25- 30	0.00	0.00	0.00	0.00	0.00	0.54	1.62	0.27	0.11	0.00	0.00	0.00	0.01	0.70	0.00	0.00	0.00	3.66																			
30- 35	0.00	0.00	0.00	0.00	0.00	0.00	0.11	0.01	0.00	0.00	0.00	0.00	0.01	1.00	0.00	0.00	1.91																				
35- 40	0.00	0.00	0.00	0.00	0.00	0.00	0.00	0.00	0.00	0.00	0.00	0.00	0.00	0.38	0.00	0.00	0.44																				
40- 45	0.00	0.00	0.00	0.00	0.00	0.00	0.00	0.00	0.00	0.00	0.00	0.00	0.00	0.70	0.14	0.00	0.84																				
45- 50	0.00	0.00	0.00	0.00	0.00	0.00	0.00	0.00	0.00	0.00	0.00	0.00	0.00	0.47	0.39	0.00	0.85																				
50- 55	0.00	0.00	0.00	0.00	0.00	0.00	0.00	0.00	0.00	0.00	0.00	0.00	0.00	0.08	0.00	0.00	0.08																				
55- >	0.00	0.00	0.00	0.00	0.00	0.00	0.00	0.00	0.00	0.00	0.00	0.00	0.00	0.00	0.00	0.00	0.00	0.00																			
Total	3.15	1.57	1.41	2.03	8.27	13.97	18.54	13.83	7.18	3.26	0.86	0.97	1.82	6.87	3.69	3.07	4.15	100.00																			

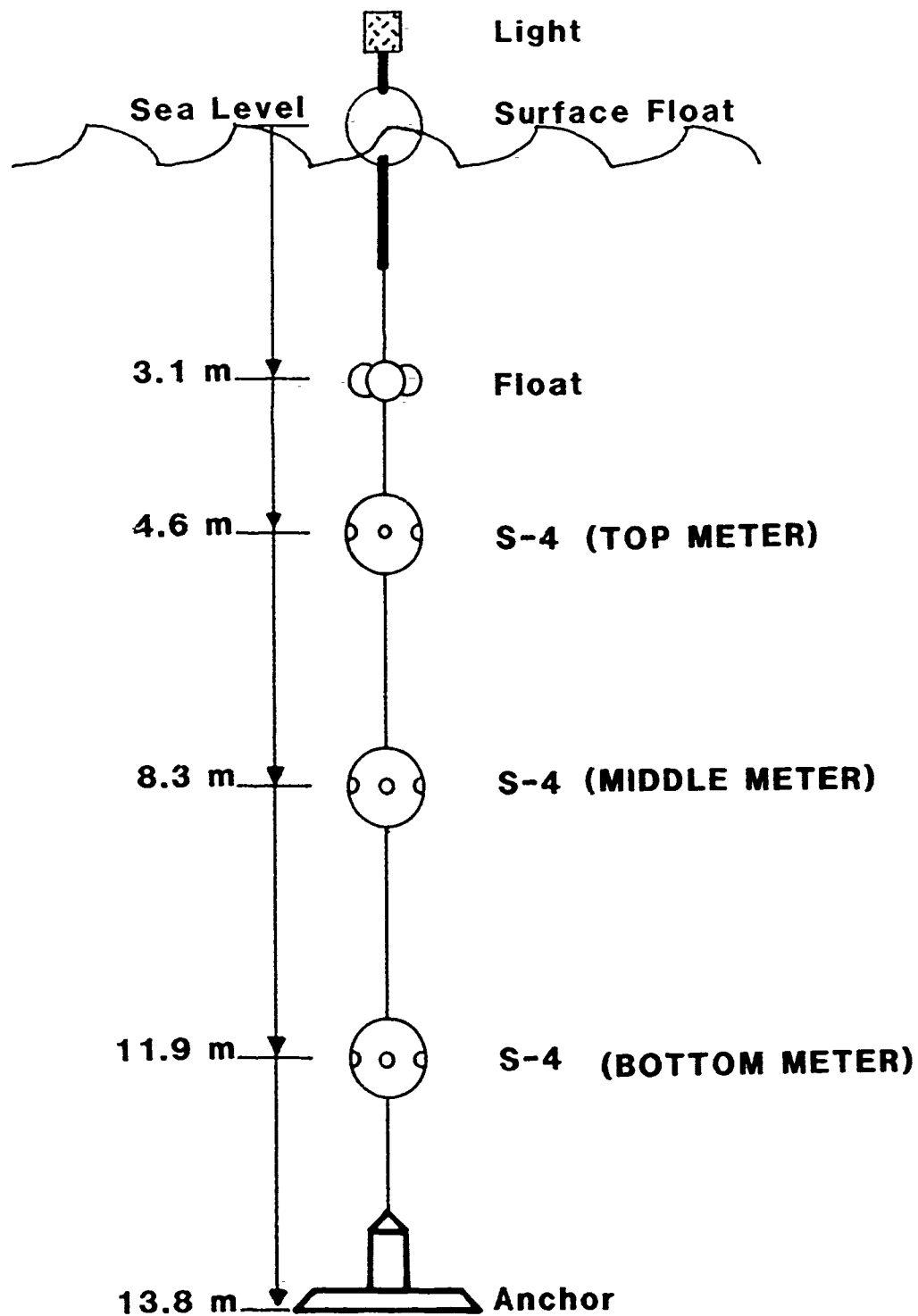


Figure 2.1. Schematic diagram of the vertical array current meter mooring near the site of the MFDGP ship operations.

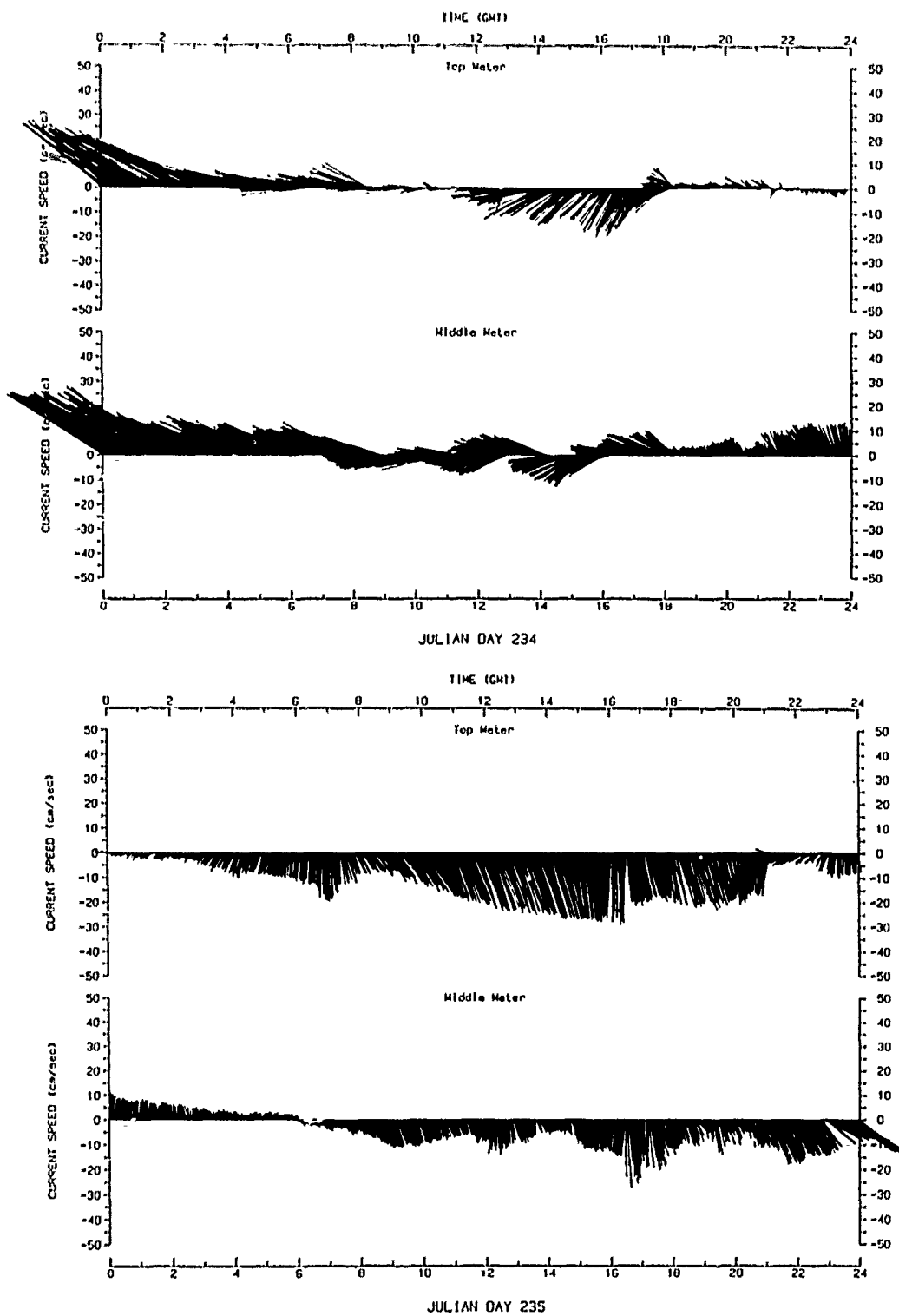


Figure 2.2. Vector plots of currents recorded by the top and middle meters for Julian Days 234 and 235.

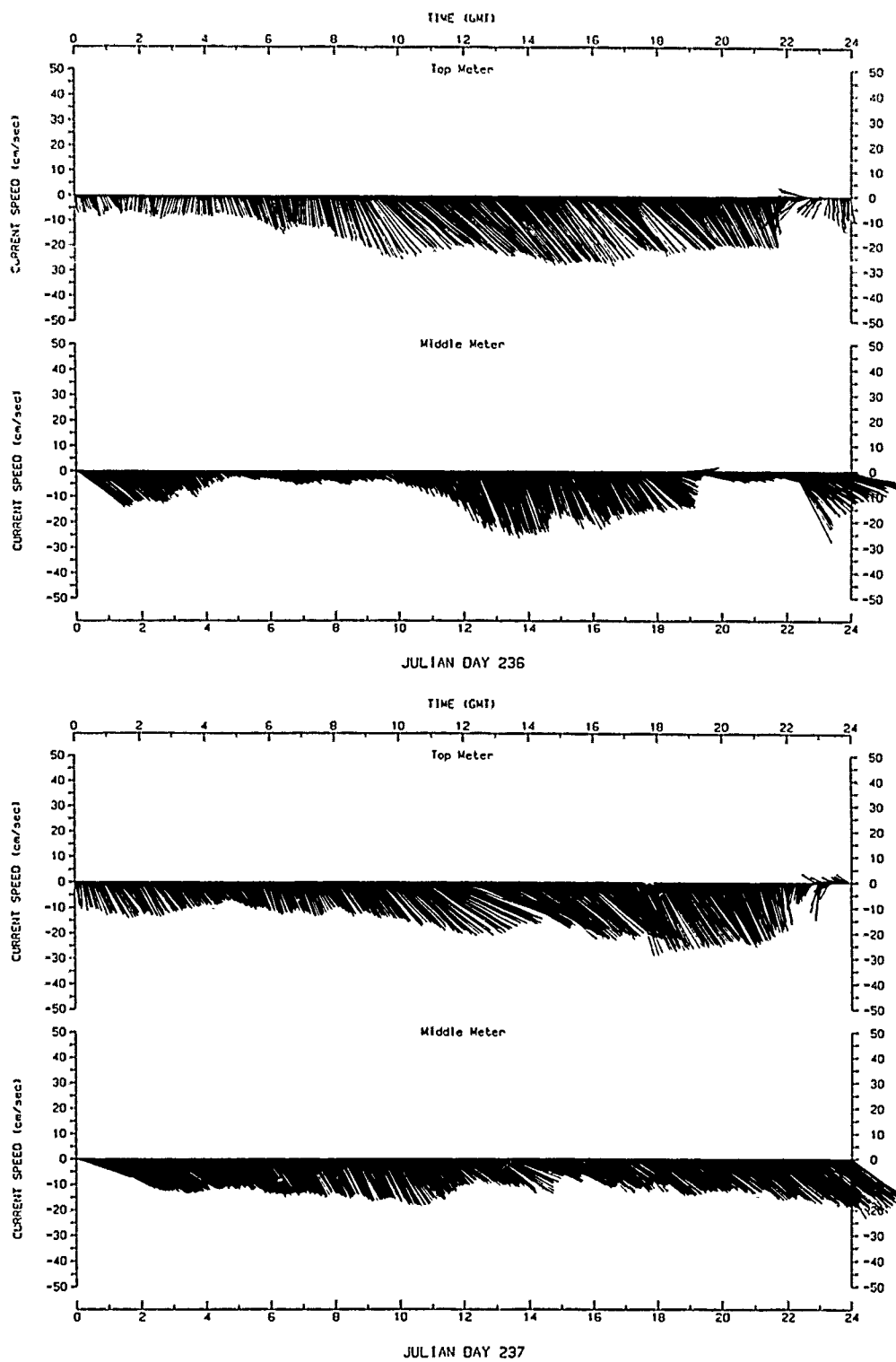


Figure 2.3. Vector plots of currents recorded by the top and middle meters for Julian Days 236 and 237.

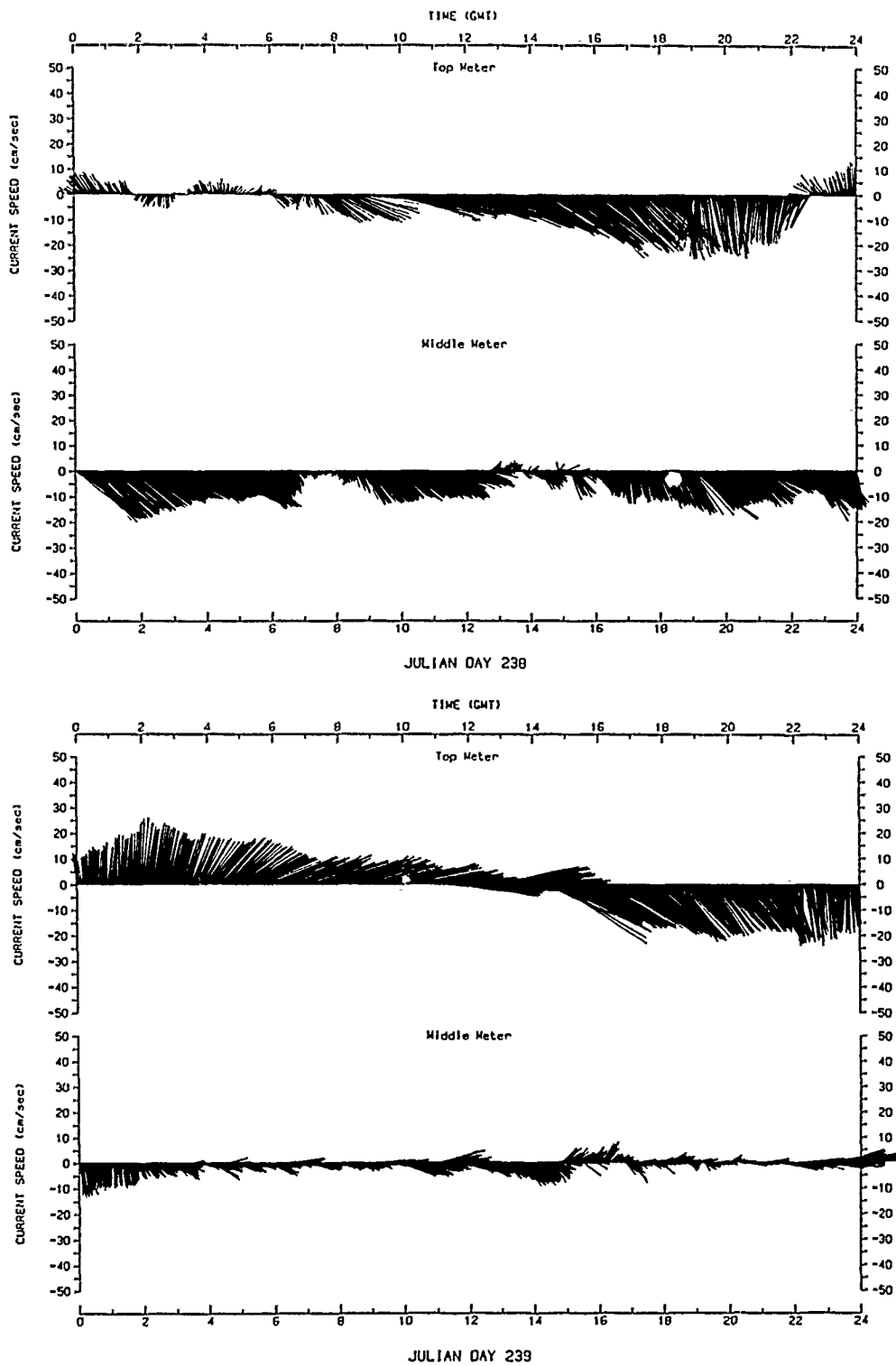


Figure 2.4. Vector plots of currents recorded by the top and middle meters for Julian Days 238 and 239.

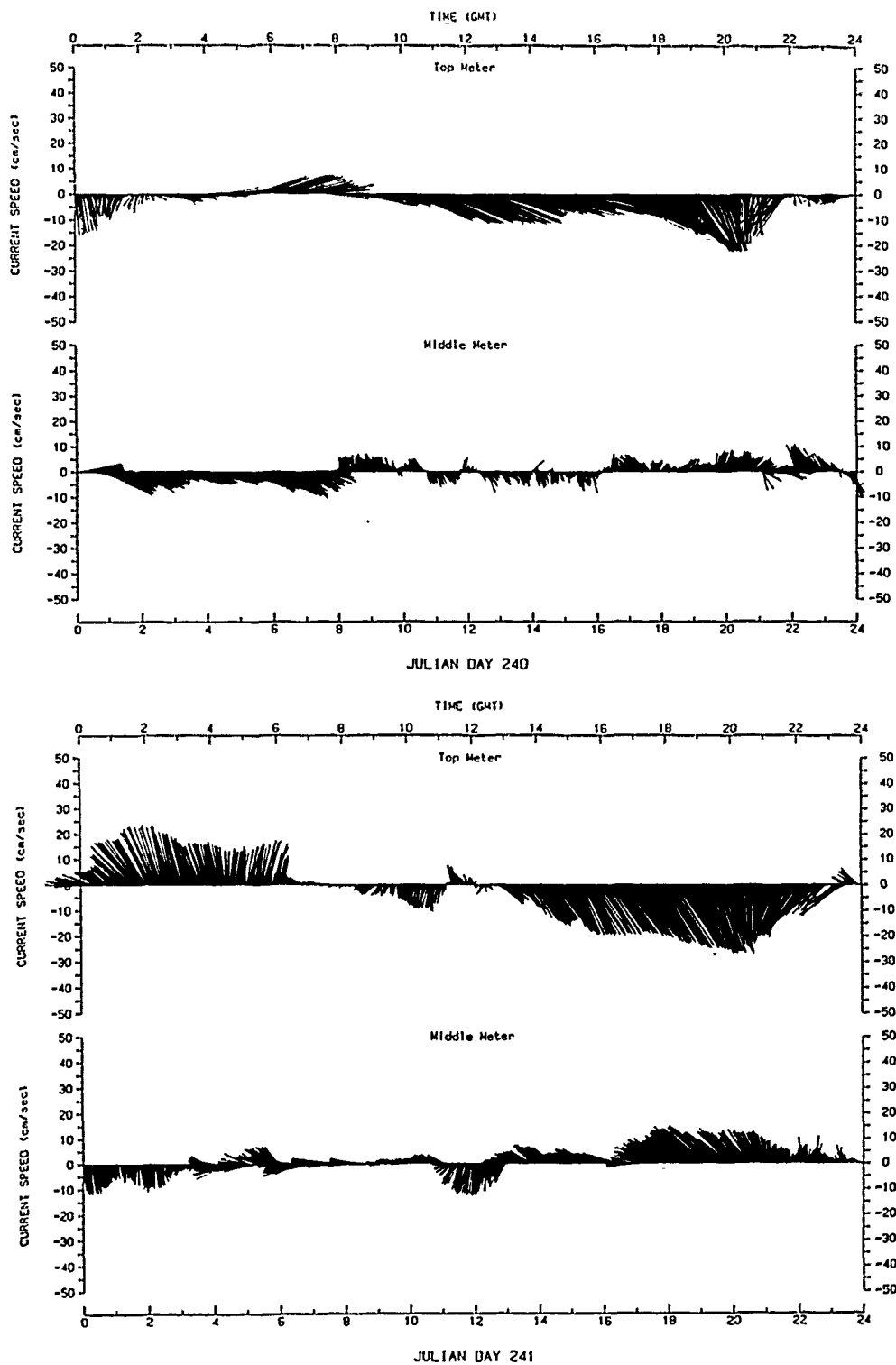


Figure 2.5. Vector plots of currents recorded by the top and middle meters for Julian Days 240 and 241.

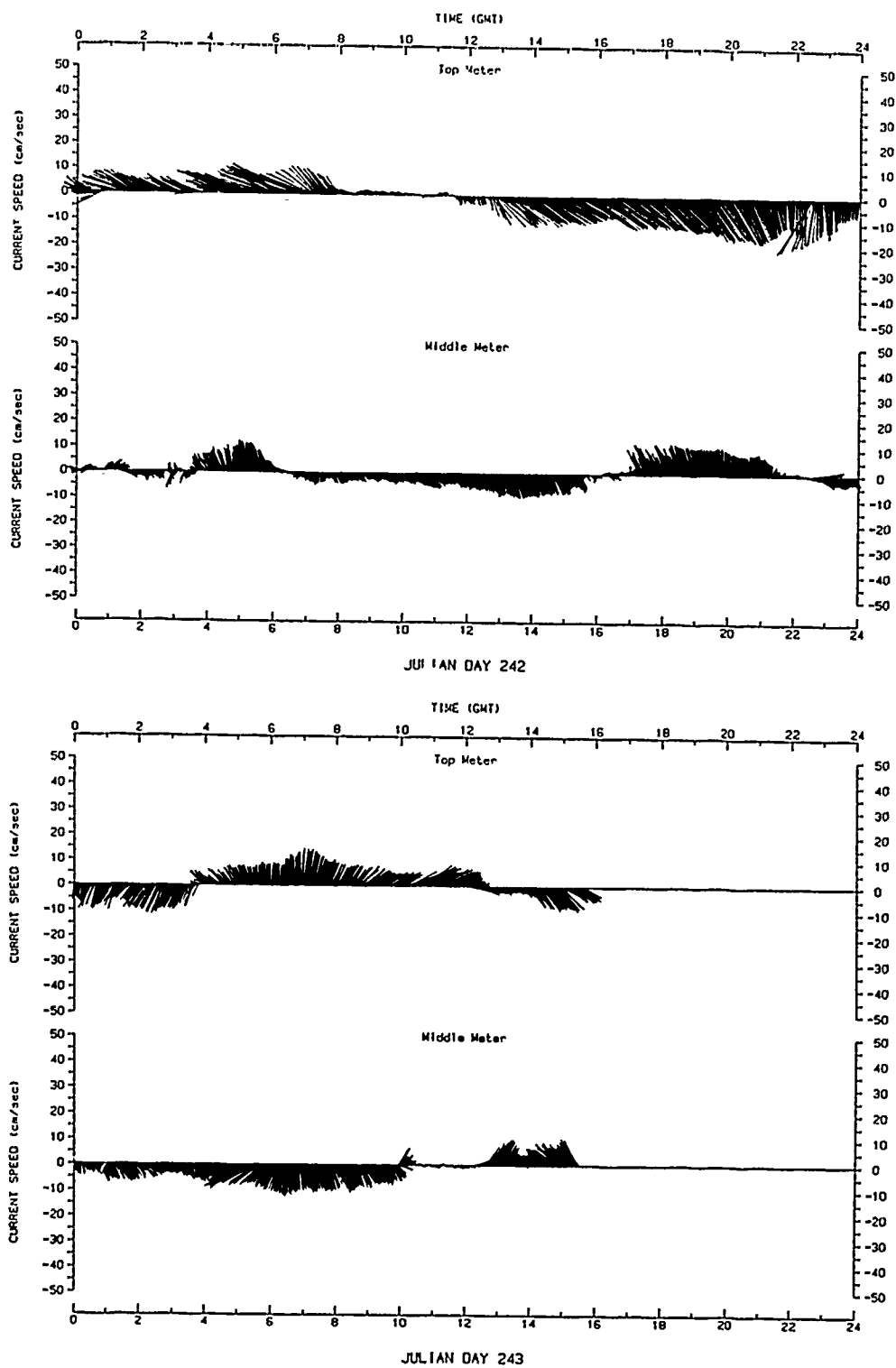


Figure 2.6. Vector plots of currents recorded by the top and middle meters for Julian Days 242 and 243.

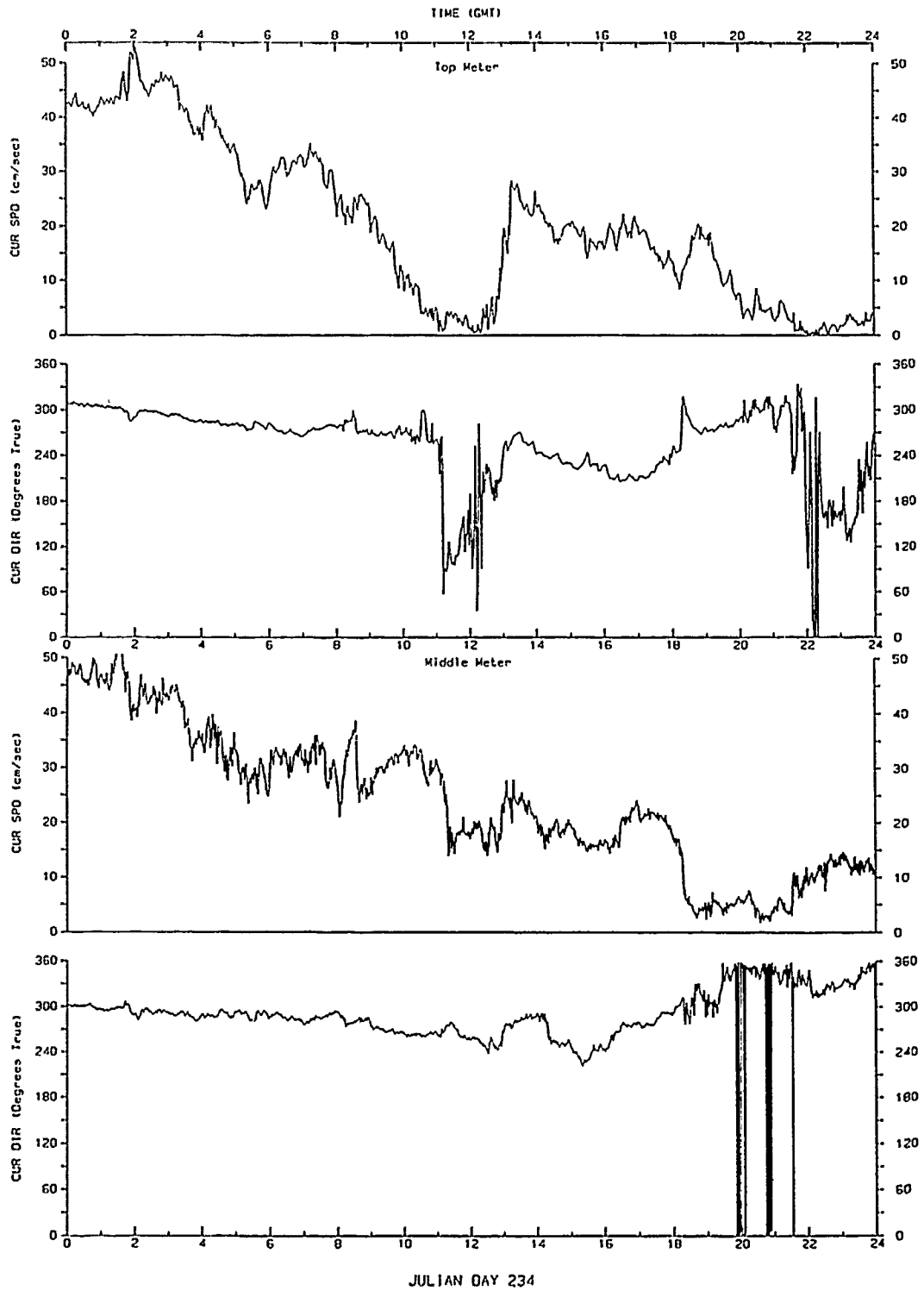


Figure 2.7. Time series of current speed and direction for the top and middle meter records for Julian Day 234.

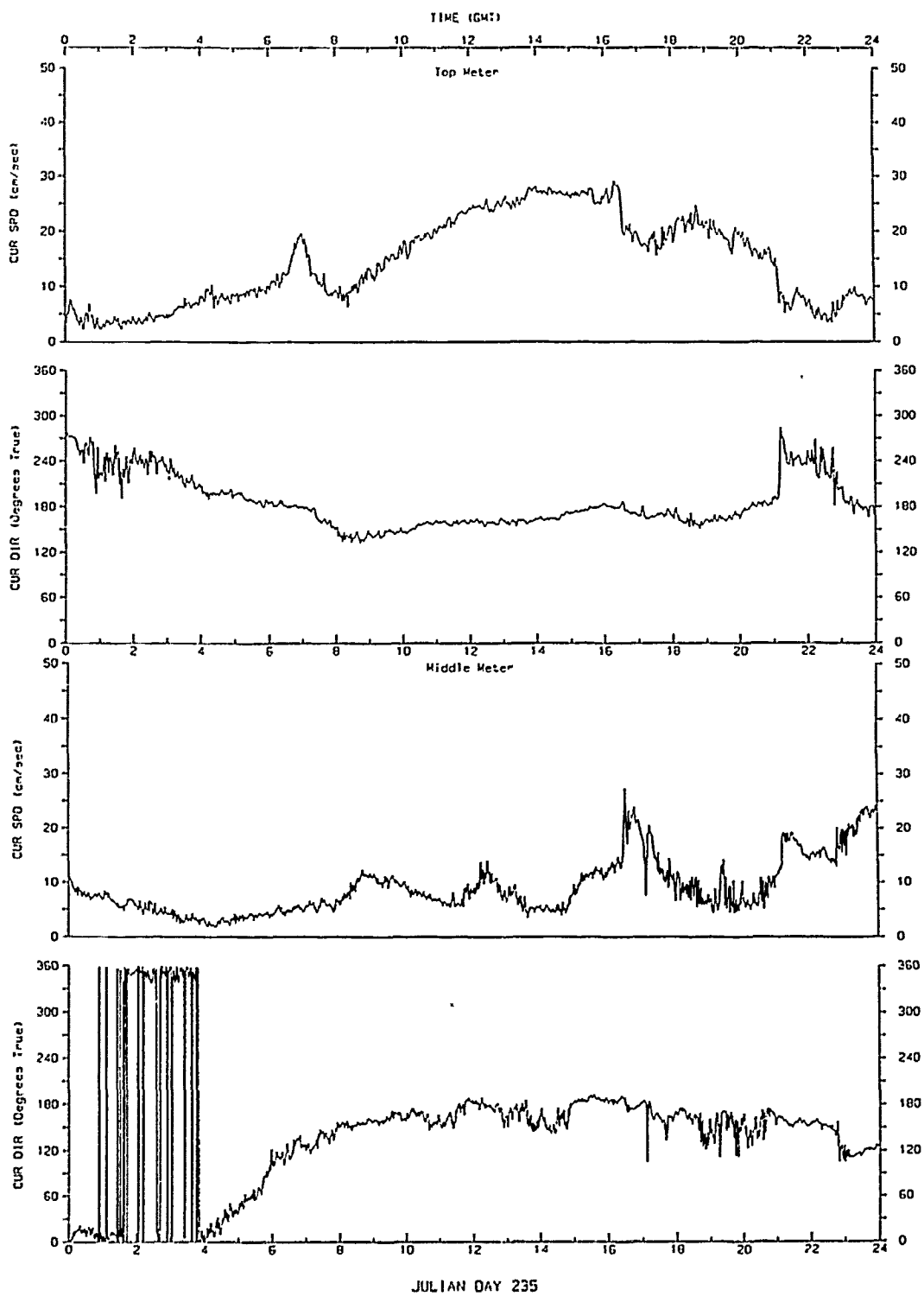


Figure 2.8. Time series of current speed and direction for the top and middle meter records for Julian Day 235.

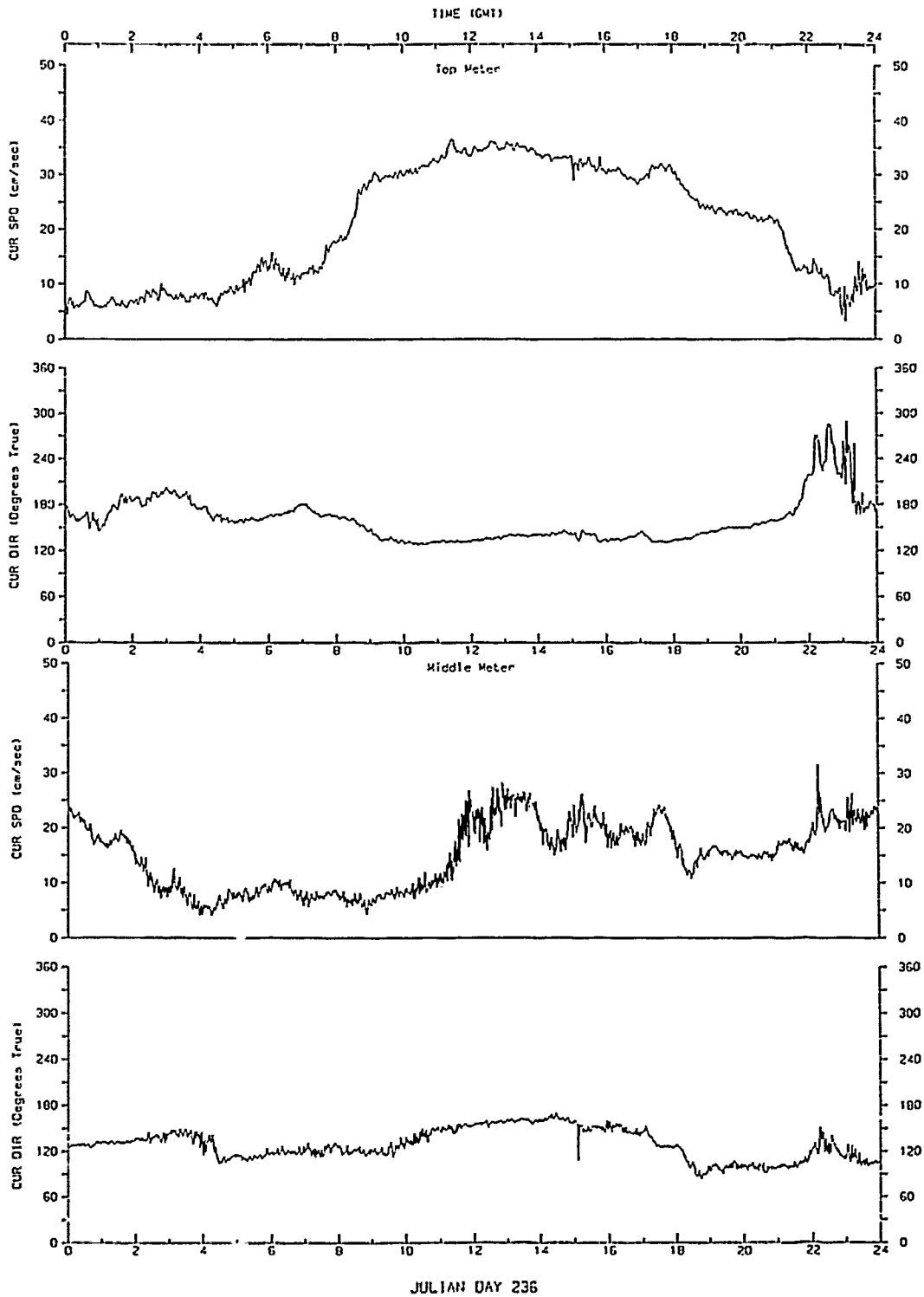


Figure 2.9. Time series of current speed and direction for the top and middle meter records for Julian Day 236.

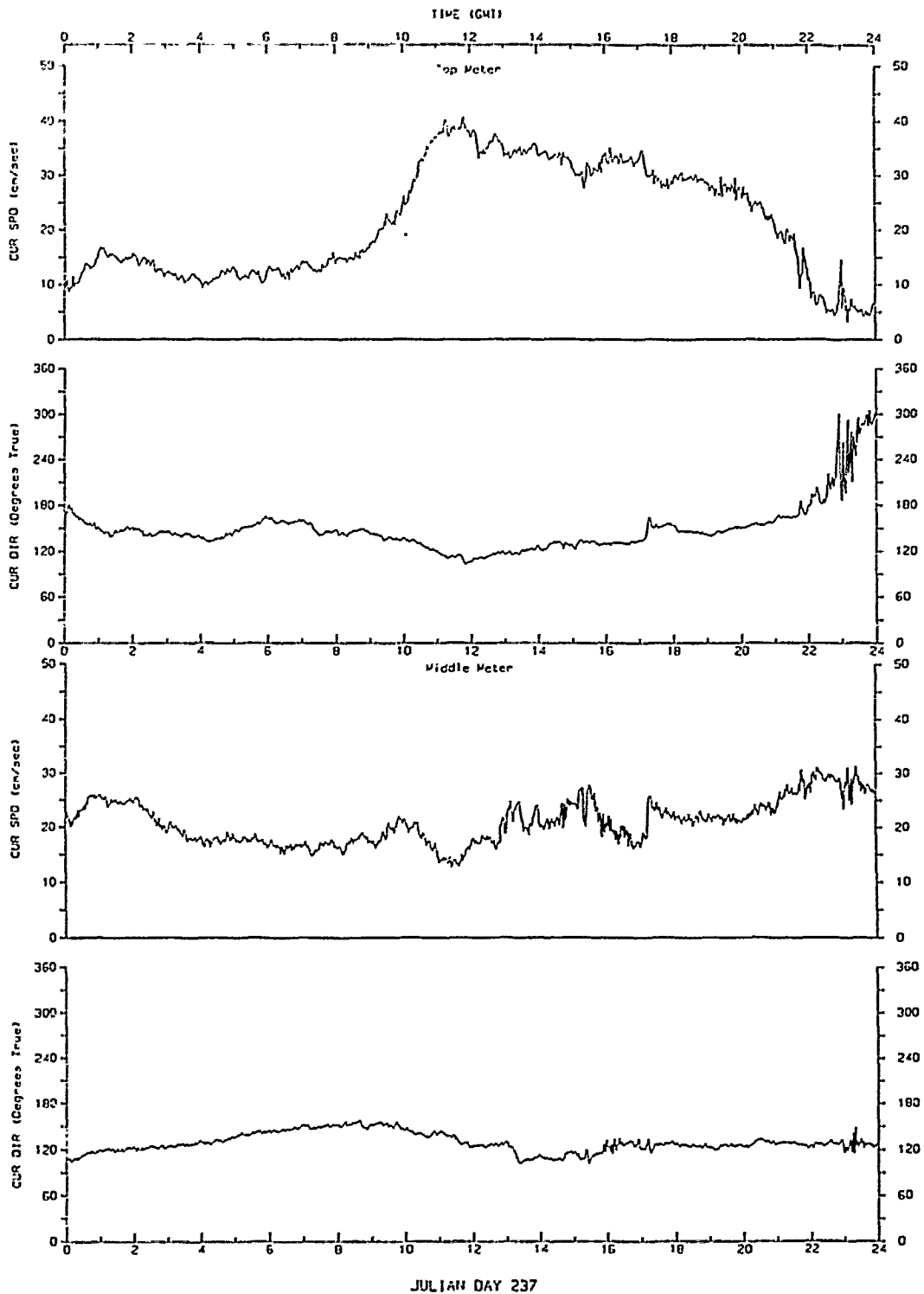


Figure 2.10. Time series of current speed and direction for the top and middle meter records for Julian Day 237.

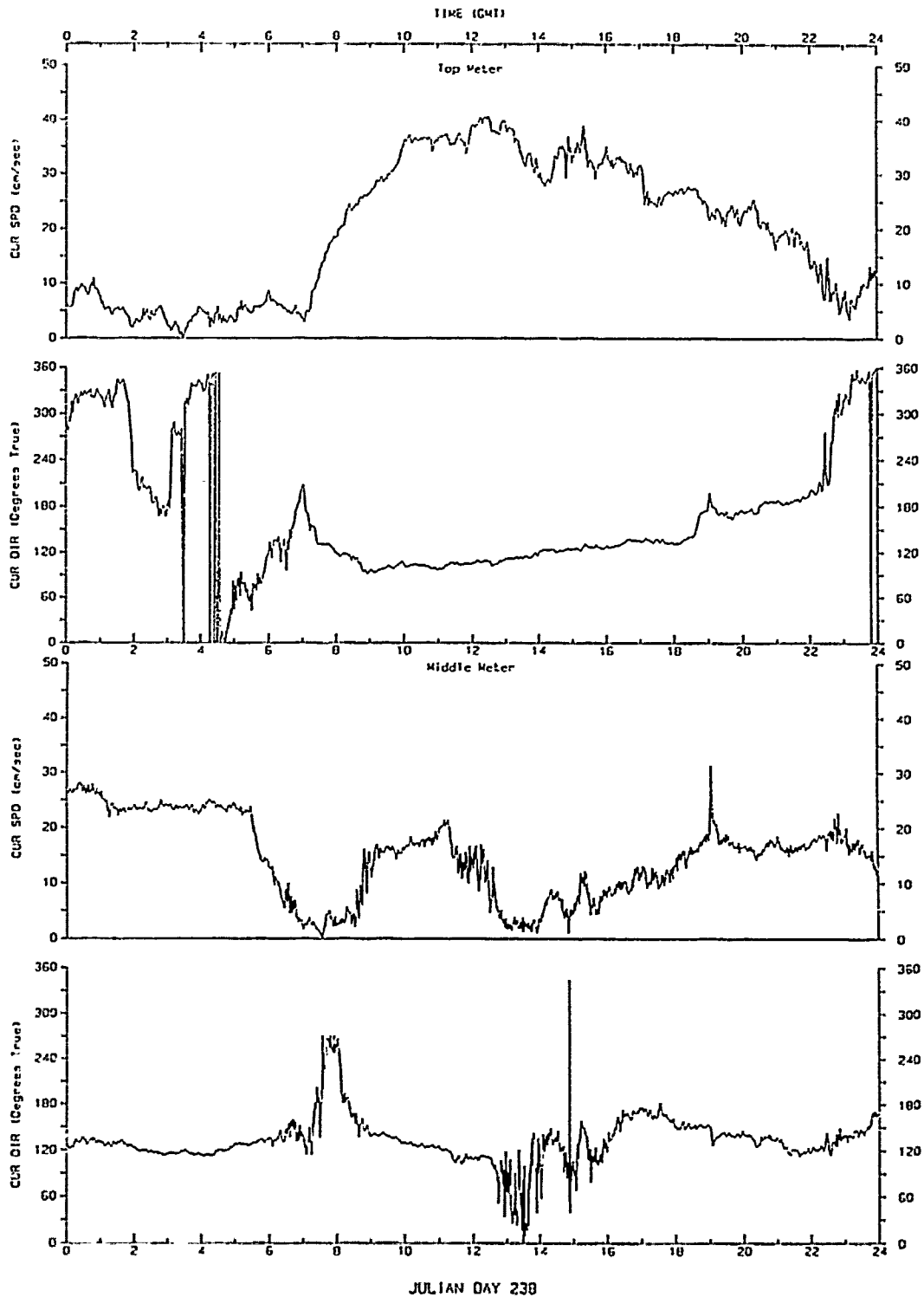


Figure 2.11. Time series of current speed and direction for the top and middle meter records for Julian Day 238.

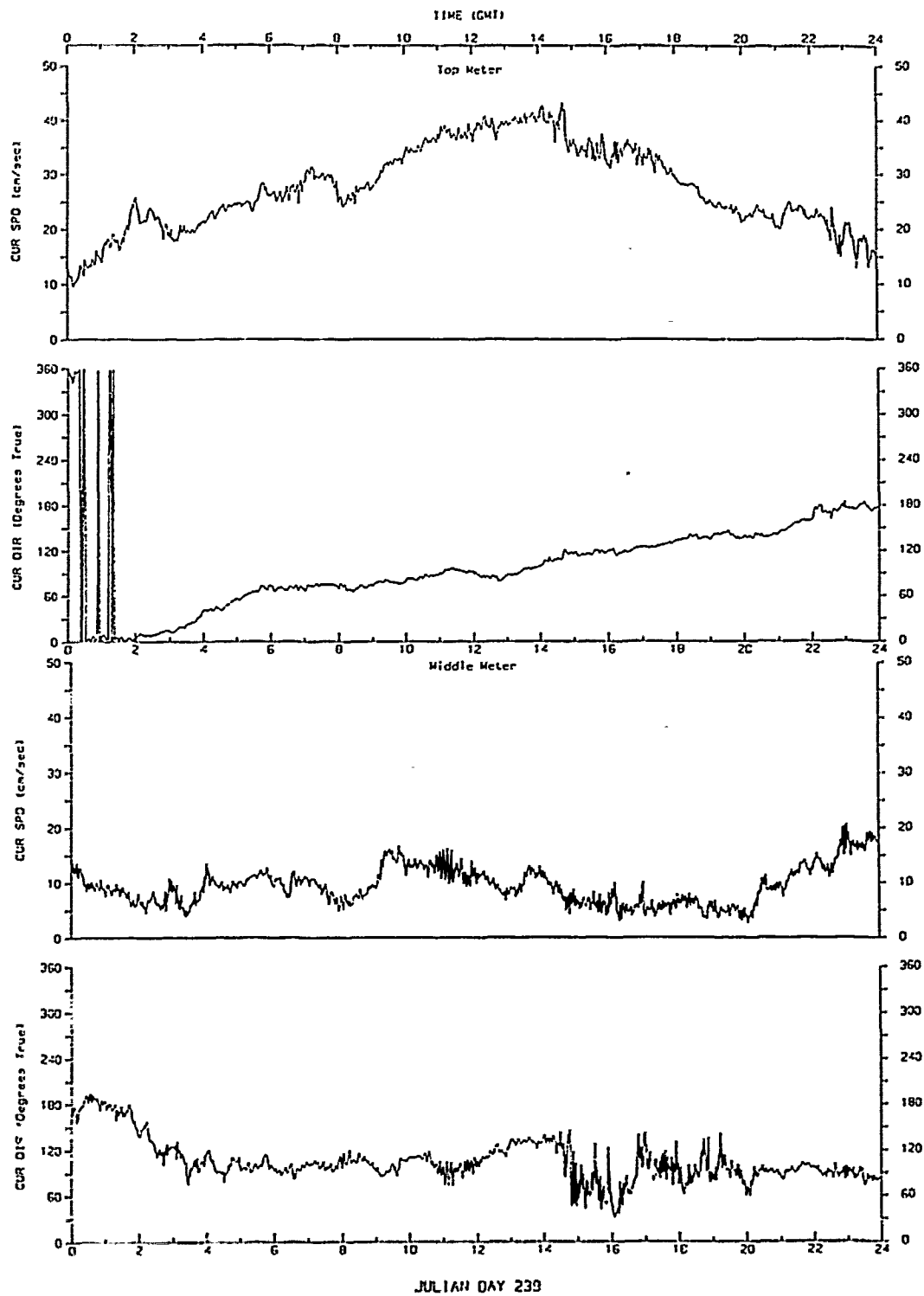


Figure 2.12. Time series of current speed and direction for the top and middle meter records for Julian Day 239.

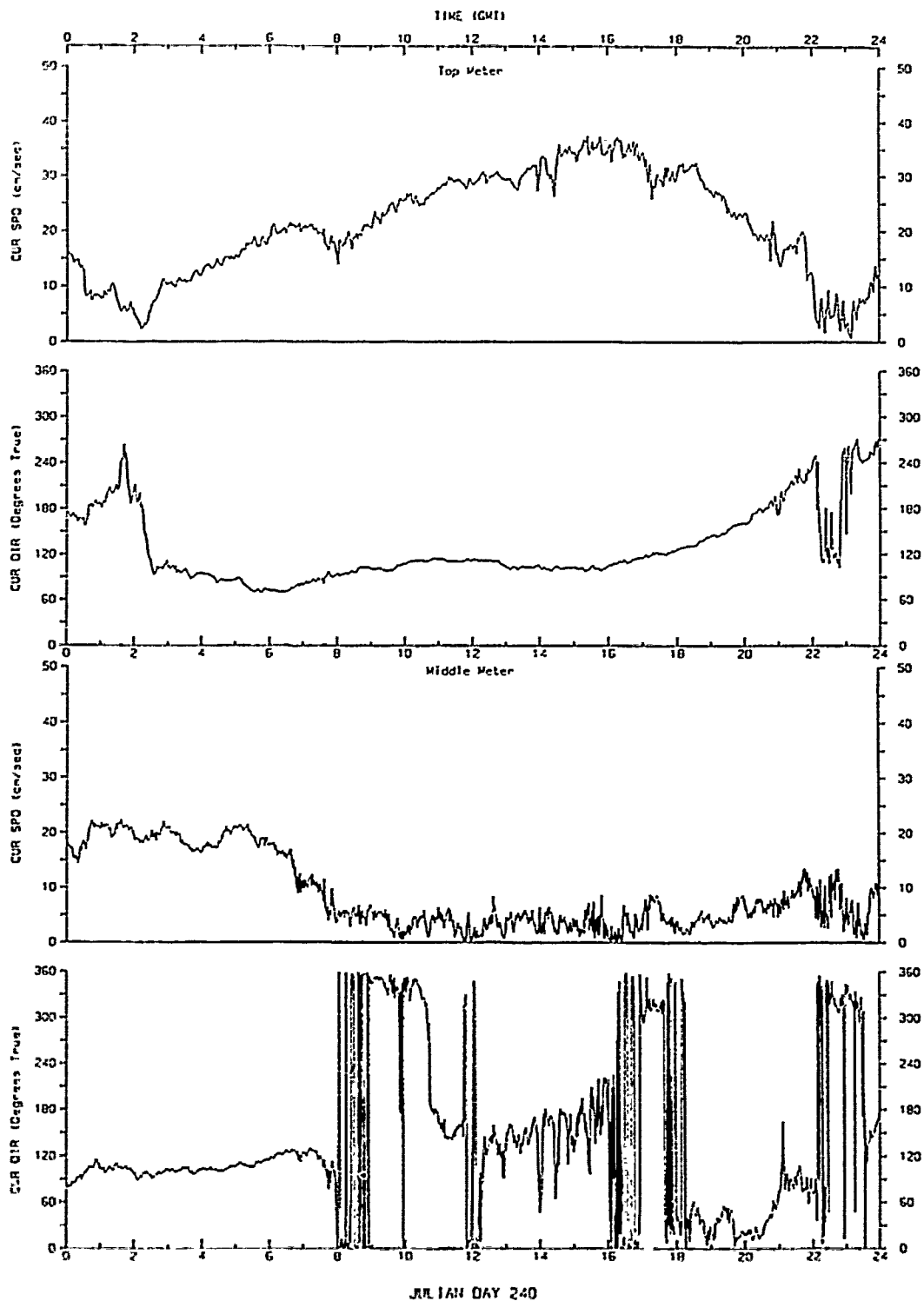


Figure 2.13. Time series of current speed and direction for the top and middle meter records for Julian Day 240.

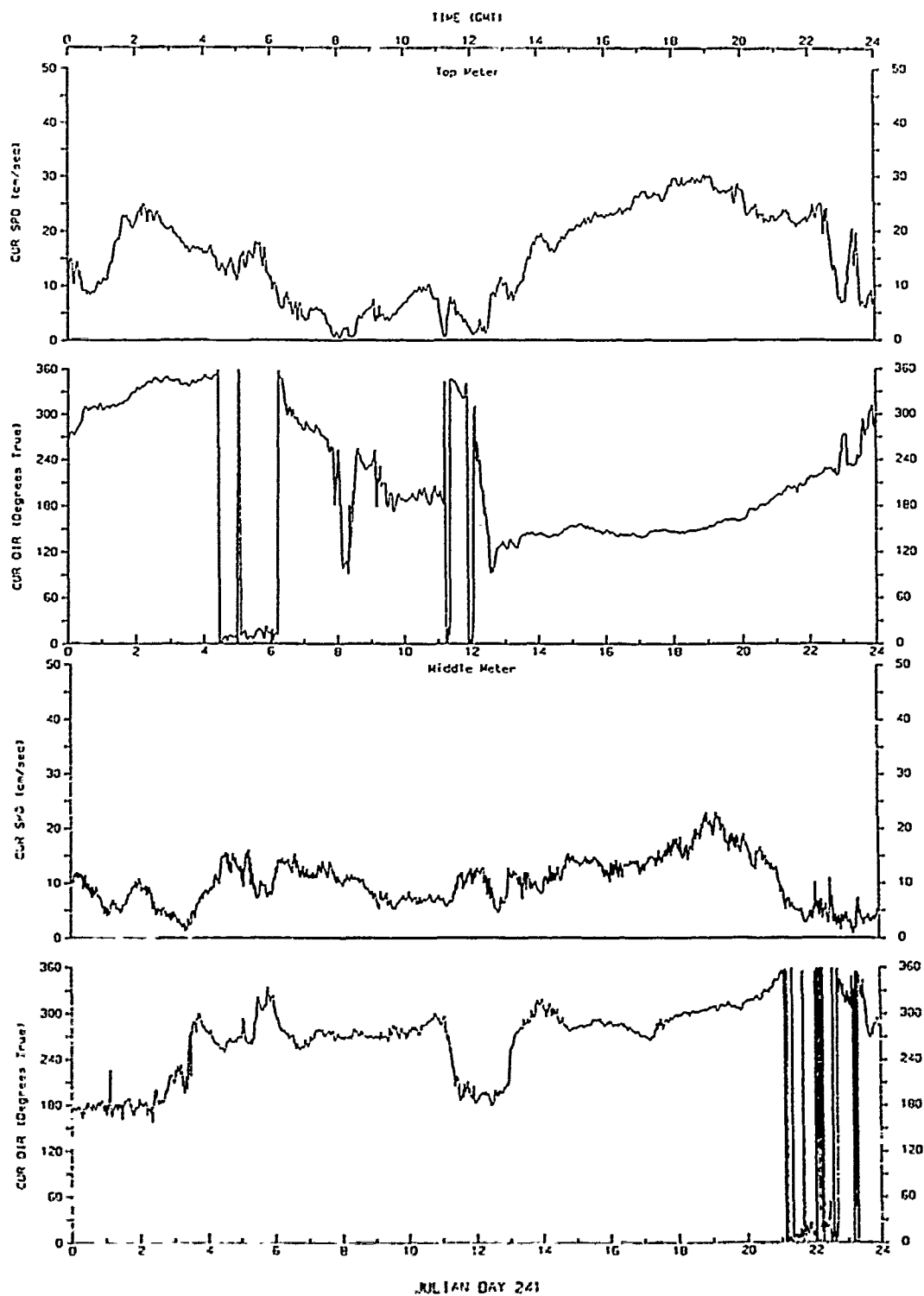


Figure 2.14. Time series of current speed and direction for the top and middle meter records for Julian Day 241.

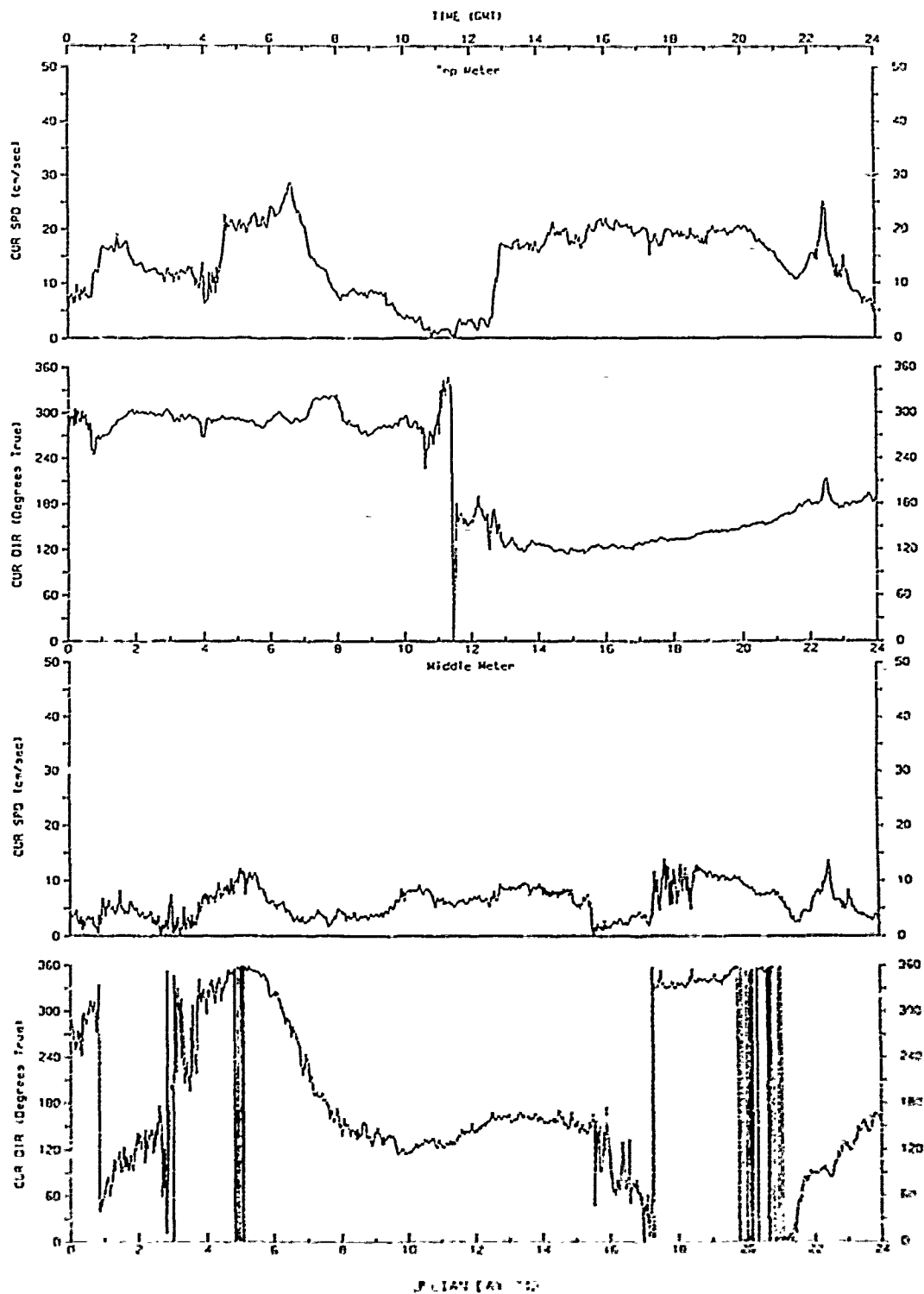


Figure 2.15. Time series of current speed and direction for the top and middle meter records for Julian Day 242.

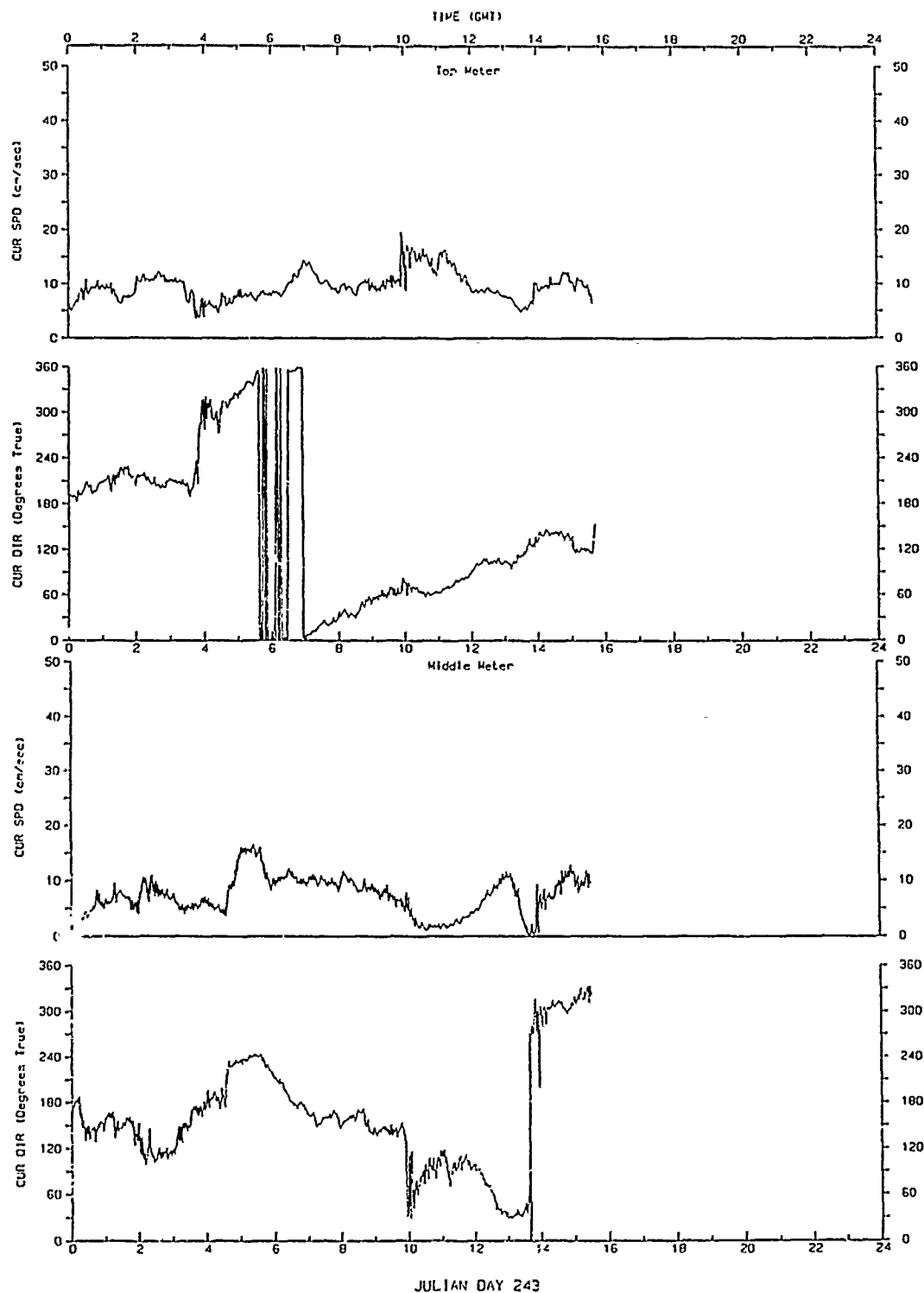
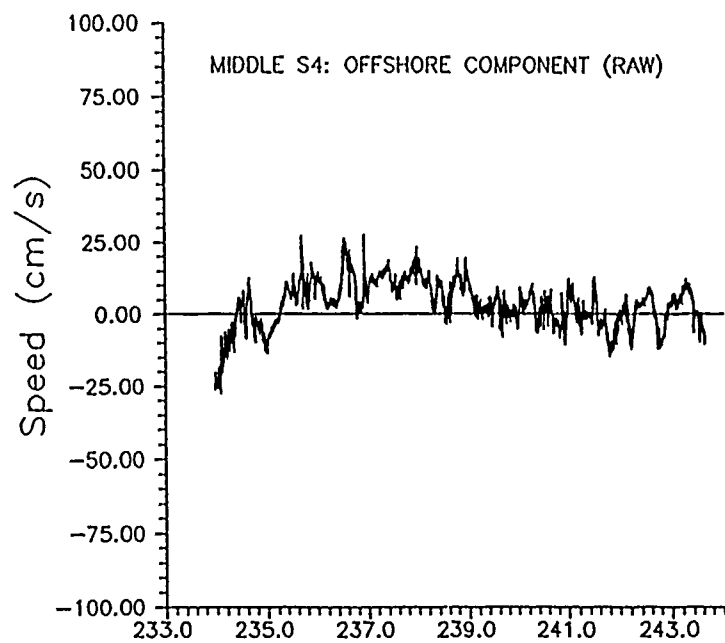
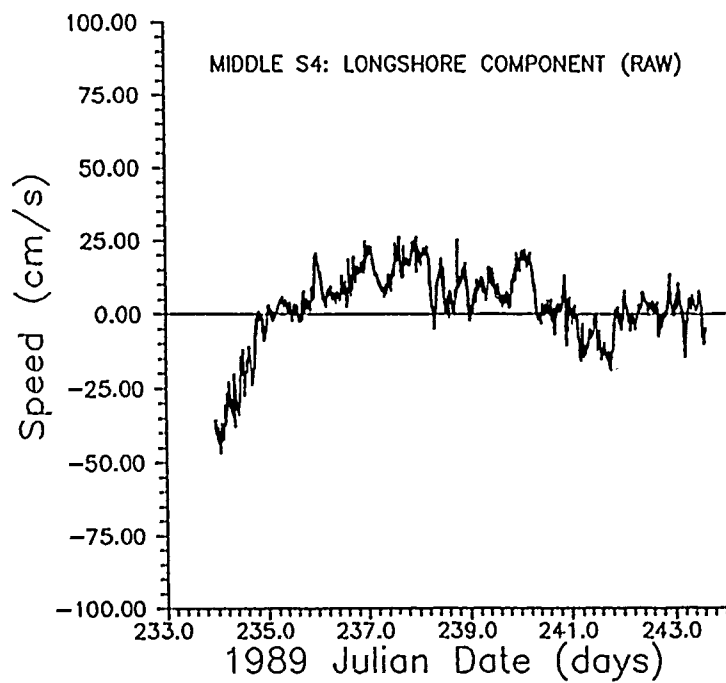


Figure 2.16. Time series of current speed and direction for the top and middle meter records for Julian Day 243.



a. Cross-shore current.



b. Longshore current.

Figure 2.21. Unfiltered time series of current components recorded by the middle current meter.

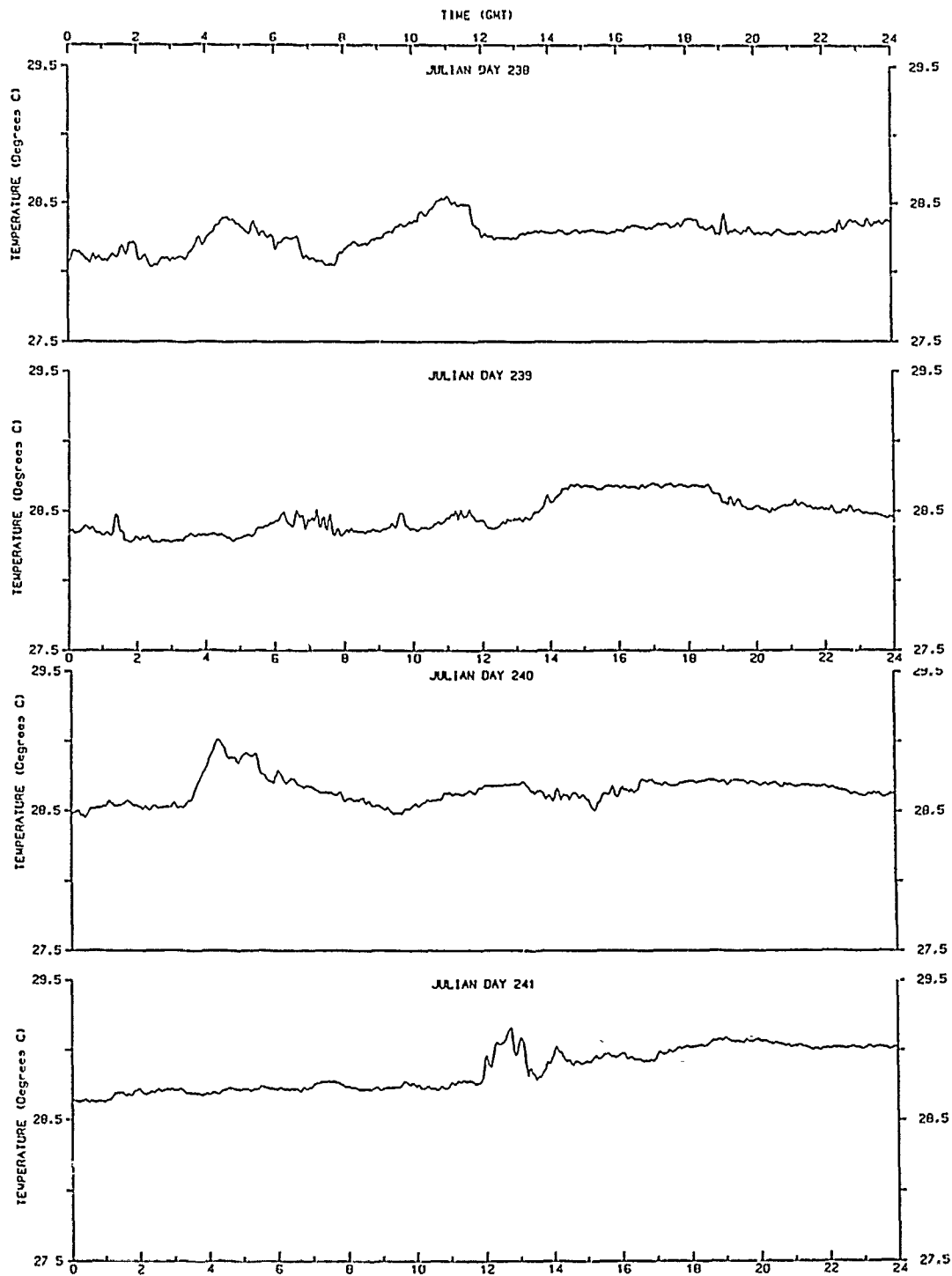


Figure 2.18. Time series of temperature for the bottom meter record for Julian Days 238, 239, 240, and 241.

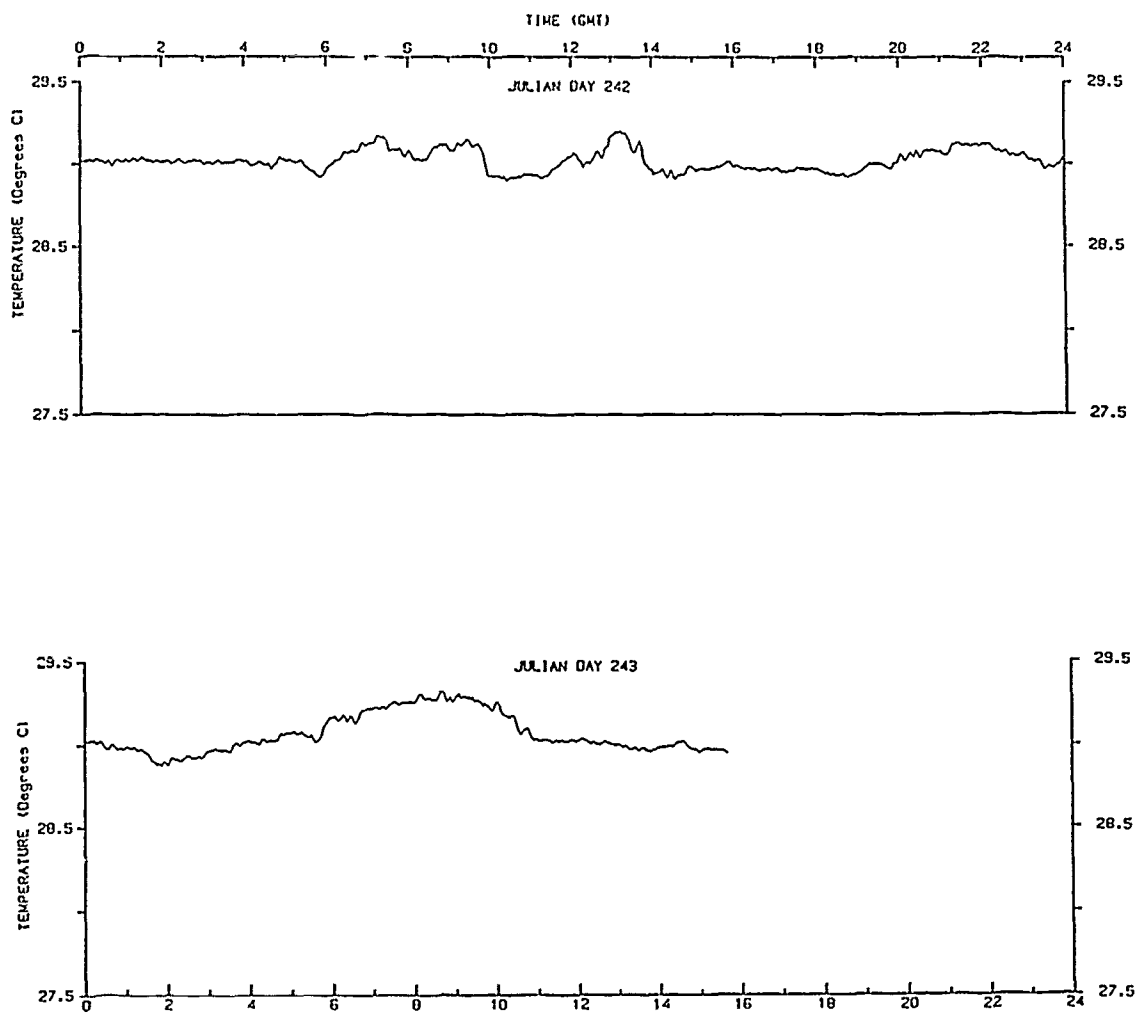
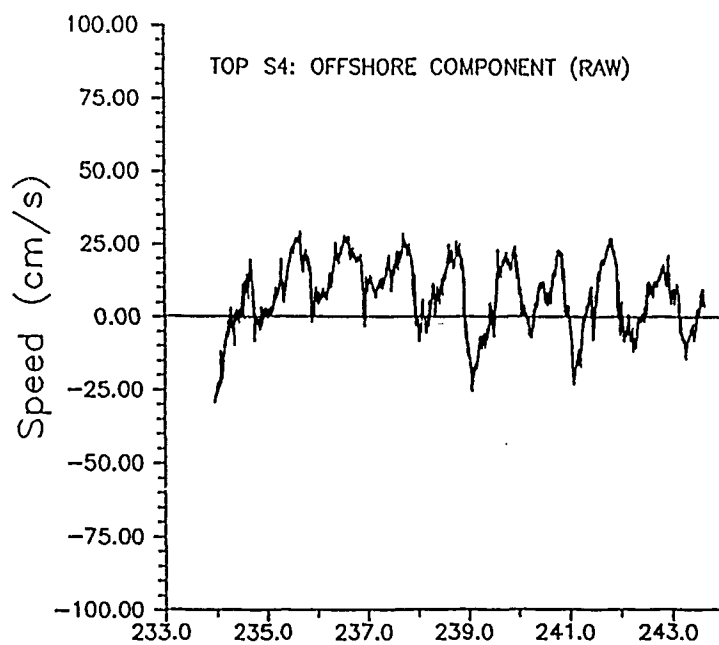
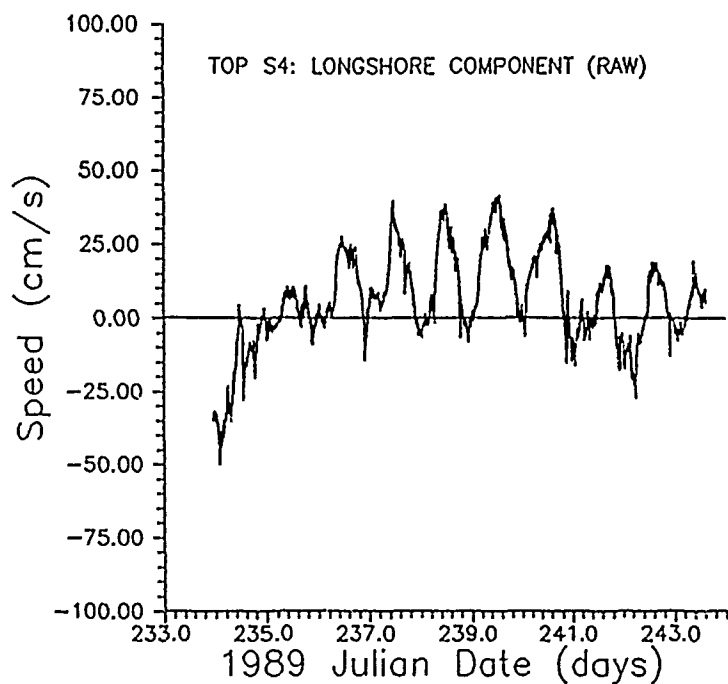


Figure 2.19. Time series of temperature for the bottom meter record for Julian Days 242 and 243.

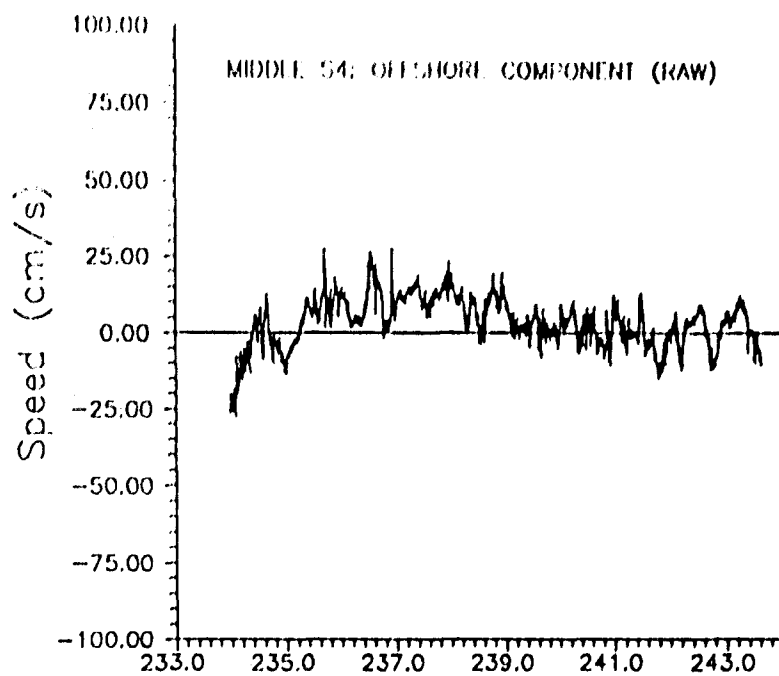


a. Cross-shore current.

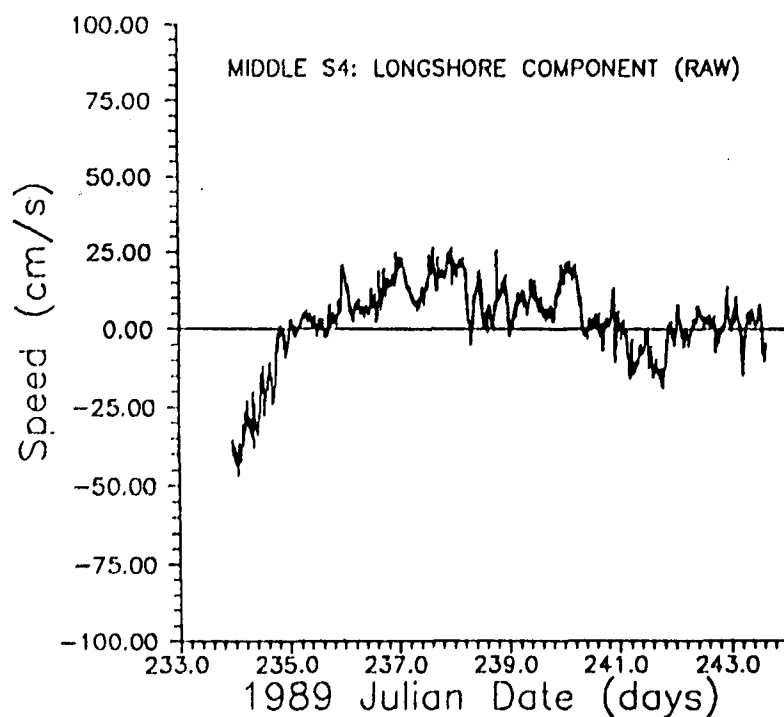


b. Longshore current.

Figure 2.20. Unfiltered time series of current components recorded by the top current meter.

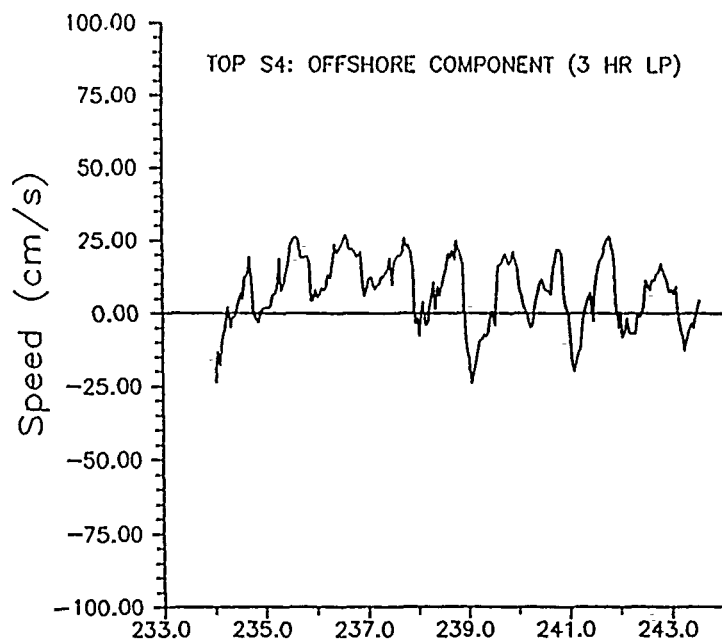


a. Cross-shore current.

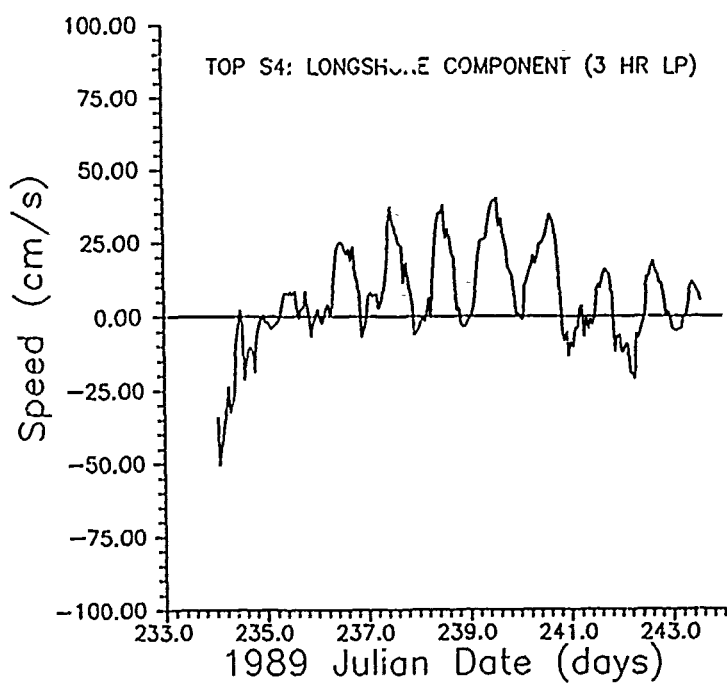


b. Longshore current.

Figure 2.21. Unfiltered time series of current components recorded by the middle current meter.

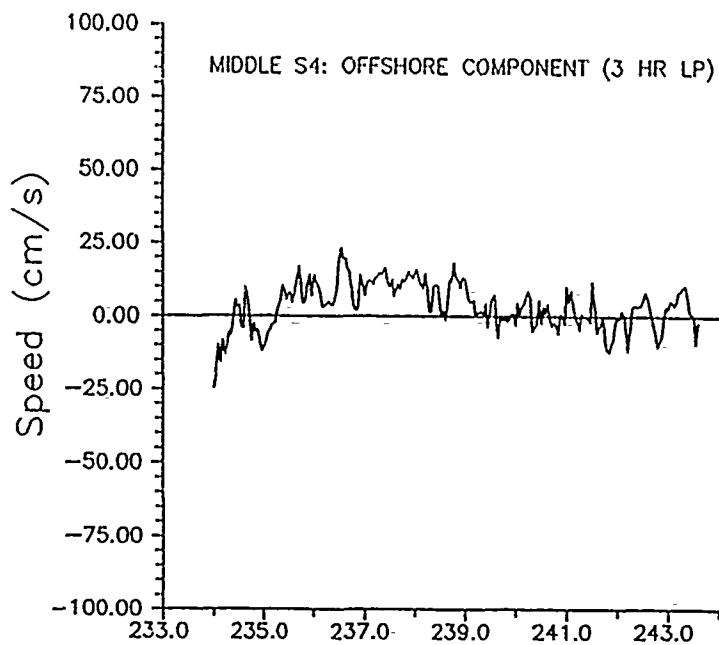


a. Cross-shore current.

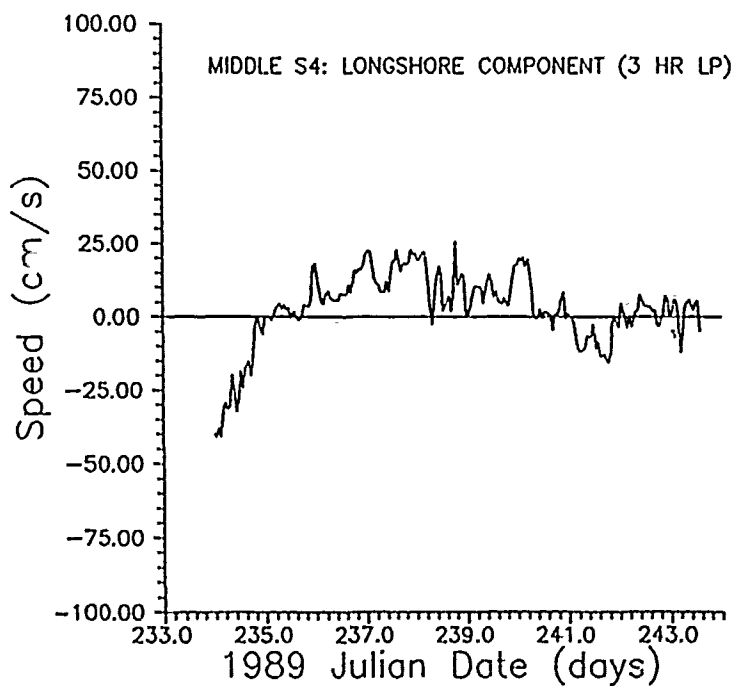


b. Longshore current.

Figure 2.22. Three-hour low-pass filtered time series current components recorded by the top current meter.

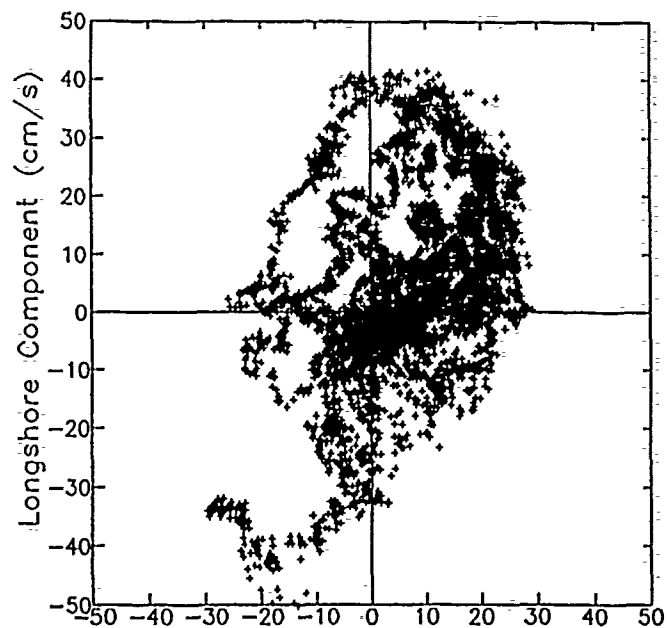


a. Cross-shore current.

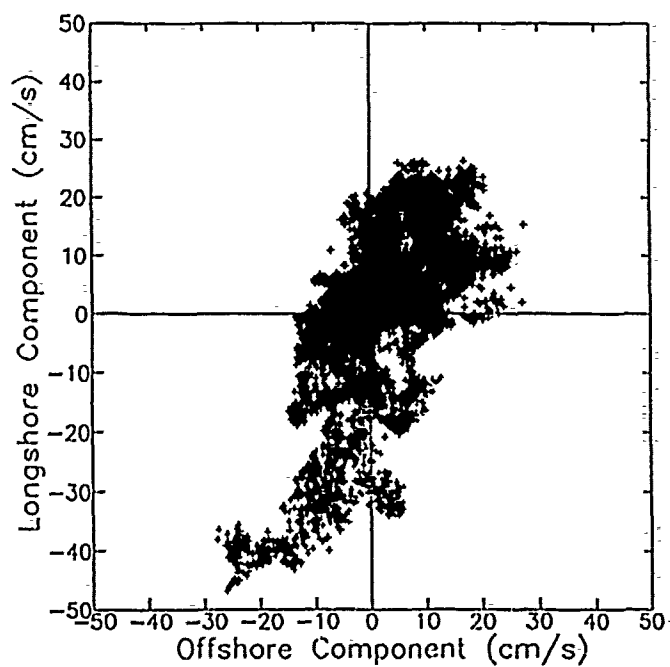


b. Longshore current.

Figure 2.23. Three-hour low-pass filtered time series of current components recorded by the middle current meter.

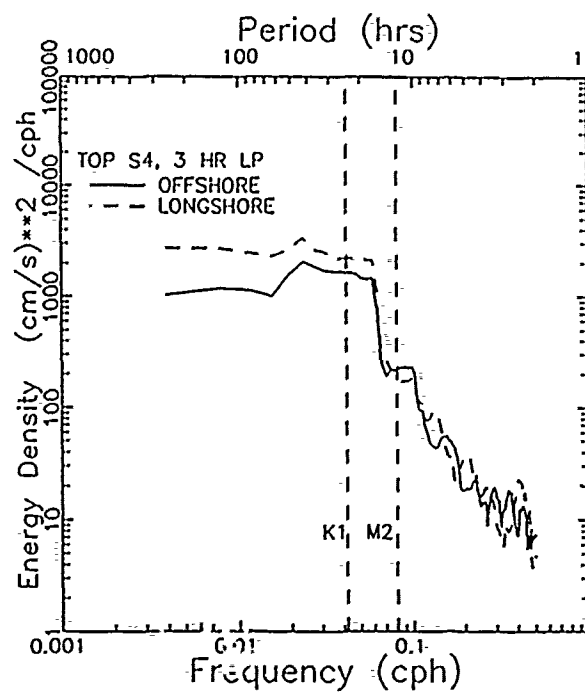


a. Top current meter.

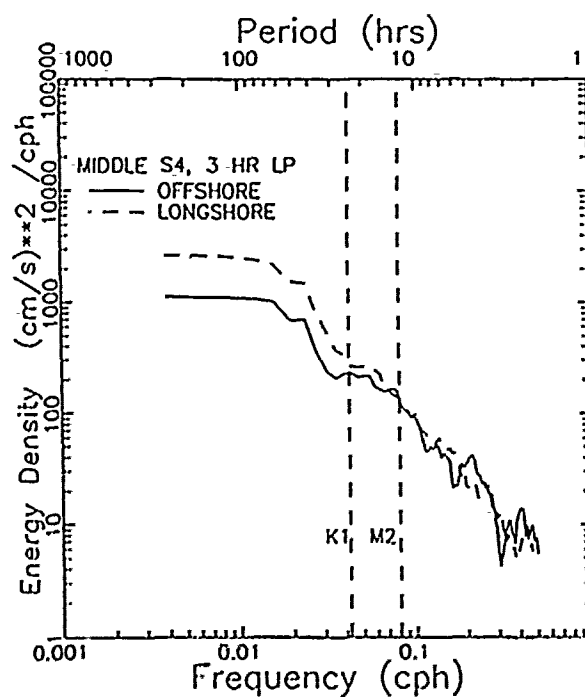


b. Middle current meter.

Figure 2.24. Scattergrams of unfiltered cross-shore versus longshore current components.

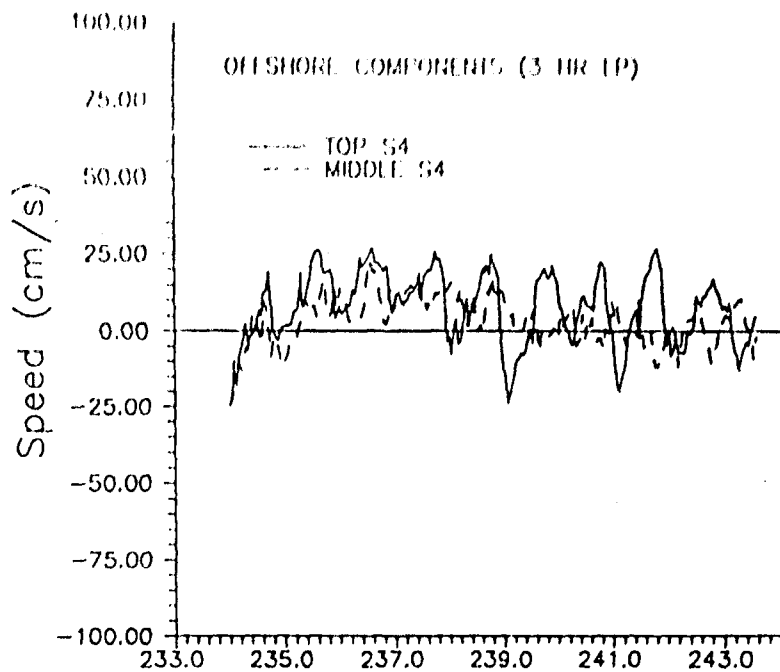


a. Top current meter.

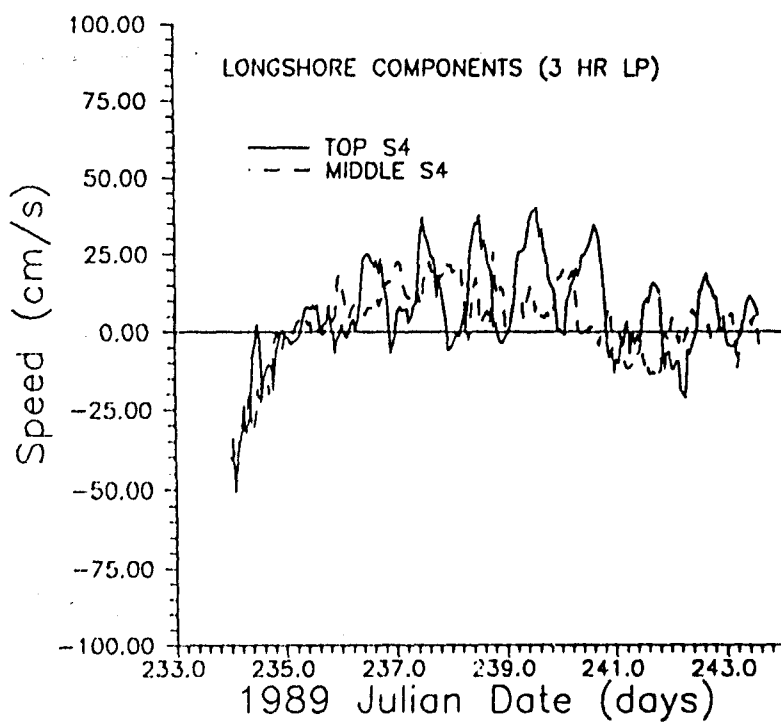


b. Middle current meter.

Figure 2.25. Auto-spectra of the cross-shore and longshore (positive eastward) current components.

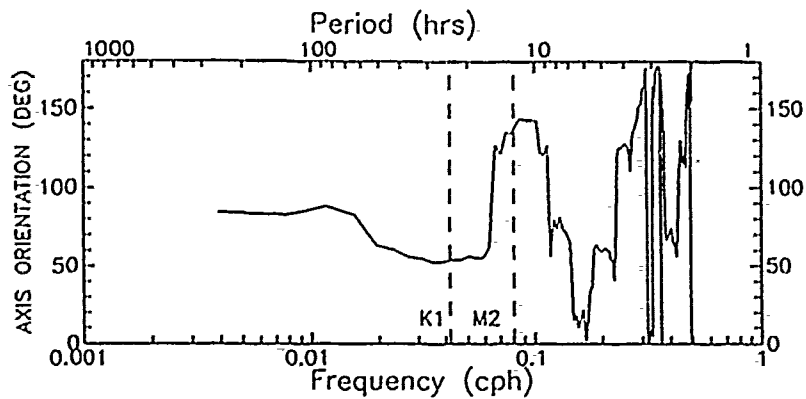


a. Top current meter.

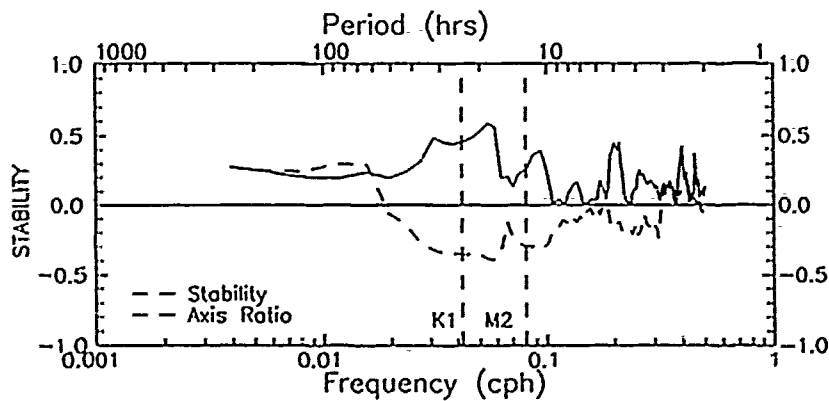


b. Middle current meter.

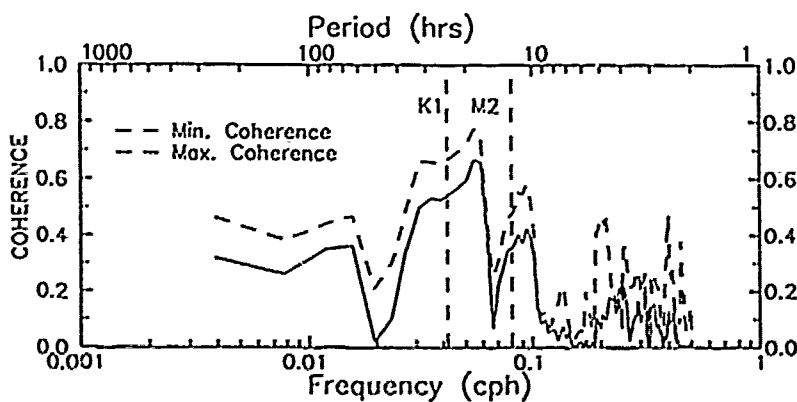
Figure 2.26. Superimposed time series recorded by the top and middle current meters.



a. Semimajor elliptical axis orientation as a function of frequency.

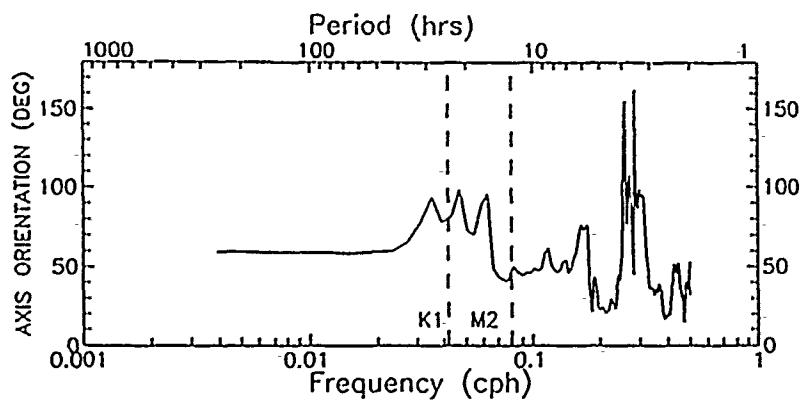


b. Stability (relative directionality) of the elliptical motion and ratio of minor to major axes ranging from (0) rectilinear to (1) circular motion.

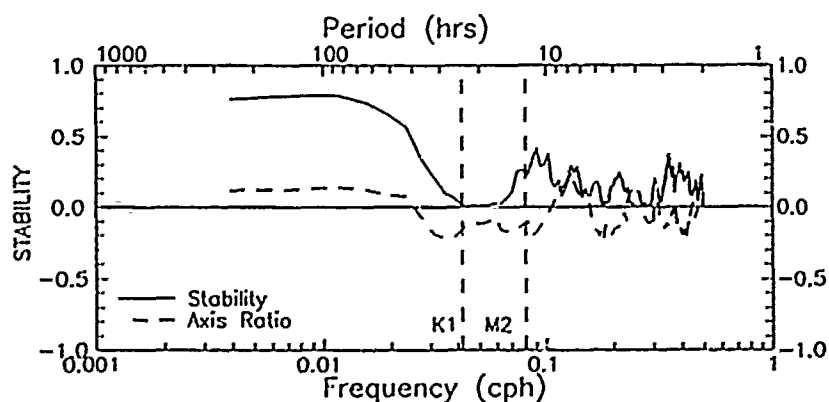


c. Maximum and minimum coherences of the rotary motion.

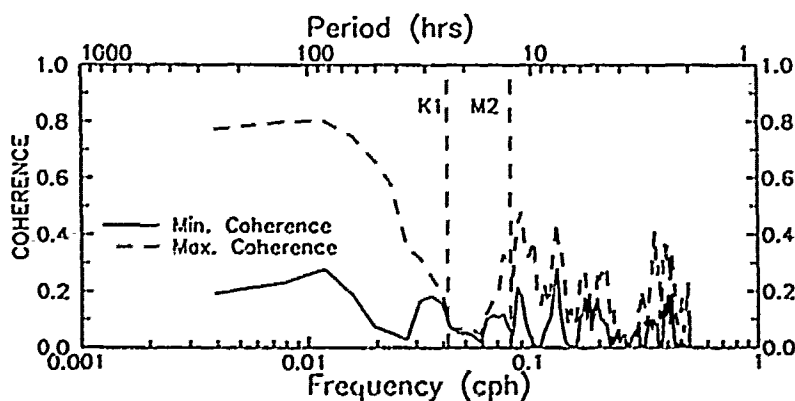
Figure 2.27. Rotary spectral characteristics for the top current meter.



a. Semimajor elliptical axis orientation as a function of frequency.



b. Stability (relative directionality) of the elliptical motion and ratio of minor to major axes ranging from (0) rectilinear to (1) circular motion.



c. Maximum and minimum coherences of the rotary motion.

Figure 2.28. Rotary spectral characteristics for the middle current meter.

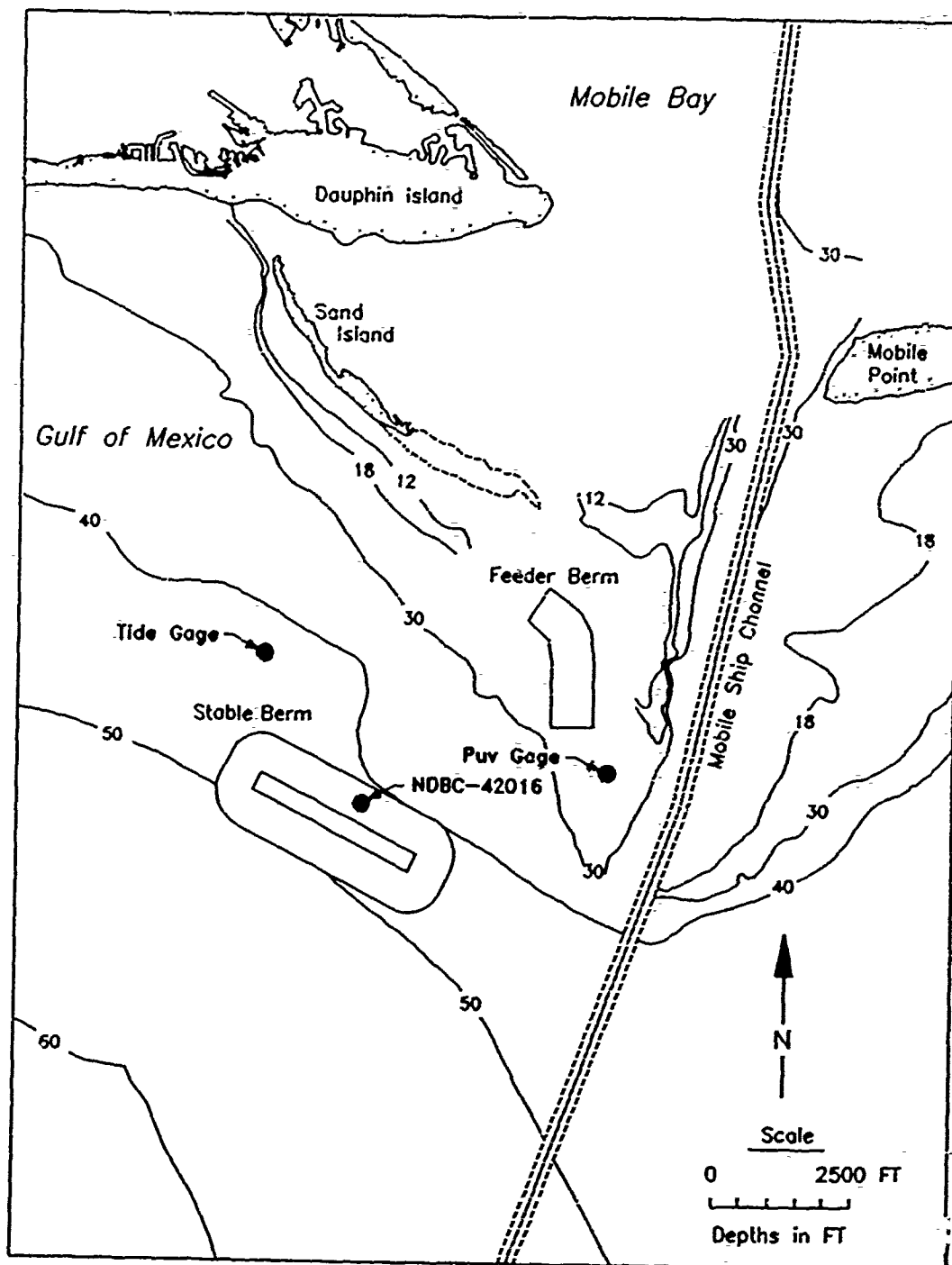


Figure 2.29. Locations of pitch-roll buoy NDBC-42016, tide gage and Puv gage off Mobile Bay.

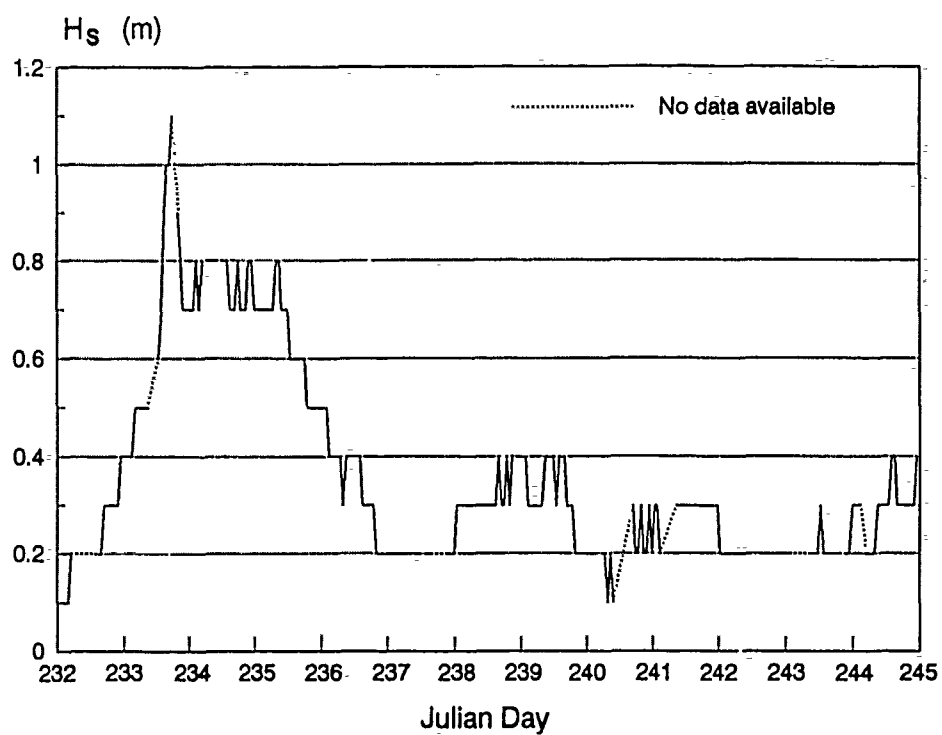


Figure 2.30. Significant wave height.

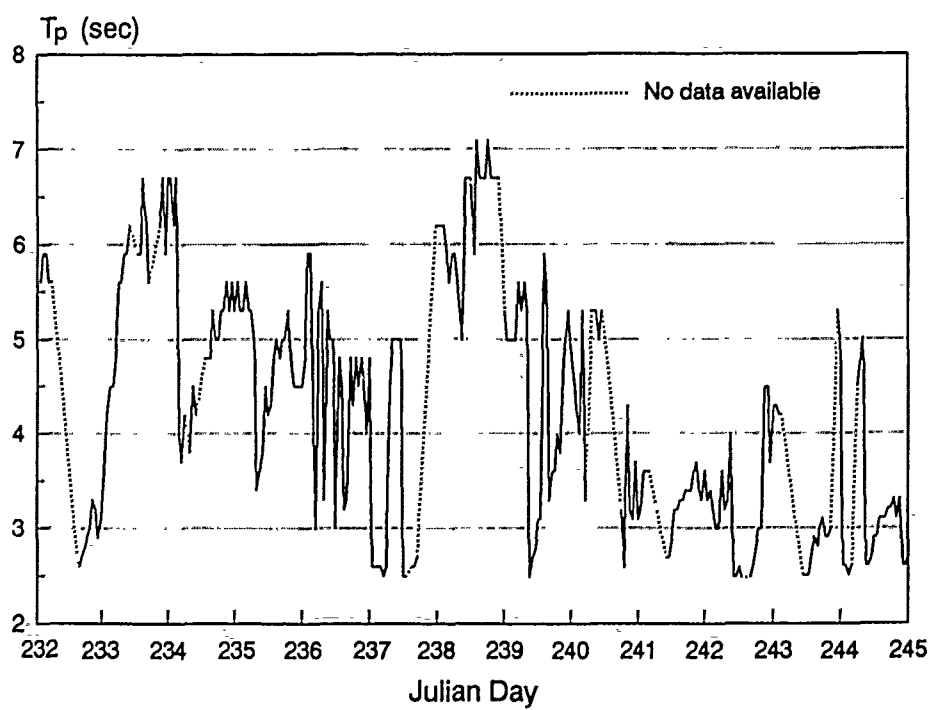


Figure 2.31. Spectral peak wave period.

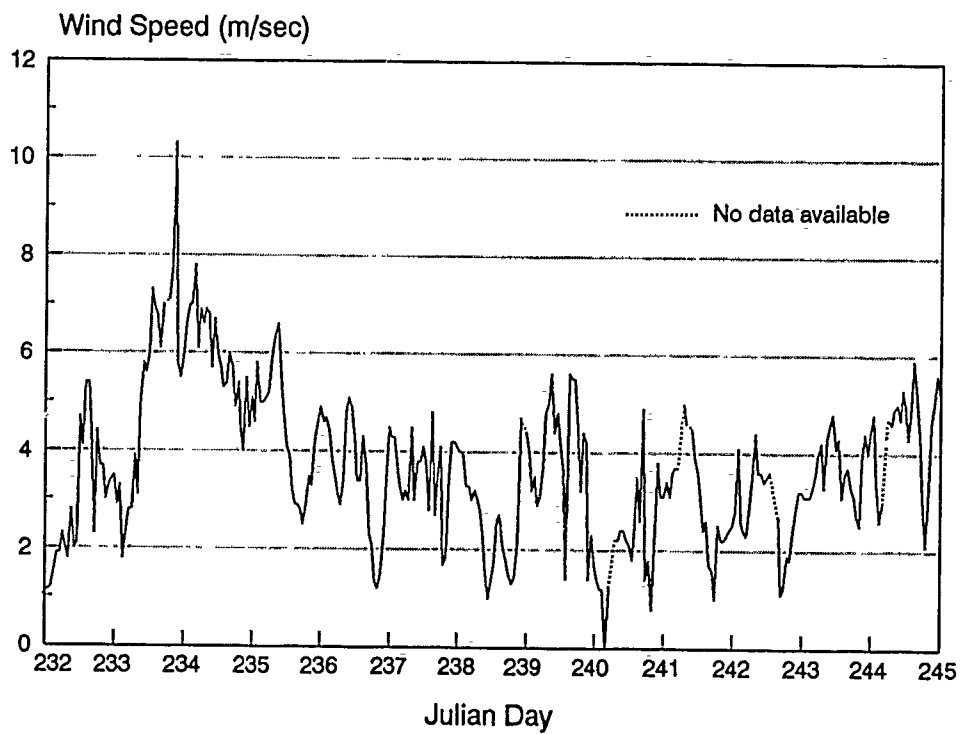


Figure 2.32. Wind speed.

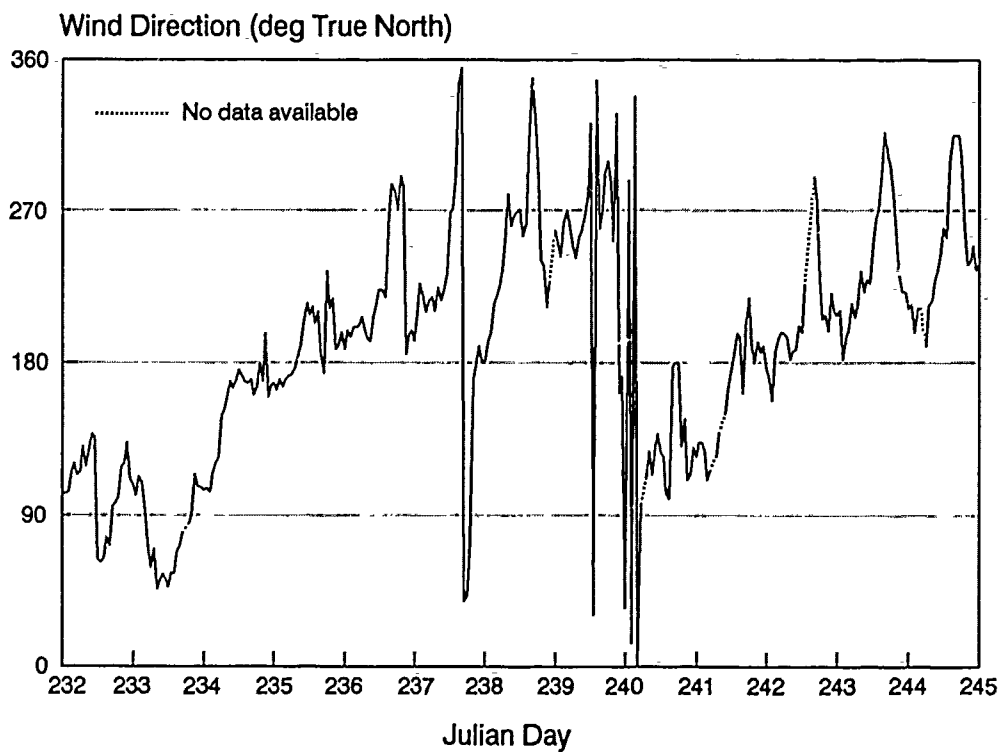


Figure 2.33. Wind direction.

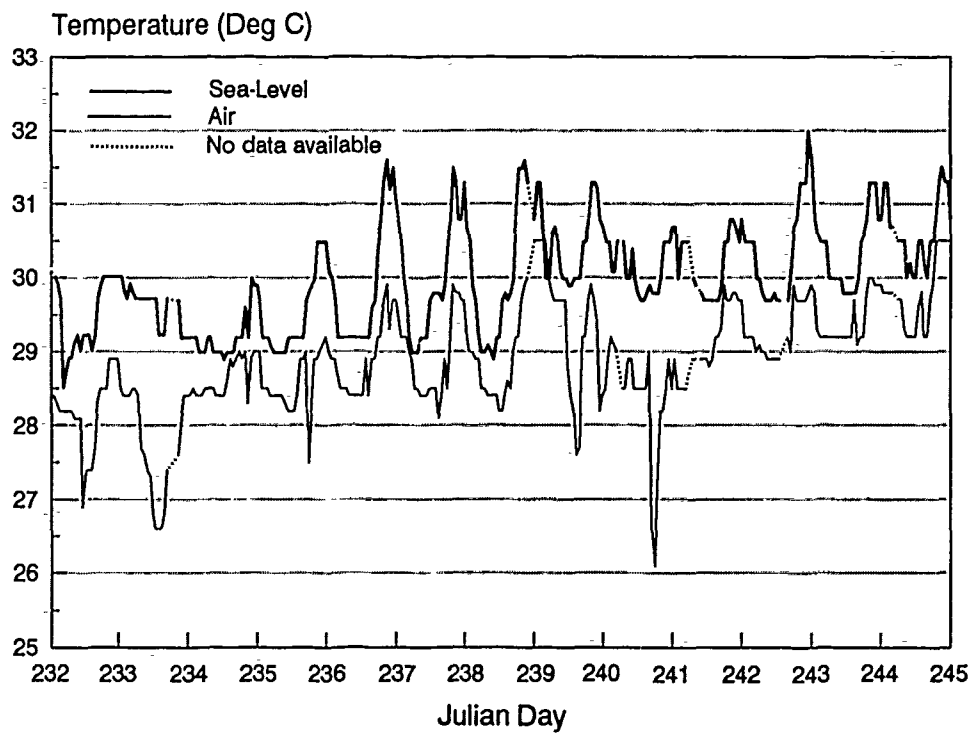


Figure 2.34. Sea level and air temperatures.

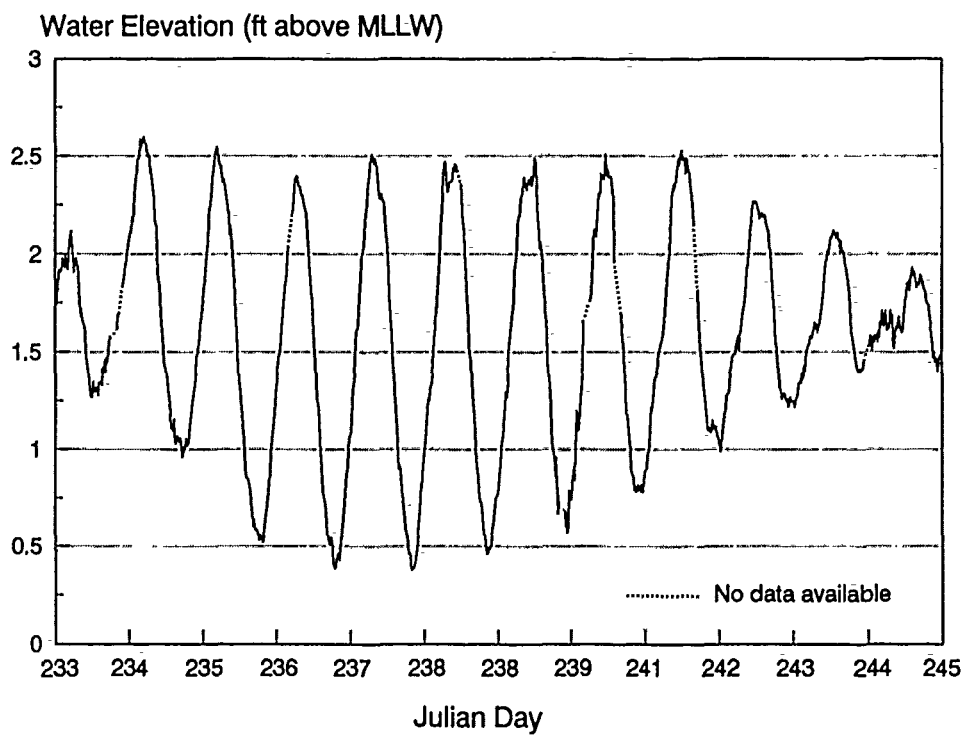


Figure 2.35. Water elevation.

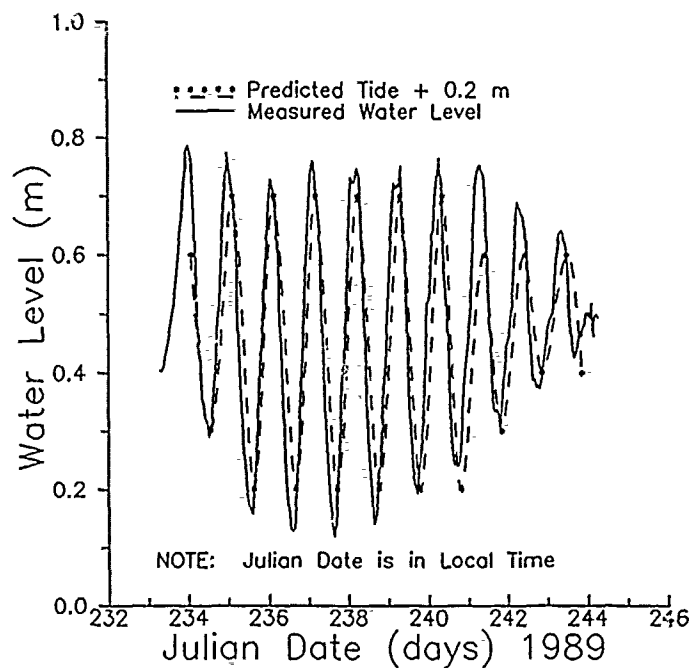


Figure 2.36. Water level measurements converted to meters and smoothed with a 3-hr low-pass convolution filter.

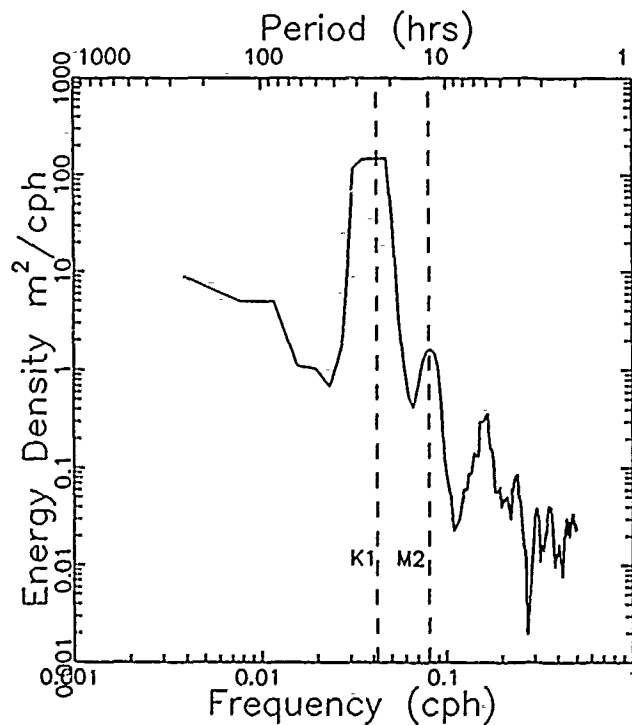


Figure 2.37. Auto-spectrum of measured water levels.

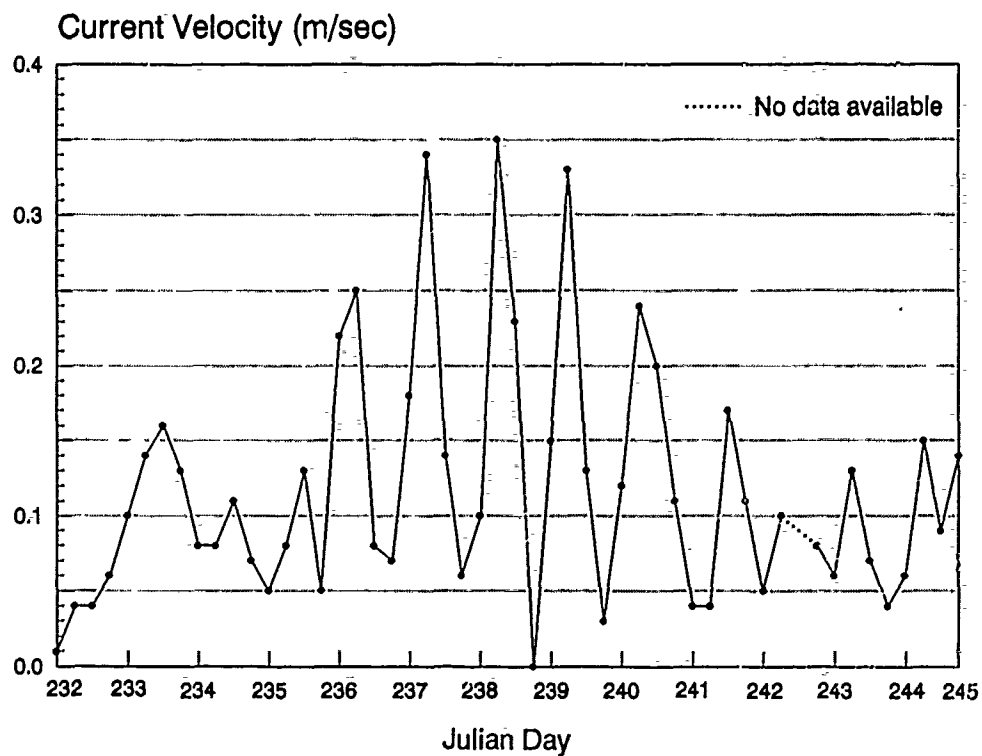


Figure 2.38. Average current velocity.

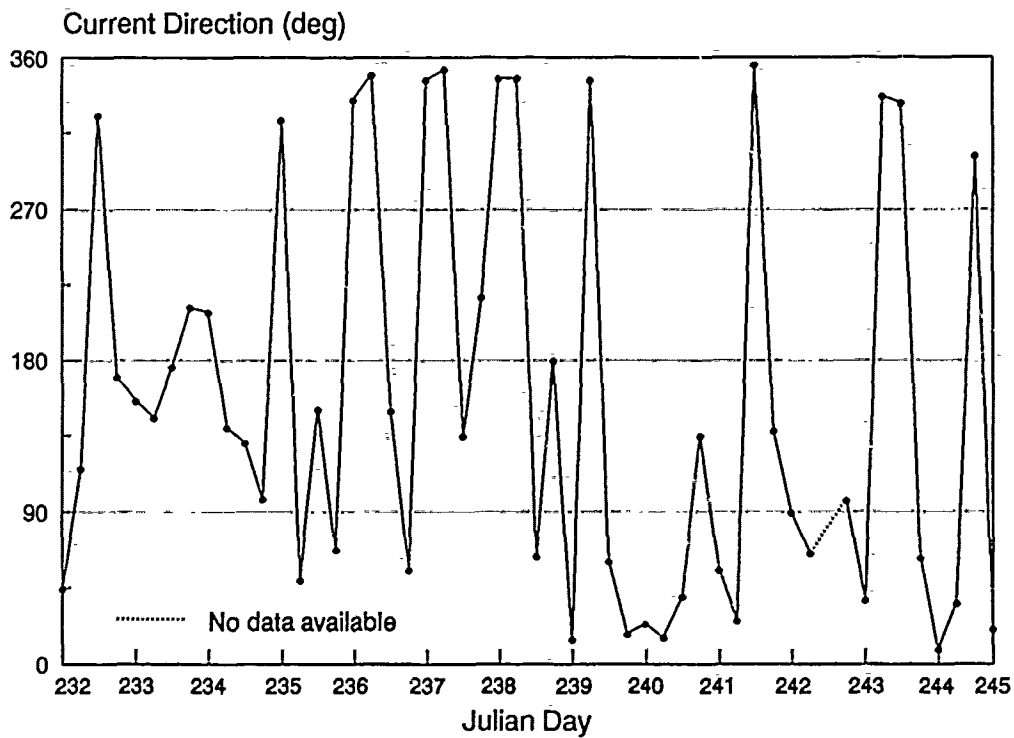
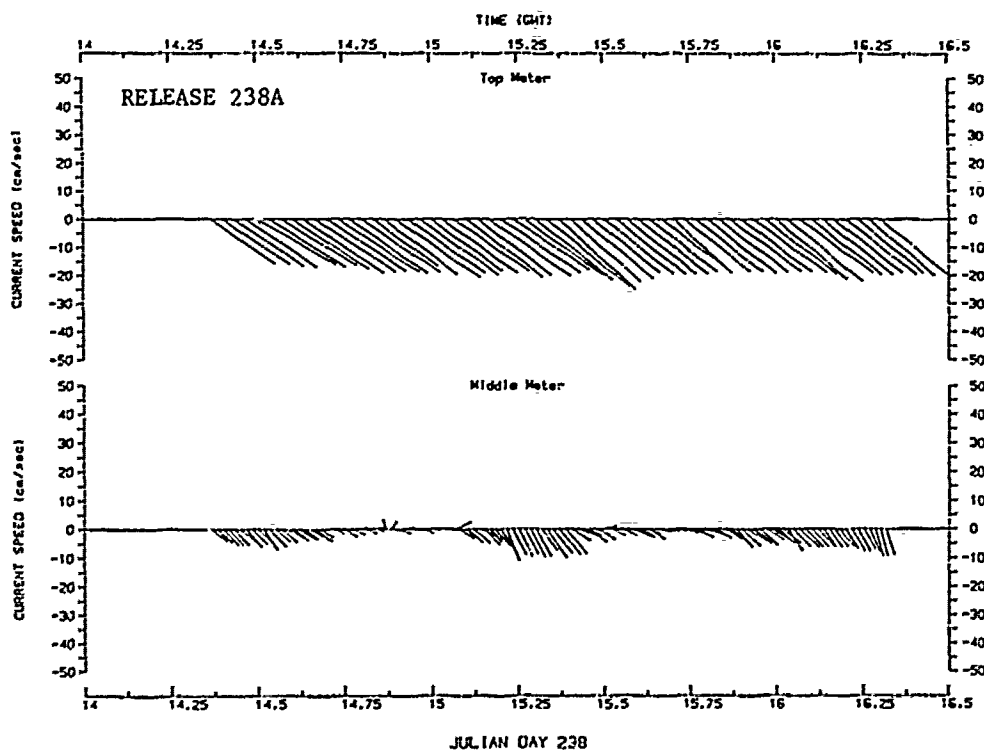
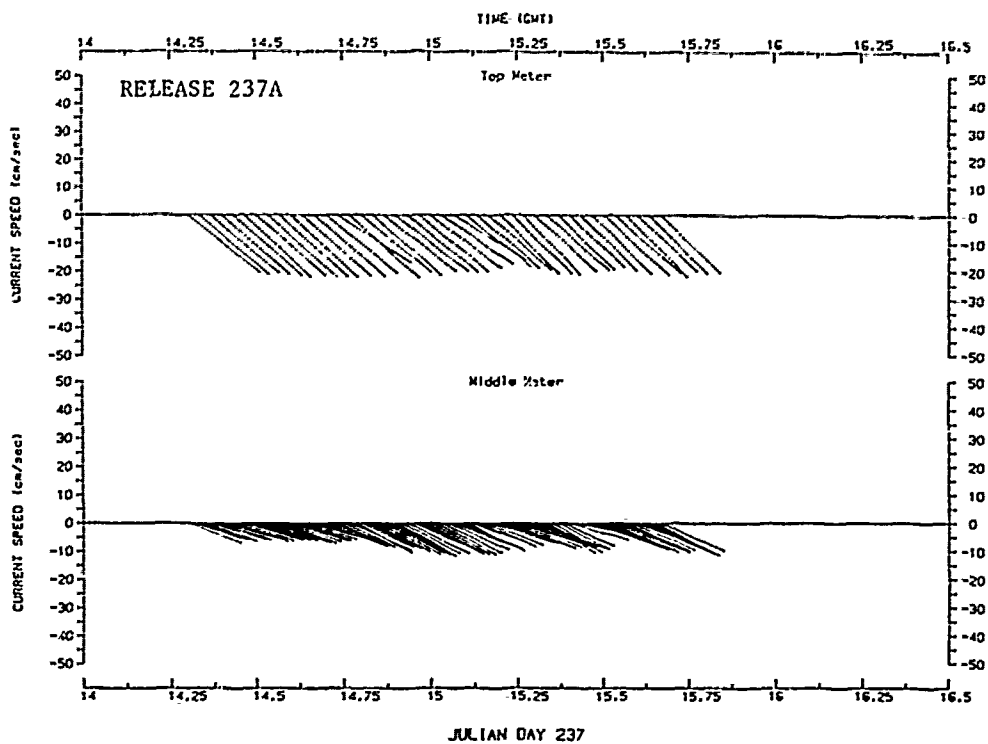
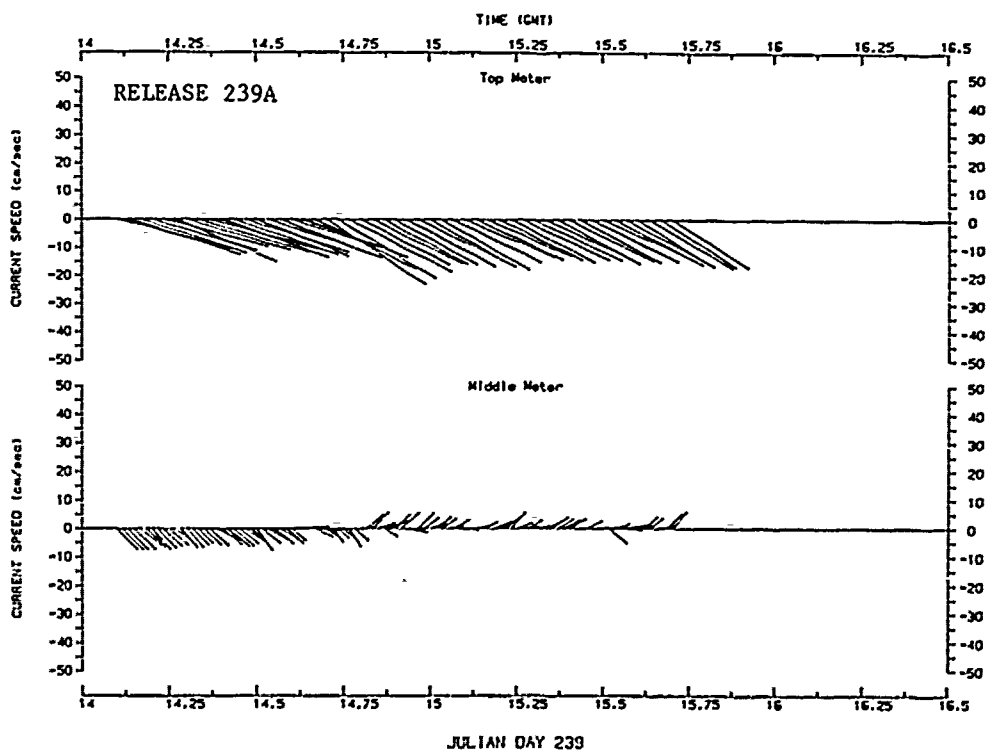
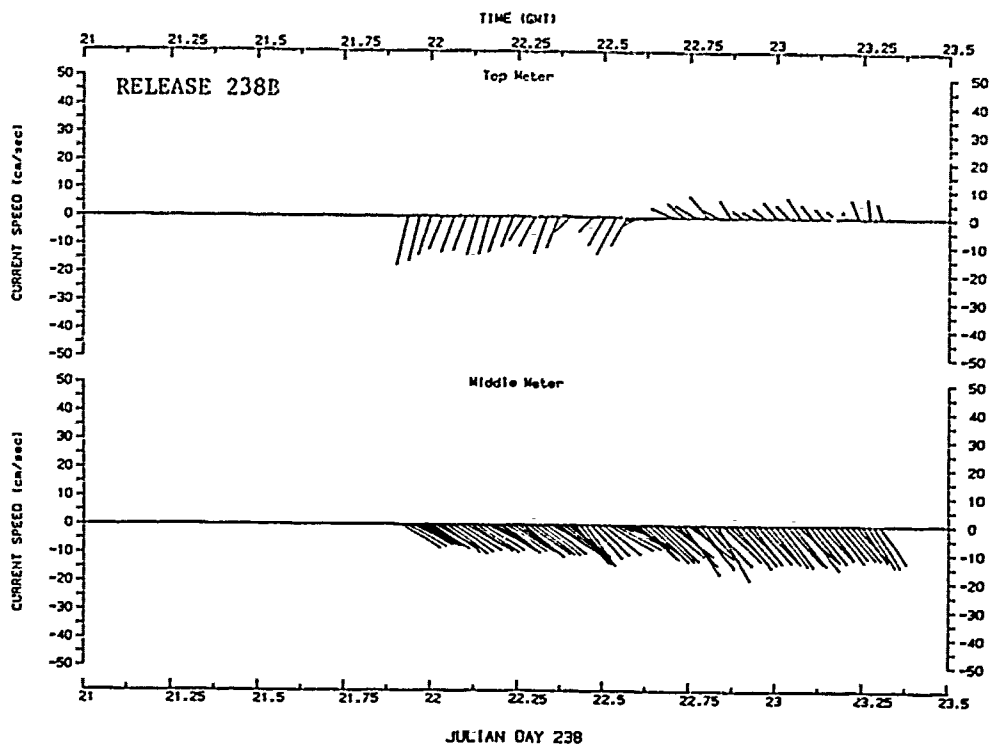
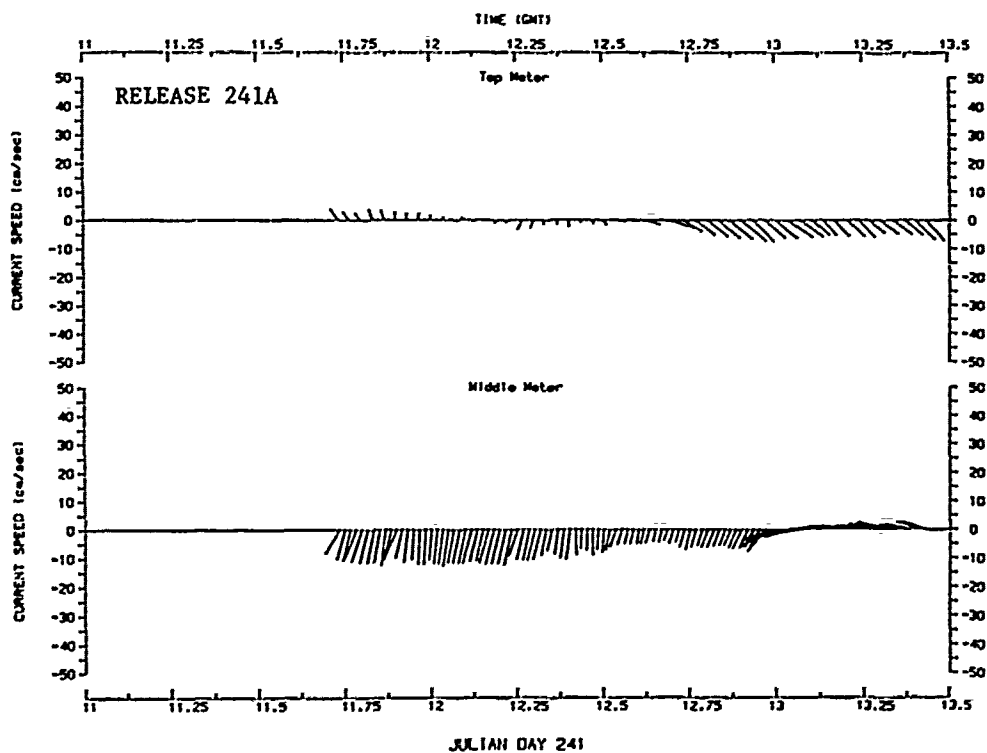
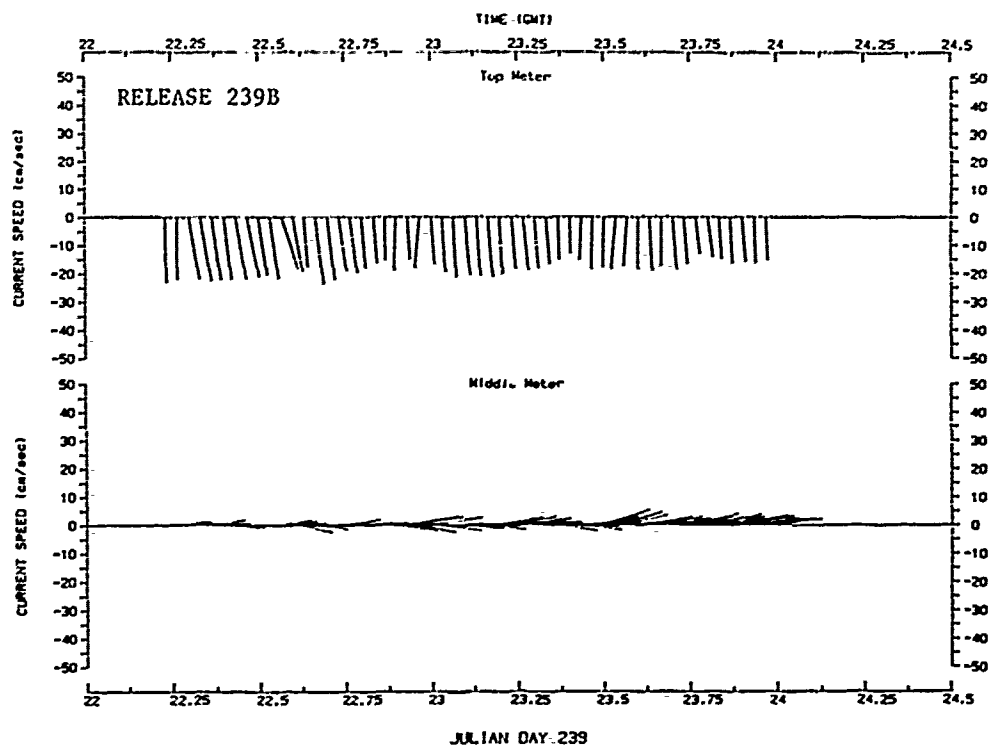


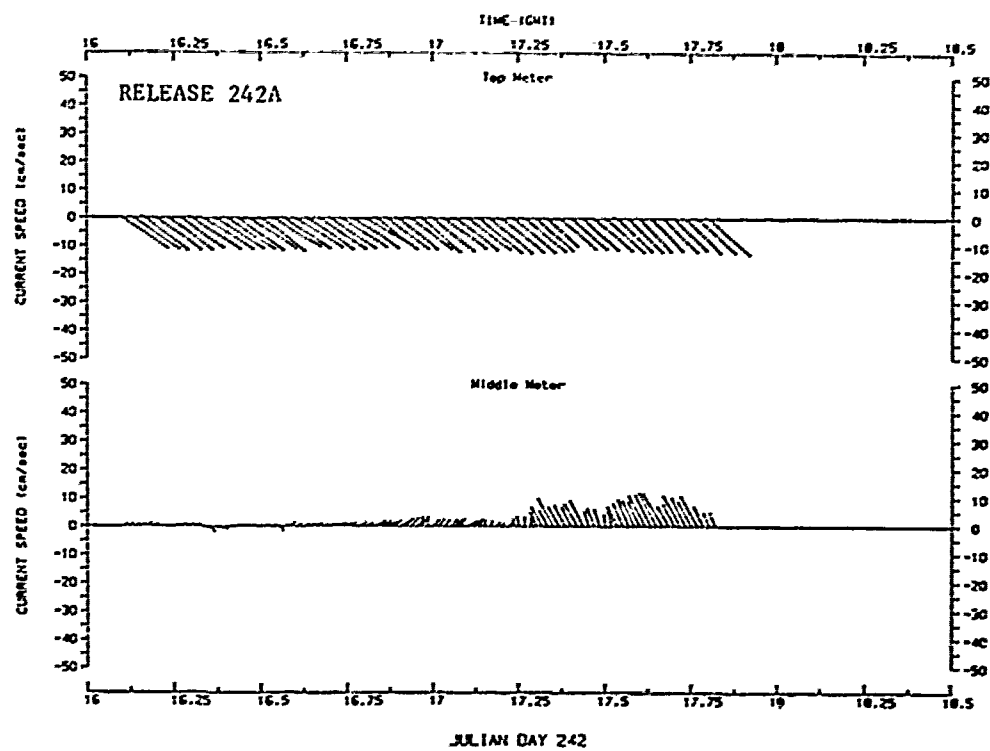
Figure 2.39. Average current direction.

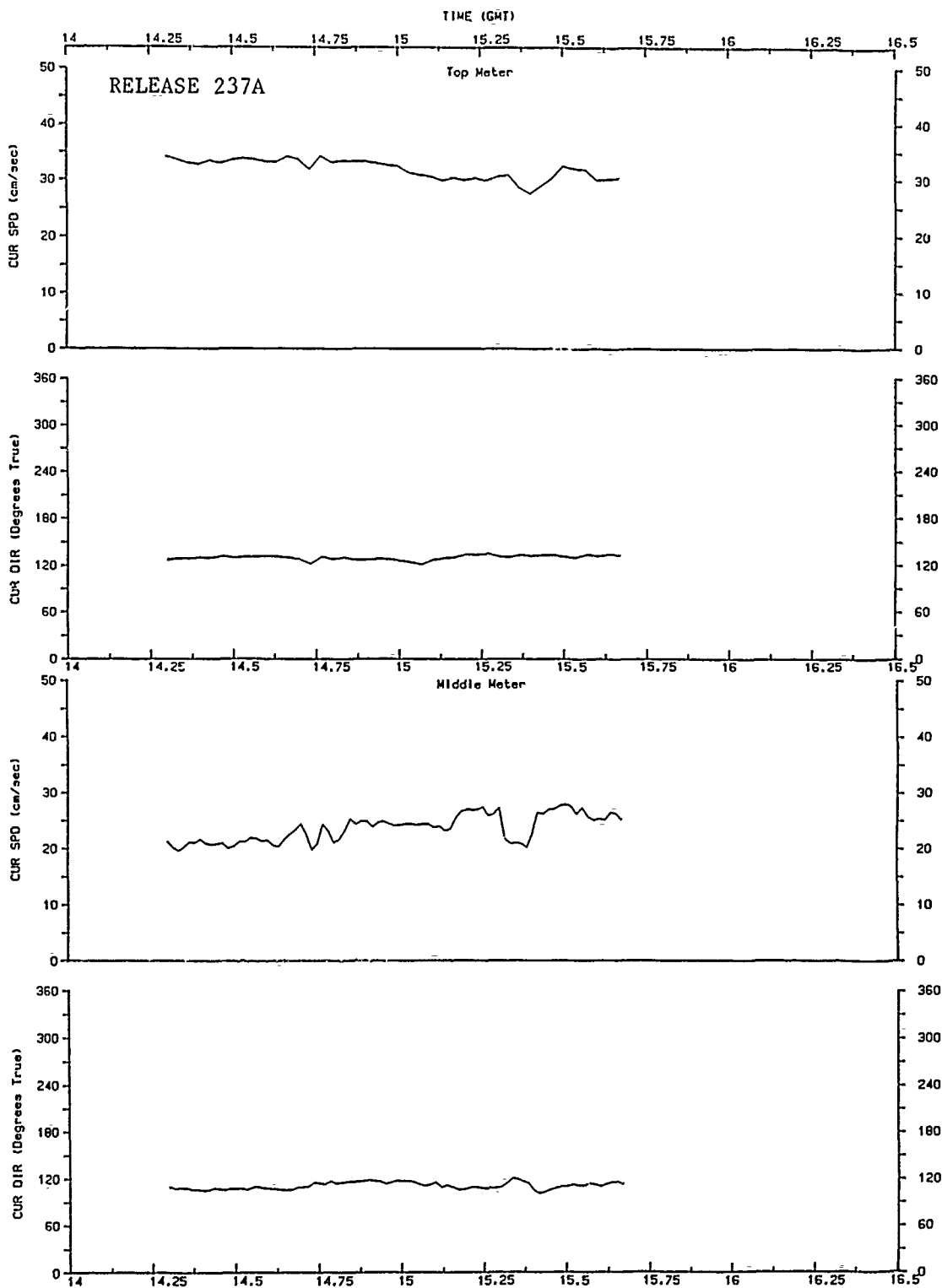
Appendix 2A: Current Vector Plots and Time Histories During Releases

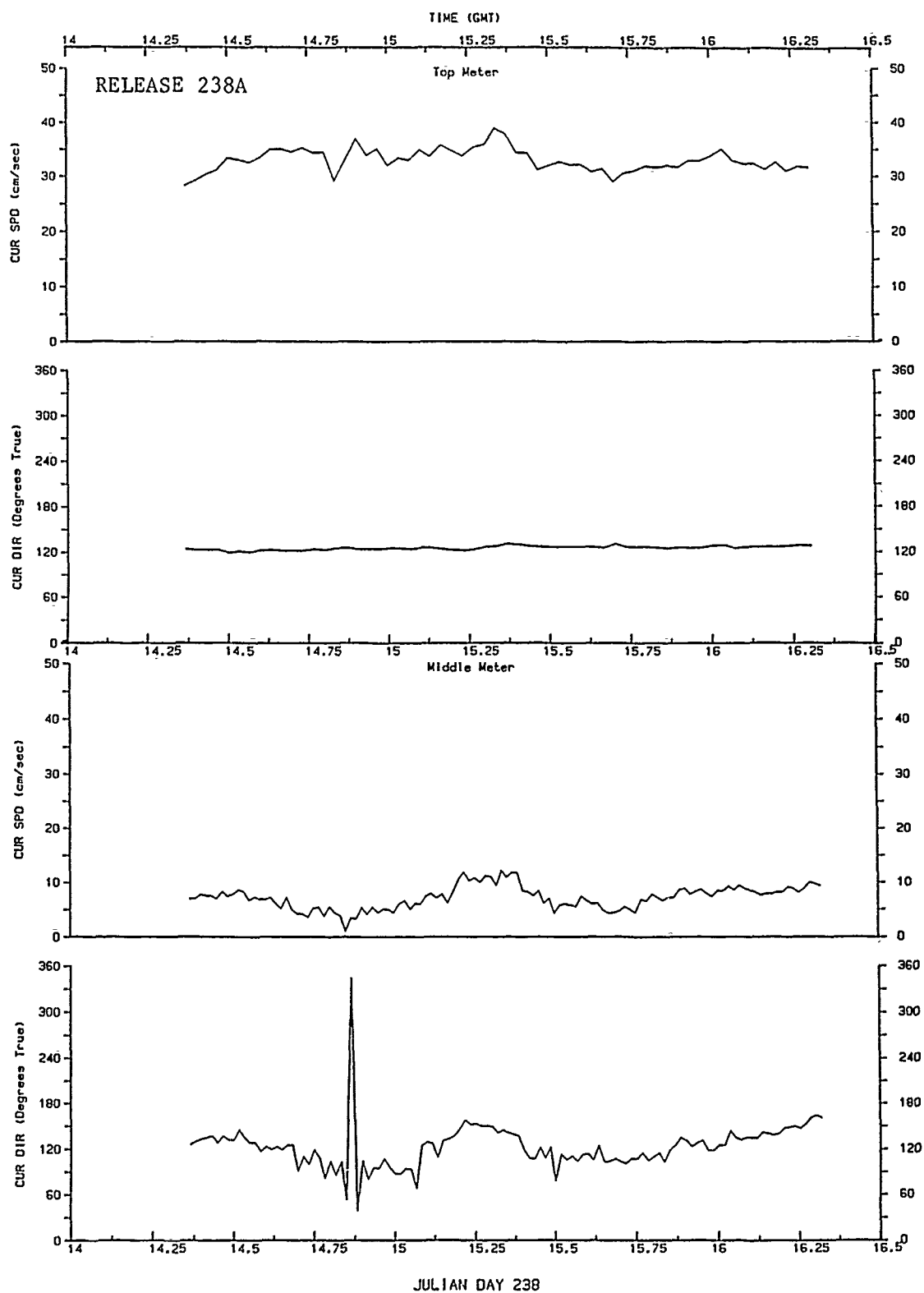


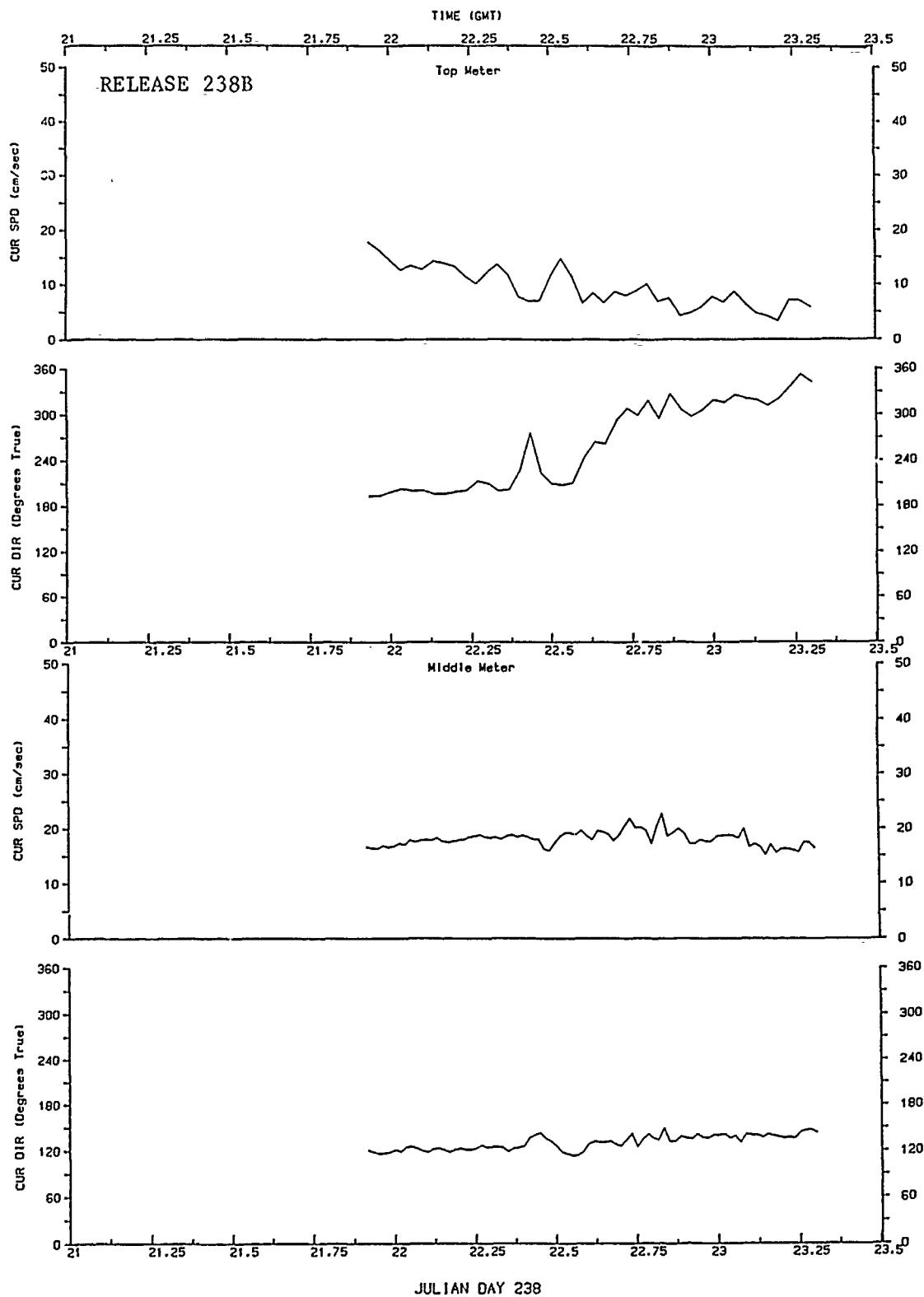


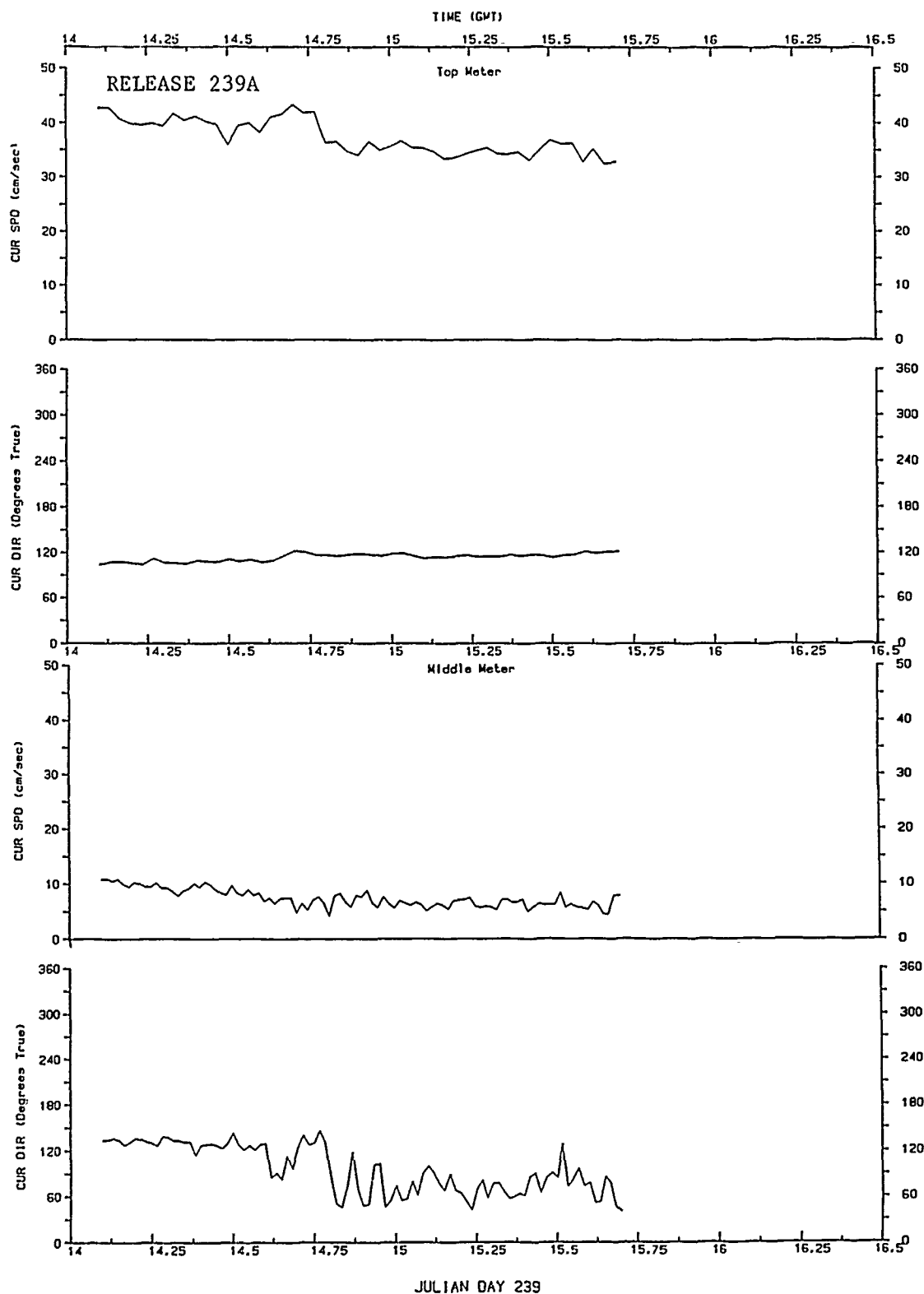


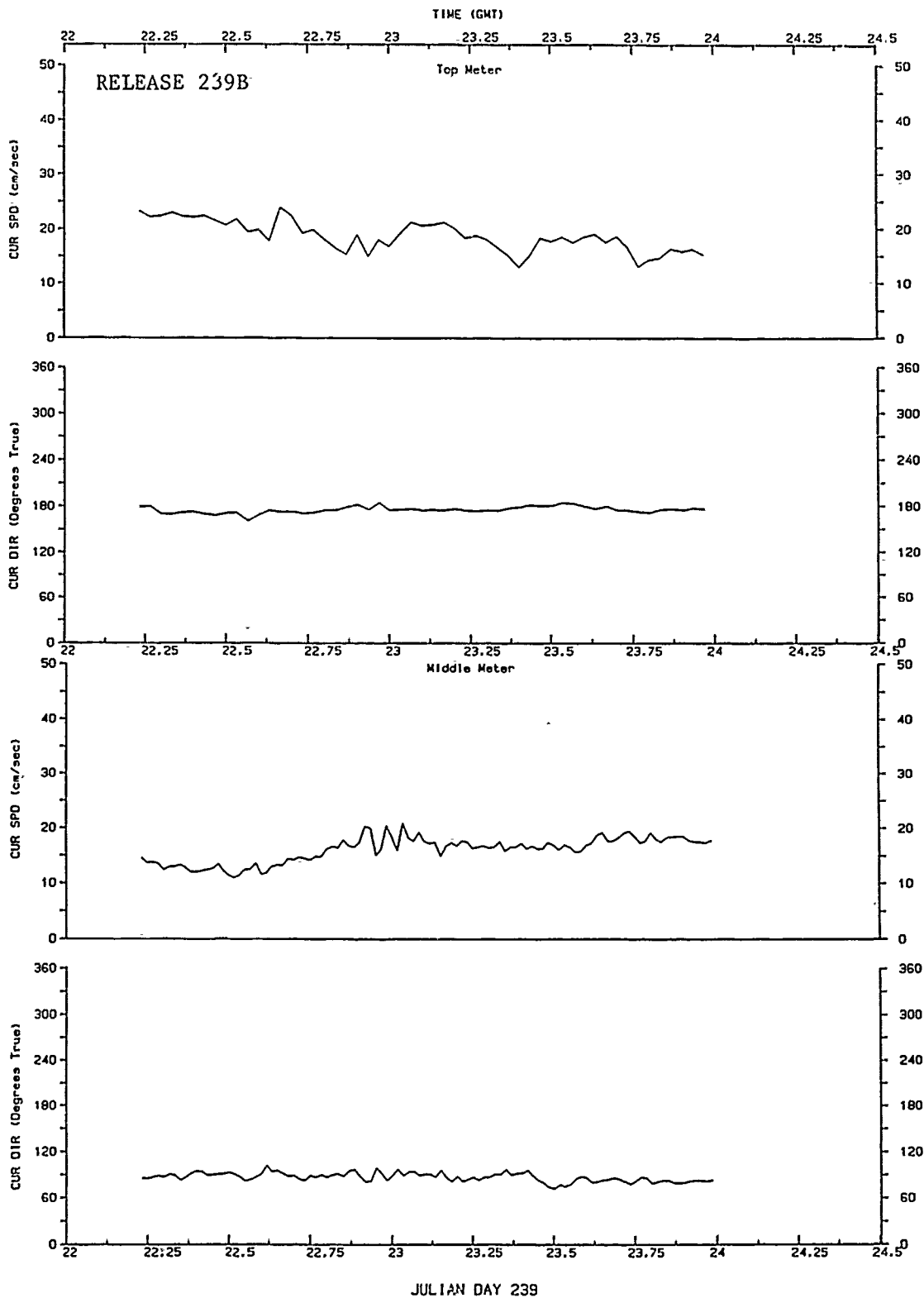


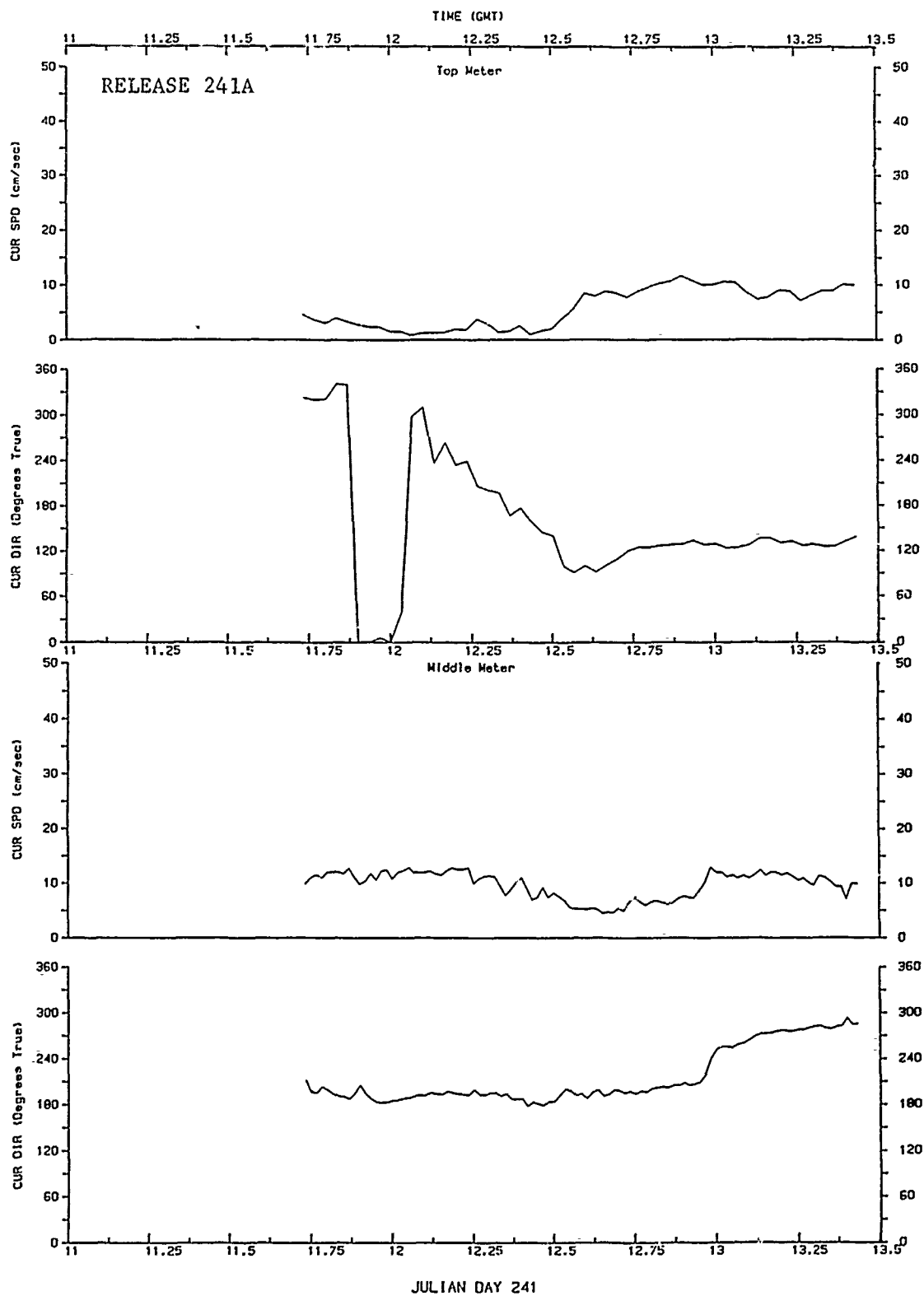


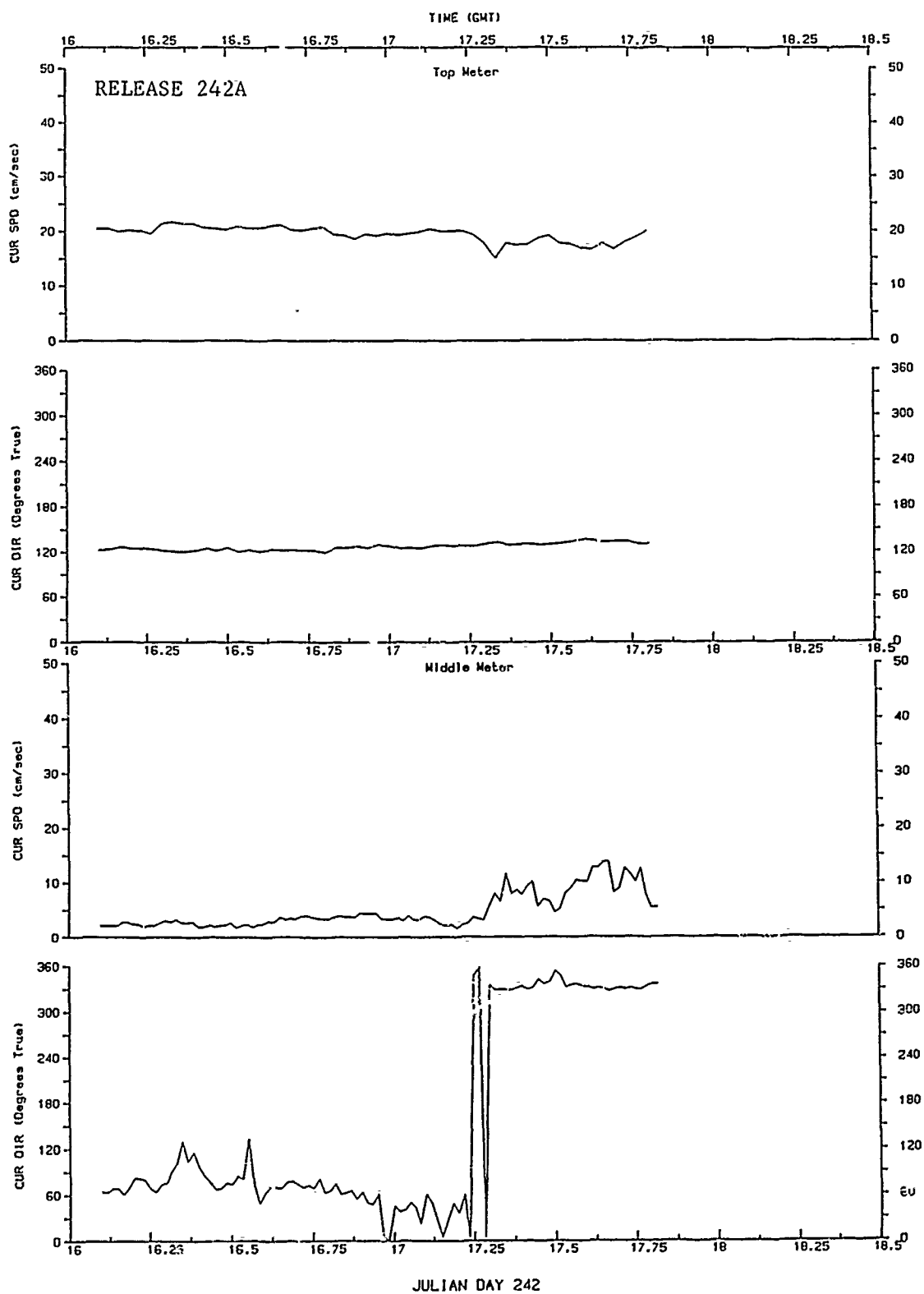












CHAPTER 3
SHIP AND BARGE POSITIONING

CAROL A. COOMES

Evans-Hamilton, Inc.
Seattle, Washington 98103

TERRI L. PRICKETT

Coastal Engineering Research Center
Waterways Experiment Station, Corps of Engineers
Vicksburg, Mississippi 39180-6199

Contents

1. Introduction
2. Ship Positioning During Survey Operations
3. Hopper Barge Tracking During Survey Operations

Aknowledgment

Tables

Figures

1. Introduction

Accurate positioning of the *R/V Pelican* was required to record the track of the ship while surveying dredged material plumes. A Motorola Mini-Range: III microwave positioning system was utilized to obtain the accuracy dictated by the Mobile, Alabama, Dredging Program Field Data Collection Project (MFDCP). In addition, the loaded hopper barge for each survey was tracked by radar before and during survey operations to maneuver the *R/V Pelican* into position near the placement site and to determine the position of the plume at the time of release. Accurate ship and barge positions were also required as basic data for interpreting dredged material behavior by the Acoustic Doppler Current Profiler (Chapter 5) and Acoustic Concentration Profiler (Chapter 6).

2. Ship Positioning During Survey Operations

Introduction

To track dredged material placement operations at Mobile, a continuously recording positioning system with an accuracy of ± 3 m was required. Loran-C, the most common positioning system of vessels, has an accuracy of ± 15 m at best, which did not meet the MFDCP criterion. A Motorola Mini-Ranger III microwave positioning system was therefore installed aboard the *R/V Pelican*, which operates at line-of-site ranges up to 37 km with a range measurement error of ± 1 to 3 m. The positioning system consisted of a range input device, a Mini-Ranger Data Processor (MRDP), and a portable computer. Procedures used to determine the position of both the survey vessel and the hopper barge are described in this chapter.

Procedure

The Mini-Ranger III Positioning System (MRS III) locates the position of a vessel with respect to two known geographical locations (reference points). It operates on the principle of pulse radar, with a radar interrogator (Receiver Transmitter (RT)) located on the vessel and a radar transponder (Reference Station) positioned at each reference site. The reference stations for the study were located at previously established survey sites (Figure 3.1) and were powered from 24-V battery sources.

The system operates at microwave frequencies and requires that line-of-site be maintained between the Reference Stations and the RT. Obstructions, such as offshore drilling rigs, will

interfere with the operation of the system, causing vertical or horizontal multipaths. Vertical multipath is a phenomenon where direct and reflected signals (from the water surface) arrive at the antenna simultaneously and cancel (e.g., reflection from the water surface). This lack of signal results in a "range hole." The overall effects of horizontal multipath are "range jumps" or "unstable readings" that result from signal cancellation when direct signals and reflections from buildings, ships, bridges, or oil tanks arrive at the antenna at the same time.

The MRS III was located in the instrument room/electronics lab of the *R/V Pelican*. The RT unit was located on an antenna directly above the electronics lab. The MRDP gathered positioning information in the form of ranges to the two known reference points, and, from those range data, computed the position of the *R/V Pelican* in Alabama State Plane Coordinates (ASPC).

Data were output to a portable computer that also recorded time in Greenwich Mean Time (GMT). The clocks on the portable computer and MRDP were set to the time generator on National Oceanographic and Atmospheric Administration data collection equipment on board the *R/V Pelican*.

The position fixing rate for the MRDP was set to 2 sec. The system provided error messages to aid in elimination of operational problems when they occurred. When problems were encountered (e.g., when the ship was within a range hole or the system received microwave interference from drilling rigs in the vicinity), the system often quickly corrected itself. When necessary, pressing the reset control on the MRDP and restarting the Execute mode usually brought the system back on-line. When both of these methods failed, a call was made to the operator of the shore-based reference stations to try to correct the problem.

The data were recorded to the portable computer in the following format: time (HR:MIN:SEC), position east (x-value), position north (y-value), and error messages. Possible errors and their explanations are:

1. LOOP - The positioning system uses tracking loop filters to refine the position calculation data. This message indicates that the system has been unable to maintain the tracking loop within limits. This may be due to inadequate range data because of inadequate power to the reference stations or failure because line-of-sight has not been maintained. The latter may include significant obstructions such as land masses or buildings that will interfere with the operation of the system. Failure to maintain adequate geometry in the work areas may also cause loop errors. The positional accuracy of the computation is dependent upon the angle of intersection of the range lines that should be maintained between 30 and 150 deg, 90 deg being the best.

2. RS - RIGHT SITE - This message indicates that the system is not receiving adequate range data from the site selected as the right site, the reference station near Fort Gaines on the tip of Dauphin Island (Figure 3.1).
3. LS - LEFT SITE - This message is the same as RS, but applies to the left site (Figure 3.1).

When an error occurred, the position data were printed in the Range-Range form instead of ASPC. When the system first entered the Run mode, it was normal to have a loop error message printed. This message indicated that the filter was acquiring the position.

The range was recorded incorrectly several times, although no error message was received. In these cases the ranges were offset by a specific amount, and a correction factor was applied at the time of editing. The most probable cause for the offset was an interference or signal bounce from rig or oil structures in the vicinity of operation. All corrected ranges were compared with bridge readings of latitude and longitude to ensure the correct position was obtained. Check readings of the Mini-Ranger at Exxon Well MO-868-1 during the course of the surveyed dredged material placement showed that the positioning system did not drift significantly during the course of the experiment.

The data files for eight surveys (237A, 238A, 238B, 239A, 239B, 241A, 242A, and 243A) and the shallow-water berm survey were edited in the following manner. The data corresponding to the time interval of 10 min prior to a release until the end of the observation for each survey were extracted from the raw data files. The extracted files were then run through a computer program to strip them of several columns of trailing zeros and comments to produce data files containing only time, Easting coordinate, and Northing coordinate in ASPC. Each file was plotted and inspected for obvious spurious points, which were then deleted. Several files showed parts of the cruise tracks to be offset from the rest of the track. The difference was calculated and applied to the offset portion.

Results

Figures 3.2 to 3.9 show the pattern of the cruise tracks for the surveys of dredged material plumes, and Figure 3.9b gives the cruise track for the shallow-water berm survey. Table 3.1 provides the times and general comments concerning each survey. Table 3.2 is a sample of the edited data file for Survey 237A.

The survey cruise tracks in Figures 3.2 to 3.9 are labeled with three specific time events: a start time denoting the ship orientation 10 min prior to the release, a dredged material release time, and an end time denoting the conclusion of all observations for the release. Tick marks on the cruise tracks indicate 15-min intervals during each survey, and arrows show the direction the *R/V Pelican* took while sampling. In addition, specific portions of five cruise tracks (238A, 238B, 239B, 241A, and 242A) have been enlarged for a clearer picture of the ship's direction during the survey. As outlined in Table 3.1, the first five surveys occurred while observing releases made at the deepwater placement site. The following three surveys were made at the shallow-water site. The survey track over the shallow-water berm followed a zig-zag pattern of 10 transects (Figure 3.10).

The Mini-Ranger malfunctioned, losing transmission on one or both of the ranges, during two surveys. Transmission was lost at the start of Survey 241A during the interval 11:35-12:07. Latitude/longitude readings recorded on the bridge as backup during this time interval were converted to ASPC and added to the Mini-Ranger file. Because the bridge readings were recorded approximately every 2 min compared with every 2 sec on the Mini-Ranger, the cruise track for this starting interval appears angular. Transmission on the Mini-Ranger failed during the entire observation for Survey 243A. Therefore, the data file and cruise track consist of converted latitude/longitude readings recorded from the bridge.

3. Hopper Barge Tracking During Survey Operations

To maneuver the *R/V Pelican* in position to commence survey operations, each hopper barge was tracked as it approached the placement site. This tracking was done by obtaining periodic fixes (distance and direction) on the barge in relation to the concurrent position of the *R/V Pelican*. Also, by tracking the barge, the exact position of the plume at the time of the release was obtained. The barge was tracked for approximately 30 min prior to the release at approximately 5-min intervals. While a release occurred, the barge position was recorded approximately every 2 min. Following the release, tracking continued in 5-min intervals for approximately 30 min. The Motorola Mini-Ranger System III tracking system described previously was used to determine the precise location of the *R/V Pelican* during monitoring operations.

Onboard instruments were used to determine the barge's position during the monitoring period. These instruments were a radar system to obtain range and bearing of the barge, a gyro-compass

to reference the heading of the ship with respect to True North, and a Loran-C navigational system to determine the latitude and longitude of the *R/V Pelican*. Loran-C coordinates were used together with the range and bearing to plot the barge track during operations and to provide a backup of the Mini-Ranger system for determining the *R/V Pelican*'s position. The Loran-C system has an estimated accuracy of ± 100 m.

In the tracking procedure, which required two people, the barge was sighted on radar, and the radar range and bearing from the bow of the ship to the barge were noted. The tug *Paul Candies* is a 140-ft vessel with a 300-ft tow line connected to a hopper barge, which is approximately 250 ft long. At great distances, the tug and barge were relatively easy to identify on radar because of their configuration. All fixes were made relative to the position of the barge. The barge ranges recorded varied between 0.02 to 3.4 nautical miles. Simultaneously, a heading of the ship in relation to True North was obtained together with latitudes and longitudes of the position of the *R/V Pelican* from Loran-C. The bearing of the barge was added to the heading of the *R/V Pelican* to calculate the barge heading relative to True North.

After the cruise, the positions of the barge were calculated from Mini-Ranger data for the nine target surveys. The Easting or x-coordinate of the barge was obtained by using the equation,

$$X_b = X_p + R \sin \theta \quad (3.1)$$

where

X_b = Easting coordinate of the barge, ft

X_p = Easting coordinate of the *R/V Pelican*, ft

R = Range from the ship to the barge, ft

θ = Barge angle with respect to True North, deg

The Northing or y-coordinate was obtained by using the equation,

$$Y_b = Y_p + R \cos \theta \quad (3.2)$$

where

Y_b = Northing coordinate of the barge, ft

Y_p = Northing coordinate of the *R/V Pelican*, ft

Table 3.3 contains a summary of barge positions for the 18 dredged material placement surveys approximately 5 to 10 min before and after the release. Release times are indicated with an asterisk. An example of a hopper barge track (Survey 239B) is given in Figure 3.11.

The volume and content of the material in the barge as estimated by the captains of the tug *Paul Candies* were obtained during tracking operations for background information relative to the acoustic data and prerelease and postrelease dredged material samples, and are summarized in Table 3.4. The number of the barge and its prerelease draft were observed as the barge came into view to obtain a visual record of the approximate volume and distribution of material within the barge. Because of uneven distributions of material in the barges, the draft sometimes varied as much as 1 ft from bow to stern.

Acknowledgment

T. L. Prickett acknowledges Mr. Douglas Evans, Evans-Hamilton, Inc., for his guidance in the navigation and tracking tasks.

Table 3.1
Mini-Ranger Information for Nine Surveys

<u>Survey No.</u>	<u>Start GMT</u>	<u>Time Release GMT</u>	<u>End GMT</u>	<u>Comments</u>
237A	14:08:00	14:18:00	15:40:00	Longitudinal transects through deepwater release.
238A	14:12:01	14:22:01	16:18:59	Transverse and far-field transects through deepwater release.
238B	21:45:00	21:55:00	23:17:58	Five transverse transects followed by four longitudinal transects through deepwater release.
239A	13:56:01	14:06:01	15:41:59	Four transverse transects followed by five longitudinal transects through deepwater release.
239B	22:05:06	22:14:00	23:59:58	Seven transverse transects through deepwater release.
241A	11:35:00	11:44:00	13:25:58	Transverse-longitudinal-transverse transect pattern through shallow-water release; mini-ranger malfunction at beginning of cruise track.
242A	15:59:04	16:06:00	17:48:58	Six longitudinal transects and one transverse transect through shallow-water release.
243A	17:53:00	18:03:00	18:58:00	Six transverse transects through shallow-water release. Mini-ranger malfunction throughout entire cruise track.
Shallow-water berm	18:24:02	--	20:59:16	Ten transects forming a zig-zag pattern across berm.

Table 3.2

Sample of Edited Mini-Ranger Data File for Cruise Track 237A

<u>Time</u> <u>GMT</u>	<u>Easting</u> <u>ft</u>	<u>Northing</u> <u>ft</u>
14:08:00	304191	55426
14:08:02	304194	55425
14:08:04	304192	55426
14:08:06	304195	55428
14:08:08	304192	55430
14:08:10	304191	55432
14:08:12	304192	55435
14:08:14	304189	55439
14:08:16	304186	55443
14:08:18	304185	55447
14:08:20	304184	55450
14:08:22	304183	55455
14:08:24	304179	55461
14:08:26	304174	55468
14:08:28	304171	55474
14:08:30	304167	55479
14:08:32	304166	55485
14:08:34	304161	55492
14:08:36	304157	55500
14:08:38	304156	55506
14:08:40	304151	55514
14:08:42	304146	55521
14:08:44	304143	55526
14:08:46	304144	55531
14:08:48	304145	55536
14:08:50	304138	55544
14:08:52	304134	55550
14:08:54	304130	55555
14:08:56	304130	55559
14:08:58	304128	55563
14:09:00	304124	55567
14:09:02	304122	55570
14:09:04	304119	55574
14:09:06	304117	55577
14:09:08	304112	55582
14:09:10	304110	55586
14:09:12	304107	55590
14:09:14	304105	55594
14:09:16	304103	55597

Table 3.3
Hopper Barge Positions During Surveys

Survey No.	Time of Reading GMT	Barge Position, ASPC, ft	
		Easting	Northing
234A	1854	304751	53105
	*1859	--	--
235A	1654	305269	53310
	1655	305528	53862
	1657	305709	54490
	*1658	--	--
236A	0006	320297	54808
	0013	313318	56884
	*0020	--	--
236B	1445	308038	50916
	1448	307487	51802
	*1450	--	--
	1453	307125	52685
236C	2204	304852	52278
	2206	304088	53886
	*2208	304061	54890
237A	1410	303579	51866
	1413	303573	53079
	1415	303596	54585
	1417	303711	56416
	*1418	--	--
237B	2206	306728	51981
	2212	303611	54561
	*2215	304014	56436
238A	1418	302782	54194
	1420	303002	55170
	*1423	--	--
	1426	303745	56977
	1430	307989	55379

(Continued)

* Barge release time.

(Sheet 1 of 4)

Table 3.3 (Continued)

Survey No.	Time of Reading GMT	Barge Position, ASPC, ft	
		Easting	Northing
238B	2150	304592	54739
	2152	304102	55575
	2154	303557	56441
	*2155	--	--
	2157	303052	58180
	2200	302615	59612
239A	1401	303571	53145
	1403	303526	54228
	1405	303561	54950
	*1406	303658	55650
	1409	304355	57580
239B	2207	305285	52706
	2209	304969	53742
	2210	304813	54440
	2211	304590	55034
	*2213	304570	56071
	2215	304197	57174
	2218	305148	57766
240A	1329	304804	52947
	1331	304359	54278
	1333	303860	55318
	1334	303788	56126
	*1335	--	--
	1339	303987	58594
	1341	306378	57721
	1343	307573	57255
240B	2031	304018	51835
	2033	303386	52934
	2035	303103	54180
	*2036	--	--
	2039	303176	56420
	2041	305665	56234

(Continued)

* Barge release time.

(Sheet 2 of 4)

Table 3.3 (Continued)

Survey No.	Time of Reading GMT	Barge Position, ASPC, ft	
		Easting	Northing
241A	1139	311085	58679
	1141	310266	59015
	1143	309394	59561
	*1144	--	--
	1145	306852	60447
	1149	309266	61351
241B	1840	313161	57263
	1842	312090	57831
	1843	311218	58251
	1845	309921	58631
	*1846	--	--
	1847	308325	59233
	1849	308644	60461
	1852	310612	59727
242A	1600	311783	57901
	1601	311099	58437
	1603	310630	58664
	1604	310041	59205
	1605	309116	59507
	*1606	--	--
	1607	308027	59983
	1608	307510	60116
	1609	306714	60639
	1611	306194	61474
242B	2325	309144	58646
	2326	308559	59145
	2327	308037	59288
	2328	307375	59710
	*2330	--	--
	2331	306544	59861
	2332	306058	60311
	2336	303911	61429

(Continued)

* Barge release time.

(Sheet 3 of 4)

Table 3.3 (Concluded)

<u>Survey No.</u>	<u>Time of Reading GMT</u>	<u>Barge Position, ASPC, ft</u>	
		<u>Easting</u>	<u>Northing</u>
243A	1758	311517	57763
	1800	310450	58596
	*1803	308990	59503
	1805	307468	60718
	1806	307947	61743
	1807	308793	61355
	1808	309488	61101

* Barge release time.

(Sheet 4 of 4)

Table 3.4
Hopper Barge Information for All Surveys

Event	Barge No.	Prerelease Barge Draft ft	Estimated Sediment Volume cu yd	Estimated Sediment Content Percent		
				Sand	Fines	Clay
234A	GL-64	17.0	--	--	--	--
235A	GL-63	20.0	--	--	--	--
236A	GL-64	20.0	--	--	--	--
236B	GL-64	20.0	--	20	80	--
236C	GL-63	16.0	4500	80	20	--
237A	GL-61	19.5	5600	80	20	--
237B	GL-64	*19.0, 20.0	--	80	20	--
238A	GL-64	20.0	--	65	35	--
238B	GL-61	21.0	5600	70	30	--
239A	GL-61	18.5	--	75	25	--
239B	GL-64	*17.0, 18.0	4500	70	30	--
240A	GL-64	18.5	4500	50	50	--
240B	GL-61	18.0	4400	70	30	--
241A	GL-61	20.0	5600	10	15	75
241B	GL-64	21.0	5600	70	30	--
242A	GL-61	**16.0, 14.0	4000	80	20	--
242B	GL-64	19.0	5200	70	30	--
243A	GL-64	20.0	5600	60	40	--

* First number indicates the draft observed at the bow, and the second number indicates the draft observed at the stern.

** Hopper barge was slightly opened, and some material had drained out before the main release.

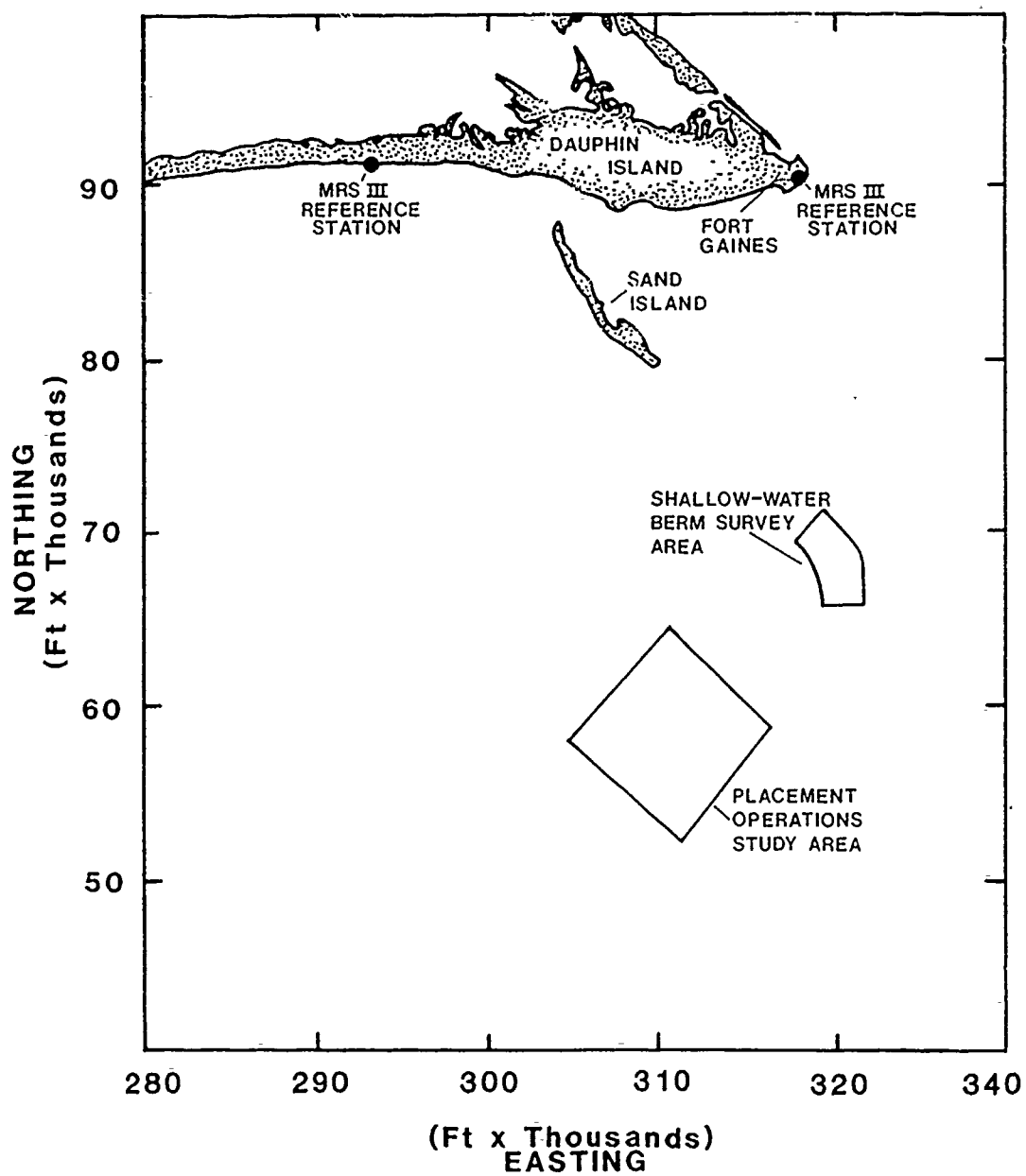


Figure 3.1. Location of the two shore-based RT units.
Scale: Alabama State Plane Coordinates.

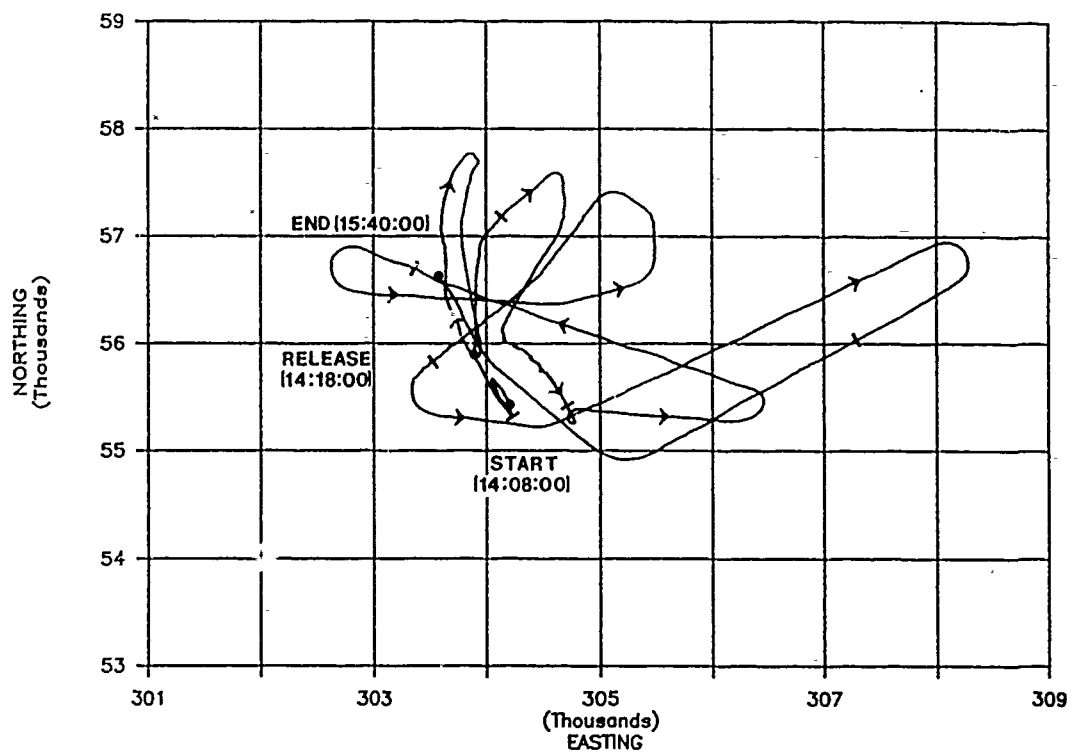
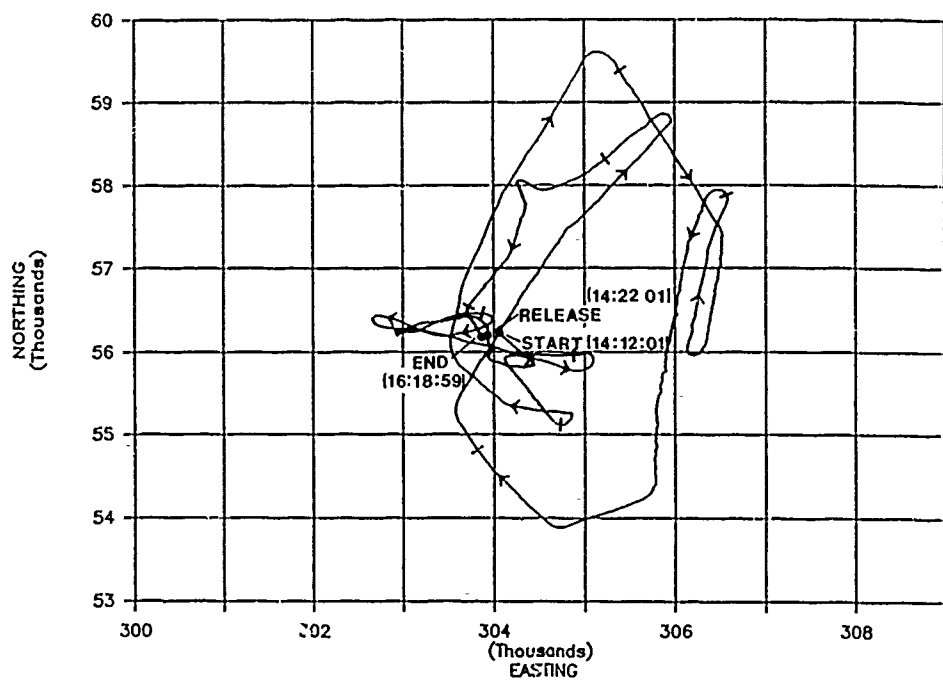
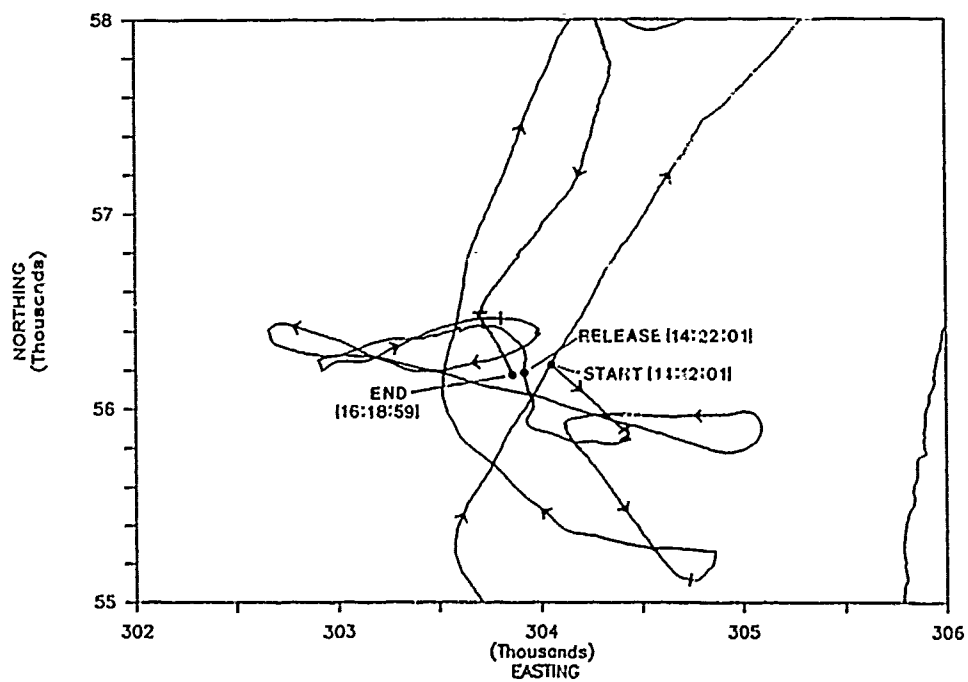


Figure 3.2. Cruise track for Survey 237A.

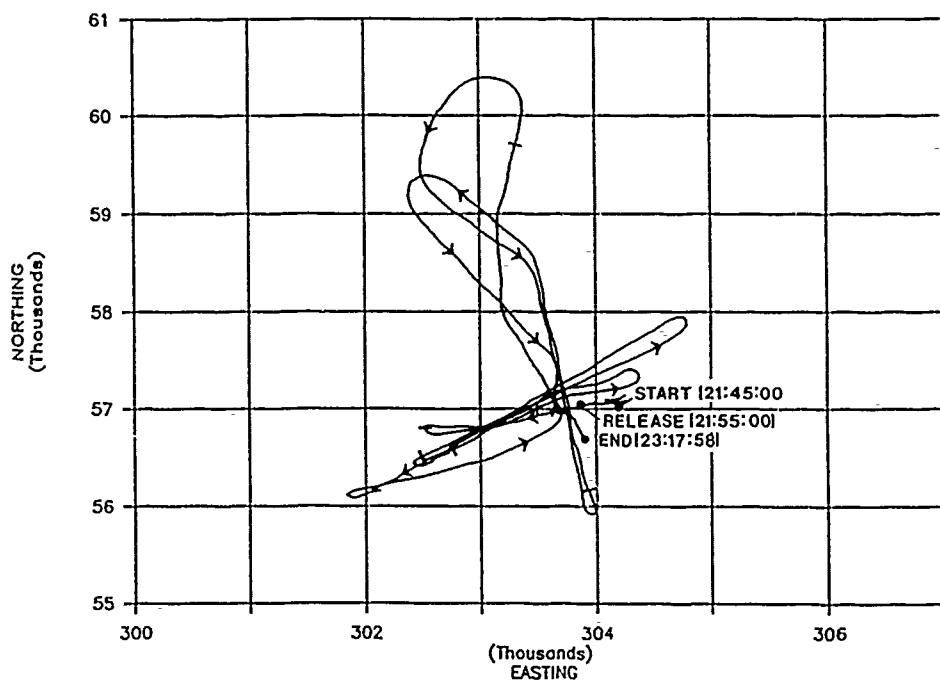


a. Complete track.

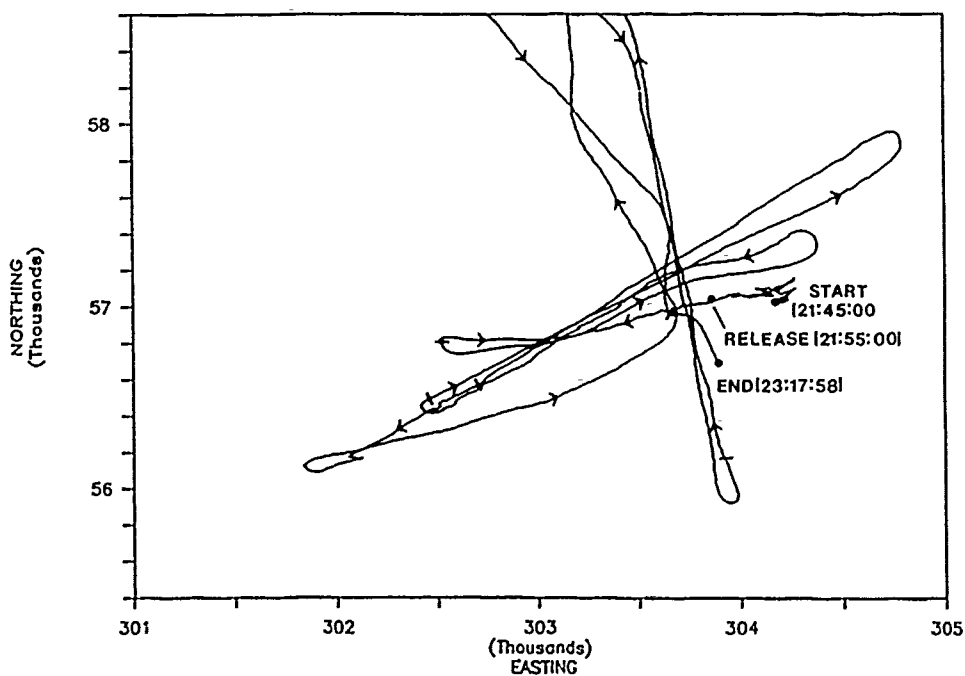


b. Enlargement of transects.

Figure 3.3. Cruise track for Survey 238A.



a. Complete track.



b. Enlargement of transects.

Figure 3.4. Cruise track for Survey 238B.

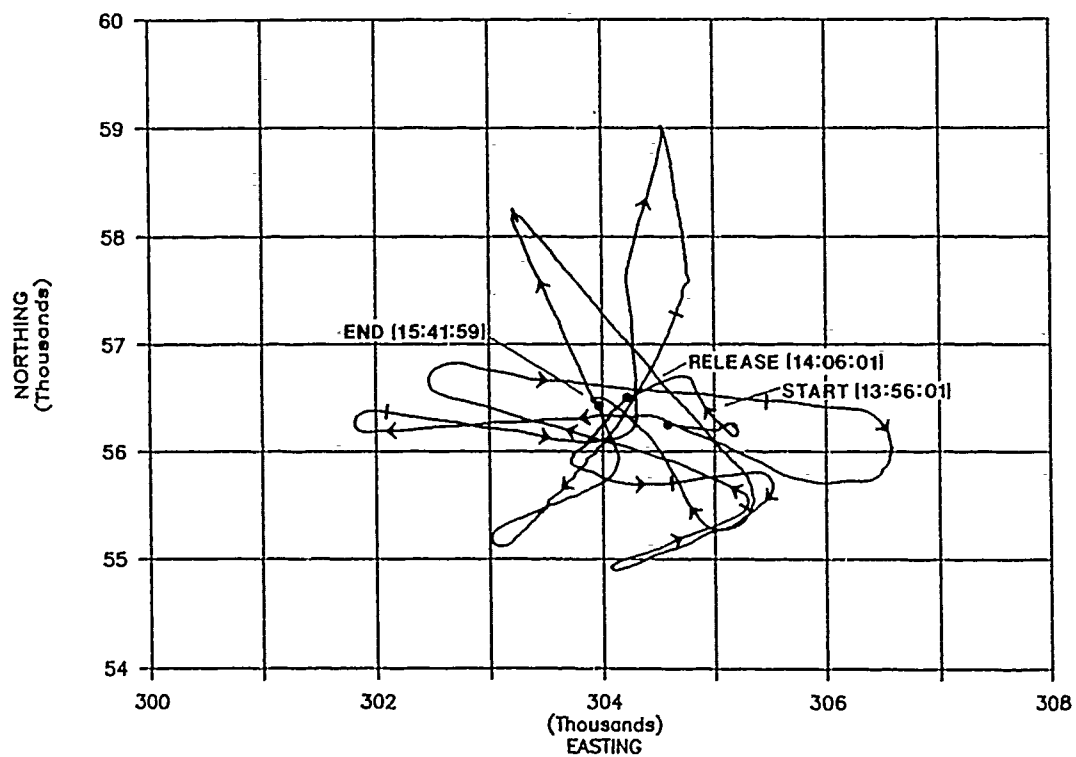
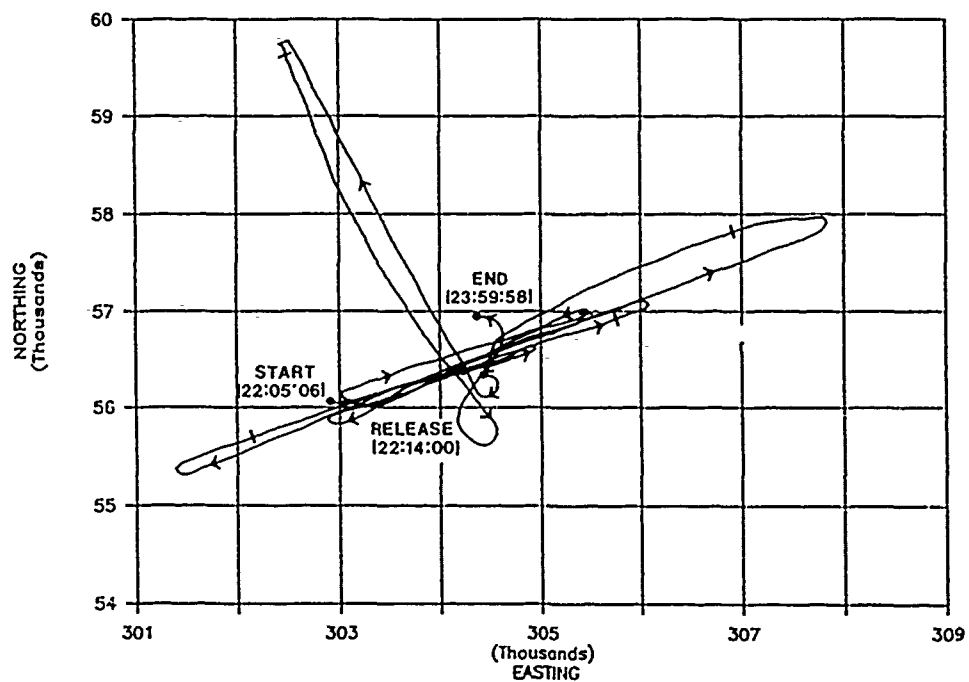
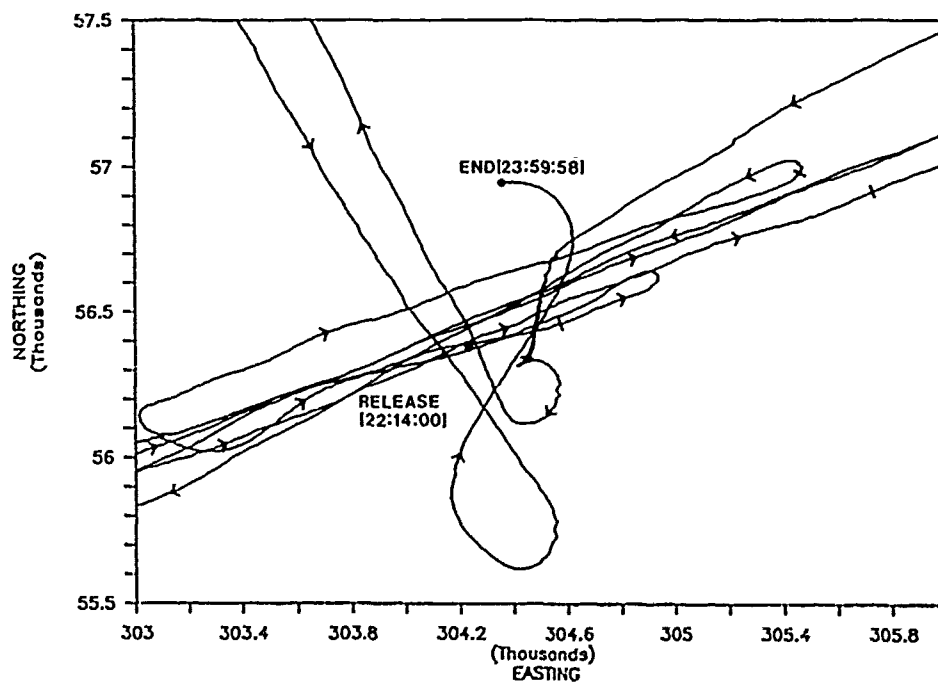


Figure 3.5. Cruise track for Survey 239A.



a. Complete track.



b. Enlargement of transects.

Figure 3.6. Cruise track for Survey 239B.

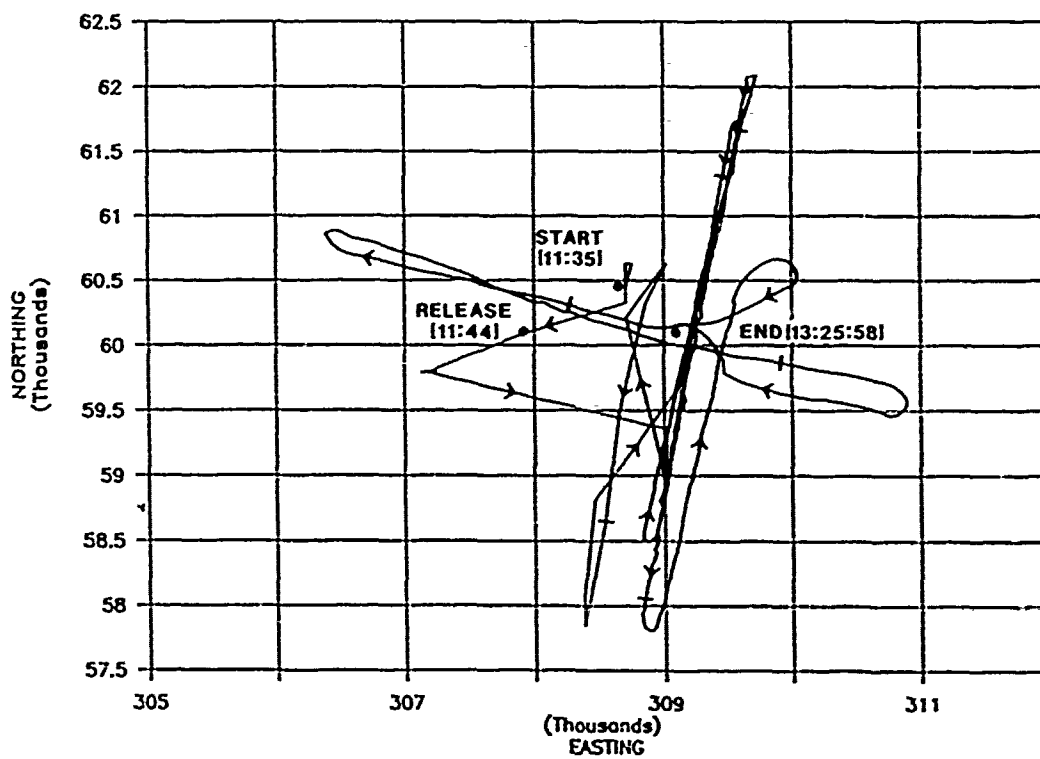
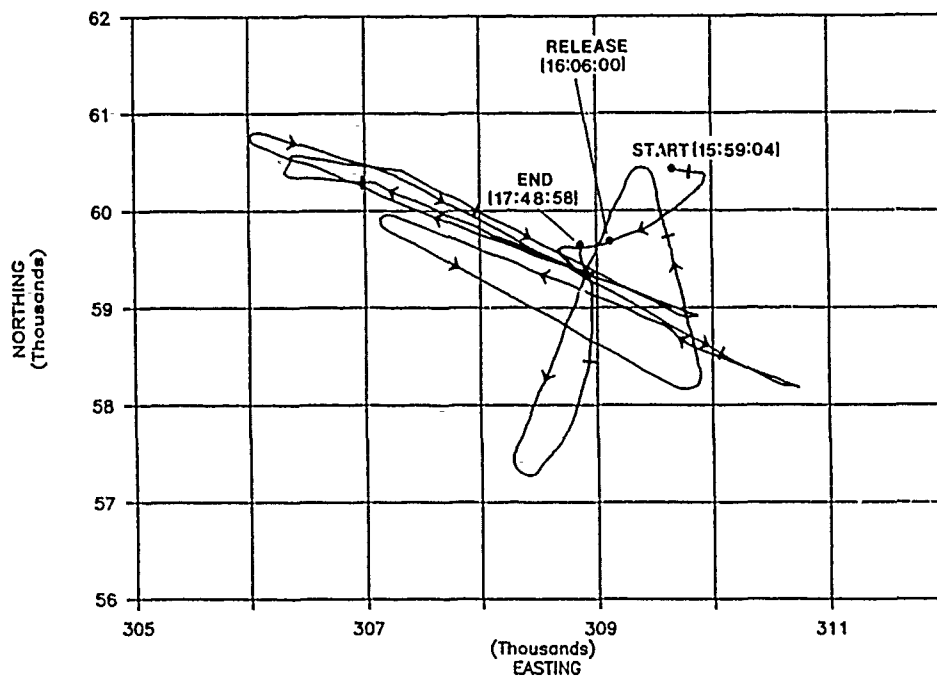
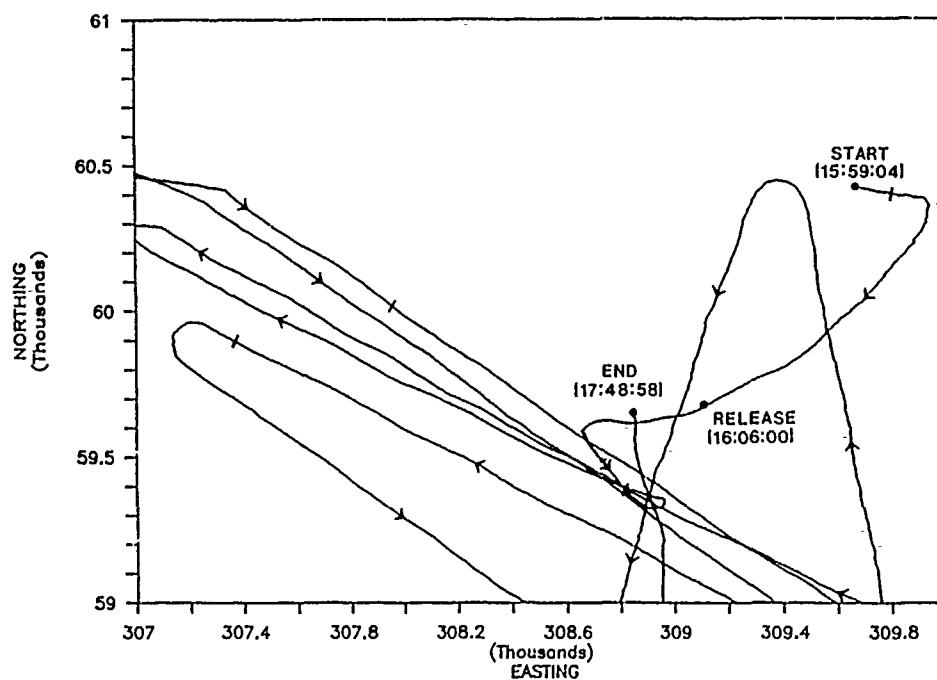


Figure 3.7. Cruise track for Survey 241A.



a. Complete track.



b. Enlargement of transects.

Figure 3.8. Cruise track for Survey 242A.

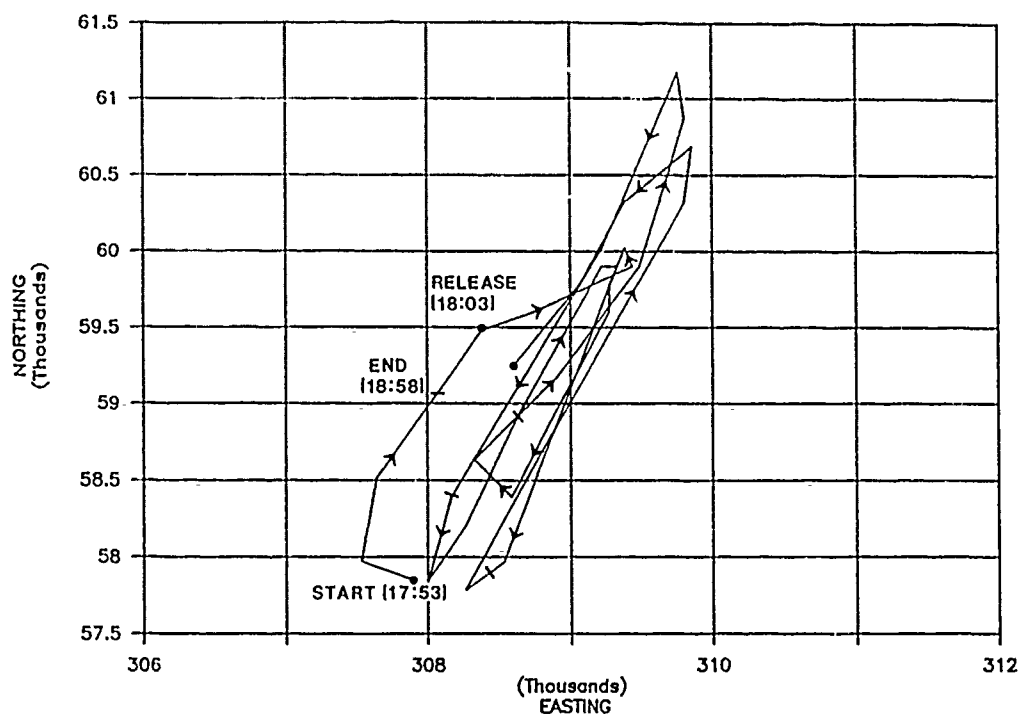


Figure 3.9. Cruise track for Survey 243A.

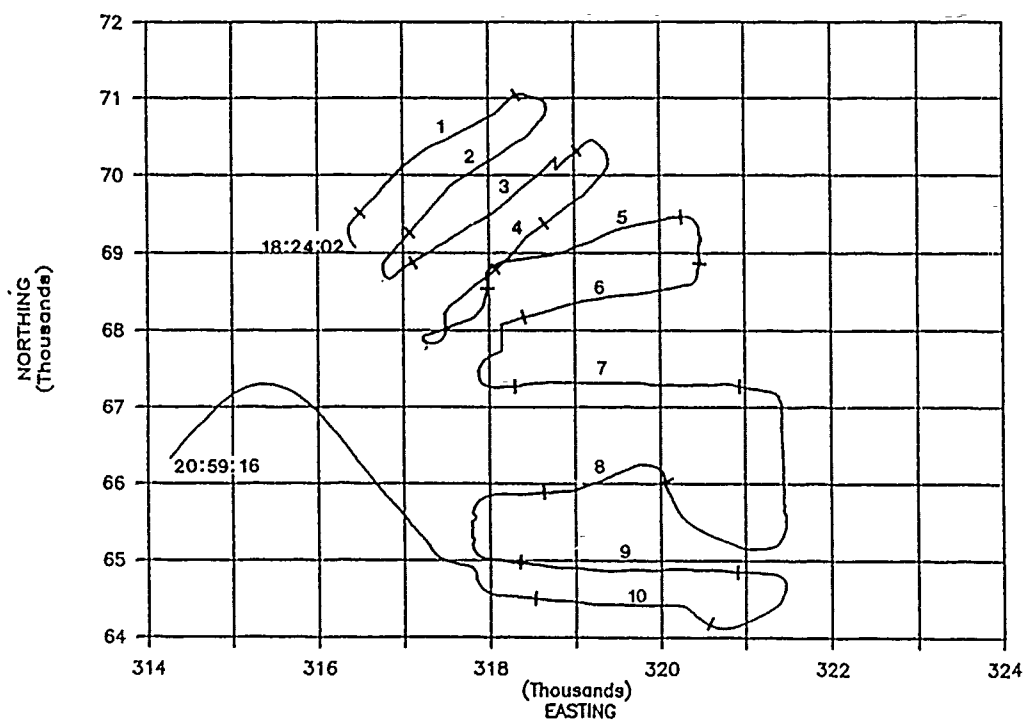


Figure 3.10. Cruise track for shallow-water berm survey.

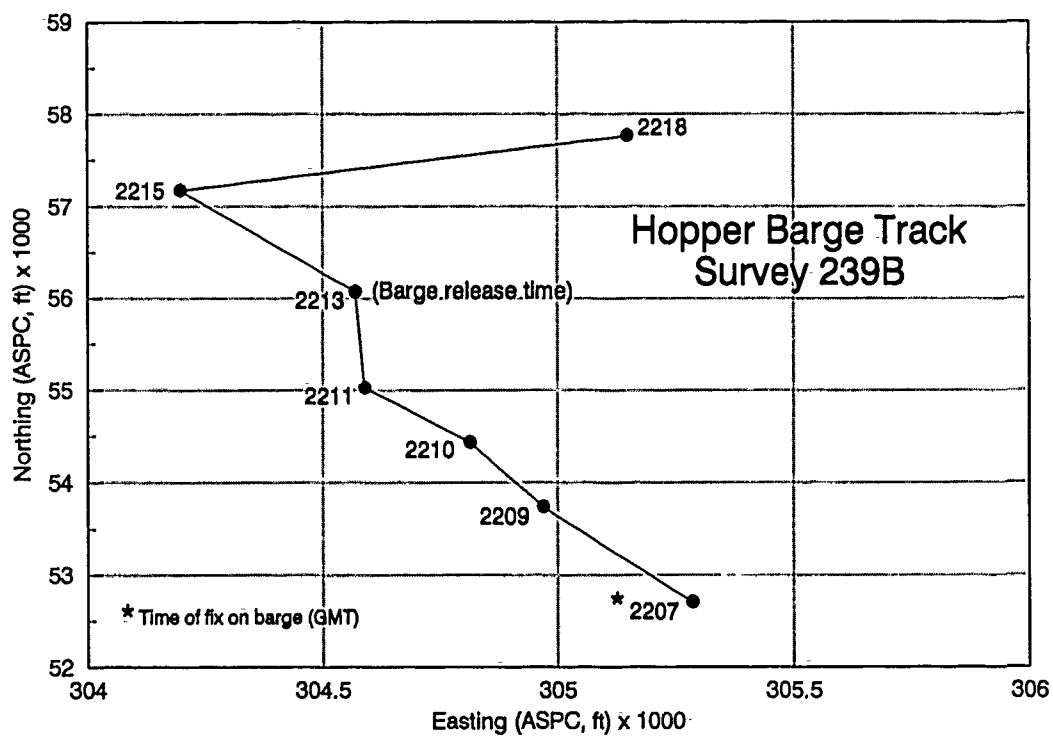


Figure 3.11. Barge track for Survey 239B as computed from periodic fixes.

CHAPTER 4

PROJECT MEASUREMENTS: IN SITU WATER PROPERTIES, SUSPENDED AND BOTTOM SEDIMENT, AND AERIAL PHOTOGRAPHY

ORSON P. SMITH

*Smith Ocean Science and Engineering, Inc.
Clayton, North Carolina 27520*

TERRI L. PRICKETT, NICHOLAS C. KRAUS

*Coastal Engineering Research Center
Waterways Experiment Station, Corps of Engineers
Vicksburg, Mississippi 39180-6199*

Contents

1. Introduction
2. In Situ Water Property Measurements, Samples, and Analysis
3. Prerelease Dredged Material Samples and Analysis
4. Postrelease Bottom Grab Samples and Analysis
5. Aerial Photographs

Acknowledgments

References

Tables

Figures

Appendices

1. Introduction

A significant portion of the effort to characterize the dispersion of dredged material in the coastal waters at the Mobile Field Data Collection site was spent measuring in situ water properties and collecting water and sediment samples for independent laboratory analysis of water properties. This information is relevant in its own right to the research objectives of the Mobile Field Data Collection Project (MFDCP), and it is also vital for calibration, verification, and interpretation of the concurrent acoustic measurements. The data are also pertinent to formulation of numerical models of open-water dredged material dispersion. Stratification of the water column at the site, nature of the sediments suspended in the water column from dispersion of dredged material, and nature of sediments found at the site of release after dispersion were carefully measured. The data collection equipment and procedures and data analysis are described in this chapter. Aerial photography taken during some of the surveyed dredged material placement operations is also described.

2. In Situ Water Property Measurements, Samples, and Analysis

Measurement and Sampling Equipment

During the data collection efforts offshore of Mobile, the equipment aboard the *R/V Pelican* included a Sea-Bird model SBE 9 data logger with sensors for measuring temperature, conductivity, pressure, dissolved oxygen, fluorescence, light transmission, and sediment concentration with an optical backscatter sensor (OBS). The manufacturers' stated resolutions of selected sensors were 0.0003 deg C temperature, 0.00004 Siemens/m conductivity, and 0.004 percent of full-depth scale (600 m). All instruments performed as anticipated with the exception of the OBS sensor. The OBS circuitry was accidentally damaged during an attempted suspended sediment calibration procedure at the start of the cruise and could not be repaired at sea. The outputs of all sensors were digitized by the SBE 9 at 32 Hz. The submersible sensor and data logger assembly were mounted within a General Oceanics rosette sampling apparatus, which was equipped with twelve 5-l Niskin sampling bottles. The rosette was lowered via a starboard davit on a single conductor cable. A shipboard microcomputer, operating Sea-Bird "Seasoft" (Sea-Bird Electronics, Inc. 1989) data acquisition software, controlled recording and real-time display of sensor data. The time and sequence of sampling were controlled by a General Oceanics rosette deck box.

Measurement and Sampling Procedures

Water depth at the field data collection site varied from 4 to 15 m. The *R/V Pelican* was either positioned at the site of a pending barge release for measurement of background conditions or placed in the plume of dredged material by visual observations of the surface and by acoustical echo amplitude indications from either the Acoustic Concentration Profiler (ACP) or Acoustic Doppler Current Profiler (ADCP). The rosette was lowered at 10 m/min or slower to within 1 to 2 m above the bottom, and closure of two Niskin bottles was signaled after a 30-sec minimum flushing period. The rosette was then raised to intermediate depths selected by review of real-time screen plots of temperature, salinity, and percent light transmission profiles, and flushed 15 to 30 sec at each depth before additional bottles were closed. Background casts typically involved closure of five bottles: two at the bottom, one at an intermediate depth, and two at the nominal surface (about 1-m depth at the pressure sensor). On deck, the first bottle at the bottom and the last bottle at the surface were sub-sampled in 8-oz glass bottles for later salinity measurements. Other full Niskin bottles were drained and flushed with the deck hose (salt water) into 10-ℓ plastic containers. The 10-ℓ containers were sterilized with 5 to 10 ml of full strength formaldehyde to minimize the effects of biological activity on later suspended sediment measurements.

The depths were recorded as measured by the Sea-Bird pressure sensor at the bottom of the rosette, about 20 cm below the bottom of the 5-ℓ Niskin bottles. Depths varied with heave of the ship, which usually was less than 0.2 m during the field data collection effort. The Niskin bottles filled from both their tops and bottoms, so the recorded depth could be considered the bottom of an approximately 1-m-deep layer from which the Niskin bottles filled.

Information including release number, cast number, date, time, position, ambient weather conditions, and depth of bottle closure was manually recorded during each cast on laboratory log sheets. A software event marker was applied to record the value of all measured parameters at the time each bottle closure was signaled. The signal to close a bottle did not result in closure until several seconds later, so the times of actual closure were 5 to 7 sec after the times noted in the marker files. The entire cast was continuously recorded as a time series of all measured parameters on a separate file. The unique serial numbers of each salinity and suspended sediment sample container were noted after each cast beside the associated Niskin bottle (rosette) number on a deck log sheet, along with the date, time, release, and cast number. The duration of each cast, from the time the rosette went over the side to its return on deck, was 15 to 20 min.

Forty-two casts were completed, which included collection of 110 suspended sediment samples and 82 salinity subsamples.

Water samples were initially taken at the bottom and intermediate depths, when the rosette was positioned in a plume of dredged material. This system was later changed to leave the rosette about 2 m above the bottom and to close bottles at that depth according to guidance from the real-time acoustics. The latter system proved to be more effective for capturing sediment during the transient plume events.

Positioning the ship in the heart of a plume of dredged material for a time interval long enough to collect a stationary series of in situ samples proved to be difficult. A number of clear water samples in 10-l containers from earlier casts were sacrificed midway through the cruise to provide additional containers. Background samples were thus reduced to one or two suspended sediment samples and one salinity sample per cast.

Analysis of Water Property Measurements

Salinity samples were tested with an AGE 2100 automatic temperature compensating salinometer at the Louisiana Universities Marine Consortium (LUMCON) laboratory complex at Cocodrie, Louisiana.* Salinities were recorded as the mean of three instrument readings. These data are presented in Table 4.1 with the associated marker file depth and time and the cast number during which the samples were collected.

The Seasoft software automatically computed temperature in degrees Celcius, salinity in practical salinity units (PSU) (e.g., Perkin and Lewis 1980), various density parameters in kilograms per cubic meter, and depth in meters. Temperature and salinity raw data were played back as depth profiles and anomalous spikes noted. The downcast (descending portion) and upcast (ascending) were next split into separate files. All of the data in the downcast files were averaged into 0.5-m-depth bins and again reviewed. Bins with obvious spikes were deleted from these averaged downcast files. A few casts lacked sufficient data points in the downcast at some depths, in which case data from the corresponding depth-bin averaged upcast were added to the file. Temperature (T), salinity (S), and potential density (σ_θ) were next plotted as depth profiles for each cast and reviewed a third time for consistency with each other and general knowledge of prevailing oceanographic conditions at the site. Potential density (σ_θ) is generally defined as the

* Personal Communication, 12 September 1989, Dr. Denise J. Reed, Marine Geologist, Louisiana Universities Marine Consortium, Chauvin, LA.

density a parcel of water would have if it were adiabatically raised to atmospheric pressure, less $1,000 \text{ kg/m}^3$ (nominal density of pure water). Salinities measured in the laboratory from samples collected during the upcast were superimposed for comparison to in situ-measured salinities. Unusual discrepancies led to correction of transposed data points and a few data point deletions.

A conventional procedure of curve-fitting salinity profiles with systematic rejection of outliers beyond a residual threshold criterion was discontinued because of complications associated with the shallow depths of the casts and the strong vertical stratification present in the water column. This procedure, routinely used for much deeper casts in the open ocean, vertically smooths the data and fits a polynomial curve to each cast for derivation of sensor-sample calibration statistics. Polynomial curves fit to the 4- to 15-m depth and 5 to 6 PSU vertical salinity variations at the site produced unrealistic profiles, and other common curve forms (e.g., power, log, and exponential curves) produced similar aberrations. Visual inspection revealed that salinities measured from bottle samples are consistently very close to the salinities concurrently measured by the conductivity and temperature sensors.

Depth profiles of temperature, salinity, sigma-theta (density), velocity of sound, light transmission, and Brunt-Väisälä frequency are displayed in Appendix 4A. Casts are noted by the survey (release) number, the cast number during that survey, and "D" for descending (downcast) data only. Data are plotted as points with a cubic spline curve (tension factor 2) superimposed. Square data points superimposed on salinity profiles indicate salinities measured in the laboratory from samples collected during the ascending (upcast) portion of the cast from the depths at which the points are plotted.

Sound velocity V_s was computed as a function of temperature, salinity, and pressure (depth) for each cast, according to Chen and Millero (1977). This parameter did not change greatly in the shallow depths encountered. The stratification revealed in the salinity and σ_θ profiles corresponds to a speed of sound variation of only a few percent.

Light transmission was reported as percentage of the transmitted beam intensity received across the 5-cm path length of the transmissometer. No statistical calibration of this transmission scale with bottle concentration data was attempted, since visual inspection indicated large scatter (poor correlation) over the range of concentrations encountered. During one cast (C244B002), the transmission was essentially zero, indicating a suspended sediment concentration higher than about 100 mg/l , the nominal limit of the transmissometer.

The buoyant stability of water masses in a stratified ocean is usually considered in terms of the rate of change of density with depth. The stability parameter, E , is defined as:

$$E = - \frac{1}{\rho} \frac{\partial \rho}{\partial z} - \frac{g}{V_s^2} \quad (4.1)$$

where

ρ = seawater density

z = vertical coordinate, positive upward

g = acceleration of gravity

V_s = velocity of sound, m/sec

The first term in Equation 4.1 is on the order of 10^{-3} for the MFDCP data, and the second term is on the order of 10^{-6} ; therefore, stability can be practically estimated by:

$$E = \frac{-1}{\rho_{s,\theta,0}} \frac{\partial \sigma_\theta}{\partial z} \times 10^{-3} \quad (4.2)$$

where $\rho_{s,\theta,0}$ is the density corresponding to σ_θ at a given depth. The Brunt-Väisälä frequency, N , conceptually is the rate at which a parcel of water displaced vertically from its equilibrium depth would oscillate up and down about its equilibrium position (Knauss 1978). It is related to stability by:

$$N = (gE)^{1/2} \quad (4.3)$$

The corresponding period of the oscillation is:

$$T_N = \frac{2\pi}{N} \quad (4.4)$$

The frequency of oscillations along density interfaces (internal waves) cannot be higher than the Brunt-Väisälä frequency, nor lower than the inertial frequency, whose corresponding period in hours, T_I , is:

$$T_f = \frac{12 \text{ hr}}{\sin \phi} \quad (4.5)$$

where ϕ is latitude in degrees. Brunt-Väisälä periods are rarely as small as a minute and are commonly several hours in the deep ocean. Profiles of sound velocity, light transmission, and Brunt-Väisälä frequency are included in Appendix 4A. Data are plotted as points with a cubic spline curve (tension factor 2) superimposed on the sound velocity and light transmission profiles.

A peak in Brunt-Väisälä frequency denotes a density interface or layer of strong vertical density gradient, which for the MFDCP data appears to correspond primarily to salinity variations. The consistent lower density above a saltier and denser layer implies that fresher water from Mobile Bay was flowing out over saltier gulf water throughout most of the field data collection effort. Significant vertical gradients of horizontal currents revealed by both moored current meters and ADCP support this hypothesis.

A Brunt-Väisälä frequency peak near 0.004 sec^{-1} , corresponding to a period of about 26 min, was observed during Survey 239B on the evening of 27 August 1989 (Julian date 239, cast C239B003) in the water column at about 5-m depth at the time a surface slick (in phase convergent zone) was observed propagating outward from the path of the tug and hopper barge. There was a notable minimum in light transmission, denoting a layer of higher suspended sediment concentration, at this same depth. The dispersion relation for internal waves in a two-layer system, assuming both layers are shallow with respect to the wavelength, reduces to

$$C^2 = \frac{gh''h'}{h'' + h'} \left(1 - \frac{\rho'}{\rho''}\right) \quad (4.6)$$

where h' and h'' are the depths of the upper and lower layers, and ρ' and ρ'' are the layer densities (Knauss 1978). An estimate of the observed internal wave's propagation speed, C , is thus about 0.4 m/sec or about 1 knot, based on water property profiles measured by cast C239B003. The slick appeared to be moving away from the track of the barge at walking speed, or about 1 to 2 mph, as observed from the stationary bridge of the *R/V Pelican*.

Laboratory Treatment and Analysis of Water Samples

Filtration. Water samples were left standing still for 72 hr to allow settling of sediment. As much as 60 percent of the water was then decanted to minimize the filtration time. The remainder of the sample, which included all the sediment, was filtered through a preweighed cellulose Millipore filter with a 0.45- μ retention rating. Because of the high suspended sediment concentration in some samples, multiple filter papers were used if necessary on individual samples. Filter papers were dried and reweighed to determine the amount of sediment retained. A correction factor to account for changes in filter paper weight caused by salt or the wetting/drying process was determined by treating clean filters with filtered water. Weights were summed for all filters as total dry weight in grams of sediment in each sample.

Grain Size Distributions. The dry filter papers obtained from the filtration procedure were combusted in a muffled furnace for 16 hr at 375 deg C. The sediment residue was treated with 30-percent hydrogen peroxide to remove organics. The small remaining amount of sediment was subjected to a multitube Coulter Multisizer analysis. The three tubes used included 280, 140, and 50- μ ratings. Continuous grain size distributions were derived using Coulter AccuComp software.

The summarized sample information of Table 4.2 is consolidated from field laboratory log sheets, deck log sheets, Seasoft event marker files, and filtered sediment dry weights. The laboratory and deck logs and marker files were used to match a cast number with each sample bottle number and identify the corresponding depth and time at which the rosette bottle was closed.

Suspended sediment concentrations assume a 5- ℓ volume of water in each Niskin bottle. No bottles that showed signs of leakage were flushed into sample containers. Spillage was never more than 10 to 20 ml, so the concentrations can be considered to have less than 1-percent error because of volume measurement.

Grain Size Statistics. The grain size distributions from the fine suspended sediments sampled during the field data collection effort were reported as percentages finer than increments of 0.5 ϕ , from 2.5 ϕ (177 μ) to 9.0 ϕ (1.95 μ). The differences in percentages finer than the consecutive size classes reported are displayed in Appendix 4B as density function of sizes in each sample. The first and last data points are understood to be the percentage finer than 1.95 μ and percentage coarser than 177 μ , respectively. The classes between these limits are (in microns): 1.95 to 2.76, 2.76 to 3.96, 3.96 to 5.5, 5.5 to 8, 8 to 11, 11 to 16, 16 to 22, 22 to 31, 31 to 44, 44 to 63, 63 to 88, 88 to 125, and 125 to 177.

Table 4.3 presents statistical parameters based on the distributions of Appendix 4B. The parameters ϕ_{16} , ϕ_{50} , ϕ_{84} , D_{40} , D_{50} , and D_{90} are the ϕ values or diameters for which the percentage denoted by the subscript is finer. The parameters $\bar{\phi}$ and \bar{D} are mean values estimated (*Shore Protection Manual* 1984) as

$$\bar{\phi} = \frac{\phi_{16} + \phi_{50} + \phi_{84}}{3} \quad (4.7)$$

and

$$\bar{D} = 2^{-\bar{\phi}} \quad (4.8)$$

The sample grain size standard deviation is estimated as

$$\sigma_{\phi} = \frac{\phi_{84} - \phi_{16}}{2} \quad (4.9)$$

and

$$\sigma_D = 2^{-\sigma_{\phi}} \quad (4.10)$$

Sample kurtosis (skewness) is computed as

$$\alpha_{\phi} = \frac{\bar{\phi} - \phi_{50}}{\sigma_{\phi}} \quad (4.11)$$

A symmetrical distribution would have no kurtosis, and the median would equal the mean. A negative kurtosis as computed here denotes a right skewness (shallow slope to the right of the peak density). Virtually all the samples are right skewed, but those with small positive kurtosis can be seen to have minimum probability density to the right of the peak.

The uniformity coefficient (Sowers and Sowers 1970) is computed as

$$C_u = \frac{D_{40}}{D_{90}} \quad (4.12)$$

Samples with C_u less than 4 are generally uniform, and those with C_u greater than 6 are generally well graded, assuming a smooth and roughly symmetrical distribution.

3. Prerelease Dredged Material Samples and Analysis

During 28-29 August 1989, personnel from the U. S. Army Engineer Waterways Experiment Station's Hydraulics Laboratory (WES/HL) obtained sediment surface samples of dredged sediment from two fully loaded hopper barges corresponding to Surveys 240B and 241B. Representative sediment samples were also obtained at different depths within one barge as it was being loaded. The barge load from which the profile samples were taken corresponds to a night release that was not monitored by the MFDCP. All samples were analyzed to determine bulk density and moisture content. Grain size distributions were determined by sieving selected samples.

The sampling team, composed of three persons, boarded two fully loaded barges to obtain water surface and grab samples of the solid material in the barge. A 1-l bottle was lowered and filled approximately 1 ft below the water level at several stations around the inside perimeter of the barge to sample the muddy water standing above the settled dredged material. These sampling locations, labeled arbitrarily, are shown in Figure 4.1. A clamshell grab sampler was lowered at the same stations to the sediment surface beneath the surface water layer to obtain samples of the settled material (Figure 4.2). Depth of the grab samples, measured in feet by a lead line, varied from station to station in both barges (Table 4.4), indicating uneven distribution of material within the barges after completion of loading. The uneven surface also indicates the material was largely consolidated (lumpy). The barge corresponding to Survey 240B had been en route to the placement site for approximately 90 min when the water surface and grab samples were taken, and the barge corresponding to Survey 241B had been en route for approximately 30 min.

Grain size analysis of the solids from one of the water surface samples in the barge load of Survey 240B indicated approximately equal amounts of fine sand and silt/clay. Moisture content ranged from 61 to 91 percent with bulk densities varying between 1.06 to 1.31 g/cm³, as shown in Table 4.4. As expected, moisture content of the grab sample material was somewhat lower, with a range of 54 to 62 percent, and bulk densities were higher, ranging from 1.27 to 1.38 g/cm³.

Grain size analysis of solids in the water surface samples from the barge load of Survey 241B showed an approximate 40:60 ratio of fine-grained sand to silt/clay. The moisture contents of samples ranged from 81 to 97 percent with bulk densities of 1.02 to 1.09 g/cm³. The grab sample material had a moisture content range of 55 to 62 percent with bulk densities of 1.30 to 1.37 g/cm³.

A representative sediment sample of the dredged material in a loaded barge was obtained using 18 containers designed by WES/HL for sampling clamshell dredge loading operations and

positioned in the empty barge prior to loading (Figures 4.3, 4.4). The sampling devices were strung together with cable at distances of 4, 11, and 21 ft, lowered into the barge, and anchored from the deck at six stations around the inside perimeter of the barge. These sampling stations were in approximately the same location as the water surface and grab samples described earlier (Figure 4.1). The samplers were filled as the material rose above the selected elevation, providing a representative sample of the material upon initial loading. The samplers were recovered, and sediment was removed for analysis after the barge released the material. The dredged material from which the samples were taken was released after daylight hours on 28 August and was not monitored by the MFDGP, but these representative samples do provide important information of material variability within a barge and the effect of compaction upon the material.

Analysis of the material removed from the profile samplers (Table 4.5) revealed primarily fine-grained sand and larger amounts of coarse sand than in previously described samples. Moisture content reached a maximum of 49 percent in the samplers placed at the 4-ft depth, but decreased to 17 percent in the samplers at the 21-ft depth. This decrease is attributable to the expulsion of pore water by compression from the overburden material during and after loading of the barge. The bulk densities increased through compaction from a range of 1.5 to 1.9 g/cm³ at the 4-ft depth to a range of 1.9 to 2.1 g/cm³ at the 21-ft depth.

4. Postrelease Bottom Grab Samples and Analysis

Following most surveys, the *R/V Pelican* returned to the location of the release site (recorded from the *R/V Pelican's* Loran C navigational system) to obtain bottom sediment samples. The samples were acquired in an attempt to measure grain size characteristics of the newly released dredged material that had settled at the disposal site. Unfortunately, it cannot be conclusively proven that samples obtained from the postrelease grabs were composed of the newly released dredged material. The location of each release site is ambiguous because of continued movement of the barge as the material was released and positioning accuracy of Loran C (+/-100 m). The bottom samples probably represent a mixture of newly released dredged material, previously released dredged material, and some native sediments as suggested by the presence of polychaete worms and oxidized wood found in some samples.

The bottom samples were obtained by using a Peterson clamshell grab sampler, that was lowered over the side of the *R/V Pelican*. In several cases, the grab sampler had to be reset and

lowered as many as four times to obtain a proper sample. Most samples were collected 1.6 to 3.2 hr after the barge release. Grab samples were not taken after Survey 234A, and a sample from Survey 239A was taken approximately 2 min after the release. Field observations associated with each sample are shown in Table 4.6.

After the MFDCP cruise, the samples were dried for several days, ground, and split by the cone quartering method. One quarter of the sample was then sieved at 1- ϕ intervals from 1 mm to 63 μ . Silts and clays remaining in the pan were analyzed on a Coulter Multisizer, using a 2-tube technique (140 and 150 μ). Grain size distributions of sand from the sieve analyses were combined with silt and clay grain size distributions using Coulter AccuComp software. Data from both techniques were combined under the assumption that particle volume and weight were equivalent measures. The grain size distribution of the sediment was recorded as cumulative percent greater than the phi size.

Most bottom grab samples consisted of a medium- to fine-grained sand containing less than 5-percent silts and clays (Table 4.7). Prerelease samples obtained from the hopper barges corresponding to Surveys 240B and 241B indicate that a larger percentage of silts and clays was released. Also, field estimates of sediment content for most surveys indicate a higher percentage of silts and clays (Table 3.4).

5. Aerial Photography

Seven hopper barge releases were photographed from the air during the period 27-31 August (Julian Days 239-243) to record the size and configuration of the surface sediment plume. The photography corresponds to Surveys 239A, 240A, 240B, 241A, 242A, 242B, and 243A.

The photography was performed by Woolpert Consultants, located in Mobile, Alabama. A Wild RC20 camera with a yellow D filter, loaded with color infrared film type 2443, was mounted from a Cessna 210 aircraft. Photographs were taken at altitudes of 1,000 to 1,100 ft above sea level during 7- to 120-min periods that included the barge release (typically lasting for 20 min). Following a release, photographs were taken at 3,100- to 6,700-ft altitudes in approximately 5-min intervals as long as the sediment plume remained visible to the pilot. A total of approximately 14.5 hr of flight time was clocked including preparation for takeoff and photography.

Many of the photographs taken during periods with little or no cloud cover contained considerable sun glare with the result that the tug, ship, and sediment plume were barely detectable in the

photographs. Also, limited visibility during periods of cloud cover, and lack of light during the late afternoon releases produced dark photographs. However, a few useful photographs were obtained. A list of the photographs including a quality rating is given in Table 4.8.

Based on the experience gained, the wide turning radius of a fixed-wing plane proved inappropriate for documenting the movement of a barge, plume, and sampling vessel. A helicopter for this type of photography is recommended for future monitoring operations. It is also recommended that several film types be tested for best recording of the plume.

Acknowledgments

T. L. Prickett acknowledges the assistance of Mr. Edward B. Hands, Coastal Engineering Research Center, in preparing the section "Postrelease Bottom Grab Samples and Analysis."

Water samples collected for laboratory measurement of suspended sediment concentration and salinity and bottom samples were treated by Dr. Denise J. Reed at the facilities of the Louisiana Universities Marine Consortium, Cocodrie, LA. The details of the laboratory procedures followed by Dr. Reed are described herein, but the timeliness and precision of the correspondence that transmitted the results were appreciated by all investigators who applied these data in their own investigations.

References

- Chen, C. T., and Millero, F. J. 1977. "Speed of Sound in Sea-Water at High Pressures," *Journal, Acoustical Society of America*, Vol. 62, pp. 1129-1135.
- Knauss, J. A. 1978. *Introduction to Physical Oceanography*, Prentice-Hall, Englewood Cliffs, NJ.
- Perkins, R. G., and Lewis, E. L. 1980 (Jan). "The Practical Salinity Scale 1978: Fitting the Data," *IEEE Journal of Ocean Engineering*, Vol. OE-5, pp. 9-16.
- Sea-Bird Electronics, Inc. 1989 (Aug). "CTD Data Acquisition Software: Seasoft Version 3.3G," Bellevue, WA.
- Shore Protection Manual*. 1984. 4th ed., 2 Vols., U.S. Army Engineer Waterways Experiment Station, Coastal Engineering Research Center, Vicksburg, MS, U.S. Government Printing Office, Washington, D.C.
- Sowers, G. B., and Sowers, G. F. 1970. *Introductory Soil Mechanics and Foundations*, 3rd ed., MacMillan Pub. Co., New York, p. 20.

Table 4.1
In Situ Salinity Sample Data

<u>Bottle No.</u>	<u>Average Salinity PSU</u>	<u>Cast No.</u>	<u>Depth m</u>	<u>Time GMT*</u>
1	28.31	C234A001	4.31	20:36:23
2	25.86	C234A001	1.26	20:38:17
3	29.20	C235A001	4.46	13:49:05
4	28.17	C235A001	1.43	13:50:48
5	29.23	C235B001	5.56	17:07:13
6	31.18	C235B002	11.35	17:10:43
7	27.20	C235B002	1.27	17:15:25
8	31.19	C235A003	11.85	18:24:00
9	29.28	C235B003	8.10	--**
10	29.00	C235B003	1.25	18:27:50
11	31.27	C235B004	11.51	18:40:25
12	29.73	C235B004	8.12	18:43:59
13	28.36	C235B004	1.48	18:48:56
14	29.23	C236A001	7.06	00:22:56
15	26.41	C236A001	1.20	00:25:01
16	30.84	C236A002	9.55	00:26:14
17	26.76	C236A002	1.75	00:28:21
18	30.38	C236A003	8.58	01:18:07
19	26.27	C236A003	1.20	--
20	31.22	C236B001	11.37	15:06:35
21	29.23	C236B001	1.27	15:11:56
22	31.26	C236B002	9.55	15:14:07
23	29.20	C236B002	1.37	15:17:24
24	31.73	C236B003	12.01	16:02:51
25	28.48	C236B003	1.10	--
26	30.66	C236B004	9.84	16:40:46
27	28.35	C236B004	1.33	16:44:24
28	31.73	C236C001	13.15	20:20:29
29	25.96	C236C001	1.30	20:25:50
30	31.44	C236C002	11.21	22:35:22
31	26.11	C236C002	1.29	22:40:58
32	33.04	C237A001	13.53	13:23:32
33	28.77	C237A001	0.98	13:27:23

(Continued)

* Greenwich Mean Time.

** Not available.

(Sheet 1 of 3)

Table 4.1 (Continued)

<u>Bottle No.</u>	<u>Average Salinity</u> <u>PSU</u>	<u>Cast No.</u>	<u>Depth</u> <u>m</u>	<u>Time</u> <u>GMT</u>
34	32.02	C237A002	12.37	14:40:33
35	28.81	C237A002	0.91	14:45:04
36	33.31	C237B001	12.77	21:49:41
37	26.51	C237B001	0.95	21:52:31
38	33.02	C237B002	11.47	22:49:56
39	25.86	C237B002	1.14	22:53:22
40	32.61	C238A001	11.45	12:46:52
41	32.89	C238A002	10.79	14:54:12
42	28.78	C238A002	1.12	14:56:51
43	33.06	C238B001	12.06	21:27:04
44	27.07	C238B001	1.12	21:30:11
45	33.14	C239A001	13.56	12:42:19
46	27.52	C239A001	1.06	12:46:11
47	32.55	C239A002	11.19	14:13:44
48	27.50	C239A002	1.28	14:19:23
49	32.64	C239B002	10.38	21:48:08
50	28.17	C239B002	0.97	21:49:54
51	33.32	C239B003	12.18	23:24:13
52	30.15	C239B003	5.77	23:26:22
53	26.92	C239B003	1.48	23:28:18
54	32.89	C240A001	11.50	13:07:30
55	28.05	C240A001	6.11	13:10:07
56	26.50	C240A001	1.16	13:12:25
57	32.01	C240A002	10.73	13:41:54
58	27.31	C240A002	4.34	13:44:36
59	26.49	C240A002	1.25	13:46:01
60	31.65	C240A003	10.20	--
61	27.21	C240A003	1.10	--
62	33.13	C240B002	11.46	19:53:32
63	27.12	C240B002	1.16	19:55:46
64	32.82	C240B003	9.75	20:39:28
65	32.60	C240B003	9.72	20:45:24
66	32.66	C241A002	10.53	11:04:56
67	27.92	C241A002	1.13	11:07:43
68	32.36	C241B001	11.13	18:17:24
69	26.84	C241B001	1.05	18:20:08
70	27.03	C241B002	5.50	--
71	27.13	C241B002	1.48	19:00:55
72	27.48	C242A001	1.25	15:44:56

(Continued)

(Sheet 2 of 3)

Table 4.1 (Concluded)

<u>Bottle No.</u>	<u>Average Salinity PSU</u>	<u>Cast No.</u>	<u>Depth m</u>	<u>Time GMT</u>
73	27.88	C242A002	7.18	16:08:52
74	28.58	C242A002	7.15	16:13:09
75	32.39	C242B001	11.08	22:46:44
76	31.70	C243A001	8.71	17:18:21
77	36.31	C244MRP1*	35.19	05:53:59
78	21.78	C244MRP1	1.61	06:00:57
79	35.50	C244MRP2	23.20	09:14:10
80	21.62	C244MRP2	1.40	09:20:11
81	35.60	C244MRP3	20.10	--
82	21.43	C244MRP3	1.10	--

* Mississippi River plume survey samples.

(Sheet 3 of 3)

Table 4.2

Suspended Sediment Sample Summary Information

<u>Survey No.</u>	<u>Cast No.</u>	<u>Bottle No.</u>	<u>Depth m</u>	<u>Time GMT</u>	<u>T deg C</u>	<u>S PSU</u>	<u>V, m/sec</u>	<u>Trans. percent</u>	<u>Sed. Wt. g</u>	<u>Conc. mg/l</u>	<u>Remarks</u>
234A	1	1002	1.3	20:38:17	30.1	25.63	1,536.0	83.2	0.0963	19.3	ARMS* site, surface
235A	1	1003	4.2	13:49:22	29.2	29.13	1,537.8	80.6	0.0450	9.0	ARMS site, bottom
235A	1	1004	1.4	13:51:03	29.3	28.00	1,536.8	85.5	0.0259	5.2	ARMS site, surface
235B	1	1005	5.6	17:07:32	29.6	29.08	1,538.8	66.1	0.0552	11.0	Bottom
235B	1	1006	2.2	17:08:18	29.8	28.75	1,538.6	67.4	0.1218	24.4	
235B	2	1008	11.2	17:11:15	29.0	20.32	1,528.4	74.0	0.0412	8.2	Maybe fouled sensors
235B	2	1009	5.9	17:13:05	29.7	20.08	1,529.6	84.7	0.0795	15.9	Maybe fouled sensors
235B	3	1012	11.8	18:24:16	29.1	24.64	1,533.1	84.2	0.0455	9.1	
235B	3	1013	4.2	18:26:54	29.6	28.94	1,538.5	92.4	0.0083	1.7	
235B	4	1015	11.5	18:40:49	29.1	21.71	1,529.9	75.4	0.0330	6.6	Maybe fouled sensors
235B	4	1016	4.4	18:46:37	29.8	21.36	1,531.1	92.0	0.0119	2.4	Maybe fouled sensors
235C	1	--**	4.3	21:03:35	29.3	29.13	1,538.1	80.2	--	--	ARMS site, no samples
236A	1	1018	7.4	00:23:18	29.5	29.45	1,539.0	92.8	0.0558	11.2	
236A	1	1019	4.2	00:24:06	29.7	28.87	1,538.7	93.7	0.0207	4.1	
236A	1	1020	1.1	00:24:39	30.0	26.51	1,536.7	56.8	0.1077	21.5	

* ARMS: Acoustic Resuspension Measurement System; discussed in Chapter 1.

** Not available.

Table 4.2 (Continued)

Survey No.	Cast No.	Bottle No.	Depth m	Time GMT	T deg C	S PSU	V _r m/sec	Trans. percent	Sed. Wt. g	Conc. mg/l	Remarks
236A	2	1021	9.4	00:26:34	29.0	30.79	1,539.2	63.7	0.0656	13.1	Same spot as 1st cast
236A	2	1022	5.4	00:27:17	29.7	29.24	1,539.1	94.3	0.0076	1.5	
236A	2	1023	1.6	00:28:05	30.0	26.70	1,537.0	77.2	0.0574	11.5	
236A	3	1024	8.6	01:18:42	29.2	30.41	1,539.2	87.8	0.0234	4.7	Bottom
236B	1	1027	11.4	15:06:52	28.8	31.76	1,539.9	77.4	0.0312	6.2	Bottom
236B	1	1028	9.2	15:08:36	29.1	30.90	1,539.5	86.2	0.0240	4.8	
236B	1	1030	1.3	15:11:40	29.6	29.02	1,538.6	84.0	0.0450	9.0	Surface
236B	2	1031	9.4	15:14:23	29.0	31.10	1,539.6	79.7	0.0407	8.1	Same spot as 1st cast
236B	2	1033	1.2	15:17:08	29.7	28.98	1,538.7	92.9	0.0088	1.8	
236B	3	1034	12.0	16:03:35	28.8	31.72	1,539.9	79.3	0.0377	7.5	Postrelease fluff sample
236B	3	1035	12.0	16:03:50	28.8	31.72	1,539.9	81.0	0.0292	5.8	Postrelease fluff sample
236B	4	1036	9.8	16:41:07	29.0	31.07	1,539.6	80.6	0.0347	6.9	
236C	1	1038	13.2	20:20:46	28.7	31.75	1,539.7	28.9	0.1562	31.2	
236C	2	1041	11.2	22:35:37	28.7	31.66	1,539.7	--	--	--	
236C	2	1042	11.1	22:35:55	28.8	31.63	1,539.7	31.5	0.1713	34.3	
236C	2	1043	8.8	22:36:59	29.1	31.42	1,540.2	89.2	0.0404	8.1	
236C	2	1044	6.6	22:38:08	29.4	30.31	1,539.6	90.7	0.0682	13.2	
236C	2	1045	4.2	22:39:20	29.8	29.26	1,539.3	89.7	0.0257	5.1	

(Continued)

Table 4.2 (Continued)

Survey No.	Cast No.	Bottle No.	Depth m	Time GMT	T deg C	S PSU	V, m/sec	Trans. percent	Sed. Wt. g	Conc. mg/l	Remarks
236C	2	1046	1.3	22:40:40	30.7	26.06	1,537.8	85.9	0.0285	5.7	
237A	1	1048	13.5	13:23:51	28.0	33.04	1,539.4	28.1	0.0369	7.4	Background
237A	2	1050	12.4	14:40:50	28.2	32.50	1,539.3	91.2	0.0218	4.4	
237A	2	1051	8.2	14:42:07	29.9	29.24	1,539.5	95.5	0.0239	4.8	
237B	1	1054	12.8	21:49:57	28.0	33.18	1,539.7	51.3	0.0791	15.8	Background
237B	2	1056	11.3	22:50:22	28.0	33.02	1,539.5	81.2	0.8319	166.4	
237B	2	1057	6.7	22:51:39	29.6	30.83	1,540.5	95.9	0.0033	0.7	
238A	1	1059	11.6	12:47:25	28.3	32.94	1,539.9	73.5	0.0108	2.2	Background
238A	1	1060	1.2	12:50:20	29.9	28.25	1,538.3	95.3	0.0036	0.7	
238A	2	--	--	14:52:00	--	--	--	--	--	--	Salinity samples only
238B	1	1061	12.2	11:27:19	28.2	33.25	1,540.1	81.6	0.0218	4.4	Background
239A	1	1063	13.6	12:42:36	28.3	33.14	1,540.2	52.6	0.0486	9.7	Background
239A	2	1065	11.0	14:13:28	28.8	32.67	1,540.7	86.4	0.0623	12.5	
239A	2	1066	11.1	14:13:44	28.8	32.66	1,540.7	85.5	0.0447	8.9	
239A	2	1067	11.1	--	--	--	--	--	0.0514	10.3	No marker file
239A	2	1068	11.0	--	--	--	--	--	0.0207	4.1	No marker file
239A	2	1069	8.7	14:16:15	29.3	31.94	1,541.0	95.8	0.0085	1.7	
239A	2	1070	8.8	14:16:41	29.3	31.88	1,541.0	95.9	0.0052	1.0	

(Continued)

Table 4.2 (Continued)

Survey No.	Cast No.	Bottle No.	Depth m	Time GMT	T deg C	S PSU	V, m/sec	Trans. percent	Sed. Wt. g	Conc. mg/l	Remarks
239A	2	1073	1.2	14:19:05	30.2	27.39	1,538.1	92.5	0.0123	2.5	
239B	1	--	--	--	--	--	--	--	--	--	Equipment check
239B	2	1074	10.4	21:47:34	28.6	33.07	1,540.8	88.7	0.0115	2.3	
239B	3	--	--	23:21:00	--	--	--	--	--	--	Salinity samples only
240A	1	1082	11.5	13:07:55	28.6	32.95	1,540.8	79.9	0.0382	7.6	
240A	1	1083	1.2	13:12:06	30.1	26.21	1,536.9	91.9	0.0288	5.8	
240A	2	1084	10.7	13:42:11	28.9	32.56	1,540.8	89.0	0.6208	124.2	
240A	2	1085	10.7	13:42:26	28.9	32.61	1,540.9	89.1	0.3144	62.9	
240A	2	1086	10.7	13:42:44	28.9	32.51	1,540.9	88.96	0.1019	20.4	
240A	2	1087	4.3	13:44:16	30.3	27.25	1,538.3	94.6	0.0317	6.3	
240A	2	1088	1.3	13:45:44	30.2	26.40	1,537.0	91.1	0.0167	3.3	
240A	3	--	--	15:16:00	--	--	--	--	--	--	Salinity samples only
240B	1	--	--	--	--	--	--	--	--	--	ARMS site, no samples kept
240B	2	1089	11.4	19:53:47	28.8	33.38	1,541.5	87.7	0.0174	3.5	Background
240B	2	1091	9.8	20:39:44	28.9	33.16	1,541.4	93.4	0.0181	3.6	
240B	2	1092	9.8	20:39:59	28.9	32.96	1,541.3	92.4	0.0200	4.0	
240B	2	1093	9.8	20:40:17	29.0	32.64	1,541.1	90.9	0.0141	2.8	
240B	2	1094	9.8	20:40:58	29.0	32.70	1,541.1	91.4	0.0282	5.6	

(Continued)

Table 4.2 (Continued)

Survey No.	Cast No.	Bottle No.	Depth m	Time GMT	T deg C	S PSU	V _r m/sec	Trans. percent	Sed. Wt. g	Conc. mg/l	Remarks
240B	2	1095	9.8	20:41:36	28.8	33.42	1,541.5	88.8	0.0285	5.7	
240B	2	1096	9.8	20:41:54	28.8	33.47	1,541.5	89.6	0.0248	5.0	
240B	2	1097	9.8	20:42:53	28.8	33.44	1,541.6	91.7	0.0092	1.8	
240B	2	1098	9.8	20:43:45	28.9	32.64	1,541.0	90.6	0.0334	6.7	
240B	2	1099	9.8	20:44:05	28.9	32.68	1,541.1	90.7	0.0379	7.6	
240B	3	1100	9.8	20:45:06	28.9	33.06	1,541.3	92.0	0.0293	5.9	
241A	1	--	--	--	--	--	--	--	--	--	ARMS site, no samples
241A	2	1101	10.5	11:05:42	28.7	32.76	1,540.7	85.8	0.5436	108.7	Background
241A	3	--	--	--	--	--	--	--	--	--	ARMS site, no samples
241B	1	1076	11.1	18:17:53	28.8	32.94	1,541.0	67.5	0.0269	5.4	Background
241B	2	1107	5.5	18:52:34	28.9	27.09	1,537.2	91.1	0.0104	2.1	
241B	2	1108	5.6	18:53:42	29.9	27.09	1,537.2	91.2	0.8989	179.8	
241B	2	1109	5.6	18:58:21	29.9	27.38	1,537.6	17.9	0.4503	90.1	
241B	2	1110	5.5	18:58:47	29.9	27.32	1,537.6	15.5	0.8909	178.2	
241B	2	1111	5.6	18:59:04	30.0	27.21	1,537.5	25.0	0.5621	112.4	
241B	2	1112	5.5	18:59:24	29.9	27.18	1,537.4	60.3	0.4957	99.1	
241C	1	--	--	--	--	--	--	--	--	--	ARMS site, no samples
242A	1	1078	5.8	15:43:34	30.0	28.34	1,538.9	89.7	0.0177	3.5	Background

(Continued)

(Sheet 5 of 7)

Table 4.2 (Continued)

Survey No.	Cast No.	Bottle No.	Depth m	Time GMT	T deg C	S PSU	V, m/sec	Trans. percent	Sed. Wt. g	Conc. mg/l	Remarks
242A	2	1103	7.2	16:08:37	30.0	28.26	1,538.6	52.2	0.1473	29.5	
242A	2	1104	7.2	16:09:07	29.9	28.31	1,538.6	53.4	0.1558	31.2	
242A	2	1105	7.2	16:09:39	29.9	28.41	1,538.6	22.8	0.1975	39.5	
242A	2	1106	7.2	16:09:56	29.9	28.76	1,538.9	19.1	0.2517	50.3	
242A	2	1113	7.2	16:10:12	29.9	28.87	1,539.1	21.6	0.2075	41.5	
242A	2	1114	7.2	16:10:29	29.9	29.09	1,539.3	59.5	0.2285	45.7	
242A	2	1115	7.2	16:11:05	29.9	28.48	1,538.8	52.6	0.1820	36.4	
242A	2	1116	7.1	16:11:44	29.9	28.46	1,538.8	53.3	0.5849	117.0	
242A	2	1117	7.2	16:12:12	29.9	28.55	1,538.9	44.8	0.2104	42.1	
242A	2	1118	7.2	16:12:29	29.9	28.46	1,538.8	49.2	0.2044	40.9	
242B	1	1077	11.0	22:46:01	29.1	32.28	1,541.0	74.2	0.0526	10.5	Background
242B	2	1001	5.0	23:33:37	30.3	28.23	1,539.2	0.0	6.5300	1306.0	
242B	2	1007	4.8	23:33:54	30.3	28.27	1,539.2	0.0	1.7663	353.3	
242B	2	1010	5.0	23:34:11	30.2	28.40	1,539.3	0.0	10.7490	2149.8	
242B	2	1014	4.9	23:34:29	30.0	28.71	1,539.2	0.0	16.7842	3356.8	
242B	2	1017	3.8	23:35:03	30.1	28.82	1,539.4	0.0	8.7464	1749.3	
242B	2	1025	3.9	23:35:22	30.3	28.48	1,539.5	0.2	4.3927	878.5	
242B	2	1026	3.9	23:35:44	30.2	28.37	1,539.3	0.2	1.2156	243.2	

(Continued)

Table 4.2 (Concluded)

Survey No.	Cast No.	Bottle No.	Depth m	Time GMT	T deg C	S PSU	V, m/sec	Trans. percent	Sed. Wt. g	Conc. mg/l	Remarks
242B	2	1029	3.9	23:36:00	30.2	28.60	1,539.4	0.0	3.1089	621.8	
242B	2	1032	3.8	23:36:15	30.3	28.38	1,539.4	0.0	3.3047	660.9	
242B	2	1037	3.8	23:36:33	30.1	28.62	1,539.3	0.1	2.2373	447.5	
242B	2	1039	3.8	23:36:50	30.1	28.92	1,539.6	0.4	2.9658	593.2	
242B	2	1040	3.8	23:37:08	30.2	28.57	1,539.3	0.8	3.4035	680.7	
243B	1	1090	8.8	17:18:02	29.2	31.65	1,540.7	55.3	0.1127	22.5	Background
244MRP	1	1064	35.1	05:54:23	25.5	36.15	1,537.4	76.2	0.0181	3.6	Mississippi River plume
244MRP	1	1071	27.4	05:56:00	26.4	36.14	1,539.5	88.8	0.0074	1.5	
244MRP	1	1072	19.9	05:57:34	28.2	35.61	1,542.7	89.4	0.0100	2.0	
244MRP	1	1075	10.0	05:59:24	29.1	31.92	1,540.6	91.4	0.0045	0.9	
244MRP	2	1047	23.2	09:14:26	28.4	35.45	1,543.0	91.0	0.0179	3.6	
244MRP	2	1049	19.8	09:16:02	28.4	35.39	1,543.0	88.7	0.0023	0.5	
244MRP	2	1052	15.5	09:18:05	28.8	33.94	1,542.2	87.0	0.0073	1.5	
244MRP	2	1053	1.5	09:19:55	30.9	21.86	1,533.9	89.1	0.0038	0.8	
244MRP	3	--	--	--	--	--	--	--	--	--	Salinity samples only

Table 4.3

Grain Size Statistics for Suspended Sediment Samples

Survey No.	Bottle No.	ϕ_{16}	ϕ_{30}	ϕ_{64}	$\bar{\phi}$	σ_{ϕ}	α_{ϕ}	D_{40}^*	D_{50}^*	D_{90}^*	\bar{D}^*	σ_D^*	C_u
234A	1002	5.56	6.38	7.77	6.57	1.11	0.17	14.3	12.2	3.4	10.5	464.3	4.2
235A	1003	4.23	5.55	6.29	5.36	1.03	-0.19	24.8	21.3	11.2	24.4	490.7	2.2
235A	1004	3.95	5.73	6.48	5.39	1.27	-0.27	22.0	19.2	9.0	23.9	415.2	2.4
235B	1005	4.42	5.78	6.62	5.61	1.10	-0.16	21.3	18.6	8.2	20.5	465.1	2.6
235B	1006	4.62	5.60	6.41	5.54	0.89	-0.06	24.4	20.8	9.8	21.5	538.5	2.5
235B	1008	3.44	4.64	6.42	4.83	1.49	0.13	58.7	40.4	9.2	35.1	356.3	6.4
235B	1009	3.52	4.87	6.12	4.84	1.30	-0.03	46.3	34.3	12.1	35.0	405.6	3.8
235B	1012	4.32	6.06	7.30	5.89	1.49	-0.11	19.7	15.4	4.7	16.8	355.6	4.2
235B	1013	4.42	5.78	6.70	5.63	1.14	-0.13	21.5	18.6	7.8	20.1	454.5	2.8
235B	1015	4.90	5.77	6.59	5.75	0.84	-0.02	21.0	18.8	7.7	18.6	558.2	2.7
235B	1016	4.60	6.30	7.50	6.13	1.45	-0.12	16.7	13.0	3.8	14.2	365.2	4.3
236A	1018	5.80	6.42	7.44	6.56	0.82	0.16	13.3	11.8	4.4	10.6	566.7	3.0
236A	1019	3.93	5.43	6.85	5.40	1.46	-0.02	31.1	23.2	6.5	23.6	363.4	4.8
236A	1020	5.69	6.29	7.25	6.41	0.78	0.16	14.8	13.1	5.4	11.8	583.8	2.8
236A	1021	4.48	5.56	6.34	5.46	0.93	-0.11	25.3	21.3	11.0	22.7	526.2	2.3
236A	1022	3.95	6.24	7.32	5.84	1.68	-0.24	20.3	13.6	5.2	17.5	311.1	3.9
236A	1023	5.16	5.91	6.56	5.87	0.70	-0.05	19.2	17.1	8.8	17.1	615.1	2.2
236A	1024	3.86	5.83	6.53	5.41	1.33	-0.32	21.3	18.0	9.0	23.6	397.0	2.4
236B	1027	4.17	5.64	6.41	5.40	1.12	-0.21	24.0	20.3	10.0	23.6	459.6	2.4
236B	1028	6.11	6.76	7.98	6.95	0.94	0.20	10.8	9.5	2.9	8.1	521.4	3.7
236B	1030	4.58	5.58	6.35	5.50	0.88	-0.08	24.7	21.1	10.9	22.1	542.6	2.3
236B	1031	3.98	5.84	7.38	5.74	1.70	-0.06	21.6	17.9	4.2	18.8	307.6	5.2

(Continued)

* D (diameter) in microns = 0.001 mm.

Table 4.3 (Continued)

Survey No.	Bottle No.	ϕ_{16}	ϕ_{10}	ϕ_{41}	$\bar{\phi}$	σ_{ϕ}	α_{ϕ}	D_{40}	D_{50}	D_{80}	\bar{D}	σ_D	C_u
236B	1033	4.80	5.91	6.72	5.81	0.96	-0.11	19.7	17.0	7.2	17.8	514.1	2.7
236B	1034	5.18	5.88	6.48	5.85	0.65	-0.05	19.2	17.4	8.9	17.4	636.6	2.2
236B	1035	5.03	5.74	6.50	5.75	0.74	0.02	21.1	19.1	7.9	18.5	600.5	2.7
236B	1036	5.03	5.65	6.29	5.65	0.63	0.01	22.1	20.3	11.5	19.9	645.5	1.9
236C	1038	4.67	5.48	6.34	5.50	0.83	0.02	25.6	22.3	10.2	22.2	561.8	2.5
236C	1041	4.94	5.85	6.63	5.81	0.84	-0.05	20.2	17.8	8.4	17.9	556.9	2.4
236C	1042	4.93	5.95	6.83	5.91	0.95	-0.05	19.4	16.6	7.1	16.7	518.2	2.7
236C	1043	3.23	5.05	6.45	4.91	1.61	-0.09	49.2	30.1	8.5	33.2	327.4	5.8
236C	1044	4.30	5.78	6.49	5.52	1.09	-0.24	21.3	18.6	8.8	21.7	468.9	2.4
236C	1045	5.36	6.45	7.45	6.42	1.04	-0.03	13.7	11.5	4.3	11.7	485.2	3.2
236C	1046	4.95	6.09	6.80	5.95	0.93	-0.16	17.5	15.1	7.9	16.2	525.8	2.2
237A	1048	5.06	5.67	6.34	5.69	0.64	0.03	21.8	20.0	11.0	19.4	641.5	2.0
237A	1050	0.00	6.12	7.31	4.48	3.65	-0.45	18.3	14.8	4.6	44.9	79.4	3.9
237A	1051	3.66	4.86	6.76	5.09	1.55	0.15	47.8	34.7	7.2	29.3	341.9	6.6
237B	1054	5.31	6.21	7.05	6.19	0.87	-0.02	15.6	13.9	6.0	13.7	547.2	2.6
237B	1056	5.04	5.92	6.49	5.82	0.73	-0.15	19.2	16.9	9.4	17.7	605.0	2.0
237B	1057	3.62	5.82	7.64	5.70	2.01	-0.06	25.6	18.1	2.9	19.3	247.9	8.9
238A	1059	3.89	6.09	7.10	5.69	1.61	-0.25	20.7	15.1	6.0	19.3	327.9	3.5
238A	1060	3.76	5.33	7.37	5.48	1.80	0.09	43.9	25.1	4.7	22.4	286.4	9.3
238B	1061	5.81	6.37	7.36	6.51	0.78	0.19	13.6	12.3	4.7	10.9	583.4	2.9
239A	1063	5.03	5.72	6.49	5.75	0.73	0.03	21.7	19.3	8.7	18.6	602.8	2.5
239A	1065	4.86	6.29	7.26	6.13	1.20	-0.13	14.9	13.1	5.2	14.2	435.8	2.9
239A	1066	5.03	5.68	6.32	5.68	0.64	-0.00	21.7	19.9	11.4	19.6	640.3	1.9
239A	1067	3.35	5.52	6.41	5.09	1.53	-0.28	28.2	21.8	9.6	29.3	345.3	2.9
239A	1068	3.92	6.02	6.98	5.64	1.53	-0.25	20.2	15.8	6.2	20.1	346.1	3.3
239A	1069	5.03	6.72	7.68	6.48	1.33	-0.18	10.9	9.7	3.8	11.2	398.4	2.9

(Continued)

(Sheet 2 of 5)

Table 4.3 (Continued)

Survey No.	Bottle No.	ϕ_{16}	ϕ_{30}	ϕ_{34}	$\bar{\phi}$	σ_{ϕ}	α_{ϕ}	D_{40}	D_{50}	D_{80}	\bar{D}	σ_D	C_u
239A	1070	4.01	5.67	7.16	5.61	1.57	-0.03	30.4	20.0	5.6	20.4	336.4	5.4
239A	1073	4.15	5.80	6.58	5.51	1.22	-0.24	20.8	18.3	7.8	21.9	430.0	2.7
239B	1074	4.47	6.39	7.30	6.05	1.41	-0.23	14.1	12.1	5.2	15.1	375.3	2.7
240A	1082	4.86	5.88	7.06	5.93	1.10	0.05	20.1	17.4	5.1	16.4	466.3	4.0
240A	1083	3.77	5.38	7.81	5.66	2.02	0.14	41.7	24.1	3.4	19.8	246.7	12.4
240A	1084	4.29	6.11	7.54	5.98	1.62	-0.08	19.1	14.9	3.9	15.8	325.3	4.9
240A	1085	4.35	5.38	6.25	5.33	0.95	-0.06	27.9	24.1	11.3	24.9	517.7	2.5
240A	1086	5.19	5.90	6.82	5.97	0.82	0.09	19.4	17.2	7.2	15.9	567.6	2.7
240A	1087	3.11	5.22	6.33	4.89	1.61	-0.21	39.5	27.1	10.8	33.8	327.8	3.7
240A	1088	4.06	5.48	7.58	5.71	1.76	0.13	32.8	22.3	4.0	19.1	295.2	8.2
240B	1089	3.61	5.17	6.71	5.16	1.55	-0.01	43.2	27.9	7.5	27.9	342.1	5.7
240B	1091	3.45	4.55	7.04	5.01	1.79	0.26	54.9	42.8	6.0	31.0	288.7	9.1
240B	1092	3.76	5.12	6.63	5.17	1.43	0.04	38.2	28.9	8.0	27.8	370.0	4.8
240B	1093	3.54	6.12	7.41	5.69	1.94	-0.22	29.1	14.8	4.7	19.4	261.4	6.2
240B	1094	4.80	6.19	7.99	6.32	1.59	0.09	17.1	14.1	2.5	12.5	331.2	6.8
240B	1095	4.74	7.36	>10	--	--	--	8.5	6.1	<2	--*	--	--
240B	1096	3.58	6.26	7.60	5.81	2.01	-0.22	16.0	13.4	3.3	17.8	248.8	4.9
240B	1097	3.28	5.86	6.61	5.25	1.66	-0.37	21.1	17.7	8.5	26.3	315.6	2.5
240B	1098	3.27	5.92	6.87	5.35	1.80	-0.32	20.7	17.0	5.9	24.5	287.6	3.5
240B	1099	3.21	5.83	8.01	5.68	2.40	-0.06	39.1	18.1	2.6	19.5	189.0	15.3
240B	1100	3.71	5.75	6.68	5.38	1.49	-0.25	28.6	19.0	8.1	24.0	356.6	3.5
241A	1101	4.57	5.41	6.59	5.52	1.01	0.11	27.7	23.5	8.1	21.8	496.2	3.4
241B	1076	4.82	6.04	6.82	5.90	1.00	-0.15	18.1	15.6	7.5	16.8	499.2	2.4

(Continued)

* Not available.

Table 4.3 (Continued)

Survey No.	Bottle No.	ϕ_{16}	ϕ_{30}	ϕ_{84}	$\bar{\phi}$	σ_{ϕ}	α_{ϕ}	D_{40}	D_{30}	D_{90}	\bar{D}	σ_D	C_u
241B	1107	2.97	3.79	5.95	4.24	1.49	0.30	85.4	73.4	9.1	53.0	355.6	9.4
241B	1108	4.48	5.57	6.48	5.51	1.00	-0.06	25.2	21.1	8.8	21.9	501.2	2.8
241B	1109	5.17	6.10	7.00	6.09	0.91	-0.01	17.4	15.0	6.1	14.7	530.4	2.9
241B	1110	4.85	5.89	6.95	5.89	1.05	0.01	20.3	17.4	6.4	16.8	482.4	3.2
241B	1111	4.78	5.52	6.33	5.54	0.78	0.03	24.9	21.8	10.8	21.4	583.7	2.3
241B	1112	4.86	5.61	6.30	5.59	0.72	-0.03	23.2	20.7	11.2	20.8	606.9	2.1
242A	1078	3.52	4.85	6.76	5.05	1.62	0.12	42.6	34.9	5.8	30.3	325.3	7.4
242A	1103	3.92	4.67	6.11	4.90	1.10	0.21	47.7	39.5	11.5	33.5	467.9	4.1
242A	1104	4.37	5.29	6.25	5.31	0.94	0.02	29.5	25.8	11.1	25.3	520.9	2.7
242A	1105	3.28	4.44	5.95	4.56	1.34	0.09	60.7	46.4	12.7	42.4	396.3	4.8
242A	1106	5.22	5.88	6.50	5.86	0.64	-0.02	19.5	17.5	8.9	17.2	641.8	2.2
242A	1113	5.25	6.06	6.91	6.07	0.83	0.02	17.8	15.4	6.8	14.8	564.1	2.6
242A	1114	5.24	6.48	7.51	6.41	1.13	-0.06	13.6	11.2	4.4	11.8	455.9	3.1
242A	1115	5.39	6.27	7.28	6.31	0.95	0.05	15.5	13.3	5.4	12.6	519.3	2.9
242A	1116	3.73	5.13	6.43	5.10	1.35	-0.03	38.3	28.6	8.9	29.2	392.1	4.3
242A	1117	4.09	5.19	6.23	5.17	1.07	-0.02	33.2	27.7	11.3	27.8	477.0	2.9
242A	1118	3.09	6.56	8.86	6.17	2.88	-0.14	20.5	10.6	0.0	13.9	135.4	--
242B	1077	3.33	4.56	6.31	4.74	1.49	0.12	55.3	42.3	10.2	37.5	356.5	5.4
242B	1001	3.88	4.94	5.86	4.89	0.99	-0.05	39.9	32.5	14.9	33.7	503.7	2.7
242B	1007	5.13	5.78	6.56	5.82	0.72	0.06	20.8	18.6	8.4	17.7	607.9	2.5
242B	1010	3.34	4.72	6.11	4.72	1.38	-0.00	53.0	38.2	12.1	37.9	383.0	4.4
242B	1014	4.20	5.24	6.28	5.24	1.04	0.00	30.8	26.7	10.7	26.5	487.7	2.9
242B	1017	3.68	5.19	6.32	5.07	1.32	-0.10	36.3	27.6	10.4	29.9	401.0	3.5
242B	1025	3.80	5.19	6.41	5.14	1.31	-0.04	33.9	27.5	8.9	28.5	403.9	3.8
242B	1026	4.69	5.64	6.77	5.70	1.04	0.06	24.1	20.4	7.2	19.2	485.9	3.4
242B	1029	4.51	5.52	6.44	5.49	0.96	-0.03	25.9	21.8	9.1	22.2	512.8	2.8
242B	1032	4.23	5.38	6.64	5.42	1.20	0.03	28.9	24.1	7.4	23.4	434.3	3.9

(Continued)

(Sheet 4 of 5)

Table 4.3 (Concluded)

Survey No.	Bottle No.	ϕ_{16}	ϕ_{50}	ϕ_{84}	$\bar{\phi}$	σ_{ϕ}	α_{ϕ}	D_{40}	D_{50}	D_{90}	\bar{D}	σ_D	C_u
242B	1037	5.18	5.97	6.98	6.04	0.90	0.08	18.8	16.3	6.1	15.2	534.5	3.1
242B	1039	4.61	5.67	6.71	5.66	1.05	-0.01	23.3	19.9	7.6	19.7	482.3	3.1
242B	1040	3.71	4.99	6.00	4.90	1.14	-0.08	42.0	31.2	13.0	33.5	453.1	3.2
243B	1090	5.48	6.18	6.97	6.21	0.74	0.04	15.9	14.2	6.5	13.5	597.0	2.4
244MRP*	1064	4.49	5.68	6.75	5.64	1.13	-0.03	22.5	19.8	6.5	20.0	457.4	3.5
244MRP	1071	4.14	6.32	7.98	6.15	1.92	-0.09	15.4	12.8	2.4	14.1	264.4	6.5
244MRP	1072	3.82	5.83	7.16	5.60	1.67	-0.14	23.9	18.0	5.1	20.6	314.8	4.7
244MRP	1075	5.22	6.21	7.26	6.23	1.02	0.02	15.8	13.9	5.3	13.3	493.2	3.0
244MRP	1047	3.68	4.76	7.16	5.20	1.74	0.26	48.4	37.3	4.8	27.2	299.4	10.2
244MRP	1049	3.45	5.59	7.17	5.40	1.86	-0.10	27.6	20.9	4.9	23.6	275.5	5.6
244MRP	1052	3.57	5.50	6.91	5.33	1.67	-0.11	32.2	22.0	6.0	24.9	314.0	5.3
244MRP	1053	4.61	6.17	7.34	6.04	1.36	-0.10	16.9	14.3	4.4	15.2	388.6	3.8

* Mississippi River plume samples.

Table 4.4
Dredged Material Surface and Grab Samples from Hopper Barge

Sample Location No.	Depth ft	Bulk Density g/cm³	Moisture Content Percent	Sediment Content			
				Percent			
				Sand*		Fine	Silt/Clay
Coarse	Medium						
Survey 240B							
1	S**	1.270	78.6	--	--	--	--
2	S	1.270	65.6	--	--	--	--
2A	S	1.306	61.0	--	--	--	--
3	S	1.056	90.1	--	--	--	--
4	S	1.073	86.9	--	--	--	--
5	S	1.070	88.9	--	--	--	--
6	S	1.218	71.4	--	--	--	--
1	10	1.270	53.8	--	--	--	--
2	2	1.305	61.9	--	--	--	--
3	2	1.345	59.8	--	--	--	--
4	12	1.377	54.6	--	--	--	--
5	2	1.344	59.6	--	--	--	--
6	4	1.328	60.7	--	--	47	53
Survey 241B							
1	S	1.035	93.4	--	--	47	53
2	S	1.016	96.7	--	1	52	47
3	S	1.018	95.8	--	--	35	65
4	S	1.025	95.2	--	--	17	83
5	S	1.094	80.8	--	--	29	71
6	S	1.044	89.8	--	--	30	70
1	1	1.379	55.8	--	3	57	40
2	6	1.338	58.6	--	--	--	--
3	16	1.325	58.4	--	--	--	--
4	12	1.301	61.8	--	--	--	--
5	2	1.356	55.3	--	--	--	--
6	8	1.369	56.2	--	--	--	--

* Coarse-grained sand particles range from 2 to 5 mm in diameter.
Medium-grained sand particles range from 0.42 to 1.99 mm in diameter.
Fine-grained sand particles range from 0.072 to 0.41 mm in diameter.

** S = Surface water samples.

Table 4.5
Dredged Material Representative Samples from Hopper Barge*

Sample Location No.	Depth ft	Bulk Density g/cm ³	Moisture Content Percent	Sediment Content Percent			
				Sand**			Silt/Clay
				Coarse	Medium	Fine	
1	4	1.509	45.0	--	4	58	38
	11	1.706	33.9	--	1	84	15
	21	1.883	26.1	--	1	41	58
2	4	1.721	27.2	--	6	77	17
	11	1.713	31.9	--	2	48	50
	21	2.036	22.0	7	25	62	6
3	4	1.748	28.3	--	3	82	15
	11	1.681	29.9	--	7	79	14
	21	1.995	19.3	1	6	86	7
4	4	1.896	23.2	2	9	82	7
	11	1.777	30.0	--	3	87	10
	21	2.020	18.1	--	9	87	4
5	4	1.947	20.2	--	10	74	16
	11	1.893	22.5	--	4	82	14
	21	2.058	16.9	1	24	72	3
6	4	1.458	49.2	--	1	61	38
	11	1.171	35.5	--	1	64	35
	21	1.905	24.8	--	4	73	23

* Hopper Barge load samples from unmonitored night release (28 August 1989).

** Coarse-grained sand particles range from 2 to 5 mm in diameter.
Medium-grained sand particles range from 0.42 to 1.99 mm in diameter.
Fine-grained sand particles range from 0.072 to 0.41 mm in diameter.

Table 4.6
Dredged Material Bottom Grab Sampler

Survey No.	Release Time GMT	Sampling Time GMT	Sample No.	Field Observations
235A	1658	1800	2002	Silt/clay, some lumps
		1802	2003	Silt/clay, some lumps
236A	0020	0137	2004	Silt/clay, one piece hard clay, 3-in. irregular shape
		0139	2005	Silt/clay, some lumps
236B	1500	1628	2006	Silt/clay, some lumps, 2-in. oxidized pine cone, 4-in. polychaete worm
236C	2208	2330	2007	Silt/clay, some lumps, 6-in. polychaete worm
237A	1418	--	2008	Uniform soupy silt/clay
237B	2215	2335	2009	Lumpy silt/clay, some sand
		2340	2010	Lumpy silt/clay, with higher sand content
		2344	2011	Lumpy silt/clay, with higher sand content
238A	1423	1605	2012	Silt/clay, no sand, one 2-in. piece oxidized wood
		1611	2013	Sandy silt/clay
		1617	2014	Sandy silt/clay, some lumps
238B	2155	2300	2015	Sandy silt/clay, some lumps
239A	1406	1345	2016	Silt/clay, very little sand, 6-in. polychaete worm
239A	1406	1408	2017	Sandy silt in large lumps

(Continued)

Table 4.6 (Concluded)

<u>Survey No.</u>	<u>Release Time GMT</u>	<u>Sampling Time GMT</u>	<u>Sample No.</u>	<u>Field Observations</u>
239B	2213	0000	2018	Silt/mud, with sandy clumps
240A	1335	1505	2019	Large sandy clumps, some fine silty/clay lumps
		1510	2020	Loose sand, some clay lumps
240B	2036	2226	2021	Clay lumps, no sand
241A	1144	1324	2022	Sandy silt, clay lumps, little sand
241B	1846	2025	2023	Lumpy clay
		2030	2024	One large lump of clay ~8 in., broken into two pieces
242A	1606	1742	2025	Silty sand, some clay lumps
242B	2330	1014	2026	Silty sand to sandy silt with clay lumps
		1017	2027	Silty sand to sandy silt with clay lumps
243A	1803	1900	2029	Almost pure fine sand, a few small clay lumps

Table 4.7
Grain Size Distribution of Bottom Grab Samples

Survey No.	Sample No.	Phi Size									
		Sand					Silt				Clay ≥ 9
		Medium 0	1	Fine 2 3 4			5	6	7	8	
235A	2002	1*	29	61	86	95	96	97	99	99	100
	2003	2	35	68	87	94	94	96	98	99	100
236A	2004	0	30	60	83	93	94	94	96	97	99
	2005	3	27	51	82	94	94	96	98	99	100
236B	2006	1	28	54	83	94	94	96	97	99	100
236C	2007	0	40	65	80	90	91	92	95	97	99
237A	2008	2	33	65	89	94	95	97	99	100	100
237B	2009	0	19	48	90	96	97	98	99	100	100
	2010	0	16	62	92	99	99	100	100	100	100
	2011	0	22	75	92	96	96	98	99	100	100
238A	2012	0	18	48	87	93	95	97	99	99	100
	2013	0	13	53	87	95	96	98	99	99	100
	2014	0	7	52	92	99	99	100	100	100	100
238B	2015	0	15	50	86	92	93	96	98	99	100
239A	2016	0	25	55	85	92	93	97	99	99	100
	2017	0	9	37	82	95	96	98	99	99	100
239B	2018	3	17	44	93	97	98	99	99	100	100
240A	2019	3	19	61	95	98	98	99	99	100	100
	2020	0	11	61	93	99	99	100	100	100	100
240B	2021	1	26	57	87	94	94	95	97	98	100
241A	2022	2	19	60	93	98	99	99	100	100	100
241B	2023	0	19	65	87	93	95	97	98	99	100
	2024	0	10	21	60	81	89	94	97	98	100
242A	2025	0	8	30	82	94	95	97	99	99	100
242B	2026	3	33	62	87	94	94	96	97	99	100
	2027	0	2	48	94	98	98	99	100	100	100
243A	2029	1	8	46	78	89	92	95	97	99	100

* Cumulative percent larger than phi size.

Table 4.8
Mobile Field Data Collection Project Aerial Photographs

Survey No.	Film Positive No.	Time GMT	Altitude ft	Photo Scale in.:ft	Quality Rating*	Remarks
239A	--**	13:55:09	--	--	H	Tug and loaded barge
		13:55:11	--	--	H	Tug and loaded barge
	--	13:56:15	1050	--	H	Tug and loaded barge
	1	14:03:07	1175	1:13200	M	Beginning of release
	2	14:03:10	1200	1:13200	H	Barge and plume
	3	14:06:44	1000	1:12000	H	Barge and plume
	4	14:06:48	1000	1:12000	H	Barge and plume
	5	14:11:46	3050	1:36000	H	Plume and <i>R/V Pelican</i>
	6	14:11:55	3070	1:36000	H	Plume and <i>R/V Pelican</i>
	7	14:18:05	4650	1:45000	M	Sediment plume
	8	14:18:18	4620	1:45000	M	Sediment plume
	9	14:18:31	4650	1:45000	X	--
	10	14:23:07	4650	1:45000	X	--
	11	14:23:23	4650	1:45000	M	Sediment plume
	12	14:27:54	4625	1:45000	L	Sediment plume
	13	14:28:05	4650	1:45000	X	--
	14	14:32:42	4700	1:45000	X	--
	15	14:32:54	4700	1:45000	X	--
	16	14:38:16	5025	1:60000	X	--
	17	14:38:28	5075	1:60000	X	--
	18	14:42:13	5050	1:57600	X	--
	19	14:42:28	5125	1:57600	X	--
	20	14:47:55	5175	1:60000	X	--
	21	14:48:07	5200	1:60000	X	--
	22	14:53:21	5125	1:60000	X	--
	23	14:53:36	5125	1:60000	X	--
	24	14:58:39	5250	1:60000	X	--
	25	14:58:56	5250	1:60000	X	--
	26	15:03:04	5125	1:60000	X	--
	27	15:03:17	5150	1:60000	X	--
	28	15:07:52	5175	1:60000	X	--
	29	15:08:07	5175	1:60000	X	--

(Continued)

* Quality Rating: H = high, M = medium, L = low, and X = not usable.

** Not available.

(Sheet 1 of 6)

Table 4.8 (Continued)

Survey No.	Film Positive No.	Time GMT	Altitude ft	Photo Scale in.:ft	Quality Rating	Remarks
240A	--	12:59:54	1250	--	H	Loaded hopper barge
	--	12:59:57	2225	--	H	Beginning of release
	1	13:34:54	1075	1:12000	H	Barge and plume
	2	13:59:56	1100	1:12000	H	Plume, <i>R/V Pelican</i> , tug and barge
	3	13:40:15	3175	1:36000	H	Sediment plume
	4	13:40:21	3175	1:36000	H	
	5	13:45:14	3250	1:36000	M	
	6	13:45:20	3250	1:36000	H	
	7	13:50:54	3225	1:36000	M	
	8	13:51:00	3225	1:36000	H	
	9	13:56:20	3250	1:36000	M	
	10	13:56:25	3225	1:36000	H	
	11	14:00:57	3150	1:36000	H	
	12	14:01:04	3150	1:36000	L	
	13	14:07:30	3300	1:37200	L	--
	14	14:07:37	3300	1:37200	X	
	15	14:10:39	3250	1:36000	X	
	16	14:10:46	3250	1:36000	X	
	17	14:17:08	3300	1:37200	X	
	18	14:17:08	3300	1:37200	X	
240B	--	20:20:24	1450	--	H	Beginning of release
	19	20:35:48	1100	1:12000	H	Barge and plume
	20	20:35:51	1100	1:12000	H	Plume, <i>R/V Pelican</i> , tug and barge
	21	20:42:03	3650	1:42000	H	Plume and <i>R/V Pelican</i>
	22	20:42:13	3700	1:42000	H	
	23	20:47:00	4675	1:54000	H	
	24	20:47:09	4625	1:54000	H	
	25	20:51:55	4650	1:54000	H	
	26	20:52:02	4650	1:54000	M	
	27	20:56:49	4675	1:54000	H	
	28	20:56:57	4650	1:54000	M	
	29	21:01:30	4625	1:54000	M	
	30	21:01:39	4620	1:54000	L	
	31	21:07:20	4625	1:53400	M	
	32	21:07:29	4625	1:53400	M	

(Continued)

(Sheet 2 of 6)

Table 4.8 (Continued)

Survey No.	Film Positive No.	Time GMT	Altitude ft	Photo Scale in.:ft	Quality Rating	Remarks
240B	33	21:12:59	4625	1:53400	M	Plume and <i>R/V Pelican</i>
	34	21:13:05	4625	1:54000	L	Sediment plume
	35	21:17:07	4675	1:54000	L	Sediment plume
	36	21:17:15	4675	1:54000	L	Sediment plume
	37	21:22:28	4675	1:54000	X	--
	38	21:22:35	4650	1:54000	L	Sediment plume
	39	21:25:52	4600	1:54000	X	--
	40	21:25:59	4575	1:54000	X	--
	41	21:31:28	4725	1:54000	L	Sediment plume
	42	21:31:37	4700	1:54000	X	--
	43	21:35:04	4725	1:54000	X	--
	44	21:35:15	4700	1:54000	X	--
241A	All positives (Nos. 0-24)				X	--
242A	--	15:47:45	1250	1:12000	H	Tug and loaded barge
	1	16:05:30	1125	1:12000	H	Sediment plume
	2	16:05:36	1125	1:54000	H	Plume, <i>R/V Pelican</i> , tug and barge
	3	16:12:28	4550	1:54000	H	Plume and <i>R/V Pelican</i>
	4	16:12:37	4600	1:54000	H	Plume, <i>R/V Pelican</i> , tug and barge
	5	16:12:45	4625	1:54000	M	Plume, <i>R/V Pelican</i> , tug and barge
	6	16:16:09	4700	1:54000	M	Plume, <i>R/V Pelican</i> , tug and barge
	7	16:16:20	4700	1:54000	H	Plume, <i>R/V Pelican</i> , tug and barge
	8	16:16:29	4700	1:54000	L	Plume and <i>R/V Pelican</i>
	9	16:20:47	4700	1:54000	L	↓
	10	16:20:57	4700	1:54000	H	
	11	16:21:06	4700	1:54000	M	
	12	16:25:48	4650	1:54000	L	
	13	16:25:56	4650	1:54000	H	
	14	16:26:05	4650	1:54000	M	
	15	16:30:19	4650	1:54000	M	
	16	16:30:29	4650	1:54000	H	

(Continued)

(Sheet 3 of 6)

Table 4.8 (Continued)

Survey No.	Film Positive No.	Time GMT	Altitude ft	Photo Scale in.:ft	Quality Rating	Remarks
242A	17	16:30:38	4650	1:54000	M	Plume and <i>R/V Pelican</i>
	18	16:35:12	4675	1:54000	M	Plume and <i>R/V Pelican</i>
	19	16:35:22	4675	1:54000	M	Plume and <i>R/V Pelican</i>
	20	16:35:32	4675	1:54000	X	--
	21	16:42:21	4625	1:54000	X	--
	22	16:42:29	4625	1:54000	M	Plume and <i>R/V Pelican</i>
	23	16:42:37	4725	1:54000	L	↓
	24	16:46:37	4700	1:54000	L	
	25	16:46:47	4725	1:55200	L	
	26	16:46:57	4725	1:55200	L	
	27	16:50:47	4700	1:54000	L	
	28	16:50:57	4700	1:54000	L	
	29	16:51:04	4675	1:54000	L	
	30	16:55:12	4675	1:54000	L	
	31	16:55:21	4675	1:54000	L	
	32	16:55:29	4675	1:54000	X	--
	33	17:00:32	4675	1:54000	X	--
	34	17:00:41	4675	1:54000	L	Plume and <i>R/V Pelican</i>
	35	17:00:52	4700	1:54000	X	--
	36	17:05:47	4700	1:54000	X	--
	37	17:06:00	4700	1:54000	L	Plume and <i>R/V Pelican</i>
	38	17:06:09	4700	1:54000	X	--
	39	17:10:19	4725	1:54000	X	--
	40	17:10:28	4725	1:54000	L	Plume and <i>R/V Pelican</i>
	41	17:10:32	4725	1:54000	L	Plume and <i>R/V Pelican</i>
	42	17:10:32	4700	1:54000	X	--
242B	41	23:23:00	1250	--	X	--
	42	23:23:06	1300	1:12000	H	Tug and loaded barge
	43	23:29:36	1100	1:12000	M	Plume and <i>R/V Pelican</i>
	44	23:29:41	1150	1:54600	H	Plume and <i>R/V Pelican</i>
	45	23:35:28	4825	1:54600	H	Plume, <i>R/V Pelican</i> , tug and barge track
	46	23:35:33	4800	1:55200	H	↓
	47	23:39:47	4800	1:55200	H	
	48	23:39:53	4825	1:55200	H	
	49	23:45:18	4825	1:55200	L	
	50	23:45:22	4825	1:55200	L	

(Continued)

(Sheet 4 of 6)

Table 4.8 (Continued)

Survey No.	Film Positive No.	Time GMT	Altitude ft	Photo Scale in.:ft	Quality Rating	Remarks
242B	51	23:50:48	4775	1:54000	X	--
	52	23:50:57	4775	1:54000	X	--
	53	23:55:55	4800	1:55200	X	--
	54	23:56:04	4825	1:55200	X	--
	55	00:00:54	4825	1:55200	X	--
	56	00:01:03	4825	1:55200	X	--
	57	00:04:22	4800	1:55200	X	--
	58	00:04:32	4850	1:55200	X	--
243A	--	--	--	--	X	--
	2	16:02:29	1125	--	X	--
	3	18:03:12	1075	1:12000	M	Sediment plume
	4	18:03:20	1075	1:12000	H	Plume, <i>R/V Pelican</i> , tug and barge track
	5	18:10:20	4700	1:54000	M	Plume, <i>R/V Pelican</i> , tug and barge track
	6	18:10:29	4700	1:54000	M	Plume, <i>R/V Pelican</i> , tug and barge track
	7	18:16:02	5475	1:64800	H	Plume and <i>R/V Pelican</i>
	8	18:16:07	5450	1:64800	H	
	9	18:19:55	5600	1:66000	H	
	10	18:20:04	5600	1:66000	H	
	11	18:25:20	5600	1:66000	H	
	12	18:25:27	5600	1:66000	H	
	13	18:29:12	5600	1:66000	H	
	14	18:29:12	5600	1:66000	M	
	15	18:34:38	5575	1:66000	M	
	16	18:34:45	5575	1:66000	H	
	17	18:40:42	5600	1:66000	H	
	18	18:40:47	5600	1:66000	M	
	19	18:45:40	5675	1:66000	M	
	20	18:45:46	5675	1:66000	M	
	21	18:50:42	5625	1:66000	M	
	22	18:50:48	5625	1:66000	L	
	23	18:55:29	5675	1:66000	M	
	24	18:55:35	5675	1:66000	M	
	25	19:00:19	5650	1:66000	L	
	26	19:00:26	5650	1:66000	L	

(Continued)

(Sheet 5 of 6)

Table 4.8 (Concluded)

Survey No.	Film Positive No.	Time GMT	Altitude ft	Photo Scale in.:ft	Quality Rating	Remarks
243A	27	19:04:58	5600	1:66000	M	Plume and R/V Pelican
	28	19:05:03	5600	1:66000	M	
	29	19:09:35	5600	1:66000	M	
	30	19:09:41	5600	1:66000	L	
	31	19:14:21	5575	1:66000	M	
	32	19:14:26	5575	1:66000	L	
	33	19:21:30	6125	1:72000	M	
	34	19:21:37	6125	1:72000	L	
	35	19:24:59	6150	1:72000	M	
	36	19:25:05	6150	1:72000	L	Sediment plume
	37	19:29:42	6200	1:72000	M	
	38	19:29:46	6200	1:72000	L	
	39	19:35:58	6600	1:78000	L	
	40	19:36:08	6600	1:78000	L	
	41	19:39:59	6625	1:78000	M	
	42	19:40:05	6625	1:78000	L	
	43	19:45:14	6625	1:78000	M	
	44	19:45:20	6625	1:78000	L	
	45	19:50:26	6650	1:78000	M	
	46	19:50:31	6625	1:78000	L	
	47	19:56:34	6600	1:78000	M	
	48	19:56:41	6600	1:78000	L	
	49	20:00:40	6675	1:78000	M	
	50	20:00:45	6650	1:78000	L	
	51	20:05:09	6675	1:78000	M	
	52	20:05:17	6675	1:78000	L	
	53	20:10:57	6700	1:78000	M	
	54	20:11:01	6700	1:78000	L	
	55	20:15:17	6625	1:78000	L	
	56	20:15:23	6625	1:78000	L	
	57	20:20:46	6625	1:78000	L	
	58	20:20:51	6625	1:78000	X	--

(Sheet 6 of 6)

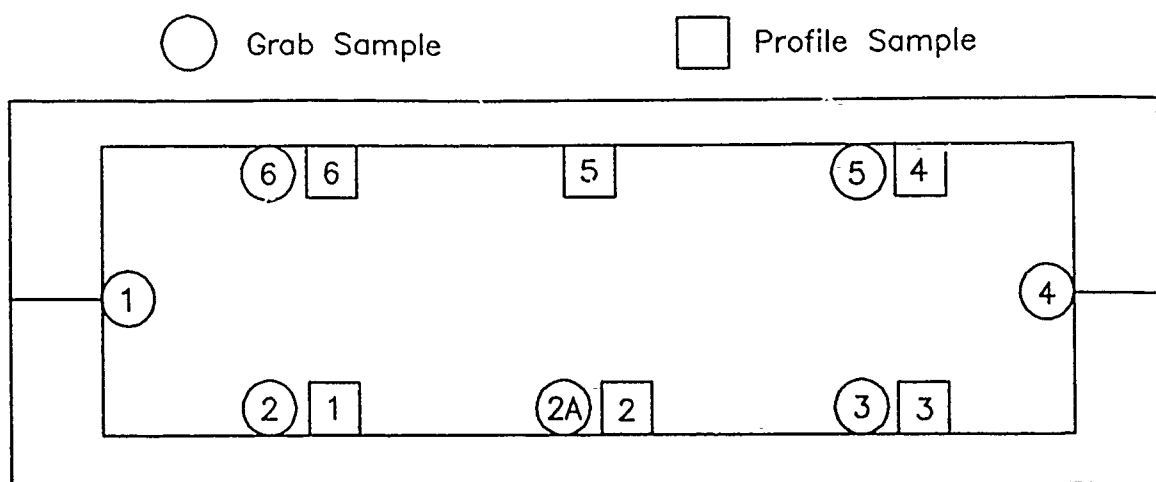


Figure 4.1. Locations of sediment grab samples and sediment profile samples. Numbers are used for sample identification.



Figure 4.2. Clamshell grab sampler used to sample dredged material in the hopper barge.

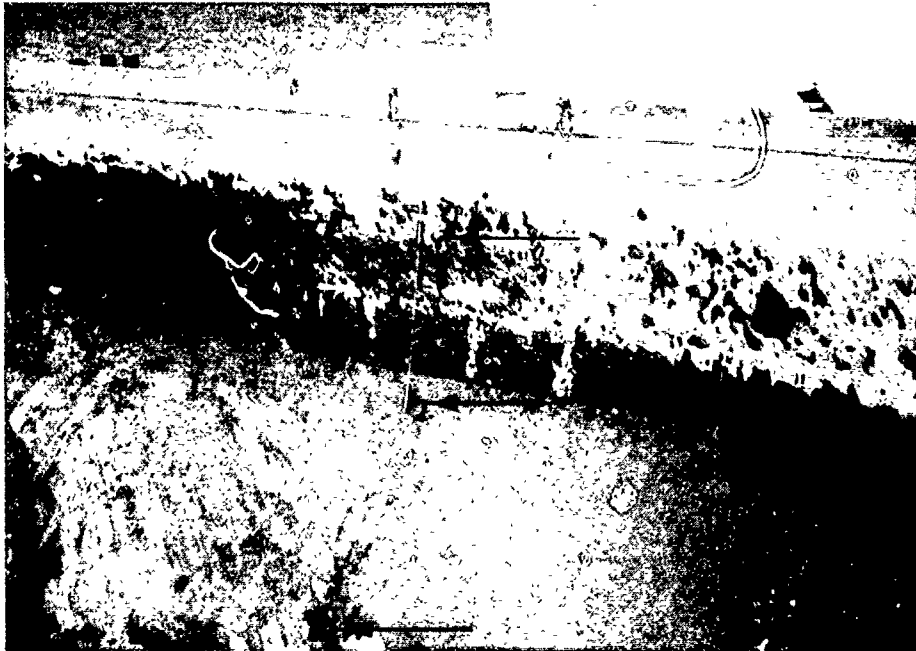


Figure 4.3. Sediment profile samplers used to collect representative sediment samples from the hopper barge. The plugs in the foreground were used to extrude the sample from the container.

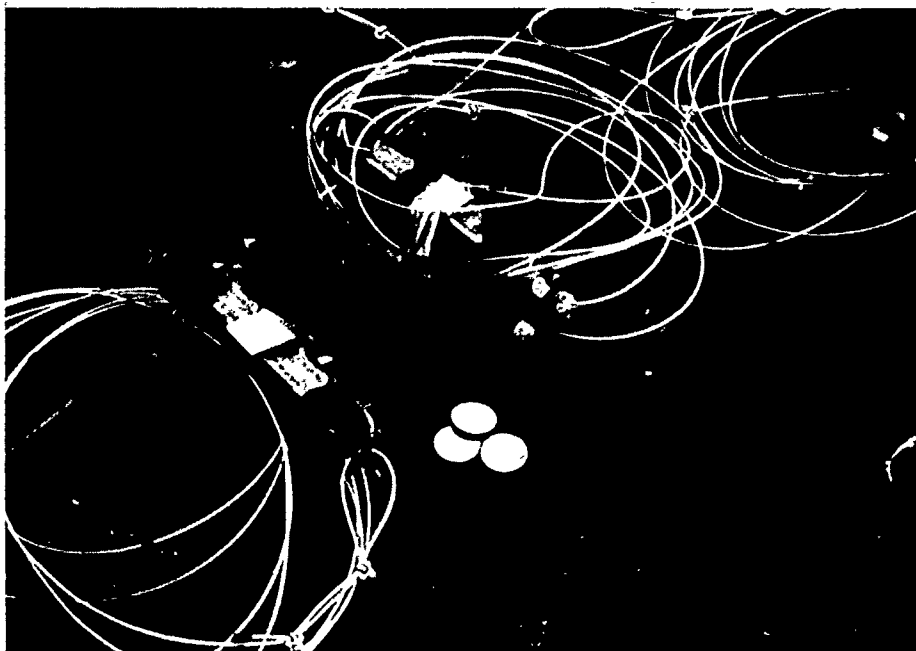
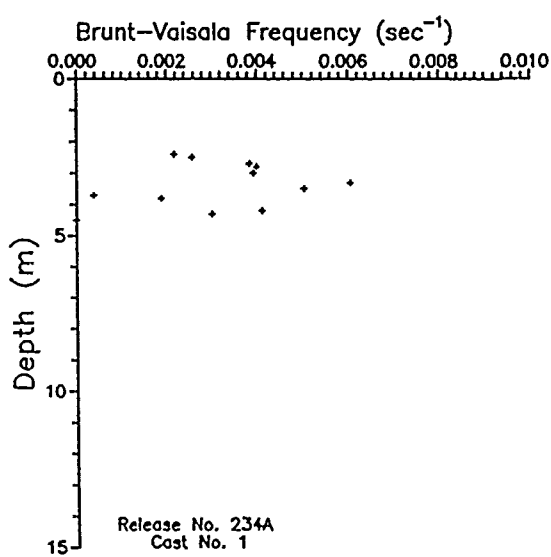
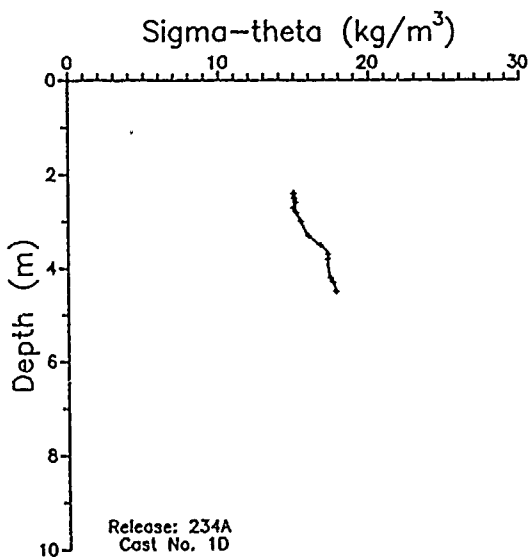
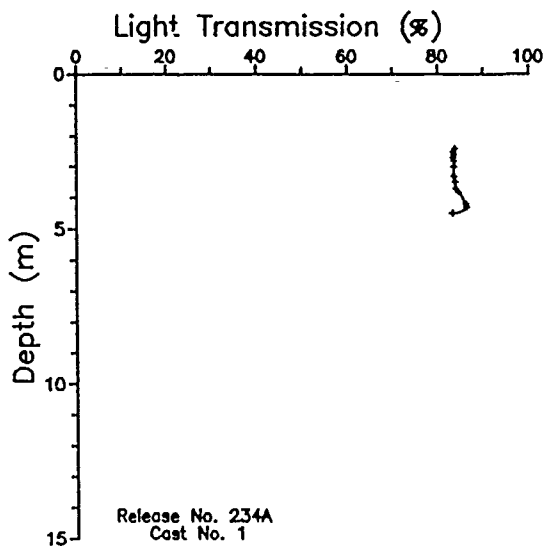
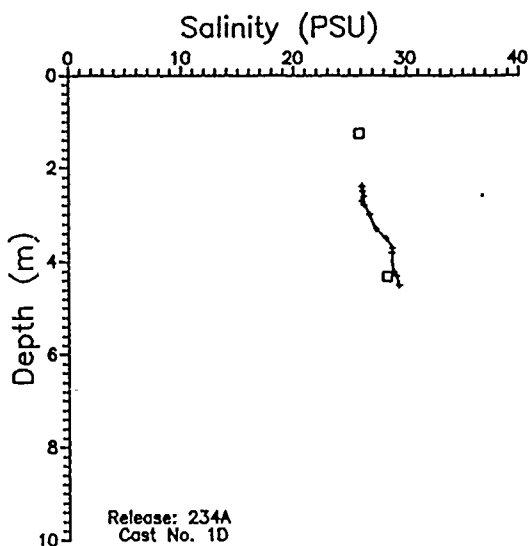
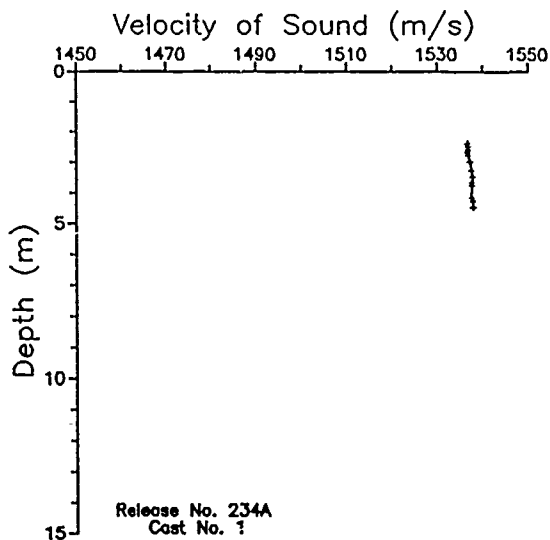
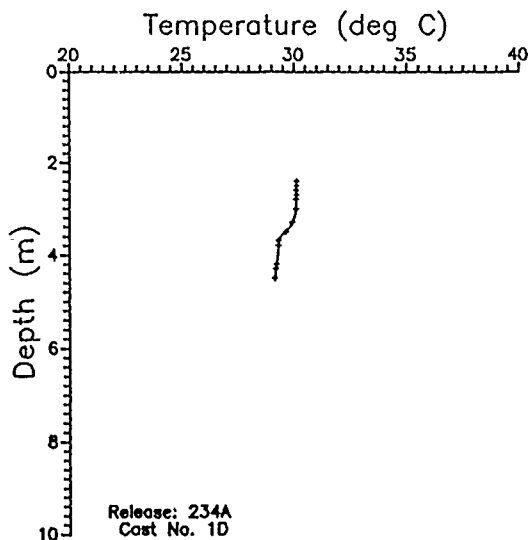
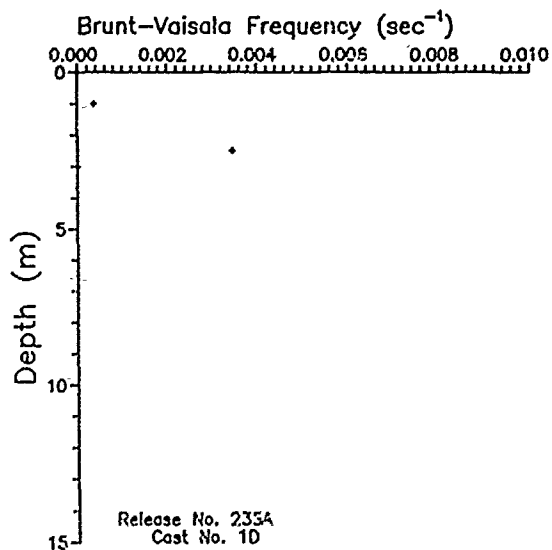
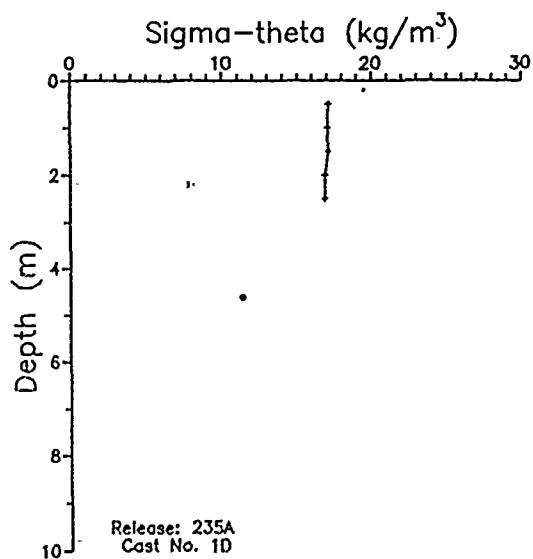
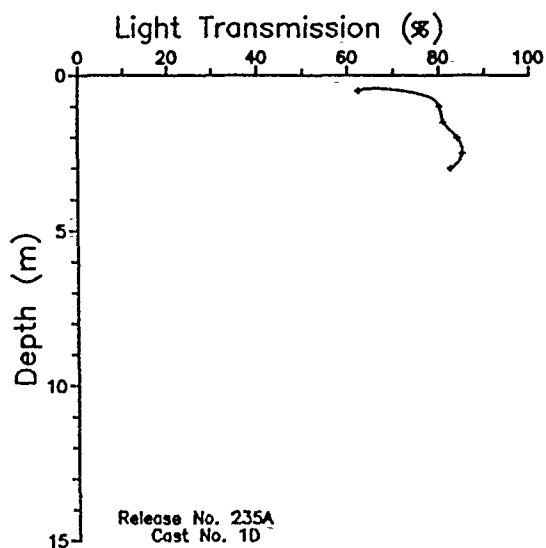
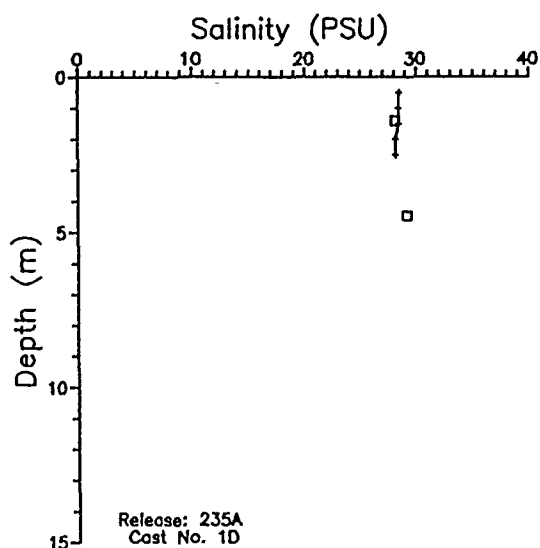
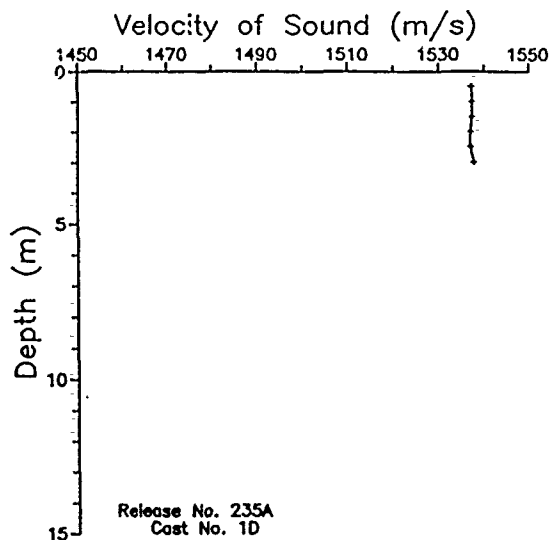
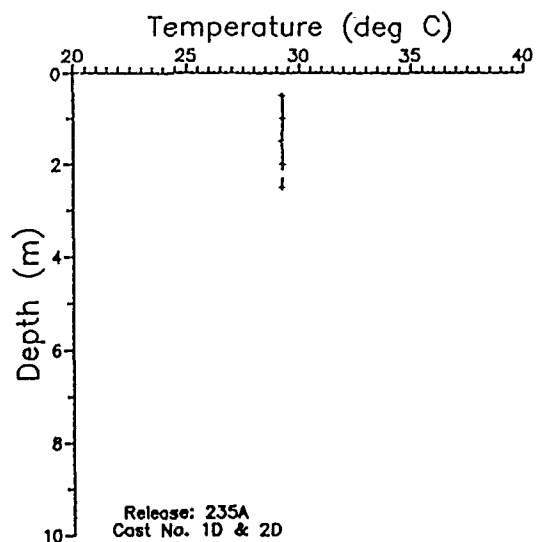
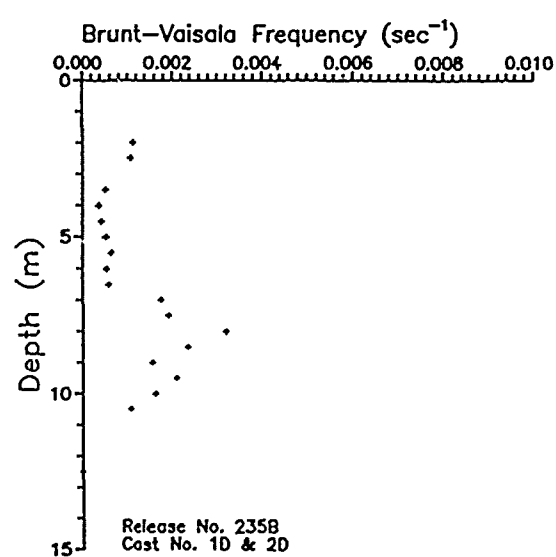
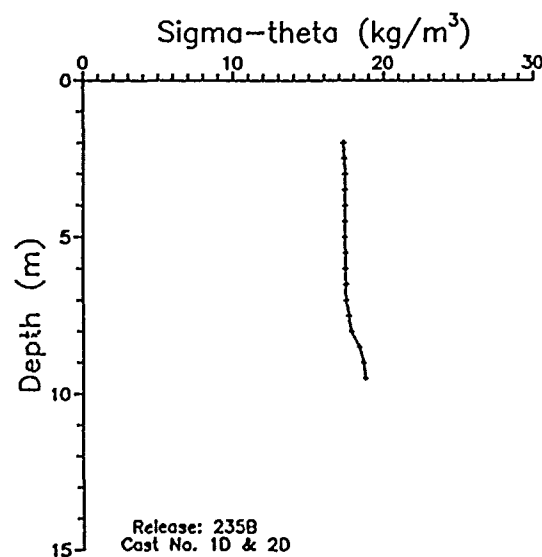
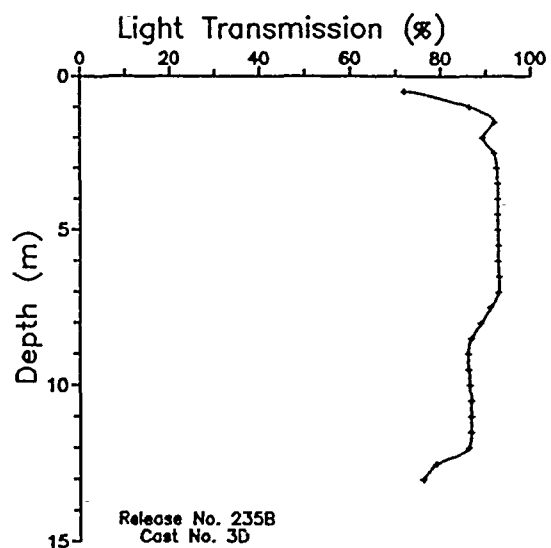
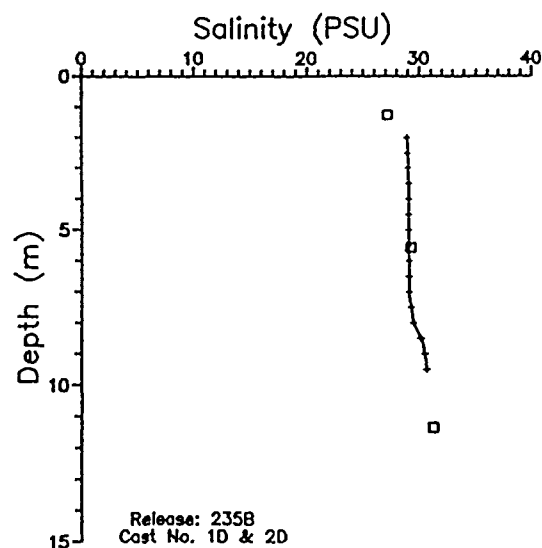
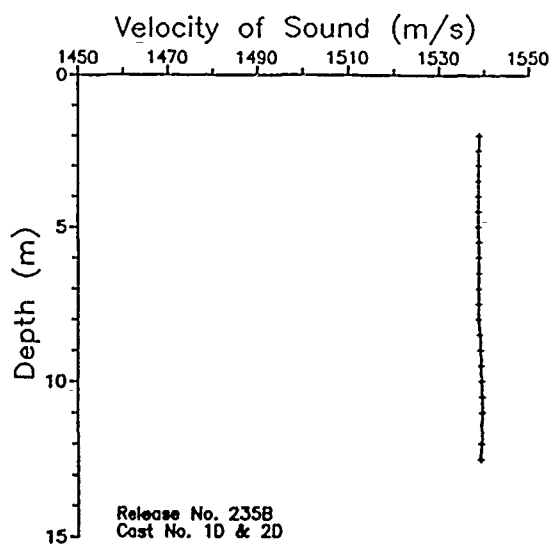
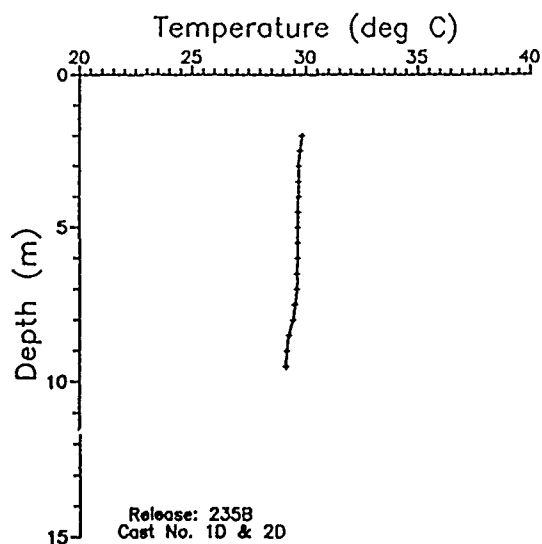


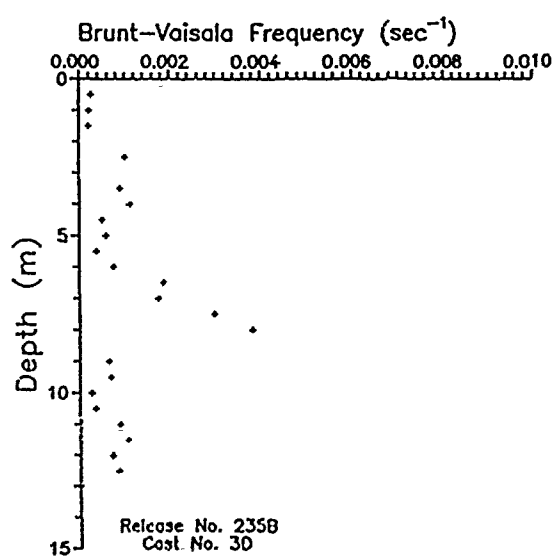
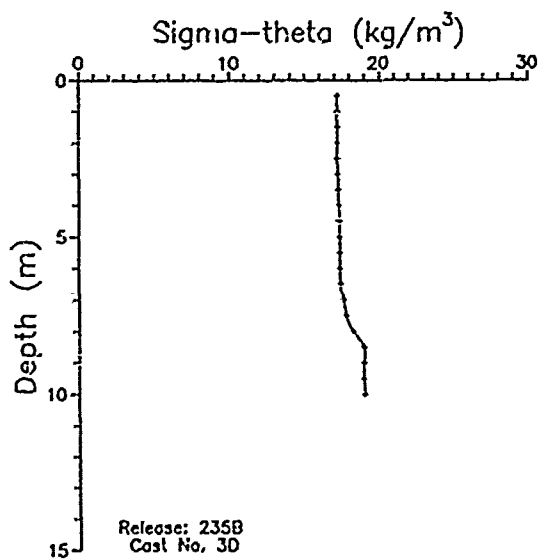
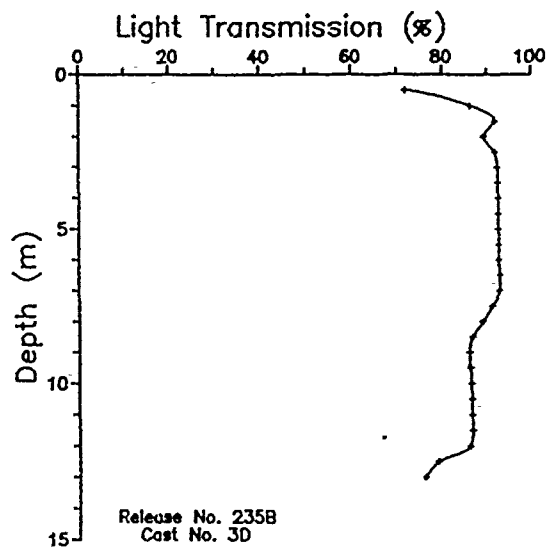
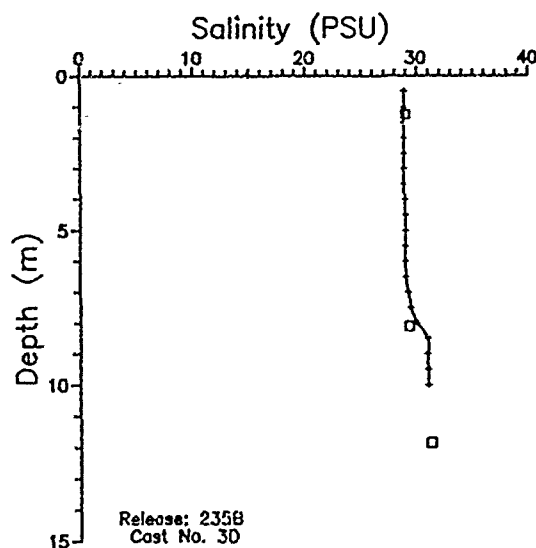
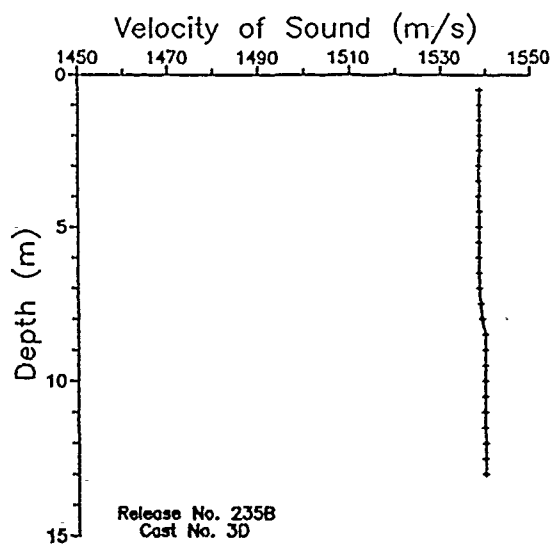
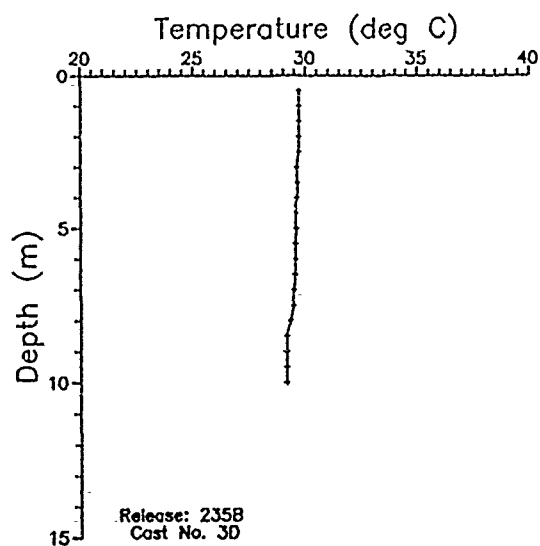
Figure 4.4. Sediment profile samplers positioned in hopper barge.

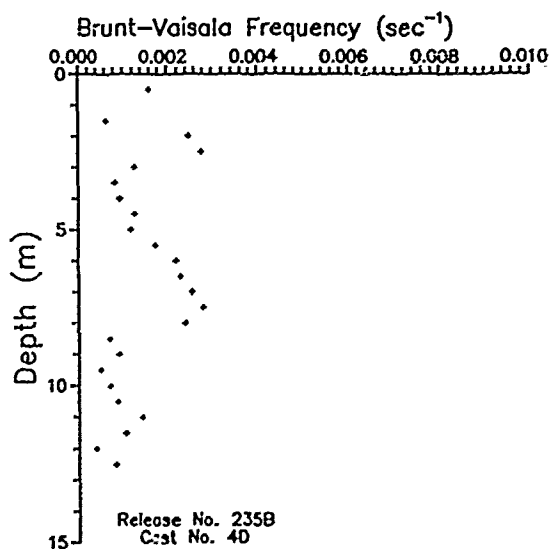
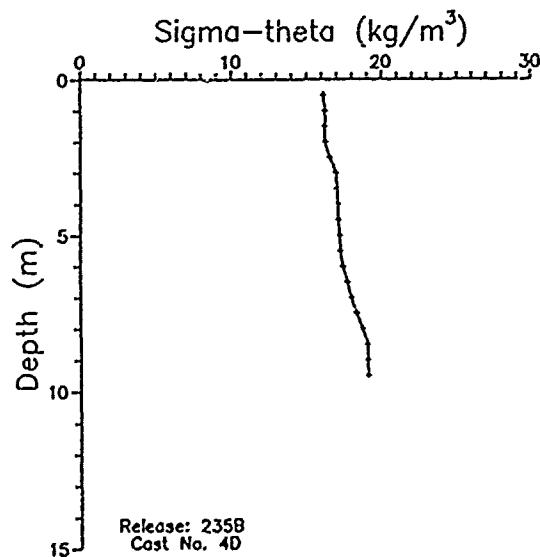
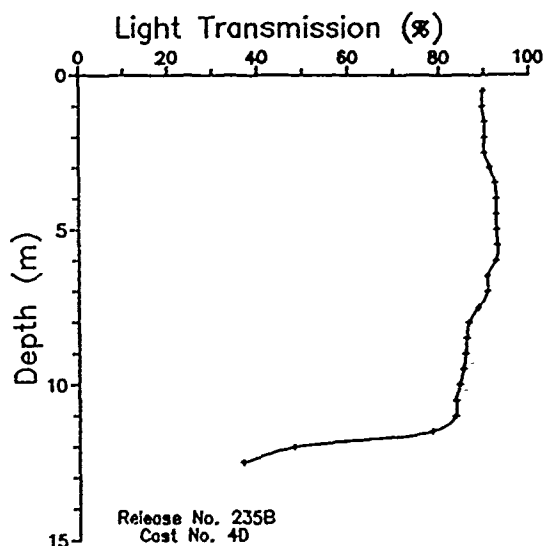
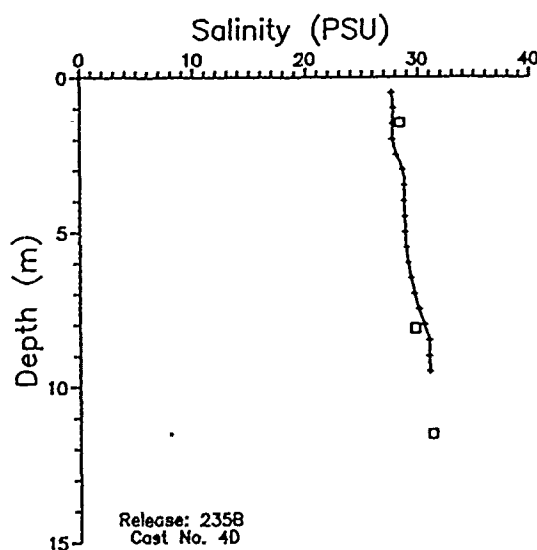
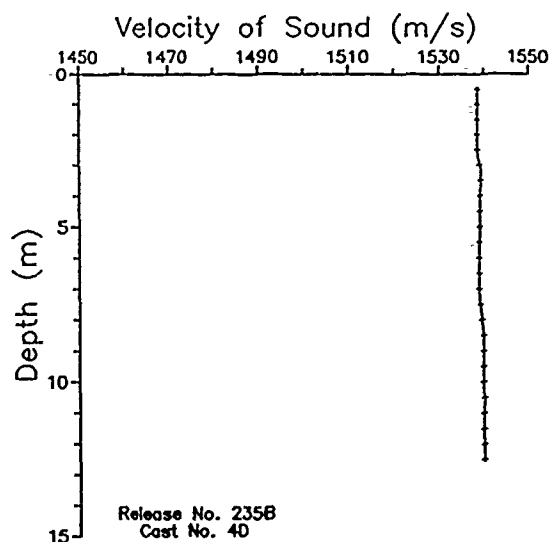
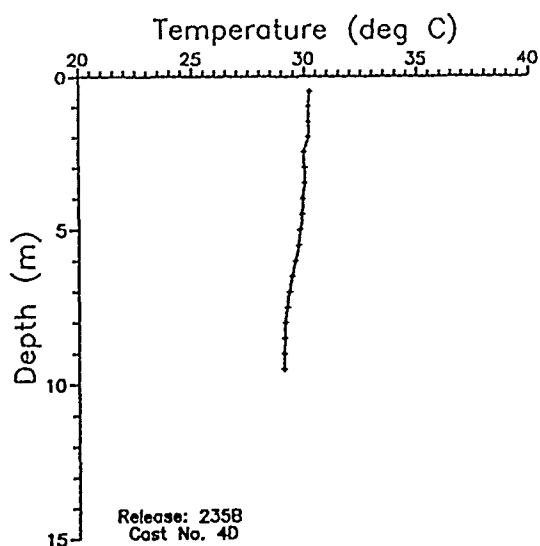
**Appendix 4A: Depth Profiles of Temperature, Salinity, Sigma-Theta,
Velocity of Sound, Light Transmission, and Brunt-Väisälä Frequency**

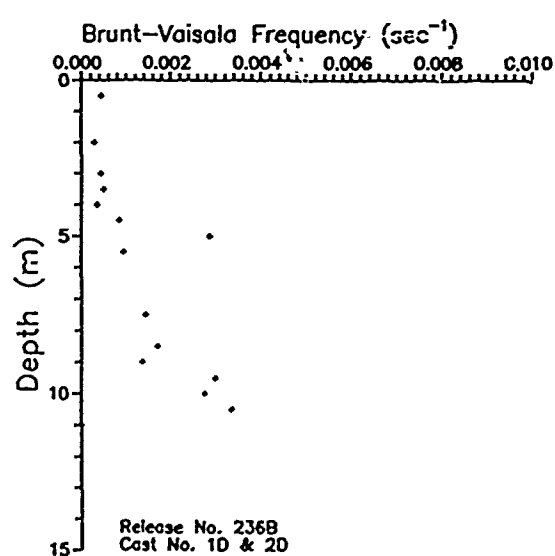
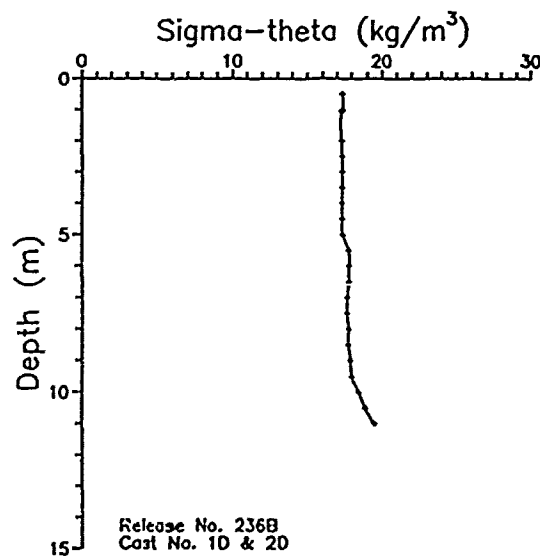
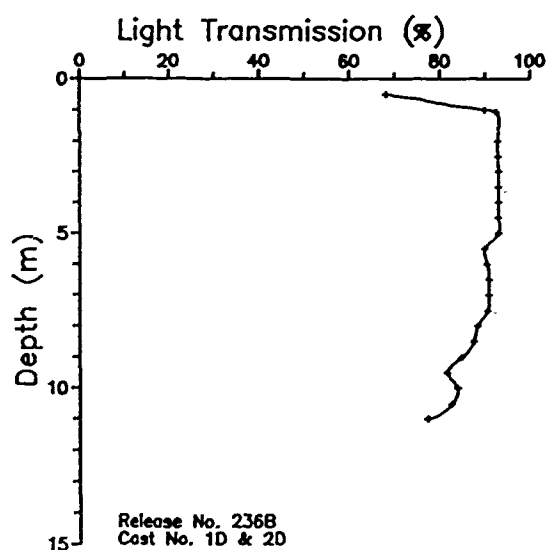
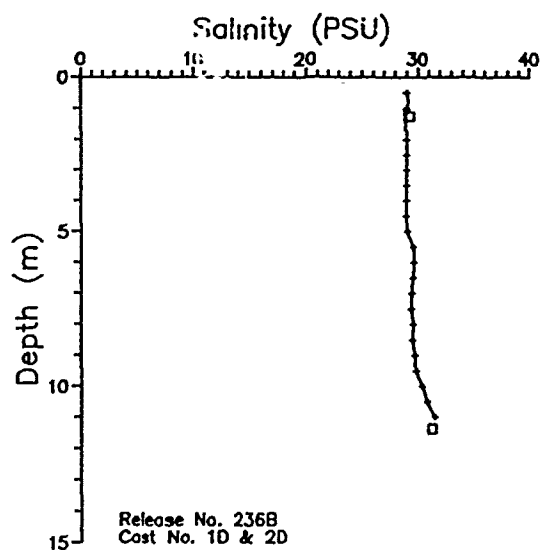
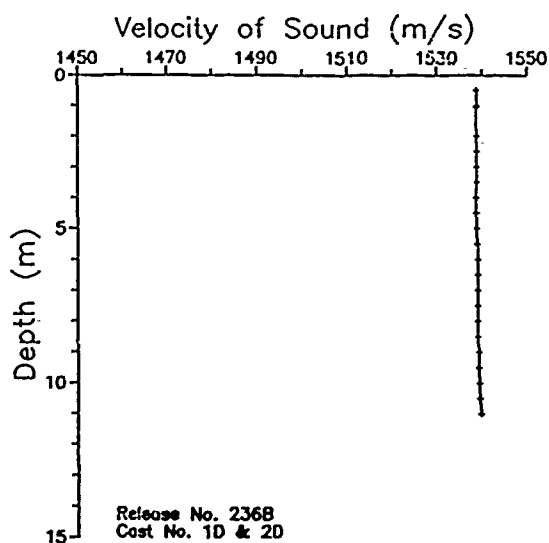
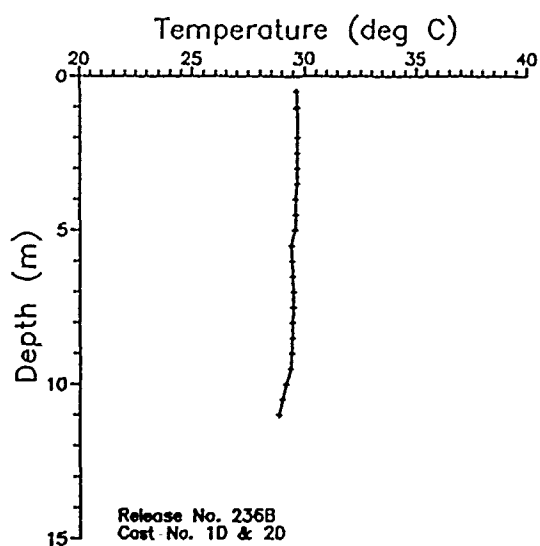


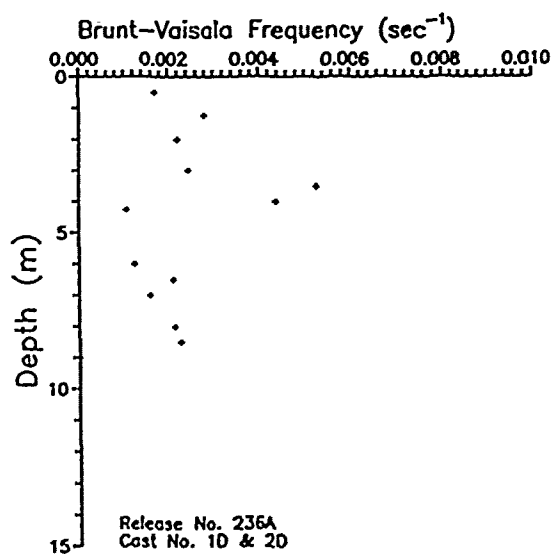
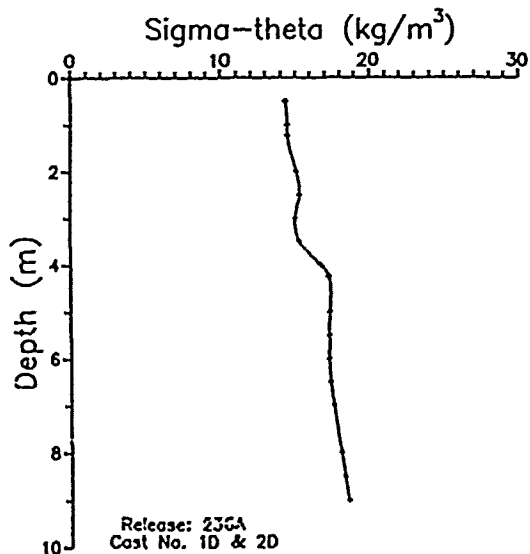
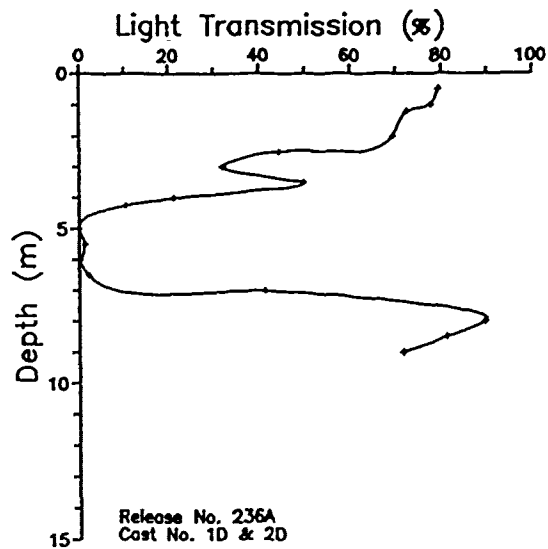
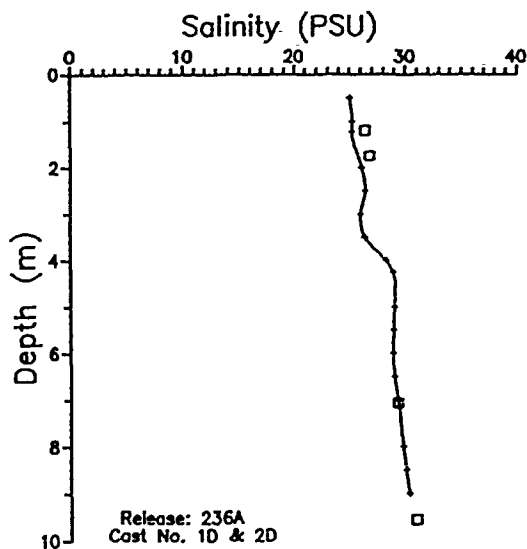
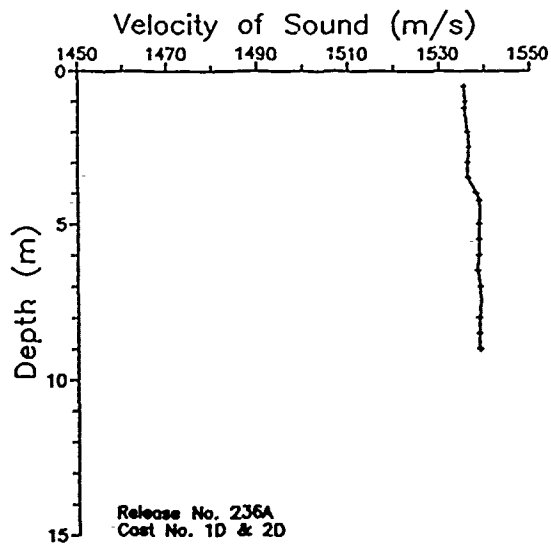
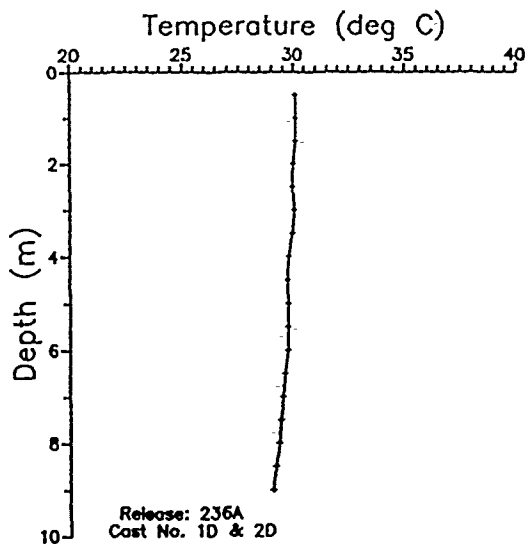


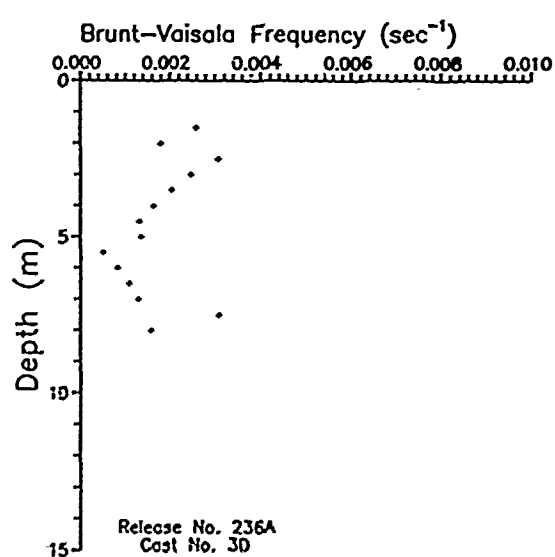
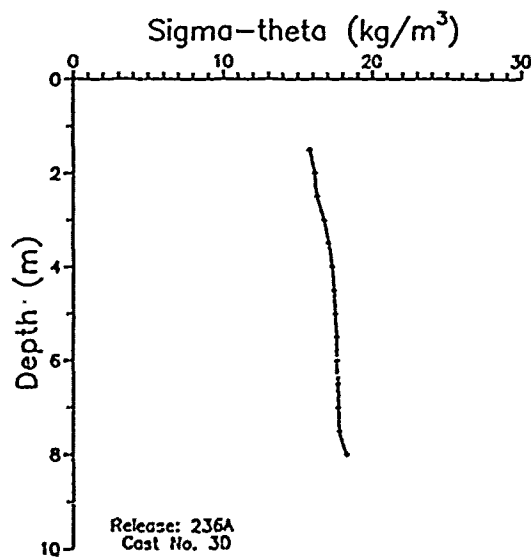
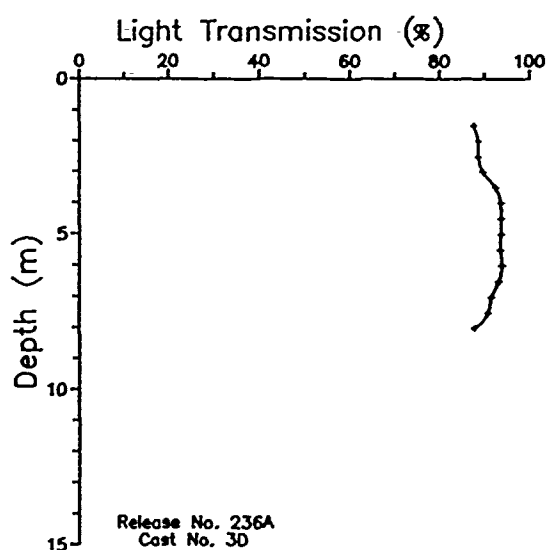
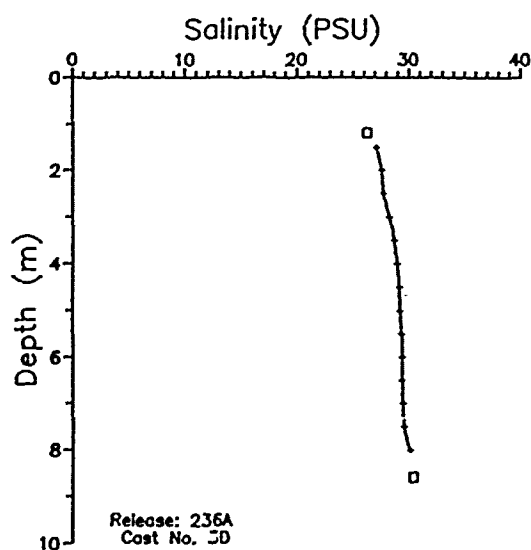
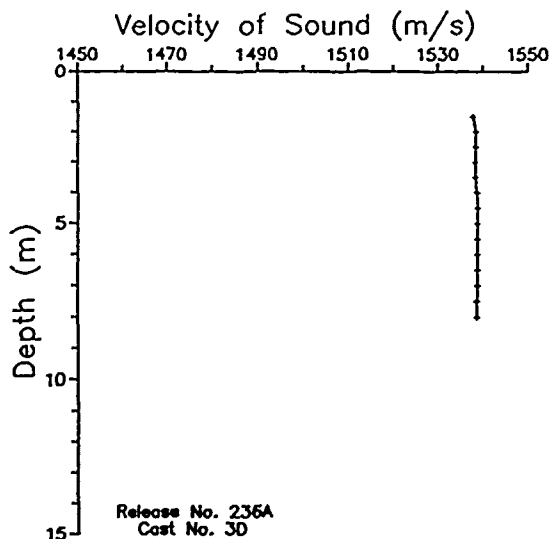
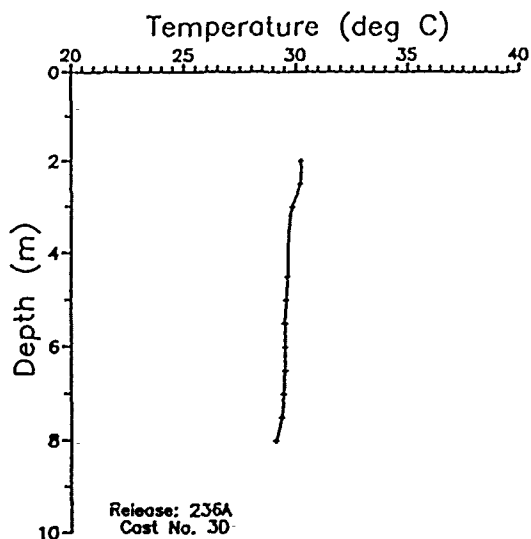


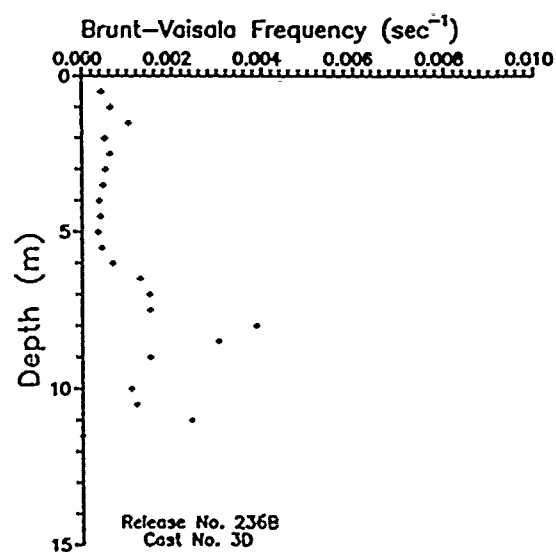
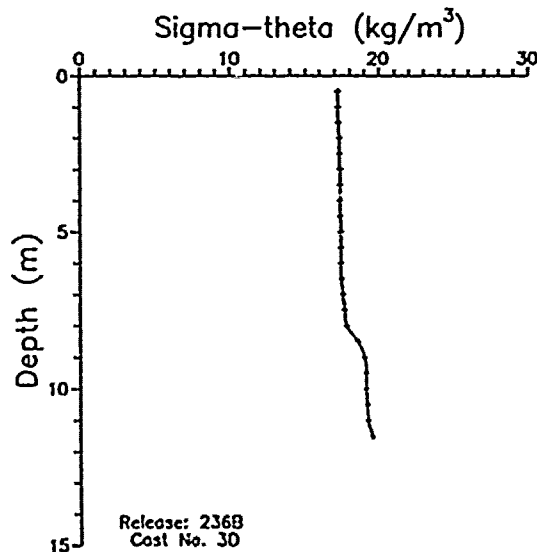
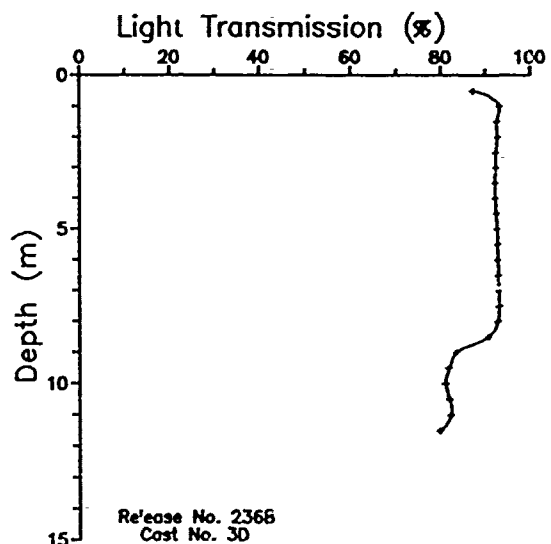
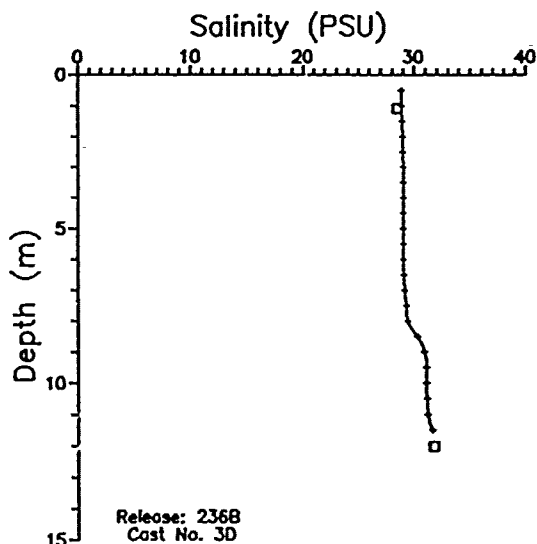
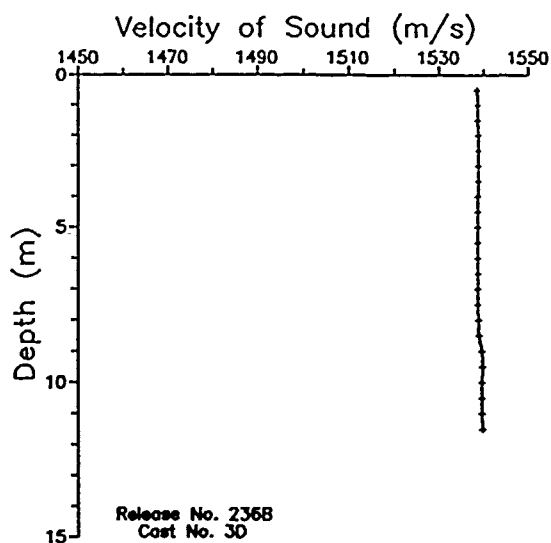
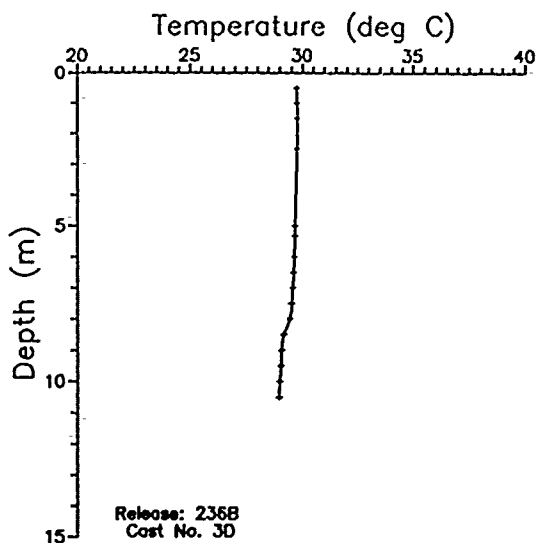


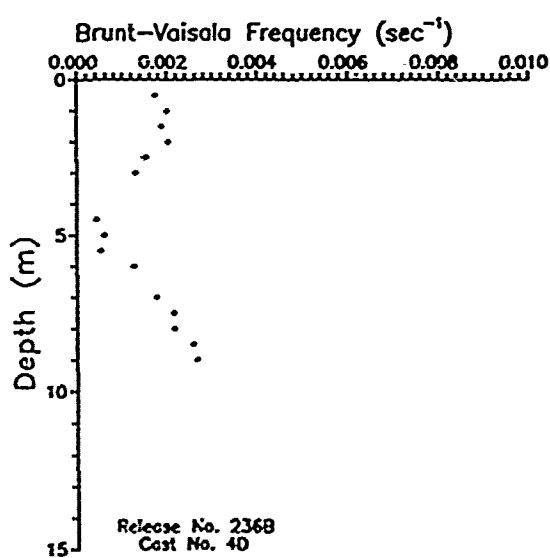
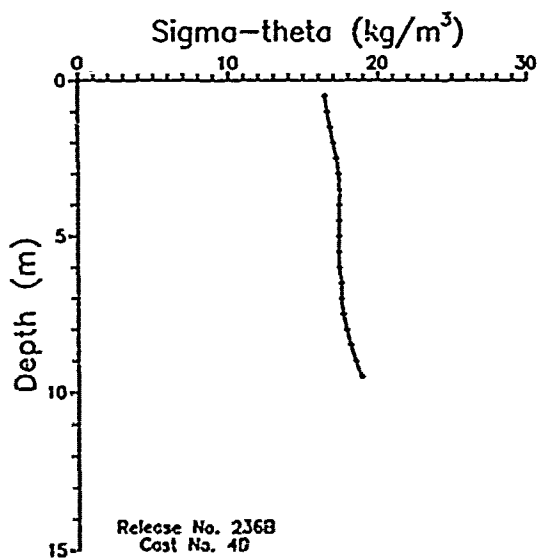
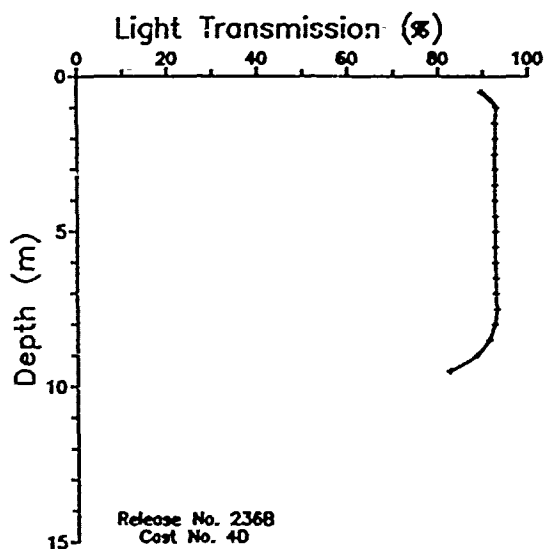
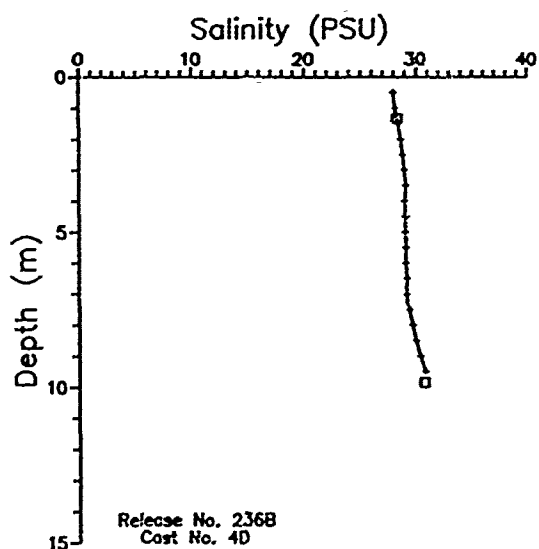
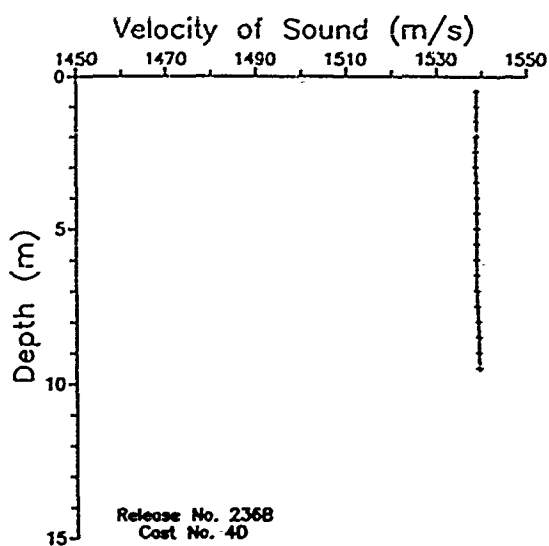
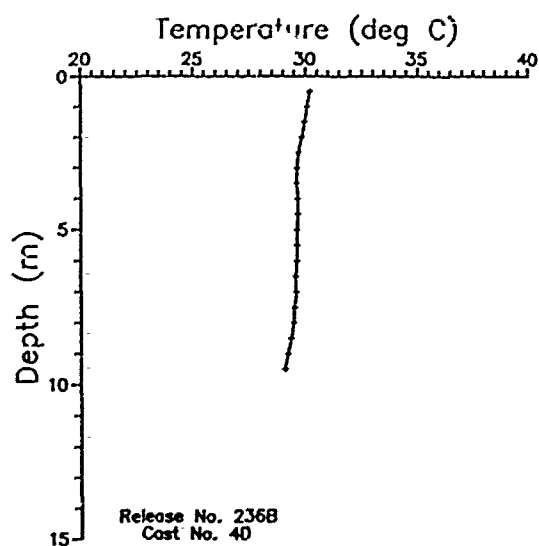


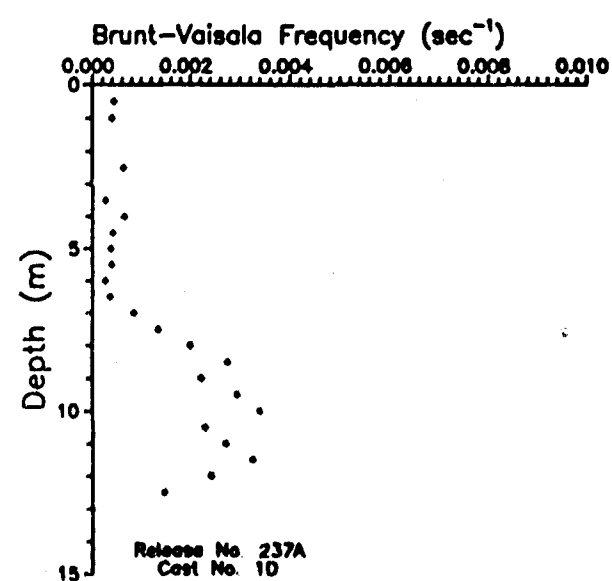
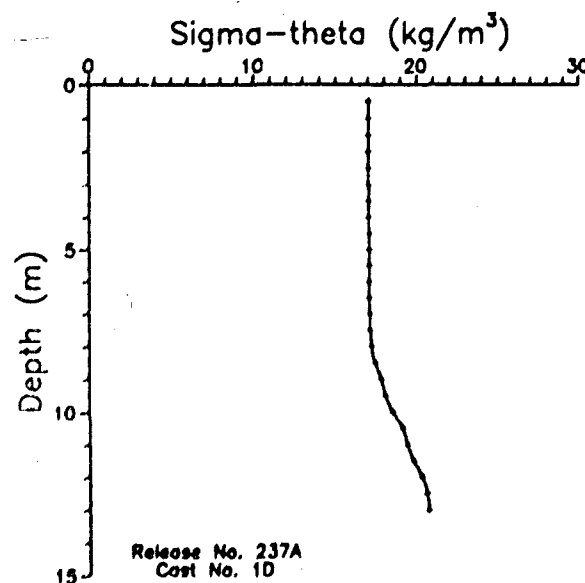
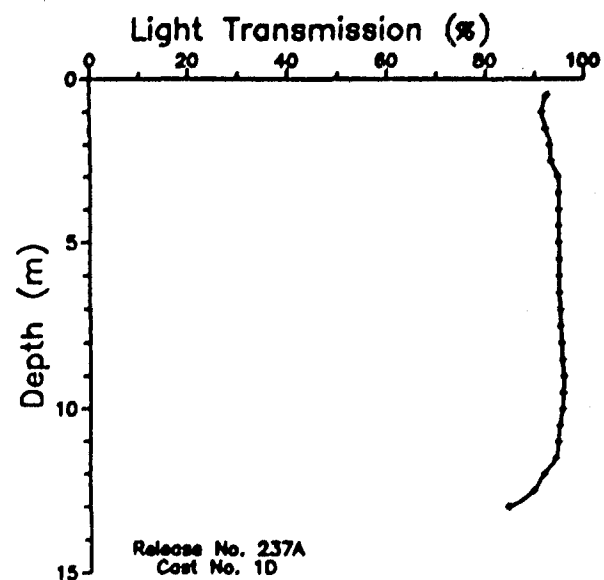
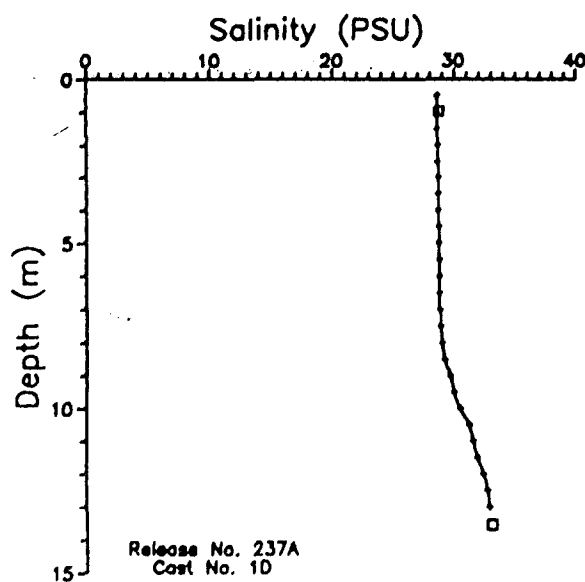
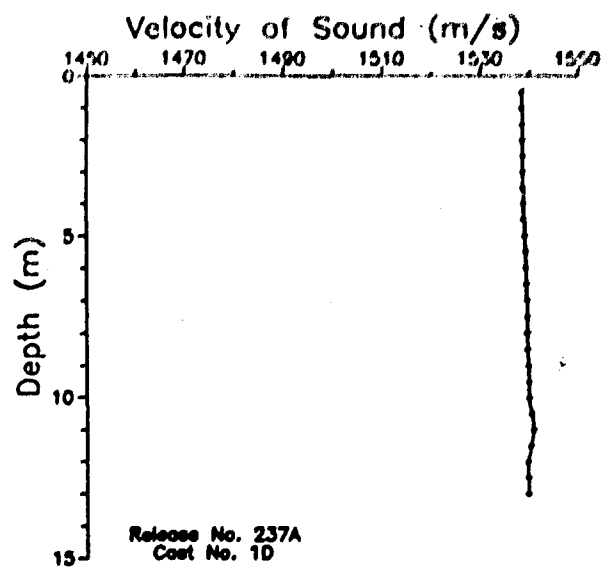
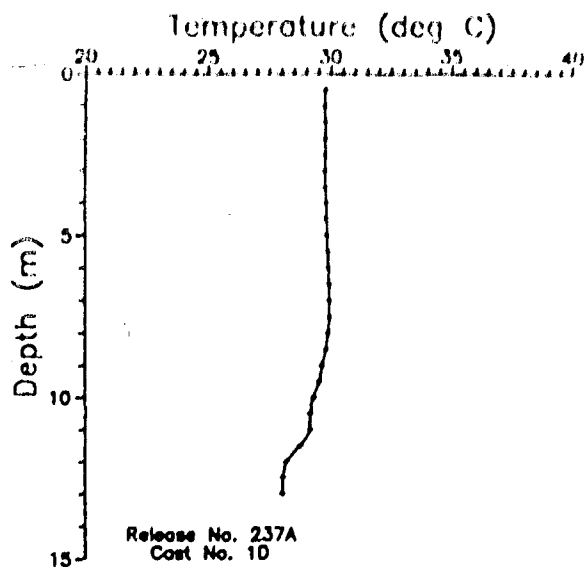


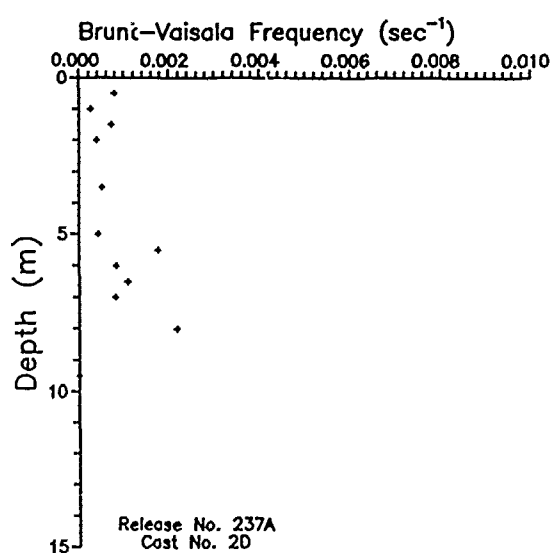
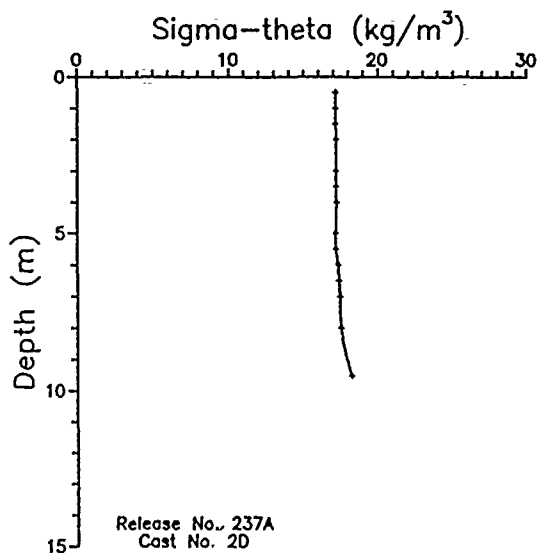
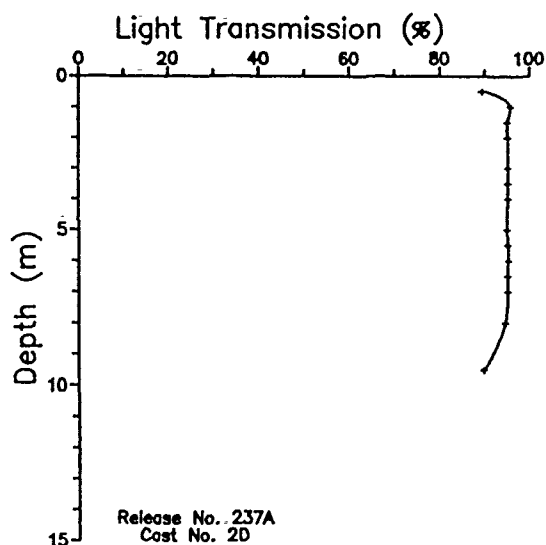
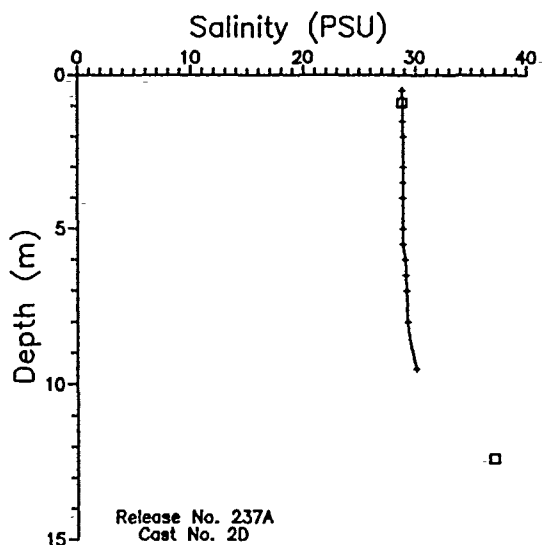
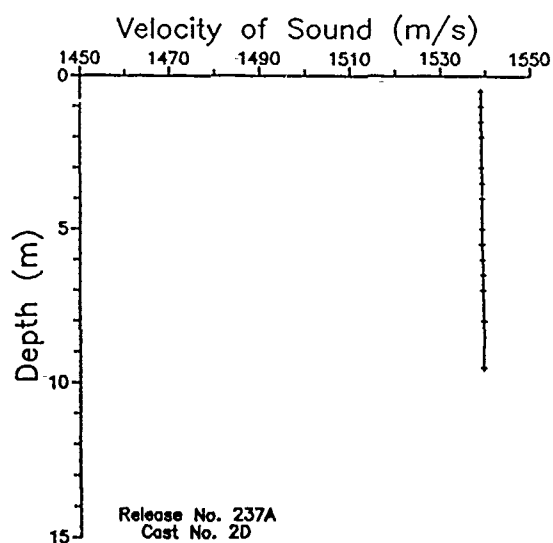
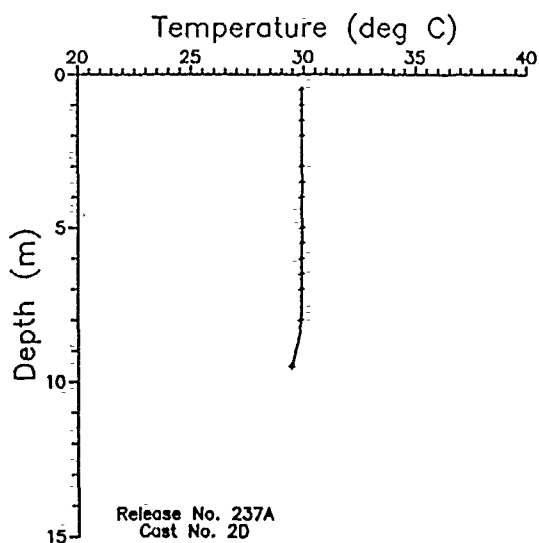


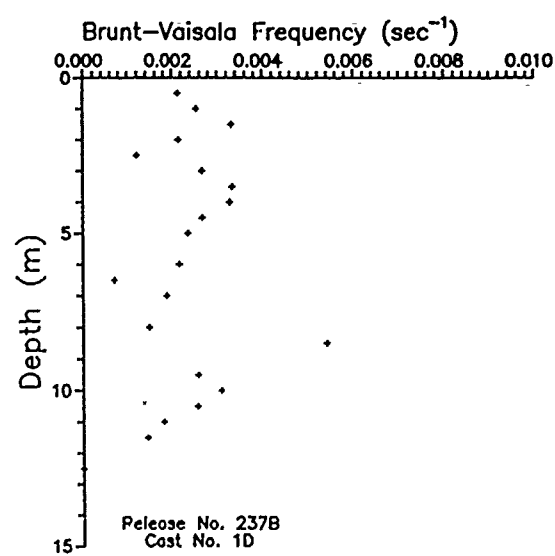
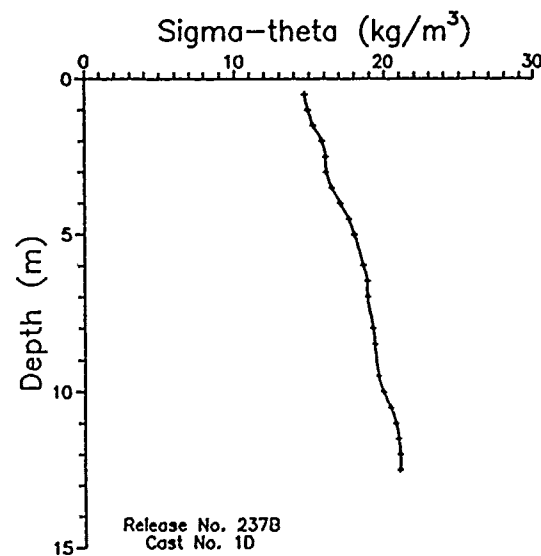
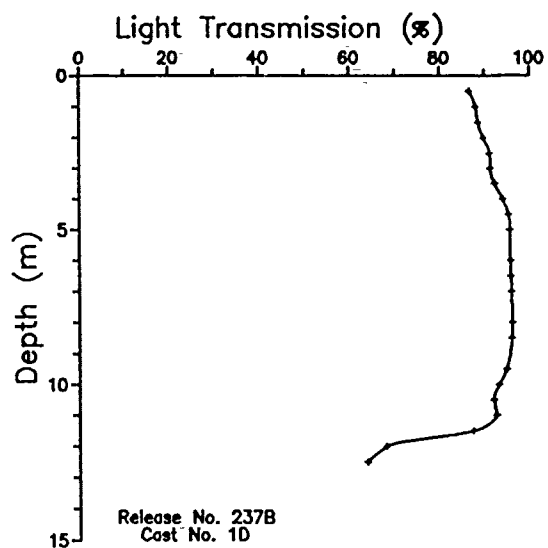
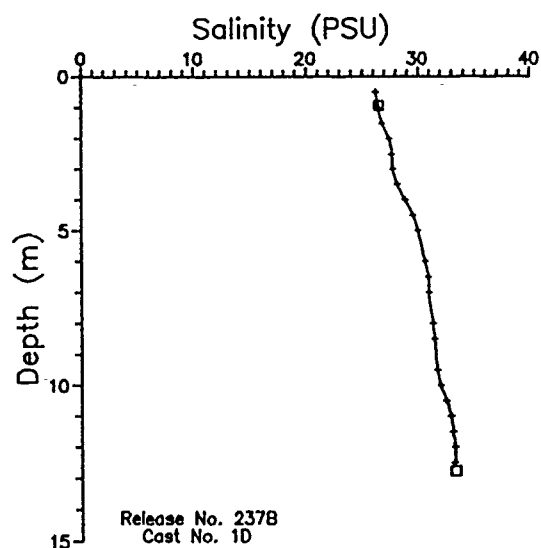
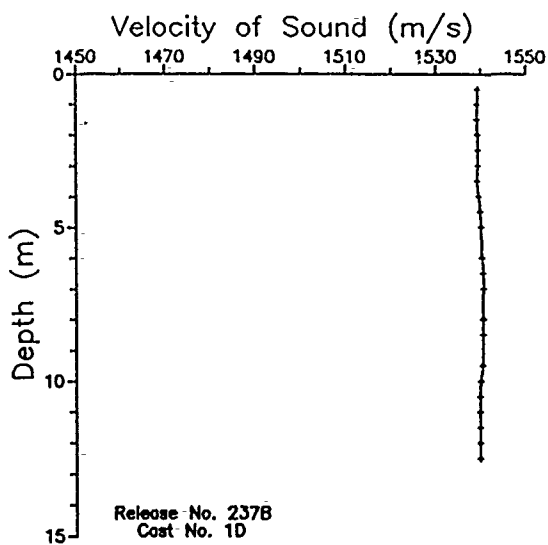
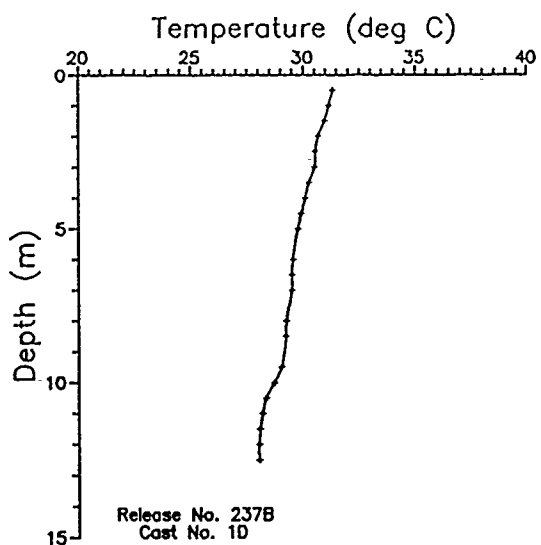


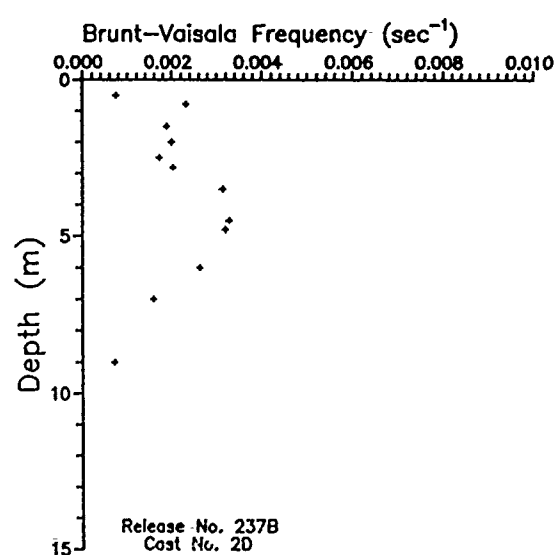
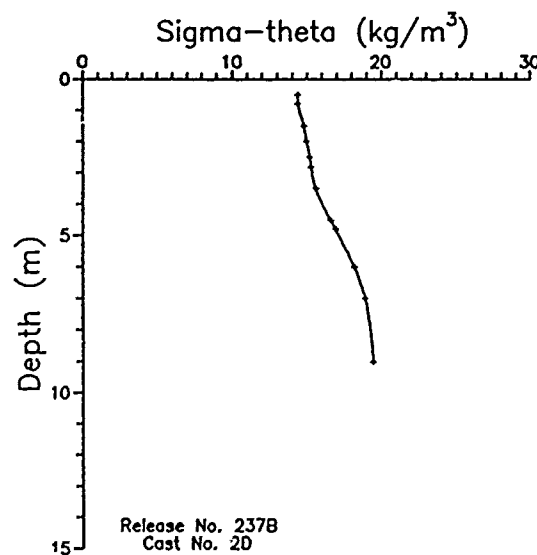
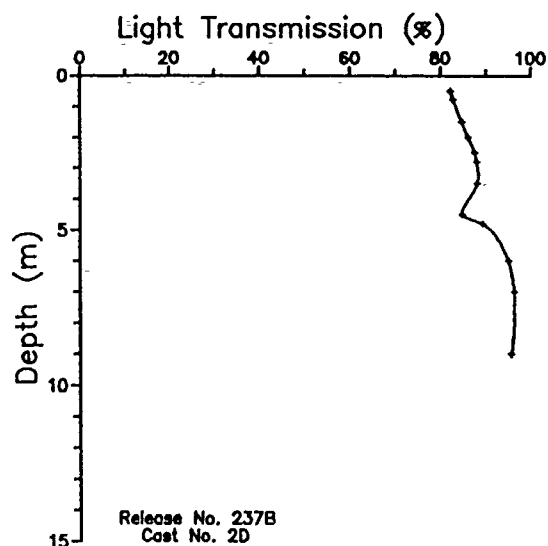
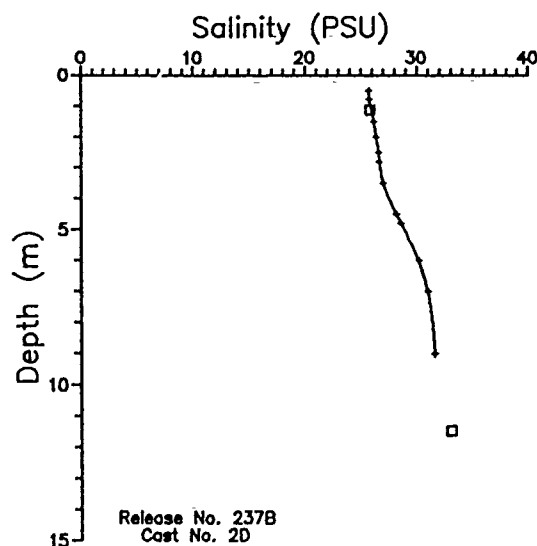
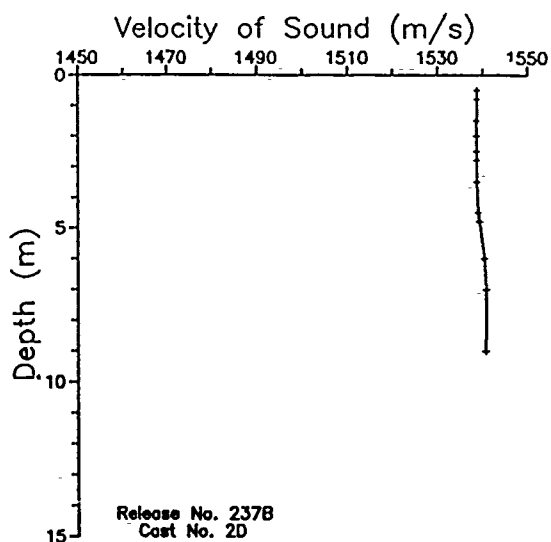
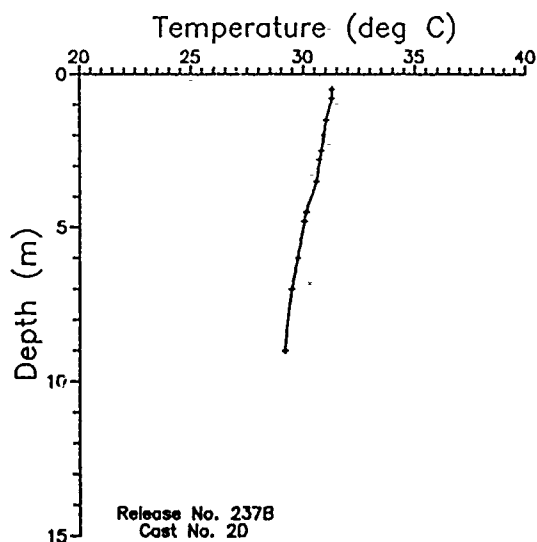


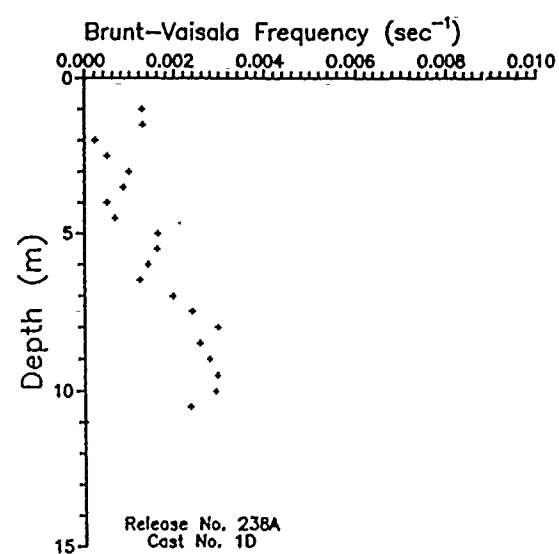
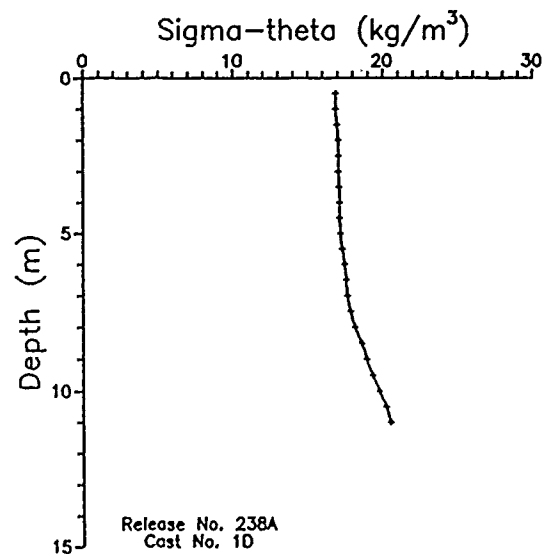
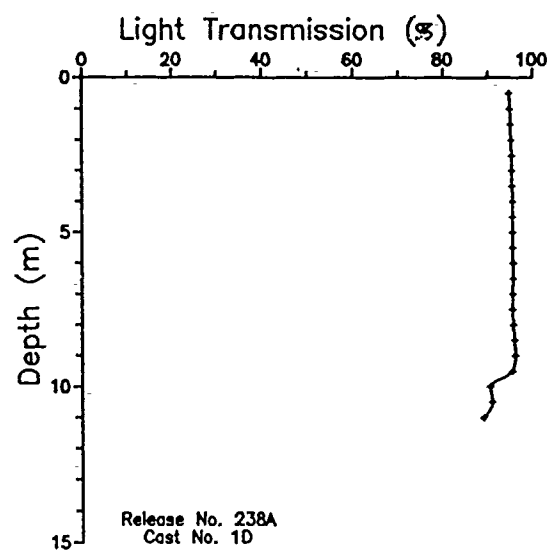
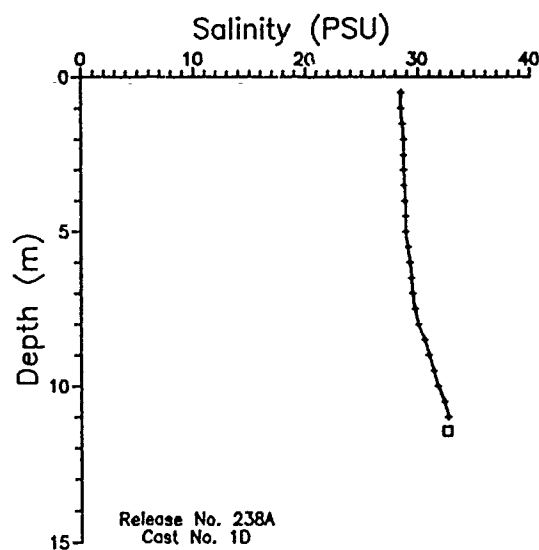
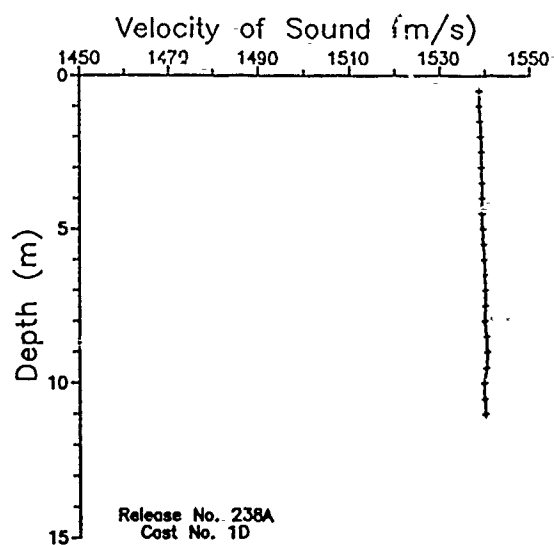
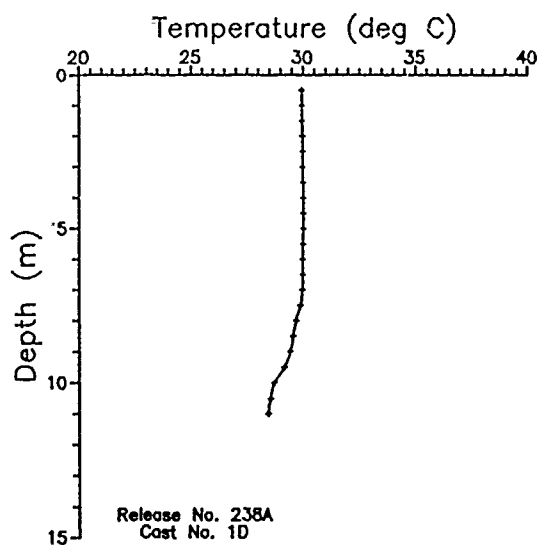


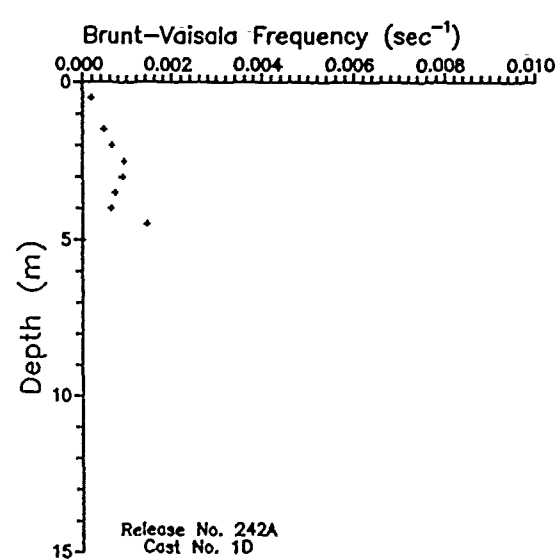
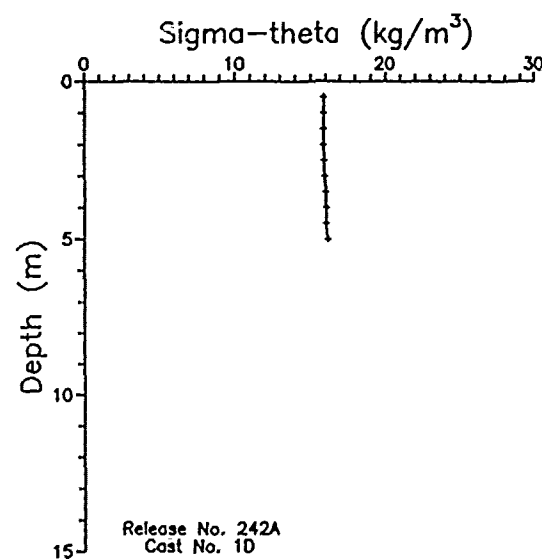
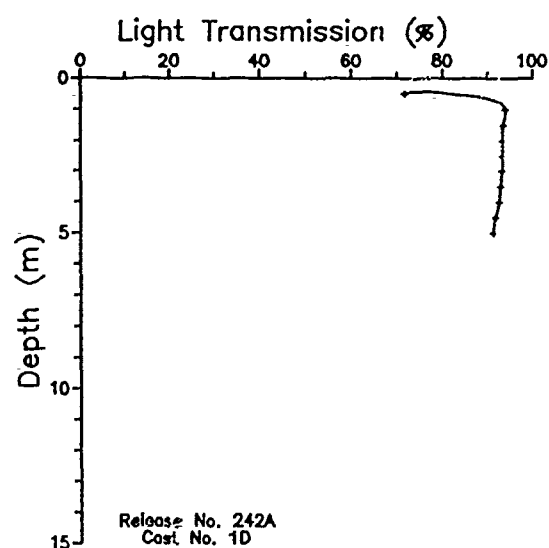
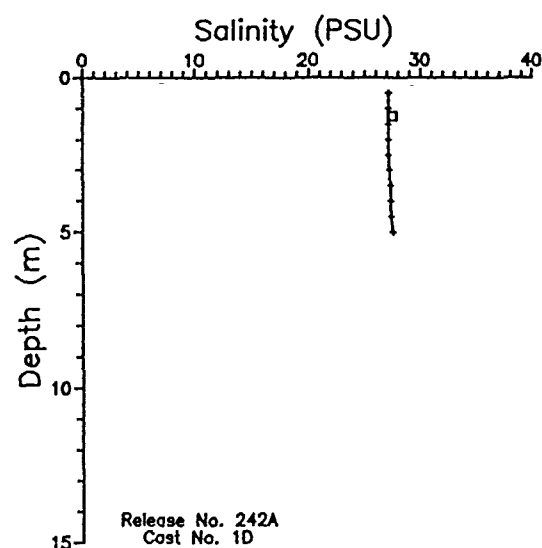
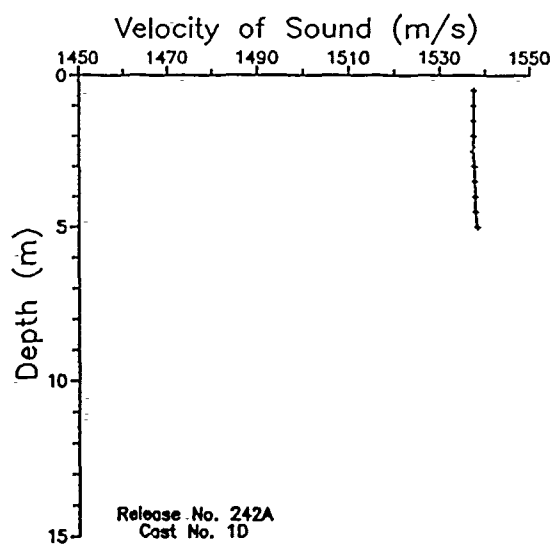
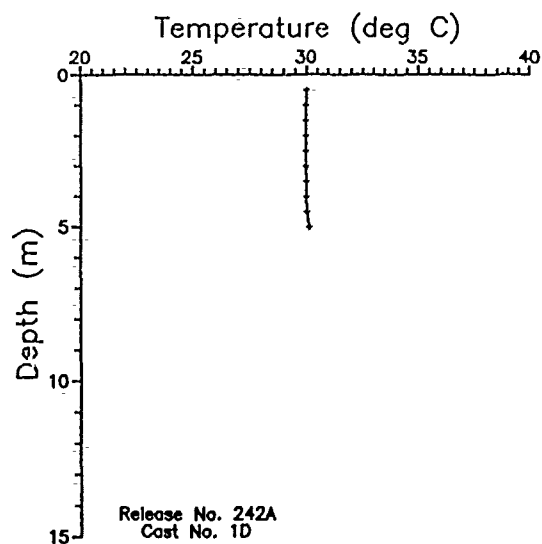


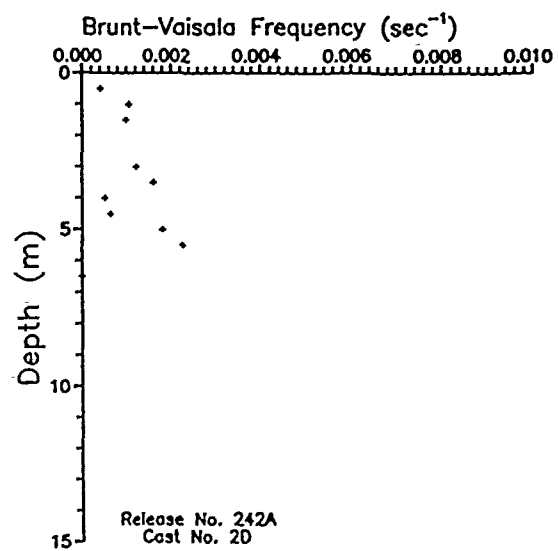
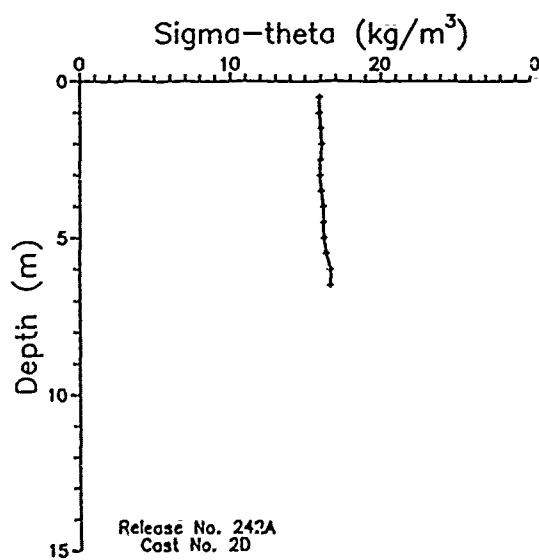
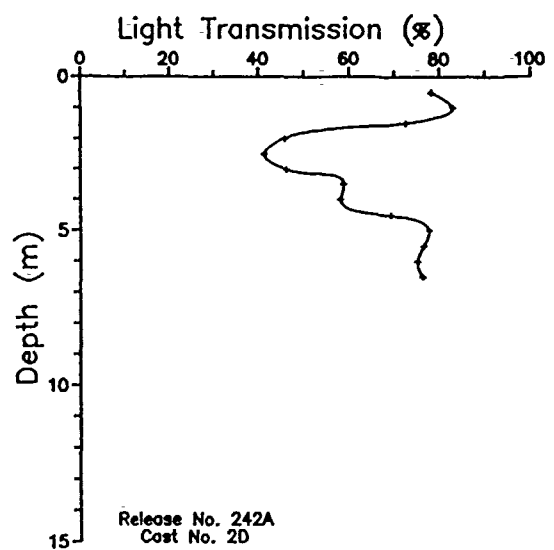
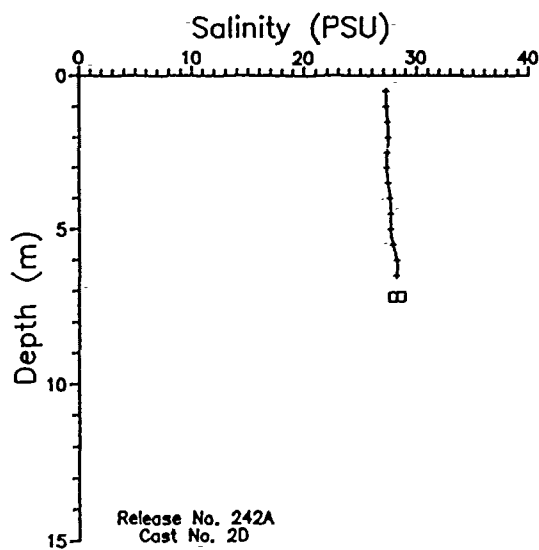
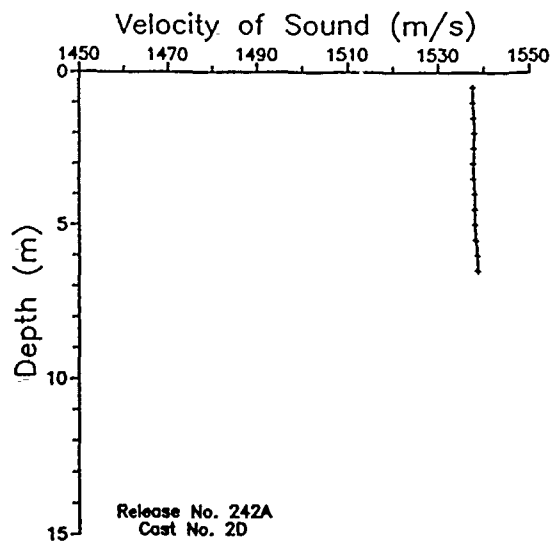
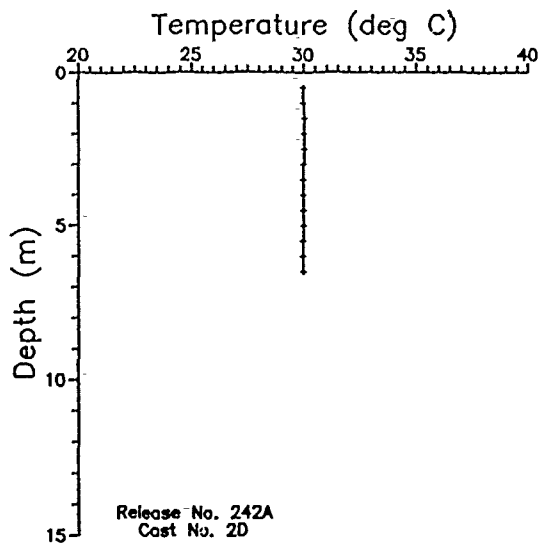


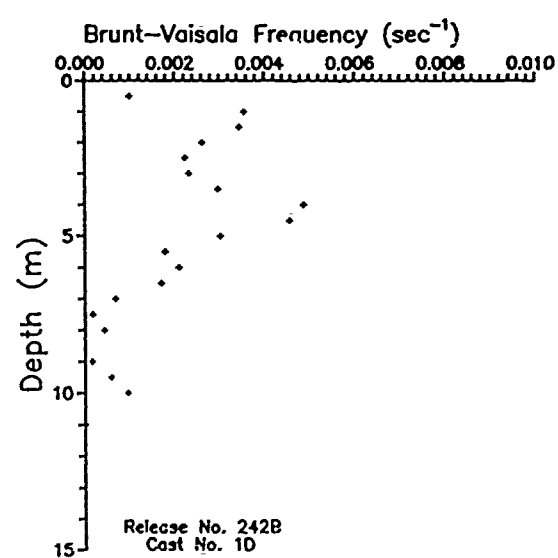
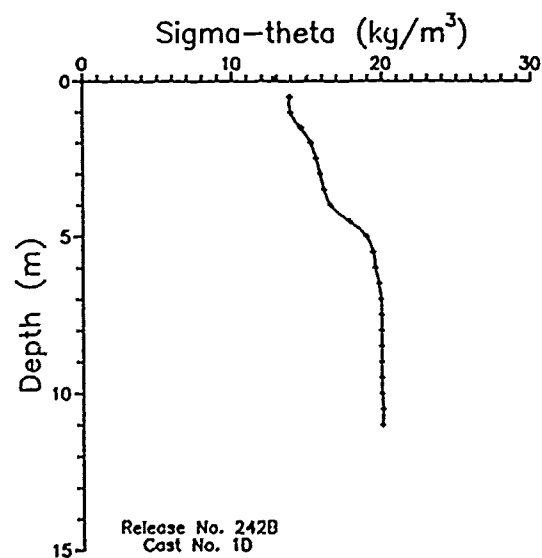
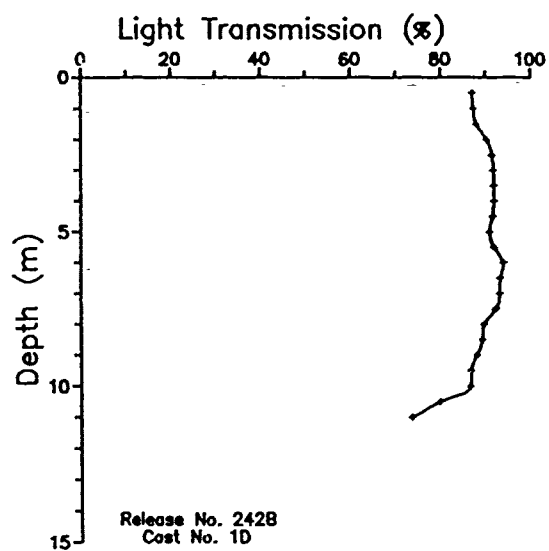
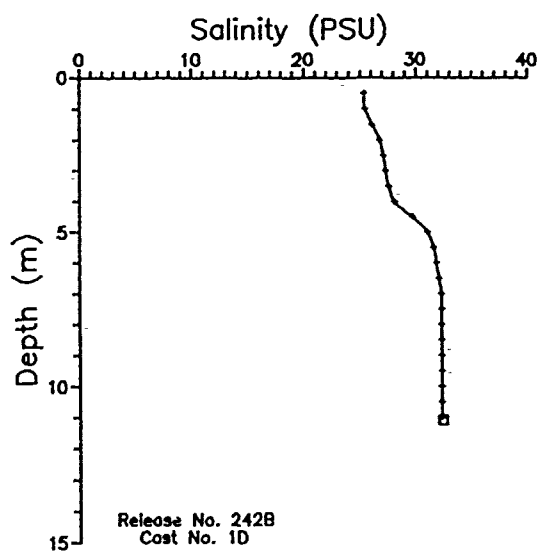
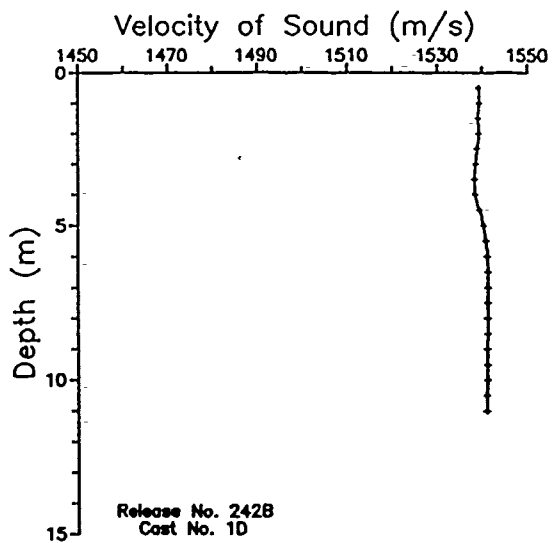
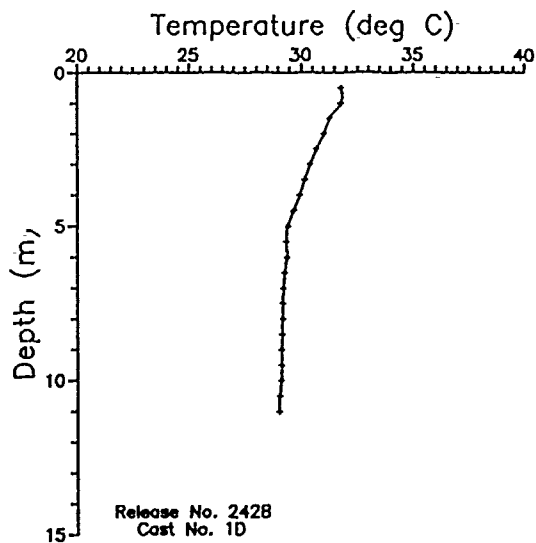


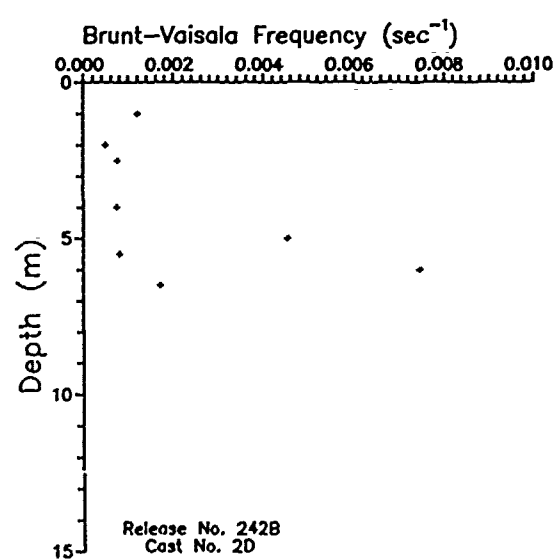
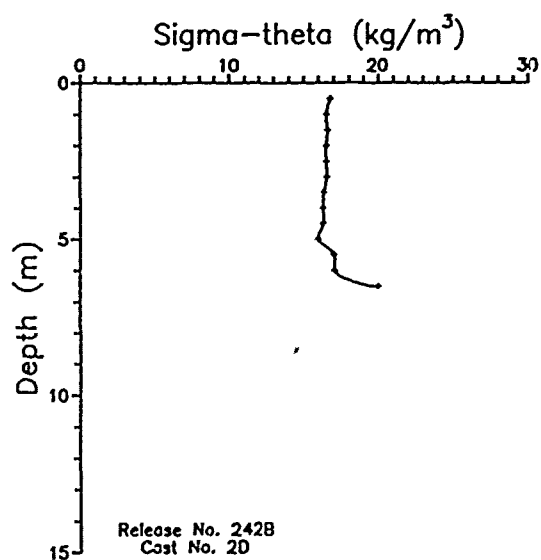
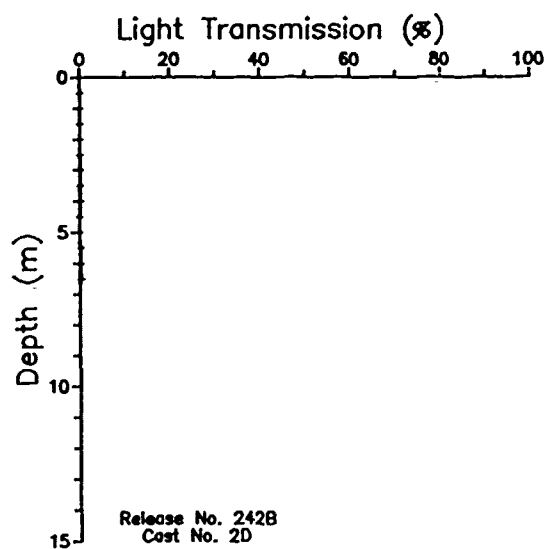
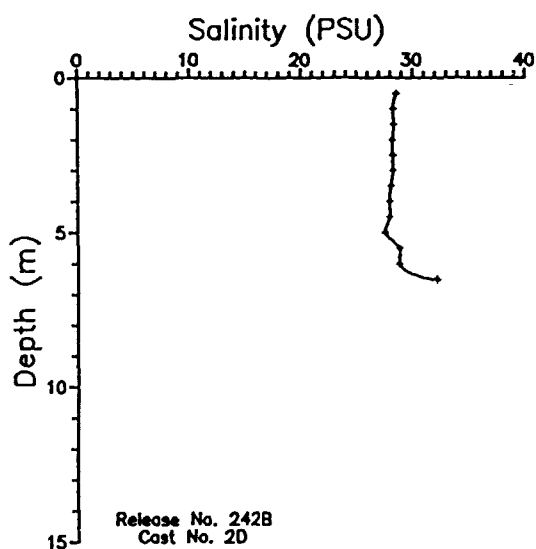
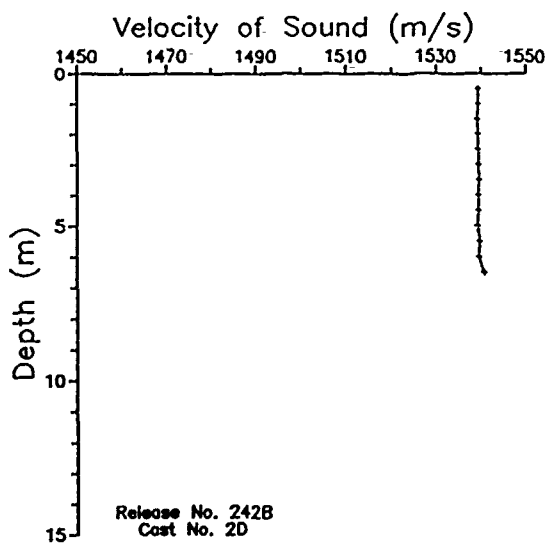
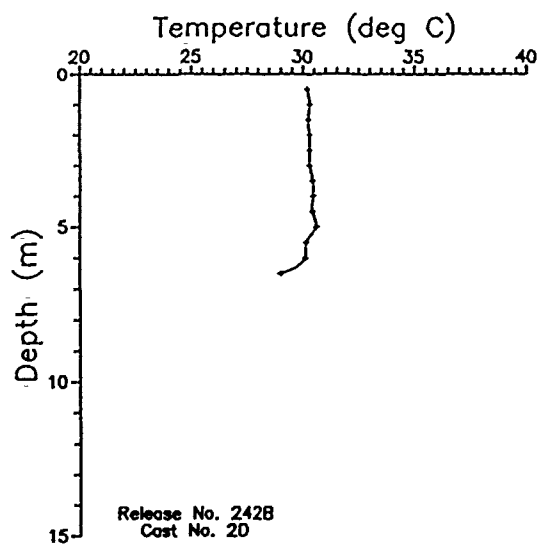


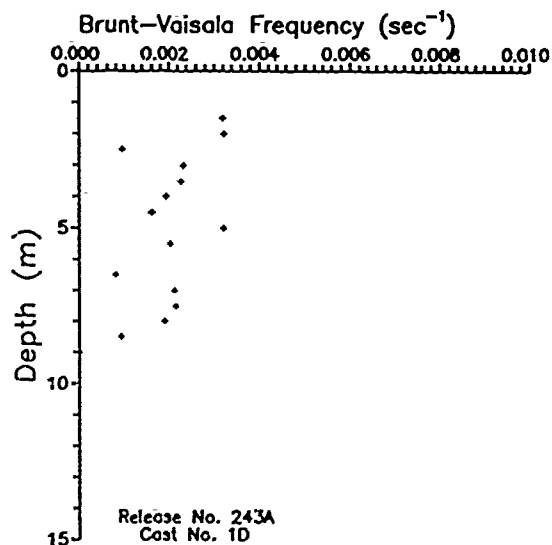
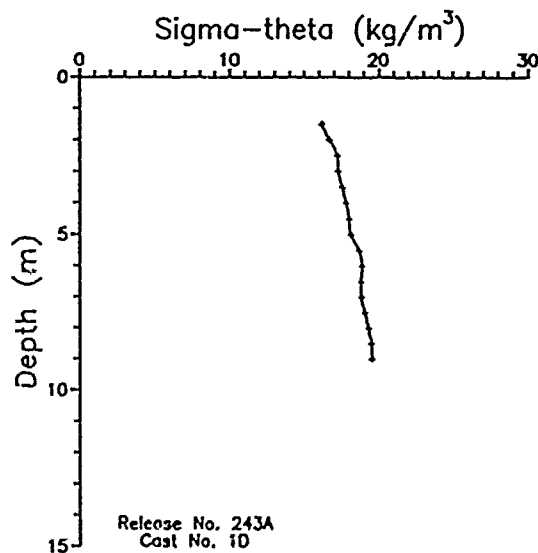
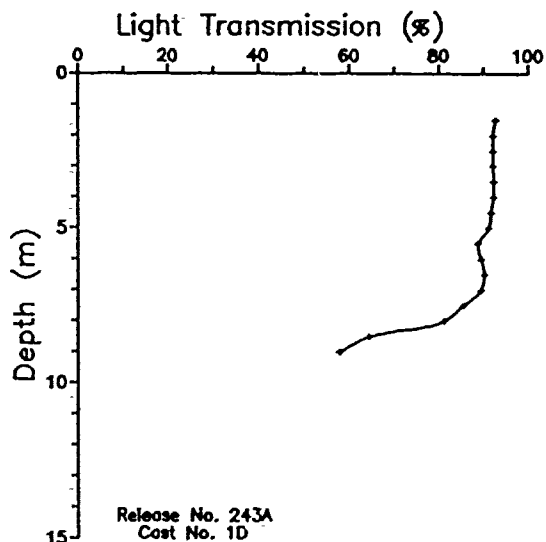
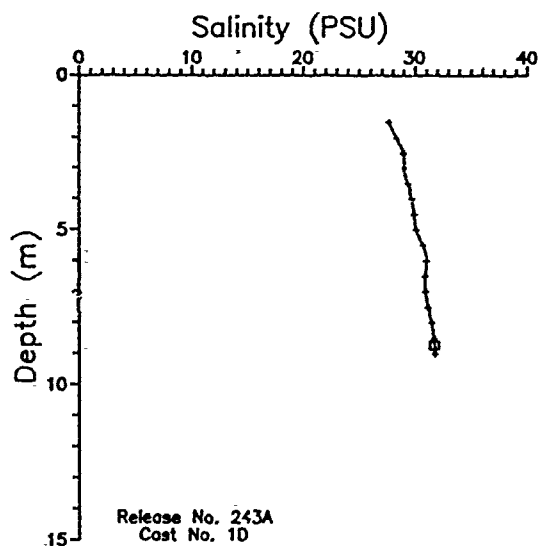
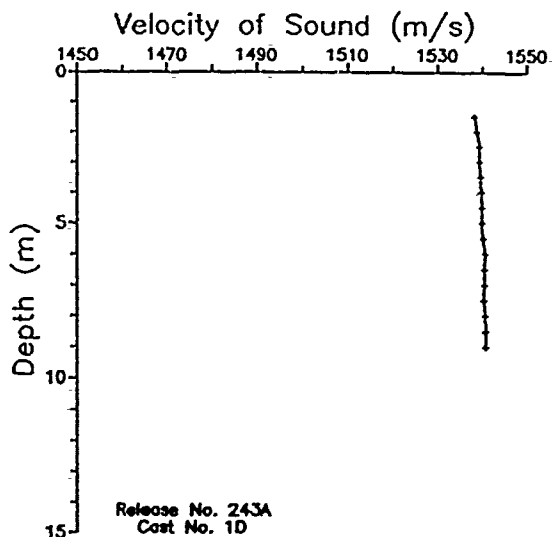
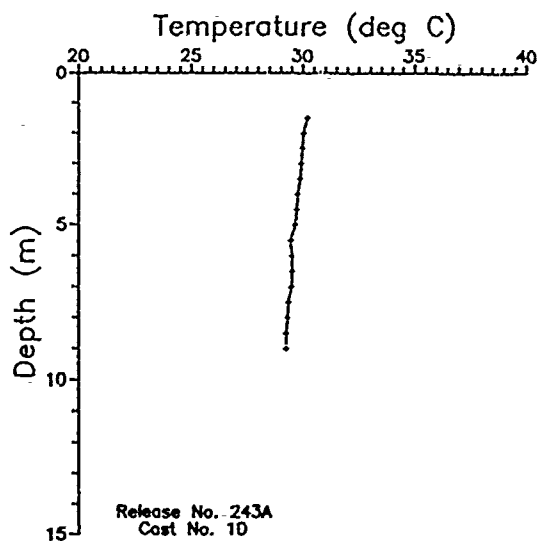


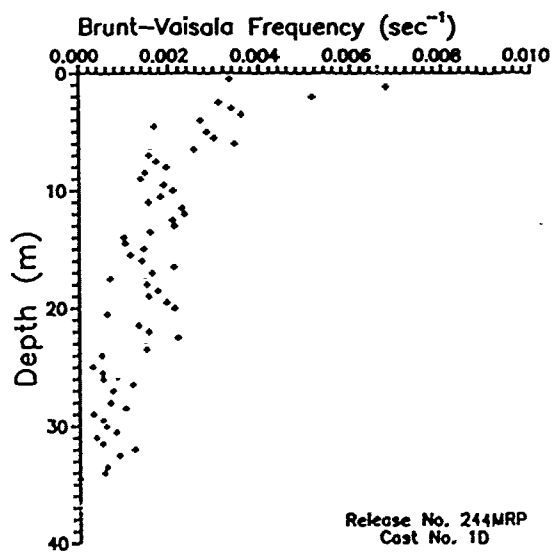
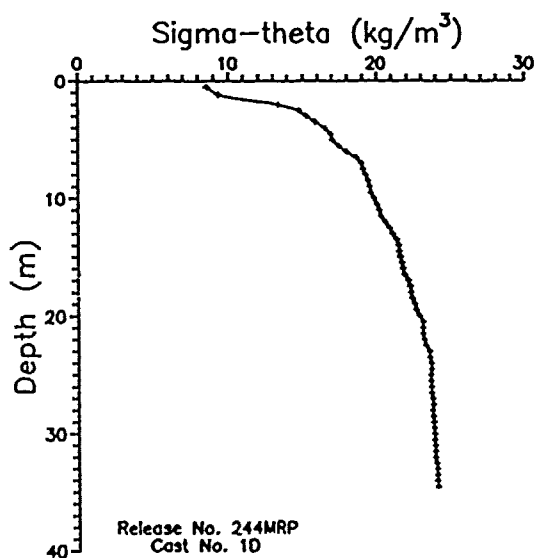
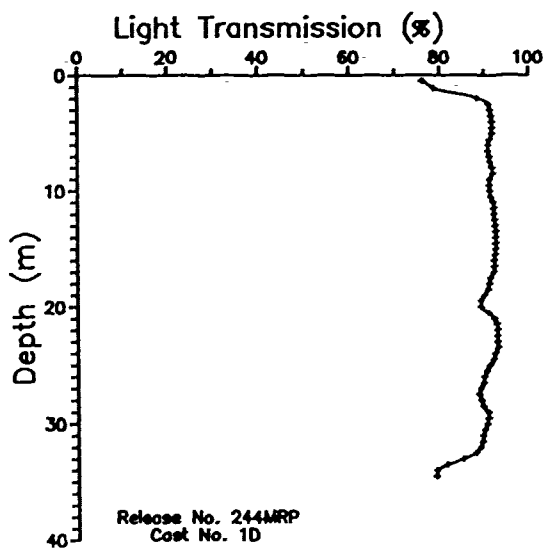
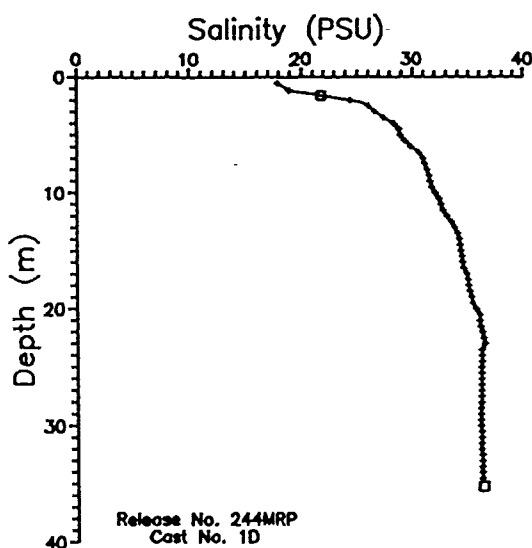
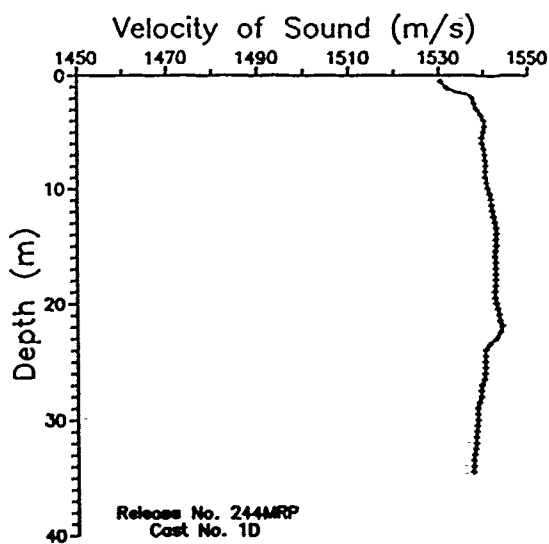
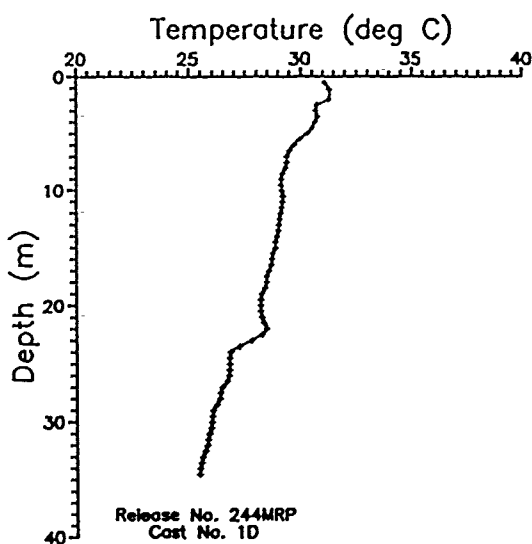


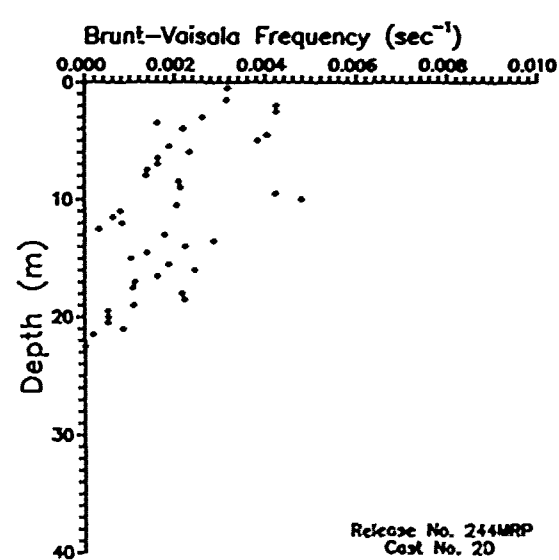
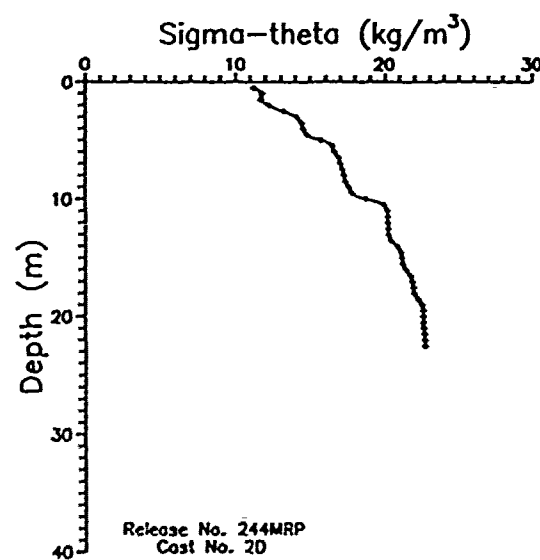
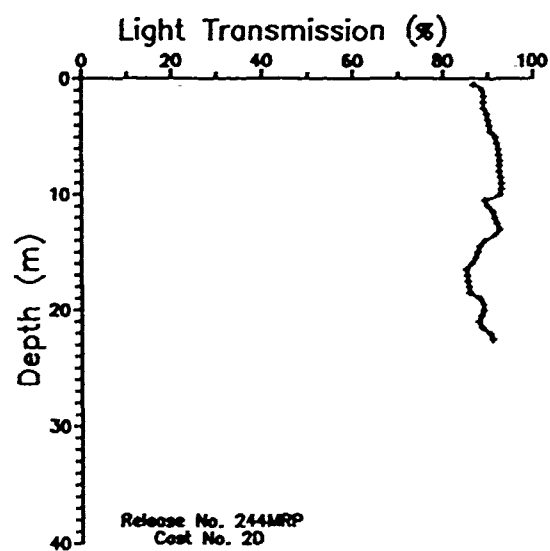
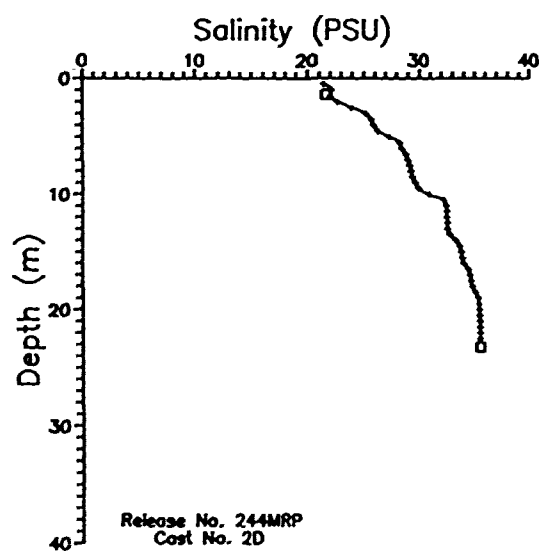
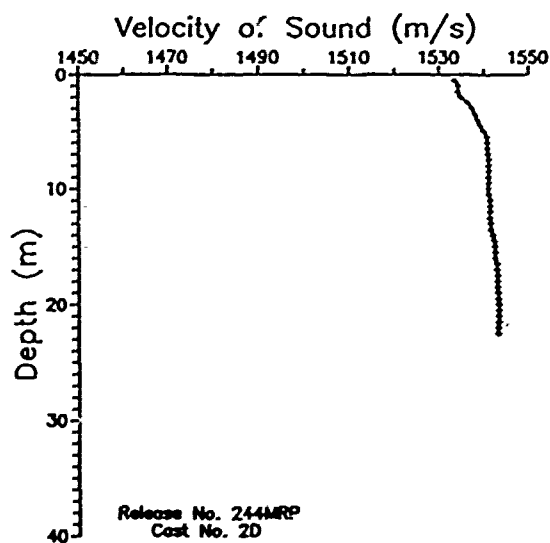
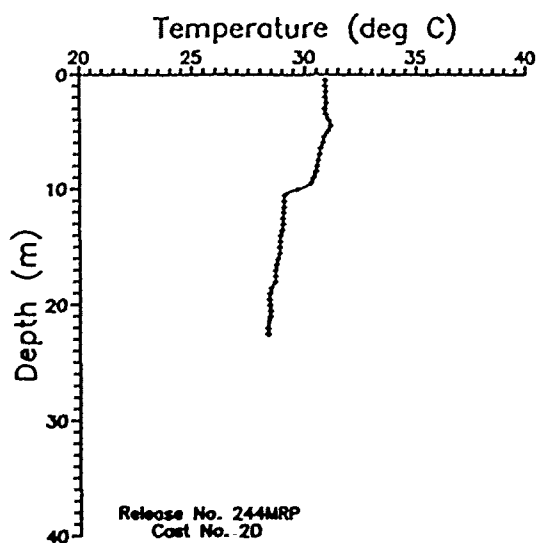


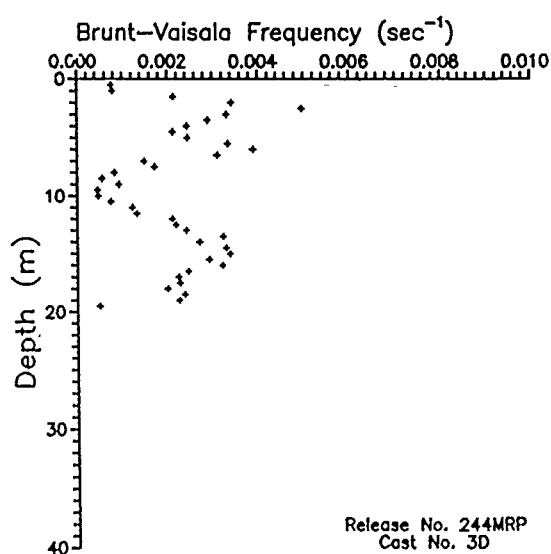
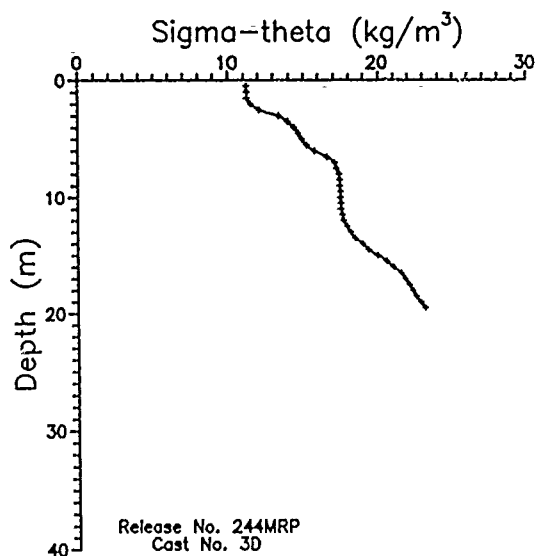
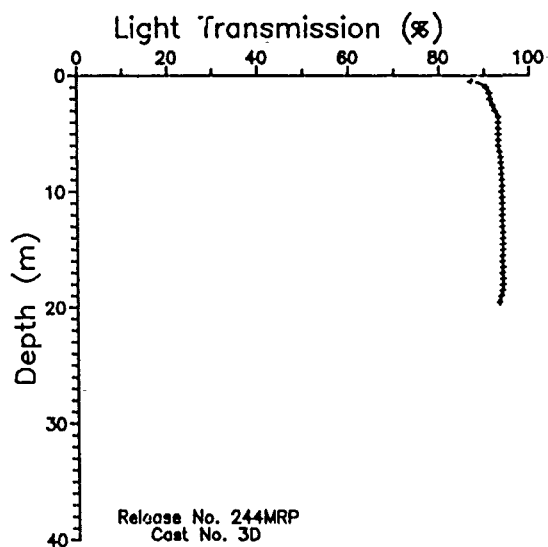
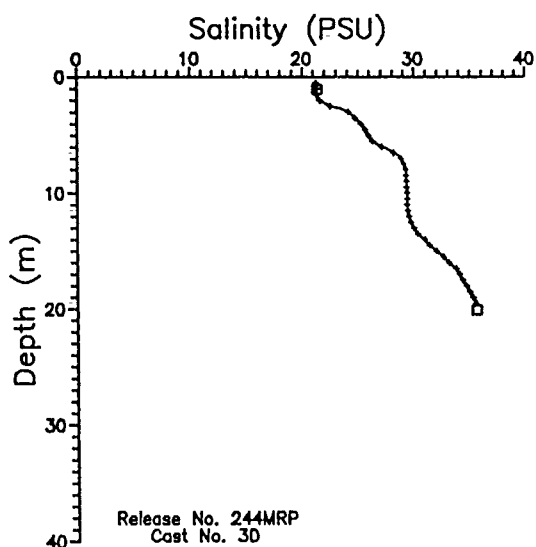
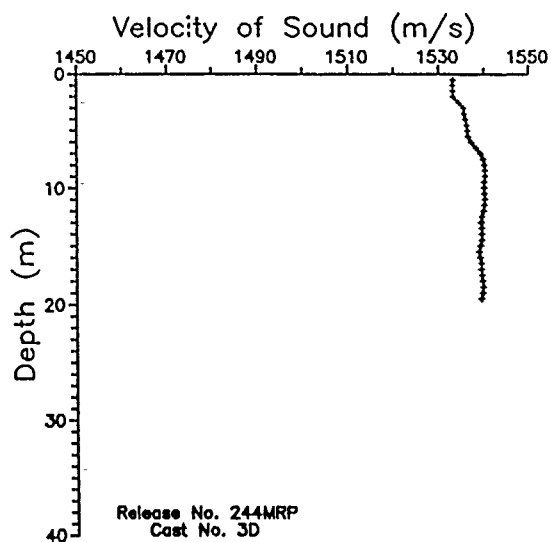
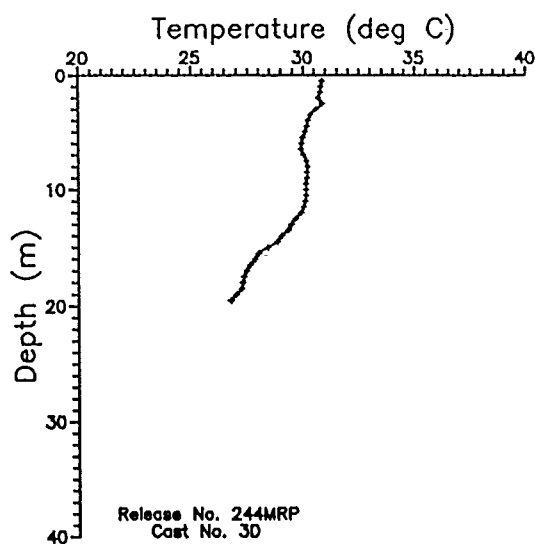




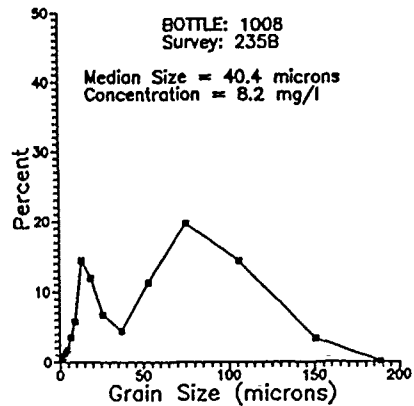
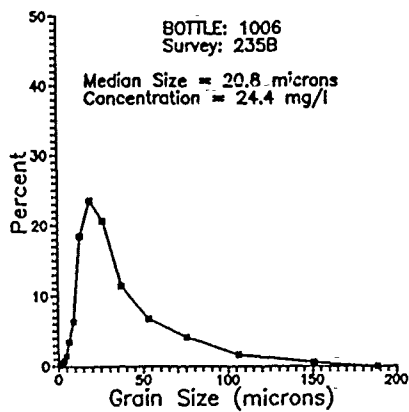
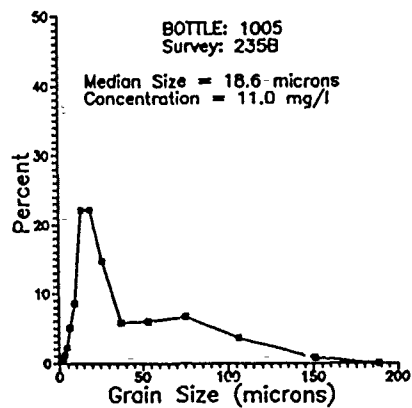
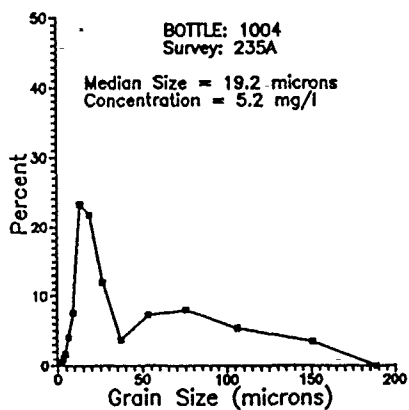
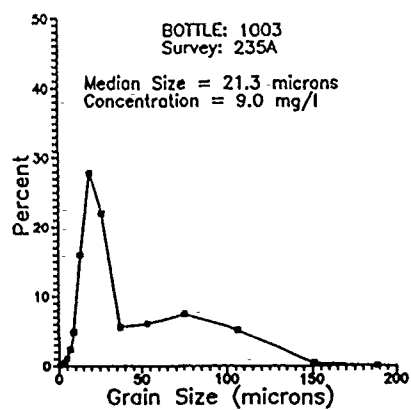
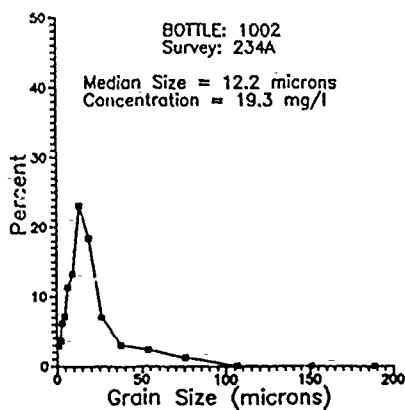


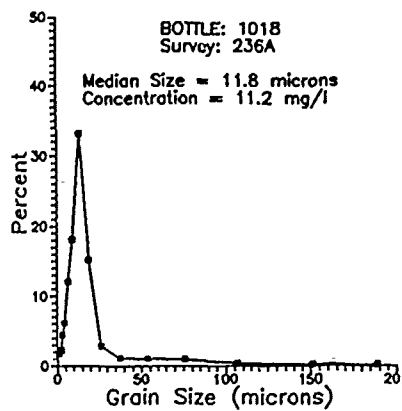
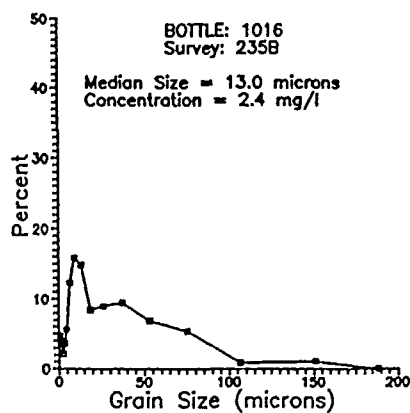
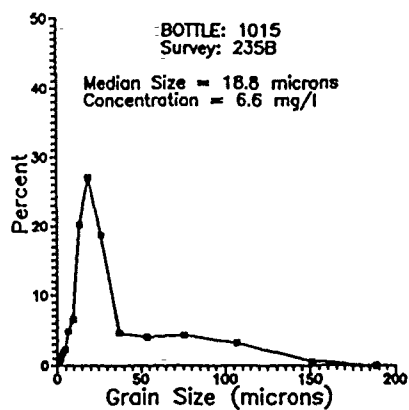
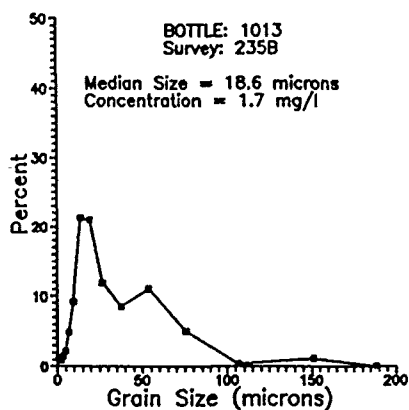
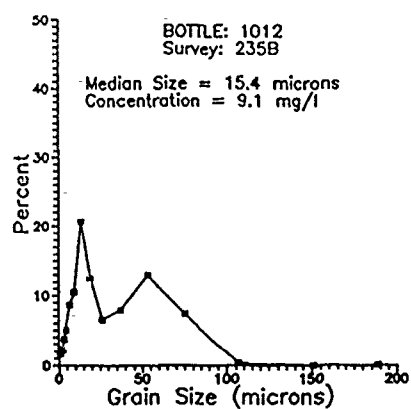
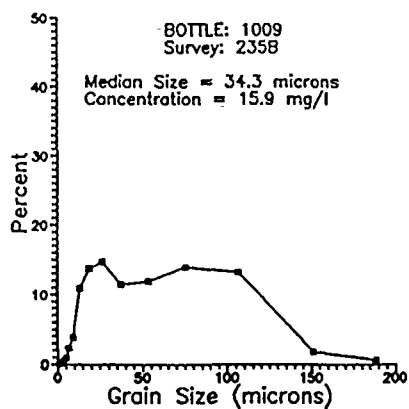


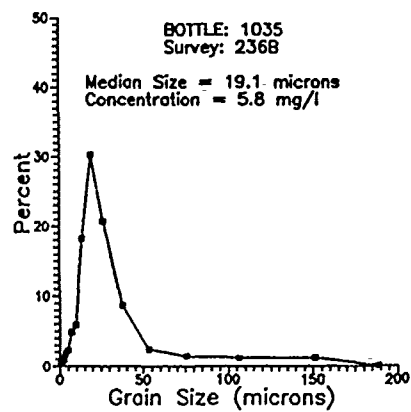
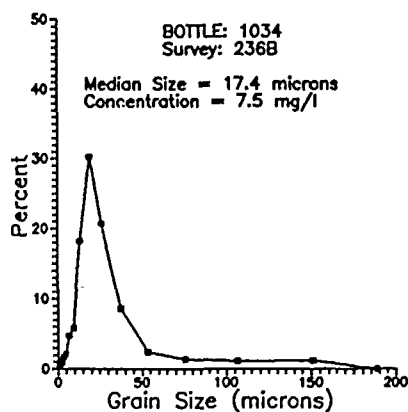
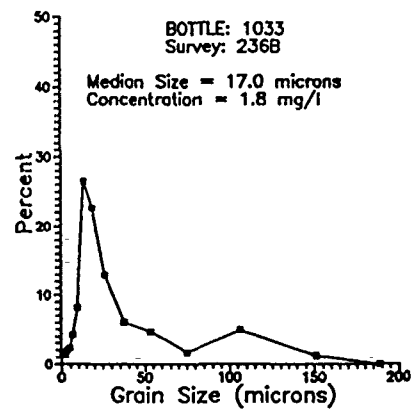
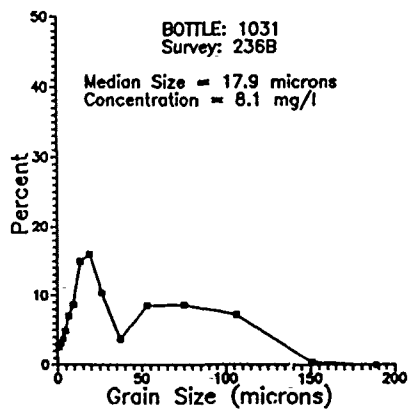
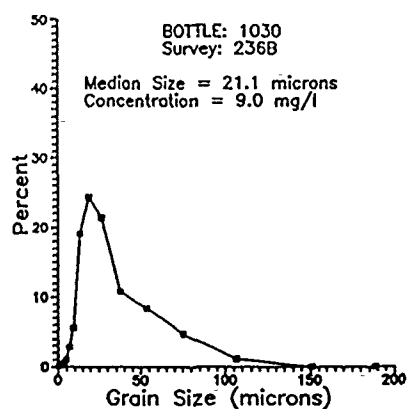
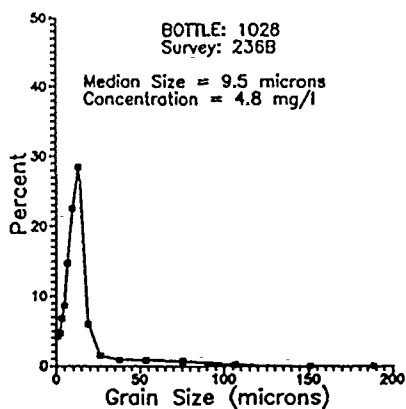


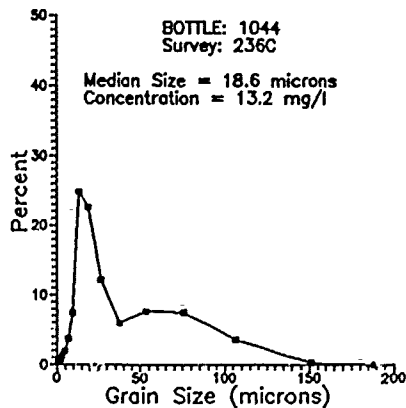
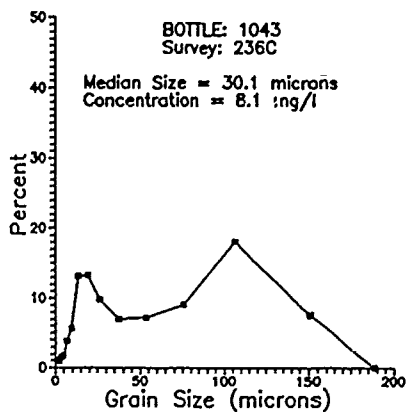
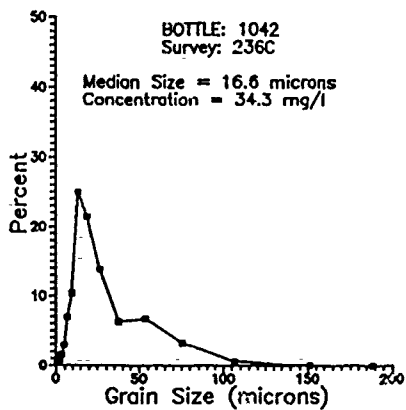
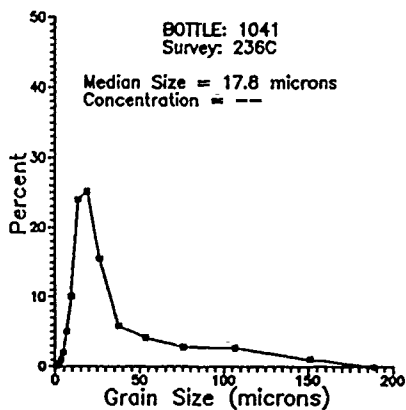
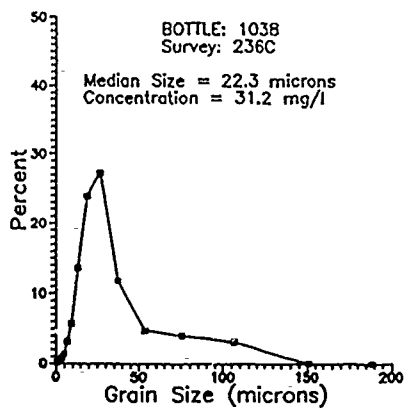
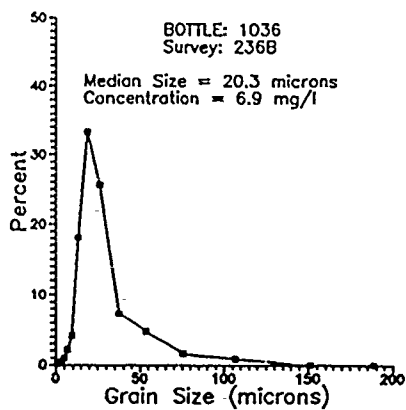


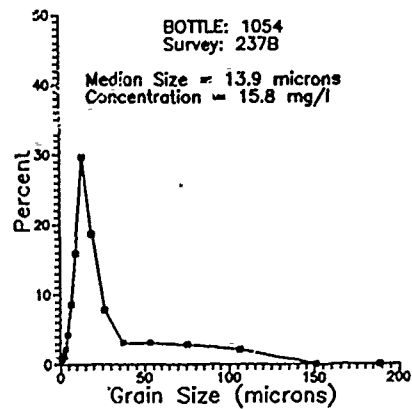
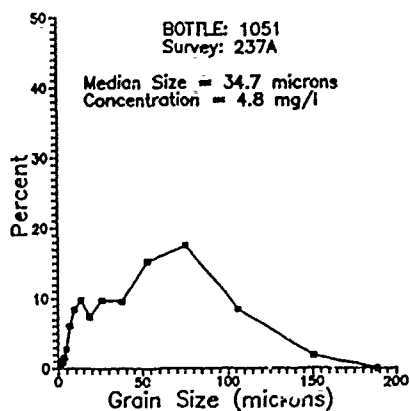
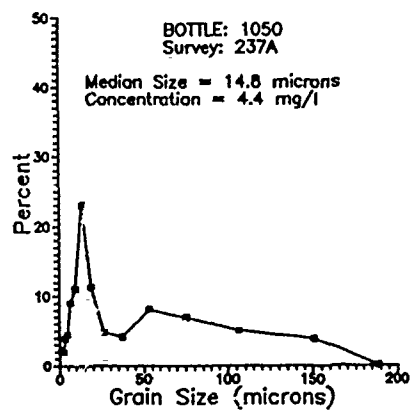
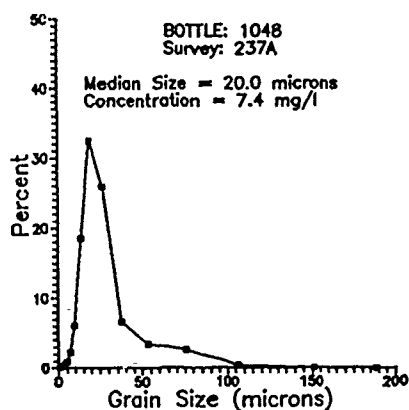
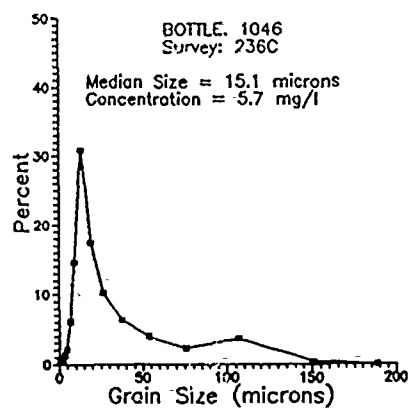
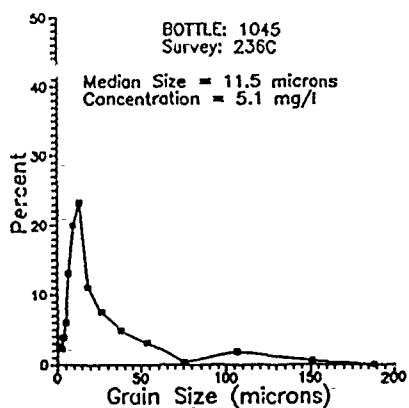
Appendix 4B: Suspended Sediment Sample Grain Size Density Functions

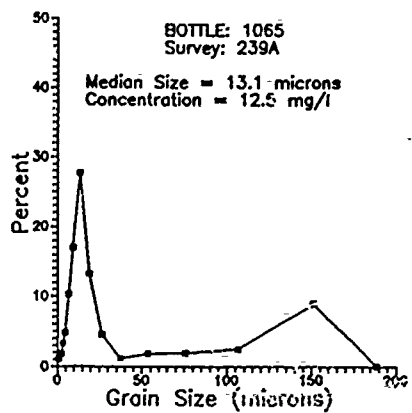
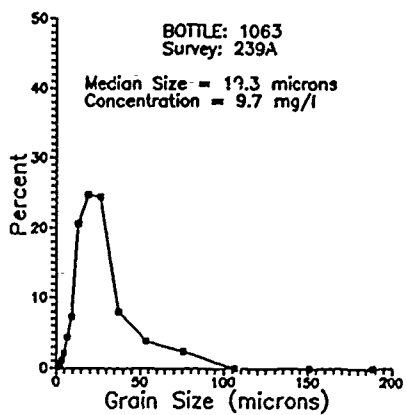
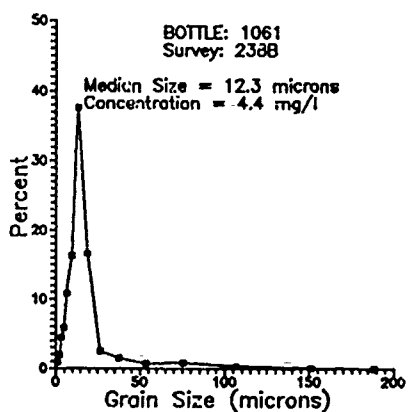
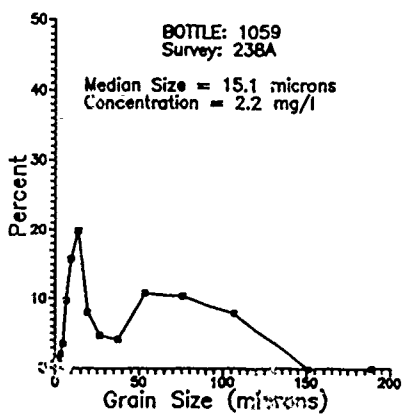
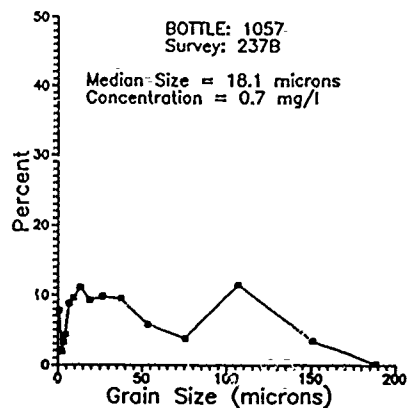
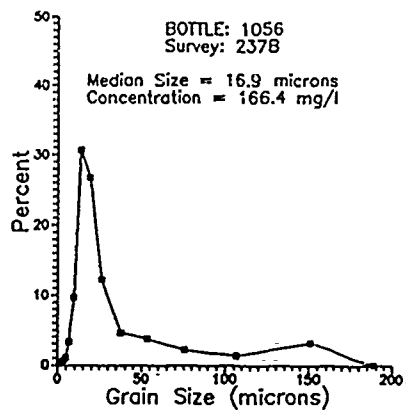


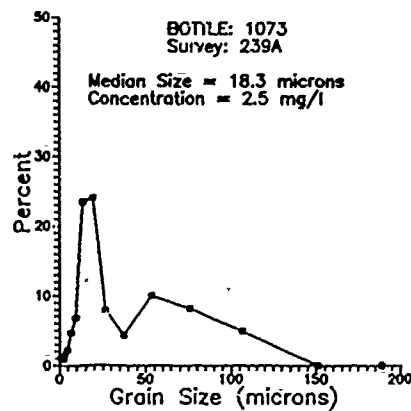
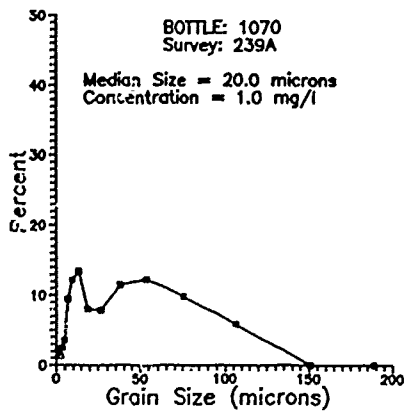
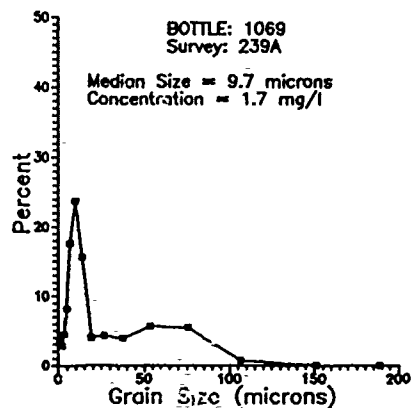
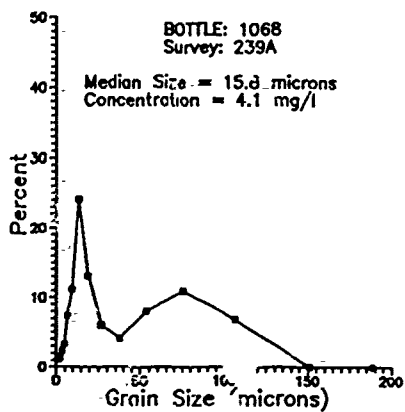
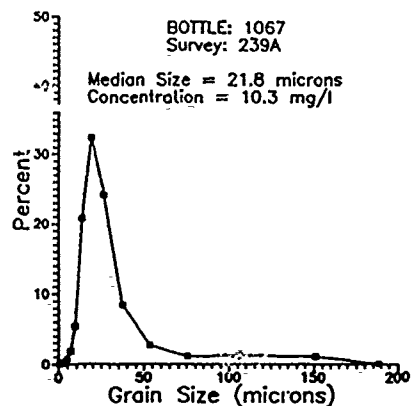
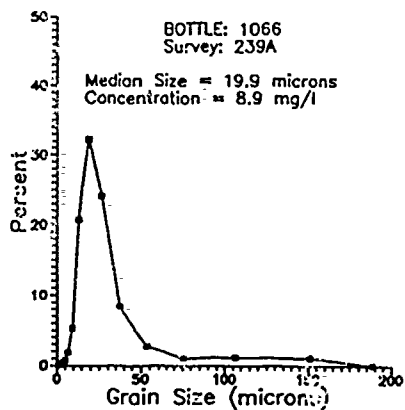


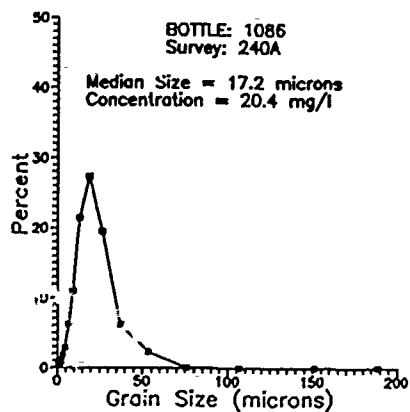
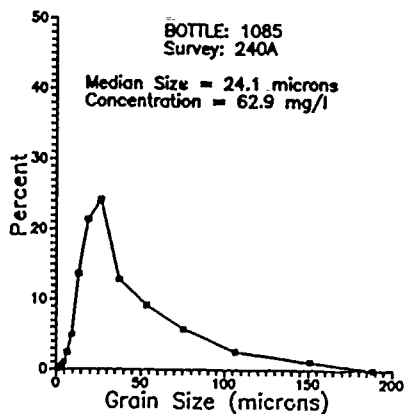
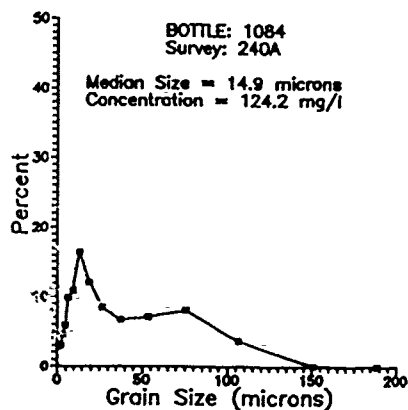
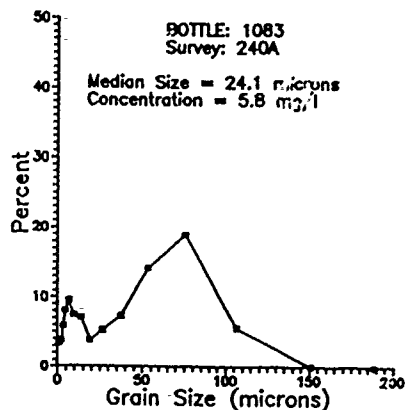
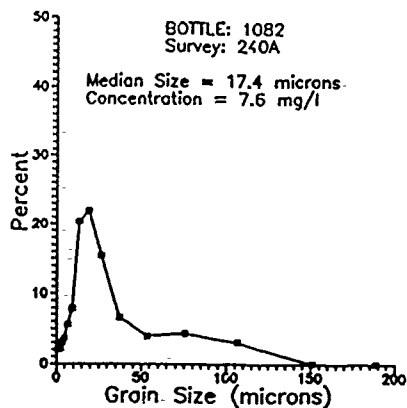
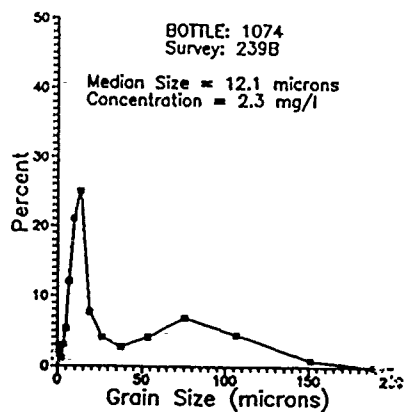


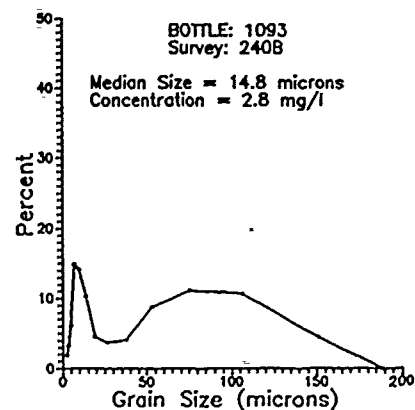
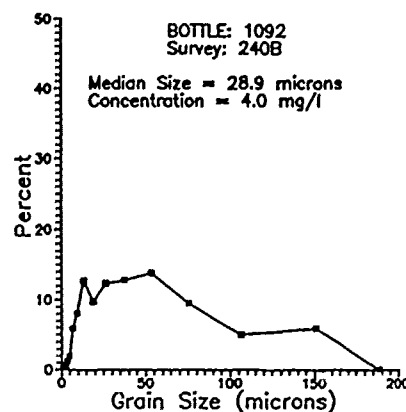
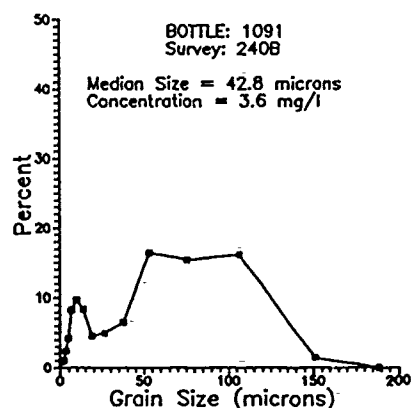
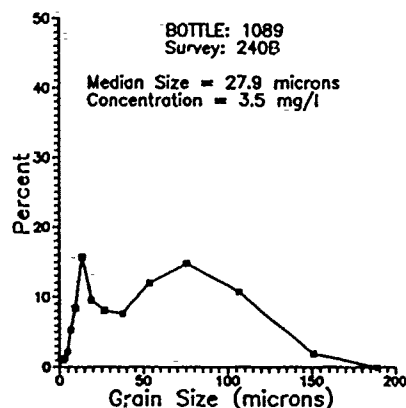
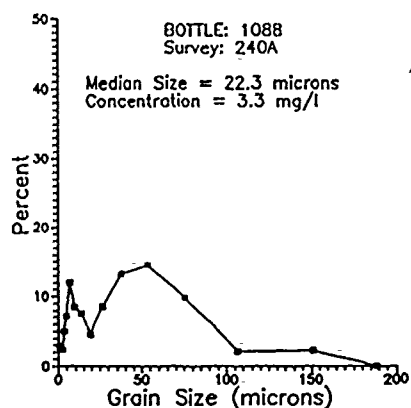
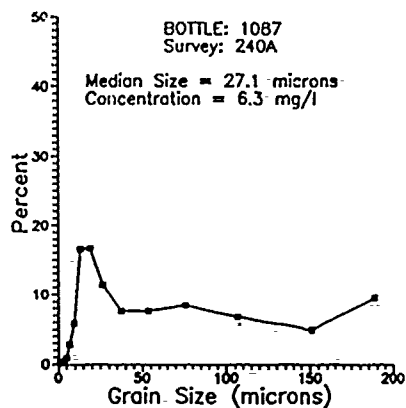


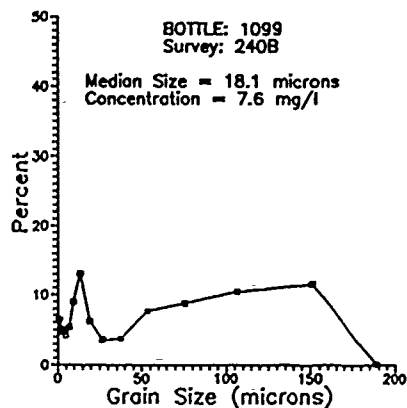
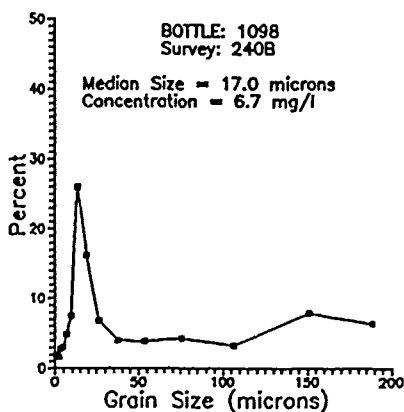
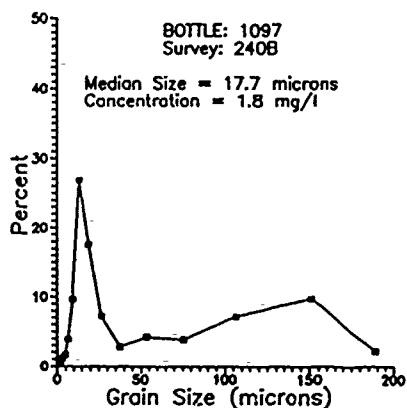
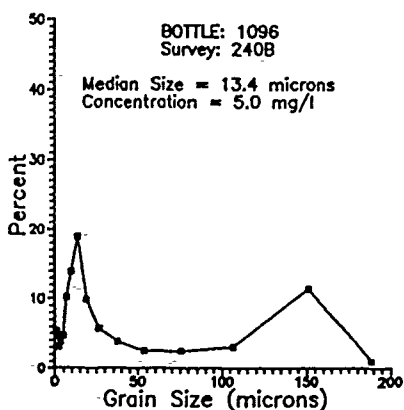
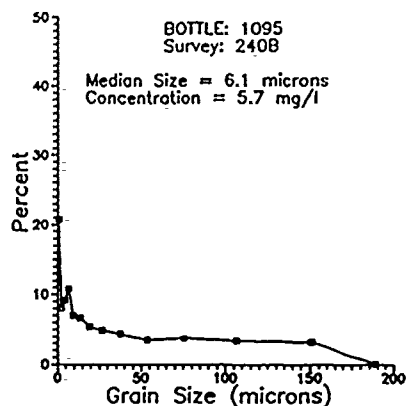
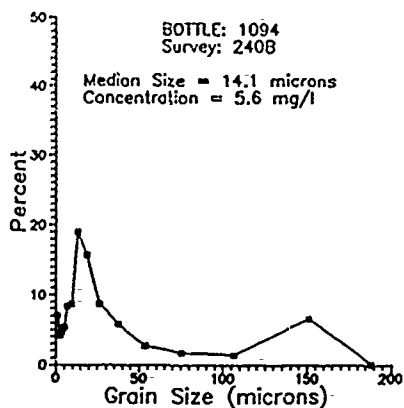


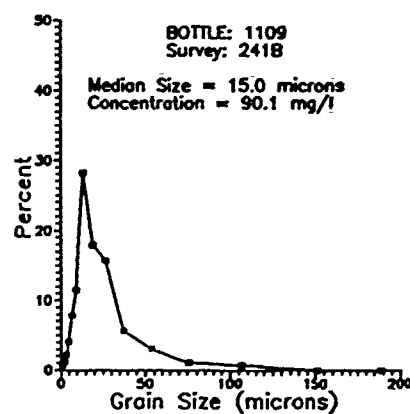
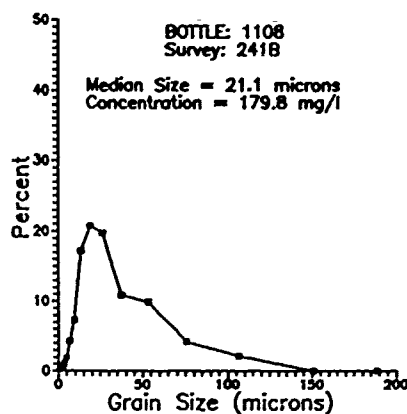
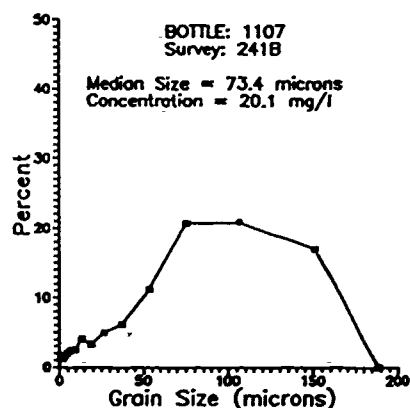
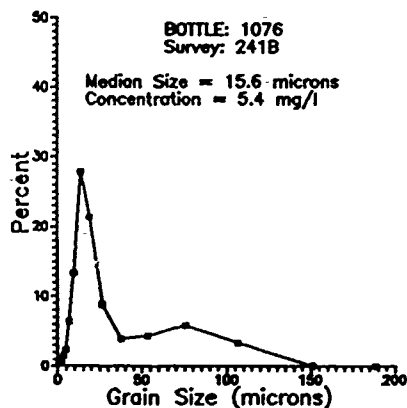
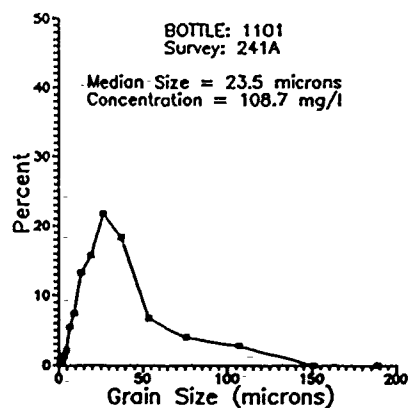
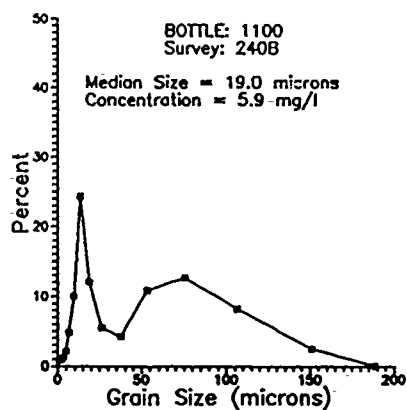


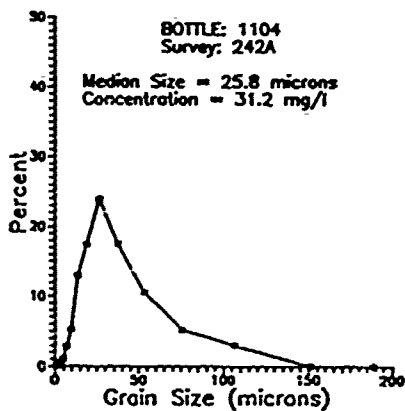
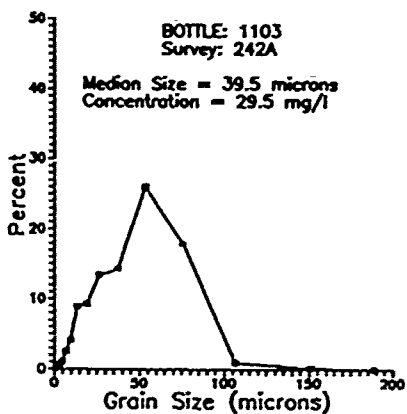
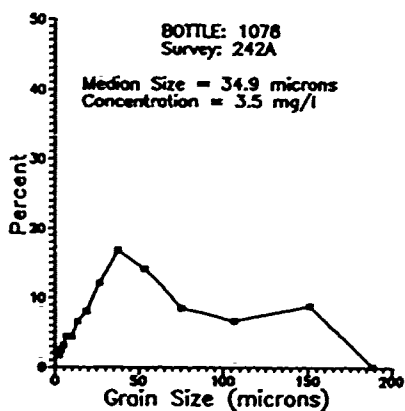
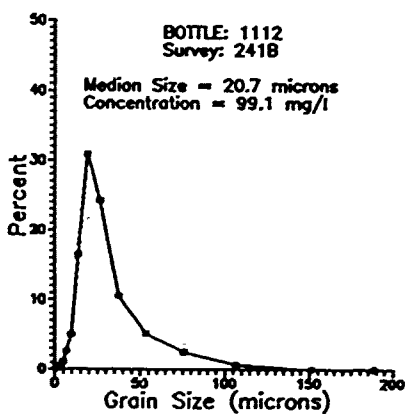
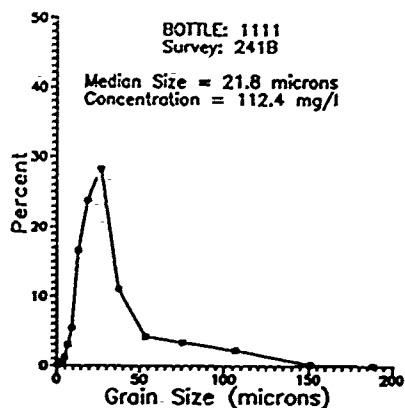
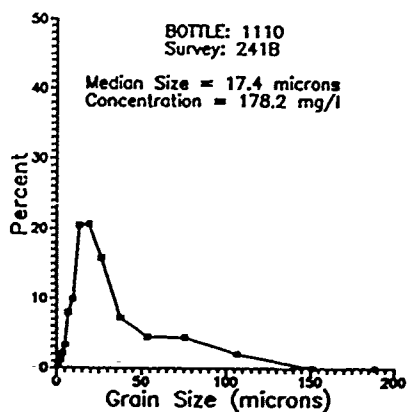


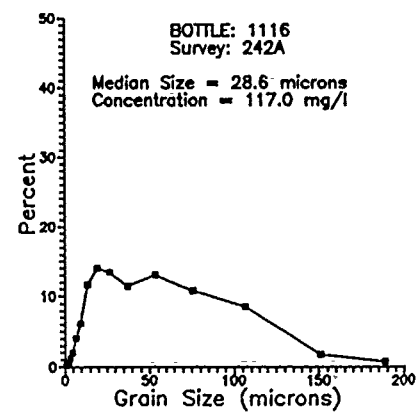
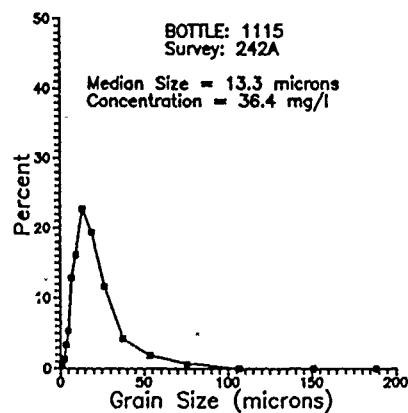
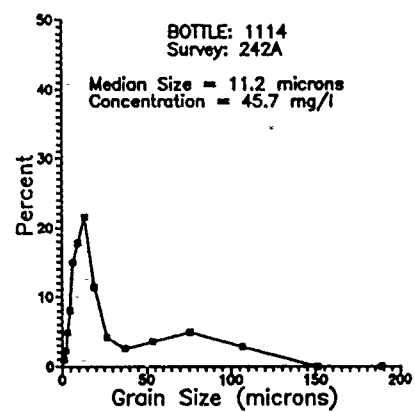
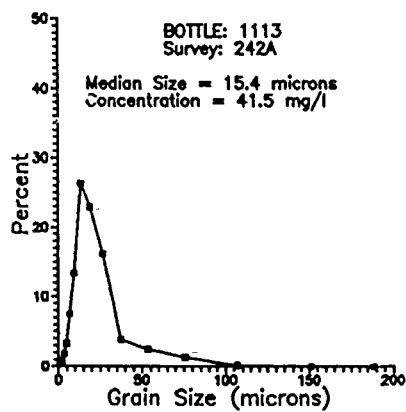
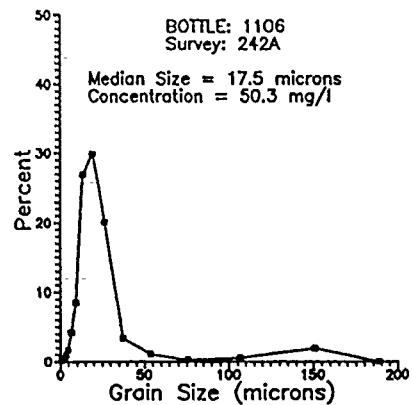
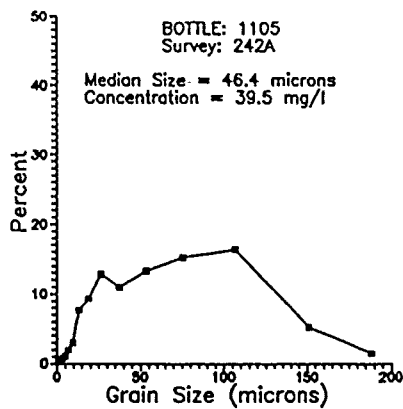


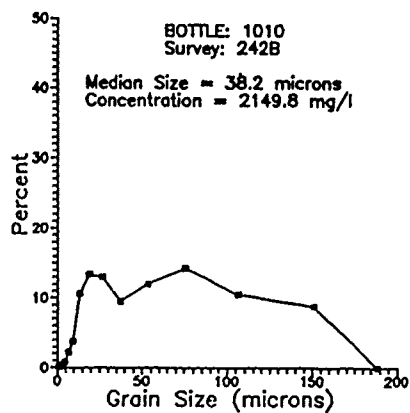
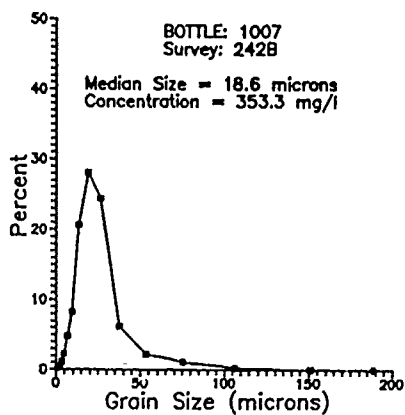
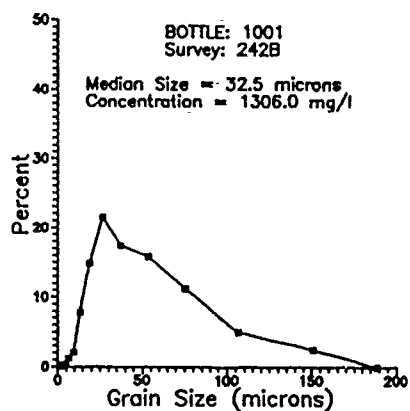
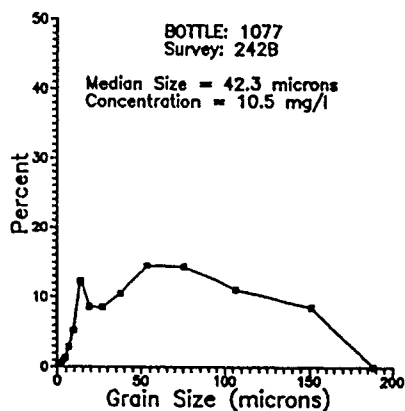
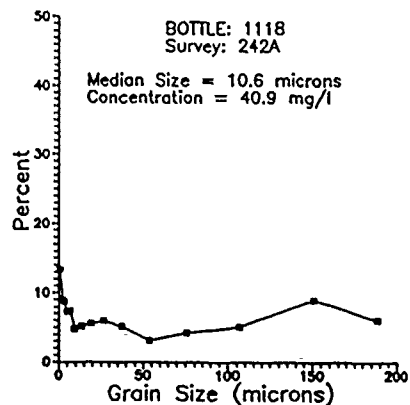
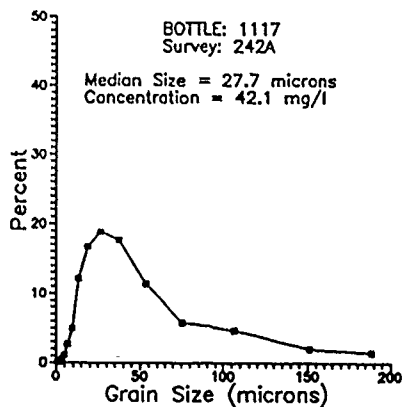


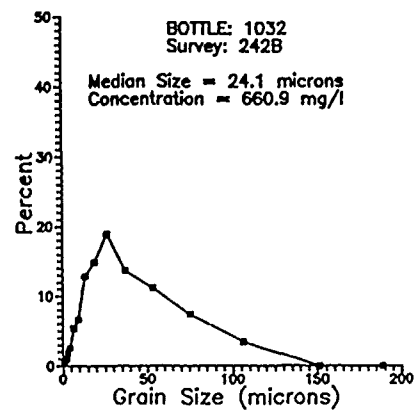
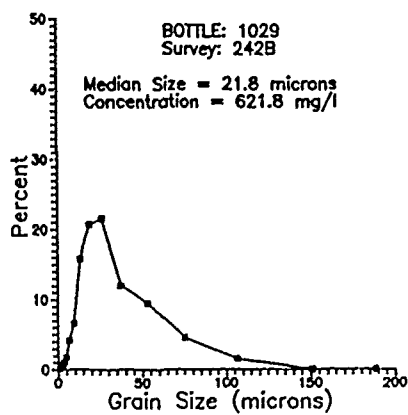
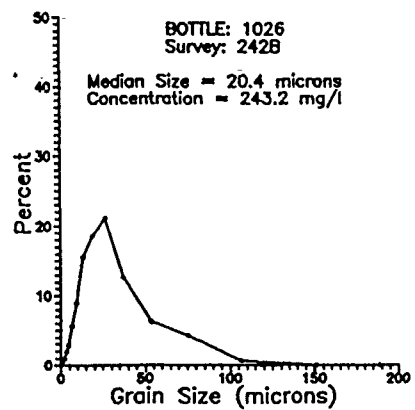
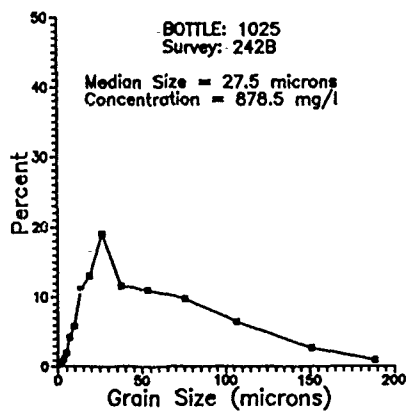
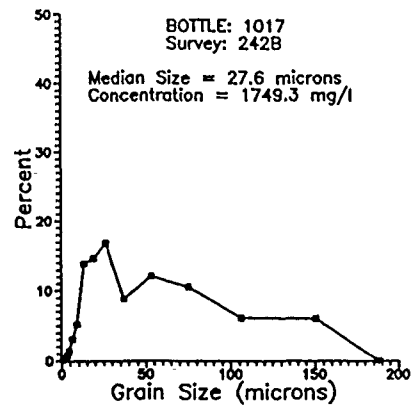
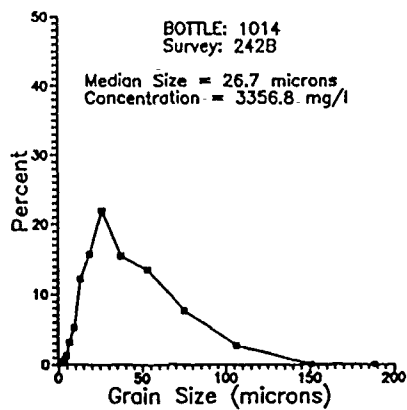


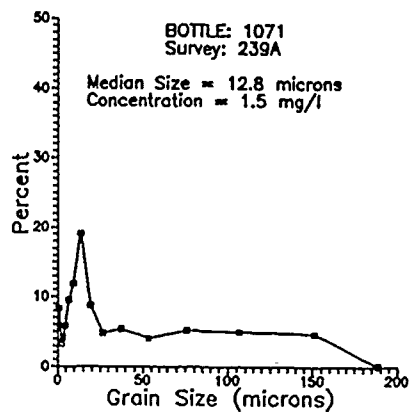
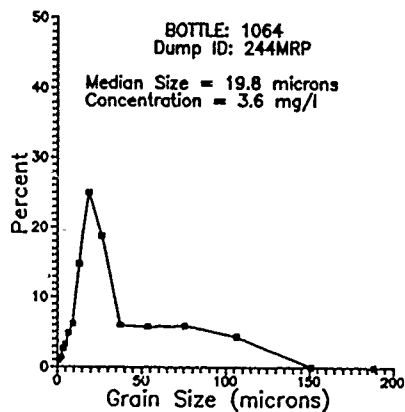
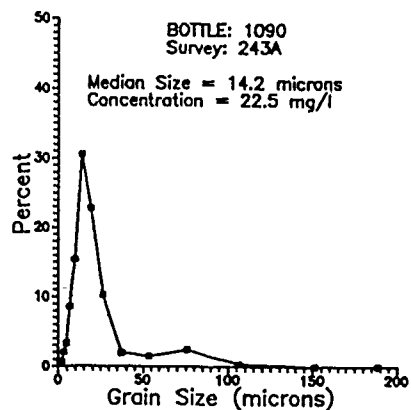
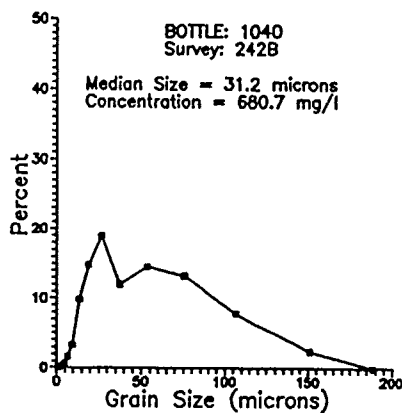
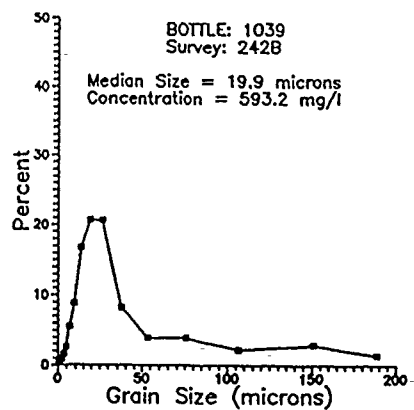
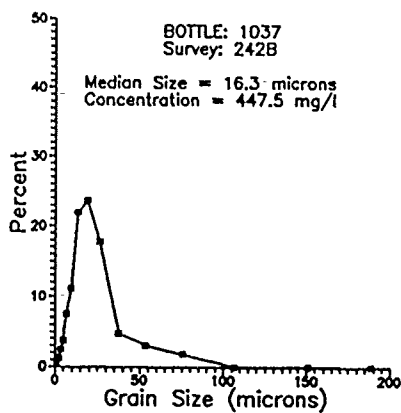


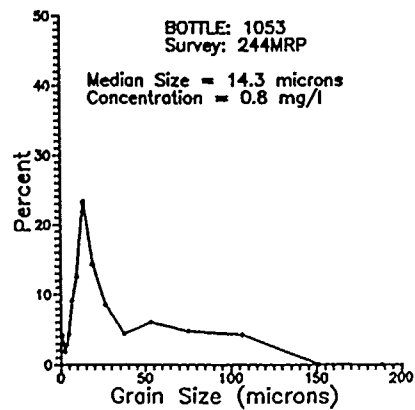
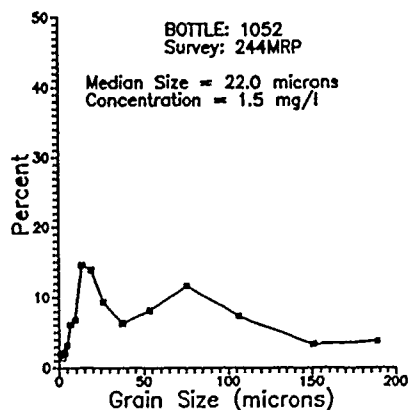
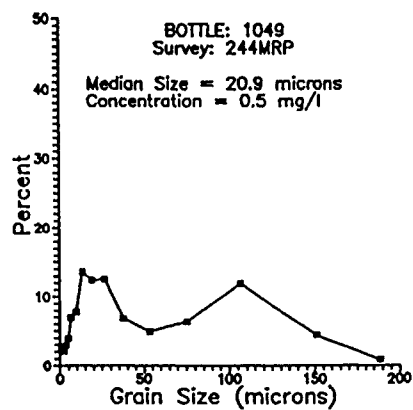
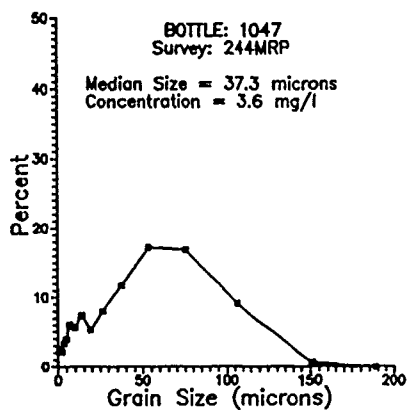
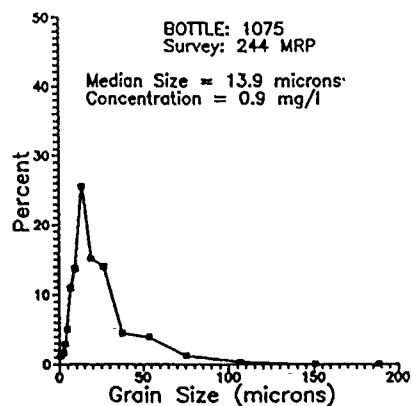
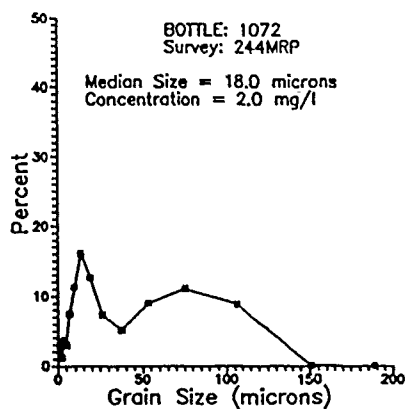












5. MEASUREMENTS WITH AN ACOUSTIC DOPPLER CURRENT PROFILER (ADCP)

ATLE LOHRMANN, CHRISTOPHER A. HUMPHREY

*RD Instruments
San Diego, California 92131*

Contents

1. Introduction
2. ADCP System: Hardware and Software
3. Measurement of Sediment Concentration
4. Simple Models of Acoustic Backscatter
5. Bottom Tracking and Navigation
6. Current Velocity
7. Vertical Velocity, Backscattering, and Internal Waves
8. Conclusions and Recommendations

References

Tables

Figures

Appendix

1. Introduction

Acoustic Doppler Current Profilers (ADCP) transmit short acoustic pulses along narrow beams at a known, fixed frequency (from a nominal 75 to 1,200 kHz, depending on the transducer). The ADCP listens to and processes the echoes from successive volumes (depth cells or bins) along the beams to determine by how much the frequency has changed. The difference in frequency between transmitted and reflected sound is proportional to the relative velocity between the ADCP and the scatterers in the water that produce the reflection (backscattering). This frequency change is called the Doppler shift. The ADCP uses an autocovariance method to compute the mean value (first moment) of the Doppler frequency, and the velocity of the scatterers is determined from this value. Data are output from the ADCP digitally and are displayed, recorded, and further processed on a microcomputer.

Sound is scattered by small particles of suspended sediment and zooplankton. These small particles tend to move with the water current, thus providing an estimate of the current velocity. Reflections from fish are infrequent and rarely affect the measurements.

The ADCP uses four beams to estimate current velocity. The standard configuration of each of these four beams is 30 deg relative to the vertical in 90-deg azimuth increments (Figure 5.1). Multiple beams are required because an ADCP measures only the velocity component parallel to the beam. Through range gating, i.e., analysis of the return signal in increments of time, it is possible to compute velocity (and backscatter) in a series of contiguous, discrete ranges along each beam. These ranges are called depth cells.

The depth cell size is determined by the durations of both the range gate and the transmit pulse length. The range gate and transmit pulse are normally set to be equal; their durations are equal to twice the spacing between depth cells (using the speed of sound to convert between length and time coordinates). The first ADCP depth cell is defined as the one closest to the ADCP, and successive bins are contiguous and partially overlapping.

The ADCP measures the velocity along each of the four beams and thus four different volumes in each depth cell. If one assumes that the current at any given depth is the same through all four beams (the homogeneous velocity assumption (RD Instruments (RDI) 1989)), then the three-dimensional (3-D) velocity vector may be computed using trigonometry. Note that any three of the four beams are sufficient to calculate the 3-D velocity vector, and the fourth beam is

redundant. This redundancy allows evaluation of the homogeneous velocity assumption and permits detection of other possible errors in data quality.

For the Mobile, Alabama, Dredging Research Program Field Data Collection Project (MFDCP), the standard configuration (Figure 5.1) was slightly modified. One of the ADCP beams was orientated at 0 deg relative to the vertical (see Figure 5.2). This orientation allowed for a more robust estimate of the vertical velocity and the acoustic backscatter of materials within the plume through the water column to the Gulf bottom. The geometry of the remaining three beams was such that they were pointed 30 deg relative to vertical: two of which were directed fore and aft (along the longitudinal ship axis) and one directed starboard (perpendicular to the longitudinal ship axis).

The fore and aft beams, when combined trigonometrically, provided an additional estimate of velocity and backscatter intensity vertically, as well as an estimate of the relative pitch of the ship (which may introduce errors in velocity estimates). The ADCP was also amplitude calibrated. This established a relationship between the sampled amplitude ("counts") and the backscatter intensity, expressed in decibels (dB). A more detailed description of the amplitude calibration procedure is given in a later section and in Appendix 5A.

The ADCP allows estimation of the ship velocity and direction by bottom tracking, which is performed by transmitting a longer acoustic pulse than that used for water velocity profiling. Bottom tracking is not constrained by the need to have high vertical resolution, and, therefore, longer pulses may be used. The longer pulse, combined with the fact that the bottom is a strong localized reflector, makes it possible for the ADCP to bottom track deeper than it can water track, resulting in a small short-term variance. Further discussion of bottom tracking is included in a later section.

A significant relation between the strength of the ADCP amplitude signal and the presence of sediment plumes was observed during the MFDCP. The analysis of the ADCP backscatter amplitude consisted of three parts: evaluation of the instrument itself, comparison of the amplitude data with the collected sediment concentration samples, and an attempt to model the backscatter.

In addition to the amplitude data, the data set from this field data collection project includes a time series of accurate ship position data from a miniranger navigation system (Chapter 3, this report). This unique opportunity to compare the ADCP Doppler current velocity measurements with an accurate reference was taken, and the results are included in this chapter. The current

velocity data were analyzed to obtain the mean velocity as well as to evaluate possible sources of error in the mean velocity measurement during each disposal event. An analysis of the plume dynamics during two of the events is included. Conclusions and recommendations are given at the end of this chapter.

2. ADCP System: Hardware and Software

Hardware

The ADCP used on the MFDCP cruise was a 1.2-MHz vessel-mounted (VM) system deployed off the side of the ship. An interface with the ship compass (Figure 5.3) allowed computation of average ship velocity (and thus the velocity of the ADCP). Table 5.1 lists some of the parameters encompassed by the data collection.

Software

The software used to process and display the current velocity and acoustic backscatter was a pilot version of RDI's transect program. This program, presently under development, produces a real-time visual picture of the processes being observed. The following is a list of the primary capabilities of this software:

- Recording and playback of raw data in real-time.
- Calculation and display of estimated range-gated backscattering levels from all four beams (using a time series of profiles to create a color contour plot for each beam).
- Calculation and display of estimated vertical and horizontal velocity structure from all four beams. The displayed data are then available to be spatially averaged by using the bottom tracking capability of the ADCP to determine the distance traveled by the ship.
- Rapid surveying of multiple transects, allowing sequential display of backscattering intensity within the plume over time.
- Integration of position data into the recorded data.

3. Measurement of Sediment Concentration

An analysis of the relationship between acoustical backscattering (scattering cross section) and sediment concentration contains four elements. Each is essential to the analysis. The first element concerns system calibration in the ADCP and how the numbers (or counts) reported by the instrument correspond to the strength of scattering from the particles inside the ensonified volume of water. The results of RDI's effort on this subject is reported in Appendix 5A. The second element is a model for the contribution of the individual particles to the total backscattering cross section, for which the particles are assumed to behave as Rayleigh scatterers. This assumption is reasonable given that the size of the particles (≈ 0.01 mm) is much smaller than the acoustic wavelength of the instrument (≈ 1.25 mm). The third element to tie the analysis together is a set of field data. During the MFDCP, more than 100 bottle water samples were collected and their contents analyzed for concentration (dry weight per volume) and particle size distribution. Of this data set, samples from seven disposal events were used in the analysis. The fourth element is an error analysis.

Calibration of ADCP for backscatter

Calibration of the ADCP involves range-dependent and range-independent contributions. The range dependency involves the effects of geometrical spreading and water absorption. This dependency was removed in the real-time display by adding terms describing absorption ($2\alpha R$) and geometrical spreading ($20 \log R$) to the receiver output (R is the range to the scattering layer along the beam in meters, and α the coefficient of absorption in decibels/meter). The range-independent (and instrument-dependent) part of the calibration was carried out before the field project. In addition, the calibration was improved upon after the project as a result of insight gained in the electronic circuitry that constitutes the response function of the ADCP. The main parameters found through the calibration procedure are the source level of the ADCP, the directional response of the transducer, and the response of the automatic gain control (AGC). Of these parameters, the directional response of the transducer is modeled once for each frequency, and the source level is measured for each beam. The AGC has proved to be much harder to characterize, and the results presented rely as much on modeling of the (temperature-dependent) circuitry as on actual calibration measurements. A typical response curve for the receiver circuitry measured at 22 deg C is shown in Figure 5.4. As can be seen, the response is linear (in log space)

over a dynamic range of 80 dB. In Table 5.2, the system parameters referred to in Appendix 5A are shown for the 1.2-MHz ADCP used on the *R/V Pelican* during the MFDCP.

Comparison with particle concentration

The accuracy of the comparison between the scattering cross section derived from the ADCP measurements and the particle concentration derived from the bottle samples involves several issues that are presently unresolved or can only be crudely estimated. Of special interest is the issue of how closely the bottle samples represent the overall sediment plume concentration. Throughout the MFDCP, the ship was nearly stationary with respect to surface currents during bottle sampling, and strong stratification and shear (vertical variation of horizontal currents) were present. Temporal variation of plume dispersion was the dominant time scale. Concentration of the falling dredged material changed on a scale of seconds to tens of seconds, and it was impossible to sample in situ concentrations faster than this time variation (Chapter 4, this report). As a result, the spatial variability in bottle-sampled particle concentration was large. The concentrations measured in this experiment show variations of up to ± 50 percent over a 1-min period, and it is difficult to estimate the actual uncertainty in the individual measurements. Ideal field sampling would close several water bottles simultaneously; however, because of the type of closing mechanism implemented for the water sampling rosette, this was not possible. Sample bottles were held open at each depth for at least 15 to 30 sec, before closing. This length of time is adequate for hydraulic flushing, but probably exceeds the time of variation in ambient concentration. Thus, for comparison to ADCP backscatter intensity measurements, a rough estimate of the uncertainty in the particle concentration obtained by the water sampling would be ± 3 dB (equivalent backscatter units).

Error analysis

Based on our knowledge of the ADCP, the range of temperatures during the field project, and the variation observed from beam to beam, we estimate the accuracy of the backscattering cross-section to be ± 3 dB. In addition to this absolute error, the problem remains of temporal and spatial variation in the amplitude data.

A first attempt at comparing the 1-sec averaged amplitude data with the measured concentrations led to a large spread in the data. A quality check and analysis procedure was implemented to improve accuracy and estimate the size and nature of the variation in the acoustic data. For the comparison between the two data sets, it was necessary to assume that the amplitude data and bottle samples were representative of the same water mass.

Temporal variation. As a first attempt at calibration, the amplitude data (sampled at 5 to 8 Hz) were averaged over the 10-sec period before the time of closing of the bottles. There are two principal reasons for this. To obtain a stable estimate of the amplitude, it is first necessary to average out the variation in the amplitude data produced by Rayleigh scattering. Second, the bottle samples must necessarily have a relatively long flushing period after they have been lowered. It is assumed that over this longer averaging period, the two data sets would more likely represent a similar temporal average. Finally, the standard deviation of the amplitude over this averaging period is used as a measure for indicating the added effect of blockage of the beam pattern. Interference could occasionally happen when the data logger, used to measure conductivity (C), temperature (T), and depth (D) (CTD), and attached to a rosette sampling apparatus (Chapter 4) blocked the transmitted pulse for one or more of the beams. By excluding all average data with a standard deviation greater than ± 3 dB, most of highly scattered data points were excluded.

In summary, the acoustic data have much better temporal resolution than the bottle samples. Because of the large spatial and temporal variations in the concentration inside the plume, bottle samples provide a crude magnitude estimate of the processes in action. This limitation also makes a comparison with acoustic data difficult. An example of the temporal variation in the amplitude data can be seen in Figure 5.5. This plot indicates the maximum variation over the 28-sec period is nearly 15 dB. Another example can be seen in Figure 5.6, where Beam 2 is blocked by the rosette.

Vertical variation. The vertical variation over the 10-sec period was calculated to quantify the uncertainty in the data and to exclude data points influenced by the bottom. Data with a standard deviation greater than ± 3 dB were excluded. This method was effective in eliminating data points that were influenced by the bottom or were found to be in the shadow of the CTD rosette.

The backscatter amplitude data proved to be sensitive to vertical variation at the start of the plume descent. Such data points pertaining to rapid evolution of the plume were not included in the comparison between concentration and acoustic scattering. An example of both the temporal and vertical variation in the volume backscattering can be seen in Figure 5.7.

For Survey 240B, Figure 5.7 shows contours of the backscatter amplitude data (expressed in decibels) as a function of time (Greenwich Mean Time (GMT)) and range (m) along the vertically oriented beam (Beam 2). Tic marks on the time axis are separated by approximately 33 sec. For this vertically oriented beam, the slant range along the beam is equal to the vertical distance from the ADCP transducer. The bottom can be seen at a depth of 10 m, where the backscattering has

a global maximum of -40 dB. The *R/V Pelican* is beginning to move over the plume at 20:36:30 GMT, and the backscattering rises steeply from the background (-70 dB) to a maximum of -44 dB. The intensity then decreases to about -65 dB until the ship drifts back into the plume at approximately 20:42:45 GMT. This plume signal is much weaker than the first, as can be seen from the slanted -60-dB contour. Toward the end of the survey shown in the plot, the plume is strongly sheared.

Data comparison. In Figure 5.8, a scatter plot between the measured concentration and the volume backscatter after quality check and calibration is shown for seven of the surveys. Data points for each of the four beams have been plotted (generating apparent vertical lines in the scattergram), and each survey includes 2 to 11 samples. The data cover a dynamic range of 40 dB both in concentration and acoustic scattering.

It is difficult to determine a curve that best represents the data set. An overall view gives the impression of a nonlinear curve with a slope that decreases with increasing concentration. However, if the survey that covers the highest concentrations (Survey 242B) is removed from the data set, a linear curve constitutes a fairly good fit. The spread is largest for low concentrations. Because the data are shown in logarithmic units, this effect can be explained by assuming a fixed or a percentage error in the concentration data.

As a first attempt to compare the ADCP backscatter data and the concentration, the results are promising. With a standard deviation in both data sets of at least ± 3 dB, a deterministic curve could be fit to the data set such that the uncertainty in the concentration derived from acoustic measurements lies within one order of magnitude. For dynamical studies or studies over large spatial scales, this accuracy would provide a much enhanced capability to characterize plumes. However, additional comparisons of backscatter and concentration are required to estimate rigorous error bounds and understand more fully the relationship between these two measures.

4. Simple Models of the Acoustic Backscatter

Because particle size distributions of the water samples are available, it is possible to make a comparison of predictions from the simplest scattering models and the measured backscatter. It is usually assumed that the scattering behavior for sediments follows the Rayleigh scattering model, as has been demonstrated in the laboratory for spherical particles of varying size, where it is assumed that the particle size is much smaller than the wavelength of the acoustic pulse. If the

reflected angle is equal to the incident angle for the scattered sound, the Rayleigh scattering cross section (disregarding density and elasticity) can be written (constant density) (Rayleigh 1945),

$$\sigma = b k^4 \sum_{i=1}^M C_i a_i^3 \quad C_i = N_i a_i^3 \quad (5.1)$$

where

σ = scattering cross section

b = empirical constant

k = acoustic wave number

C_i = concentration by weight of particles in size class i

a_i = radius of one particle in size class i of a total of M size classes

N_i = number of particles per unit volume in size class i

If the particle size distribution does not change (i.e., $N_i / \sum N_i = \text{constant}$), the cross section is proportional to the total number of particles and hence to the particle concentration.

It is not possible to simplify the calculation by using the median or mean radius of the particles in the calculation and still be consistent with this scattering model. If only statistical parameters are available, the appropriate value to use for the "mean volume" in Equation 1 is:

$$a^3 = \frac{\sum C_i a_i^3}{C} \quad (5.2)$$

where a^3 is a weighted mean volume, C_i is the partial concentration associated with particles of radius a_i , and C is the total concentration.

Because the scattering cross section in this model depends on the 6th power of the radius, the scattering is heavily weighted toward the large particles. This weighting implies that knowledge of the size distribution becomes important for the relationship between acoustic scattering and concentration.

Based on the size distribution of the sediments collected with the water bottles, a scatter plot between the model prediction and the actual scattering is shown in Figure 5.9. This plot shows a larger spread than Figure 5.8, which corresponds to a 3rd-power scattering law. All power laws between 1 and 6 were tested for comparison, with a minimum spread obtained using the 3rd-power

law. Of interest also is the spread to be expected in a scatter plot between the acoustic signal and concentration if a 6th-power law is applied. Figure 5.8 shows the results based on the size distributions observed in the project. Comparison of the previous scattergram (Figure 5.8) reveals a similarity in trend to the theoretical calibration curve (Figure 5.9). The spread is sufficiently small that knowledge of the backscattering strength is adequate to predict the concentration within one order of magnitude (see Figure 5.8).

In the data, there is neither support for the 6th-power scattering model nor evidence to refute the model. If the scattering model is correct, one might conclude that density variations and the effective scattering cross section of the individual particles must be taken into account to reduce the spread in the data.

5. Bottom Tracking and Navigation

The ADCP measures the Doppler shift of an emitted pulse. The source of the sound is the transducer element fixed to the transducer head. On a moving vessel, the transducer head moves with the vessel; thus, the Doppler shift is a vector combination of both the water current and the velocity of the vessel itself. In the following, this combined velocity is referred to as the "water velocity."

The purpose of the special ADCP mode called "bottom tracking" is to measure the motion of the vessel with respect to the bottom. The estimate of the vessel velocity is then subtracted from the water velocity to yield the current velocity. If the water is too deep or if it is impossible to automatically detect the bottom on the basis of the acoustic echo, the velocity of the vessel will remain unknown, and the true current velocity cannot be calculated. In these cases, another way of determining the ship velocity must be found. One option is to use the time derivative of the position data. For ships operating in areas with full ocean depth, this is the most common method of deriving the vessel velocity.

Just as the position data can be used to measure the velocity of the ship, the bottom track data can be integrated to yield the position of the ship relative to a starting point (dead reckoning). This technique is used in volume transport measurements with the ADCP.

During the MFDCP, ADCP bottom tracking data and positioning data from a highly accurate Mini-Ranger navigation system were recorded. To determine errors and accuracy involved with

each of the methods described above, the recorded data were analyzed, and the results are reported in the following.

Bottom tracking

The bottom track pulse is distinguished from the water track pulse by processing that takes place within the ADCP. Instead of processing the echo at fixed range gates, the processing is configured to locate steep gradients in the echo strength, thereby measuring the Doppler shift of the echo from the bottom and area in the vicinity of the bottom. Whereas the water track transmit pulse usually needs to be short to retain vertical resolution, the bottom track transmit pulse is usually long. This long pulse is required to reduce the single ping variance of the Doppler shift; also, the sound beam must ensonify the bottom over the entire beam to avoid changing the effective beam angle. Based on previous calibration projects, this long pulse illuminating the bottom will produce an accurate and stable estimate of ship velocity.

Analysis of bottom track and navigation data

The ADCP provides ship velocity measurements, whereas navigation data provide an estimate of ship position. By integrating the ADCP bottom track data, a relative ship position can be determined and compared with navigation data. Similarly, differentiation of navigation data yields relative ship velocity, which can be compared with ADCP bottom tracking velocity. Before a direct comparison of the two data sets could be performed, the data had to be corrected for three systematic errors.

1. The transducer was mounted somewhat irregularly on a pipe over the side of the *R/V Pelican*, and the error in the installation angle (referred to as transducer misalignment) had to be determined. The misalignment was assumed to be equal to the difference between the mean of the direction of course from the bottom track velocity and the mean of the direction of course based on navigation data. These angles, expressed in degrees, are given in Table 5.3.
2. For precise comparison, ADCP data must be corrected for the speed of sound. The nominal conversion factor between the recorded Doppler shift and engineering units is based on the value 1536 m/sec for the speed of sound (defined by the conditions: $T = 26$ deg C, and 35 ppt salinity). For the bottom track data set collected during the MFDCP, the speed of sound was taken to be equal to this value.
3. The navigation data have to be checked for quality. The ship was stationary during microwave positioning checks, during which time no tracking checks were possible. Positions were recorded every 2 sec. Rotating the transceiver antenna affected reliability of the positioning, as did the position of the ship (there were some shadow zones). The task of checking the quality of the navigation data was carried out by staff of Evans-Hamilton, Inc., and the analyzed data were judged to be quite reasonable (Chapter 3, this report).

Comparisons of ADCP bottom track data to the navigation data were performed for seven transects to estimate errors and accuracy of each method and to create a postprocessing template for additional event processing. Unweighted least squares fits were computed for the following: ship position (from navigation data) and ship velocity estimated from the integrated ADCP data (bottom track velocity); ADCP ship velocity and ship velocity estimated from ship position; and ship heading computed from integrated ADCP bottom track data and from navigation data. The results of these analyses are tabulated in Tables 5.4 through 5.7.

In general, the two methods (ADCP and navigation) exhibited a high linear correlation. The data were unweighted because errors in each measurement method were assumed to be uniform over all measurements. Plots of ADCP and navigation-determined tracks versus time were made for both position and velocity to determine variation as a function of time. Data pairs were aligned to within one second in accordance with the 1-sec standard for accuracy between the different clocks used in the project. In the following, all velocity time series plots are a function of elapsed time in minutes (0 min corresponding to the start time of the survey).

Before comparison of position data, the ADCP bottom tracking data (recorded in beam coordinates) were converted to north and east components of the true ship velocity using the heading information and transducer misalignment correction. The velocity components were converted to relative north and east position components by integration with respect to time. The data were converted to feet in accordance with the coordinate system used by the Mini-Ranger positioning system, referenced to the Alabama State Plane Coordinate System (ASPCS).

Before comparison of the velocity data, the ADCP bottom track velocity components were converted to east and north components, and the navigation data were converted to velocity by differentiation with respect to time. The total velocity from each source was then computed and compared. Results of this analysis are discussed next.

Bottom track data. Data measured by the ADCP using bottom tracking were recorded at 2-1/2-sec intervals and saved in separate files for each survey in ASCII format (ADCP bottom tracking data file name: ADCP####.BTM (the four-character string #### corresponds to a survey number)). The data format for each line of the file is [HR:MN:SC VX VY HEADING], where:

HR:MN:SC = Eight-character string corresponding to the local hour, minute, and second of each velocity measurement

VX = Component of velocity perpendicular to the main axis of the ship (positive starboard) in units of 0.125 cm/sec.

VY = Component of velocity along the main axis of the ship (positive forward) in units of 0.8 cm/sec.

HEADING = Ship heading measured in degrees from north.

Navigation data. Navigation data for the *R/V Pelican* provided ship position and were recorded at 2-sec intervals and saved in separate files in ASCII format for each survey (navigation data file name: EDT#### (the four character string #### corresponds to a survey number)). The data format for each line of the file is [HR:MN:SC EP NP], where:

HR:MN:SC = Eight-character string corresponding to the local hour, minute, and second of each position measurement

EP = East (easting) position in feet

NP = North (northing) position in feet

Plots of the ship tracks from the navigation (Mini-Ranger) system for surveys covered in this chapter are shown in Figures 5.11 through 5.17 at the end of the chapter. The ADCP data were converted to feet and referenced to the ASPCS.

The results of intercalibration of ship velocity, position, and heading from ADCP bottom tracking and navigation data are presented for Surveys 237A, 238A, 238B, 239A, 239B, 241A, and 242A.

Ship direction. The direction of the ship velocity as reported by the ADCP combined with the heading data was compared with the direction of the velocity vector derived by differentiating the northern and eastern components of position (from navigation data). The velocity time series plots (Figures 5.18-5.31) suggest that while the ship is turning (sustained low mean ship speed), computation of ship heading from position data may be unreliable.

Scatter plots of ship heading computed from ADCP bottom track and navigation data are shown in Figures 5.32, 5.33, 5.34, 5.35, 5.36, 5.37, and 5.38. The linear regression between the two

sources of ship heading are tabulated in Table 5.4 and demonstrates a high correlation for the events processed.

Ship speed. Results of the linear regression analysis are given in Table 5.5. The scatter plot of ADCP bottom track speed as a function of speed calculated with the navigation data is shown in Figures 5.39, 5.40, 5.41, 5.42, 5.43, 5.44, and 5.45. The data show high correlation for most of the surveys. Although the time series plots (Figures 5.18, 5.20, 5.22, 5.26, 5.28, and 5.30) show noise in both sets of velocity data, the Mini-Ranger navigation data show larger variance in ship velocity. This analysis suggests that ship velocity measurements derived from navigation data may be less accurate than ADCP bottom track velocity measurements.

Ship position. Times series plots for the estimates of ship position from the ADCP bottom track data and the navigation data are shown in Figures 5.46 through 5.52. Linear regression between the north and east position estimates for the events considered also exhibited high linear correlation, as shown in Tables 5.6 and 5.7. The large value and uncertainty for the offset results from the difference between the ADCP position and the origin of the navigation grid.

An offset bias was added to the ADCP position data to align the data at the initial point in the time series. This offset bias is equivalent to aligning ADCP data to the navigation coordinate grid. Note that both the navigation and ADCP position data are relatively free of high-frequency noise.

This analysis indicates ADCP bottom track velocity data, integrated to compute position, provide stable and accurate position information comparable with position data obtained from land-based navigational sources.

Results from individual events. Results of the intercalibration of navigation and bottom track data are presented in Tables 5.4 through 5.7. Scatter plots and time series plots are also presented in Figures 5.11 through 5.52.

6. Current Velocity

Measurements of current structure (velocity and direction) in the area around the dredged material placement site are shown in Figures 5.53 through 5.68. These plots show little horizontal variation in the current velocity. Synthesis of current structure data was achieved by first subtracting the velocity of the ship from the collected current velocity data. For each depth bin, the current velocity was then averaged over the entire event. The small horizontal variation in the current structure near the disposal sites was disregarded. Depth bins within 2 m of the bottom

were rejected from analysis. The vertical variation shows a relatively weak shear in some events, with typical current speeds of 30 cm/sec near the surface and 10 cm/sec near the bottom. Because of the small horizontal variation, the data have been synthesized into one vertical profile from each survey.

It was observed during the data collection that the direction and magnitude of the measured current (as illustrated with current sticks on the computer monitor) exhibited a weak dependency on the speed of the ship. It became clear that there was a coupling between the two parameters, and an analysis to quantify the interaction of the current and ship speed was undertaken.

The problem is caused by the influence of the ship on the flow field below the hull of the ship. Conceptually, the ship can be thought of as "pulling" the water along in the direction of its motion. This action leads to a net apparent current in the direction of the travel of the ship. The effect has not been previously reported among ADCP users, and the result was therefore surprising. Research on this phenomenon is presently being conducted. Most likely, the effect was particularly strong during the MFDCP because of the shallow water (compared with the keel depth and displacement of the ship) and because the ADCP was mounted off the side of the ship.

The analysis of the coupling was achieved by linear regression between each of the components of the current velocity and the ship velocity. The influence of the ship motion on the undisturbed current field is stronger near the surface (2 to 3 percent of ship speed) and decays toward the bottom, and it is stronger in shallower water than in deeper water. The error is large enough that the current data need to be corrected before they can be used to characterize the undisturbed flow field. There is no effect on the bottom track measurements because the bottom is unperturbed by the ship motion. Typical results of the linear regression data collected are shown in Table 5.8 (shallow depth, Survey 242A) and Table 5.9 (medium depth, Survey 238B).

7. Vertical Velocity, Backscattering, and Internal Waves

The ADCP provides two independent estimates of the vertical current velocity. One estimate is derived directly from the vertical beam, and the other is derived from a linear combination of the fore and aft ADCP beams (Beams 3 and 4) directed 30 deg from the vertical. Comparison of backscattering amplitude to vertical velocity measurements, examination of plume dispersion, and the generation of internal waves were performed using time series plots and contour plots as a function of depth and time (or space).

Survey 240B

During Survey 240B, the ship entered the plume at a speed of 2 m/sec and then slowly drifted through the plume sideways with a speed of 0.2 to 0.3 m/sec. Figure 5.69 shows the backscattering for the vertically oriented beam (Beam 2) in depth cell 2 (4.3 m). The first part of the plot (starting at 150 sec) shows that the plume had very high initial concentration and is probably confined to a very small area. After 320 sec, a central plateau appears with an interval of slightly lower backscattering with only small temporal variations. The plume at this time appears to be spread over a large area, and material is well mixed. At an elapsed time of 800 sec, the ship has drifted out of the plume, and the backscattering amplitude returns to the value it had before plume entry (-80 dB).

Figure 5.70 is also from Survey 240B and shows plots of forward and transverse ship velocity along with the bottom track and water velocities in bin 2 (vertical beam). Note that the bottom track and the water track velocities have been multiplied by a factor of 10 to aid visual comparison. Two observations can be made from this figure. One is that the ship speed is small during the time the *R/V Pelican* drifted through the plume and, consequentially, the parameters in the figure (to first order) represent a single point in the horizontal. The other is that the water track velocity along the vertical beam is greater than the bottom track velocity. This latter observation is important because it rules out the possibility that the vertical velocities are artifacts of vertical misalignment in the transducer installation.

There are three mechanisms by which vertical velocities could be introduced given conditions during the field data collection. The first is the fall speed of the particles through the water. The fall speed of individual particles is expected to be of order 1 to 5 cm/sec for the first 10 min after the initial placement of the material (after the descent of the collective body of material immediately after release). The second mechanism is the existence or generation of internal waves. The third mechanism is the generation of potential flow around the vessel that disturbs the background flow field. The strong peak in vertical current seen in Figure 5.71 (-10 cm/sec) at elapsed time of 150 sec can be explained only as generated by this potential flow field. The effect is particularly severe at this time because the ship is making a sharp turn and partially yawing (transverse motion).

Figures 5.71 and 5.72 show the two independent estimates of the vertical current velocity within a temporal subset of the previous figures. The subset corresponds to the time when the ship is drifting through the plume. This correspondence allows for maximum dynamic range in the plot

and rules out the possibility of significant interference by the potential flow. Figure 5.71 shows data from the vertical beam (Beam 2), and Figure 5.72 shows combined data from Beams 3 and 4. Both figures show the vertical current velocity from bins 2 and 5 along with the bottom track velocity. The current velocity is equivalent to the water velocity minus the bottom track velocity shown in Figure 5.70. As expected, the vertical current for bins 2 and 5 is generally of the same shape, with larger negative velocities for the deeper bin 5. The bottom track velocity is close to zero. Although the two figures show much of the same structure, the differences between the two estimates of the vertical velocity imply that the horizontal distance between the sampling volumes for the three beams is important. From these figures, it appears that the vertical current is dominated by the propagation of internal waves that have an amplitude of 5 to 10 cm/sec. This domination is unfortunate, because it makes direct measurement of the fall velocities difficult.

The first contour plot (Figure 5.73) shows backscatter amplitude as a function of depth and time. The temporal range is a subset of that used in Figures 5.69 through 5.72. The spacing of contour lines over time gives an indication of plume dispersion. The initial closely packed contour lines indicate a denser scattering field and the presence of a plume structure. The later widely spaced contour lines indicate dispersion and settling of the dredged material.

The second contour plot (Figure 5.74) shows the vertical current from the vertically oriented beam (Beam 2) as a function of depth and time. The temporal range is identical to that used in Figure 5.73. The relatively high velocities in the interval from 150 to 350 sec show the presence of the released dredged material moving rapidly downward through the vertical water column. Again, the large velocities after the initial placement are believed to be a manifestation of an internal wave propagating away from the area.

Survey 238B

Instead of examining the temporal variation as the ship drifts into the plume, Survey 238B was analyzed from the perspective of temporal change of the plume taken as a whole. The plume was traversed several times after the initial placement, and each transect (although taking 3 to 5 min) can be seen as representing the state of the plume at a given averaged elapsed time. From a dynamical point of view, the transverse sampling method is a more powerful type of presentation if the aim is to understand development of the plume.

To assure that the presentation was as correct as possible, all the position data were projected onto a straight line representing a suitable cross section of the plume. This projection ensures that

variation in the ship speed or changes in the angle of the transect do not distort the horizontal image of the plume. The line runs in the direction from 225 to 75 deg (positive) true north.

The first plot (Figure 5.75) shows the backscattering (in relative units) from bin 3 (depth 5.3 m) for each of the five transects. The first transect (marked 1) shows the highest concentration of scattering material and a narrow horizontal baseline. Subsequent transects (marked 2, 3, 4, and 5) show lower backscatter amplitude and larger horizontal extent. The last phenomenon is even more pronounced in the data from bin 6 (Figure 5.76), where the whole plume shifts over to the positive side of the plot. The reason is that the plume material is being advected by the average horizontal current. The strong eastward current in the bottom layer during this event explains both why the bottom layer is shifted more than the top layer and why the bottom layer of the plume moves toward the positive side of the plot (toward 75 deg).

Figure 5.77 illustrates the observed vertical velocity during the first 2-1/2 transects that were made across the plume. The internal wave believed to be generated at the time of the placement propagates out from the placement site and produces a relatively large vertical velocity. The maximum velocity is observed in bin 3 (depth 5.3 m). The density gradient at this level is of order two sigma-theta units per meter (1 sigma-theta unit is approximately equal to 1 kg/m³). For a two-layered fluid, the wave may be regarded as propagating freely on the interface, following the standard dispersion relation with reduced gravity.

The wavelength λ of the interface wave is of order 100 m, and the wave has propagated 350 m from the time of the first transect until the ship passed over the wave the second time. The propagation velocity (group speed) c_g of the wave is,

$$c_g = \sqrt{\frac{g'}{k}} \quad (5.3)$$

where

$$g' = g(\rho_1 - \rho_2 / \rho_2),$$

$$\rho_1 = \text{density of the upper layer}$$

$$\rho_2 = \text{density of the lower layer}$$

$$k = 2\pi/\lambda \quad (\lambda = \text{wavelength})$$

The reduced gravity g' is $2 \cdot 10^3$ m/sec², and $c_g = 0.56$ m/sec is obtained, indicating the wave will take 630 sec to propagate 350 m. By comparison, the time between the initial positive peak in the vertical velocity and the negative peak observed at the end of the second transect was 580 sec.

It thus appears that a simple two-layer model can explain the propagation well within the uncertainty in the density gradient, the propagation distance, and the wavelength.

The contour plots in Figures 5.78 through 5.81 show the development of the backscattering values for the four first transects. The plume material is behaving as expected, falling as a narrow downward jet of material at the outset, then evolving into an upside-down mushroom-shaped cloud. The material spreads out from the bottom cloud in elapsed time (as seen in successive Figures 5.78 through 5.81). Simultaneously, the concentration in the main jet is reduced, and the whole plume is advected with the horizontal current. Small internal waves can be seen to propagate on top of the expanding mushroom-shaped cloud.

The vertical velocity component (Figures 5.82 to 5.84) shows the rapid evolution of internal waves in the first few minutes after placement. There is a maximum in the vertical velocity at the point of maximum density gradient. After the first transect was completed, the vertical velocity field became quite noisy (except for the trailing edge of initial wave seen in the right-hand corner of pass 2). The upward movement of the cloud, the small internal waves generated by the upward motion near the bottom, and the falling particles in the initial jet all disturb the total field enough to make the vertical velocity measurement obscure after the initial pass. The times for each transect after the data sampling was initialized (21:55:38) were:

	<u>sec</u>
Pass 1 (from right to left):	0 - 330
Pass 2 (from left to right):	467 - 740
Pass 3 (from right to left):	852 - 1132
Pass 4 (from left to right):	1,357 - 1,627

8. Conclusions and Recommendations

Bottom track

Comparison of the bottom tracking data and navigation data shows, in general, good correspondence. During the first phase of each placement event, the bottom track data are influenced by the high backscatter in the water. There also are some spikes in the navigation data that have not been filtered out, and there are some small problems related to correct estimation of integration times. However, for the purpose of this initial study, bottom tracking data have been shown to be adequate both as a measure of the ship speed and as a tool for navigation when position devices are unavailable.

Current velocity

The current velocities were relatively weak during the MFDCP, and one surprise was encountered in analysis of the data. This previously unreported phenomenon was the apparent interference of the ship on the current field, which could amount to 3 percent of the ship speed. There are two alternatives for avoiding this problem. One is to correct the data with a software procedure that accounts for the presence of the ship, and the other is to use ships smaller than the *R/V Pelican* in shallow-water areas.

Sediment concentration

Two independent results in this chapter point toward the feasibility of using acoustic backscatter as a tool for determining sediment concentration. One is the comparison with the bottle sample data, which shows that for the MFDCP data set, the concentration can be found within an order of magnitude from the measured volume backscattering. The other result is the qualitative correspondence between the contour plot of the plume transects and knowledge of plume dynamics. Although not pointing directly to the relationship between backscatter and concentration, it is difficult to believe that the backscatter is a poor measure of the concentration from examination of the contour plots.

The next step in the application of acoustic instrumentation is measurement of suspended sediments in the controlled laboratory environment. In the laboratory, the particle size, distribution, and type can be controlled, and uncertainty in the acoustic measurements reduced to a minimum. An experiment to relate the volume backscatter and the sediment concentrations for several size classes and different types of particles might also be conducted. This experiment would provide valuable information about the limitation and applicability of the measurement technique and potentially lead to the routine application of acoustic instrumentation in this area. Such a firm development in instrumentation would be of great benefit in the measurement of particulates in pollution studies (e.g., sewage), which is a situation acoustically similar to the measurement of sediment.

References

- Rayleigh, J.W.S. 1945. *Theory of Sound*, Vol. 2, Dover Publications, Inc., New York.
- RD Instruments. 1989. "Acoustic Doppler Current Profilers, Principles of Operation: A Practical Primer", San Diego, CA.

Table 5.1
ADCP Characteristics for the MFDCP

Parameter	Value
ADCP model	RD-DR1200 direct-reading ADCP
Frequency	1,228 kHz
Depth cell size	1 m
Measurement ensemble size	28 pings (+/-3 pings)
Measurement ensemble duration	3 sec
Single-ping measurement error	13 cm/sec
Measurement bias	0.5 to 1.0 cm/sec
Ensemble measurement error	2.5 cm/sec
ADCP transducer depth	1.8 m
ADCP beam width	1.5 deg
Transducer side-lobe level	-55 dB

Table 5.2

ADCP System Configuration for Amplitude Calibration

<u>System Configuration</u>	
<u>Property</u>	<u>Value</u>
ADCP frequency	1,200 Hz
Ks	5,650,000.0
ADCP input voltage	110.0 VAC
Chassis temperature	30.0 deg C
Salinity	28.0 ppt
Depth of the transducer	1.8 m
Sound velocity at transducer depth	1,538.3 m/sec
Water absorbtion coefficient (α)	0.474
Blanking	0.5 m
Pulse length	1.0 m
Depth cell length	1.0 m

Beam Configuration

<u>Parameter</u>	<u>Beam 1</u>	<u>Beam 2</u>	<u>Beam 3</u>	<u>Beam 4</u>
K2	9.520	10.630	9.530	10.270
Kc	0.428	0.428	0.428	0.428
K1	47.428	51.829	46.424	43.593
Nc	28.400	28.400	30.500	26.300
ϕ^* , deg	30	0	30	30

* ϕ : Beam angle measured from vertical.

Table 5.3

Transducer Misalignment

<u>Survey</u>	<u>237A</u>	<u>238A</u>	<u>238B</u>	<u>239A</u>	<u>239B</u>	<u>241A</u>	<u>242A</u>	<u>243A</u>
Angle (deg)	6.78	8.69	8.51	10.62	10.27	9.48	3.38	4.78

Table 5.4

Ship Heading Linear Regression (ADCP = $m \cdot \text{Navigation} + b$)

<u>Survey</u>	<u>m*</u>	<u>Uncertainty in m</u>	<u>b</u>	<u>Uncertainty in b</u>	<u>r</u>
237A	0.99	+/- 0.01	8.99	+/- 28.57	0.988
238A	0.96	+/- 0.01	16.35	+/- 43.68	0.962
238B	0.96	+/- 0.01	16.06	+/- 29.77	0.987
239A	0.98	+/- 0.01	14.89	+/- 23.08	0.991
239B	0.96	+/- 0.01	16.15	+/- 27.14	0.982
241A	0.98	+/- 0.01	13.86	+/- 28.20	0.979
242A	0.98	+/- 0.01	4.51	+/- 44.30	0.978

* m = slope, b = offset, and r = linear correlation coefficient.

Table 5.5

Ship Speed Linear Regression (ADCP = $m \cdot \text{Navigation} + b$)

<u>Survey</u>	<u>m</u>	<u>Uncertainty in m</u>	<u>b</u>	<u>Uncertainty in b</u>	<u>r</u>
237A	0.96	+/- 0.01	9.11	+/- 53.24	0.965
238A	0.92	+/- 0.01	3.57	+/- 67.75	0.924
238B	0.98	+/- 0.02	4.53	+/- 93.95	0.890
239A	0.96	+/- 0.01	4.61	+/- 68.85	0.950
239B	0.99	+/- 0.01	1.65	+/- 42.54	0.970
241A	0.99	+/- 0.03	4.73	+/- 175.44	0.740
242A	0.95	+/- 0.01	15.46	+/- 53.79	0.950

Table 5.6

Northing Ship Position Linear Regression ($ADCP = m \cdot \text{Navigation} + b$)

<u>Survey</u>	<u>m</u>	<u>Uncertainty in m</u>	<u>b</u>	<u>Uncertainty in b</u>	<u>r</u>
237A	0.97	+/- 0.00	-296,704.33	+/- 1,859.94	0.998
238A	1.00	+/- 0.00	-305,618.34	+/- 31,395.63	0.995
238B	1.00	+/- 0.01	-304,539.37	+/- 41,934.60	0.991
239A	0.99	+/- 0.00	-300,020.71	+/- 13,534.91	0.999
239B	0.99	+/- 0.00	-301,881.06	+/- 6,158.94	0.999
241A	0.97	+/- 0.00	8534.83	+/- 18,085.04	0.998
242A	1.01	+/- 0.00	-316,114.49	+/- 14,447.30	0.998

Table 5.7

Easting Ship Position Linear Regression ($ADCP = m \cdot \text{Navigation} + b$)

<u>Survey</u>	<u>m</u>	<u>Uncertainty in m</u>	<u>b</u>	<u>Uncertainty in b</u>	<u>r</u>
237A	0.98	+/- 0.01	-53,719.42	+/- 6,862.43	0.992
238A	0.97	+/- 0.01	-54,025.98	+/- 7,135.21	0.992
238B	0.99	+/- 0.00	-56,788.45	+/- 1,535.90	0.999
239A	0.97	+/- 0.00	-54,886.85	+/- 5,479.97	0.995
239B	0.99	+/- 0.00	-55,713.50	+/- 4,481.23	0.997
241A	0.99	+/- 0.01	922.92	+/- 7,732.47	0.992
242A	1.18	+/- 0.01	-70,314.49	+/- 11,000.29	0.988

Table 5.8

Linear Regression Between Ship Speed and Current Speed (Survey 242A)

Depth, m	$U_c = A_u U_s + B_u$		$V_c = A_v V_s + B_v$	
	A_u	r	A_v	r
3	0.037	0.77	0.030	0.33
4	0.038	0.77	0.033	0.37
5	0.045	0.74	0.027	0.24
6	0.031	0.62	0.020	0.18
7	0.032	0.63	0.014	0.16

Table 5.9

Linear Regression Between Ship Speed and Current Speed (Survey 238B)

Depth, m	$U_c = A_u U_s + B_u$		$V_c = A_v V_s + B_v$	
	A_u	r	A_v	r
4	0.023	0.49	0.019	0.29
5	0.027	0.47	0.021	0.26
6	0.018	0.32	0.017	0.23
7	0.016	0.34	0.012	0.15
8	0.013	0.29	0.004	0.06
9	0.011	0.26	0.006	0.08

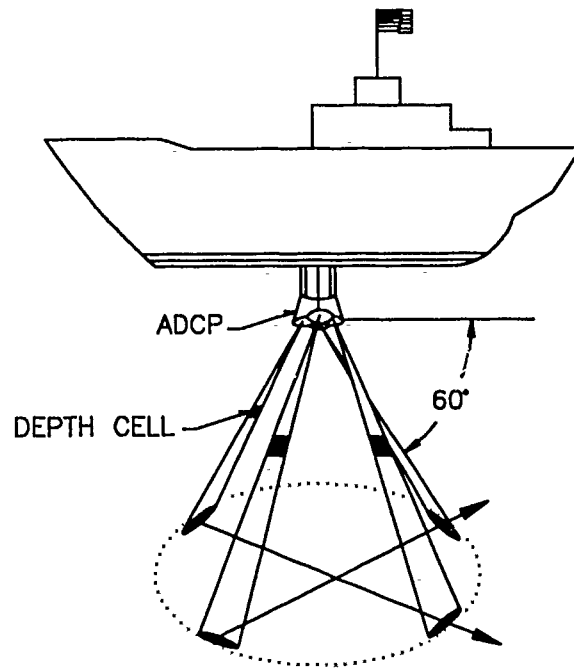


Figure 5.1. Standard ADCP beam configuration.

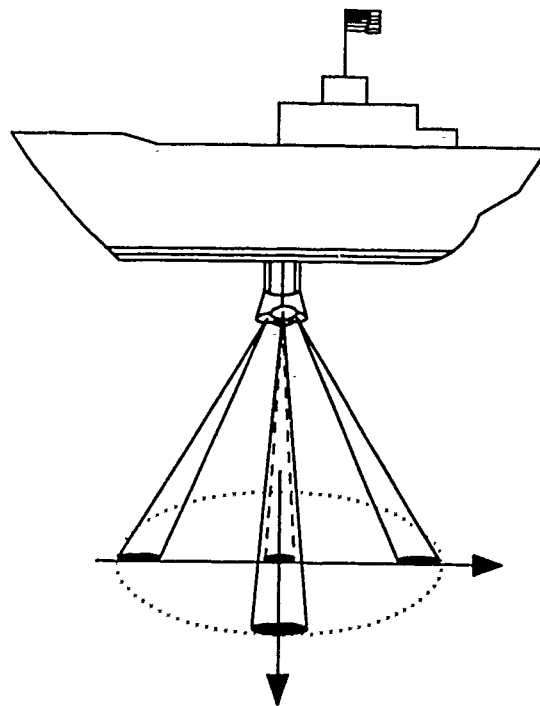


Figure 5.2. ADCP beam configuration used during the MFDCP.

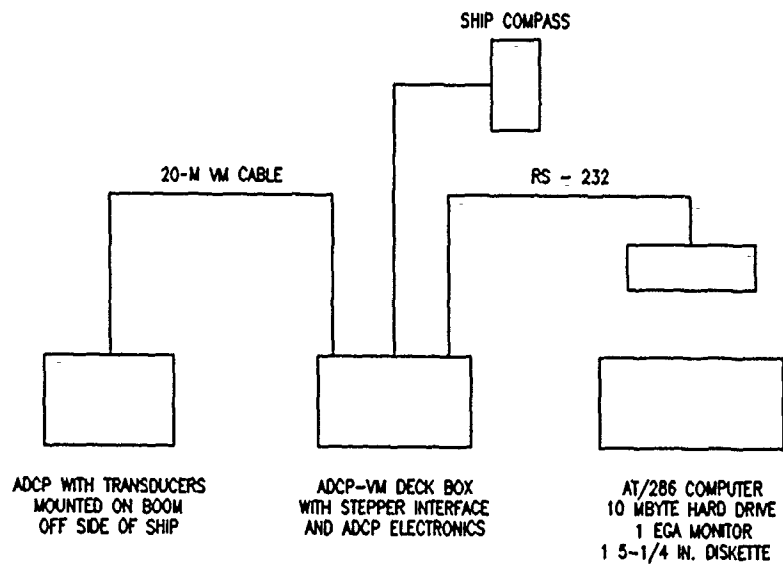


Figure 5.3. ADCP hardware configuration on the *R/V Pelican*.

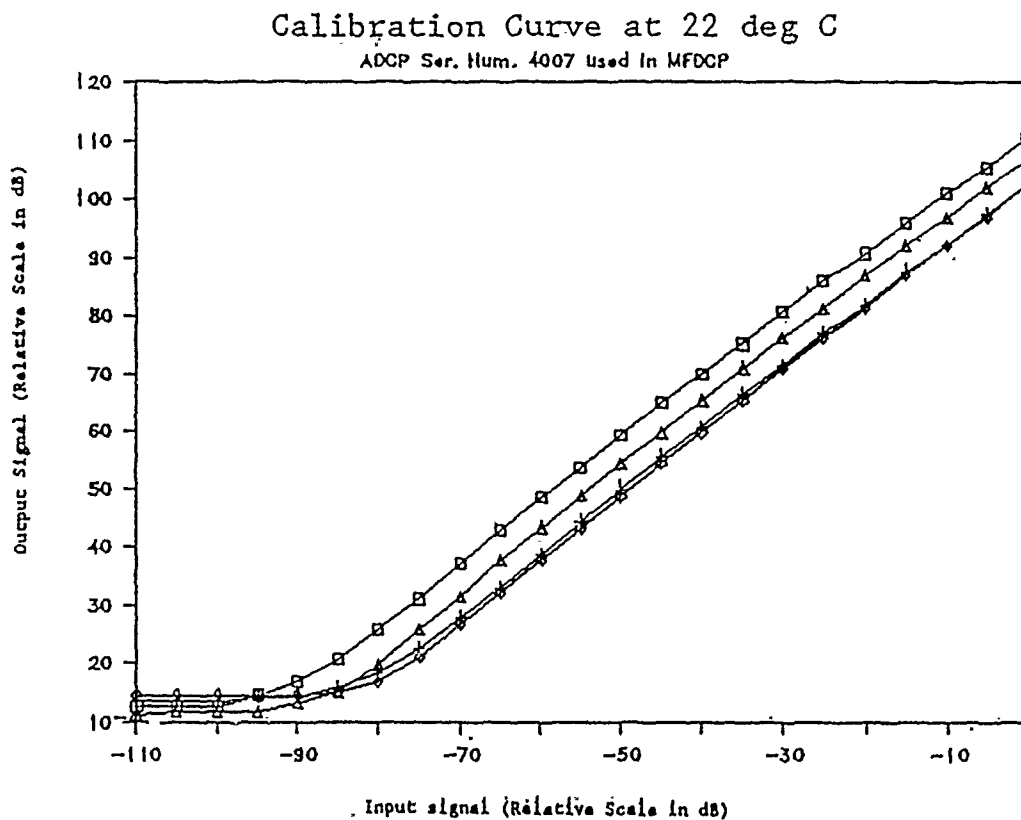


Figure 5.4. Response of ADCP receiver circuitry measured at 22 deg C.

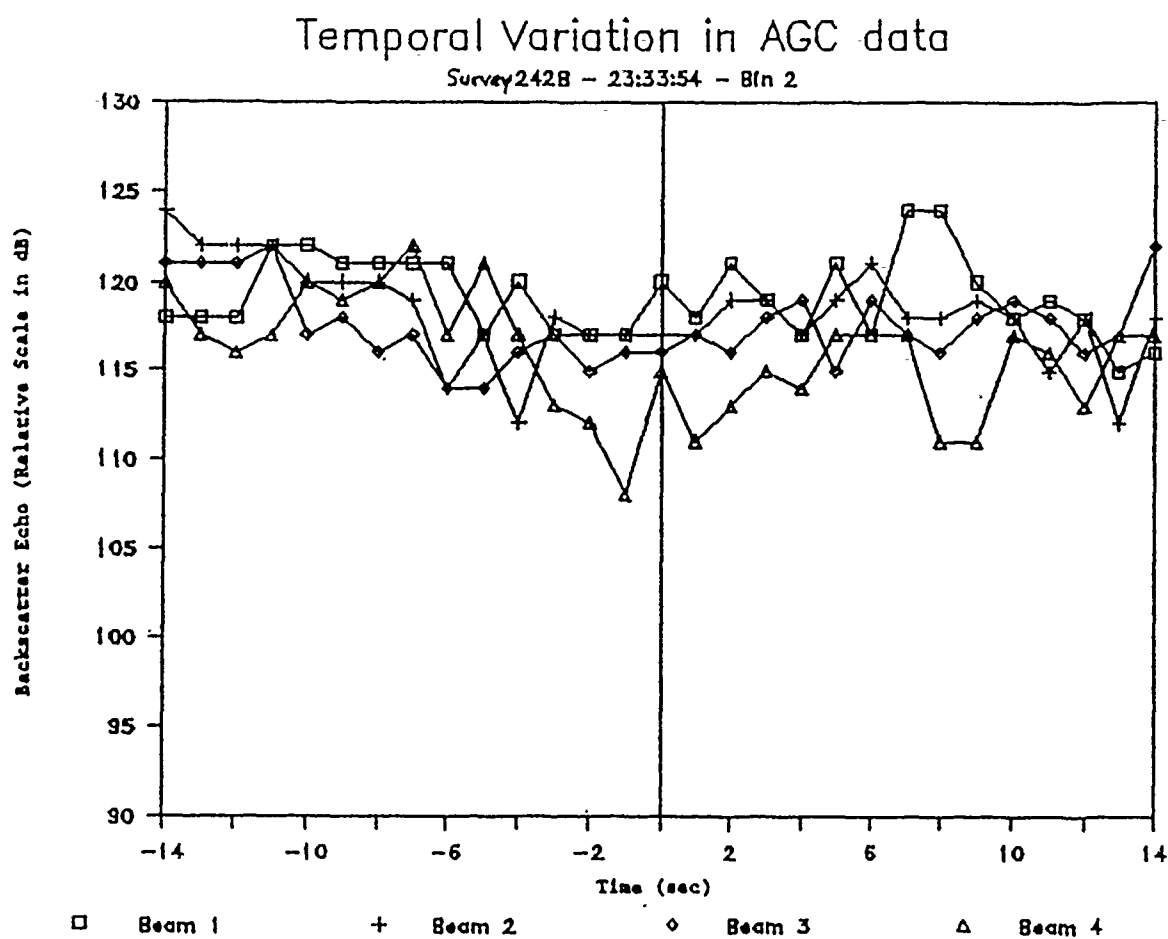


Figure 5.5. Temporal variation of ADCP amplitude (Backscatter Echo) for bin 2 of all four ADCP beams for a 28-sec period.

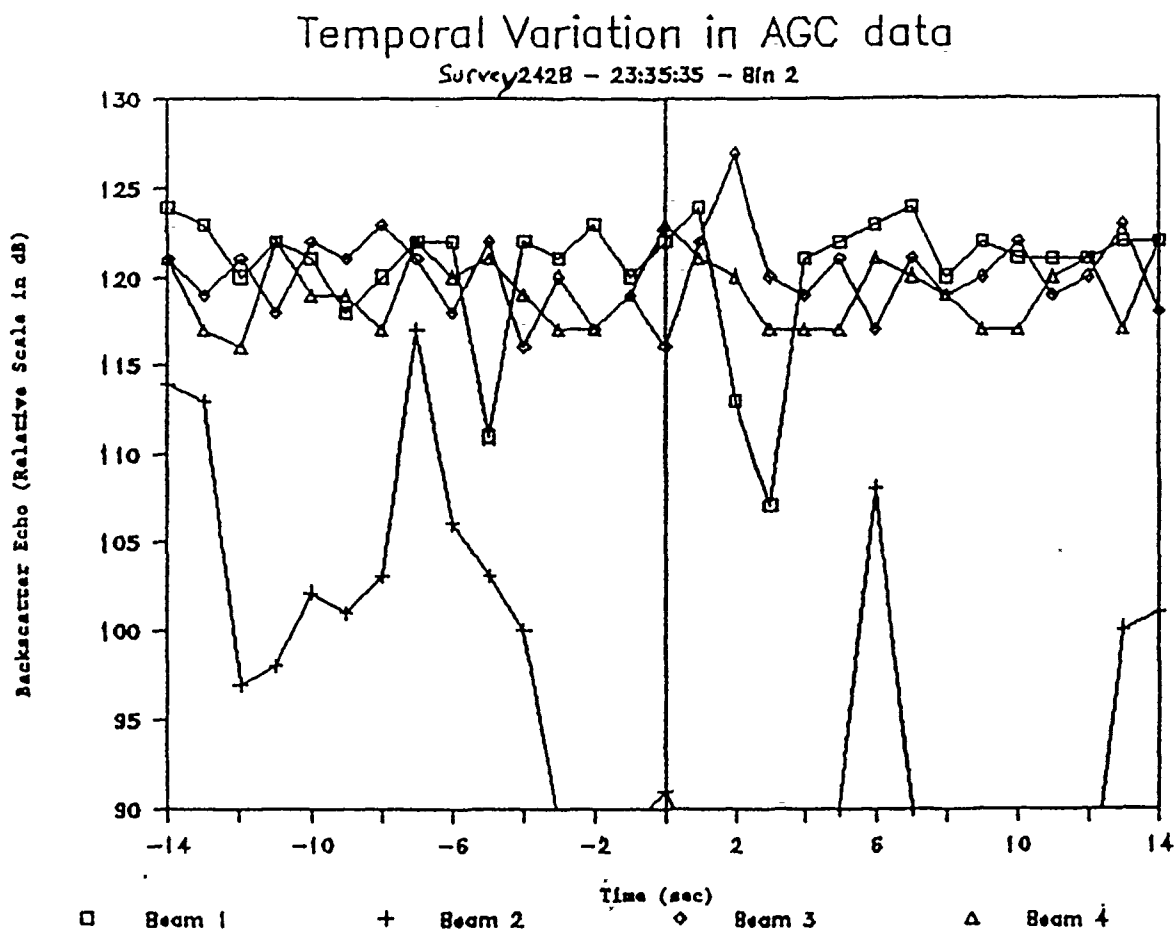


Figure 5.6. Temporal variation of ADCP amplitude (Backscatter Echo) for bin 2 of all four ADCP beams for a 28-sec period. Beam 2 (the vertical beam labeled with "+") is in the shadow of the CTD rosette.

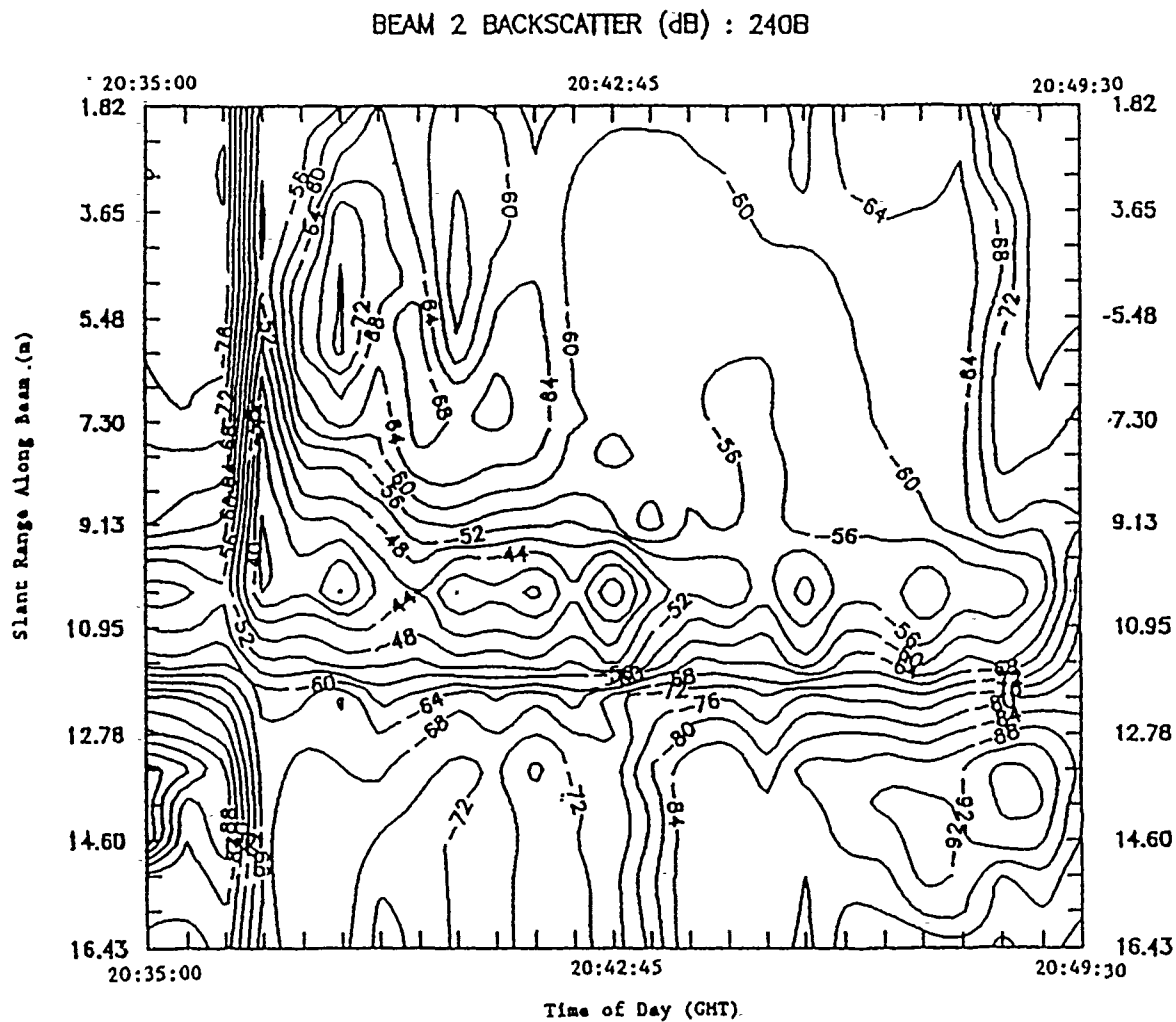


Figure 5.7. Contour plot of backscatter amplitude data in decibels as a function of time and slant range along Beam 2 (m). For this vertically oriented beam, slant range is equal to distance from the transducer.

Calibration of 1200 kHz ADCP — MFDCP

Average Amplitude Data (10 sec)

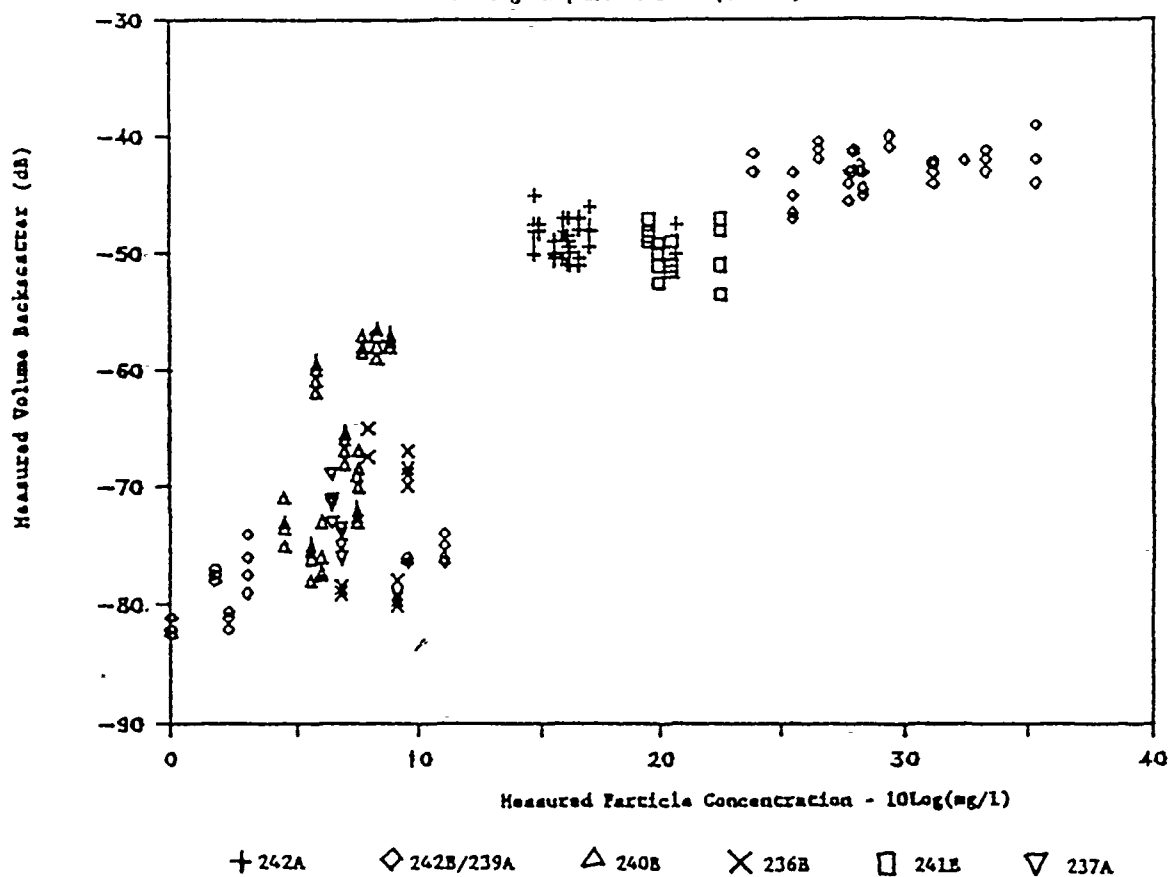


Figure 5.8. Scatter plot between measured particle concentration and the volume backscatter, after quality check and calibration, for seven release surveys. Data for all four beams have been included, generating apparent vertical lines in the scattergram.

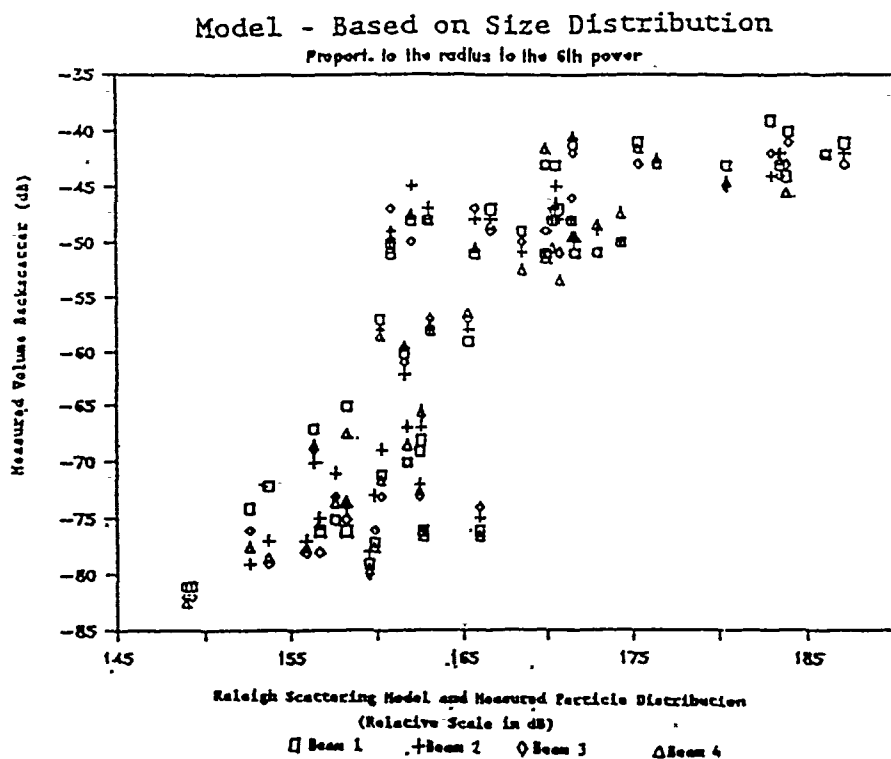


Figure 5.9. Measured volume backscatter and Rayleigh scattering model.

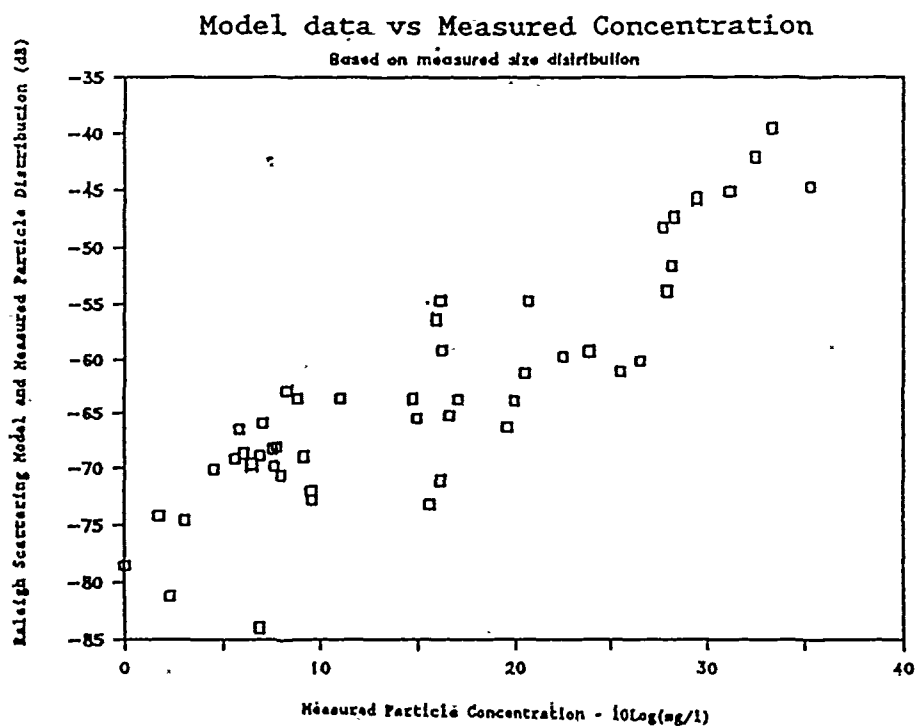


Figure 5.10. Rayleigh scattering model and measured particle concentration.

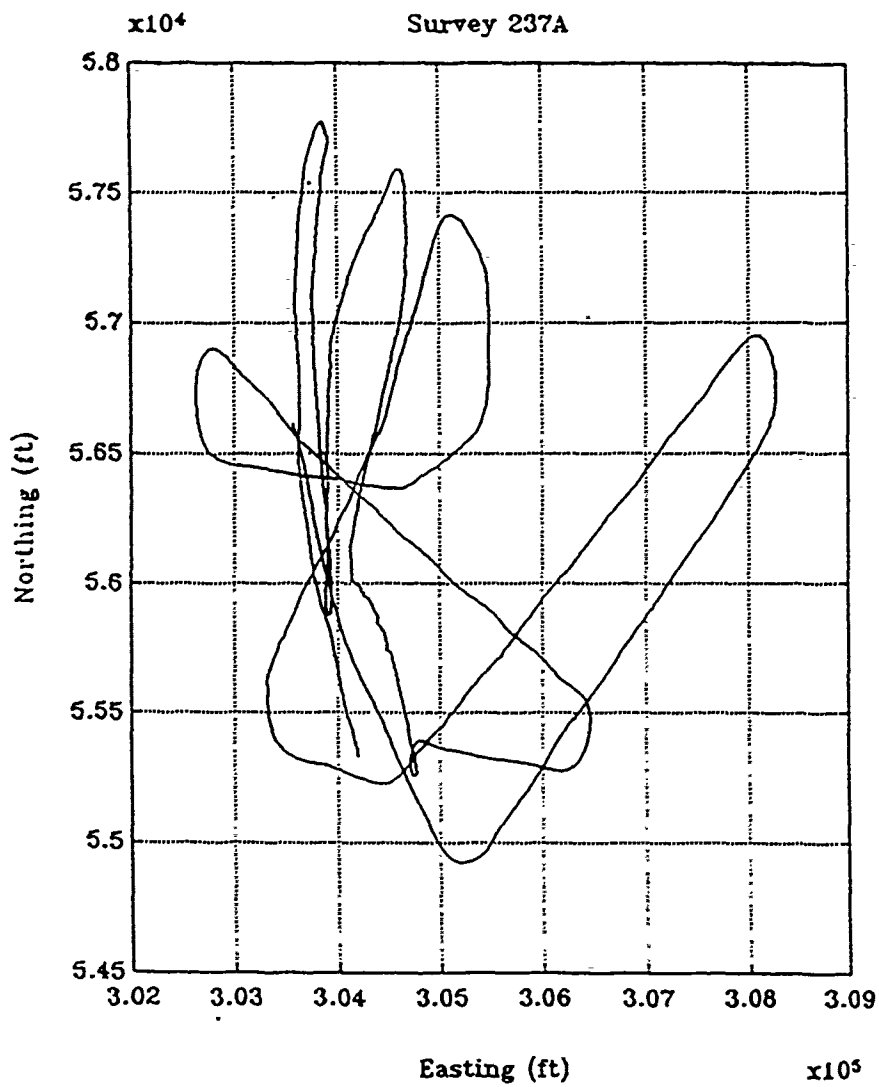


Figure 5.11. Survey 237A: ship tracks from navigation (Mini-Ranger) data.

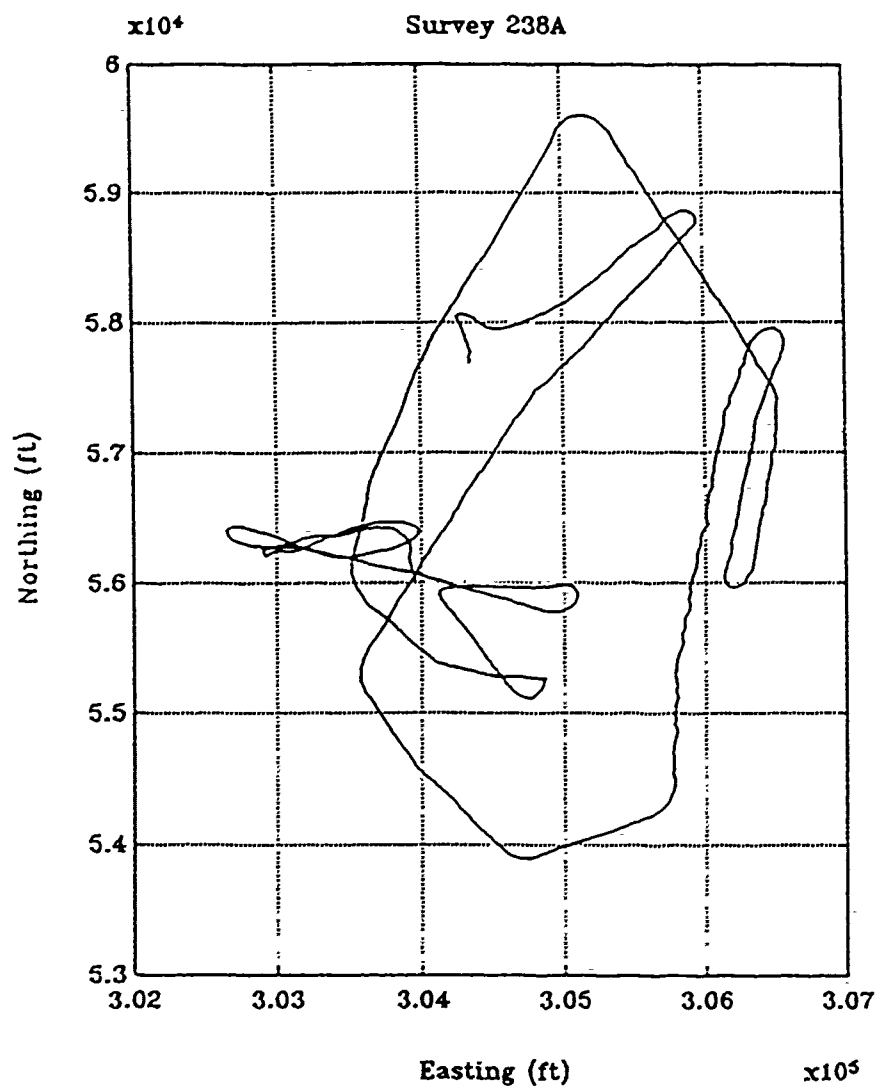


Figure 5.12. Survey 238A: ship tracks from navigation (Mini-Ranger) data.

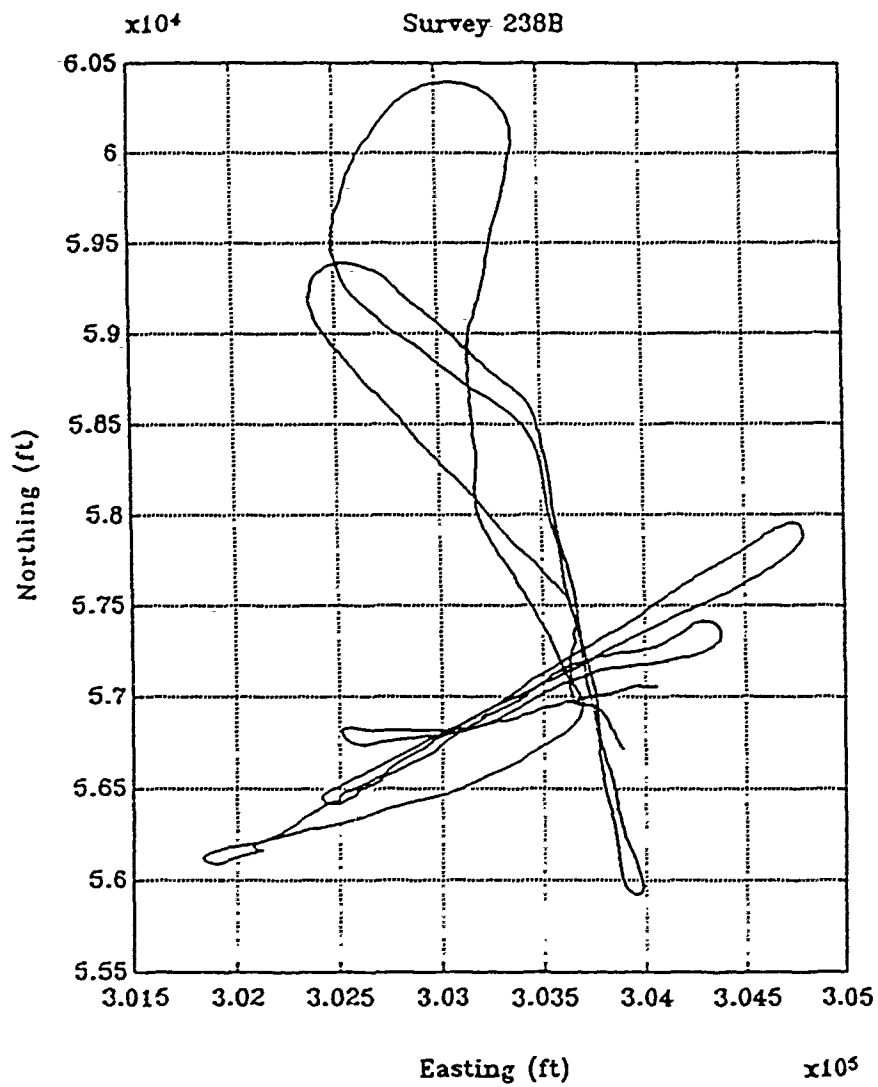


Figure 5.13. Survey 238B: ship tracks from navigation (Mini-Ranger) data.

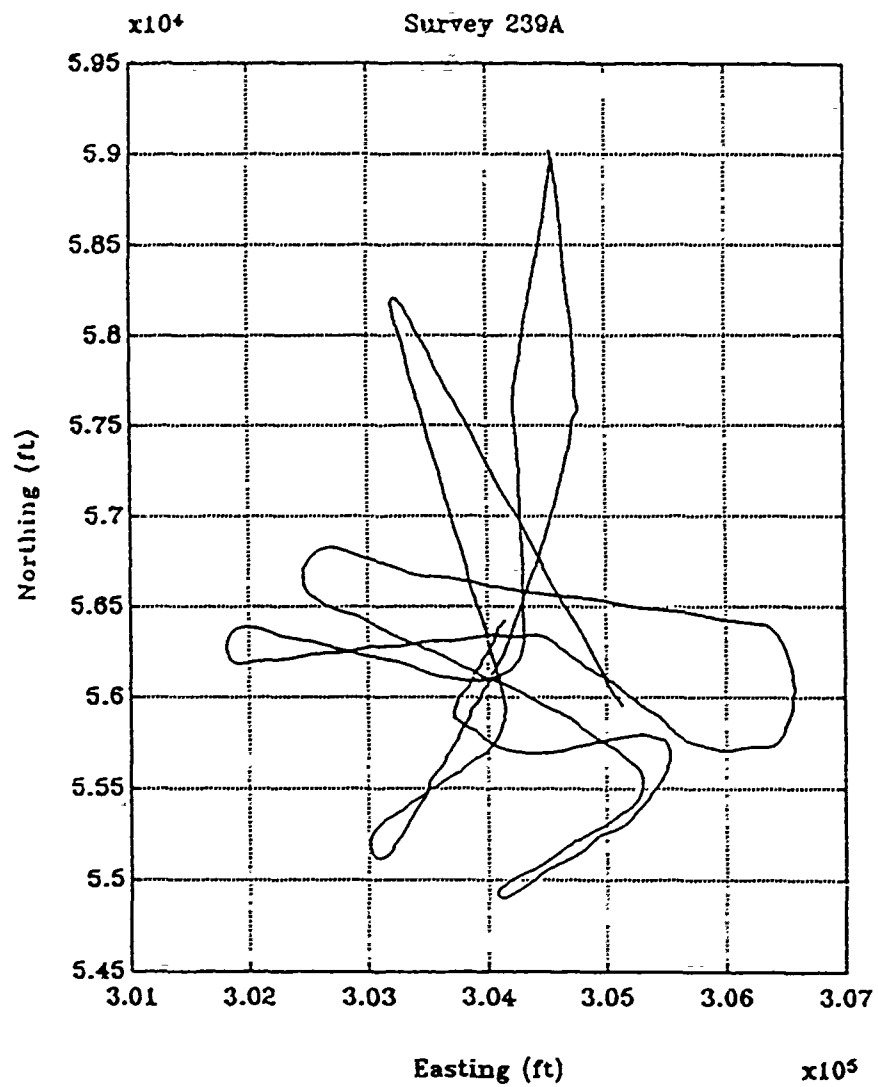


Figure 5.14. Survey 239A: ship tracks from navigation (Mini-Ranger) data.

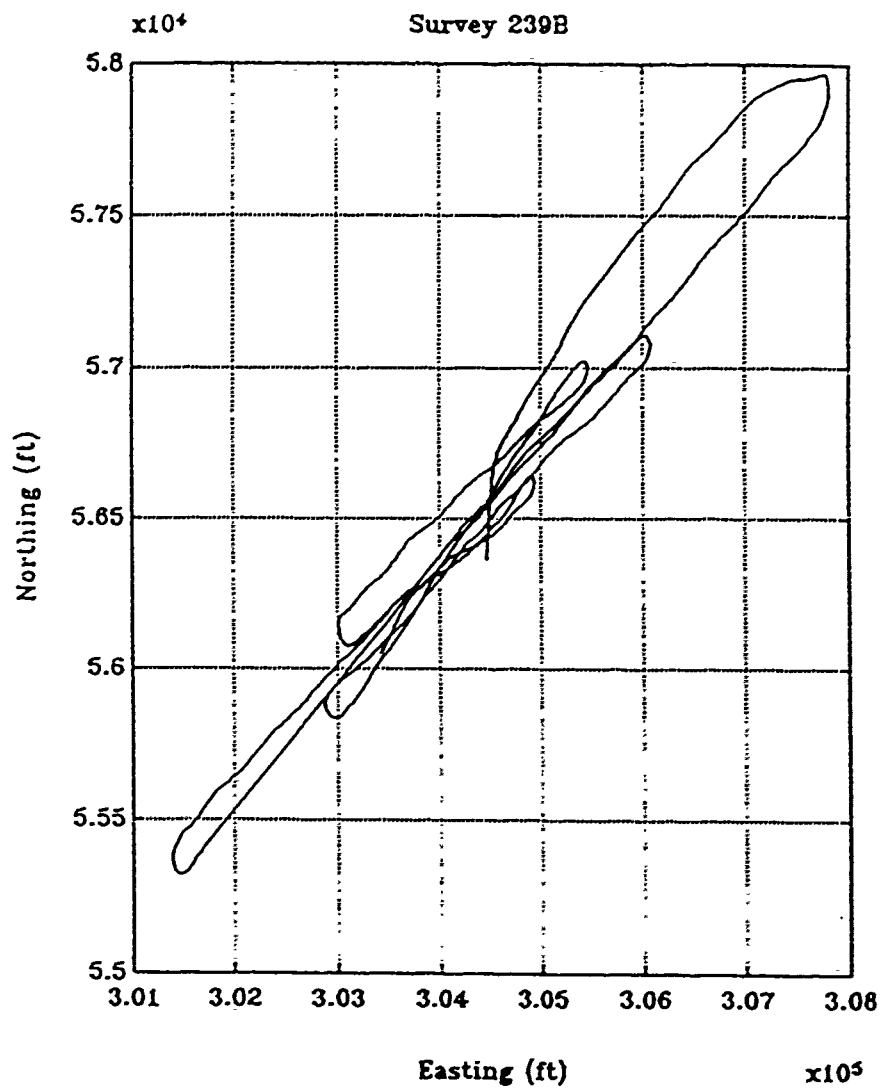


Figure 5.15. Survey 239B: ship tracks from navigation (Mini-Ranger) data.

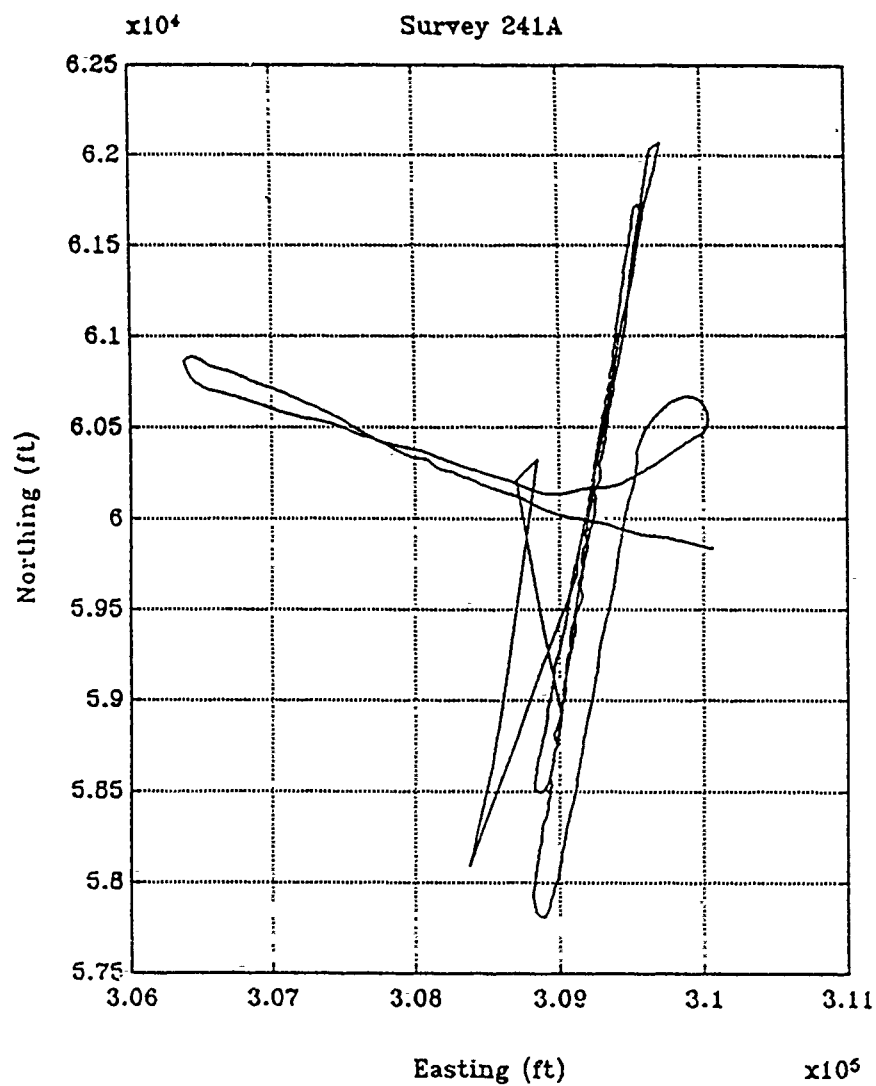


Figure 5.16. Survey 241A: ship tracks from navigation (Mini-Ranger) data.

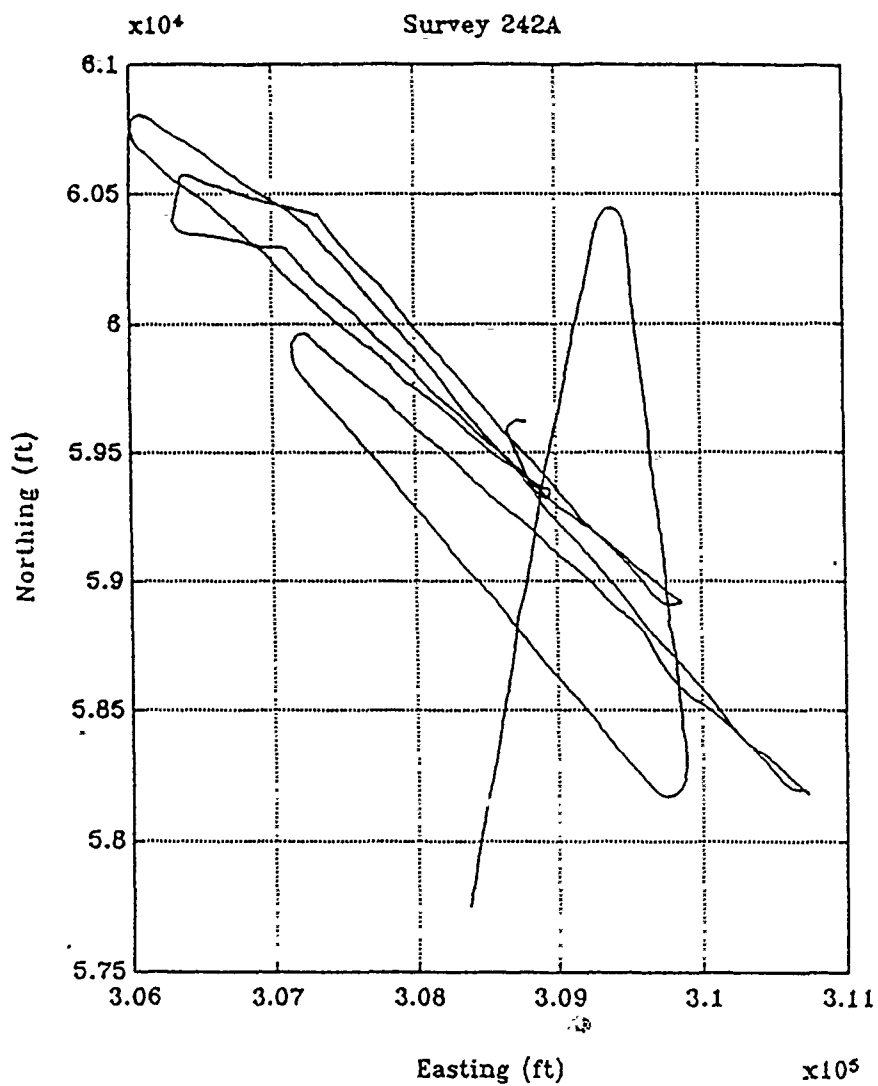


Figure 5.17. Survey 242A: ship tracks from navigation (Mini-Ranger) data.

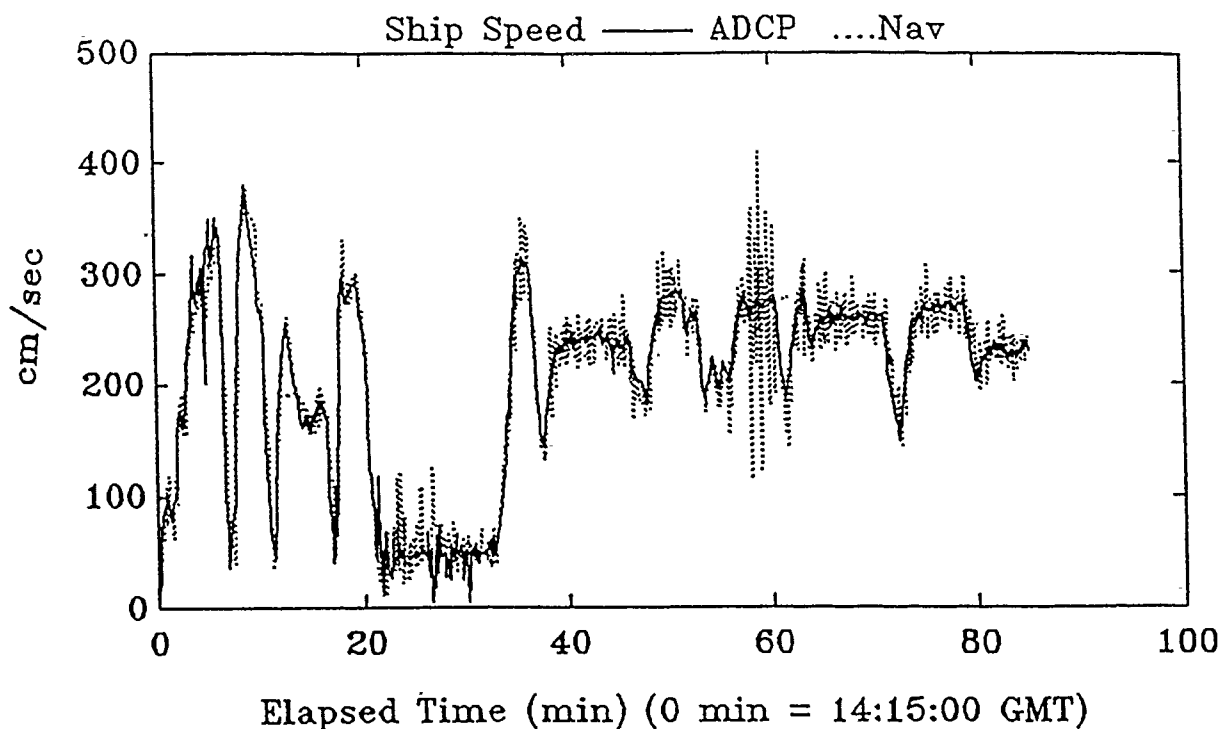


Figure 5.18. Survey 237A: time series of ship speed data.

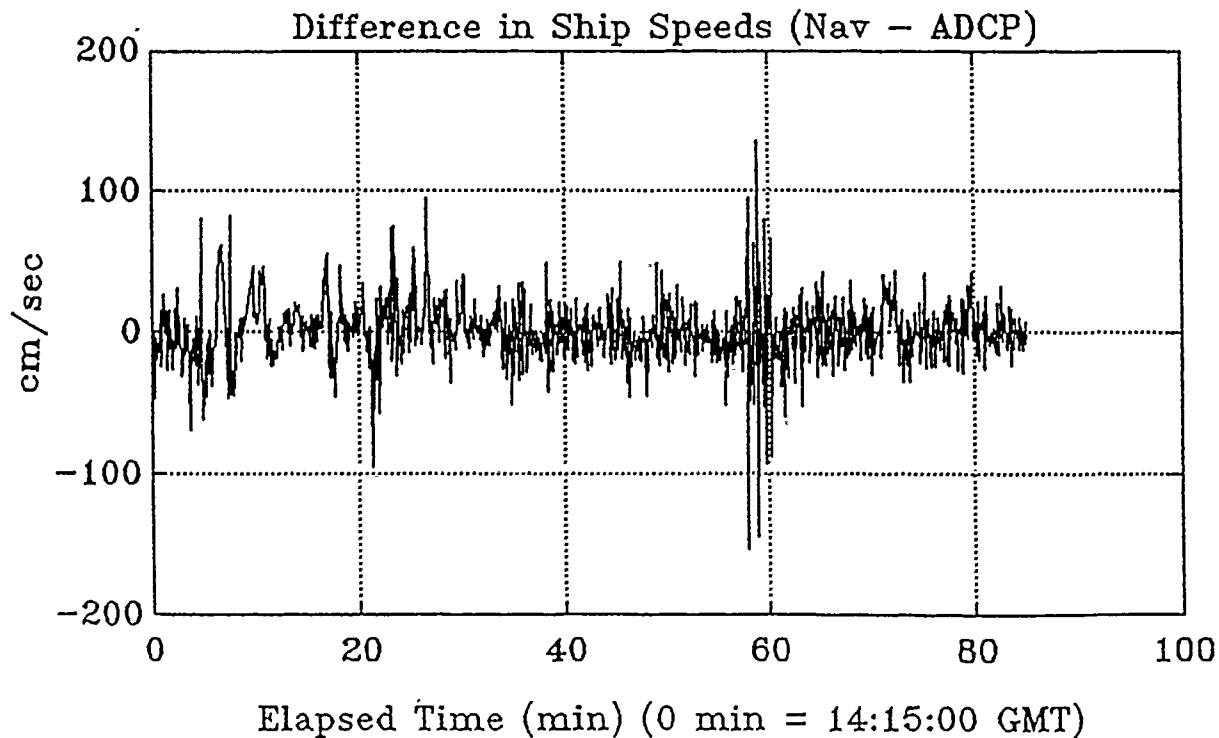


Figure 5.19. Survey 237A: time series of the difference in ship speed.

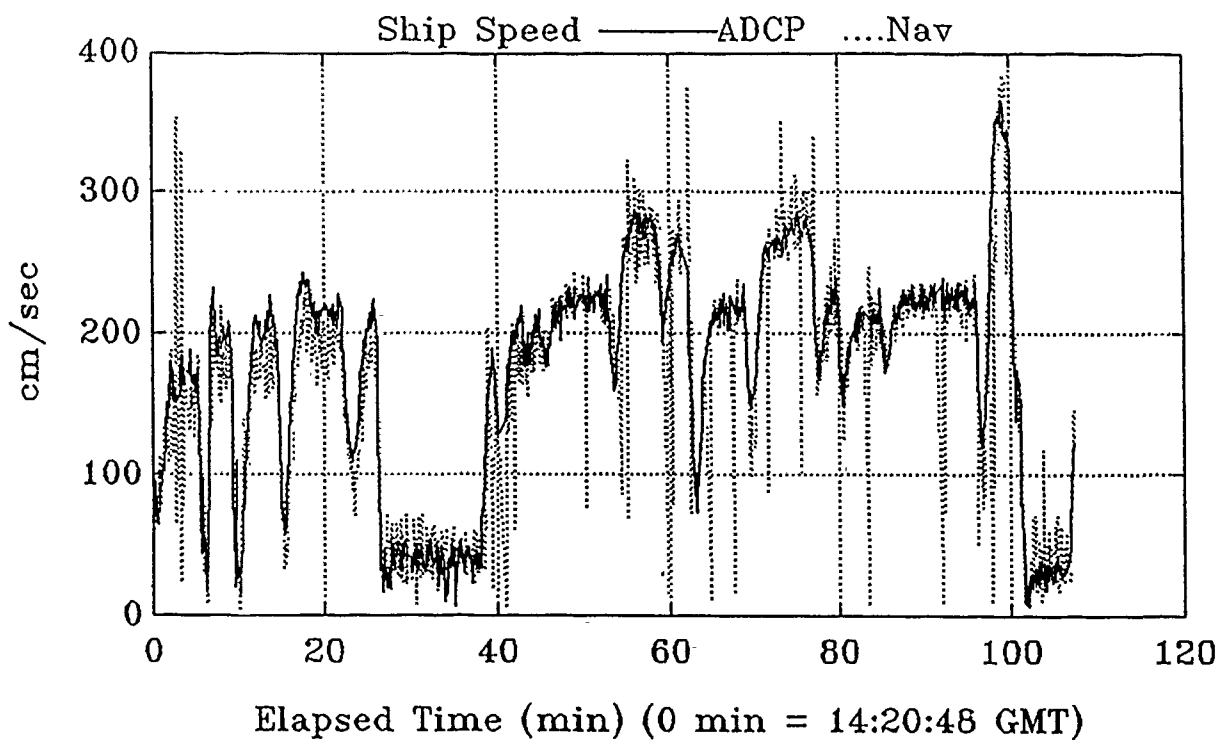


Figure 5.20. Survey 238A: time series of ship speed data.

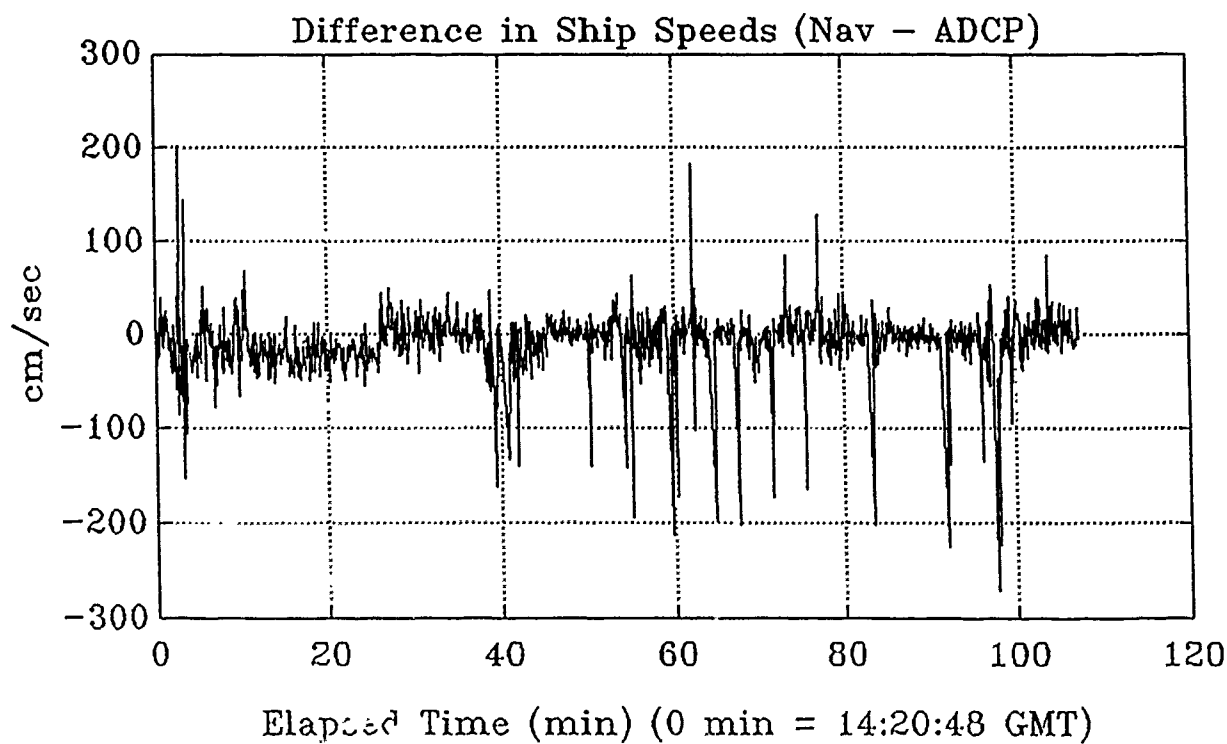


Figure 5.21. Survey 238A: time series of the difference in ship speed.

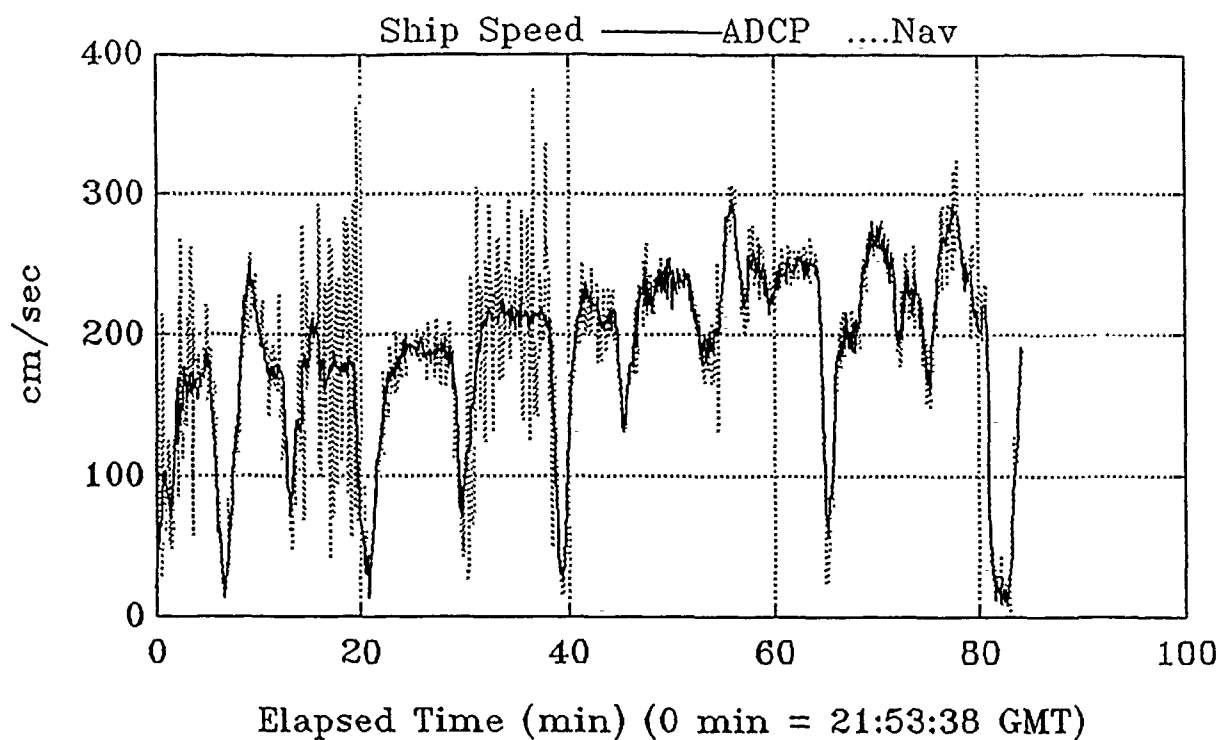


Figure 5.22. Survey 238B: time series of ship speed data.

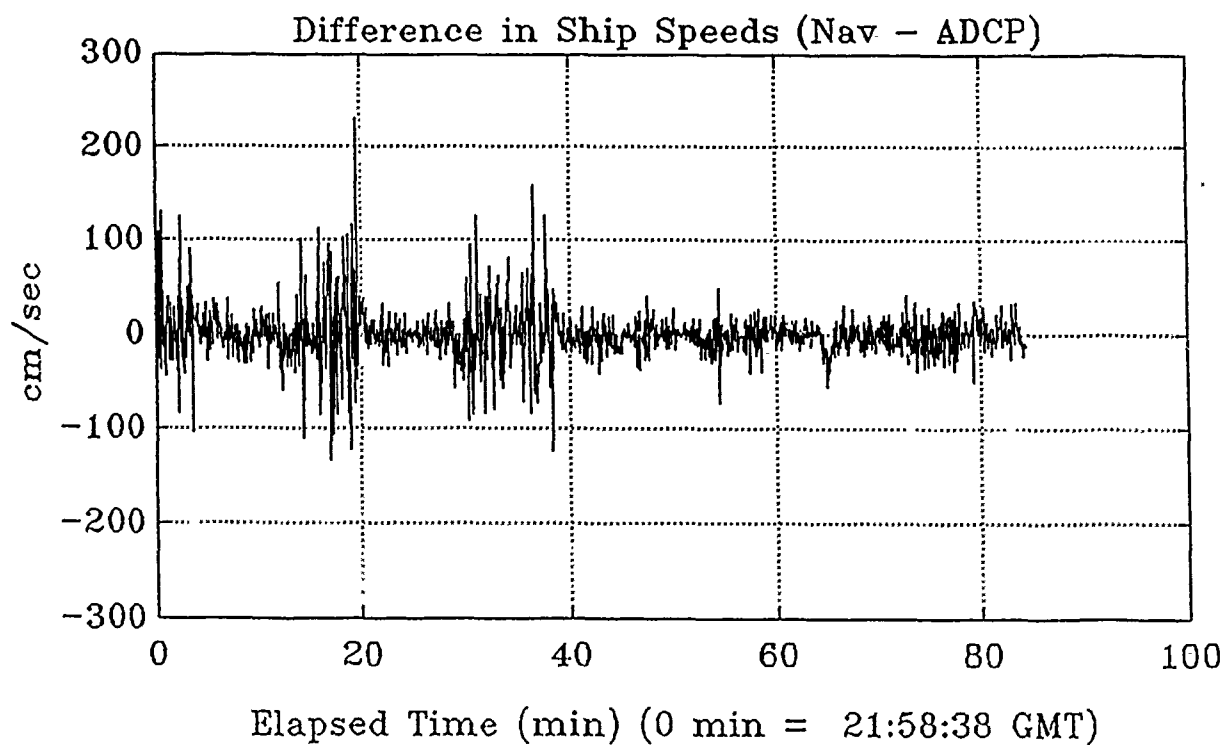


Figure 5.23. Survey 238B: time series of the difference in ship speed.

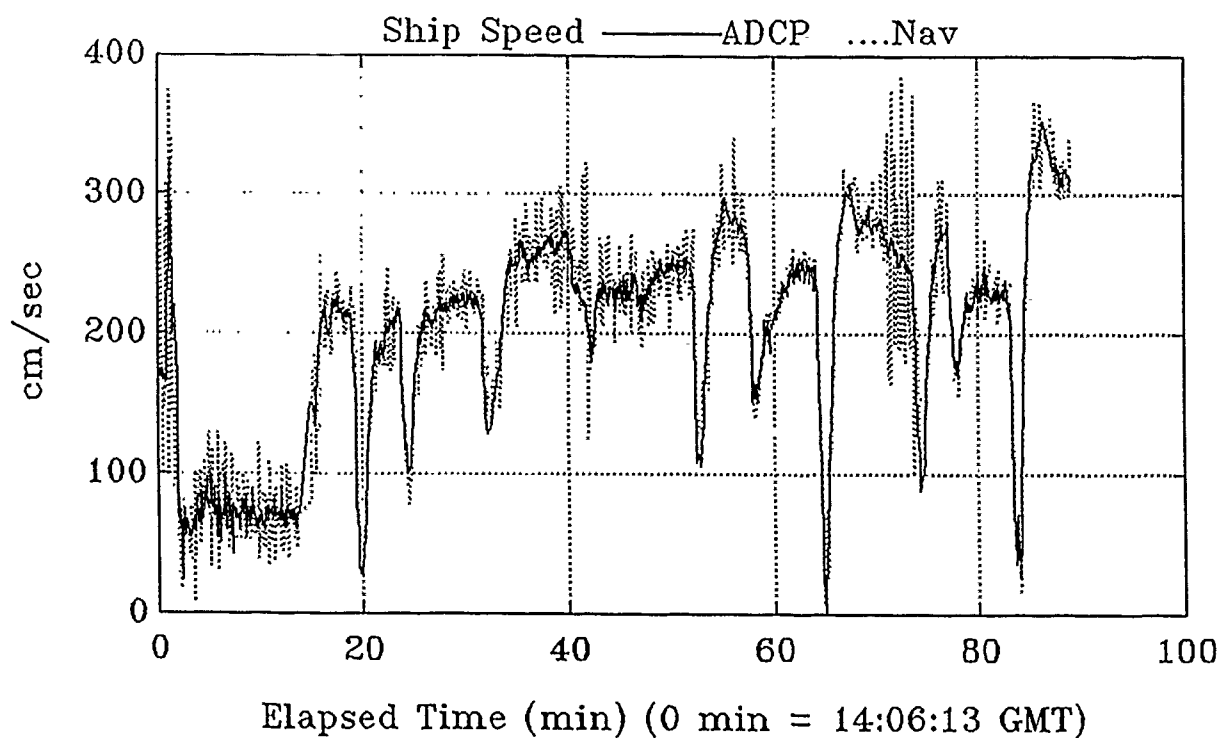


Figure 5.24. Survey 239A: time series of ship speed data.

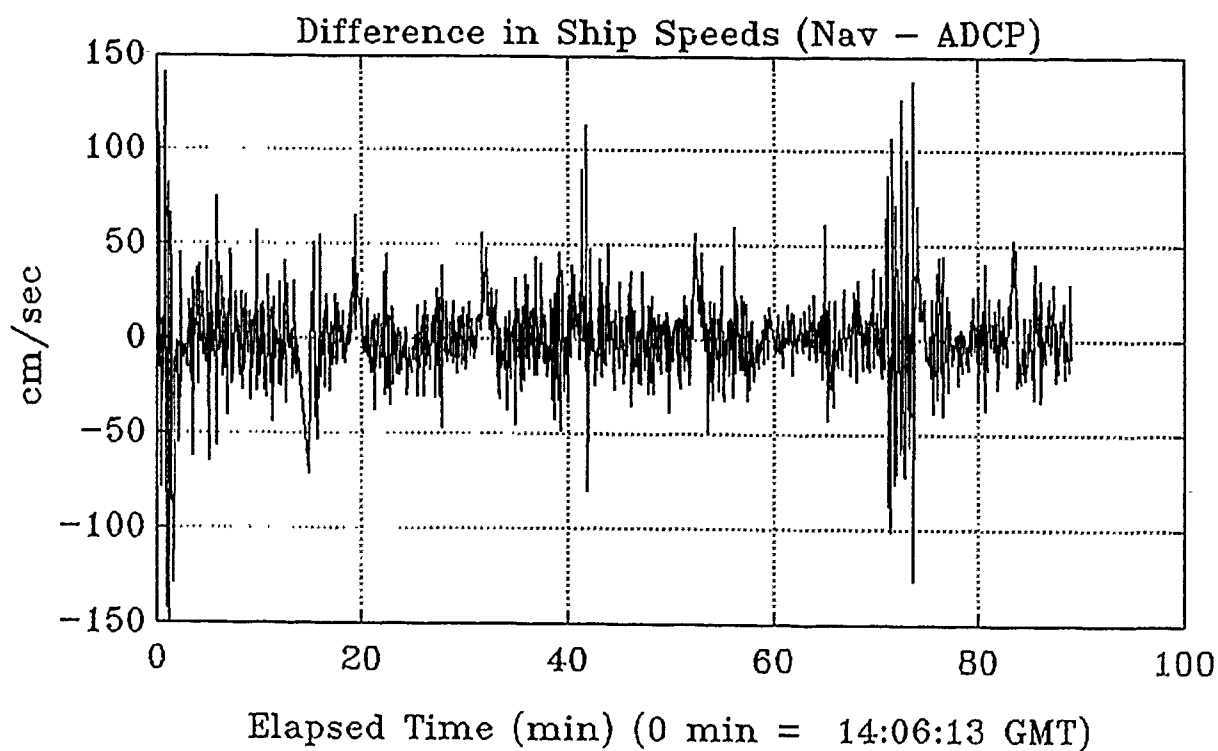


Figure 5.25. Survey 239A: time series of the difference in ship speed.

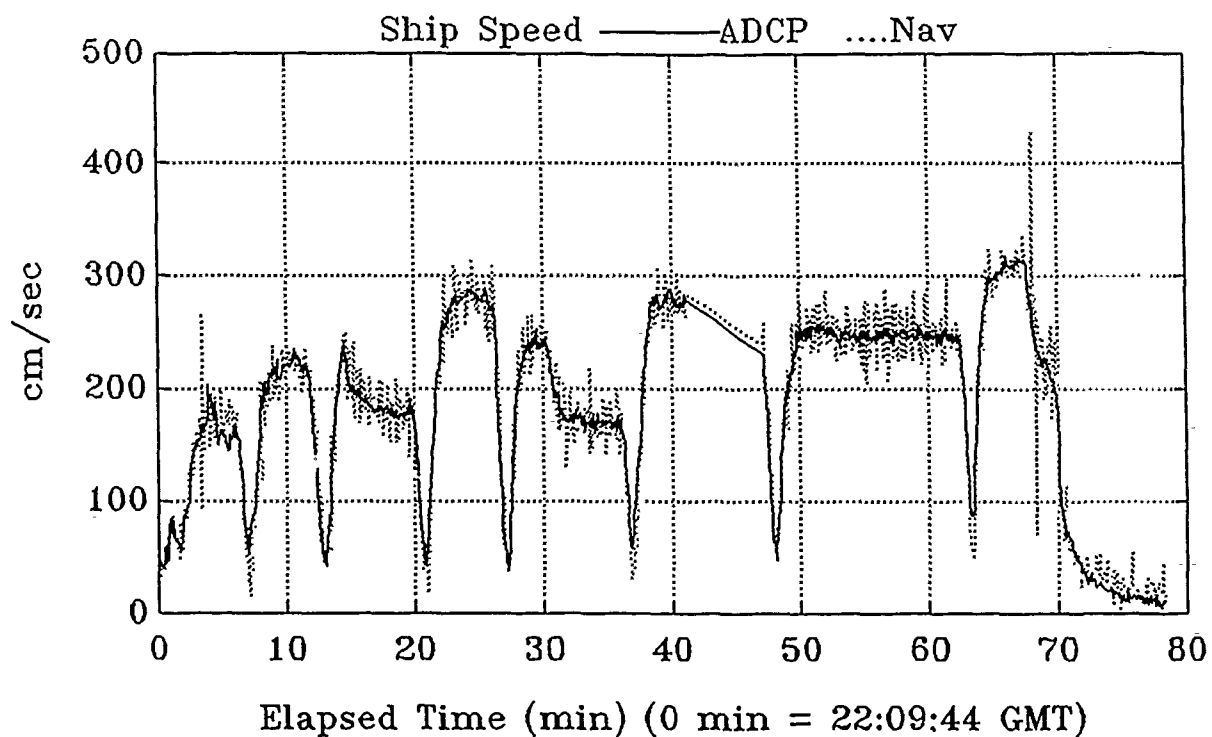


Figure 5.26. Survey 239B: time series of ship speed data.

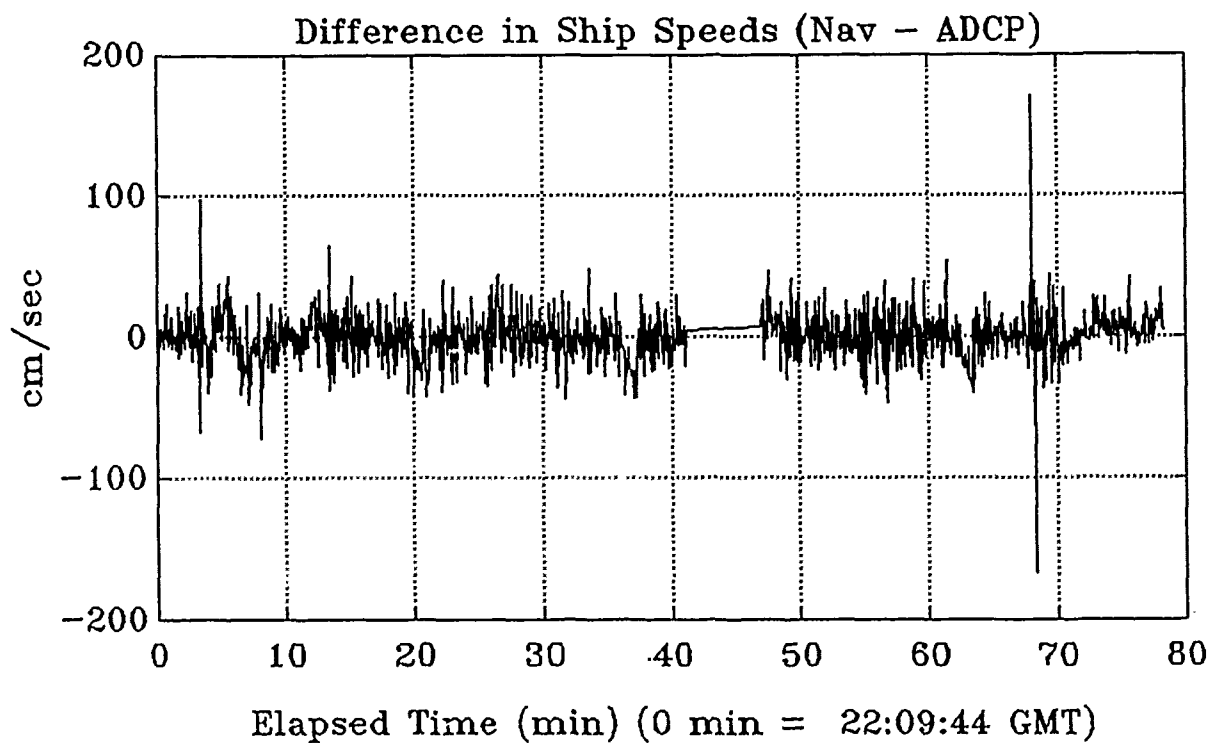


Figure 5.27. Survey 239B: time series of the difference in ship speed.

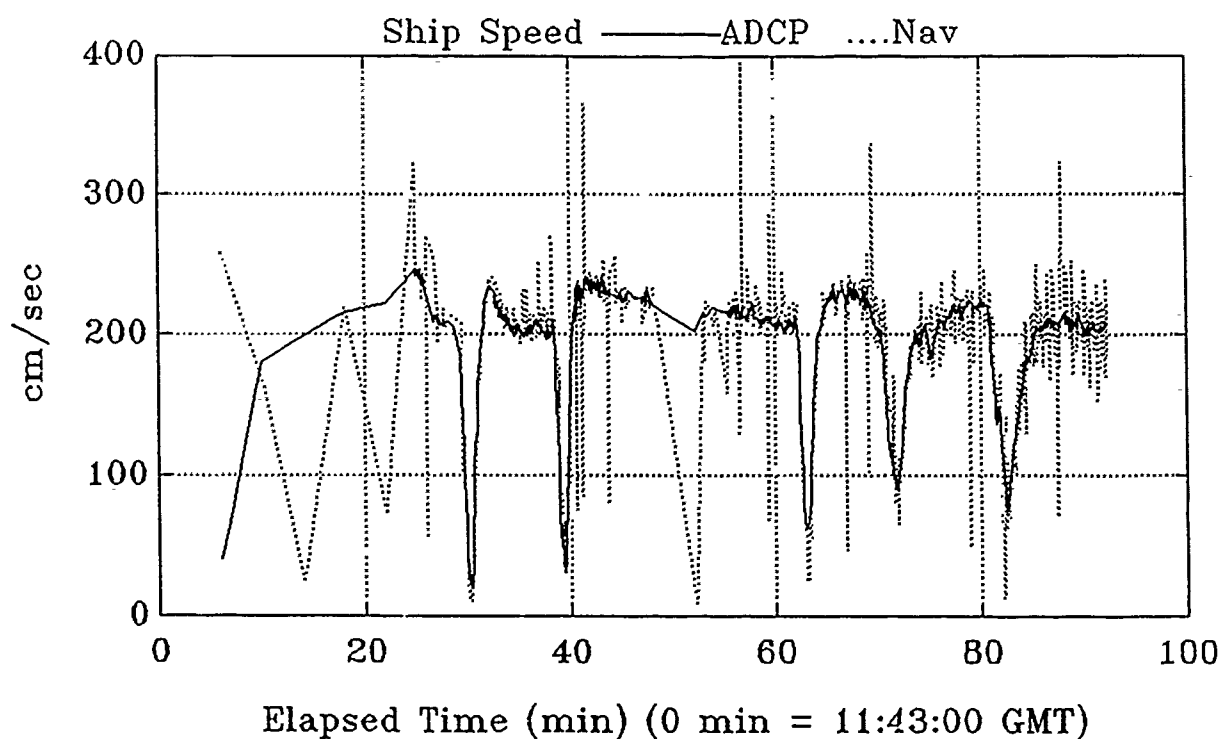


Figure 5.28. Survey 241A: time series of ship speed data.

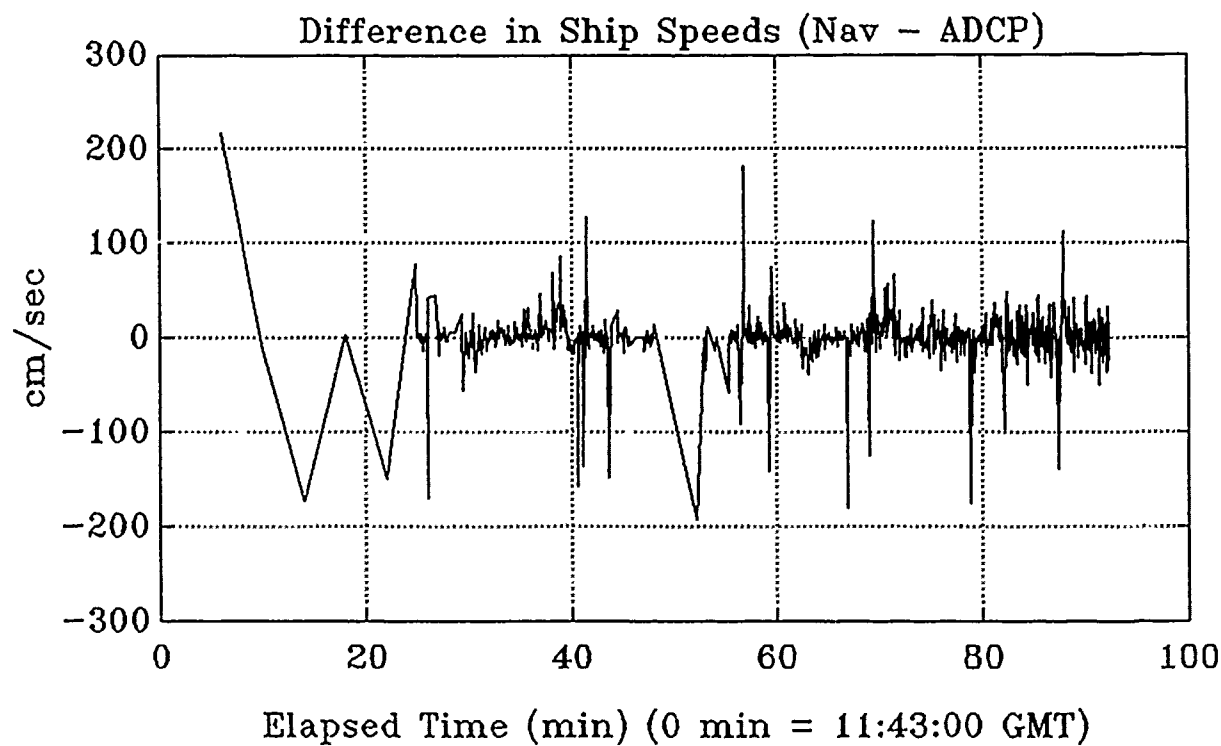


Figure 5.29. Survey 241A: time series of the difference in ship speed.

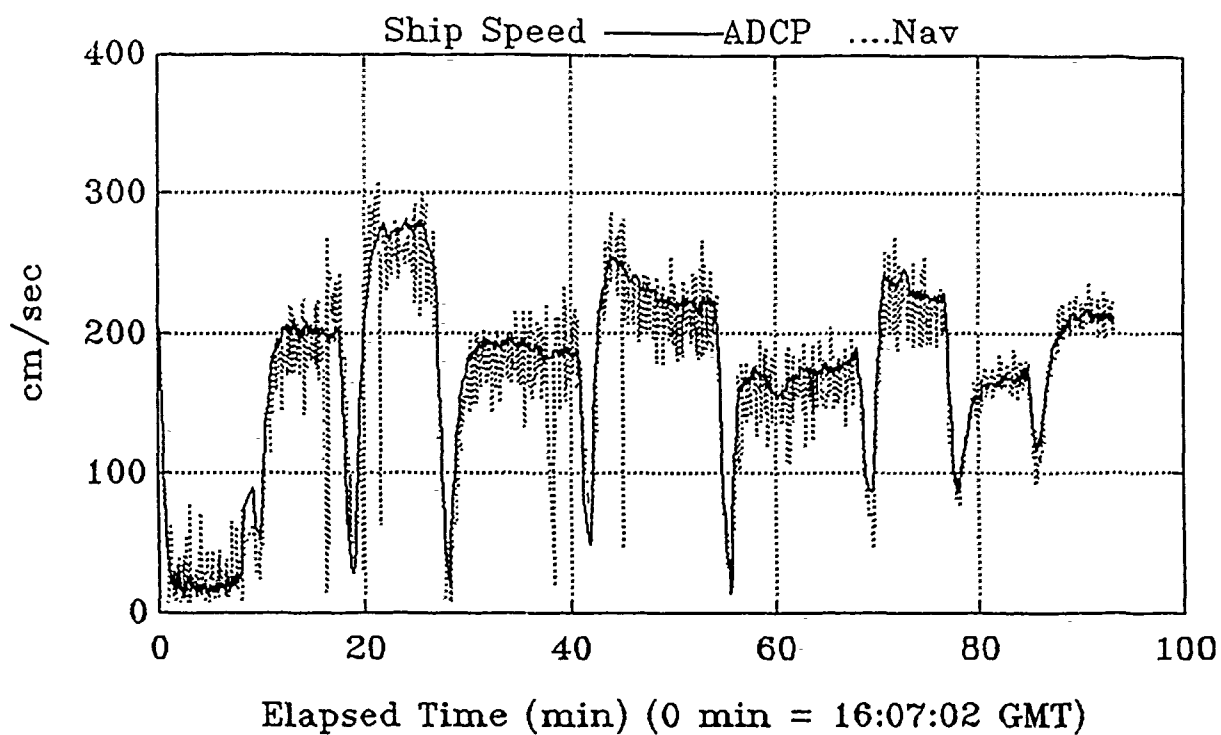


Figure 5.30. Survey 242A: time series of ship speed data.

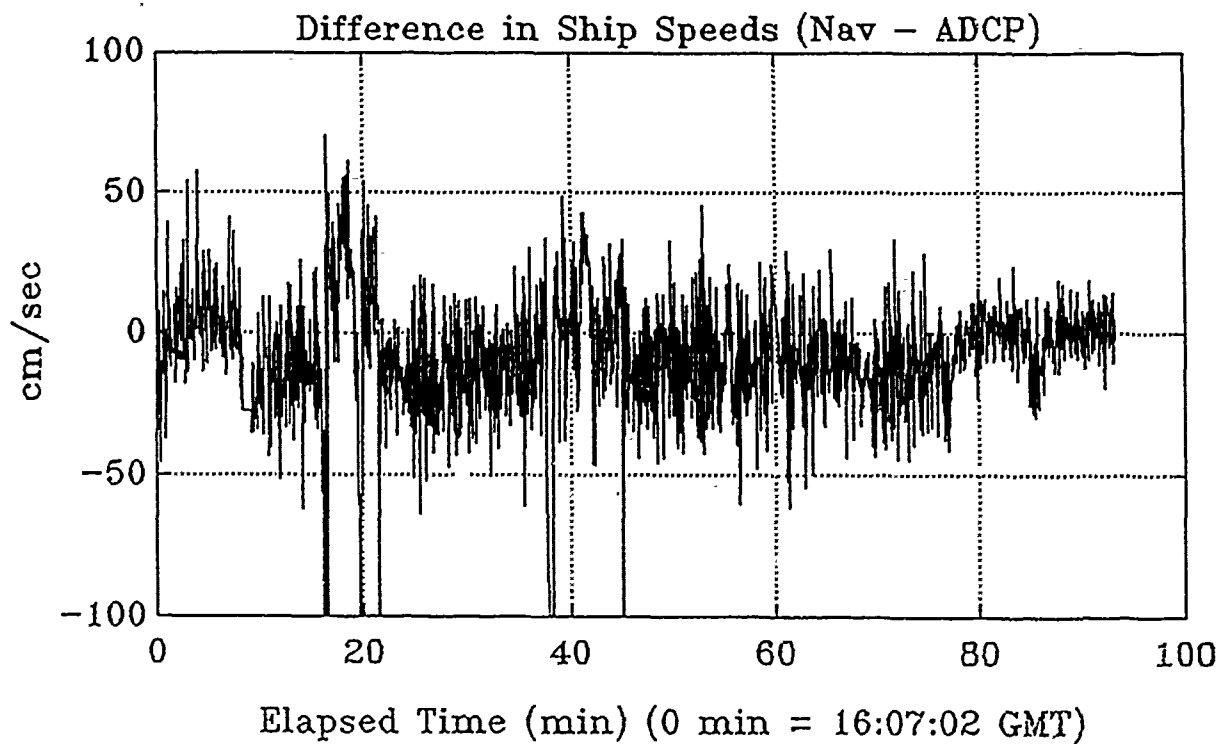


Figure 5.31. Survey 242A: time series of the difference in ship speed.

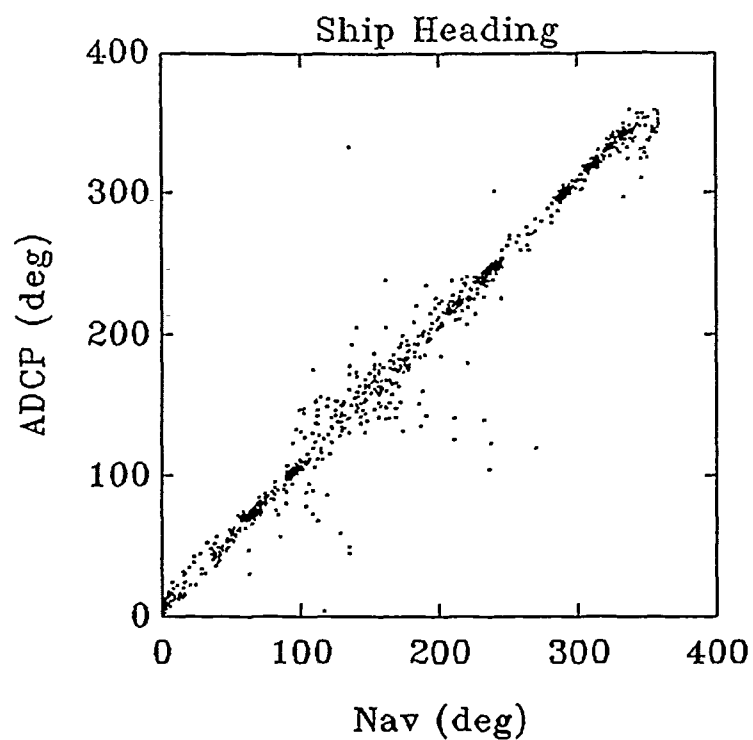


Figure 5.32. Survey 237A: comparison plot of ship heading.

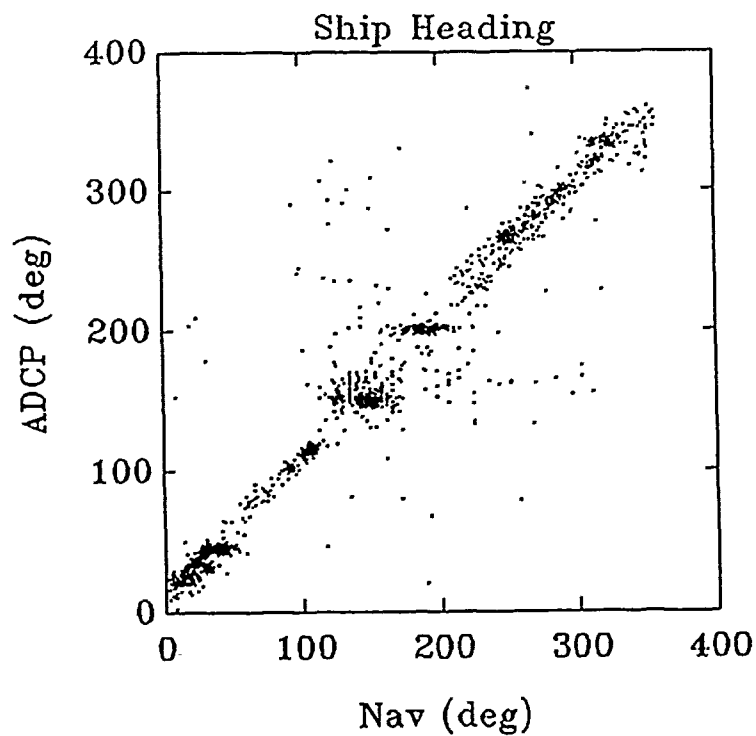


Figure 5.33. Survey 238A: comparison plot of ship heading.

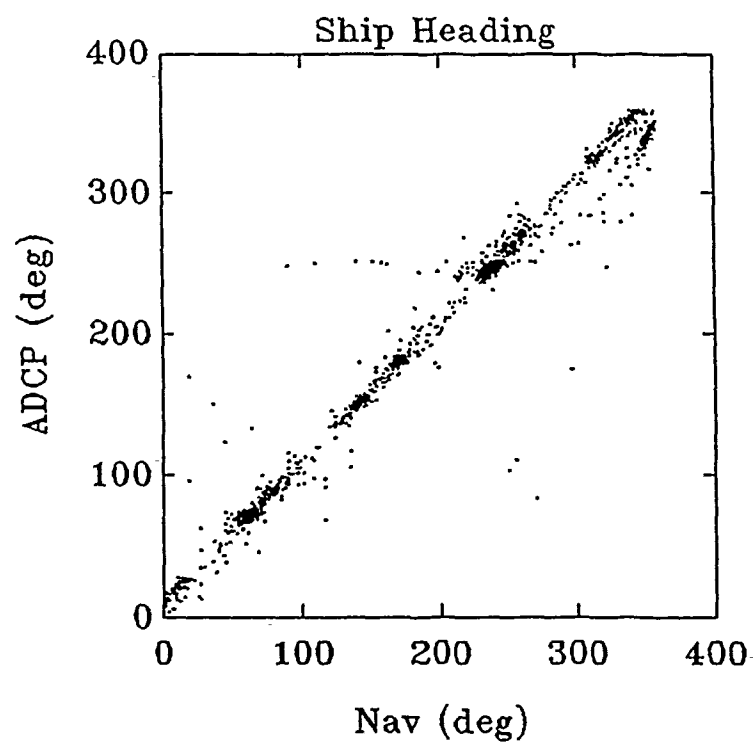


Figure 5.34. Survey 238B: comparison plot of ship heading.

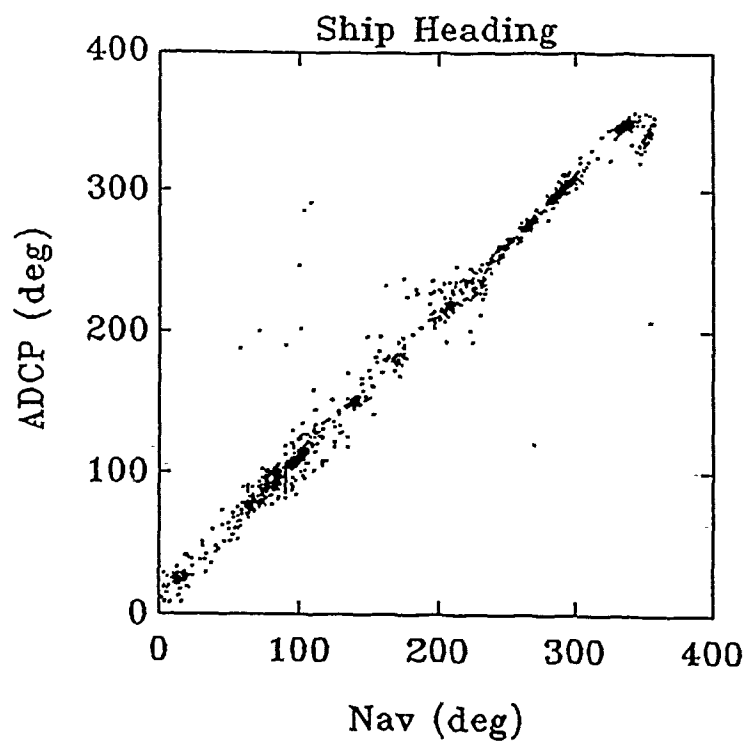


Figure 5.35. Survey 239A: comparison plot of ship heading.

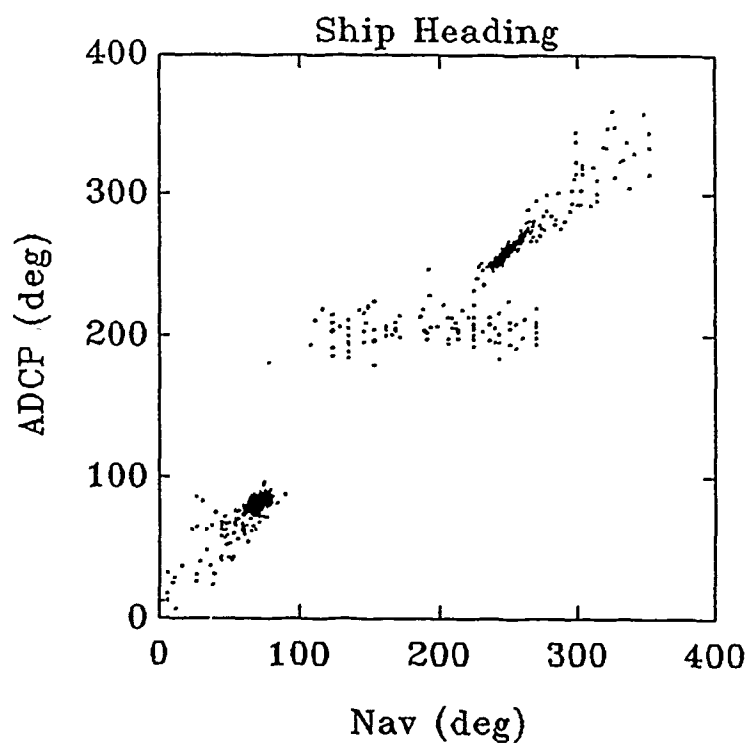


Figure 5.36. Survey 239B: comparison plot of ship heading.

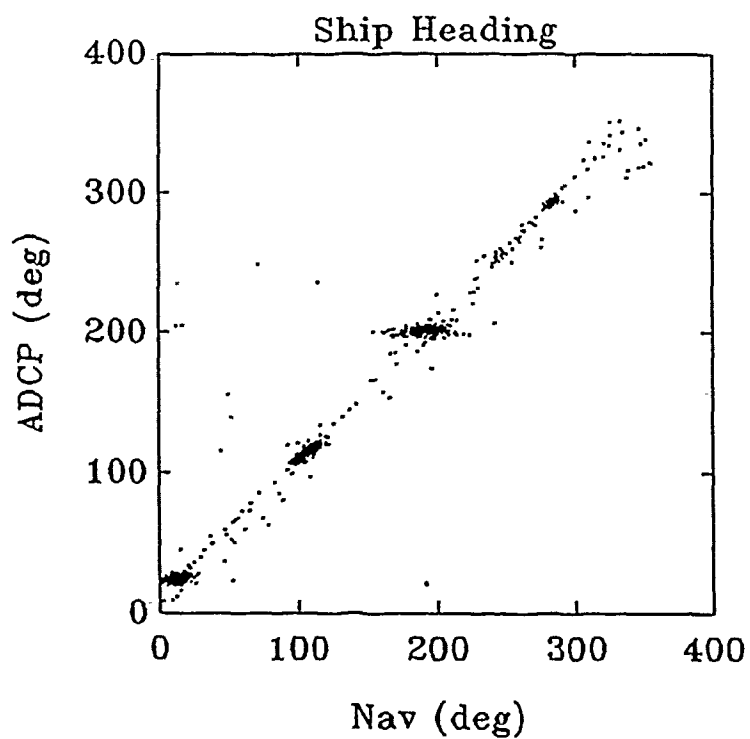


Figure 5.37. Survey 241A: comparison plot of ship heading.

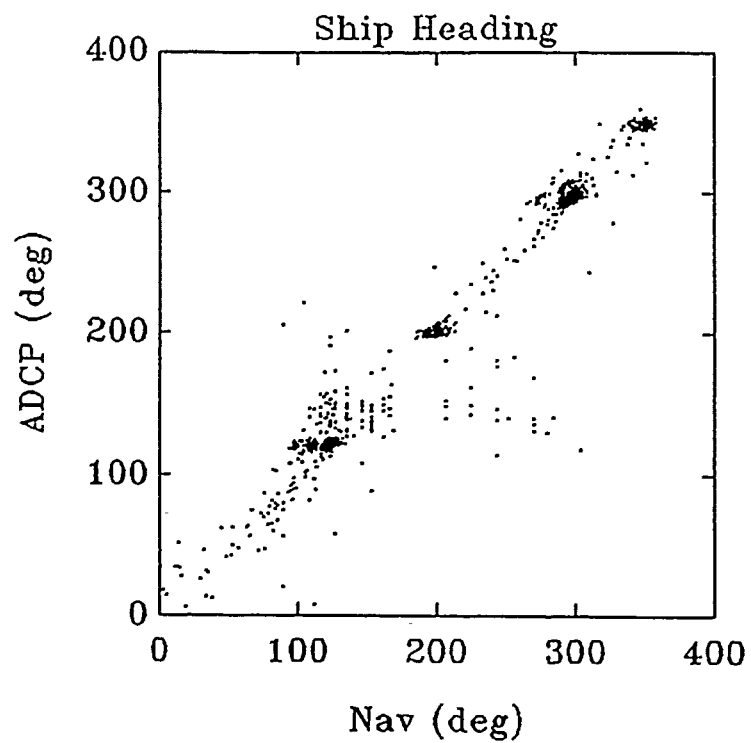


Figure 5.38. Survey 242A: comparison plot of ship heading.

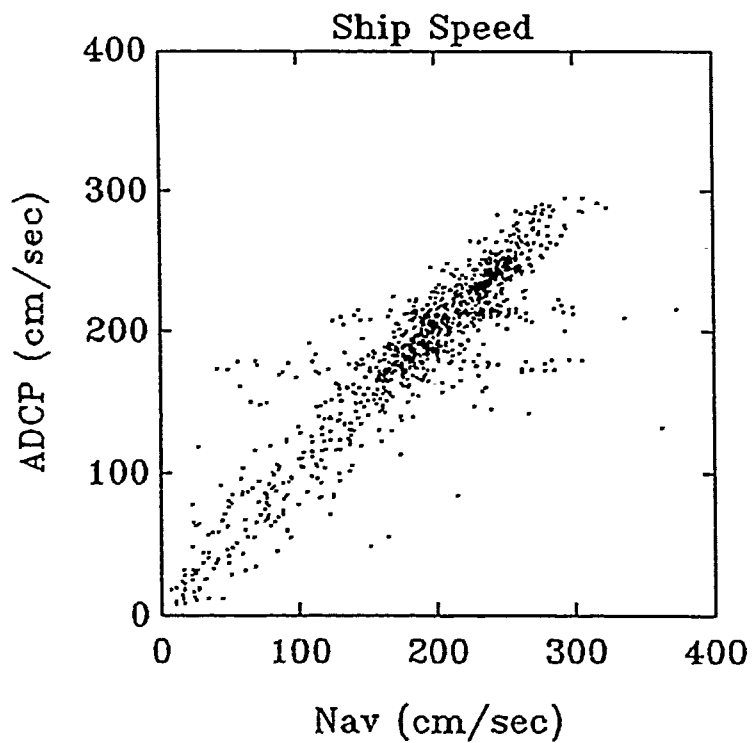


Figure 5.39. Survey 237A: comparison plot of ship speed.

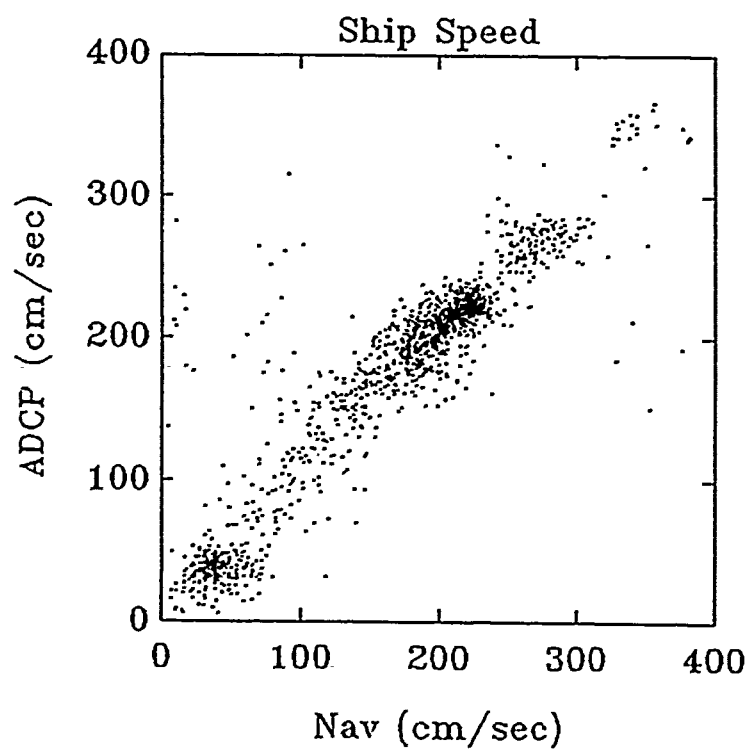


Figure 5.40. Survey 238A: comparison plot of ship speed.

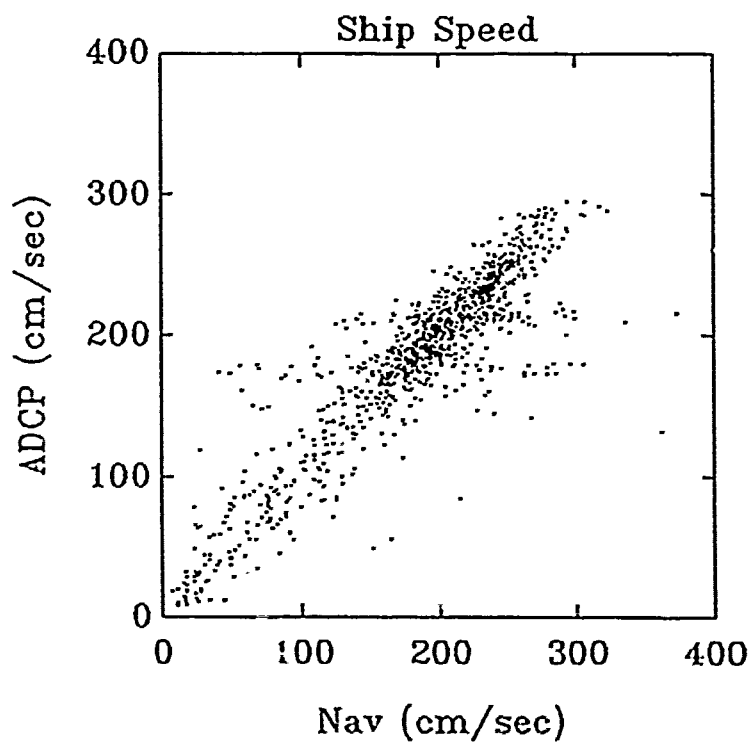


Figure 5.41. Survey 238B: comparison plot of ship speed.

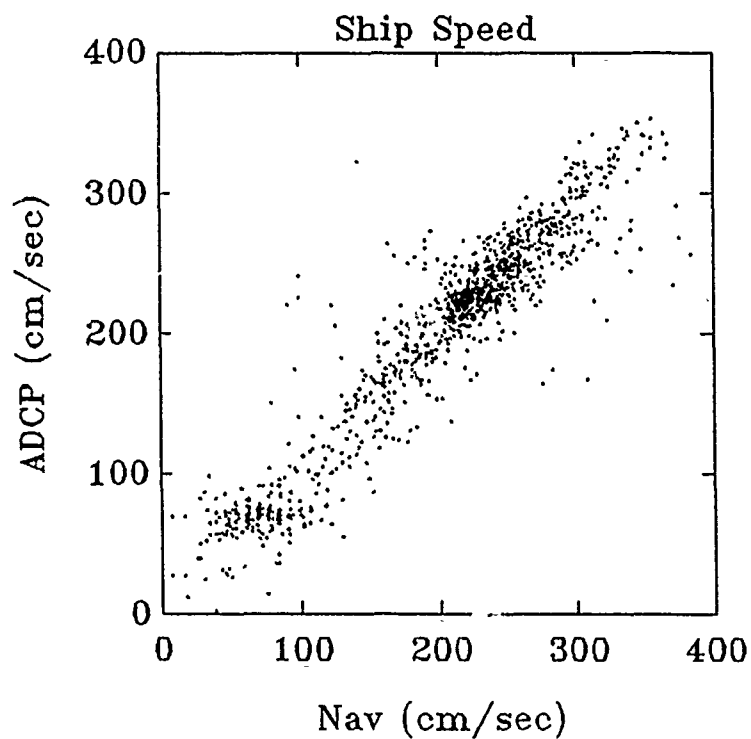


Figure 5.42. Survey 239A: comparison plot of ship speed.

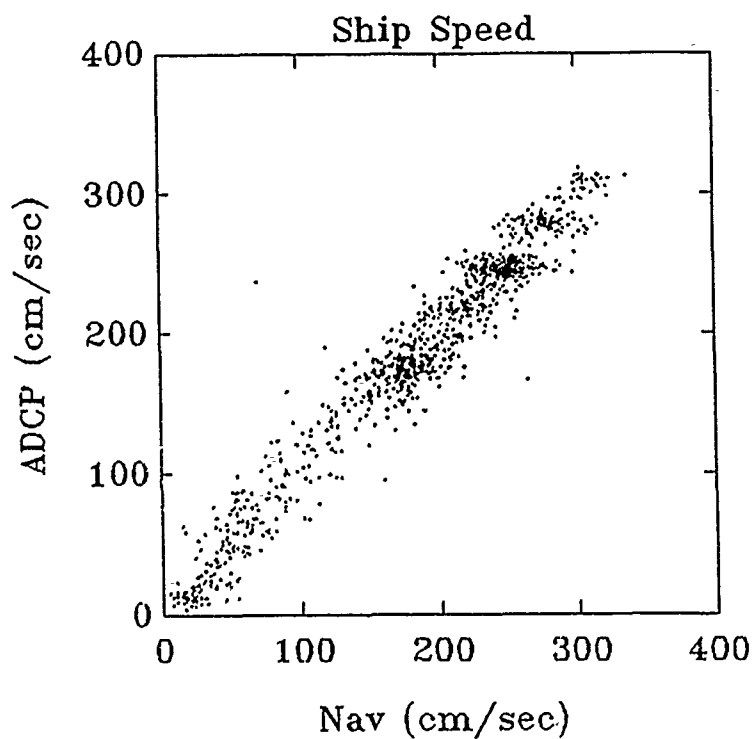


Figure 5.43. Survey 239B: comparison plot of ship speed.

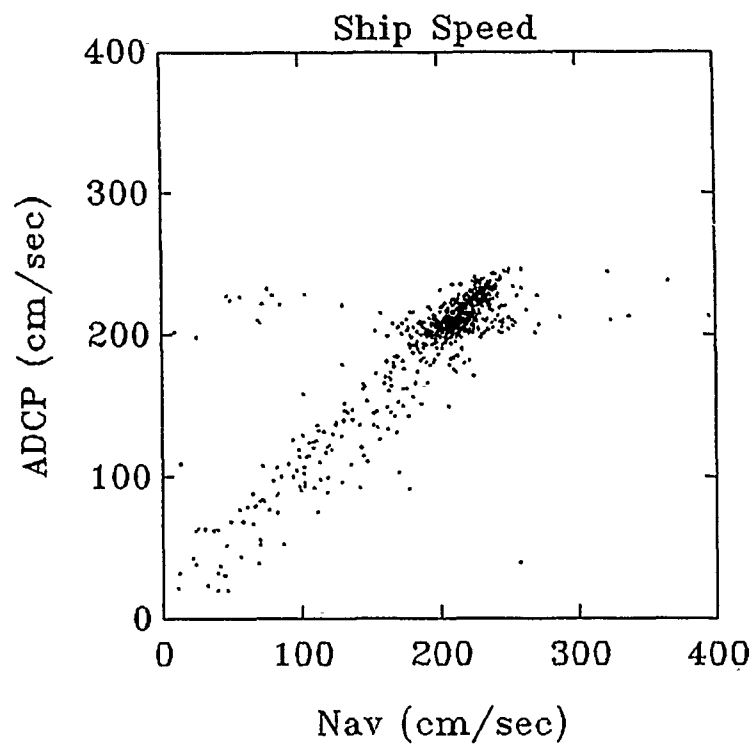


Figure 5.44. Survey 241A: comparison plot of ship speed.

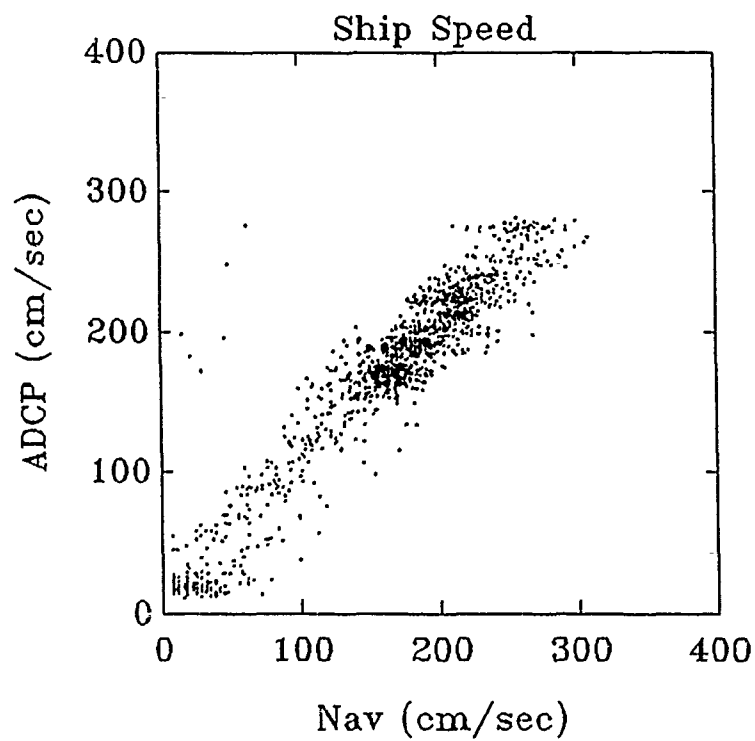


Figure 5.45. Survey 242A: comparison plot of ship speed.

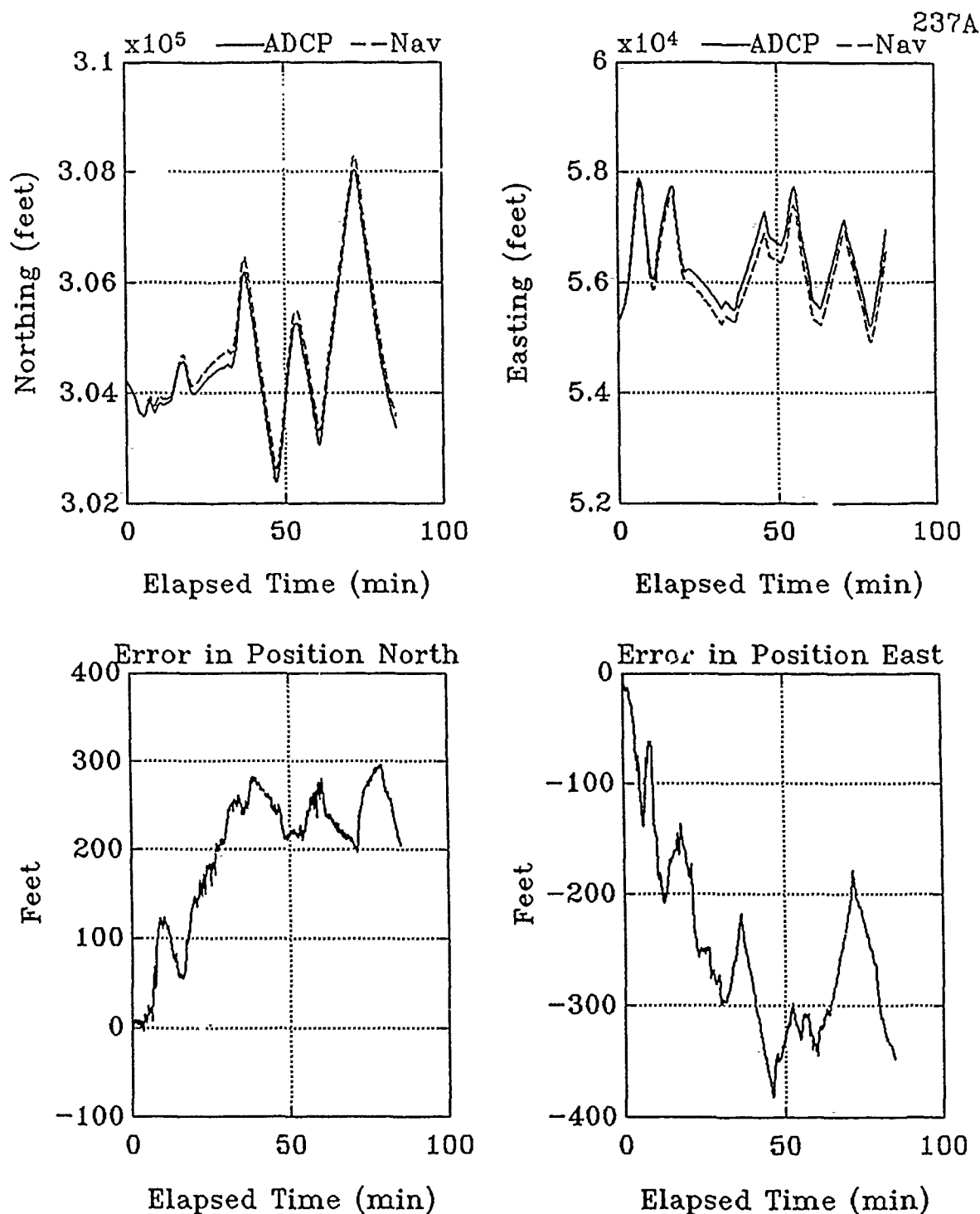


Figure 5.46. Survey 237A: time series for the estimates of ship position from the ADCP bottom track data and the navigation data. Clockwise from upper left: (a) North ship position (ADCP solid line, Navigation dashed); (b) East ship position (ADCP solid line, Navigation dashed); (c) Error in north position estimates (Navigation - ADCP); (d) Error in east position estimate (Navigation - ADCP). Elapsed time is given in minutes from the start of the survey (0 min = 14:15:00 GMT).

238A

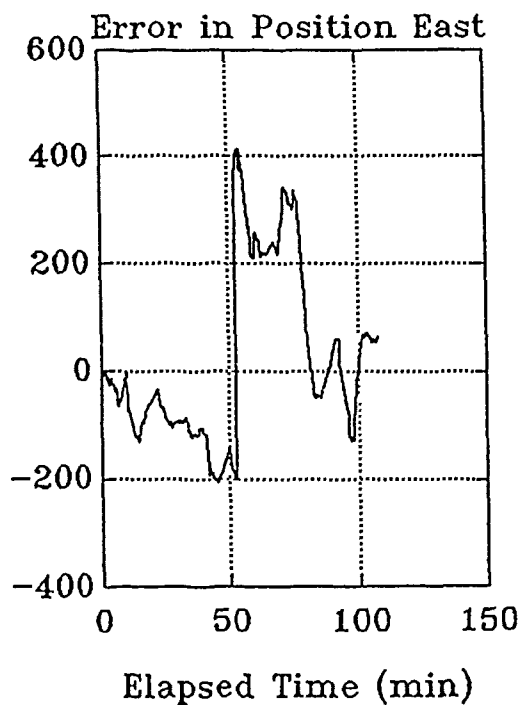
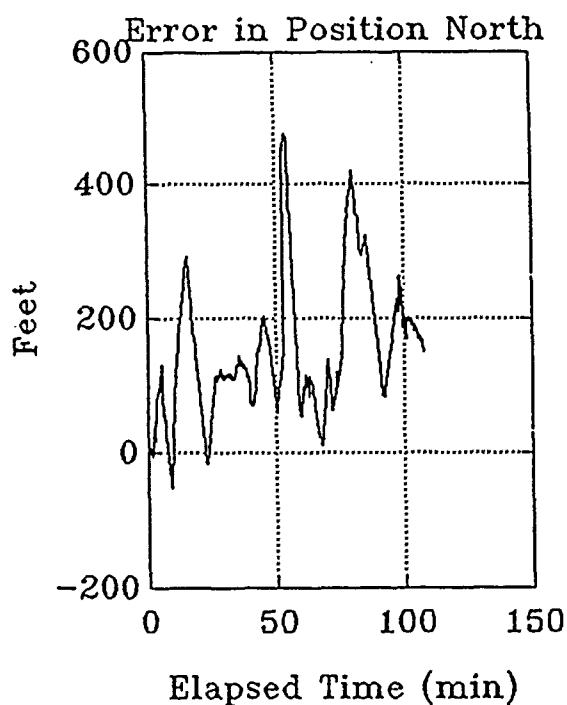
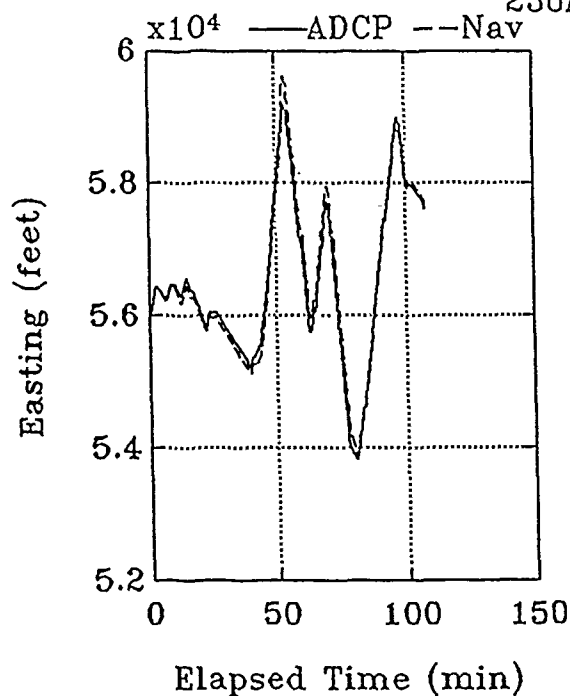
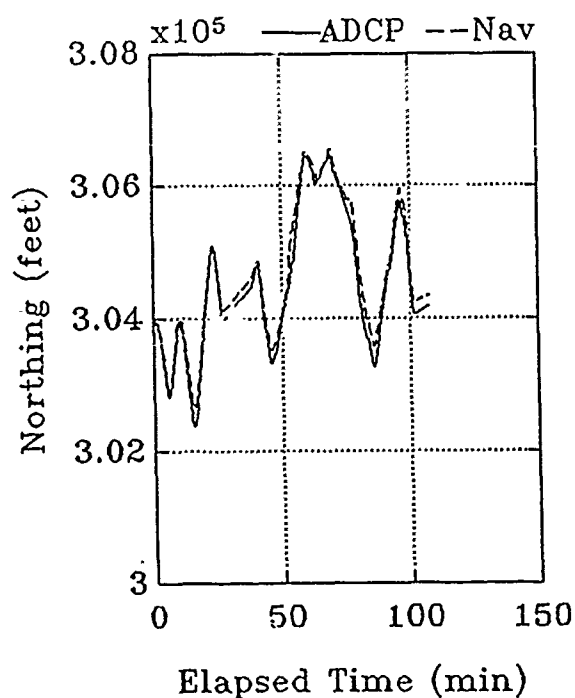


Figure 5.47. Survey 238A: time series for the estimates of ship position from the ADCP bottom track data and the navigation data. Clockwise from upper left: (a) North ship position (ADCP solid line, Navigation dashed); (b) East ship position (ADCP solid line, Navigation dashed); (c) Error in north position estimates (Navigation - ADCP); (d) Error in east position estimate (Navigation - ADCP). Elapsed time is given in minutes from the start of the survey (0 min = 14:20:48 GMT).

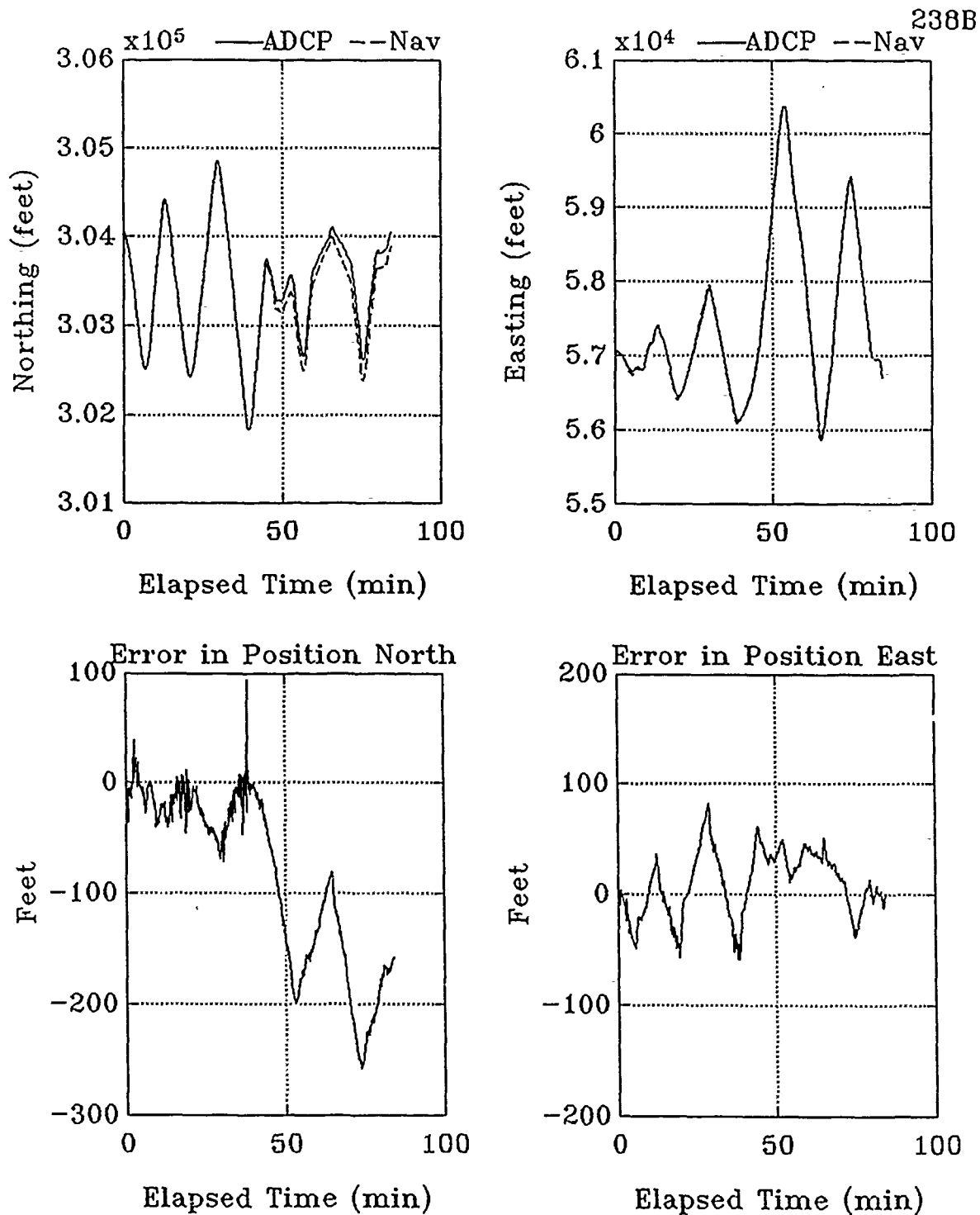


Figure 5.48. Survey 238B: time series for the estimates of ship position from the ADCP bottom track data and the navigation data. Clockwise from upper left: (a) North ship position (ADCP solid line, Navigation dashed); (b) East ship position (ADCP solid line, Navigation dashed); (c) Error in north position estimates (Navigation - ADCP); (d) Error in east position estimate (Navigation - ADCP). Elapsed time is given in minutes from the start of the survey (0 min = 21:53:38 GMT).

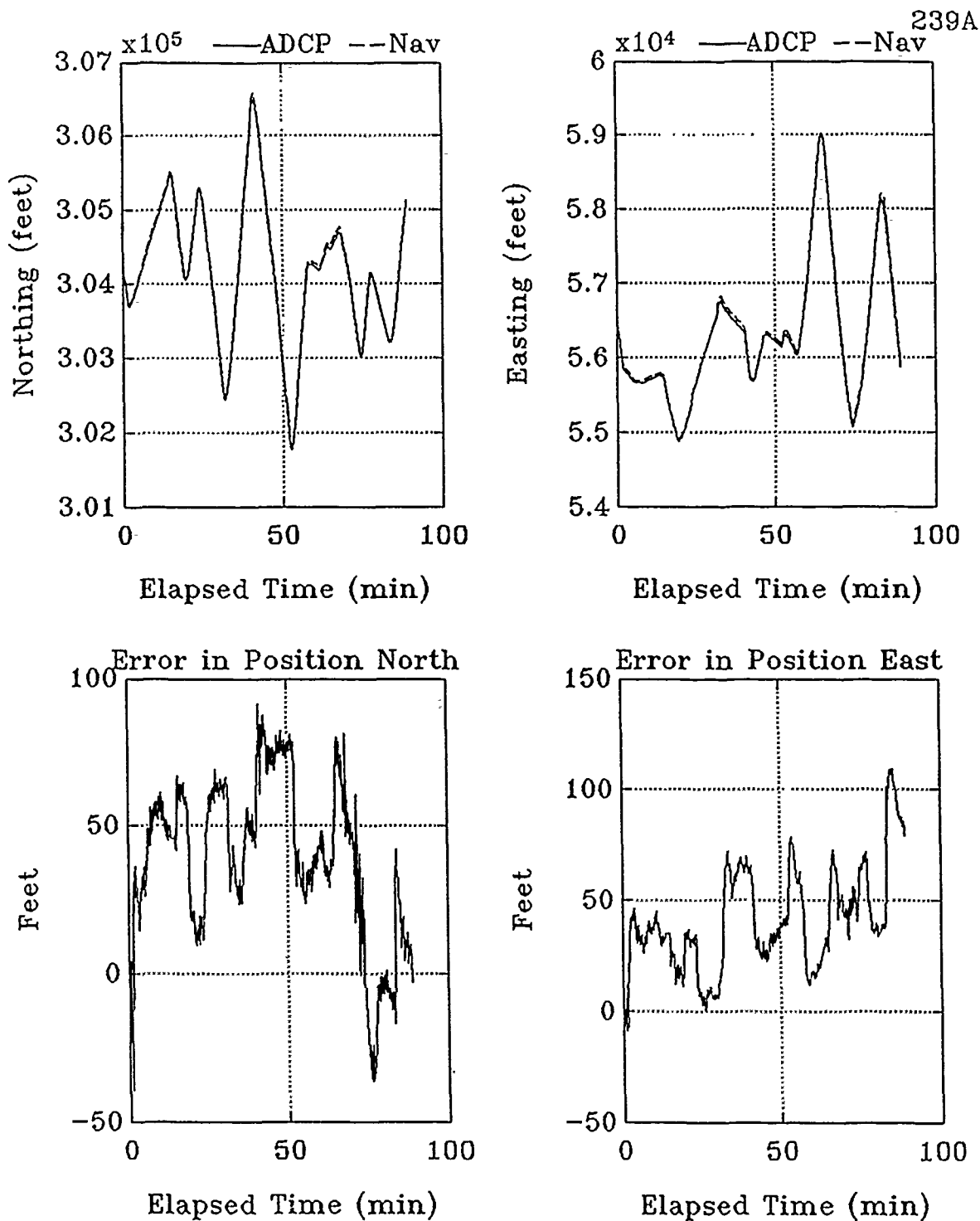


Figure 5.49. Survey 239A: time series for the estimates of ship position from the ADCP bottom track data and the navigation data. Clockwise from upper left: (a) North ship position (ADCP solid line, Navigation dashed); (b) East ship position (ADCP solid line, Navigation dashed); (c) Error in north position estimates (Navigation - ADCP); (d) Error in east position estimate (Navigation - ADCP). Elapsed time is given in minutes from the start of the survey (0 min = 14:06:13 GMT).

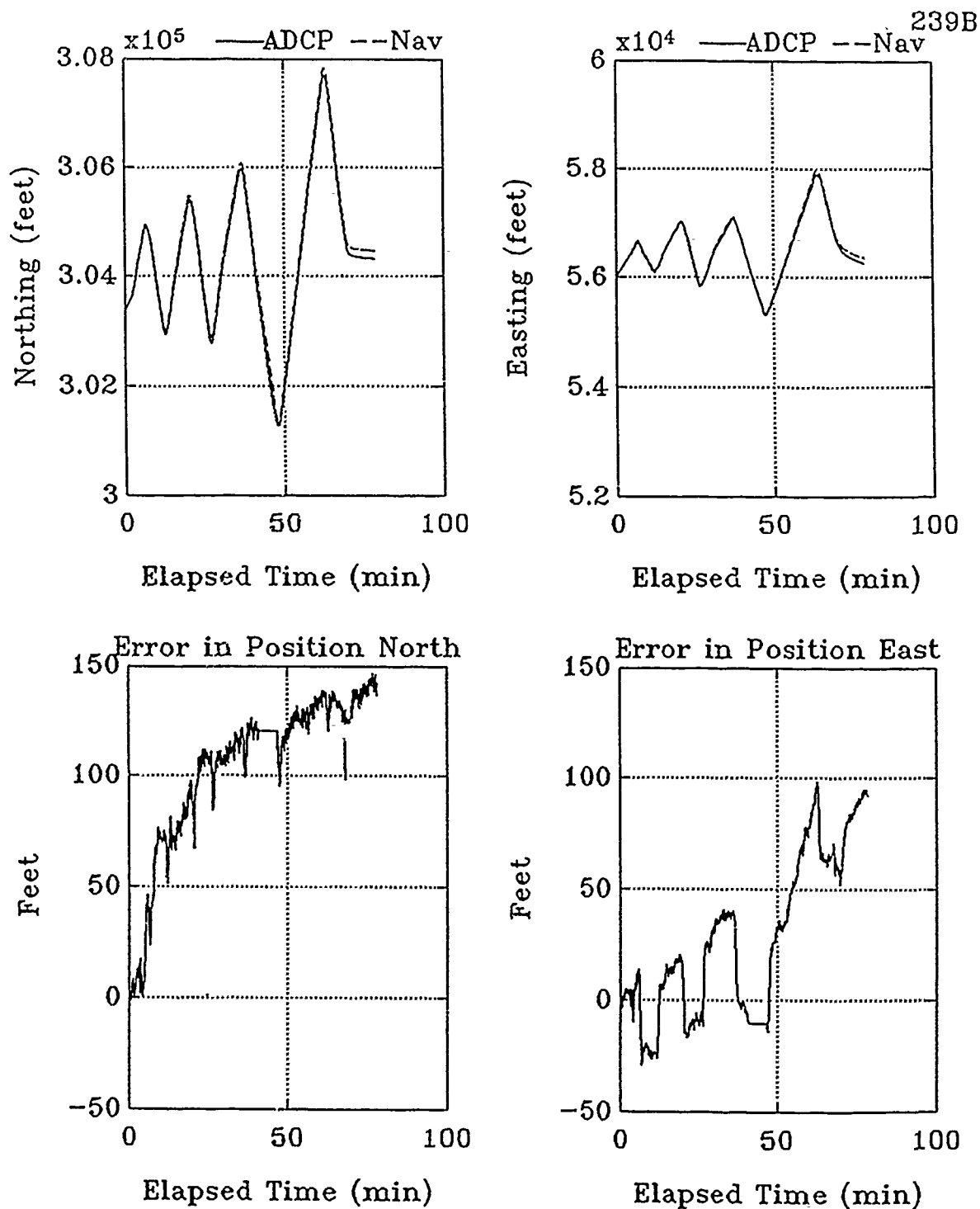


Figure 5.50. Survey 239B: time series for the estimates of ship position from the ADCP bottom track data and the navigation data. Clockwise from upper left: (a) North ship position (ADCP solid line, Navigation dashed); (b) East ship position (ADCP solid line, Navigation dashed); (c) Error in north position estimates (Navigation - ADCP); (d) Error in east position estimate (Navigation - ADCP). Elapsed time is given in minutes from the start of the survey (0 min = 22:09:44 GMT).

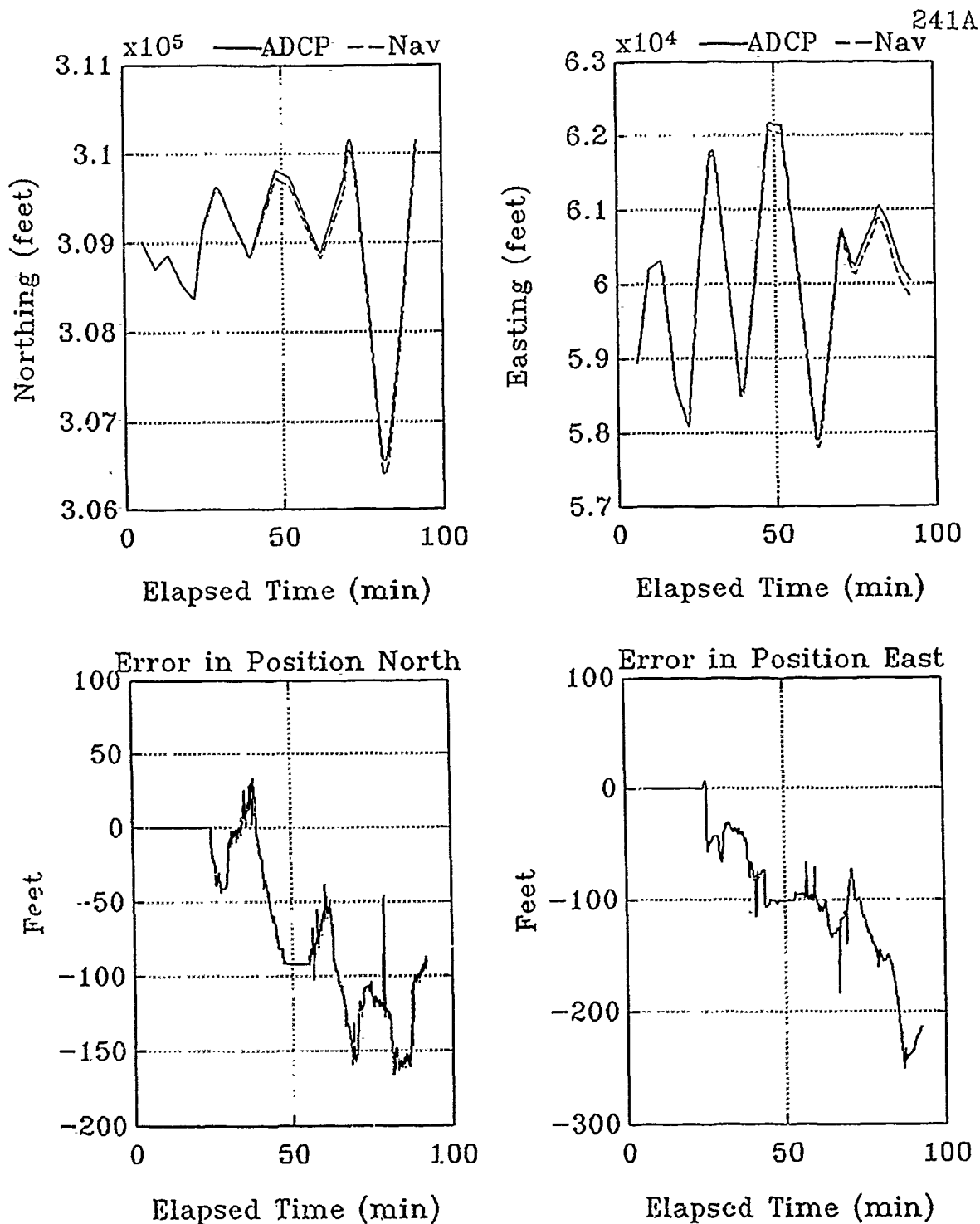


Figure 5.51. Survey 241A: time series for the estimates of ship position from the ADCP bottom track data and the navigation data. Clockwise from upper left: (a) North ship position (ADCP solid line, Navigation dashed); (b) East ship position (ADCP solid line, Navigation dashed); (c) Error in north position estimates (Navigation - ADCP); (d) Error in east position estimate (Navigation - ADCP). Elapsed time is given in minutes from the start of the survey (0 min = 11:43:00 GMT).

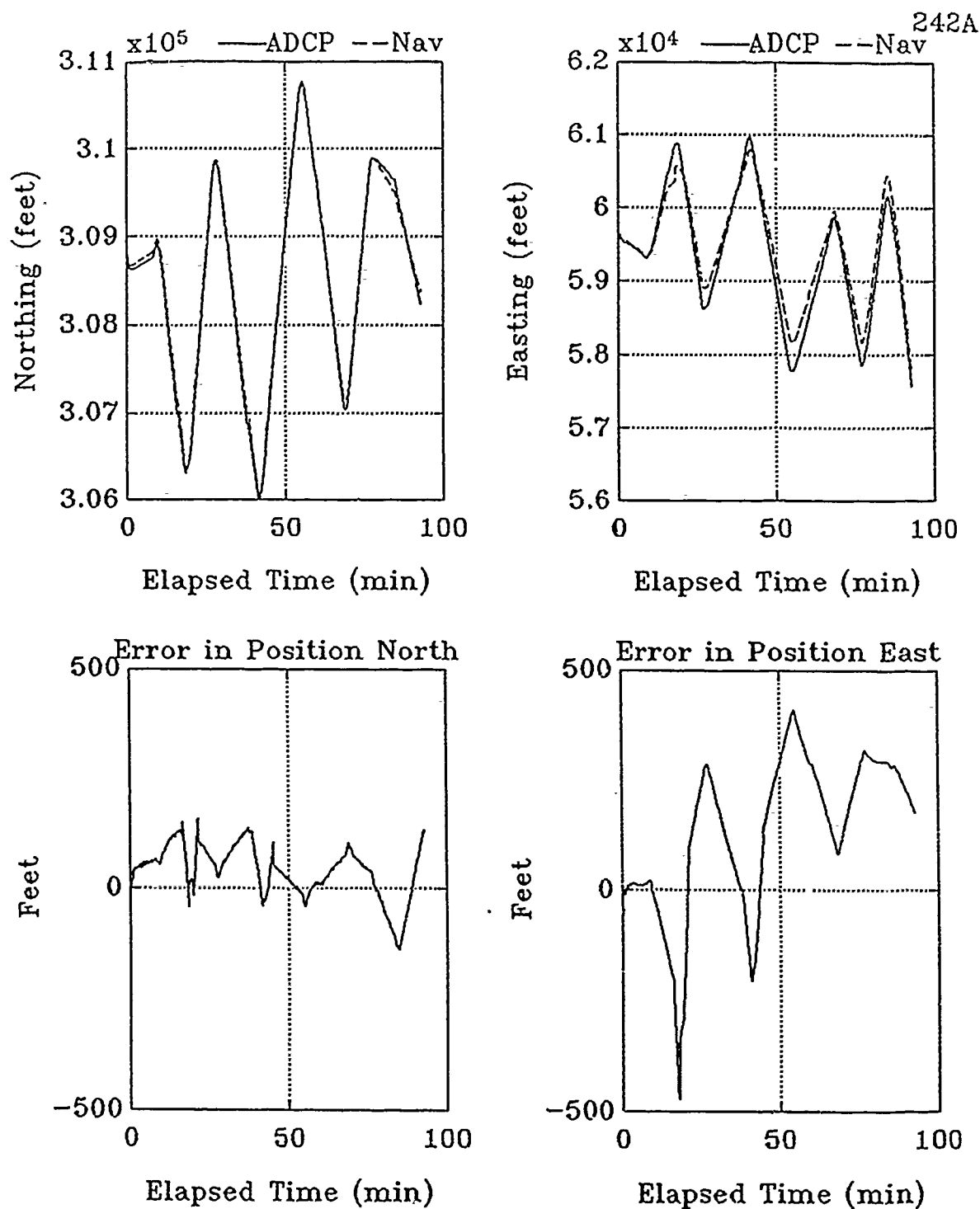


Figure 5.52. Survey 242A: time series for the estimates of ship position from the ADCP bottom track data and the navigation data. Clockwise from upper left: (a) North ship position (ADCP solid line, Navigation dashed); (b) East ship position (ADCP solid line, Navigation dashed); (c) Error in north position estimates (Navigation - ADCP); (d) Error in east position estimate (Navigation - ADCP). Elapsed time is given in minutes from the start of the survey (0 min = 16:07:02 GMT).

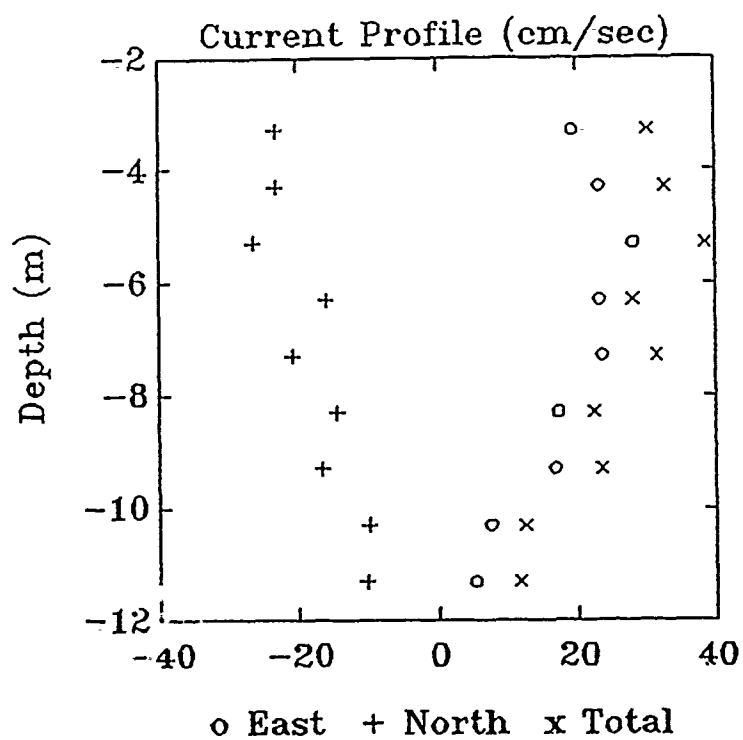


Figure 5.53. Survey 237A: vertical current profile.

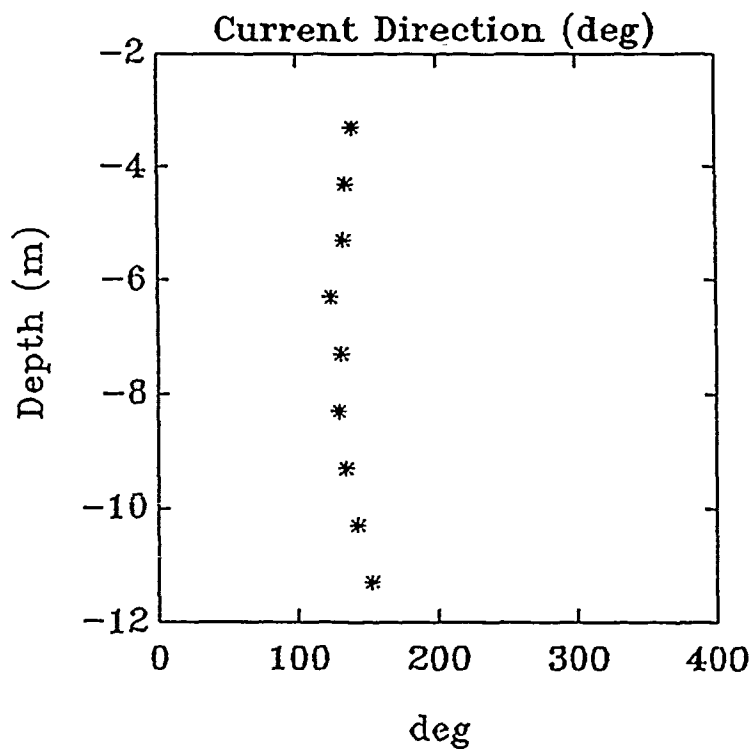


Figure 5.54. Survey 237A: current direction (degrees from north).

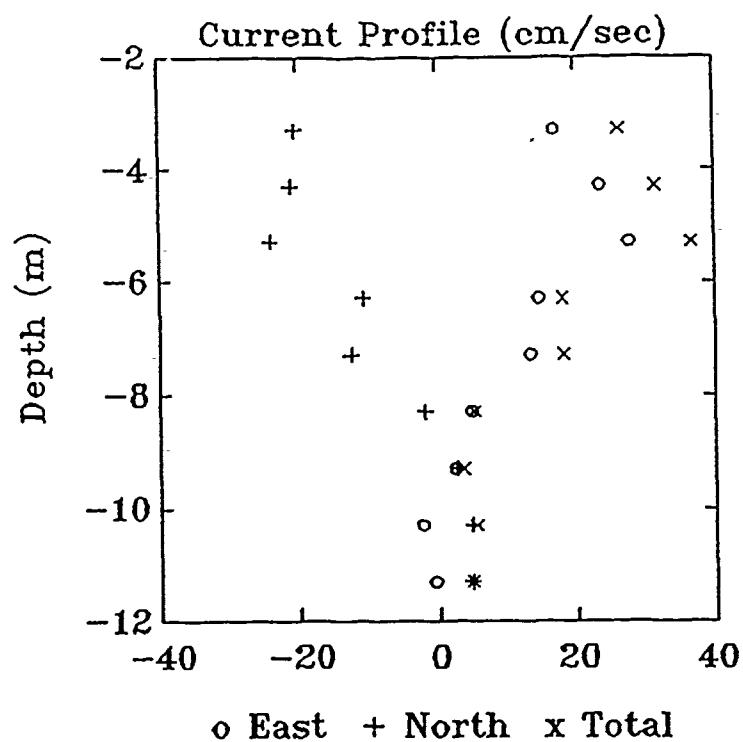


Figure 5.55. Survey 238A: vertical current profile.

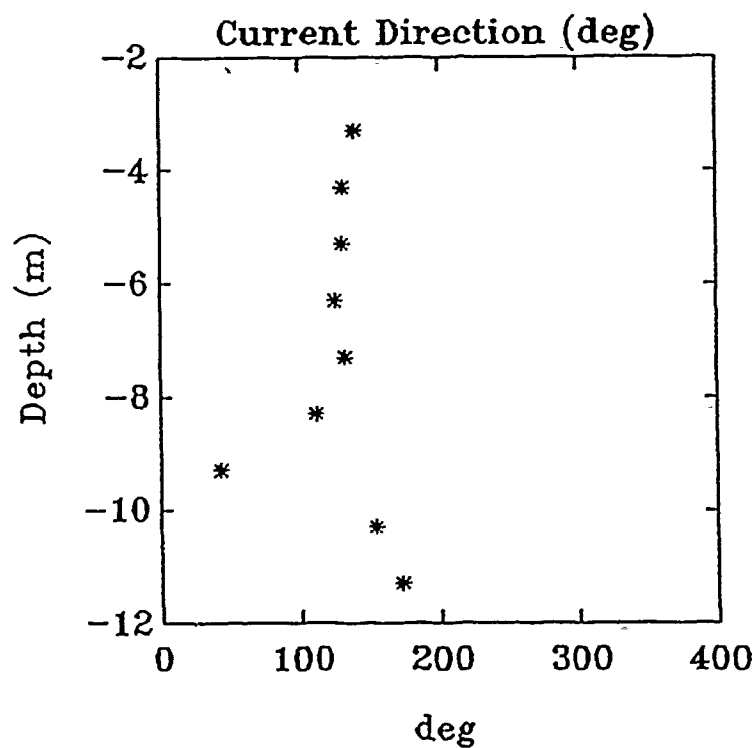


Figure 5.56. Survey 238A: current direction (degrees from north).

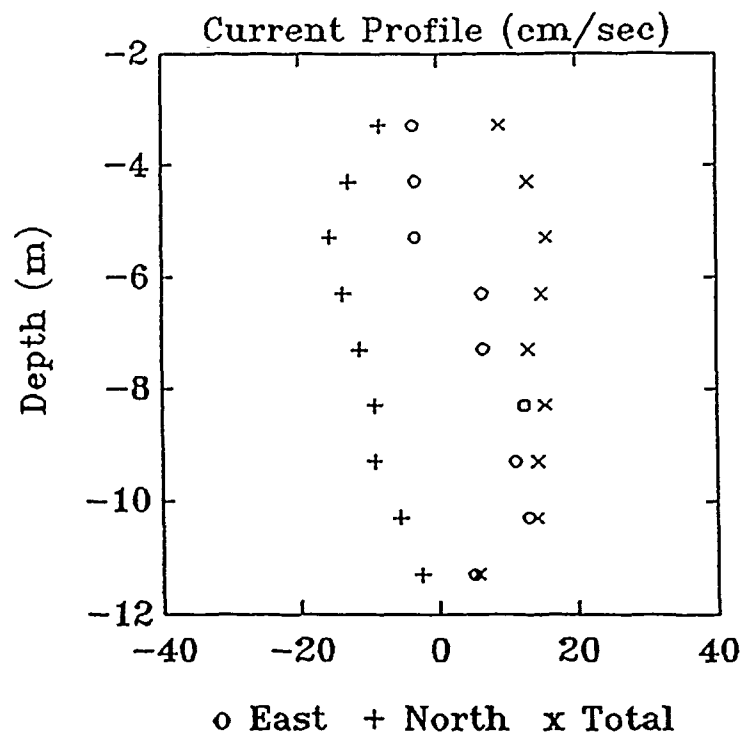


Figure 5.57. Survey 238B: vertical current profile.

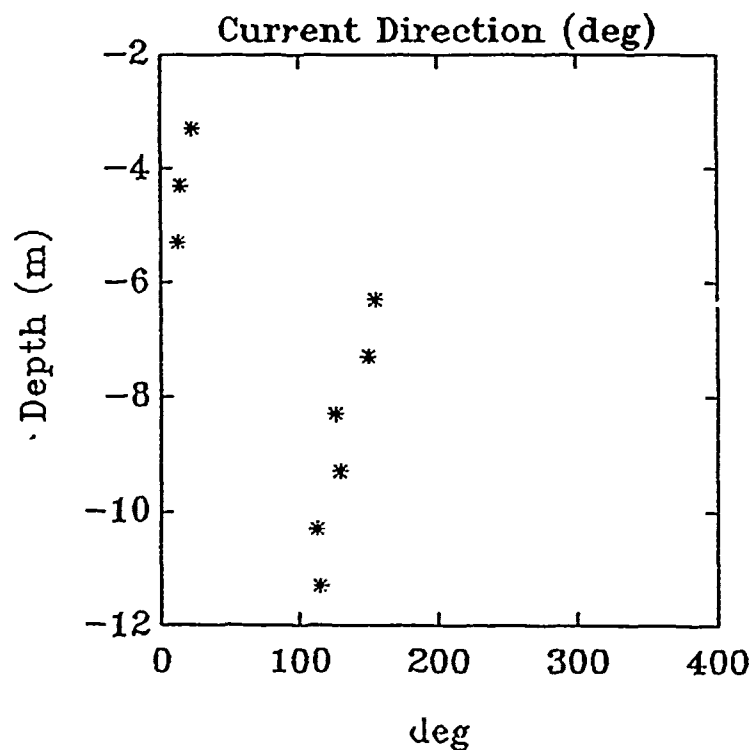


Figure 5.58. Survey 238B: current direction (degrees from north).

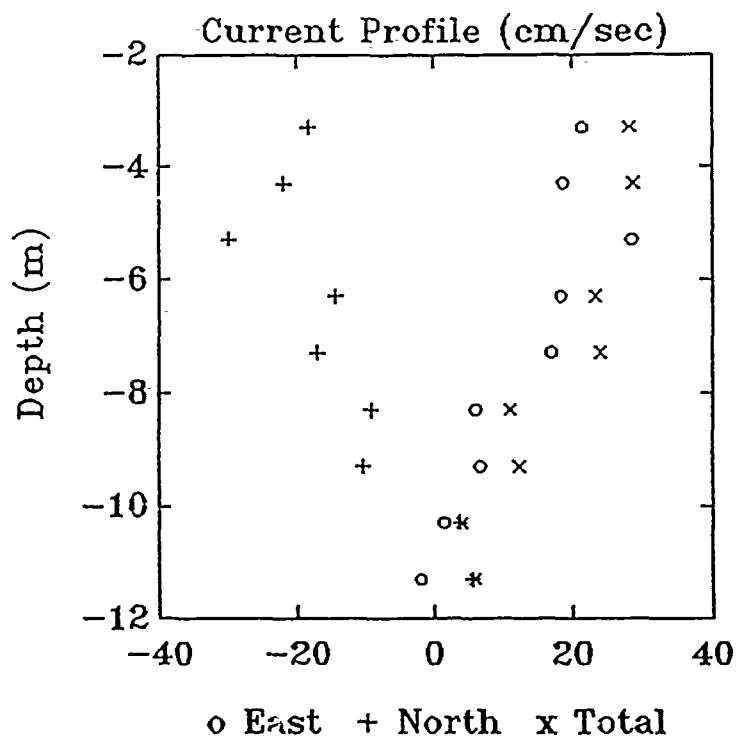


Figure 5.59. Survey 239A: vertical current profile.

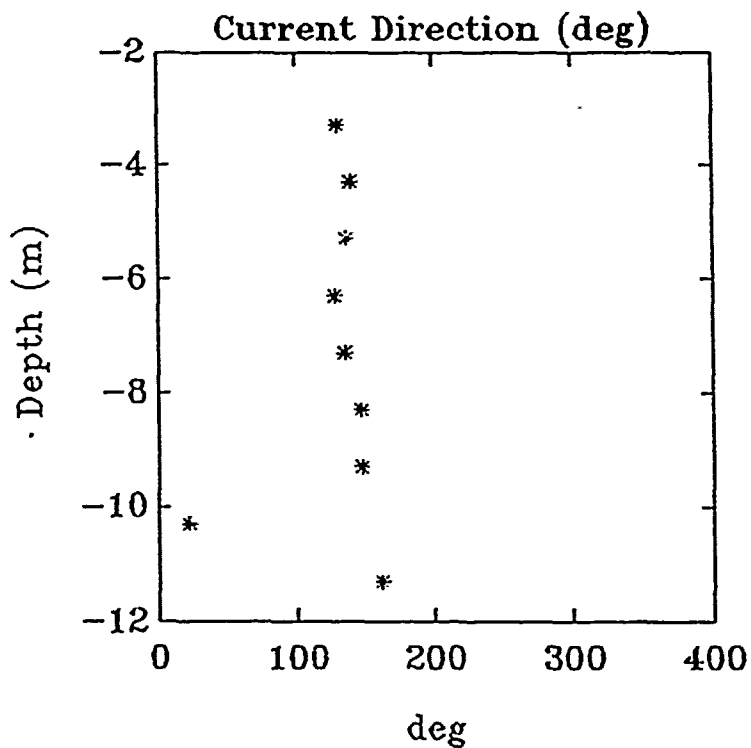


Figure 5.60. Survey 239A: current direction (degrees from north).

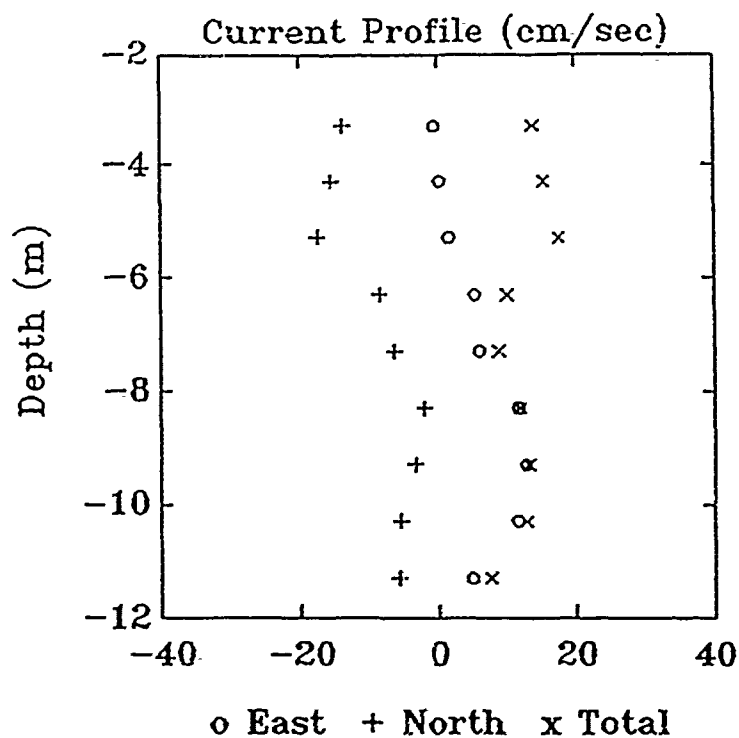


Figure 5.61. Survey 239B: vertical current profile.

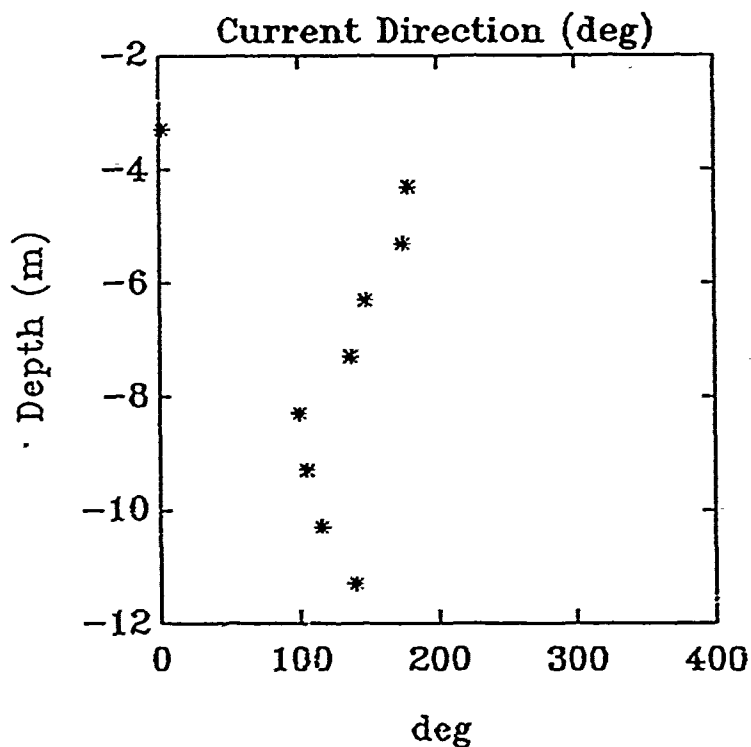


Figure 5.62. Survey 239B: current direction (degrees from north).

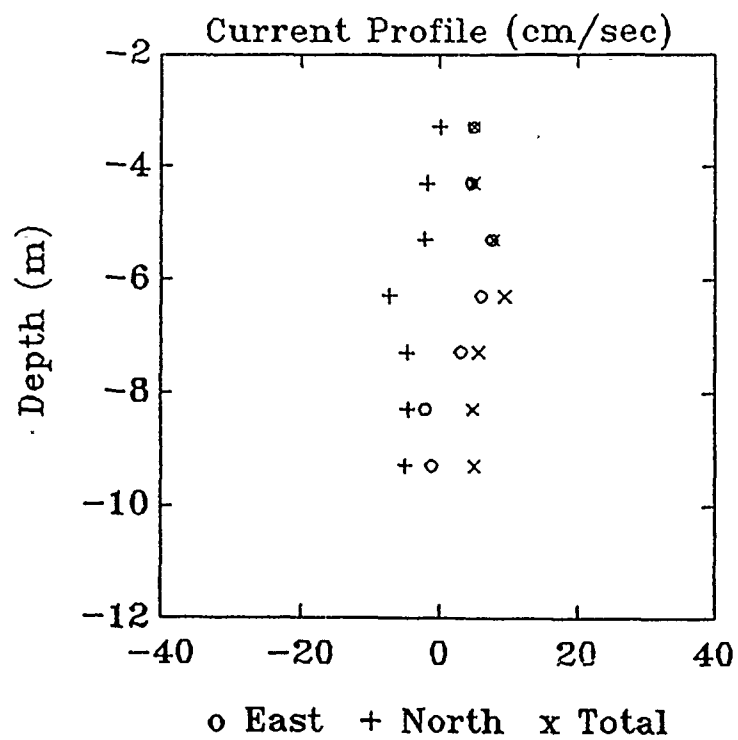


Figure 5.63. Survey 241A: vertical current profile.

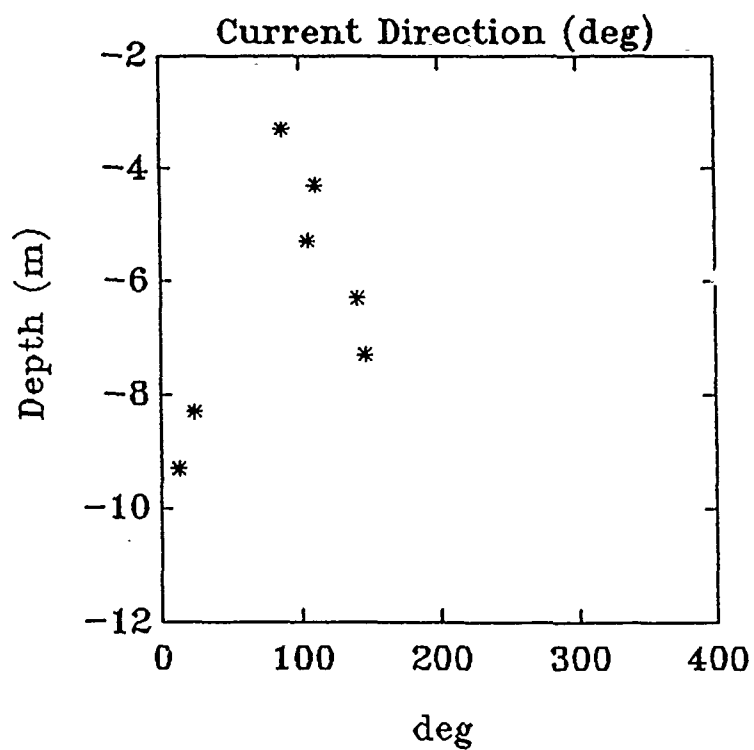


Figure 5.64. Survey 241A: current direction (degrees from north).

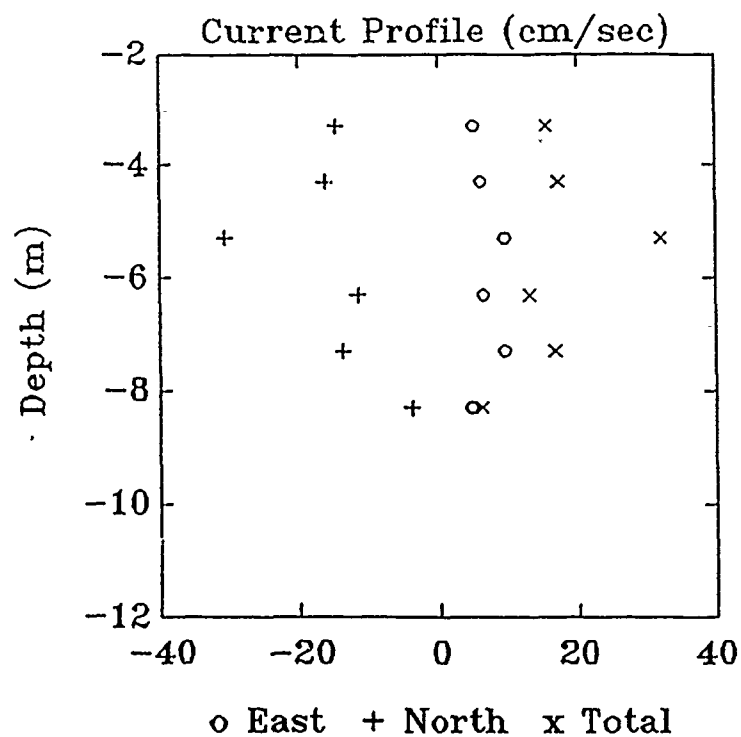


Figure 5.65. Survey 242A: vertical current profile.

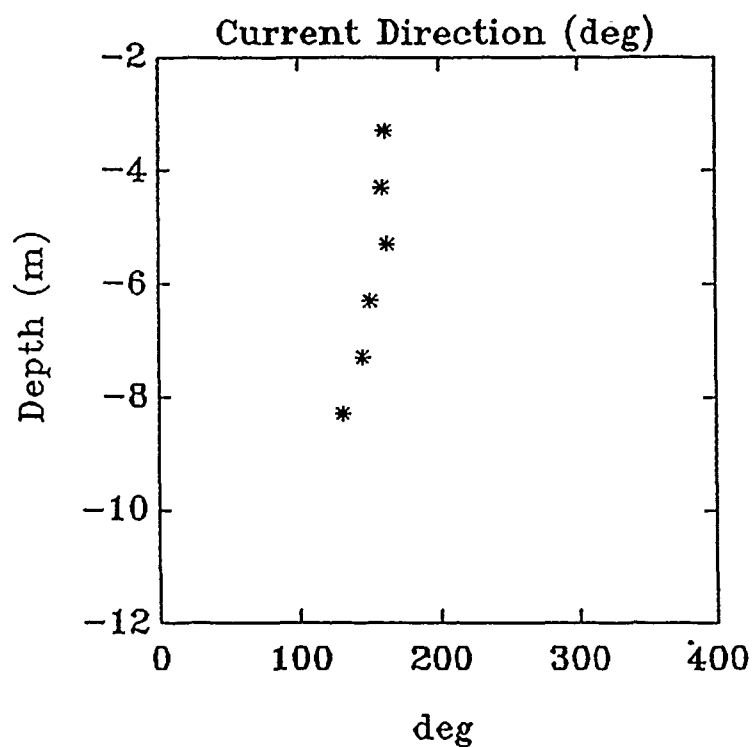


Figure 5.66. Survey 242A: current direction (degrees from north).

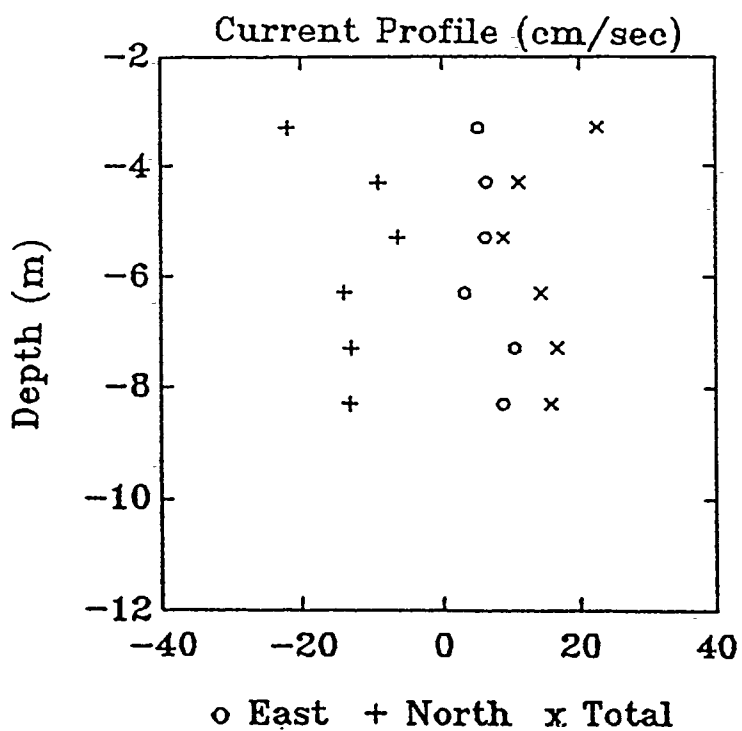


Figure 5.67. Survey 243A: vertical current profile.

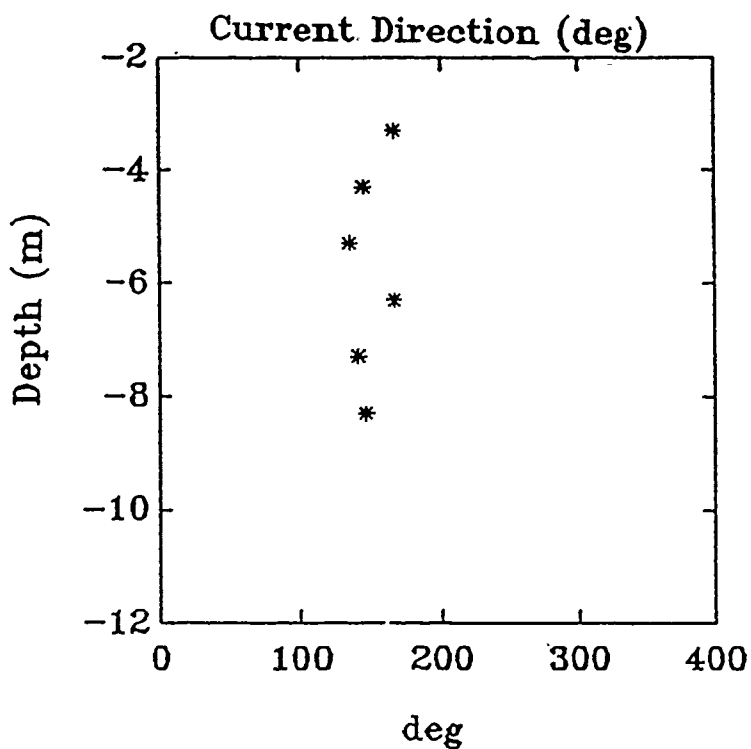


Figure 5.68. Survey 243A: current direction (degrees from north).

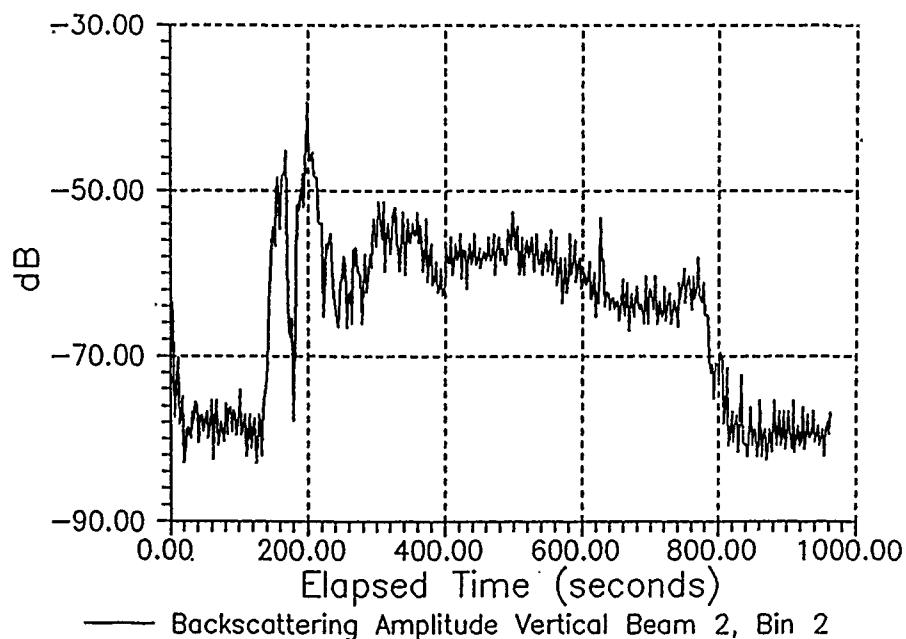


Figure 5.69. Backscattered amplitude data received by the ADCP bin 2 (4.45 m), Beam 2 (vertical beam) as the *R/V Pelican* passed through the plume. Backscattering level of -75 to -80 dB corresponds to the background level.

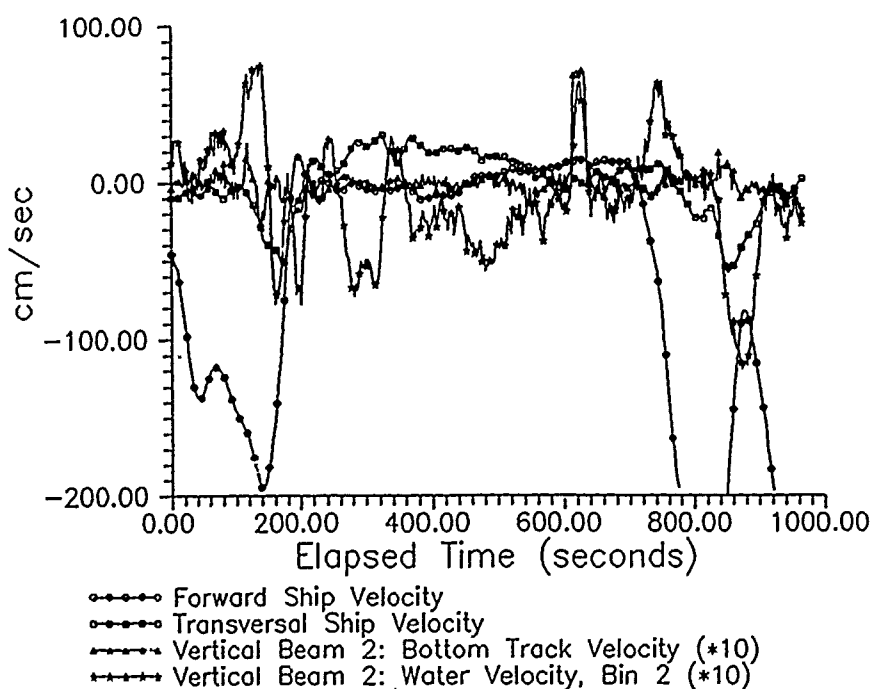


Figure 5.70. Forward velocity and transverse velocity of the bottom relative to the ship in addition to the water track velocity observed along the vertical beam. Vertical velocities have been multiplied by a factor of 10.

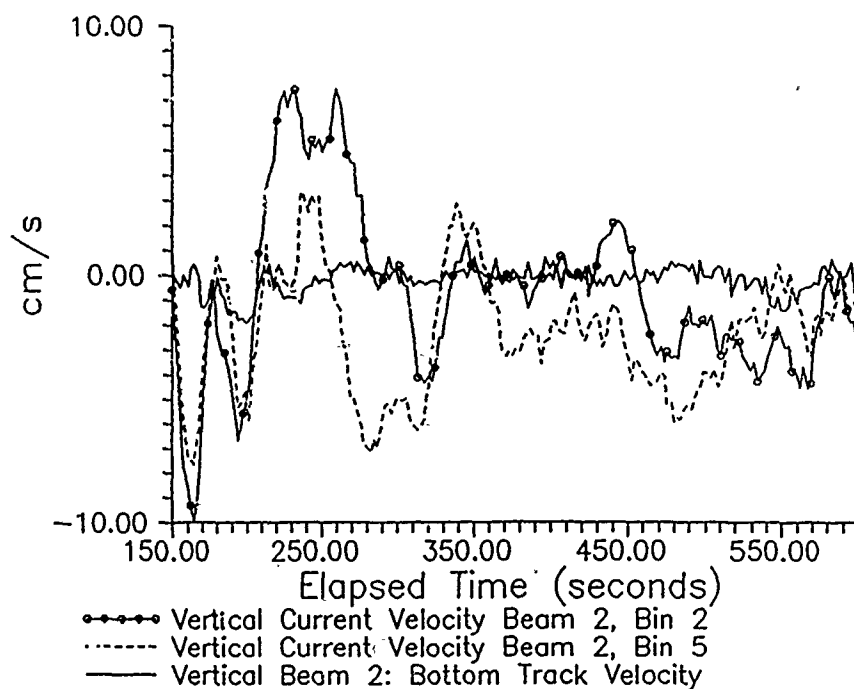


Figure 5.71. Subset of Figure 5.70 when the boat drifted through the plume. The lines depict the bottom track velocity and the vertical current velocity from bins 2 and 5 calculated from the vertical beam (Beam 2).

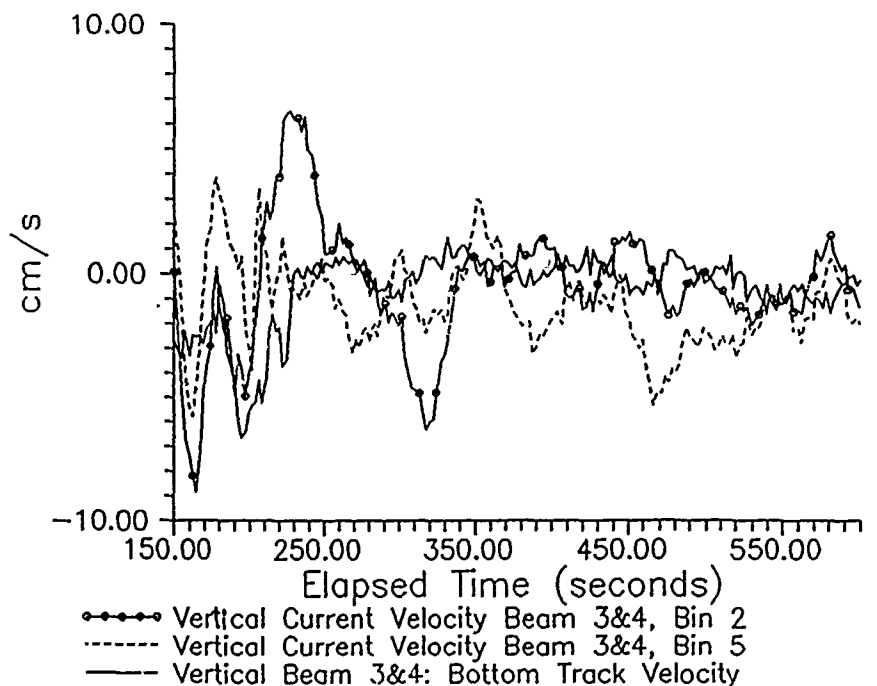


Figure 5.72. Subset of Figure 5.70 when the boat drifted through the plume. The lines depict the bottom track velocity and the vertical current velocity from bins 2 and 5 calculated from Beams 3 and 4 (pointing in the direction of the ship).

BACKSCATTERED AMPLITUDE: VERTICAL BEAM 2 (dB)

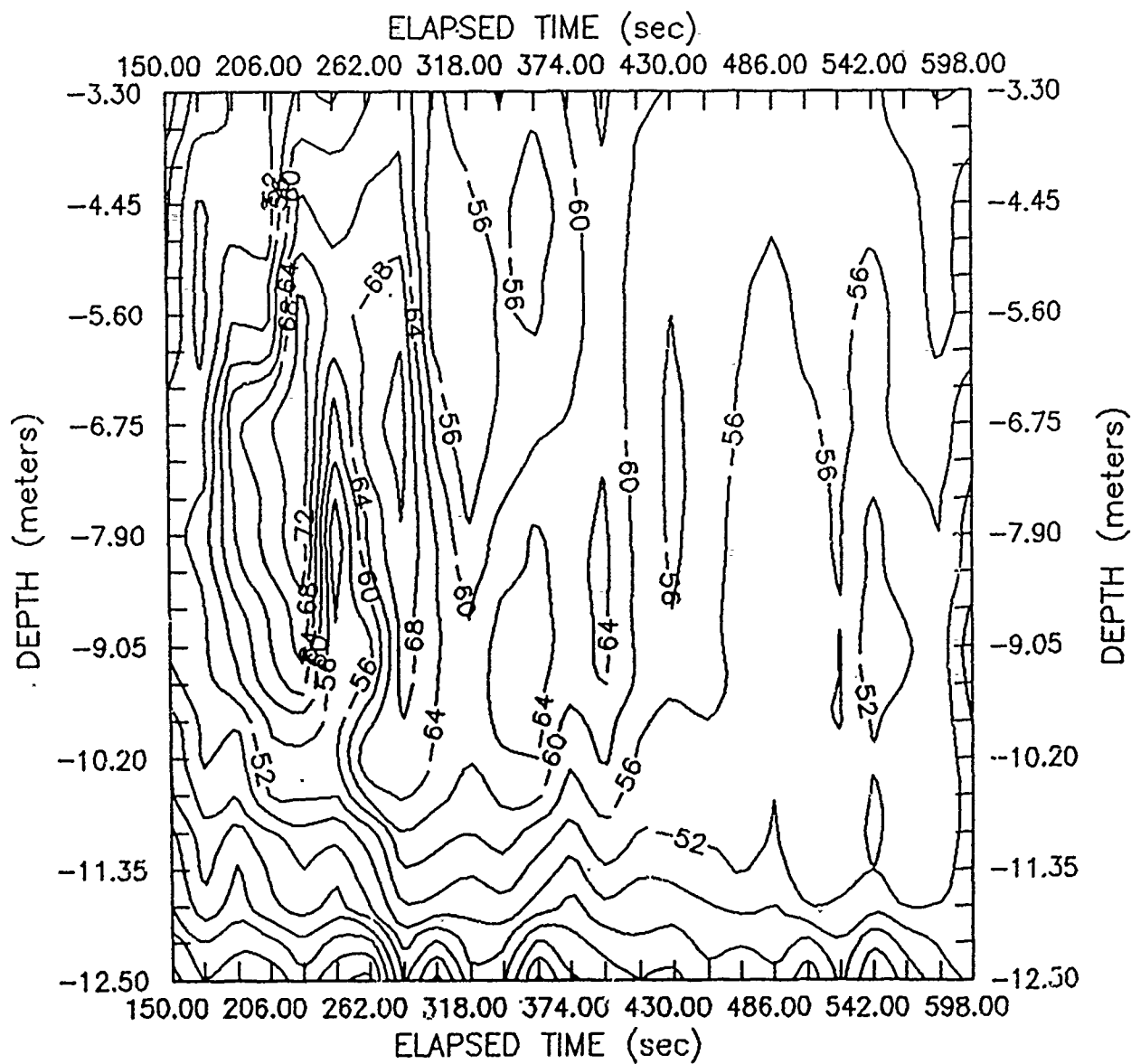


Figure 5.73. Variation in backscattering (from vertical Beam 2) as the *R/V Pelican* drifts through the plume. Temporal subset is same as in Figures 5.71 and 5.72.

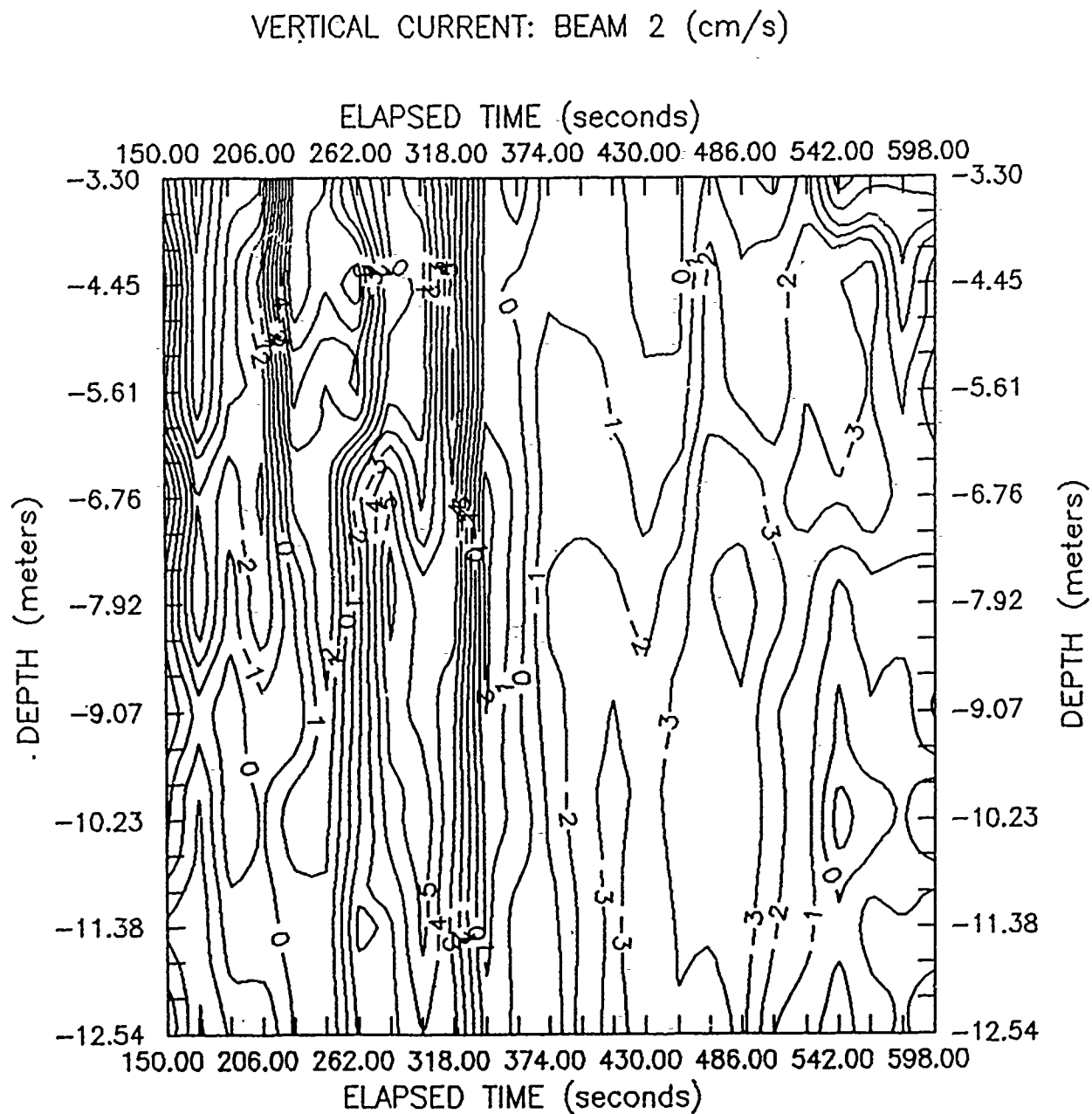


Figure 5.74. Variation vertical current velocity (from vertical Beam 2) as the R/V Pelican drifts through the plume. Temporal subset is the same as in Figures 5.71 and 5.72.

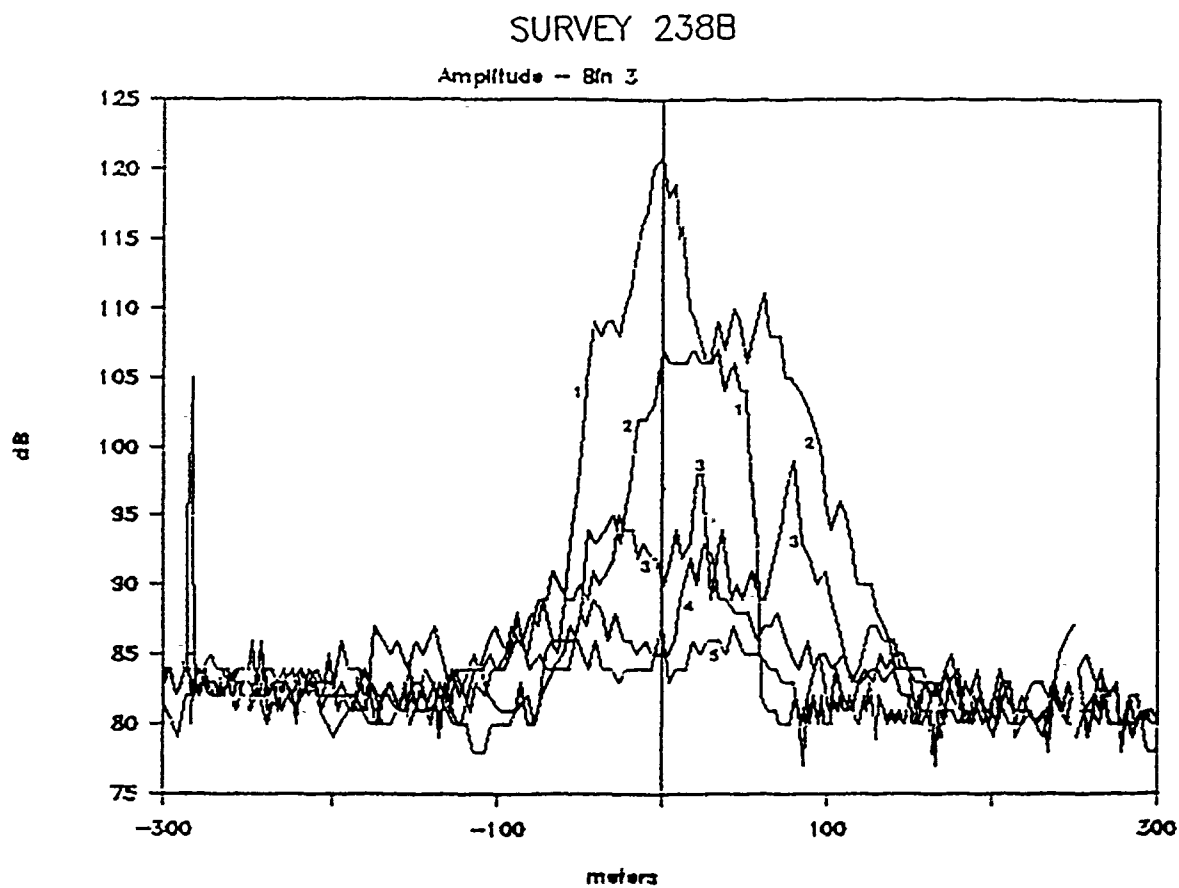


Figure 5.75. Survey 238B: amplitude data collected along five transects. The amplitude is in decibels (relative units) and is taken from bin 3 (5.3 m) along Beam 2 (vertical beam).

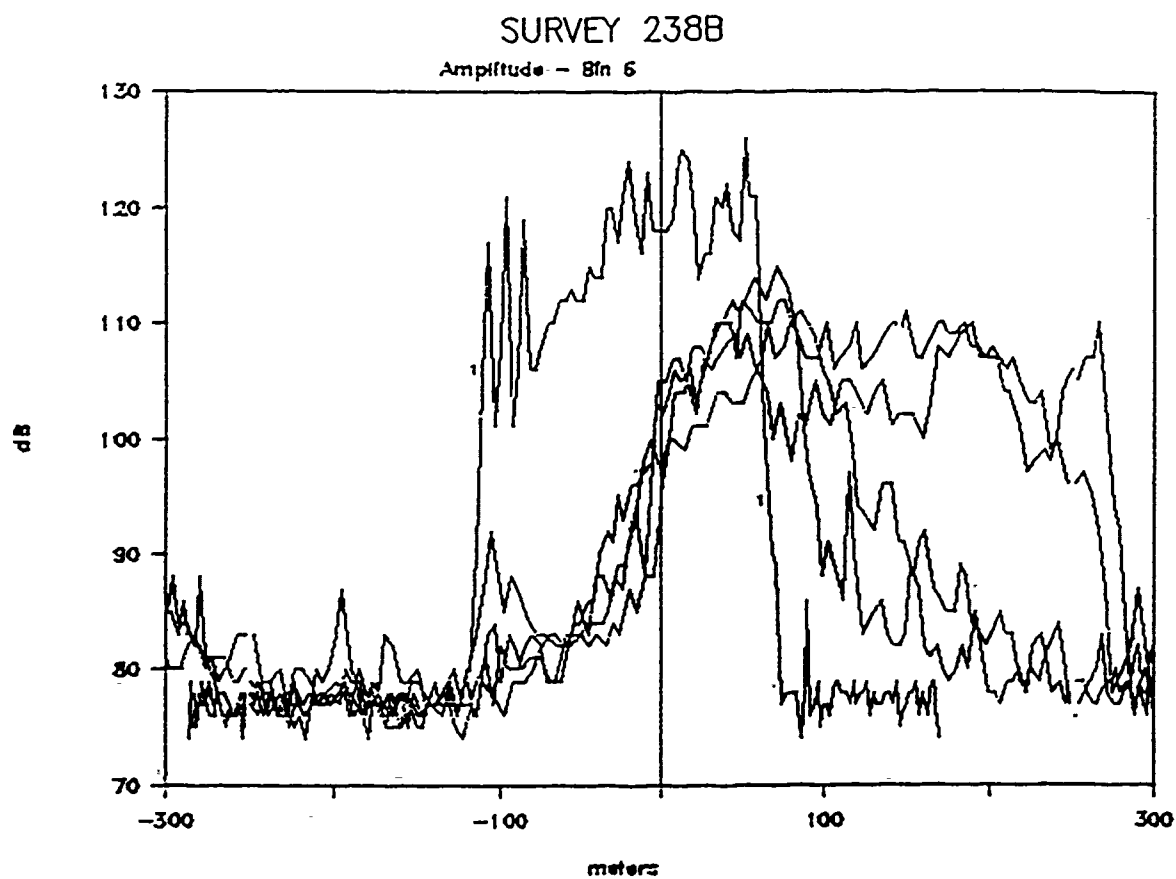


Figure 5.76. Survey 238B: amplitude data collected along five transects. The amplitude in decibels (relative units) is taken from bin 6 (8.3 m) along Beam 2 (vertical beam).

BACKSCATTER AMPLITUDE (dB) SURVEY 238B PASS 1

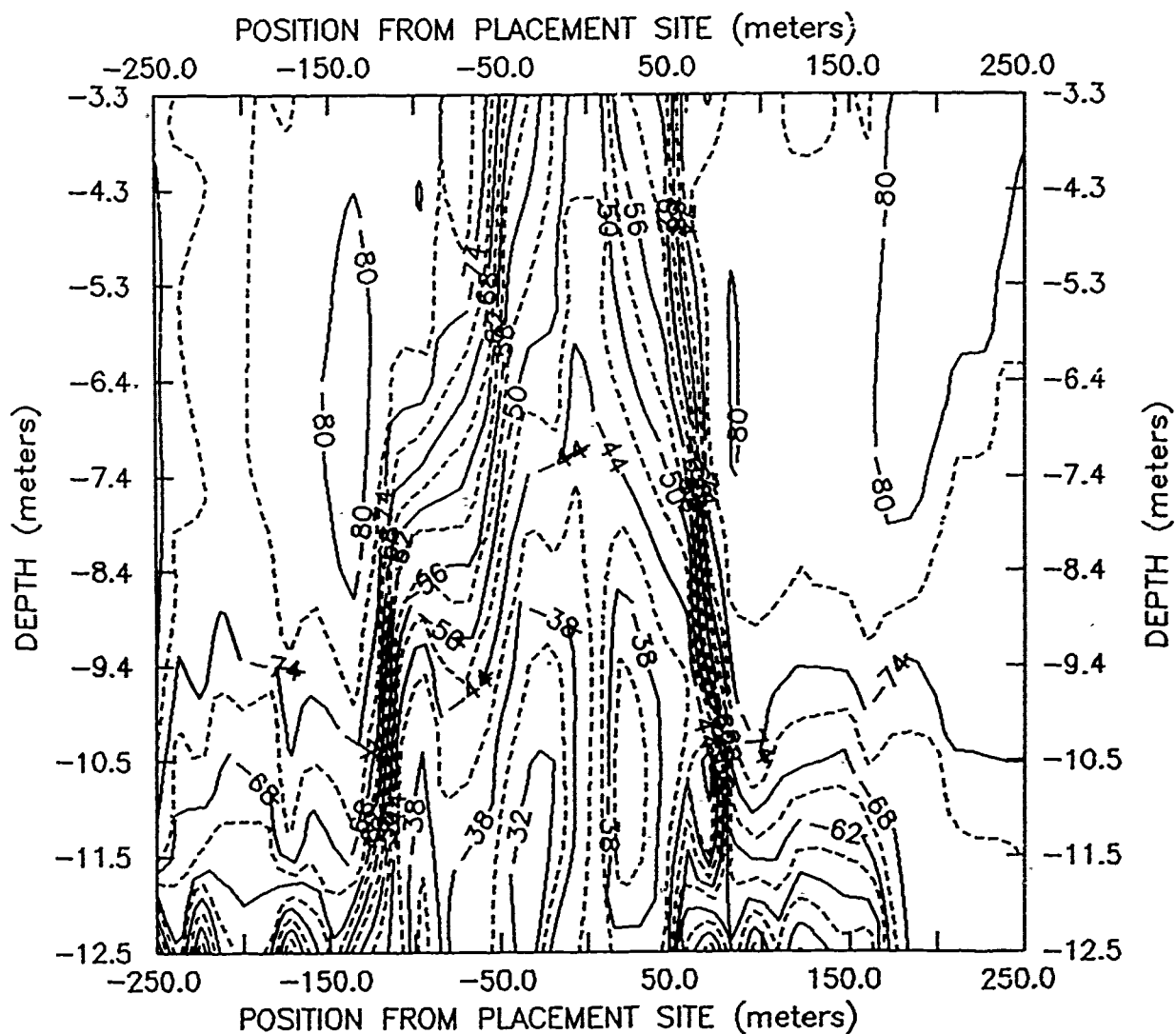


Figure 5.78. Survey 238B: contour plot showing the variation of the backscattering strength as a function of horizontal distance from the placement site during the first transect across the plume. The data have been projected onto a section that runs in the direction from 225 to 75 deg (positive) true north.

BACKSCATTER AMPLITUDE (dB) SURVEY 238B PASS 2

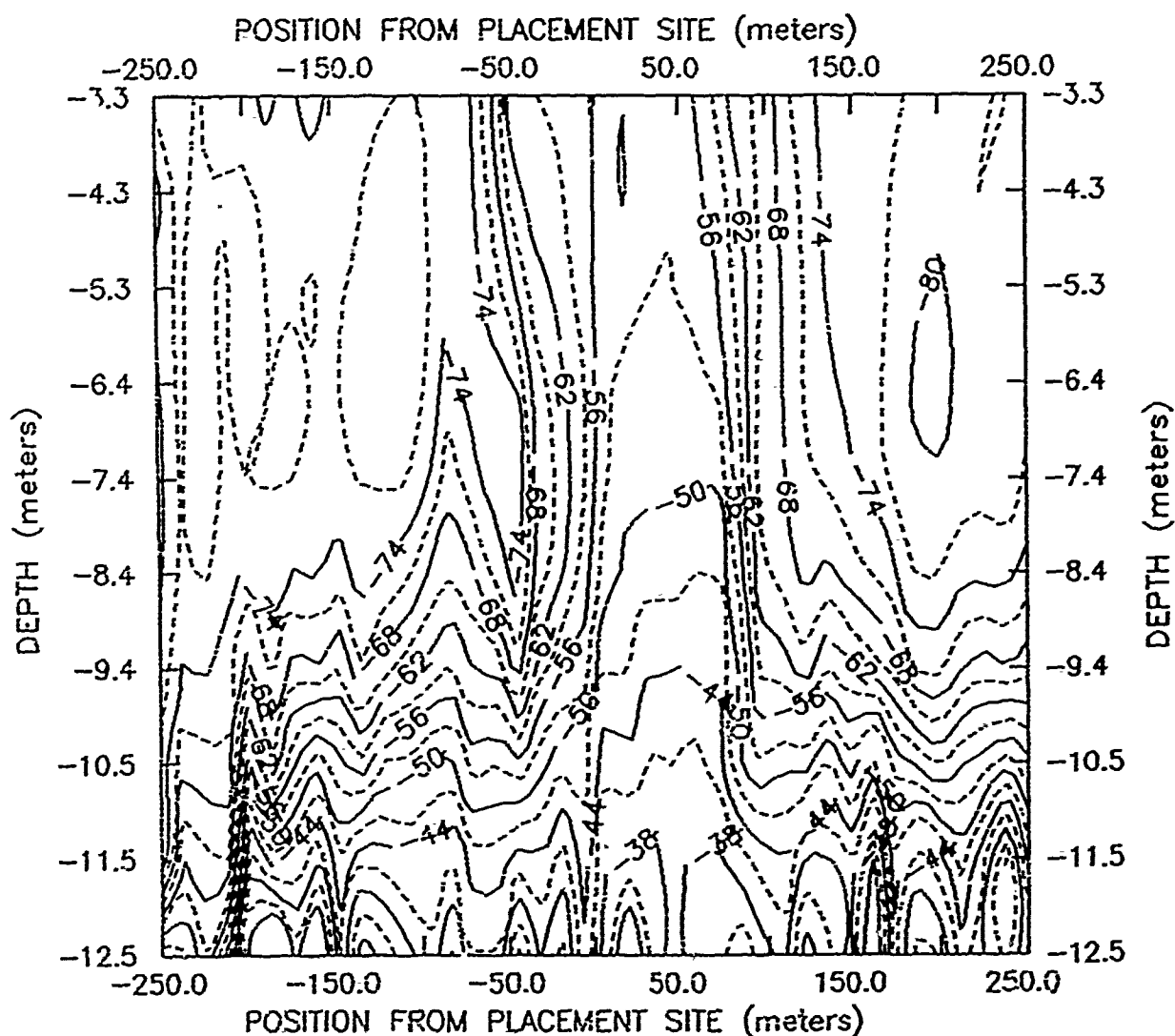


Figure 5.79. Survey 238B: contour plot showing the variation of the backscattering strength as a function of horizontal distance from the placement site during the second transect across the plume. Same projection as Figure 5.78.

BACKSCATTER AMPLITUDE (dB) SURVEY 238B PASS 3

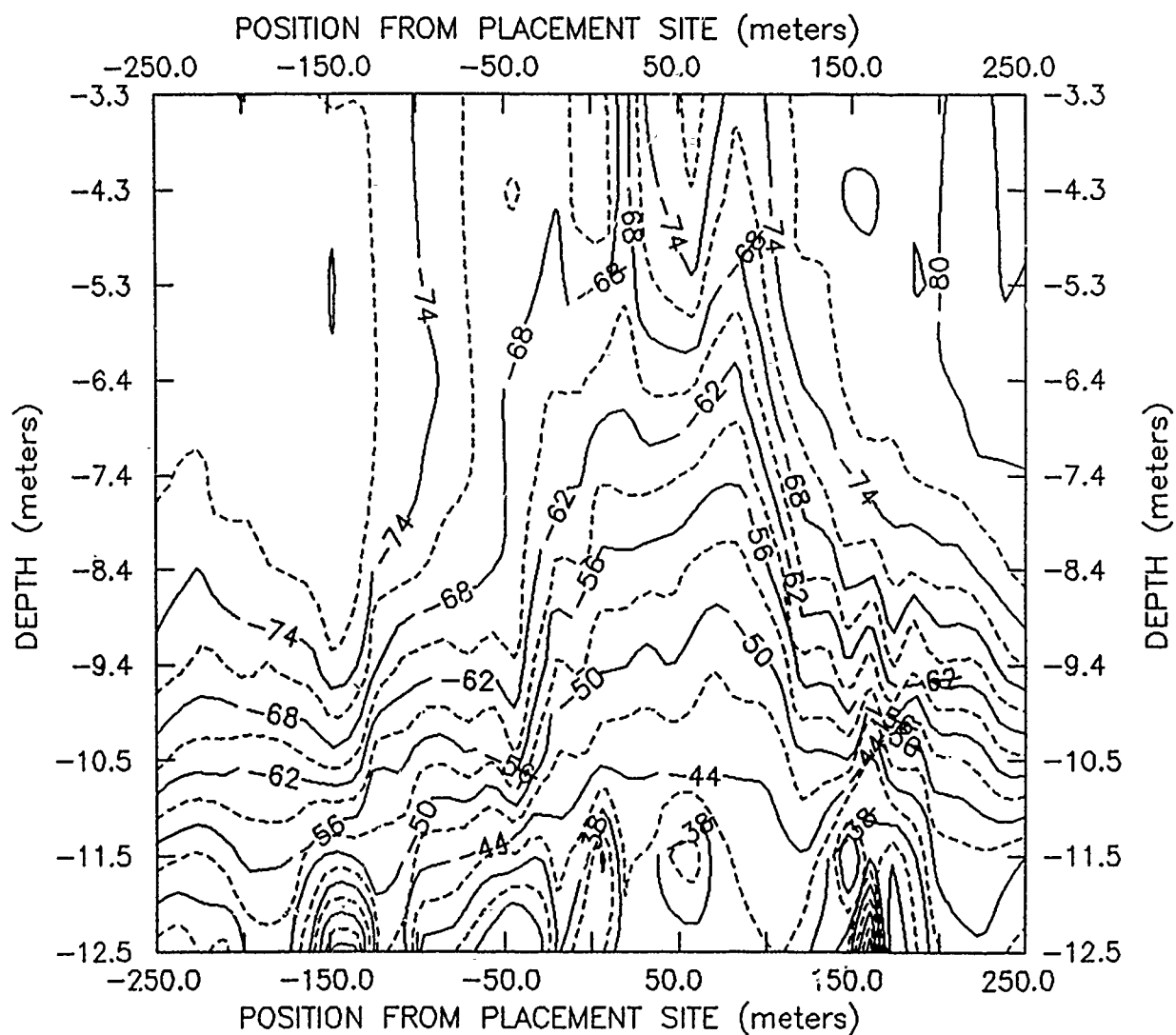


Figure 5.80. Survey 238B: contour plot showing the variation of the backscattering strength as a function of horizontal distance from the placement site during the third transect across the plume. Same projection as Figure 5.78.

BACKSCATTER AMPLITUDE (dB) SURVEY 238B PASS 4

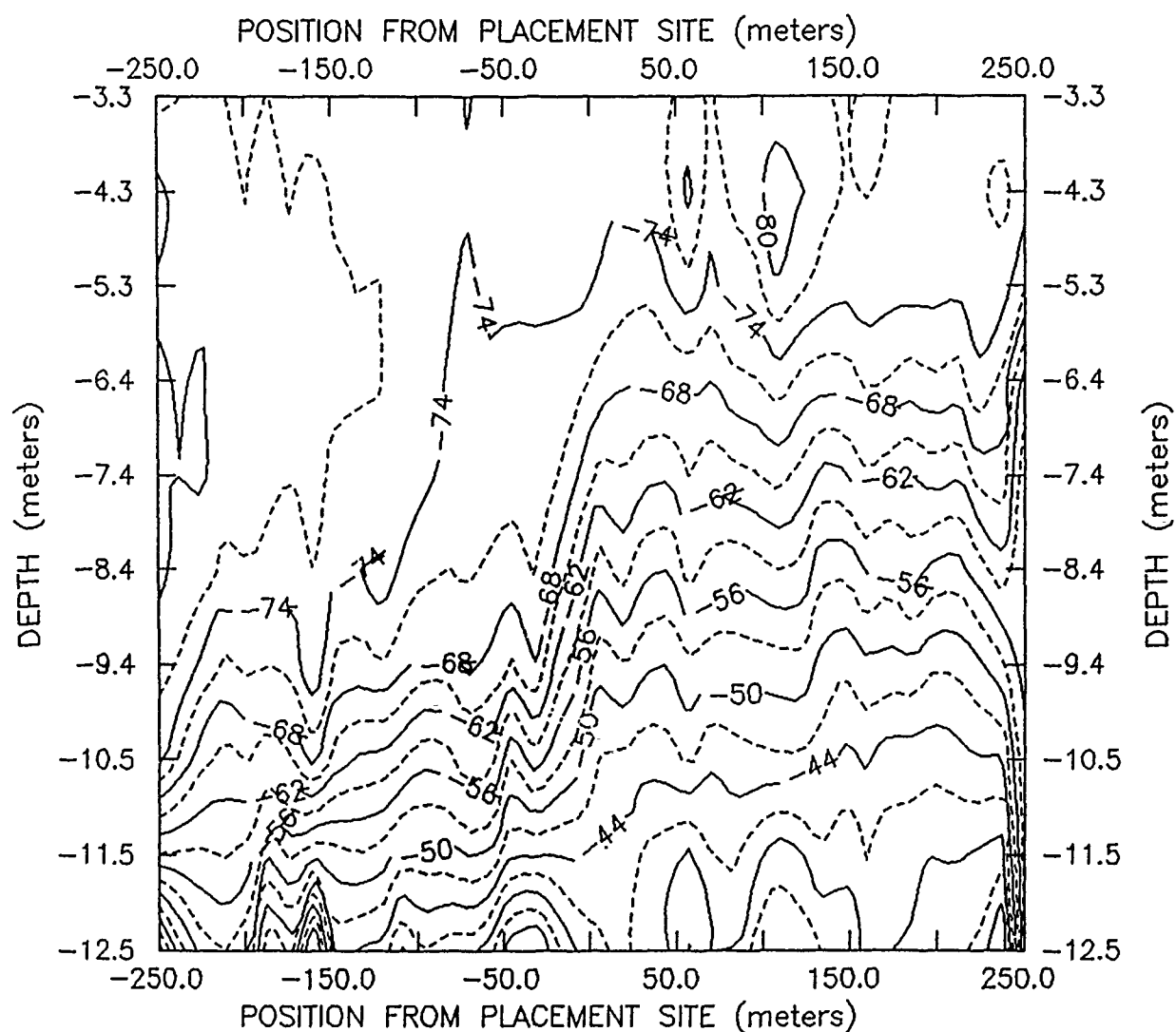


Figure 5.81. Survey 238B: contour plot showing the variation of the backscattering strength as a function of horizontal distance from the placement site during the fourth transect across the plume. Same projection as Figure 5.78.

VERTICAL VELOCITY (cm/sec). SURVEY 238B PASS 1

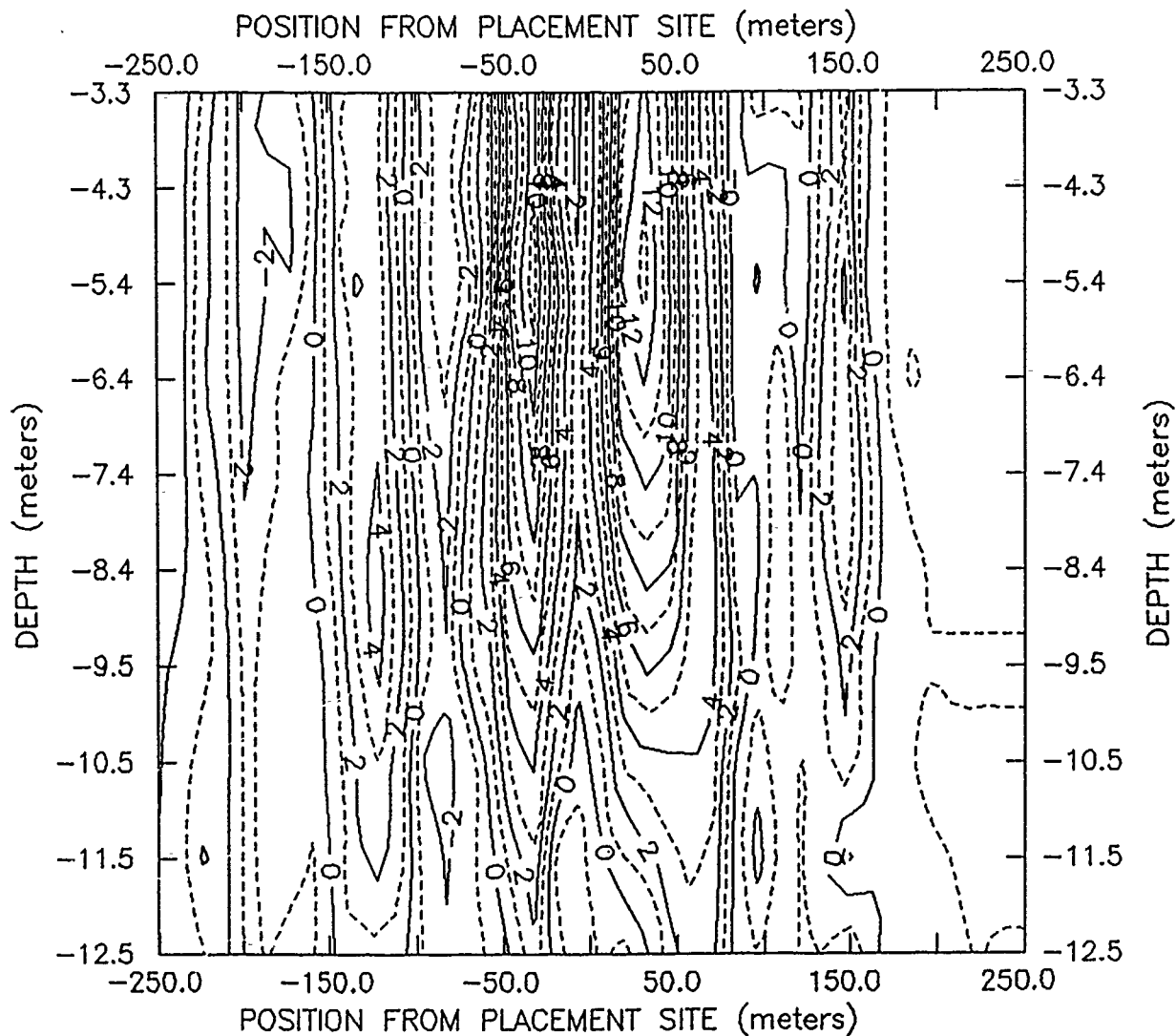


Figure 5.82. Survey 238B: contour plot showing the variation of the vertical velocity as a function of horizontal distance from the placement site during the first transect across the plume. Same projection as Figure 5.78.

VERTICAL VELOCITY (cm/sec) SURVEY 238B PASS 2

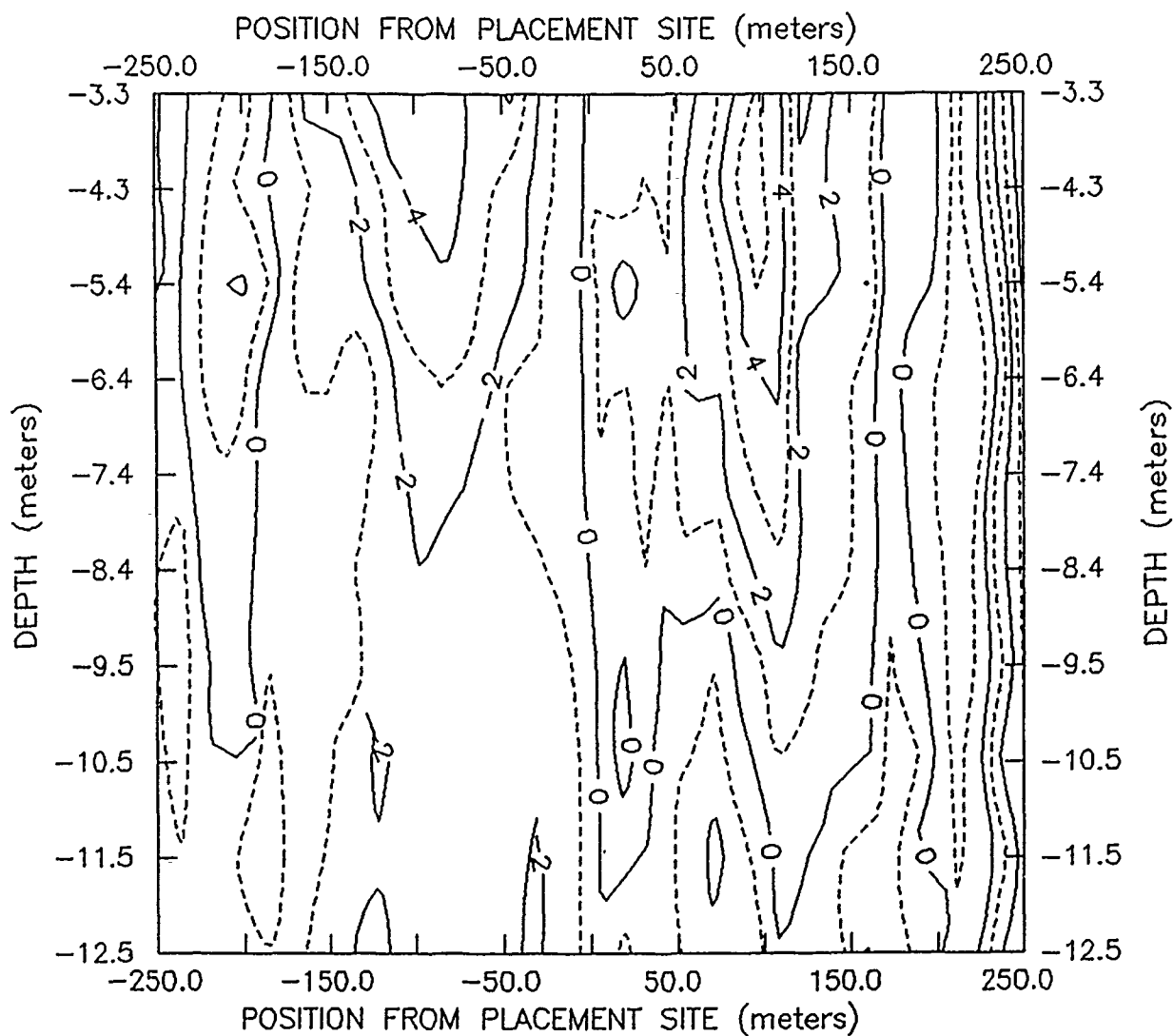


Figure 5.83. Survey 238B: contour plot showing the variation of the vertical velocity as a function of horizontal distance from the placement site during the second transect across the plume. Same projection as Figure 5.78.

VERTICAL VELOCITY (cm/sec) SURVEY 238B PASS 3

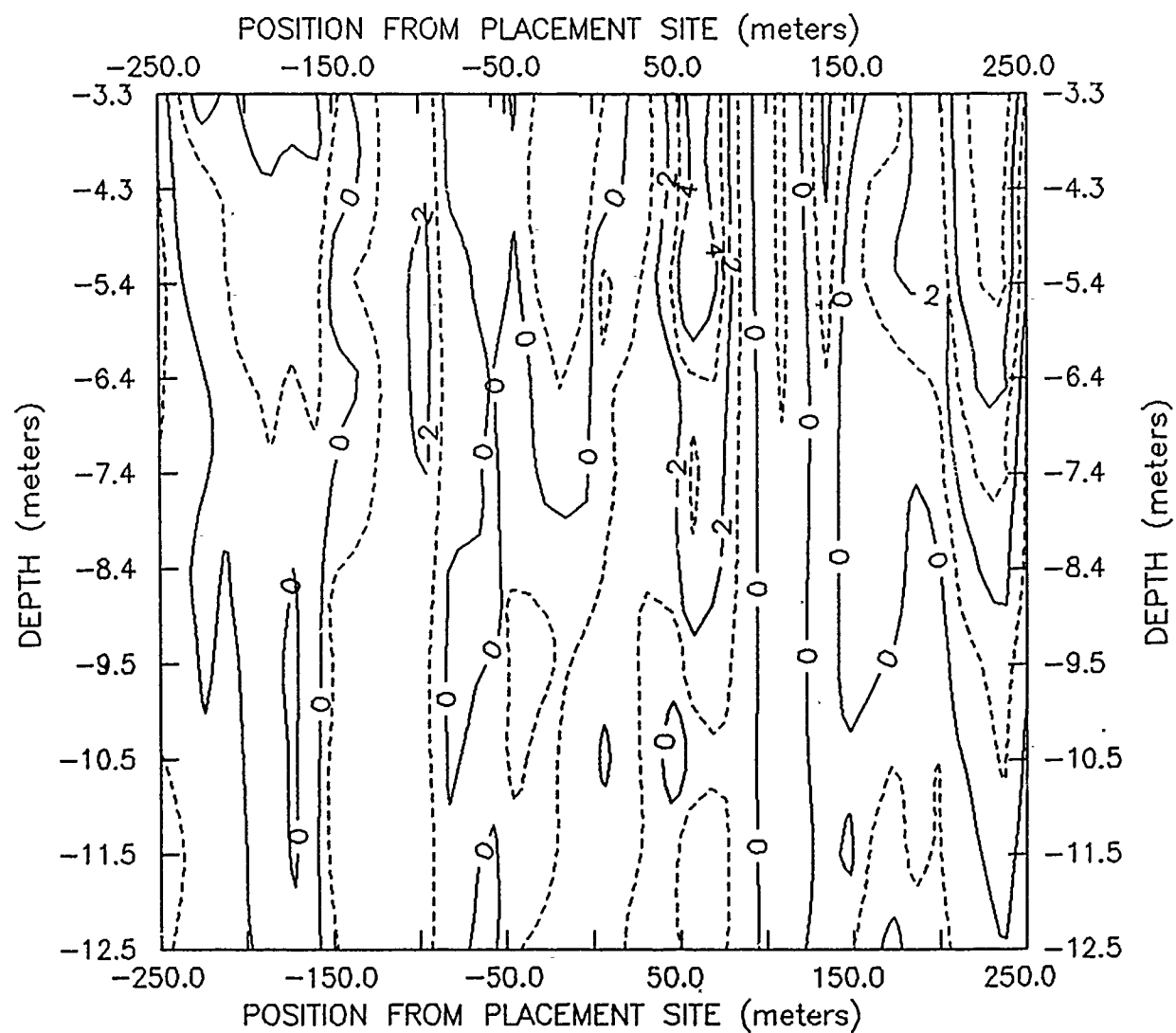


Figure 5.84. Survey 238B: contour plot showing variation of vertical velocity as a function of horizontal distance from placement site during third transect across the plume. Same projection as Figure 5.78.

Appendix 5A: Beam Amplitude Calibration

(RDI Technical Bulletin ADCP-89-04)

Introduction

This appendix describes how to perform a beam amplitude calibration on an RD Instruments (RDI) Acoustic Doppler Current Profiler (ADCP) to obtain absolute backscatter strength. Descriptions of the parameters involved in the calibration and derivation of the backscatter coefficient equation are also included. In this appendix the different ADCP models are labeled as follows: "VM" refers to the vessel-mounted ADCP; "SC" refers to the self-contained ADCP; and "DR" refers to the direct read ADCP.

An Overview of Measuring Backscatter Strength and Echo Amplitude

An uncalibrated RDI ADCP can measure relative backscatter strength at different ranges along each acoustic beam. The measurement is relative because it allows only comparison of backscatter strength from one discrete range cell to the backscatter strength from other range cells along the same acoustic beam. A beam amplitude calibration must be done on the ADCP to obtain absolute backscatter strength so that measurements can be compared with other beams or with other ADCPs. Once the ADCP is calibrated, one can compute absolute backscatter (± 3 dB) using ADCP calibration data and known (or assumed) values for speed of sound, geometric spreading, and absorption. An ADCP calibration has three tests:

1. Test 1 - The power each transducer beam puts into the water at a specific supply voltage level is measured. This measurement is used to calculate the acoustic energy in the water.
2. Test 2 - The noise factor of the ADCP is determined. The noise factor is a measure of how much worse an actual receiver is as compared with a perfect receiver.
3. Test 3 - The conversion factor from the ADCP's echo amplitude measurement (in counts) to power (in decibels) is determined. Since echo amplitude is not linear with temperature, the slope is determined at three temperatures. The three temperatures (over the range of 0 to 40 deg C) are chosen depending on the expected operating environment.

The temperature at the ADCP's electronics chassis contributes the most to the echo amplitude slope changes. The temperature of the transducer head and beams have very little effect. Therefore, the temperature of the electronics during deployment must be known. The temperature is easily found for DR and SC ADCPs because the transducer has a thermistor that measures the temperature of the water at the transducer head. If the ADCP is completely submerged, this temperature will be nearly the same as in the ADCP's electronics chassis. Since

the VM-ADCP electronics chassis is separated from the transducer, the temperature of the chassis must be measured. The rack-mounted ADCP chassis often has higher temperatures than the room; therefore, the chassis should have a temperature measurement device.

Backscatter Coefficient Equation

This section describes the Backscatter Coefficient Equation (S_v). The following tabulation lists a description of each term within the equation and explains how it is obtained. Derivation of the Backscatter Coefficient Equation is included in a later section of this appendix. The Backscatter Coefficient Equation is for a single beam:

$$S_v = 10 \log \left[\frac{4.47 * 10^{-20} K_2 K_s T (10^{K_1(Z_c - N_c)/10} - 1) R^2}{c L K_1 10^{-2\alpha R/10}} \right] \quad (5A.1)$$

Term	Description
S_v	Backscatter Coefficient (decibels)
K_2	System Noise Factor - This is the factory-measured noise factor of the ADCP. An Amplitude Calibration Sheet (furnished with the ADCP) lists this value for each beam of the ADCP as a ratio. This ratio is the reference noise floor for the ADCP system.
K_s	Fixed Value Based on System Frequency - This value is the ratio of the ADCP system's IF (or AGC) bandwidth, B, to the square of the transducer's diameter, d. Therefore, $K_s = B/d^2$ and is equal to:

K_s	ADCP Frequency, kHz
$1.09 * 10^5$	75
$4.17 * 10^5$	150
$7.69 * 10^5$	300
$1.56 * 10^6$	600
$5.65 * 10^6$	1200

T	Temperature (degree kelvins) - The temperature of the transducer.
-----	---

(Continued)

(Sheet 1 of 4)

(Continued)

<u>Term</u>	<u>Description</u>
<i>Kc</i>	Slope of Echo Amplitude Curve - This number is given on the Amplitude Calibration Sheet (supplied) for each beam at three separate temperatures. With a Beam Amplitude Calibration, the user is also provided the echo amplitude curves for each beam. <i>Kc</i> must be chosen for the temperature closest to the actual temperature of the ADCP electronics chassis. In most cases, the temperature measured by DR and SC-ADCPs at the transducer will be close to the temperature of the chassis. For VM-ADCPs, the temperature of the chassis will have to be measured.
<i>Ec</i>	Total Echo Amplitude Counts - Echo amplitude data are output for each beam at each depth cell (bin) location. The depth cell and beam of interest will need to be chosen for analysis.
<i>Nc</i>	Noise (Echo Amplitude Counts with no signal present) - This value is the number of Echo Amplitude Counts of the noise floor. Do this test to determine noise floor counts.
<p>NOTE: This test should be done at the site where backscatter measurements will be taken. If this is not possible, the user can still do this test by taking the following precautions:</p> <ol style="list-style-type: none">(1) The electronics chassis must be at the same temperature it will be at the measurement site. This is due to the variability of measured echo amplitude with temperature.(2) DR or VM users operating on a vessel must stop the boat while the test is being done. The boat motion causes flow noise. Flow noise will cause a bias in the measurement of the noise floor and make the calculation of true backscatter strengths impossible.(3) The user should make sure there is no other equipment running that may generate a signal that the ADCP could receive. This interference will cause a bias in the measurement of the noise floor.	
<i>c</i>	Speed of Sound - This factor is the speed of sound at the scattering layer being measured. The user must calculate this number. It should take into account changes in salinity, temperature, and depth.
<i>L</i>	Transmit Pulse Length in meters
<i>K1</i>	Power into the Water - This value scales the acoustic power into the water at a given supply voltage. RDI provides <i>K1a</i> for each beam on an Amplitude Calibration Sheet. The user must scale <i>K1a</i> for the supply voltage during the deployment. As supply voltage levels change, so will the power into the water. <i>K1a</i> is measured at 40 VDC for all systems. Choose the appropriate formula from the three that follow to correct the <i>K1a</i> value.

(Continued)

(Sheet 2 of 4)

(Continued)

Term	Description
<u>SC users:</u>	

$$K1 = \left[\frac{V2 - 5.76}{34.24} \right]^2 * K1a \quad (5A.2)$$

where:

$$V2 = (\text{Counts from high volts in leader data}) * (0.17)$$

NOTE: Remember that $K1$ needs to be scaled periodically, because the supply voltage is from batteries and battery voltage decreases as deployment time progresses.

DR users:

$$K1 = \left[\frac{(ACrms * 1.397) - 6.3}{35.1} \right]^2 * K1a \quad (5A.3)$$

where

$ACrms$ = Measured RMS AC voltage at the ADCP. Using an ACrms Voltmeter, measure the voltage at pins 19 and 20 of the ADCP connector when not plugged into the pressure case. This is done so any voltage loss through the cable can be ignored. For systems operating at 220 AC volts, divide the $ACrms$ by two before entering it in the formula.

VM users:

$$K1 = \left[\frac{(ACrms * 1.397) - 4.27}{37.14} \right]^2 * K1a \quad (5A.4)$$

where

$ACrms$ = Measured RMS AC voltage at the ADCP. Using an ACrms Voltmeter, measure the voltage at the AC receptacle that the ADCP will be plugged into. For systems operating at 220 AC volts, divide the $ACrms$ by two before entering it in the formula.

(Continued)

(Sheet 3 of 4)

(Concluded)

Term	Description
α	Absorption Coefficient (in water) in decibels/meter - The user must provide this measurement. This value accounts for the loss in echo strength through attenuation in the water.
R	Slant Range - This value is the range to the scattering layer along the beam in meters. Use the following formula to calculate the value of R .

$$R = \left[\frac{BK + \left| \frac{PL - BL}{2} \right| + (N * BL) + \frac{PL}{4}}{\cos \theta} \right] * \frac{c}{1475.1} \quad (5A.5)$$

where

BK = blank beyond transmit, m

PL = transmit pulse length, m

BL = depth cell length, m

N = depth cell number of the scattering layer being measured

θ = angle of transducer beams to vertical, usually 30 deg

c = weighted average of the speed of sound between the transducer and depth cell of interest. The ADCP has a default speed of sound of 1,475.1 m/sec. This term corrects for speeds of sound other than 1,475.1 m/sec.

(Sheet 4 of 4)

Derivation of the Backscatter Coefficient Equation

The Sonar Equation - The following equation presents Signal-to-Noise (S/N) ratio as a function of backscatter, range, and other ADCP parameters.

$$\frac{S}{N} = \frac{PE}{4\pi} \frac{G}{R^2} 10^{-\alpha R/10} \frac{\pi[R\phi]^2}{4} \frac{ct}{2} \frac{10^{S_v/10}}{R^2} 10^{-\alpha R/10} \frac{Gk^2}{4\pi} E \frac{1}{KTBF} \quad (5A.6)$$

Term:	1	2	3	4	5	6	7	8	9	10
-------	---	---	---	---	---	---	---	---	---	----

where

S/N = signal-to-noise ratio

P = electrical power to transducer, W

E = transducer efficiency

G = transducer gain or directivity

R = range to scatterers along the beam, m

α = water absorption, dB/m

ϕ = effective two-way beam width, rad

c = speed of sound, m/sec

t = transmit pulse length, sec

S_v = backscatter coefficient (dB)

k = wavelength of transmitter, m

K = Boltzmann's constant, J/deg K

T = temperature, deg K

B = noise bandwidth, Hz

F = receiver noise factor

The following tabulation describes each term in Equation 5A.6:

Term	Description
1	Power density of a spherically spreading pulse on the surface of 1-m sphere
2	Corrects for directivity of the transducer and adjusts for range (one-way)
3	Corrects for absorption of the out-going pulse
4	Instantaneous ensonified area of water
5	Instantaneous ensonified depth of water
4 * 5	Gives instantaneous ensonified volume of water
6	Corrects for backscatter strength and adjusts for range (one-way)
7	Corrects backscattered signal for absorption
8	Capture area of the transducer
9	Corrects for transducer efficiency
1 to 9	Give signal power (S)
10	Noise power (N)

For a circular piston $G = (\pi d/k)^2$ and $\phi^2 = (4k/\sqrt{2}\pi d)^2$, where d is the transducer diameter. Substituting for G and ϕ^2 and combining terms:

$$\frac{S}{N} = \frac{PE \pi c t}{4\pi R^2} 10^{S_v/10} 10^{-2\alpha R/10} \frac{\pi d^2 E}{4} \frac{1}{KTBF} \quad (5A.7)$$

and

$$S_v = 10 \log \left[\frac{5.09 S/N R^2 KTBF}{PE c t 10^{-2\alpha R/10} d^2 E} \right] \quad (5A.8)$$

Defining the term PE as $K1$ - power into the water, the term F/E as $K2$ - system noise factor, and the term $Ks = B/\omega^2$ - system dependent parameters, we obtain

$$S_v = 10 \log \left[\frac{5.09 S/N R^2 KT Ks K2}{K1 c t 10^{-2\alpha R/10}} \right] \quad (5A.9)$$

Substituting $K = 1.38 \cdot 10^{23}$ J/deg K, and $t = 0.00157L$, where L is the transmit length in meters

$$S_v = 10 \log \left[\frac{4.47 * 10^{-20} S/N R^2 T K_s K_2}{K_1 cL 10^{-2\alpha R/10}} \right] \quad (5A.10)$$

The term S/N can be determined from the ADCP AGC output.

Now define E_c as counts representing $S+N$ power, N_c as counts representing N power (no signal present), and K_c as the conversion factor decibels/count, as follows

$$E_c = 10 \log(S+N)/K_c \quad (\text{in counts}) \quad (5A.11)$$

$$S+N = 10^{K_c E_c / 10} \quad (5A.12)$$

$$S = 10^{K_c E_c / 10} - N \quad (5A.13)$$

$$N = 10^{K_c N_c / 10} \quad (5A.14)$$

$$S/N = 10^{K_c (E_c - N_c) / 10} - 1 \quad (5A.15)$$

Finally, substituting Equation 5A.15 into Equation 5A.10:

$$S_v = 10 \log \left[\frac{4.47 * 10^{-20} (10^{K_c (E_c - N_c) / 10} - 1) R^2 T K_s K_2}{K_1 cL 10^{-2\alpha R/10}} \right] \quad (5A.16)$$

6. SEDIMENT PLUME MEASUREMENTS WITH AN ACOUSTIC CONCENTRATION PROFILER

W. PAUL DAMMANN, JOHN R. PRONI

*Atlantic Oceanographic and Meteorological Laboratories,
National Oceanic and Atmospheric Administration
Miami, Florida 33149*

Contents

1. Introduction
2. Background
3. Equipment and Procedures
4. Analysis and Results
5. Conclusions
6. Discussion and Recommendations

References

Tables

Figures

Appendix

1. Introduction

In August 1989, the U.S. Army Corps of Engineers conducted a series of dredged material discharge studies off Mobile Bay, Alabama, called the Mobile Field Data Collection Project (MFDCP). The objectives of the MFDCP included (a) measurement of discharge sediment plume concentration distributions, (b) measurement and analysis of physical processes affecting distribution and transport of discharged material, and (c) evaluation of acoustical methods for the study of concentration distributions and material transport. One important instrument used in the studies was the Acoustic Concentration Profiler (ACP). The ACP was operated by personnel from the National Oceanic and Atmospheric Administration (NOAA), Atlantic Oceanographic and Meteorological Laboratories (AOML), Ocean Acoustics Division, located in Miami, Florida. Of the eighteen discharge events monitored during the MFDCP (Chapter 1, this report), eight have been selected for analysis. These are denoted as plume Surveys 237A, 238A, 238B, 239A, 239B, 241A, 242A, and 243A. In addition, a shallow-water berm survey performed on Julian day 238 is analyzed.

The MFDCP produced a rich data set on discharge plume characteristics, concentrations, transport, and movement and on acoustical methodologies for the study of such features and processes. In addition to the principal objectives listed in the preceding paragraph, several subobjectives may be noted. These include (a) identifying and measuring, where possible, any discharge parameters or processes for which formerly only poor estimates, or only laboratory estimates, are available for use in numerical plume models, (b) examination of at least some of the processes whereby dredged material might potentially be transported out of the placement site; (c) development of initial thoughts for the evolution of an acoustical device for real-discharge-time or post discharge-time monitoring of dredged material placement and retention, and (d) identification of any processes that are not yet included in existing numerical plume dynamics numerical simulation models.

2. Background

The AOML has carried out acoustical studies on dredged material discharges in various locations including Lake Ontario, the New York Bight, and the Miami deepwater dump site (for example, Proni et al. 1989). These studies together with the MFDCP have revealed or confirmed many plume characteristics and processes. A key point to recognize about acoustical methodologies is that a great deal may be learned about dredged material discharges even if the relationship between the plume material scattered acoustical intensity and plume concentration is only specified in a statistical sense. It is sufficient in many circumstances to assume only that the scattered sound intensity is proportional to the concentration or the mean concentration plus a small random concentration component. In acoustical Doppler systems, for instance, the main assumption is that enough scattering is present to produce a plume-related echo. However, a calibration research effort and development program for acoustical devices for making concentration measurement is greatly needed.

3. Equipment and Procedures

The ACP used during the MFDCP consisted of a Datasonics model DFT-210 dual-channel acoustic transceiver with internal preamplifier (pre-amp) enhancements, operating at 20 and 200 kHz. The transducers were mounted in a streamline towbody aimed vertically downward and towed at a constant depth of 1 m below the surface of the water approximately 15 ft outboard of the vessel's starboard beam at a location a few feet forward of amidships. Two Raytheon digital chart recorders were used to record echographs from the DFT-210. The receiver output was recorded simultaneously with an IRIG-B time code and synchronizing pulses on standard VHS video cassette tapes using two JVC video tape recorders and a Sony audio signal processor, and separately onto two Sharp digital audio tape (DAT) recorders. The time code was generated by a Systron Donner time code generator and frequency multiplexed with a 1-msec 15-kHz key pulse. The system configuration is diagrammed in Figure 6.1, and the towbody configuration is shown in Figure 6.2.

Upon arrival at the placement site each operating day, the ACP towbody was deployed and remained in the water as described for the entire working day. Each morning, the time code generator was synchronized to universal time by radio monitoring of station WWV at 5, 10, 15, or

20 MHz. New tapes were loaded into all of the tape recorders approximately 30 min prior to each survey. Data recording began when the tug was within 5 min of arriving at the placement site. The transceiver transmitted pulses of 0.1-msec duration at both frequencies simultaneously every 0.250 sec throughout each survey. The equipment remained active until all transects were completed and water samples obtained. Receiver pre-amp gains were adjusted between transects to increase the overall dynamic range of the recorded data set. Table 6.1 shows the start time and elapsed times of the ACP tape records during the MFDCP.

The data recorded on the DATs were processed as follows. The time code channel was monitored by a time code reader to find areas of specific interest on the tapes. The 10-kHz double side band signal was played back into a band pass filter that removed 60-cycle noise and provided anti-aliasing protection for the following stage, which consisted of an analog demodulator. The demodulator output was further filtered and amplified for input to a 12-bit analog to digital (A/D) converter interfaced to an IBM-AT compatible computer. Synchronizing pulses multiplexed with the time code were used to initiate A/D sampling bursts. Each burst consisted of 128 samples taken at equal time/depth intervals within a pulse, and the range to the last sample was used to determine the necessary sample rate such that,

$$sample\ rate = 127 \frac{c}{(2 \cdot range)} \quad (6.1)$$

where c is the speed of sound in seawater (1,500 m/sec), and the range was 13 m. Entering these values into Equation 6.1 yields a sampling rate of 7,327 samples per second used for digitizing all data included herein.

The digitized data consist of a series of records each containing 128 16-bit integer words. Each consecutive 2-byte integer represents a root-mean-square (rms) voltage V_{rms} at the output of the receiver accurate to 12 bits. The integer values range from 0 to 4,095 and are linearly proportional to V_{rms} such that:

$$V_{rms} = \frac{Integer}{4,095} \quad (6.2)$$

20 MHz. New tapes were loaded into all of the tape recorders approximately 30 min prior to each survey. Data recording began when the tug was within 5 min of arriving at the placement site. The transceiver transmitted pulses of 0.1-msec duration at both frequencies simultaneously every 0.250 sec throughout each survey. The equipment remained active until all transects were completed and water samples obtained. Receiver pre-amp gains were adjusted between transects to increase the overall dynamic range of the recorded data set. Table 6.1 shows the start time and elapsed times of the ACP tape records during the MFDGP.

The data recorded on the DATs were processed as follows. The time code channel was monitored by a time code reader to find areas of specific interest on the tapes. The 10-kHz double side band signal was played back into a band pass filter that removed 60-cycle noise and provided anti-aliasing protection for the following stage, which consisted of an analog demodulator. The demodulator output was further filtered and amplified for input to a 12-bit analog to digital (A/D) converter interfaced to an IBM-AT compatible computer. Synchronizing pulses multiplexed with the time code were used to initiate A/D sampling bursts. Each burst consisted of 128 samples taken at equal time/depth intervals within a pulse, and the range to the last sample was used to determine the necessary sample rate such that,

$$\text{sample rate} = 127 \frac{c}{(2 \cdot \text{range})} \quad (6.1)$$

where c is the speed of sound in seawater (1,500 m/sec), and the range was 13 m. Entering these values into Equation 6.1 yields a sampling rate of 7,327 samples per second used for digitizing all data included herein.

The digitized data consist of a series of records each containing 128 16-bit integer words. Each consecutive 2-byte integer represents a root-mean-square (rms) voltage V_{rms} at the output of the receiver accurate to 12 bits. The integer values range from 0 to 4,095 and are linearly proportional to V_{rms} such that:

$$V_{rms} = \frac{\text{Integer}}{4,095} \quad (6.2)$$

For a cloud of particulate scatterers such as a sediment plume, the reverberation level is given by,

$$RL = SL - 20\log_{10}(r) - 2\alpha r + S_v + 10\log_{10}\left(\frac{c\tau\psi}{2}\right) \quad (6.8)$$

where SL is the source level (dB reference to $1\mu\text{Pa/V}$), r is range in meters, α is the absorption coefficient in decibels per meter, S_v is the volume scattering strength in decibels, τ is the transmitted pulse duration in seconds, and ψ is the equivalent solid angle of a uniform beam containing the same integrated power as the actual transmitted beam and is given in steradians. For further information on decibel units, refer to Urick (1975). Also, for more information on scattering strength, refer to Clay and Medwin (1977).

Combining Equations 6.5 and 6.8 gives the relation used to calculate volume scattering strength:

$$S_v = 20\log_{10}(V_{rms}) - RR - G - SL + 20\log_{10}(r) + 2\alpha r - 10\log_{10}\left(\frac{C\tau\psi}{2}\right) \quad (6.9)$$

For conical beam transducers such as those used in the ACP,

$$10\log_{10}\left(\frac{c\tau\psi}{2}\right) = 10\log_{10}\left(\frac{c\tau\theta}{2}\right) - 31.6 \quad (6.9a)$$

where θ is the angle between the reference axis of the transducer, and the first point on the beam diagram at a level of -3 dB referenced to the axis level (Urick 1975). A more complete derivation of the theoretical background for these procedures is presented in Appendix 6A.

4. Analysis and Results

The first 3 min of each of the eight placement surveys selected for detailed analysis were processed to provide contour plots of volume reflection coefficient as a function of depth and distance. In addition to each contour plot, a series of graphs was plotted at 1-m intervals to give reflection coefficients as a function of horizontal distance across the plume. These plots corresponding to the eight selected surveys are available from the authors of this chapter and from the DRP Technical Area 1 Manager, Dr. Nicholas C. Kraus, WES. An additional five 3-min transects were plotted for Survey 239B in order to provide a total of five transects across the plume. A short narrative of each survey follows.

Survey 237A

This plume was monitored using a longitudinal track (along the major axis of the plume). The placement occurred at the deep in approximately 14 m of water. At depths between zero and 6 m, background scattering was slight and patchy, and it was one to two orders of magnitude less than at depths greater than 6 m. The plume was first detected by both systems at about 14:18:30 GMT. The plume dominated the upper water column over the first 40 m traversed into the plume, and the plume material filled the entire water column beyond that distance. The 20-kHz system appears to have been overcome by attenuation inside the plume during the initial stages, and the 200-kHz system was also affected, but not as severely. During the first 2 min inside the plume, the 200-kHz system showed little variation in scattering throughout the water column, and, as scattering diminished, the plume became more patchy.

Survey 238A

This is the first of the transverse monitoring operations chosen for analysis. The placement occurred in about 14 m of water at the deep site. Background scattering was slight and patchy above 10 m and clear below. Both the 20- and 200-kHz systems detected a large bottom surge while approaching the plume, the leading edge appeared to be 2 to 3 m high, and the horizontal extent was at least 20 m at 14:24:10 GMT (more about this feature is discussed under Survey 239B). Attenuation was again extremely severe at 20-kHz and significant at 200-kHz.

Survey 238B

This was another transverse operation at the deep site at approximately 14-m depth. Background scattering was slight and patchy above 5 m. A bottom surge is clearly seen upon entry and exit of the plume on both the 20- and 200-kHz records. The plume boundaries are visible, although 20-kHz attenuation is severe inside the plume and 200-kHz attenuation is notable.

Survey 239A

This survey was a transverse-monitored placement at the deep site in approximately 13 m of water. The background scattering was moderate above 6 m. Bottom surge and plume boundaries were recorded on both systems. Attenuation is again severe at 20-kHz and significant at 200-kHz in the midsection of the plume.

Survey 239B

This operation used transverse monitoring, and seven transects were performed at the deep site in about 14 m of water. The background scattering was slight and patchy above 5 m. Survey 239B contains several features of dredged material discharges that were not observed

before the MFDCP. This data set has been selected for a more extensive discussion because of these features.

Examination of Survey 239B reveals novel features that have been clearly identified for the first time during the MFDCP. This survey also illustrates the increase in data interpretation capability when more than one acoustical frequency is used to obtain data simultaneously on dredged material discharges. Figures 6.3 through 6.7 are color contour plots of the 200 kHz reflection coefficient for consecutive ship passes over the discharge plume. The data in these figures indicate the existence of the following features:

1. A bottom surge is created with a tall leading edge, and the surge is detected both upon entering and exiting the plume.
2. The effect of the bottom manifests itself upon the movement of the plume and becomes evident at about the 8-m depth horizon. This depth horizon is located approximately 5 m above the bottom, and the nominal bottom depth is 13 m. The effect of the bottom upon the dynamical plume behavior is manifested as a large change in the slope of the outer plume boundary.
3. A gross apparent inhomogeneity is observed in the plume structure in the initial two passes; the authors hypothesize that this inhomogeneity is the result of a region of bubbles intertwined with the discharged dredged particulate material.
4. Over time, the plume seems to separate into two distinct lobes settling at different rates.
5. A strong current shear effect acts to horizontally separate the upper and lower water column portions of the plume over the duration of the survey.

To evaluate the validity of the bubble hypothesis advanced in 3 above, a comparison of the 200- and 20-kHz data was made for consecutive ship passes over the discharge plume. Figure 6.8 shows the reflection coefficients at 6-m depth for the 20-kHz (top) and 200-kHz (bottom) signals for transect number 1 (22:13 to 22:16 GMT). The gap seen on the 20-kHz record, extending from approximately 105 to 118 m, appears as a sharp dip in the 200-kHz record at about 115 m. Figure 6.9 shows reflection coefficients for both frequencies at 6 m for the second pass through the plume (22:17:30 - 22:20:30 GMT); the gap seen in the 20-kHz record extending from about 150 to 160 m is not evident on the 200-kHz record. Figure 6.10 shows similar data for the third pass through the plume (22:25 - 22:28 GMT). No gaps appear evident in either record at this time. This type of frequency-dependent absorption that is transient in nature lends support to the hypothesis of a dispersing cloud of bubbles present in the water column. It is important to note that immediately following many of the releases, the surface of the water was visually observed to effervesce as if air had been entrained in the discharged material and was released

upon immersion. The contour plot shown in Figure 6.11 shows the 20-kHz reflection coefficients for the second transect. The feature over the horizontal distance extending from 150 to 160 m is the same feature seen as a gap in Figure 6.9. Notice that, over the horizontal extent of that feature, from a depth of 4 to 6 m, the signal level steadily drops at a rate in excess of the surrounding plume. This drop in signal level is indicative of a region of localized excess absorption that extends to a depth of at least 6 m, implying that the hypothesized bubble cloud extends to at least that depth.

Subsequent passes through Survey 239B reveal both the horizontal dispersion of the plume material and current shear effects upon the dispersing plume. A portion of the water column may act as a "ceiling" for plume material below it (~8 m), while another portion (~5 m) acts as a "floor" for dispersing plume material above it.

Other important features such as internal waves and midwater surge fronts are also evident in these data, but detailed discussion of such is beyond the scope of this report.

Survey 241A

This survey consisted of a release in the shallow-water site in approximately 10 m of water followed by transverse monitoring. The plume boundaries are clear on both the 20- and 200-kHz records. Bottom surge is not as evident upon entering the plume, but is more clearly seen upon exiting. Absorption is high in the middle of the plume, with the 20-kHz signal again being more greatly affected.

Survey 242A

This survey occurred at the shallow site in about 10 m of water. Background scattering was very low. In this survey the ship entered the discharge plume and remained there for a period in excess of 10 min. The 200-kHz signal color contour plot of reflection coefficients for the first 3 min of the time period 16:06 to 16:09 is shown in Figure 6.12. Line contour plots and depth interval plots corresponding to the color contour plot are found in Appendix 6B. An expansion of the plume width with depth is clearly evident as the *R/V Pelican* entered the discharge plume. An apparently buoyant area of return is seen to overlie the initial plume expansion slope, this area could be bubbles. An incipient bottom surge is also visible. Note that for a vertical increment Δz of 2 m, a horizontal increment Δx of about 10 m is observed, yielding an estimate for the entrainment coefficient e of $\Delta z/\Delta x = 0.2$. Figure 6.13 shows the reflection coefficients for the 7- and 8-m depth horizons for the 200-kHz acoustical system. It is possible to obtain an estimate of e from these figures by dividing the depth difference of 1 m by the horizontal displacement of the

10^9 iso-reflection line of 5 m. Figure 6.14 is a line contour plot of the 20-kHz signal data corresponding to the same time period as in Figure 6.12. It may readily be seen that the suspected bubble feature discussed above coincides with a region of heavy absorption of the 20-kHz sound. This absorption of the 20-kHz sound further supports the bubble hypothesis.

Survey 242A provides sufficient acoustical, concentration, and transmissivity data to make rough estimates of confidence limits for measurements of the three data types. Using concentration estimates C_i provided from the samples gathered during Survey 242A (Chapter 4, this report), one obtains a mean concentration C_{avg} of 47.4 mg/l, a standard deviation in concentration σ_c of 25.2 mg/l, and a coefficient of variation $\sigma_c/C_{avg} = 0.53$. For the acoustical data set, using first-approximation acoustical processing, the average scattering coefficient (Appendix 6A) $R_{avg} = 7 \cdot 10^7$, the standard deviation in the reflection is $\sigma_a = 6 \cdot 10^7$, and $\sigma_a/R_{avg} = 0.9$. For the optical transmissivity data set, $\%T_{avg} = 42.5$, $\sigma_t = 15.4$, and $\sigma_t/\%T_{avg} = 0.36$. All three data sets are, therefore, properly dispersed in a statistical sense.

Survey 243A

This operation consisted of transverse sampling at the shallow site in approximately 10 m of water. Background scatter was slight. This survey showed clear signs of a bottom surge upon entry and less so upon exit. There was clearly strong absorption at 20 kHz in the midsection of the plume, with significant absorption at 200 kHz as well.

Shallow-Water Berm Survey

The 200- and 20-kHz data were recorded from 17:57 to 19:57 GMT on Julian Day 237. The 200-kHz system detected a weak background with no significant change in structure over the course of the survey. The 20-kHz system detected weak background scattering with an apparent increase in scattering from fish schools in the shallower portions of the survey. From these data it is concluded that there were no notable sand suspension events along either the shallower or deeper regions during the period of the survey.

Summary

The eight plume surveys analyzed show striking similarity in the overall make-up of plume features. Nearly all of the surveys showed evidence of horizontally propagating bottom surges during the first 5 min after release of the material. At least one edge of each plume showed a measurable growth in the horizontal width of the plume with increasing depth. Significantly greater absorption occurred in the upper water column for the 20-kHz signal than for the 200-kHz signal in the main body of each plume during the early stages of the survey.

Signal Comparison

Comparisons of acoustic scattering strength with concentrations measured from water bottle samples were performed on five discharge events (Surveys 240A, 240B, 241B, 242A, and 242B). These surveys were used because the in situ samples were taken at constant depth throughout each survey, reducing the number of degrees of freedom in the data from each survey, and the data contained a wide range of concentration values with which to compare. Table 6.2 lists the 20- and 200-kHz scattering strengths with the respective times, depths, and measured concentrations for the above five surveys. Figures 6.14 and 6.15 show the 20- and 200-kHz volume scattering strength (S_v) plotted against concentration for the five surveys. The wide dynamic range of values makes visualization of the correlation between S_v and concentration difficult if the values are plotted on a linear scale. Figures 6.16 and 6.17 show the same data plotted in decibel and log form. Plotted in this fashion, it becomes evident that from the 200-kHz data, there is a direct relationship between mean scattering strength and mean concentration from each survey at that frequency. At the time the samples were taken, the 20-kHz echoes were contaminated by echoes from the sampling rosette which resulted in the apparent lack of sensitivity of the 20-kHz data at that time to changes in concentration.

5. Conclusions

The MFDCP provided a rich data set on dredged material discharges for evaluating acoustic instruments that measure discharge plumes and particulate transport. Data were obtained on many key plume parameters including those of basic importance in numerical plume modeling. One example of these type of data is field measurement of the turbulent entrainment parameter. Numerical models may now be compared with a complete field data set on dispersion, this complete data set includes plume concentration, relative plume concentration, plume particulate distribution parameters, ambient density profiles, ambient current profiles, and meteorological parameters. The objectives of the ACP component of this general study have been achieved. Numerous discharge plume profiles of high quality using 20- and 200-kHz signals were obtained. These data may now be intercompared with other acoustical and nonacoustical data. Initial calibration curves have been obtained, and the effects of bubbles on acoustic echoes have been observed.

6. Discussion and Recommendations

The MFDCP yielded a unique data set and can surely be regarded as the most careful, extensive, and complete dredged material discharge study to date. From the point of view of evaluation of the applicability of acoustical methodologies to the study of dredged material discharges, the MFDCP was a pioneering effort. NOAA has now performed five cooperative acoustical studies of dredged material discharges with the U.S. Army Engineer Waterways Experiment Station. These studies are as follows;

1. Lake Ontario Discharge Study (1976).
2. New York Bight Discharge Study (1977).
3. James River Discharge Study (1982).
4. MFDCP (1989-present).
5. Miami Harbor Discharge Study (1990).

The data from these studies form a powerful set for research and model evaluation purposes.

It is now clear that the detection of dredged material discharge plumes can be accomplished acoustically. The essential remaining task is calibration of acoustical systems. In a strict sense, calibration of an acoustical system means establishment of a relationship whereby the scattered acoustical intensity is directly interpretable in terms of the concentration of the particulate load giving rise to the scattering. Attempts have been made both in the laboratory "and in the field" to establish a calibration of sorts. In the laboratory, measurements may be made using relatively homogeneous and well-defined particulate samples, particles of fixed size distribution and of fixed physical character (e.g., size, rigidity, elasticity, and shape). In the field, the situation is highly inhomogeneous and variable. Indeed, it must be borne in mind that, in evaluating the utility of acoustical devices, all other measurement approaches for plume particulate concentrations suffer from similar or worse problems than does acoustics. In particular, bottle samples, transmissivity, radioactivity, and other methods have method-specific measurement problems compounded by the natural spatial variability of the plume.

The MFDCP has provided information on the field calibration of the 20- and 200 kHz ACP systems. Data from the MFDCP have clearly shown the presence of bubble clouds intertwined with dredged material discharge plumes. The 20-kHz system performance is much

more affected by the presence of the bubbles, thus, the field calibration data of the 20-kHz system is much more variable than the 200-kHz system.

The following is a set of recommendations for analysis and future work.

Plume Analysis

The discharge surveys should be analyzed for the provision of data on parameters used in and basic to the operation of existing Corps numerical models of discharge plumes. For example, preliminary analysis of MFDCP acoustical data has yielded an estimate of about 0.2 for the turbulent entrainment coefficient. This coefficient could be computed for most of the discharge surveys.

Numerical simulation models should be run for the MFDCP discharge surveys. Comparison of model predictions with this extensive data set would be most interesting and valuable for model validation.

The influence of the ocean bottom on the flow and dynamics of discharge plumes should be carefully analyzed. It is clear from the MFDCP data that the influence of the bottom on flow dynamics of the plume extends to meters above the bottom.

A careful analysis of the effect of water column density profile characteristics and ambient current characteristics upon the passive dispersion phase of the plume discharge should be made. The existence of vertical shear and dispersion floor and ceiling effects has been indicated in the MFDCP data.

Acoustical System Analysis

Future analysis of MFDCP data should continue investigating differences between the 20- and 200 kHz data. A calibration effort should be undertaken for multiple acoustical frequencies as it is likely that a final design acoustical system for real-time monitoring and research will use multiple frequencies.

Intercomparison of ACP and Acoustic Doppler Current Profiler (ADCP) data should be made. The ADCP operated at a frequency of 1.2 MHz, thus providing yet a third frequency to compare with 20- and 200-kHz data.

A refined detailed analysis of acoustical data and concentration samples should be made.

The preceding is but a portion of the analysis which may be made with the MFDCP data.

References

- Clay, C. S., and Medwin, H. 1977. *Acoustical Oceanography: Principles and Applications*, John Wiley & Sons, New York.
- Proni, J. R., Dammann, W. P., Craynock, J. F., and Fergen, R. 1989. "Oceanic Wastewater Outfall Characteristics Measured Acoustically," *Eighth International Ocean Disposal Symposium*, Dubrovnik, Yugoslavia.
- Urick, R. J. 1975. *Principles of Underwater Sound for Engineers*, McGraw-Hill, New York.

References

- Clay, C. S., and Medwin, H. 1977. *Acoustical Oceanography: Principles and Applications*, John Wiley & Sons, New York.
- Proni, J. R., Dammann, W. P., Craynock, J. F., and Fergen, R. 1989. "Oceanic Wastewater Outfall Characteristics Measured Acoustically," *Eighth International Ocean Disposal Symposium*, Dubrovnik, Yugoslavia.
- Urick, R. J. 1975. *Principles of Underwater Sound for Engineers*, McGraw-Hill, New York.

Table 6.2
Scattering Strengths and Water Bottle Concentrations

<u>Survey Number</u>	<u>Time GMT</u>	<u>200-kHz S_v</u>	<u>20-kHz S_v</u>	<u>Depth m</u>	<u>Concentration mg/l</u>
240A	13:42:11	-71.3	-52.6	10.7	124.2
240A	13:42:26	-74.6	-49.9	10.7	62.9
240A	13:42:44	-78.8	-50.5	10.7	20.4
240A	13:44:16	-56.7	-39.5	4.3	6.3
240A	13:45:44	-67.9	-58.5	1.3	3.3
240B	20:39:44	-111.0	-51.3	9.8	3.6
240B	20:39:59	-101.0	-48.9	9.8	4.0
240B	20:40:17	-116.0	-51.1	9.8	2.8
240B	20:40:58	-112.0	-39.6	9.8	5.6
240B	20:41:36	-88.3	-37.5	9.8	5.7
240B	20:41:54	-85.2	-37.7	9.8	5.0
240B	20:42:53	-83.6	-34.4	8.8	1.8
240B	20:43:45	-78.7	-34.6	9.8	6.7
240B	20:44:05	-87.4	-35.4	9.8	7.6
240B	20:44:56	-90.8	-44.7	9.8	5.9
241B	18:52:34	-68.2	-44.6	5.5	2.1
241B	18:53:42	-68.9	-50.7	5.6	179.8
241B	18:58:21	-65.4	-49.0	5.6	90.1
241B	18:58:47	-65.8	-47.6	5.5	178.2
241B	18:59:04	-66.6	-48.4	5.6	112.4
241B	18:59:24	-68.0	-52.8	5.5	99.1
242A	16:08:37	-56.8	-53.9	7.2	29.5
242A	16:09:07	-57.9	-50.0	7.2	31.2
242A	16:09:39	-59.8	-46.1	7.2	39.5
242A	16:09:56	-61.9	-50.6	7.2	50.3

(Continued)

Table 6.2 (Concluded)

Survey Number	Time GMT	200-kHz S_v	20-kHz S_v	Depth m	Concentration mg/l
242A	16:10:12	-65.3	-52.3	7.2	41.5
242A	16:10:29	-62.6	-51.9	7.2	45.7
242A	16:11:05	-64.2	-51.6	7.2	36.4
242A	16:11:44	-66.2	-48.4	7.2	117.0
242A	16:12:12	-69.5	-51.4	7.2	42.1
242A	16:12:29	-70.9	-54.9	7.2	40.9
242B	23:33:37	-57.9	-68.0	5.0	1306.0
242B	23:33:54	-56.4	-79.3	4.8	353.3
242B	23:34:11	-59.0	-66.3	5.0	2149.8
242B	23:34:29	-61.5	-50.9	4.9	3356.8
242B	23:35:03	-55.9	-41.6	3.8	1749.3
242B	23:35:22	-55.8	-61.3	3.9	878.5
242B	23:35:44	-52.3	-55.2	3.9	243.2
242B	23:36:00	-56.2	-43.2	3.9	621.8
242B	23:36:15	-55.5	-37.7	3.8	660.9
242B	23:36:33	-60.6	-37.4	3.8	447.5
242B	23:36:50	-63.4	-44.4	3.8	593.2
242B	23:37:08	-59.4	-41.8	3.8	680.7

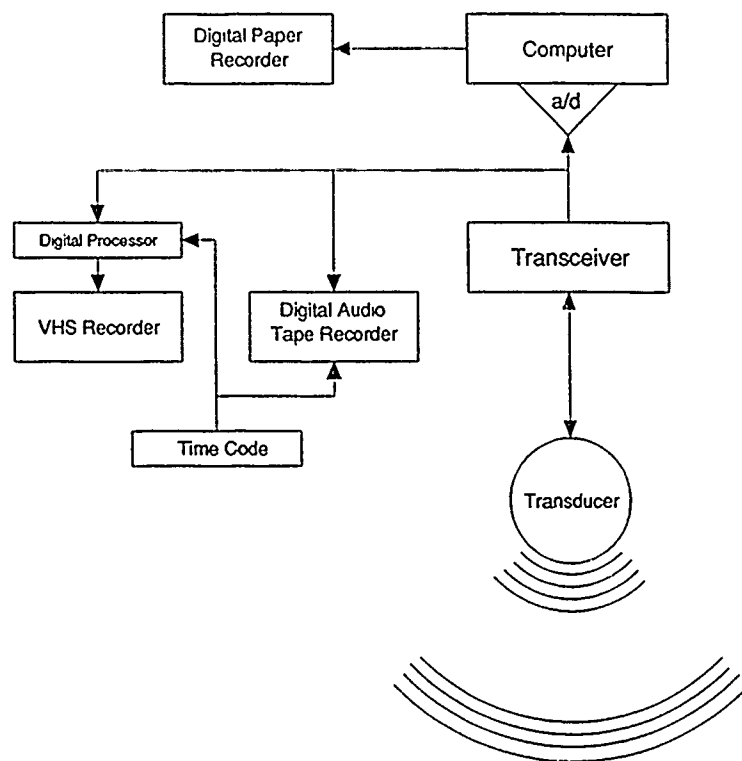


Figure 6.1. ACP system diagram.

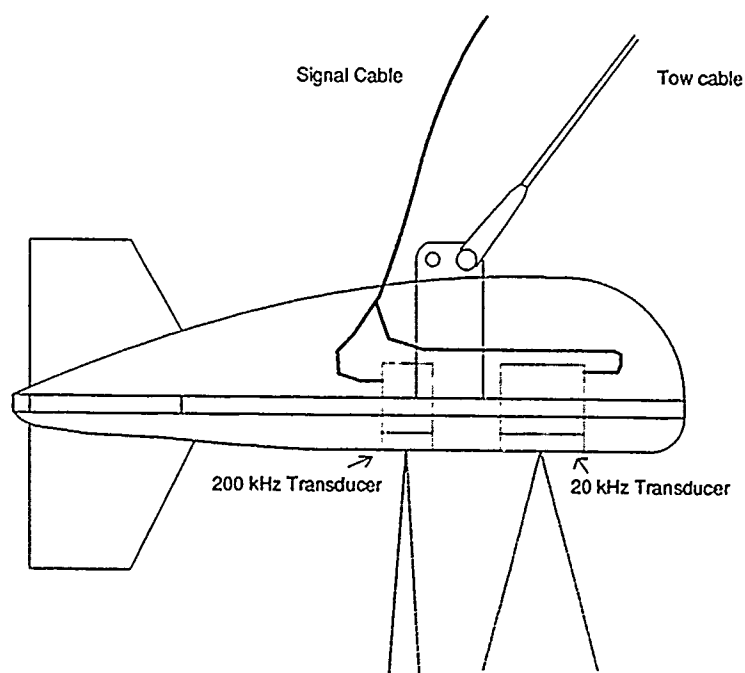




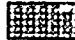

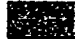

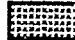

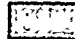







Figure 6.2. ACP towbody configuration.

KEY

Color codes for acoustic backscatter intensity
(dB) in Figures 6.3 to 6.7 and Figure 6.12.

	ABOVE	-30
	-36 -	-30
	-42 -	-36
	-48 -	-42
	-54 -	-48
	-60 -	-54
	-66 -	-60
	-72 -	-66
	-78 -	-72
	-84 -	-78
	-90 -	-84
	-96 -	-90
	-102 -	-96
	-108 -	-102
	-114 -	-108
	BELOW	-114

239B 2213:00-2216:00 Z 200 KHz
REFLECTION COEFFICIENT ($\times 10^{-7}$)

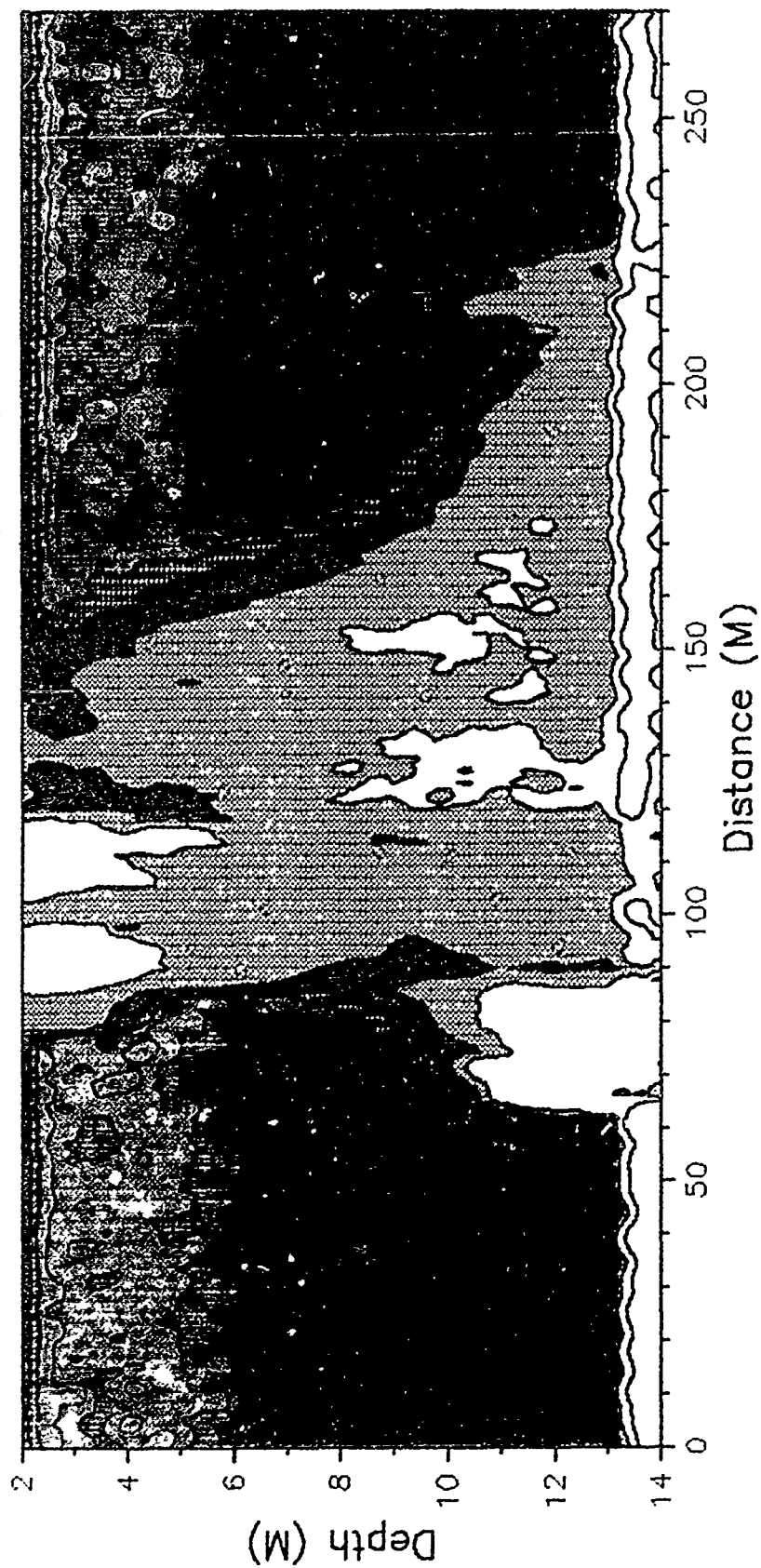


Figure 6.3. Survey 239B 200-kHz S_v Pass 1.

239B 2217:30-2220:30 Z 200 KHz
REFLECTION COEFFICIENT ($\times 10^{-7}$)

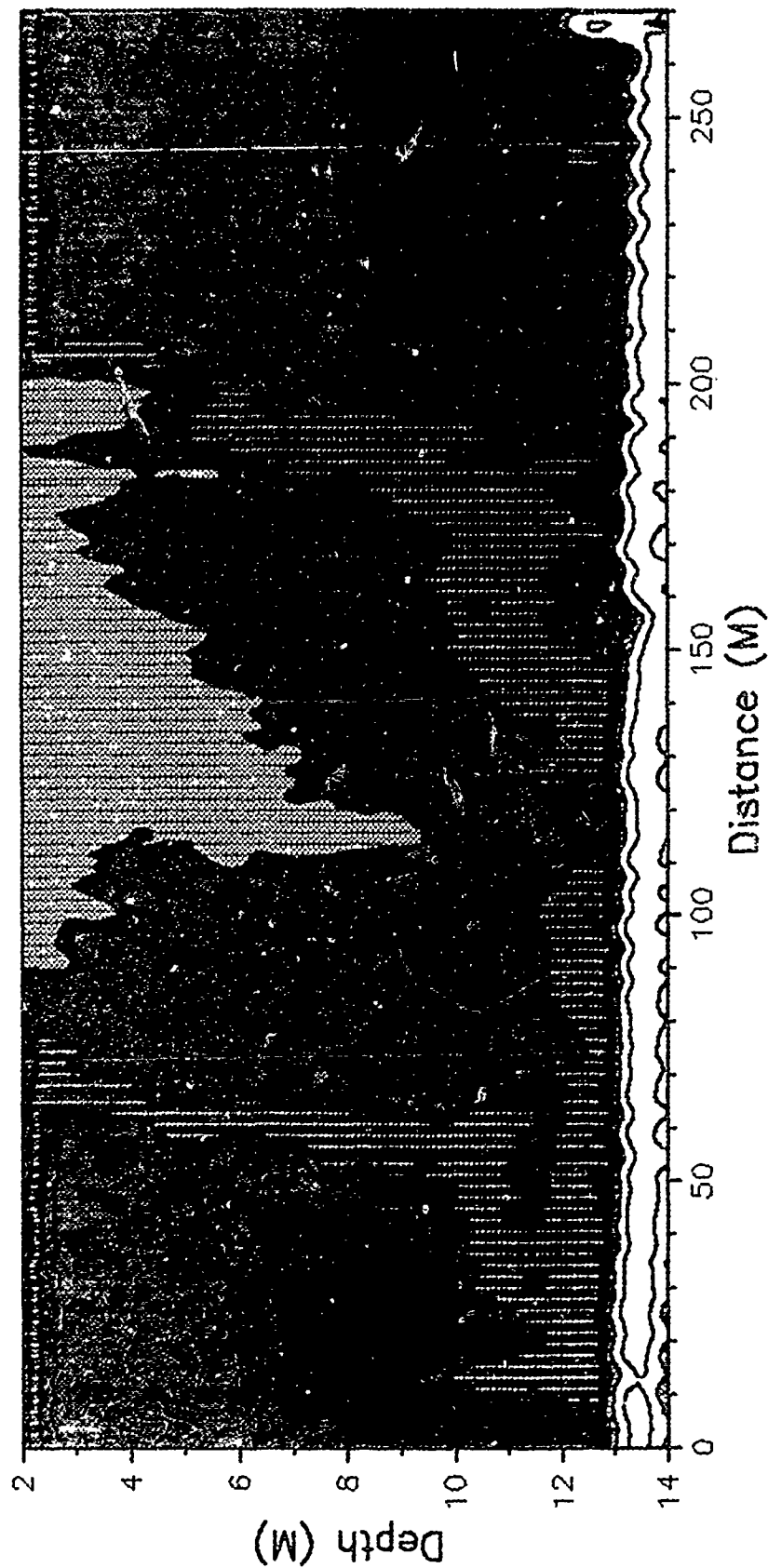


Figure 6.4. Survey 239B 200-kHz S_v Pass 2.

239B 2225:00-2228:00 Z 200 KHz
REFLECTION COEFFICIENT ($\times 10^{-7}$)

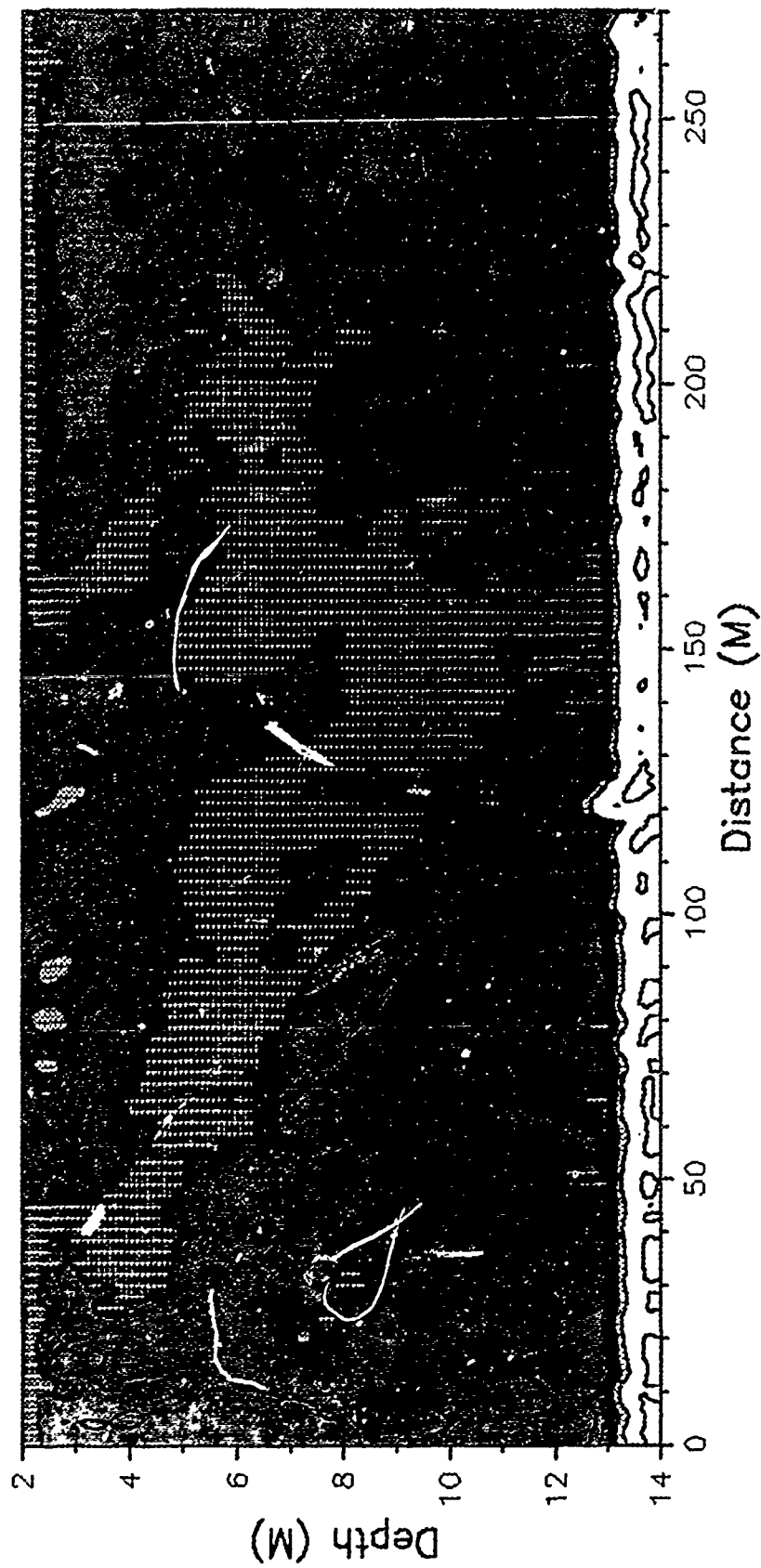


Figure 6.5. Survey 239B 200-kHz S_v Pass 3.

239B 2232:30-2235:30 7. 200 KHz
REFLECTION COEFFICIENT ($\times 10^{-7}$)

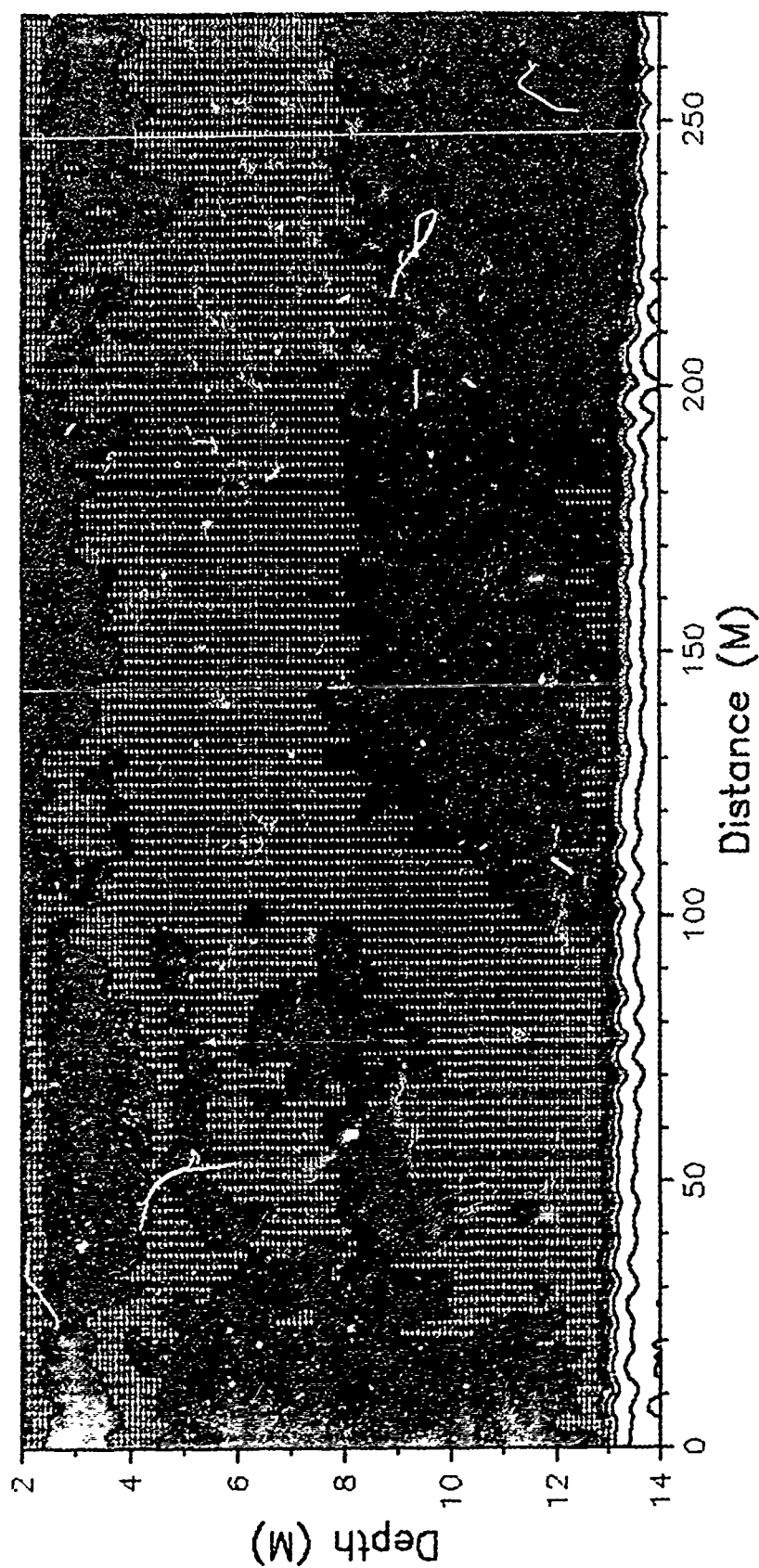


Figure 6.6. Survey 239B 200-kHz S_v Pass 4.

239B 2239:00-2242:00 Z 200 KHz
REFLECTION COEFFICIENT ($\times 10^{-7}$)

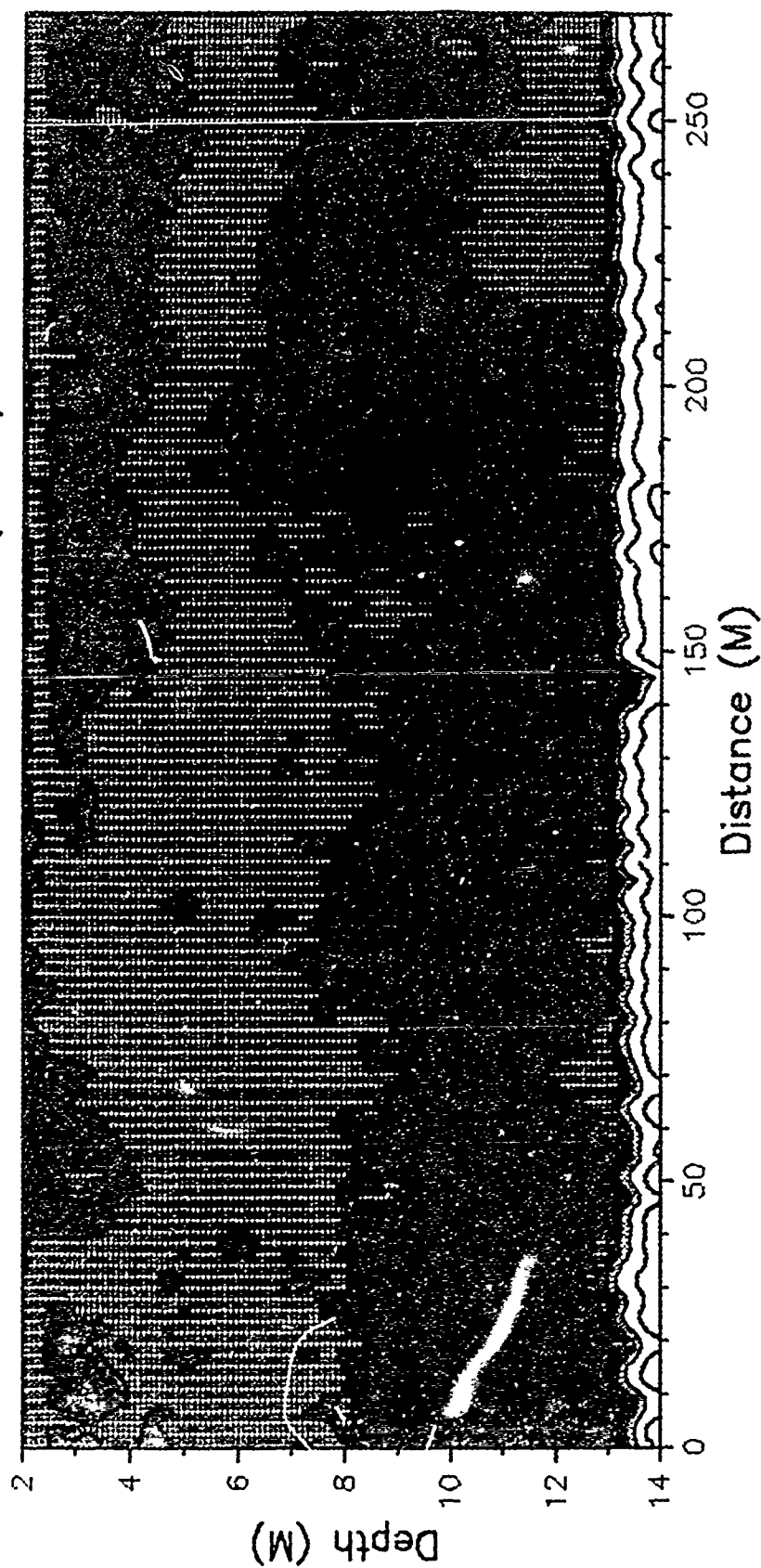
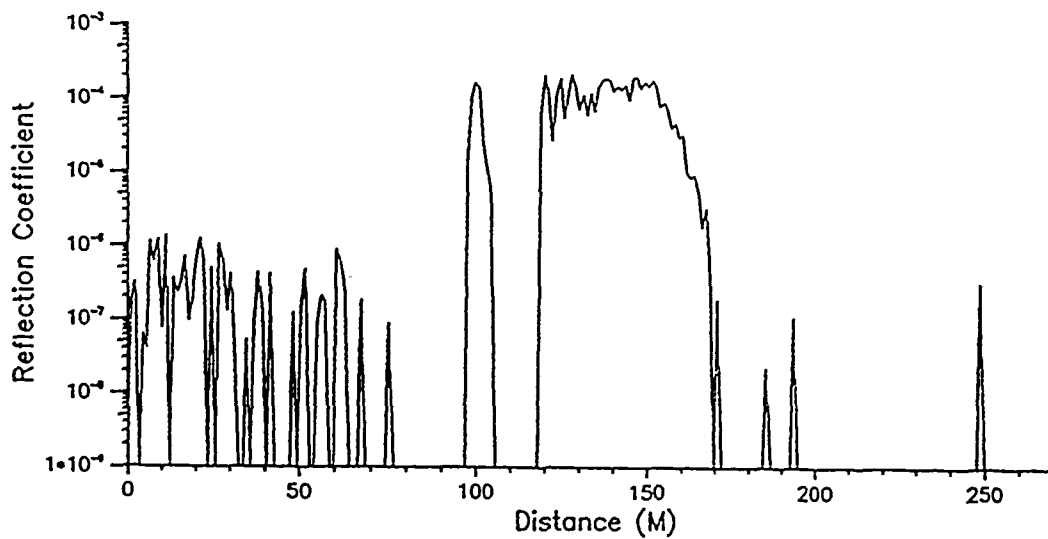


Figure 6.7. Survey 239B 200-kHz S_v Pass 5.

239B 2213:00–2216:00 Z 20 KHz Background time = 2213:00 Z
 Depth = 6.0 meters



239B 2213:00–2216:00 Z 200 KHz Background time = 2213:00 Z
 Depth = 6.0 meters

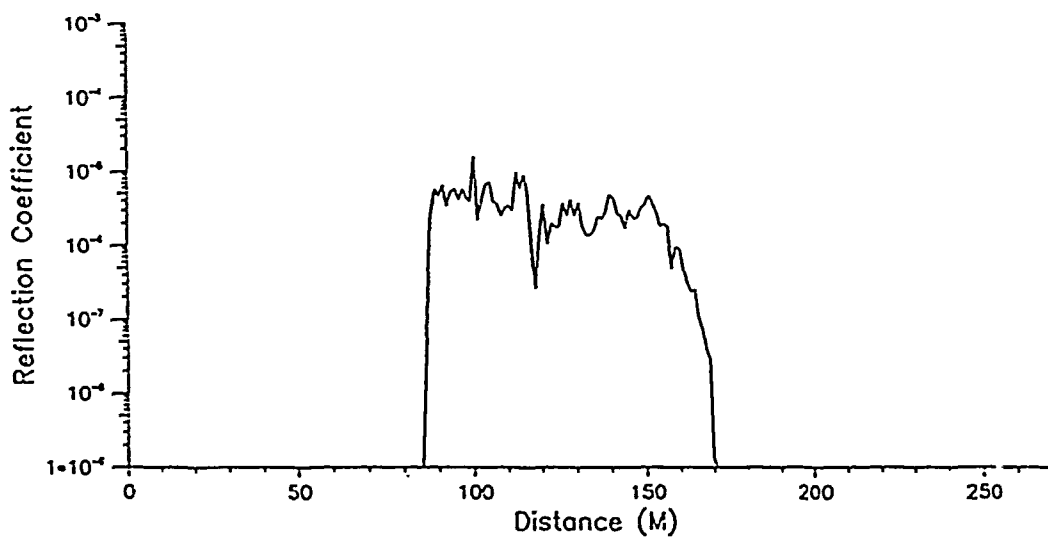
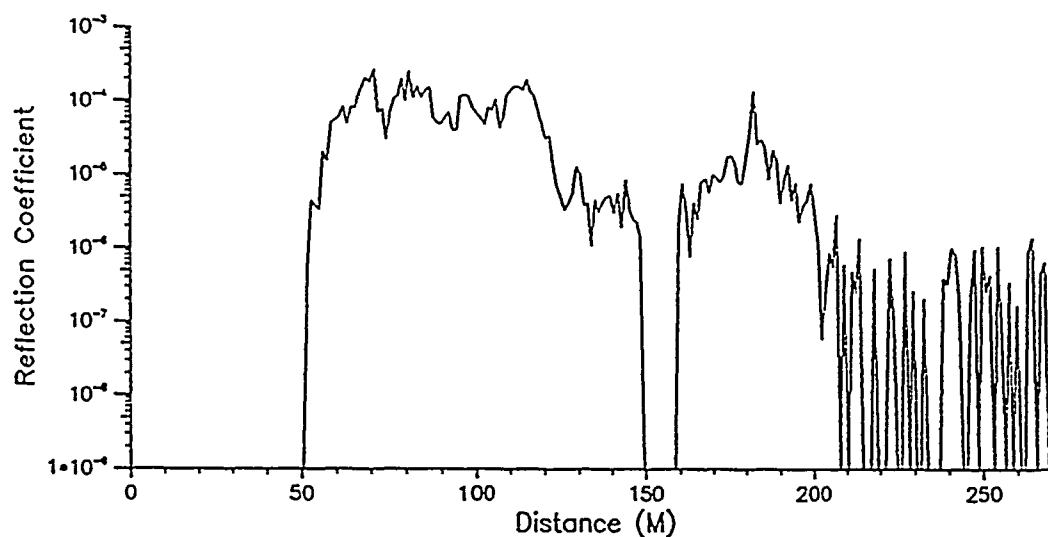


Figure 6.8. 239B 6 m S_v , Pass 1.

239B 2217:30-2220:30 Z 20 KHz Background time = 2220:00 Z
 Depth = 6.0 meters



239B 2217:30-2220:30 Z 200 KHz Background time = 2220:00 Z
 Depth = 6.0 meters

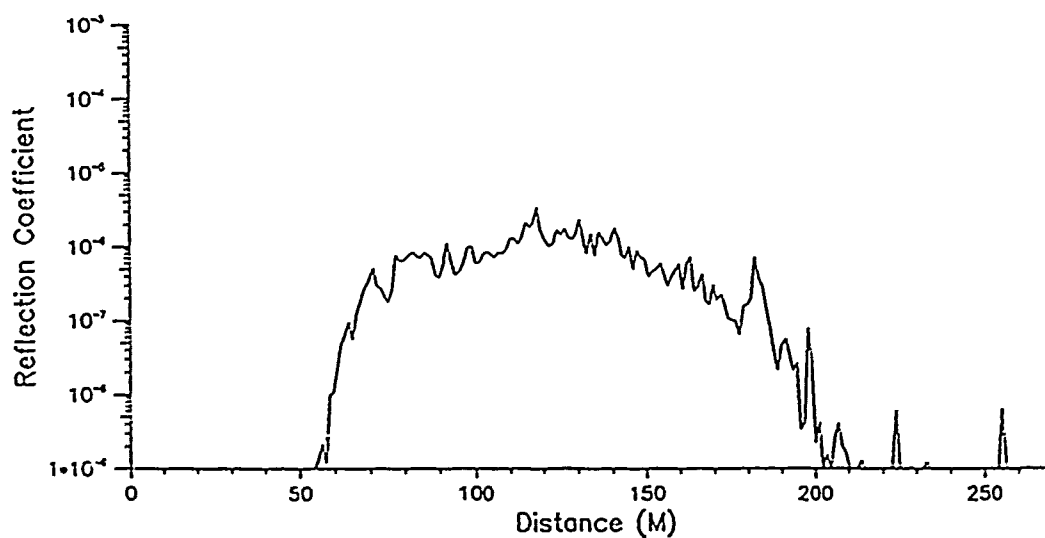
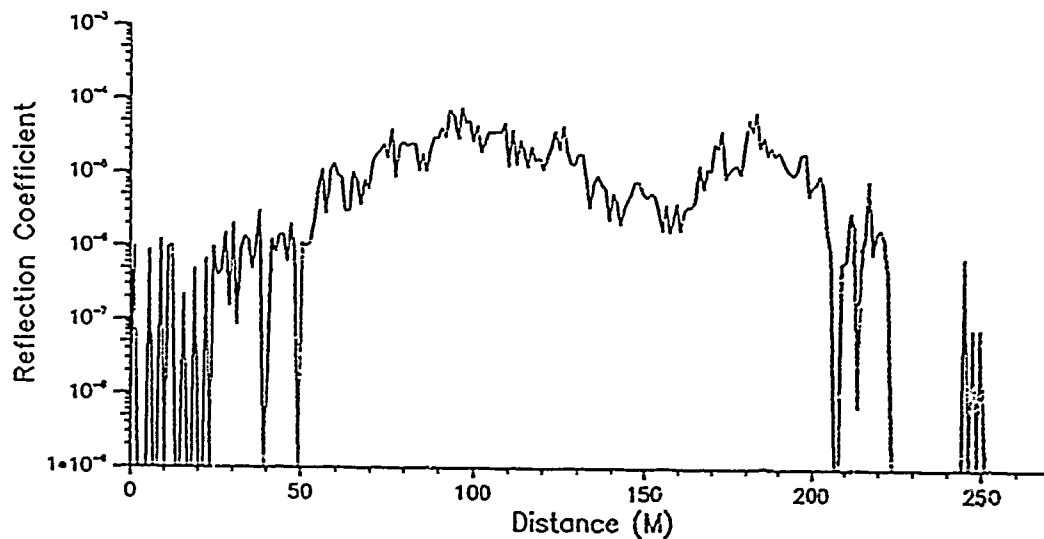


Figure 6.9. 239B 6 m S_{v} , Pass 2.

239B 2225:00-2228:00 Z 20 KHz Background time = 2225:00 Z
 Depth = 6.0 meters



239B 2225:00-2228:00 Z 200 KHz Background time = 2225:00 Z
 Depth = 6.0 meters

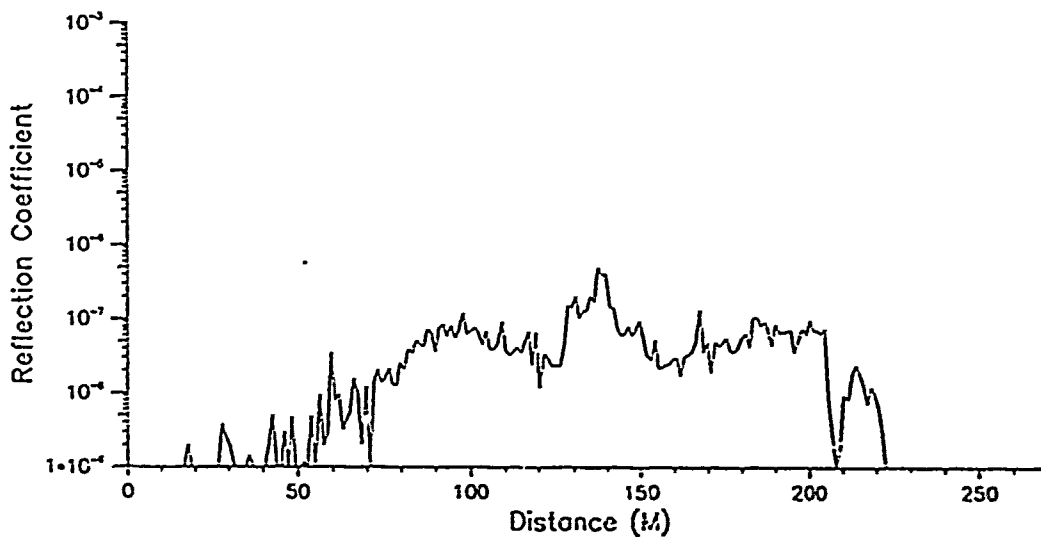


Figure 6.10. 239B 6 m S_v , Pass 3.

239B 2217:30-2220:30 Z 20 KHz Background time = 2220:00 Z
REFLECTION COEFFICIENT ($\times 10^{-7}$)

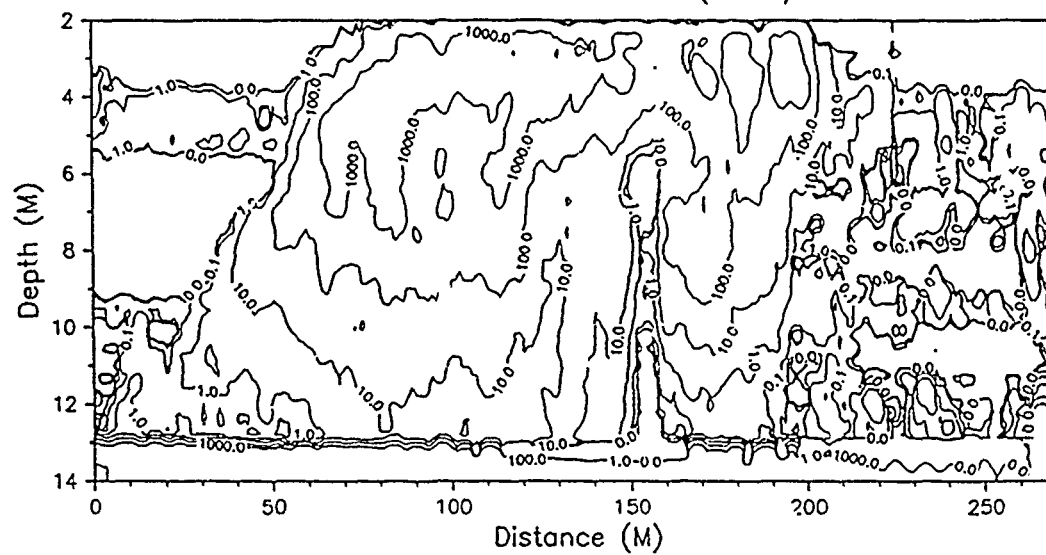


Figure 6.11. Survey 239B 20-kHz S_v Pass 2.

242A 1606:00-1609:00 Z 200 KHz Background time = 1606:00 Z

REFLECTION COEFFICIENT ($\times 10^{-7}$)

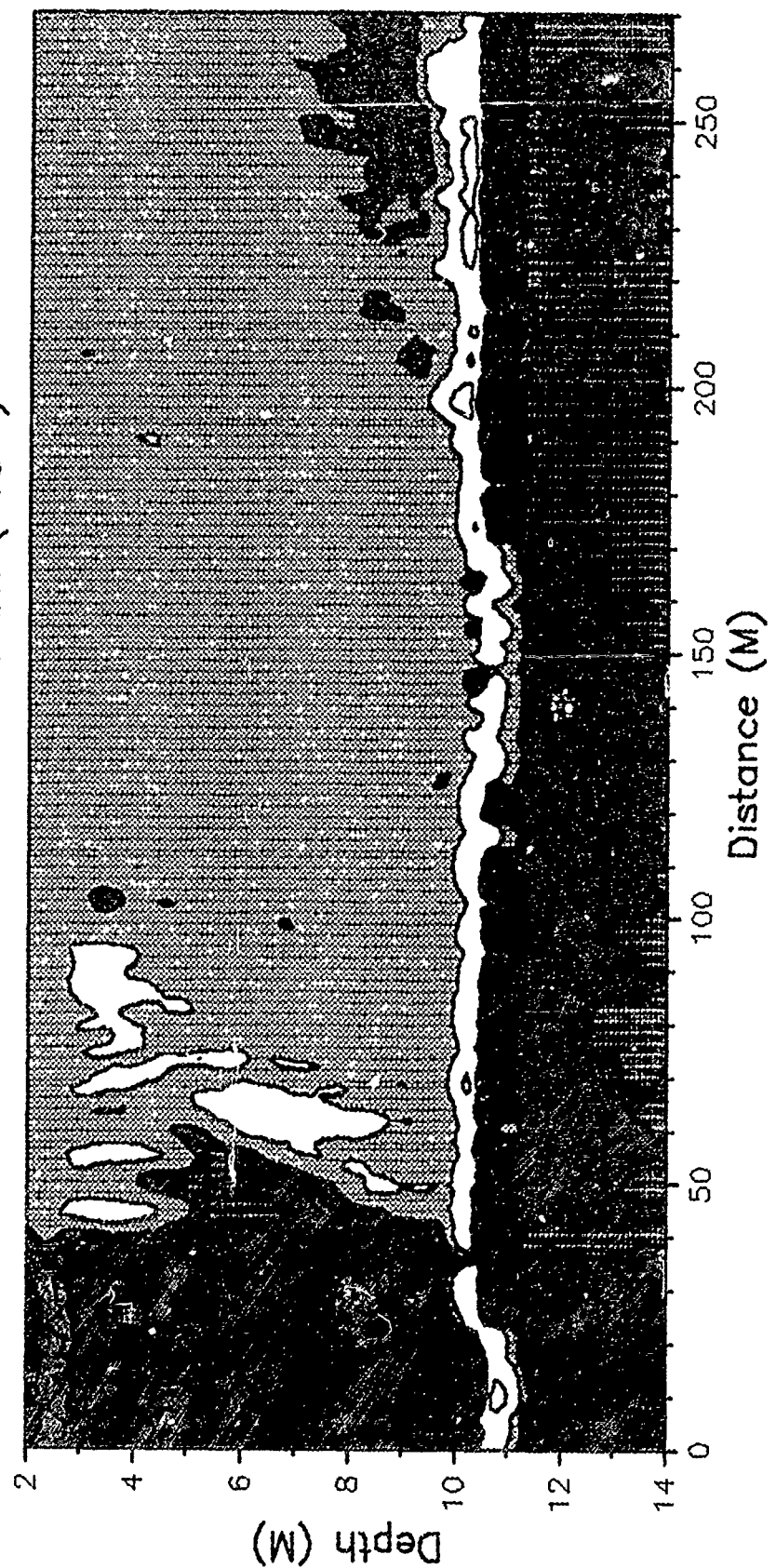
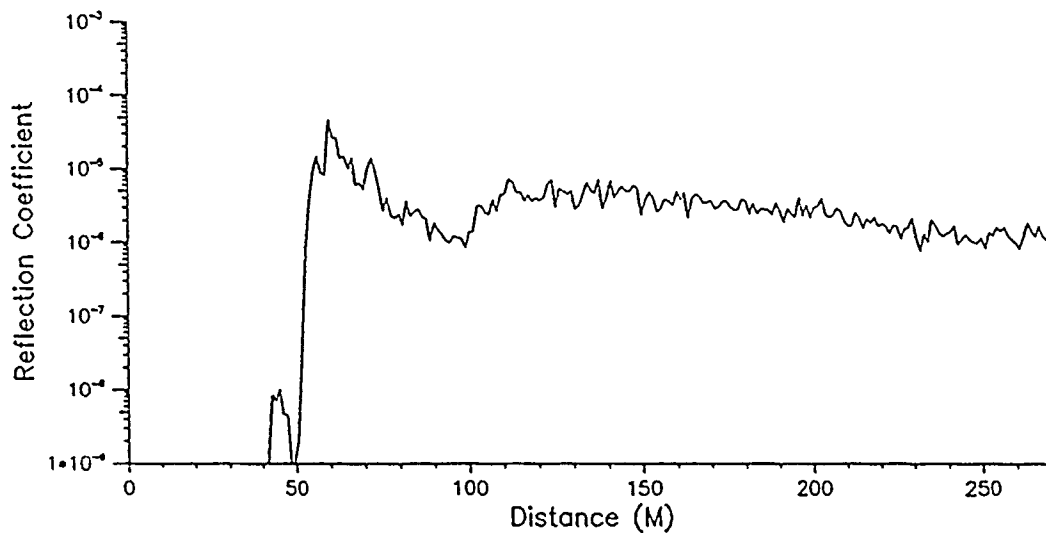


Figure 6.12. Survey 242A 200-kHz S_y Pass 1.

242A 1606:00-1609:00 Z 200 KHz Background time = 1606:00 Z
 Depth = 7.0 meters



242A 1606:00-1609:00 Z 200 KHz Background time = 1606:00 Z
 Depth = 8.0 meters

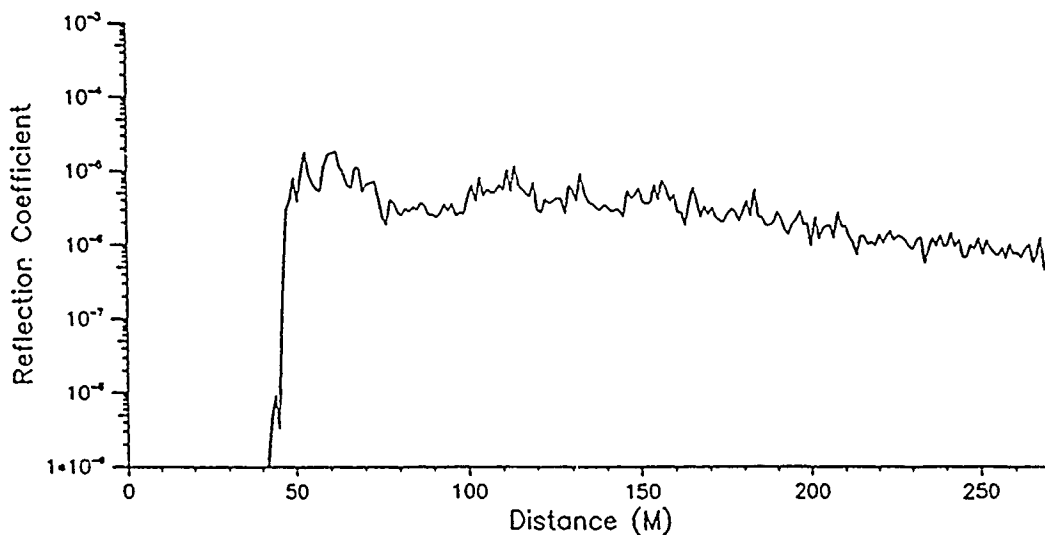


Figure 6.13. Survey 242A 200-kHz 7 and 8 m S_v .

Scattering Coefficient vs. Concentration

20 kHz

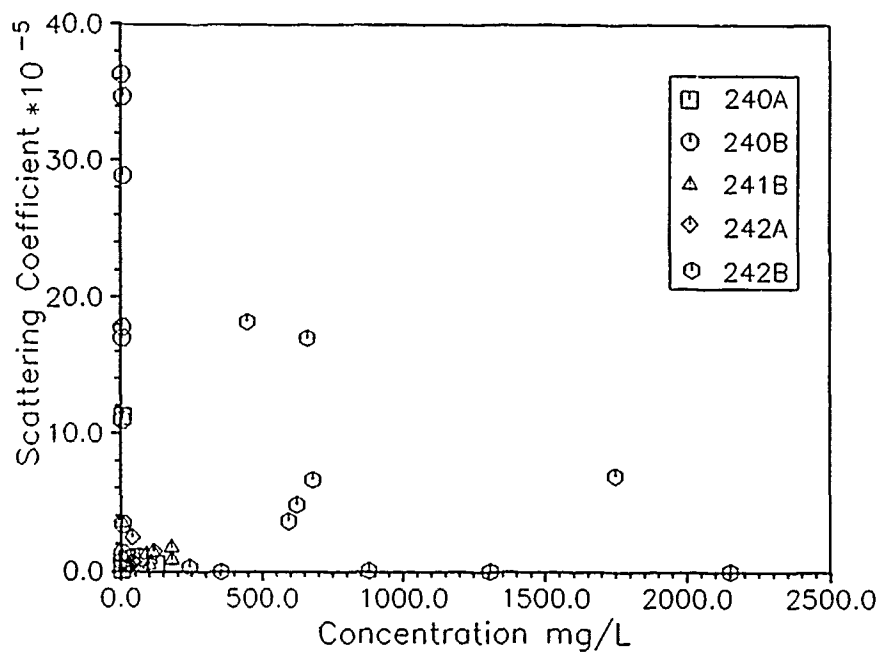


Figure 6.14. 20-kHz S_v versus concentration.

Scattering Coefficient vs. Concentration

200 kHz

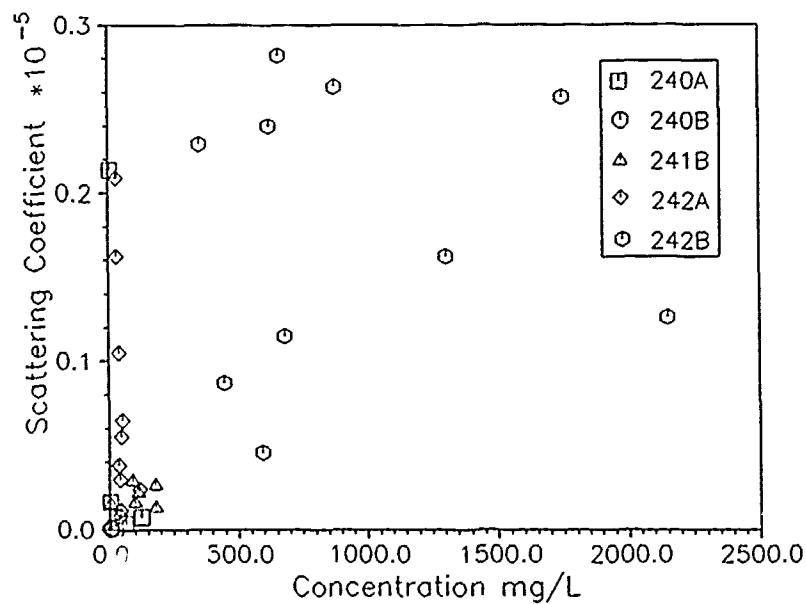


Figure 6.15. 200-kHz S_v versus concentration.

Scattering Strength vs. Log Concentration

20 kHz

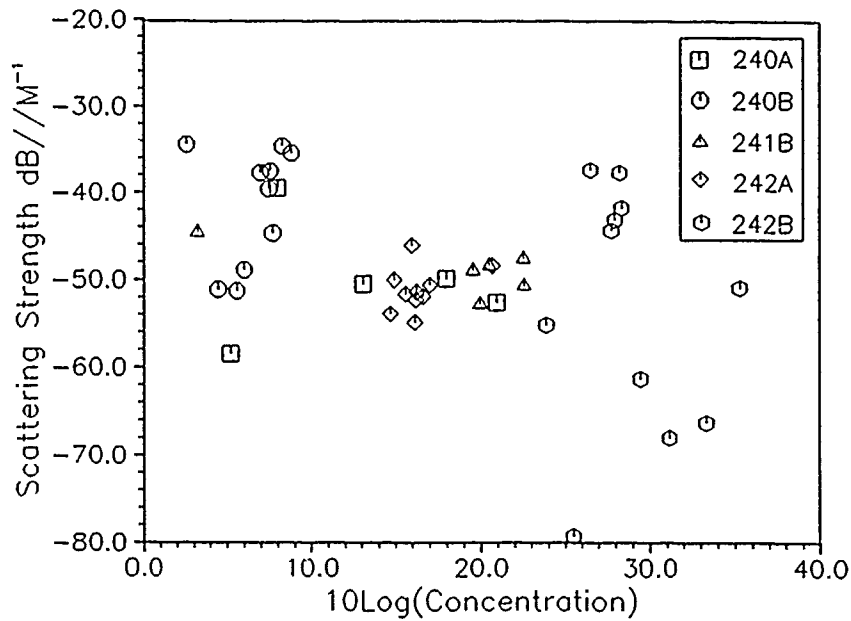


Figure 6.16. 20-kHz S_v versus log concentration.

Scattering Strength vs. Log Concentration

200 kHz

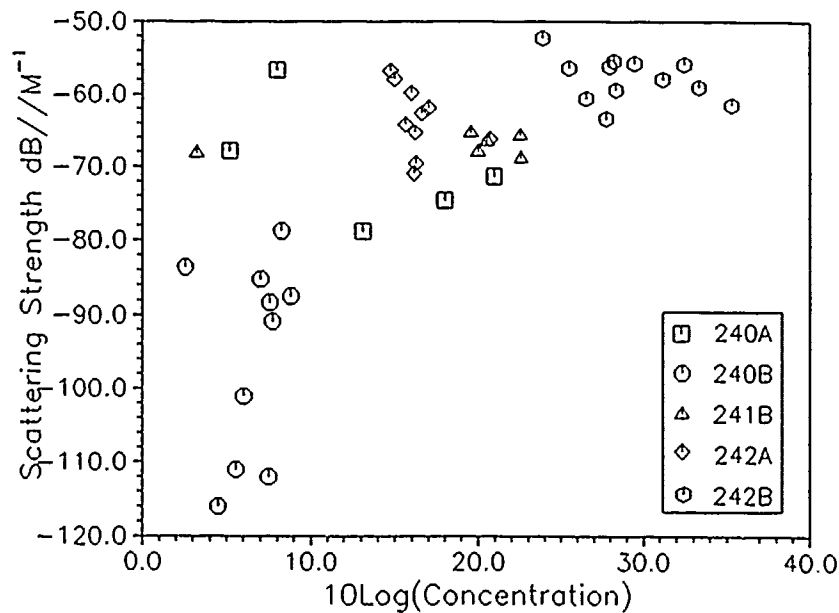


Figure 6.17. 200-kHz S_v versus log concentration.

Appendix 6A: Theoretical Background

Scattering Coefficient

The scattering coefficient R is the ratio of the scattered acoustic intensity I_s measured at a distance of 1 m from the center of the scattering volume in the direction of the transducer to the incident plane wave intensity I_i referenced to the same 1-m range,

$$R = \frac{I_s}{I_i} \quad (6A.1)$$

where the plane wave intensity is given by,

$$I = \frac{p^2}{\rho c} \quad (6A.2)$$

in which ρ is the mass density of seawater (1.024 kg/m³).

The scattering strength S_v is the decibel equivalent of the scattering coefficient such that:

$$S_v = 10 \log_{10} (R) \quad (6A.3)$$

In acoustically measuring particulate concentration, the approach taken is to relate particulate concentration to acoustic cross-section-per-unit volume s_v . Clay and Medwin (1977)* assert that,

$$s_v = \sum N_i \sigma_{bsi} \quad (6A.4)$$

where N_i is the number of particles per unit volume in the i^{th} size class, and σ_{bsi} is the backscattering cross section (m²) of those particles. The scattering coefficient is proportional to the cross-section-per-unit volume such that the scattering strength is given by:

$$S_v = 10 \log_{10} (s_v r_l) \quad (6A.5)$$

where r_l is the reference distance of 1 m.

For particles of similar shape and orientation in any given size class in a plume of scatterers, the backscattering cross-section-per-unit particle volume κ_i at orientation (θ, ϕ) is given by:

$$\kappa_i (\theta, \phi) = \frac{\sigma_{bsi}}{v_i} \quad (6A.6)$$

* See References at the end of main text.

where v_i is the volume of a particle of size class i . For a large number of particles oriented randomly, the mean backscattering cross-section-per-unit particle volume is given by,

$$\bar{\kappa}_i = N_i^{-1} \sum_{j=1}^{N_i} \kappa_i(\theta_j, \phi_j) \quad (6A.7)$$

Further, defining the probability density of orientations within the plume for particles of size class i as $p_i(\theta, \phi)$ gives,

$$\bar{\kappa}_i = \int_0^\pi \int_0^{2\pi} p_i \kappa_i d\theta d\phi \quad (6A.8)$$

and

$$S_v = \sum N_i \bar{\kappa}_i v_i = N \bar{\kappa} \bar{v} \quad (6A.9)$$

where $N = \sum N_i$.

The mass m_i of a particle of size class i is given by,

$$m_i = \bar{\rho}_i v_i \quad (6A.10)$$

where $\bar{\rho}_i$ is the mean density of a particle of size class i . The mass concentration C of particles in a fluid volume is given by,

$$C = \sum N_i m_i = \sum N_i \bar{\rho} v_i = N \bar{\rho} \bar{v} \quad (6A.11)$$

where C is in units of mass per unit volume. Dividing Equation 6A.11 by Equation 6A.9 yields,

$$C = \frac{S_v \bar{\rho}}{\bar{\kappa}} = A S_v = \frac{AR}{r_1} \quad (6A.12)$$

where A is an empirical coefficient of proportionality with units of mass per unit area.

Dilution Ratio

The dilution ratio δ between two scattering volumes with different concentrations C_1 and C_2 can be calculated from ratios of scattering coefficients R_1 and R_2 measured directly from the two volumes using the equation,

$$\delta_{21} = \frac{C_2}{C_1} = \frac{R_2}{R_1} \quad (6A.13)$$

Entrainment Coefficient

One key model parameter is the turbulent entrainment coefficient ϵ . An approximate argument may be constructed such that ϵ is directly measurable from real-time acoustical data. In particular, it may be shown that,

$$\epsilon = \frac{da(z)}{dz} \quad (6A.14)$$

where a is the radius of the descending discharge plume at depth z . The quantity ϵ may be read directly, even from simple acoustical real-time paper records. Thus it will be of interest in future data analysis to compute ϵ for the eight discharge surveys selected for in-depth review. Because an excellent database was gathered in the Mobile Field Data Collection Project in addition to the acoustical data, interesting interdata types of analyses may be performed in the future. For example, in Survey 242A the research vessel entered the discharge plume and remained there for more than 10 min. Conductivity, temperature, depth, transmissivity, and concentration were simultaneously measured by in situ water sampling.